HyspIRI Headquarters Update

Woody Turner
HyspIRI Co-Program Scientist
Earth Science Division
NASA Headquarters
May 16, 2012

Earth Science Budget: FY13 Request

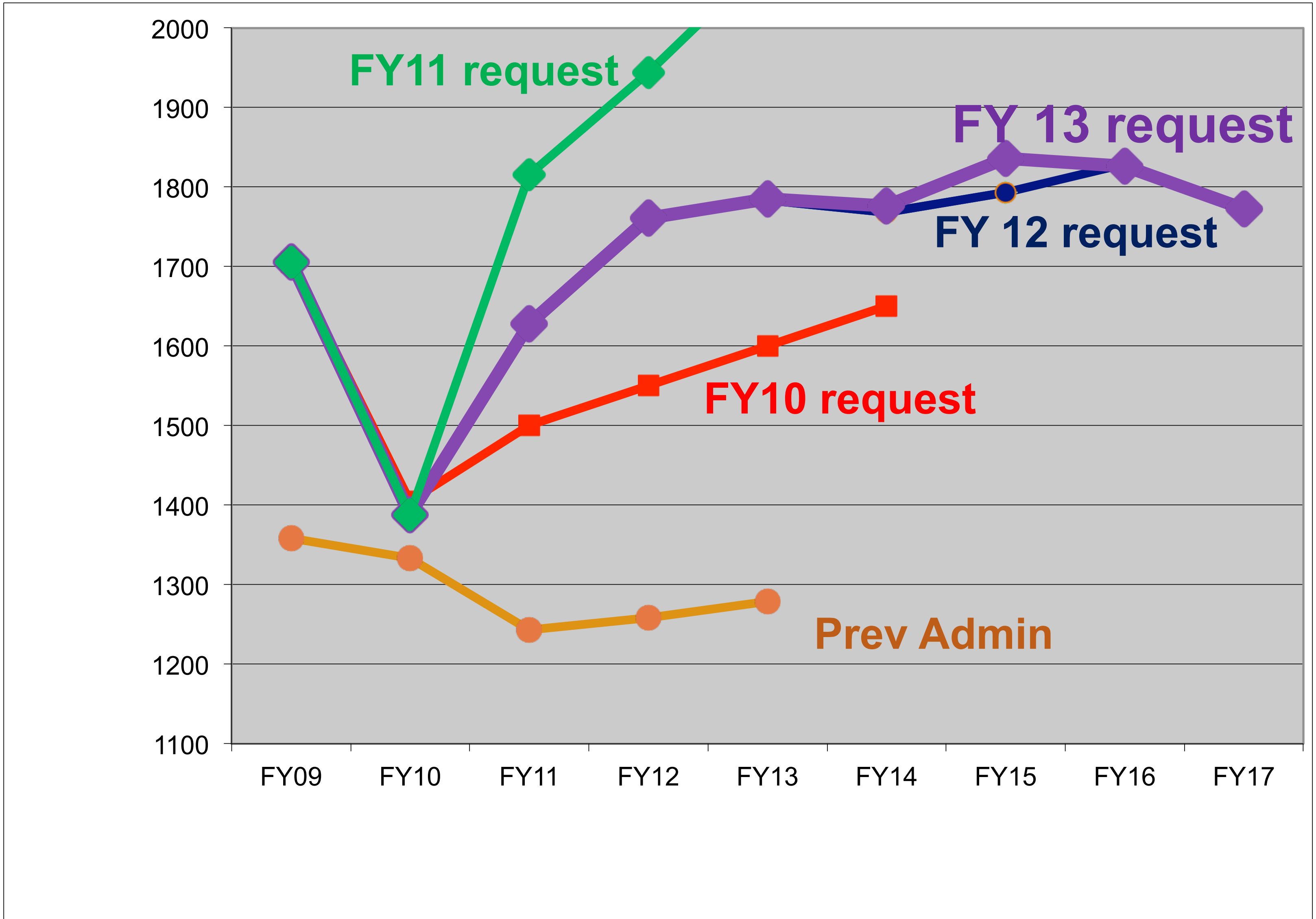

Update

- 4th HyspIRI Science Workshop in August 2011
- HyspIRI Mission Applications Reps: JPL/Simon Hook, MSFC/Jeff Luvall
- Pre-Formulation Workshop in December 2011
  - *"Is still the most 'shovel ready' mission among the Tier II's"* – Steve Volz
  - Flat line funding for at least two years, to be revisited every year
  - Current launch date still after 2020
  - Explore partnerships to accelerate launch of elements of the HyspIRI mission
- HyspIRI Preparatory Airborne Activities and Associated Science and Applications Research solicitation released in December 2011
  - 49 proposals received, preparing for peer review panel
- NRC Mid-Term Assessment of NASA's Implementation of Decadal Survey released in May 2012
- HyspIRI Independent Cost Estimate with The Aerospace Corporation
- Weekly teleconferences by Steering Committee
- Science Study Group (SSG) and International Science Group calls
- Be ready for opportunities

Summary of HyspIRI Mission Concept and Instruments

Simon J. Hook *, Robert O. Green *, Elizabeth M. Middleton **, Carl Bruce *, Marc Foote * and The HyspIRI Group

16 May 2012

*Jet Propulsion Laboratory, California Institute of Technology
**Goddard Space Flight Center

NRC Decadal Survey
HyspIRI Mission Concept

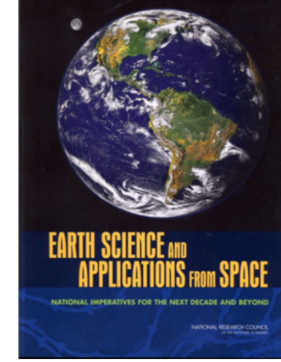

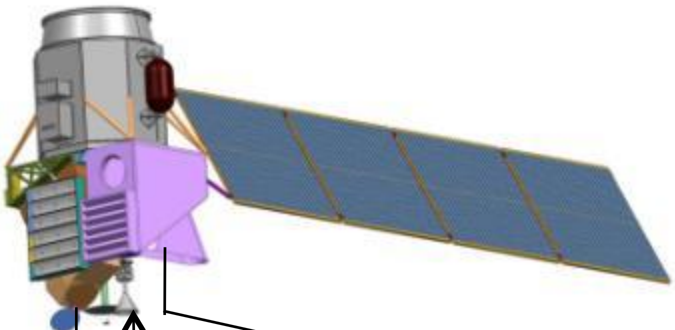

Visible ShortWave InfraRed (VSWIR) Imaging Spectrometer

Intelligent Payload Module Low Latency Data

Multispectral Thermal InfraRed (TIR) Scanner

Map of dominant tree species, Bartlett Forest, NH

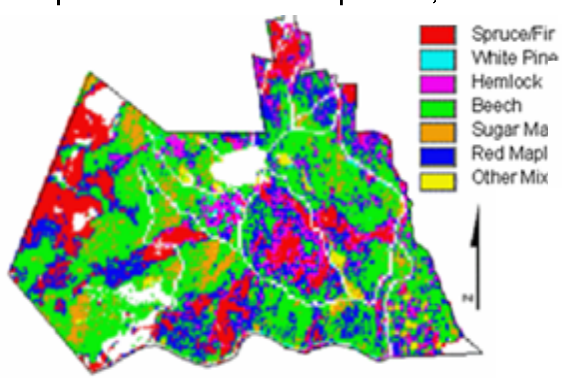

Soil C:N Ratio

White Mountain National Forest, NH

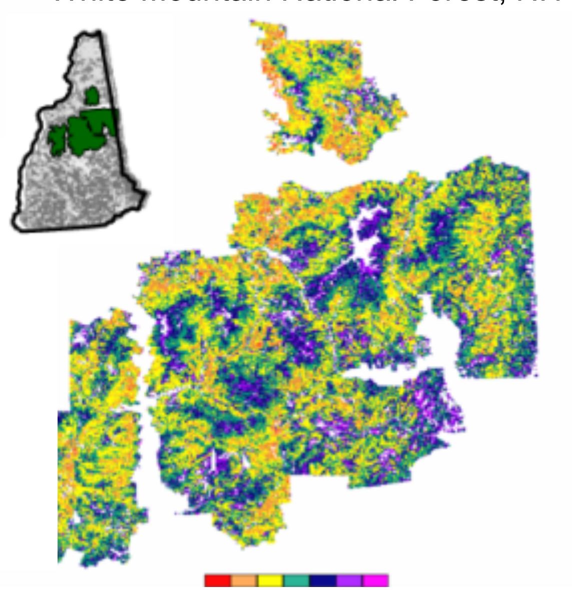

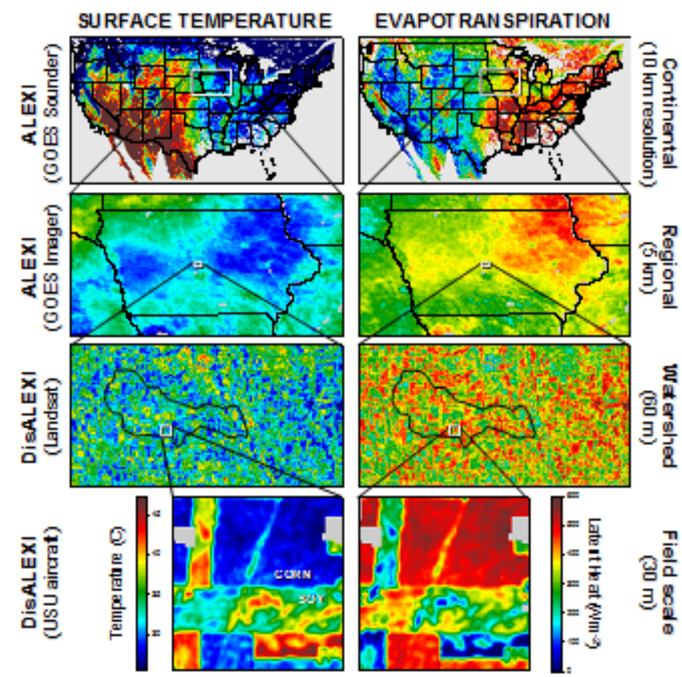

HyspIRI Measures the Optical Spectrum

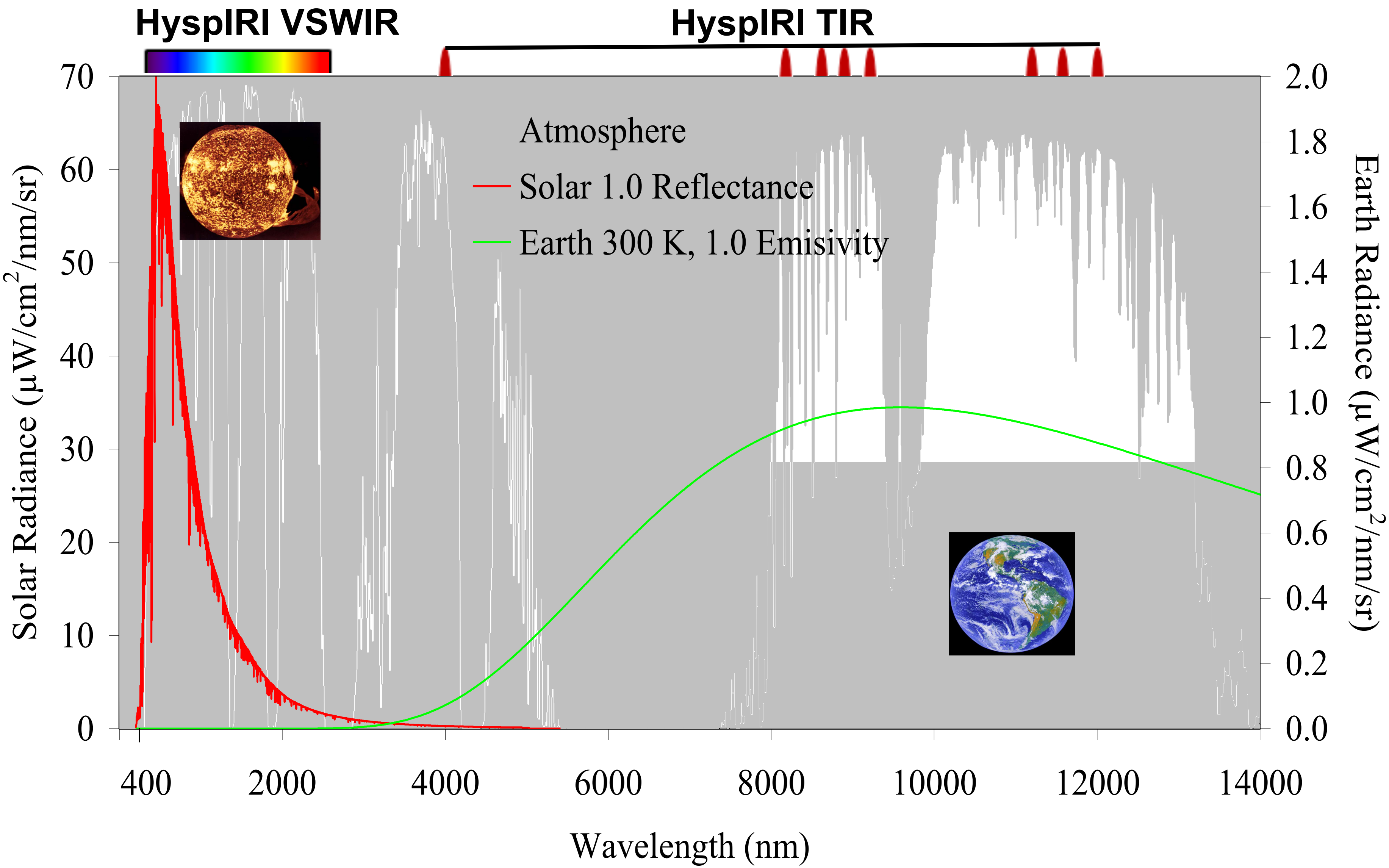

Antecedent Science Examples

Example: Imaging Spectroscopy Mapping Wetland Dominants 2010

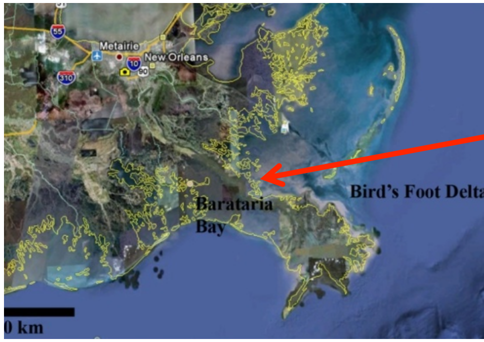

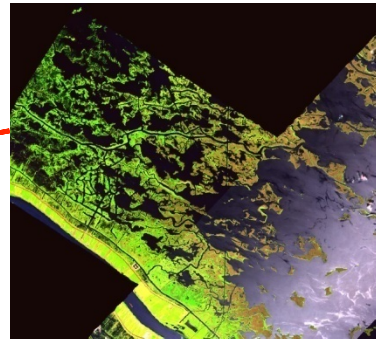

AVIRIS Vegetation Spectra

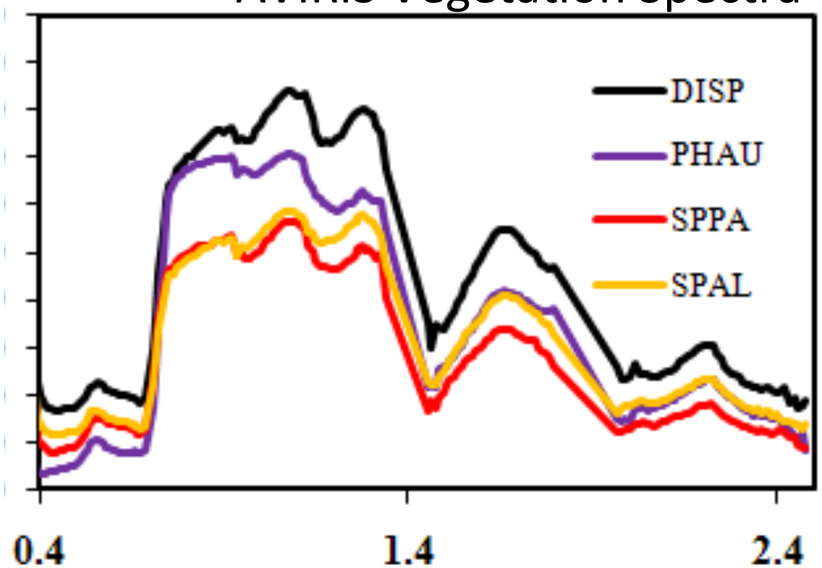

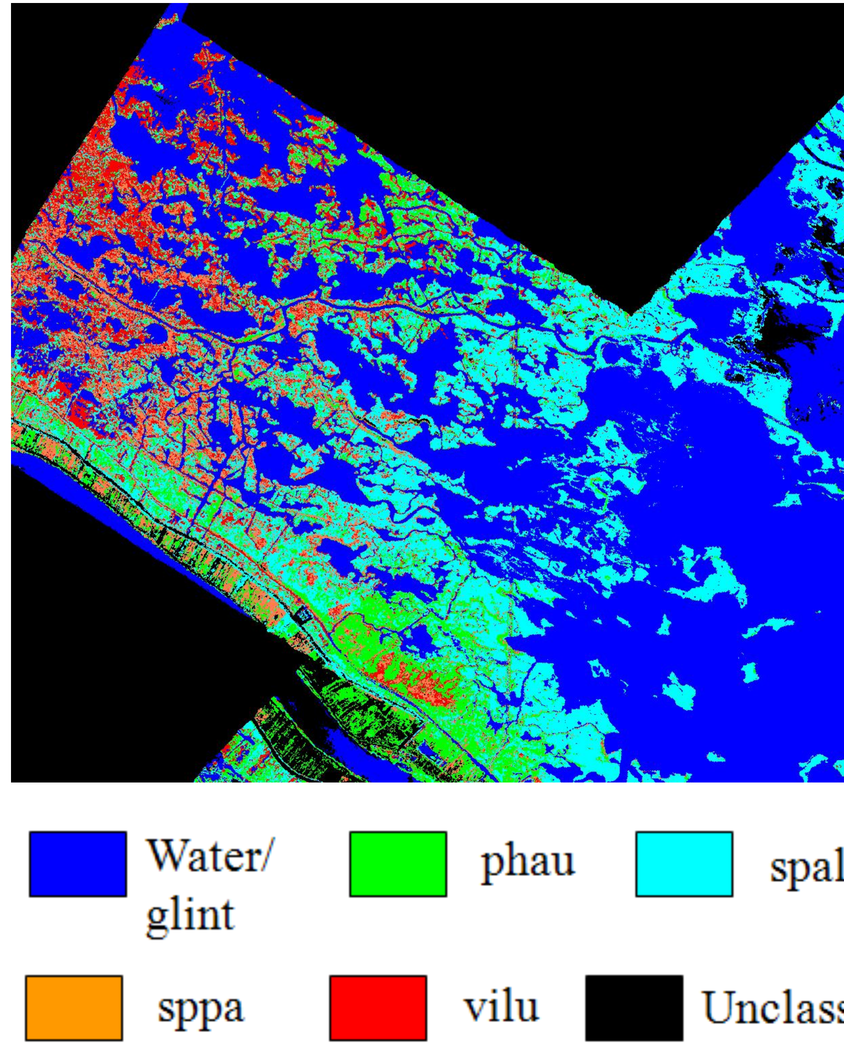

Vegetation mapped cleanly across scene boundaries

- ***Phragmites (phau)***
- ***Spartina alterniflora (spal)***
- ***Spartina patens (sppa)***
- ***Vigna luteola (vilu)***

D. Roberts, UCSB

Spectroscopy for Species/Functional-type, Biogeochemistry and Physiological Condition

PLSR weighting for foliar Nitrogen

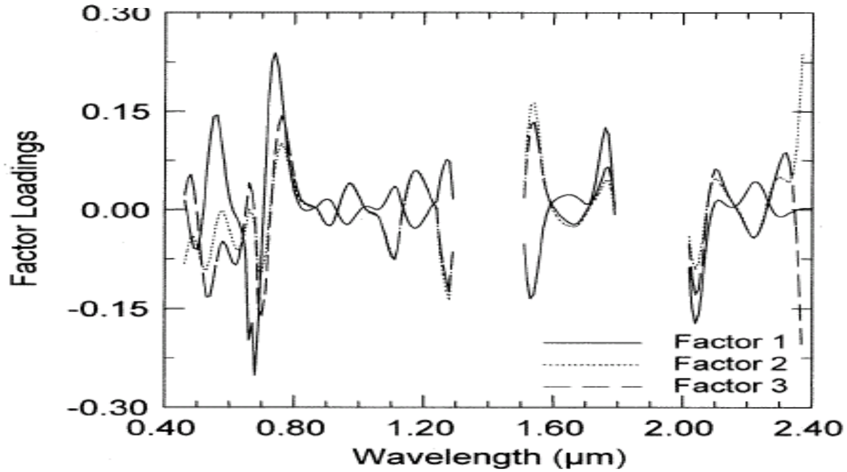

PLSR wavelength selection for one species

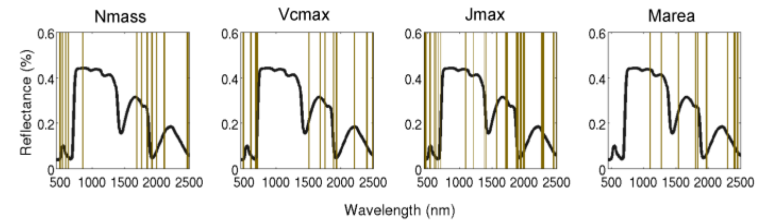

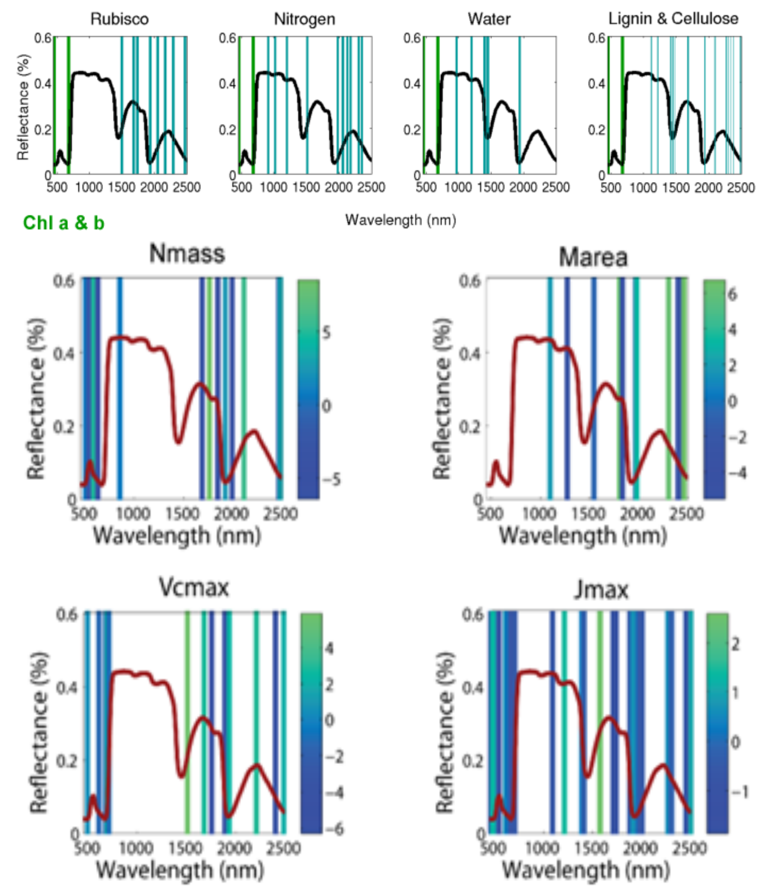

Measuring spectral shift from Lignin : Cellulose ratio

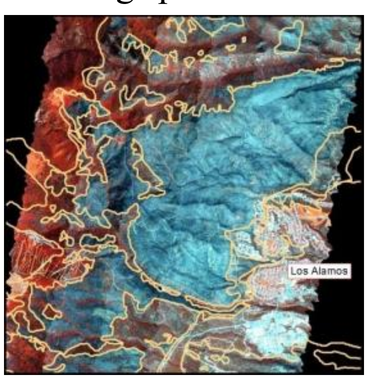

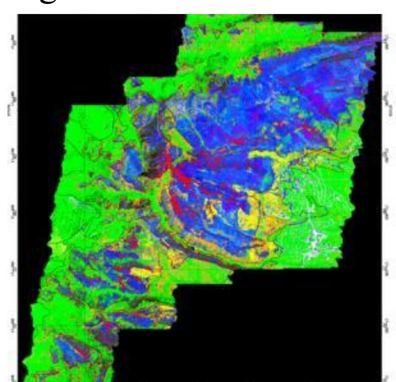

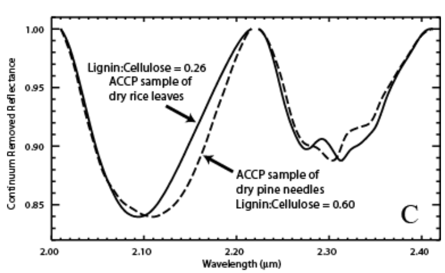

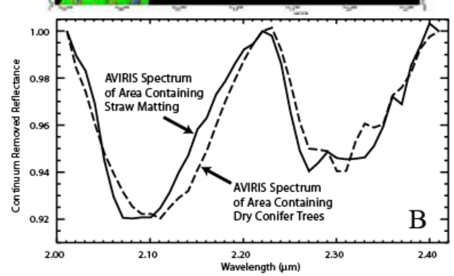

Surface Compositional Derived with Imaging Spectrometer Measurements

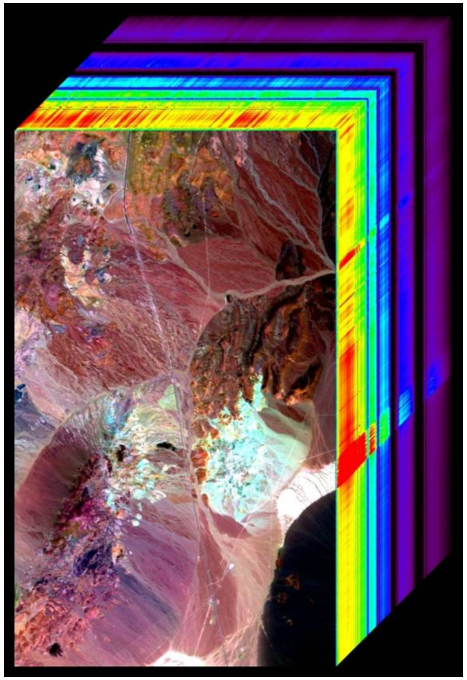

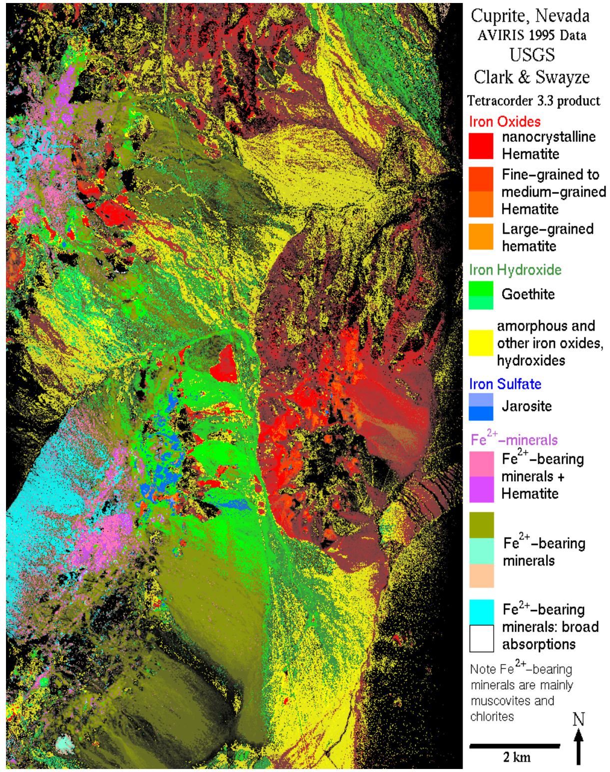

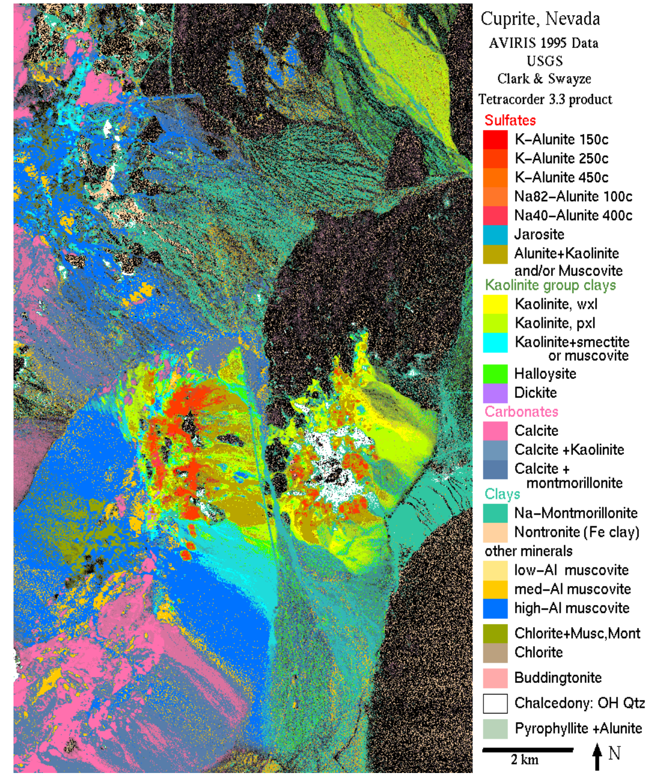

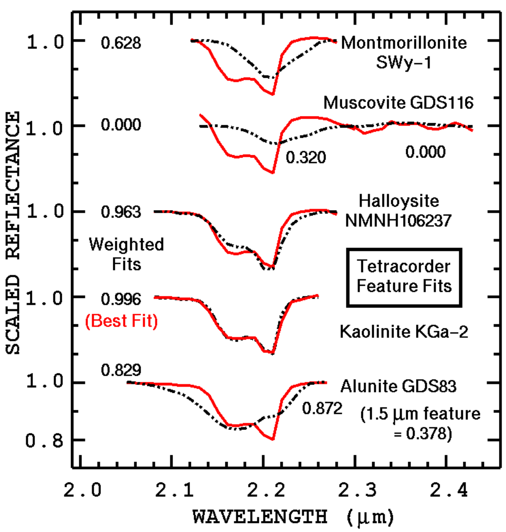

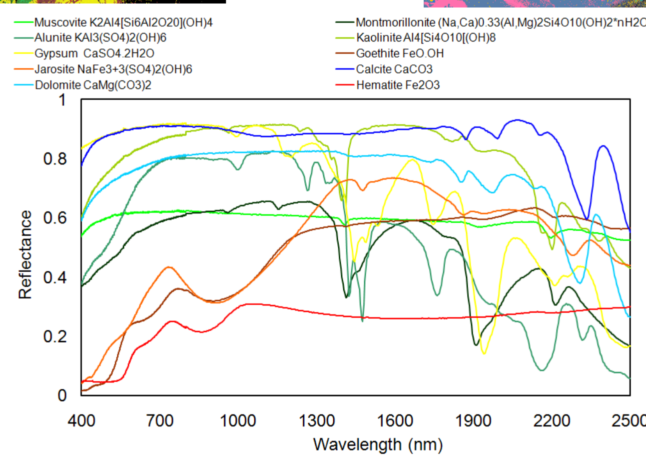

Albedo and Black Carbon/Dust Effects on Snow/Ice

What is causing the downwasting and retreat of Himalayan glaciers and elsewhere?

For snow and ice in the Himalaya, increasing temperatures and increasing dust and soot combine in unknown proportions to accelerate melt through their changes in albedo. Imaging Spectroscopy is the only approach that allows us to attribute changes in albedo into effects from temperature and dust/black carbon and at a fine enough spatial resolution that heterogeneous terrain can be resolved. Multi-band sensors such as NPOESS VIIRS have neither capacity.

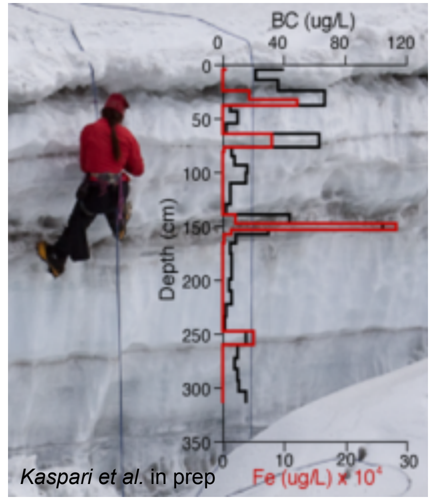

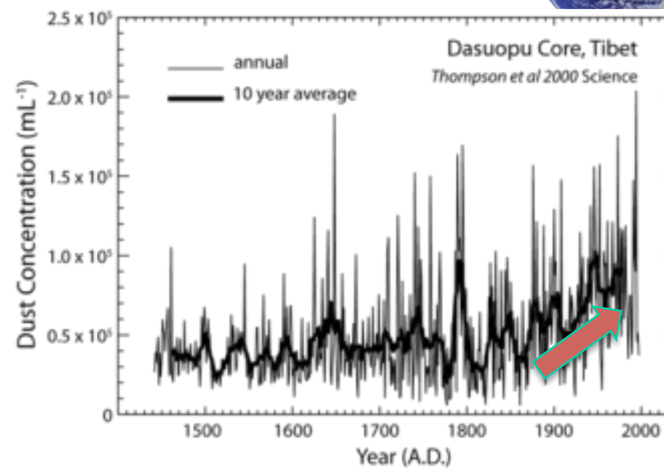

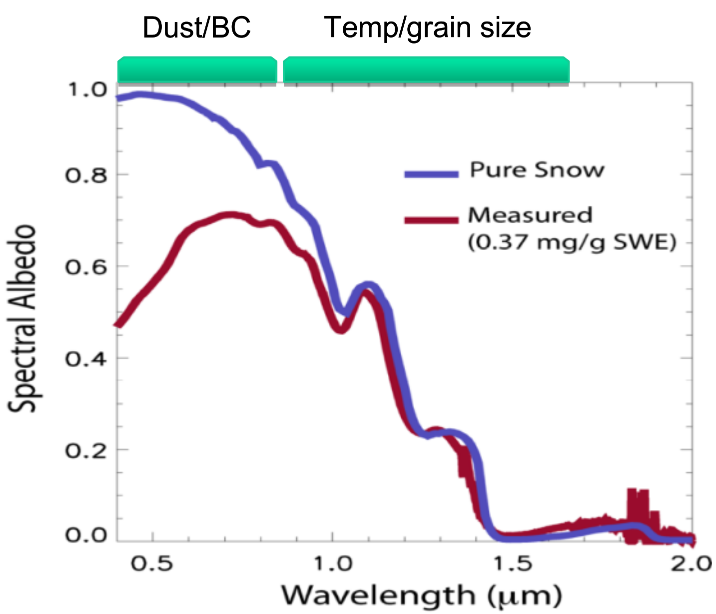

Required Measurement: Global glacial covered area, full solar spectrum, < 100 m spatial, <20 days revisit

HyspIRI: Coral, Benthic Composition, and Aquatic Vegetation

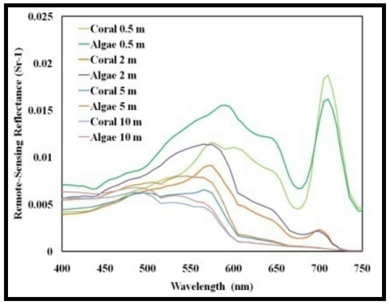

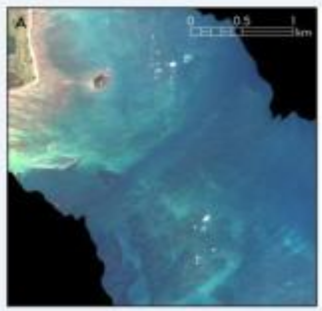

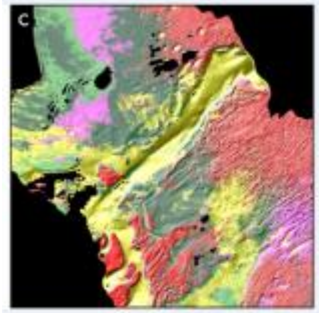

Variation in shallow water HyspIRI-type spectral signatures in coral environments.

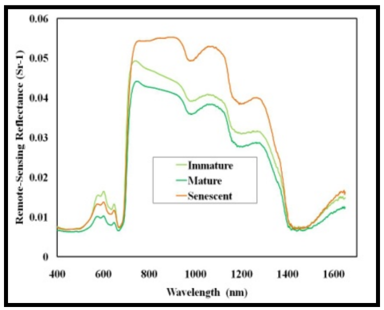

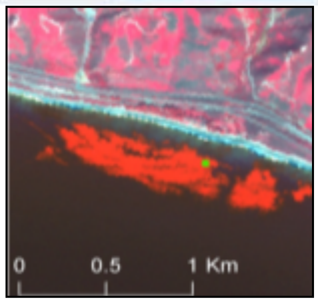

Variation in HyspIRI-type spectral signatures of floating aquatic vegetation (e.g. Kelp)

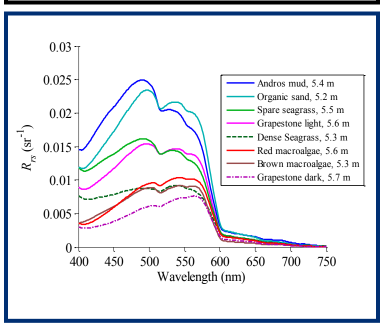

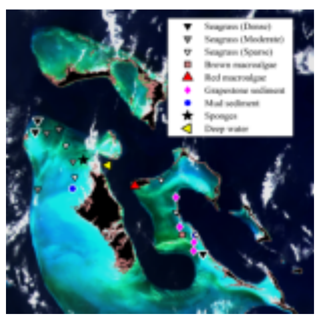

Variation in shallow water HyspIRI-type spectral signatures in seagrass beds and benthic habitat materials

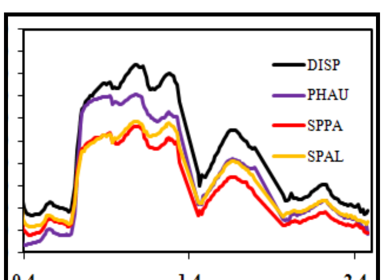

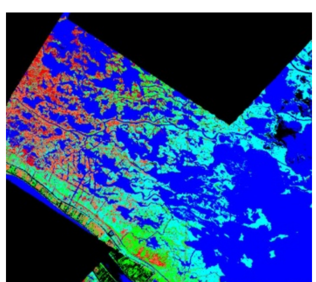

Emergent vegetation signatures are well suited to the HyspIRI measurement. For example mapping in the Gulf of Mexico coastal region with AVIRIS measurements.

TQ1. Volcanoes/Earthquakes

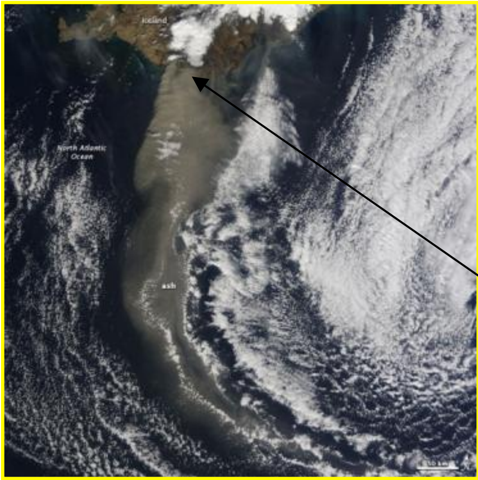

Eyjafjallajökull Iceland Volcano Eruption

April 19 2010 MODIS image of ash plume.

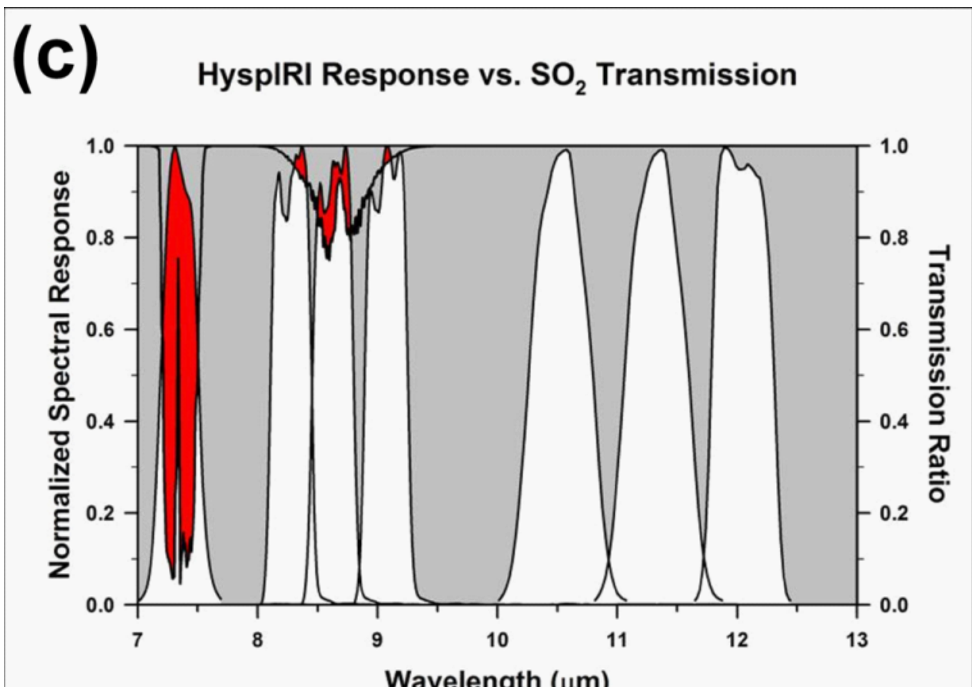

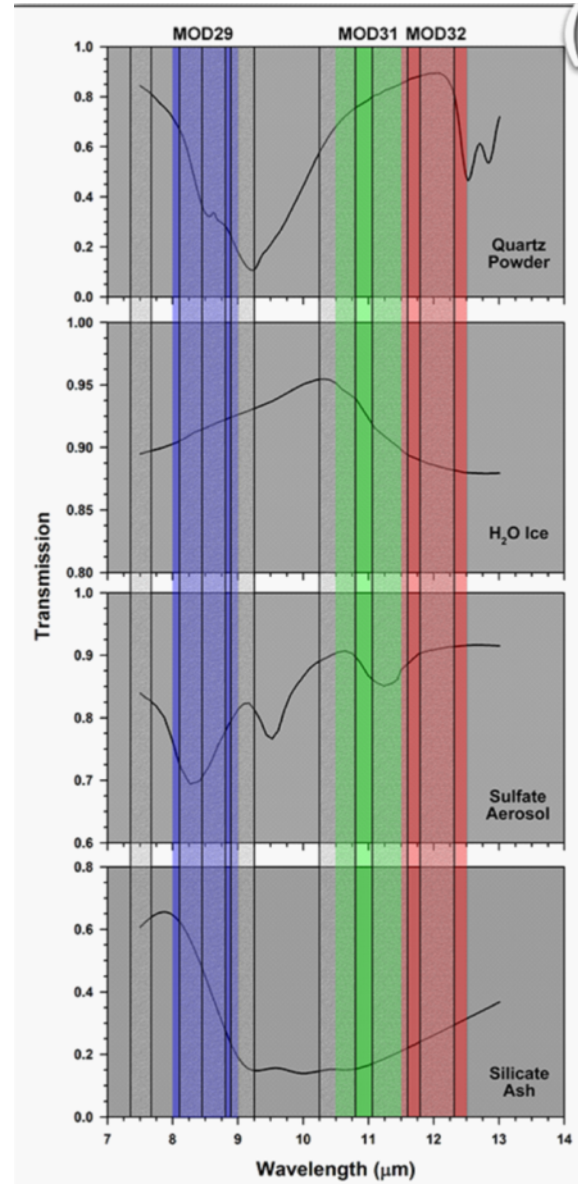

Characterizing and Understanding Volcanic Eruptions

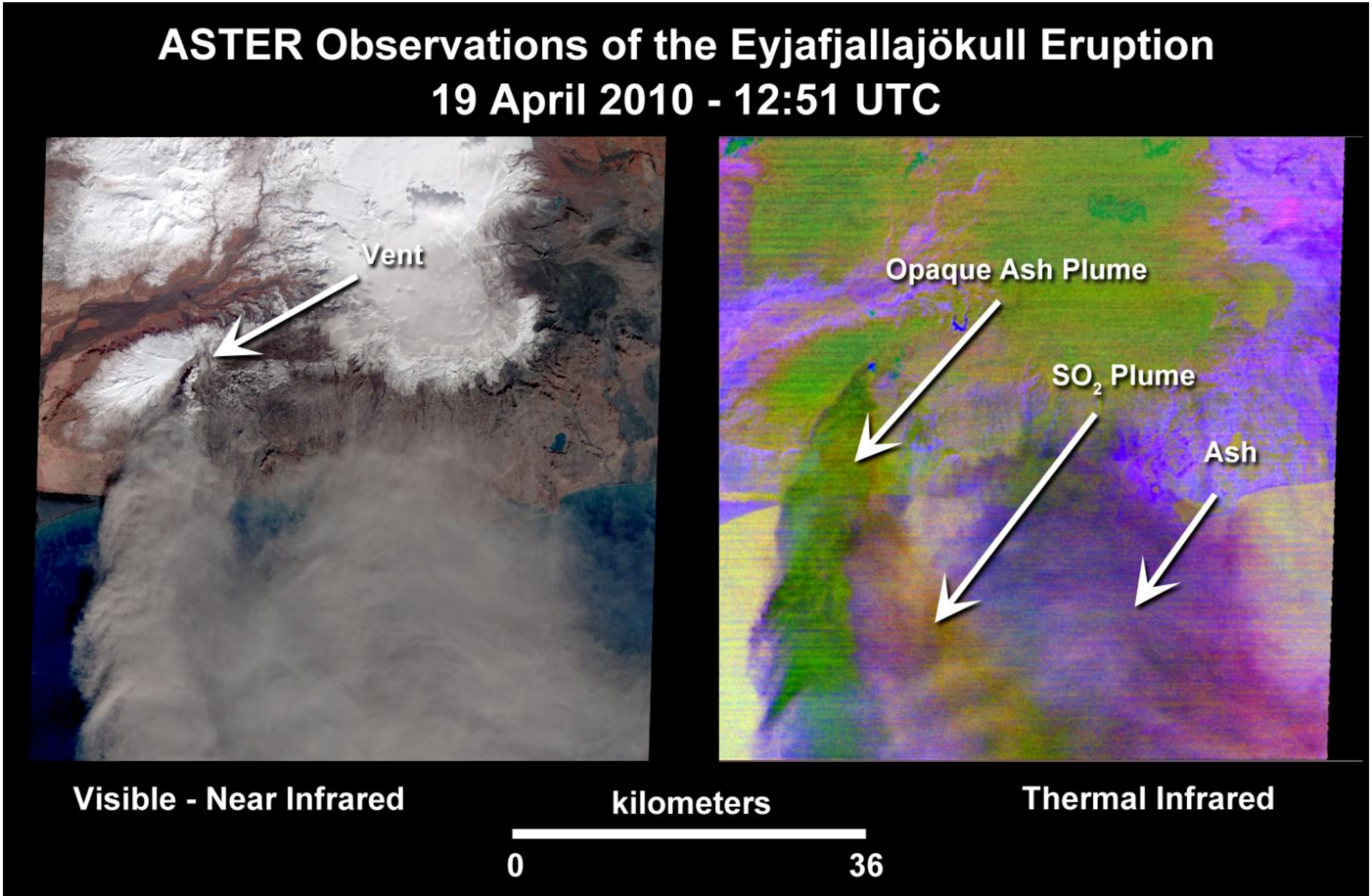

Annual TIR imaging opportunities in a 5-day near-repeating orbit, 1 yr. simulation

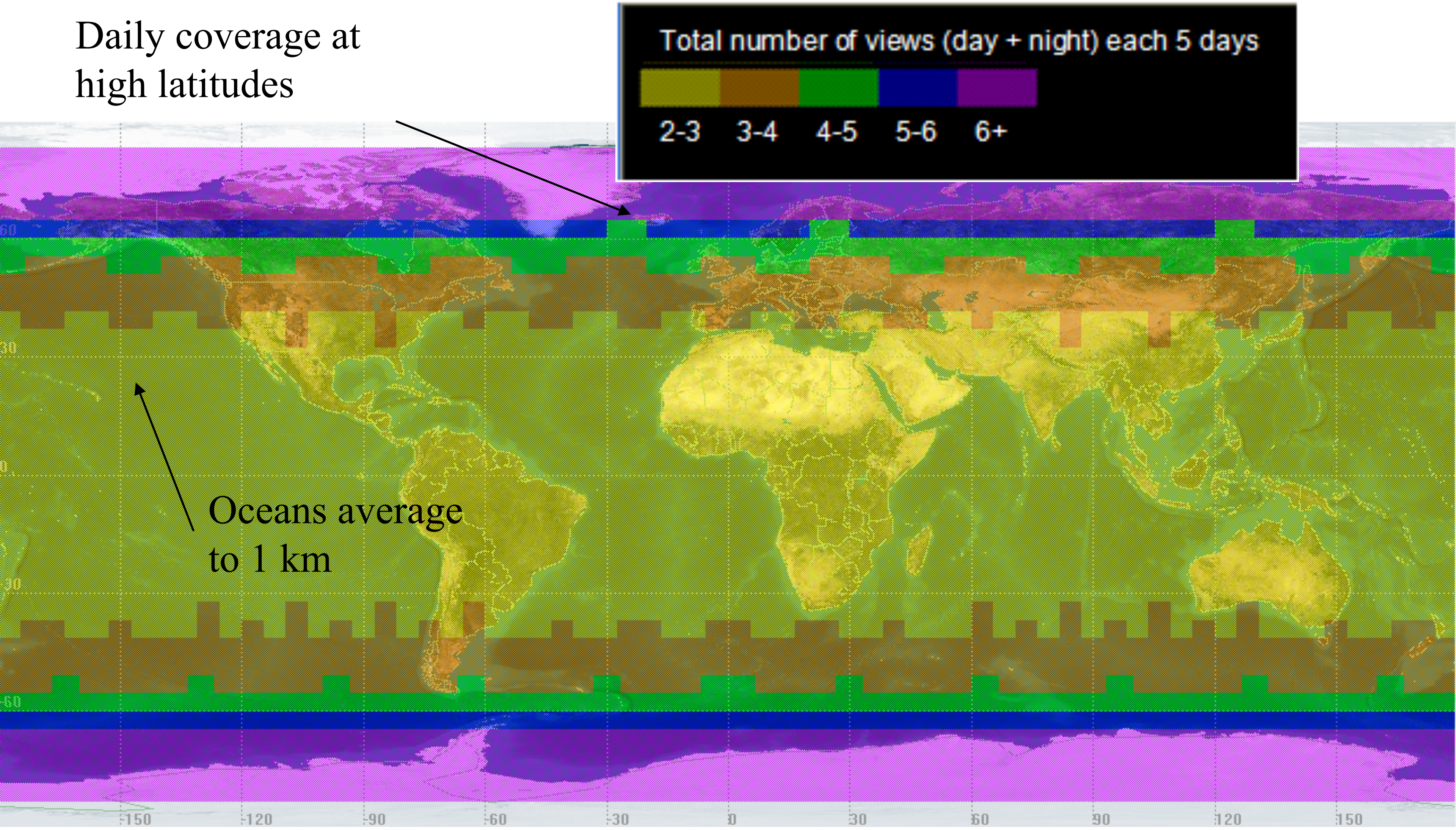

Nominal orbit: average alt. 626.8 km, inclination 97.8°. TIR imager FOV: +/- 25.46° (60 m pixel GSD at nadir, 9272 cross-track pixels).

TQ2. Wildfires

Large error in carbon budget exists due to poor knowledge of Carbon release from fires

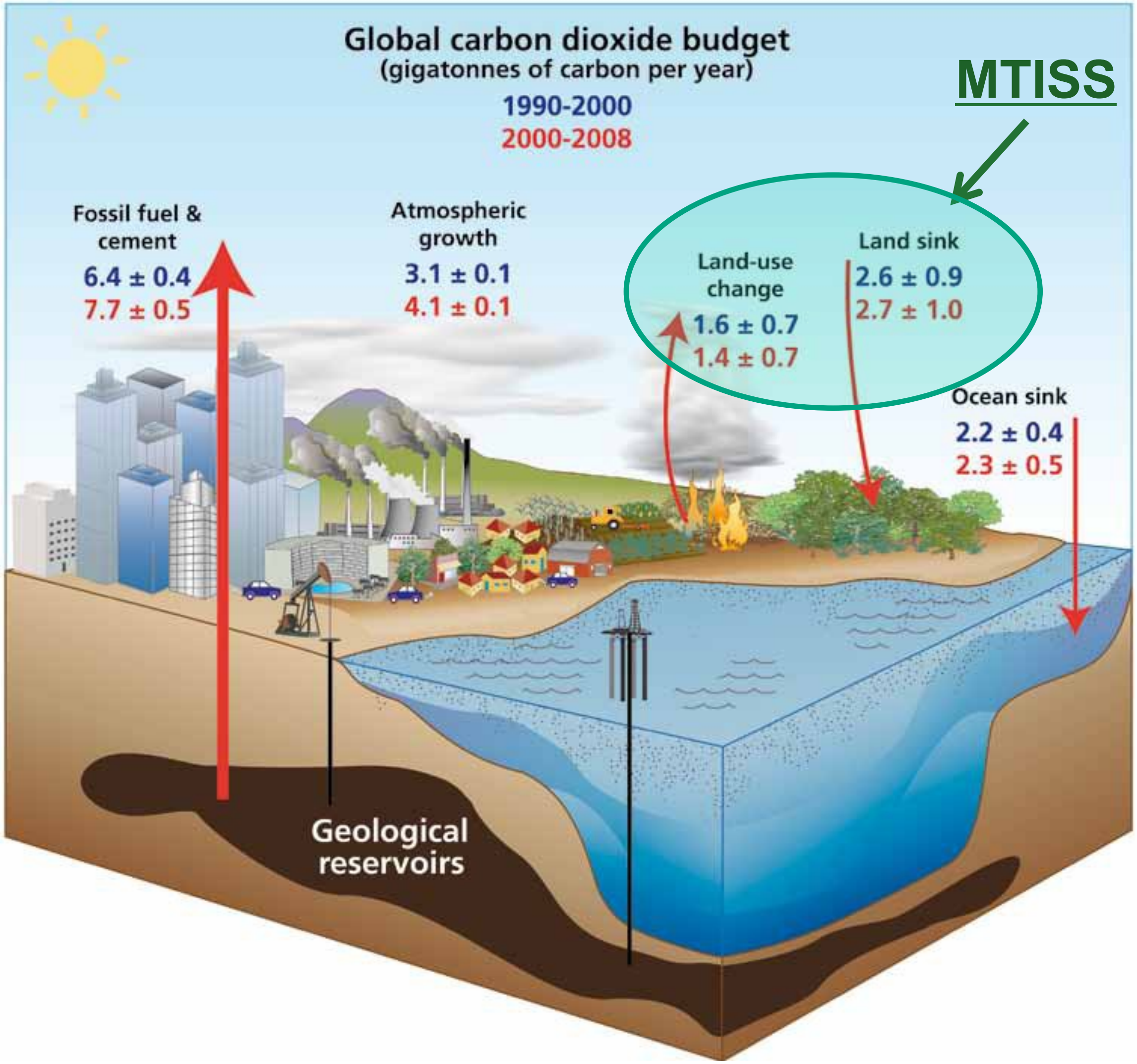

Global CO2 budget for 1990-2000 (blue) and 2000-2008 (red) (GtC per year). Emissions from fossil-fuel and land-use change are based on economic and deforestation statistics. Atmospheric CO2 growth is measured directly. The land and ocean CO2 sinks are estimated using observations for 1990-2000 (Denman *et al.* IPCC 2007). For 2000-2008, the ocean CO2 sink is estimated using an average of several models, while the land CO2 sink is estimated from the balance of the other terms.

HyspIRI-TIR Provides Orders of Magnitude Improvement in Measurement Capability

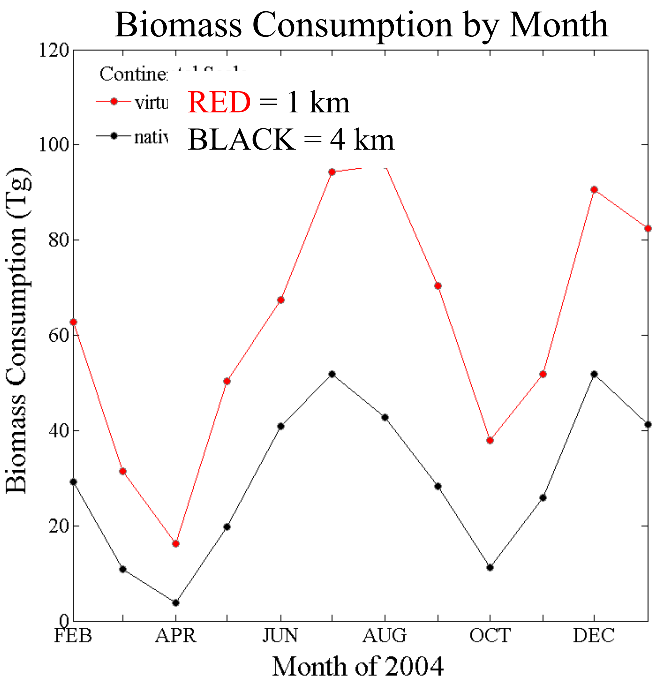

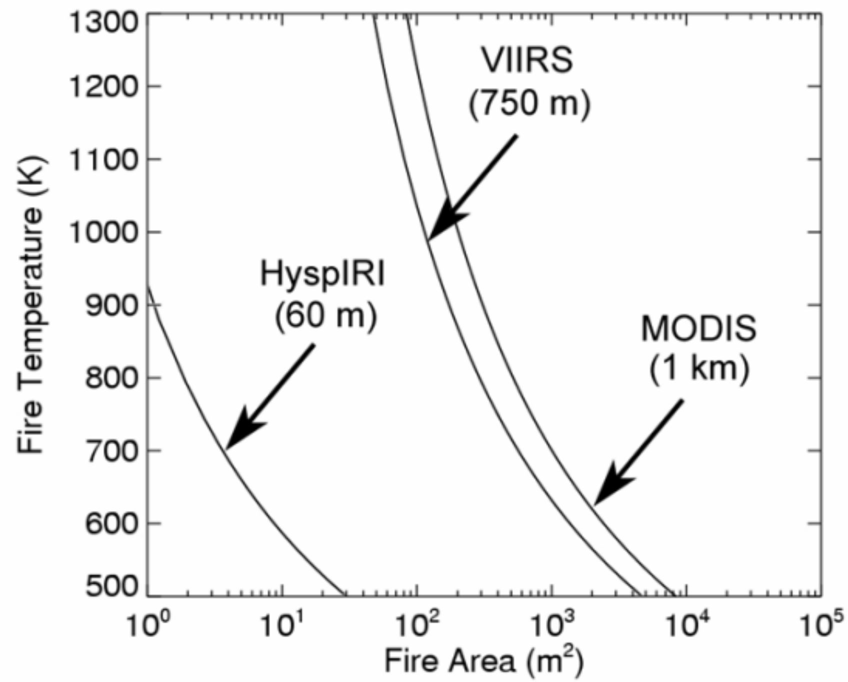

- HyspIRI-TIR measures very small fires as well as large fires. Small fires have a disproportionately large carbon contribution
- Global carbon contribution from peat, agricultural and deforestation fires unknown because cannot be measured with current sensors but see a large discrepancy between 1km MODIS and 4km GOES

Measuring carbon fire emissions requires measurements in the Mid and Thermal Infrared

- Greater sensitivity due to shift in emission peak with temperature
- Measure radiance rather than temperature and avoid mixed pixel problem

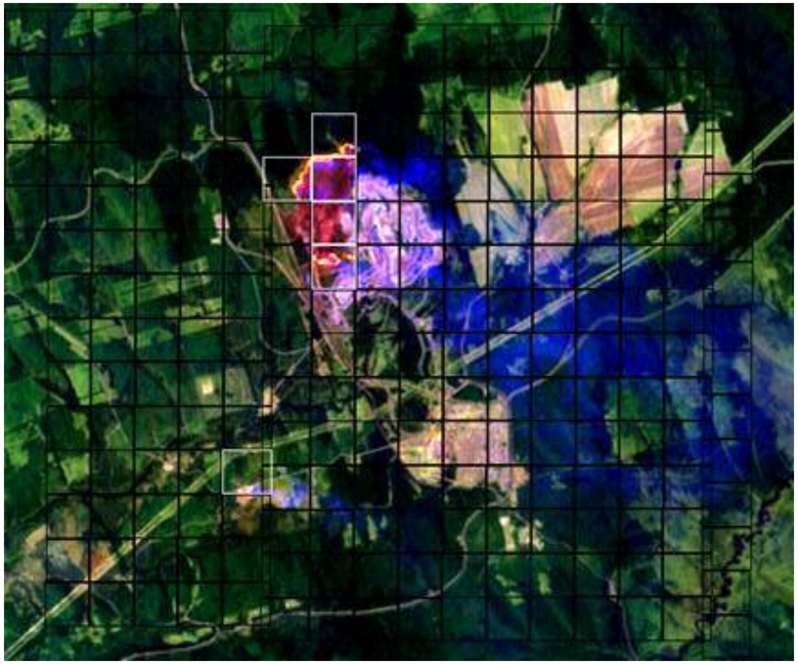

MODIS only detects white boxes (1kmX1km) does not provide information on the fire front or smouldering part of fire

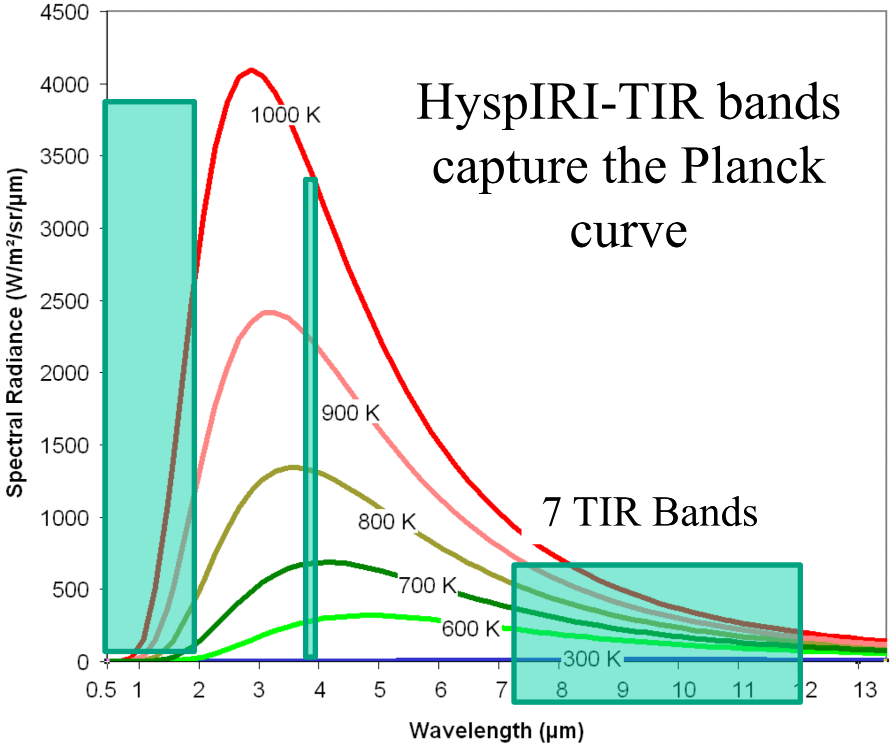

Thermal emission peaks in the MIR (3-5 µm) region for fire temperatures ranging from ~ 650 K (weak smouldering) to ~ 1400 K (strong flaming). MIR is far more sensitive to hot targets than TIR.

6/15/12

Refining carbon emissions from wildfires by using a remotely sensed fire severity product

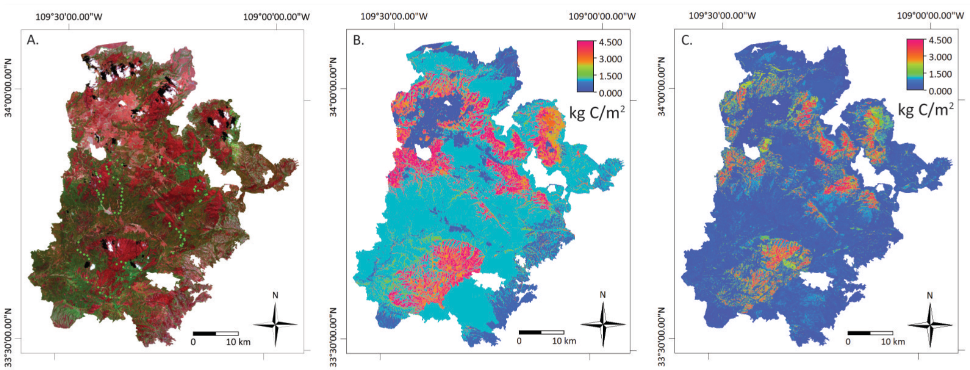

A. False Color Composite of Wallow fire

B. C emission from modeling

C. C emission from modeling and RS

Fire	Burned area (ha)	Estimation methodology	Total C emission (Tg)	Area normalized C emission (kg/m²)	% C emitted relative to the modeling approach
Wallow (AZ)	218 000	Modeling	3.44	1.57	1
		Modeling & RS	1.52	0.70	0.45
Canyon (CA)	5900	Modeling	0.12	2.02	1
		Modeling & RS	0.09	1.60	0.73

Veraverbeke & Hook (2012) submitted

Problem: Carbon emissions from wildfires account for 20-40 % of the total global carbon emissions, however, uncertainties in these estimates are large.

Result: Using field and satellite data over two wildfires in the southwestern US, we have demonstrated that complementing traditional modeling approaches to estimate wildfire emissions with a remotely sensed fire severity product derived from spectral unmixing of VSWIR and MIR leads to significantly lower carbon emission estimates. For the mixed severity Wallow fire (AZ) estimates were 55 % lower and for the dominantly high severity Canyon fire (CA) estimates were 27 % lower.

Significance: Current models that estimate carbon emissions from wildfires are subject to large uncertainties. Using remotely sensed fire severity products these uncertainties can be reduced.

Instrument Concepts

HyspIRI VSWIR Science Measurements

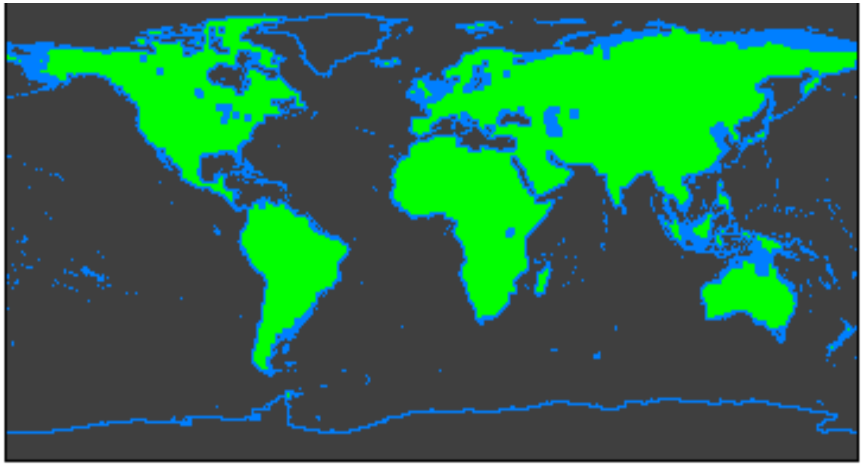

HyspIRI is a global mission, measuring land and shallow aquatic habitats at 60 meters and deep oceans and ice sheets at 1km every 19 days (VSWIR). This will allow seasonal coverage for most of land surface

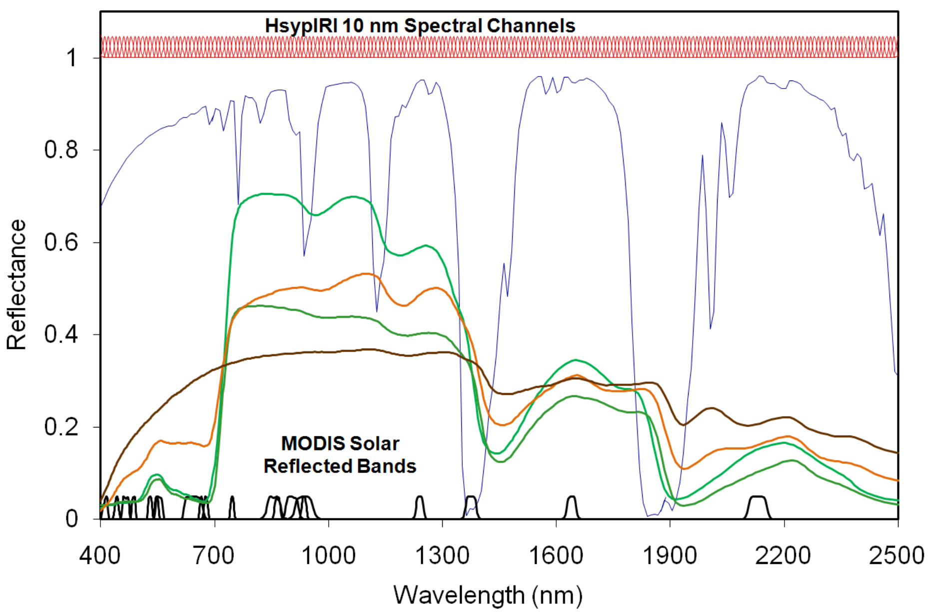

HyspIRI's VSWIR imaging spectrometer directly measures the full solar reflected spectrum of the Earth from 380 – 2500nm at 10 nm.

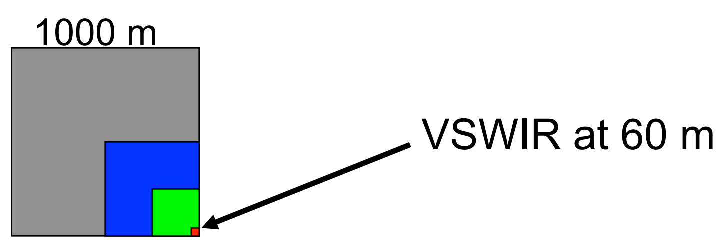

Seasonal and Annual Cloud Probability Maps Validate the HyspIRI Coverage Requirements

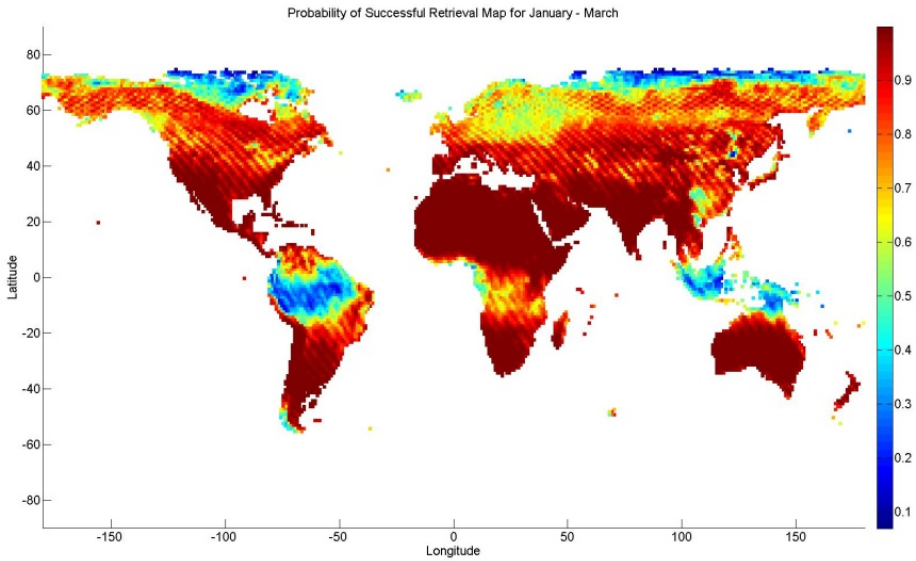

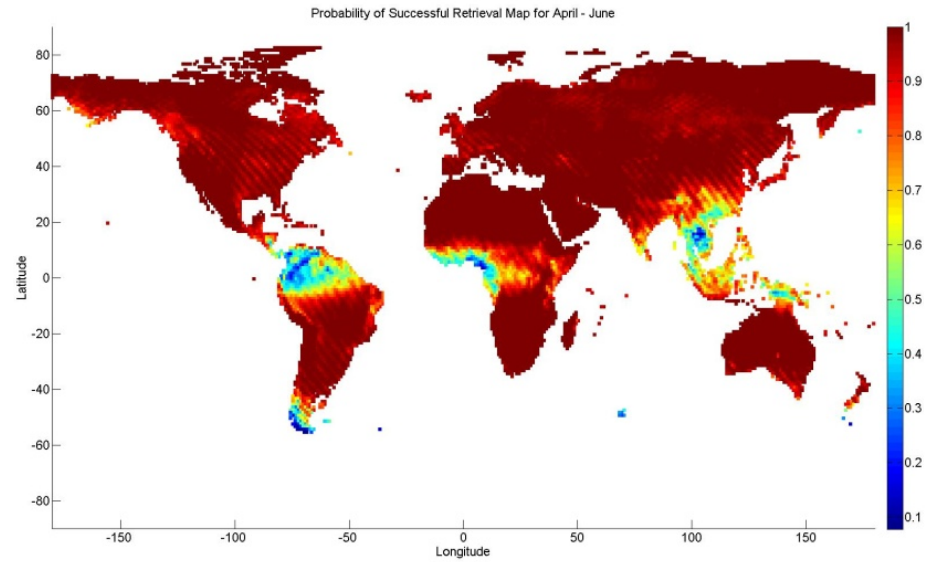

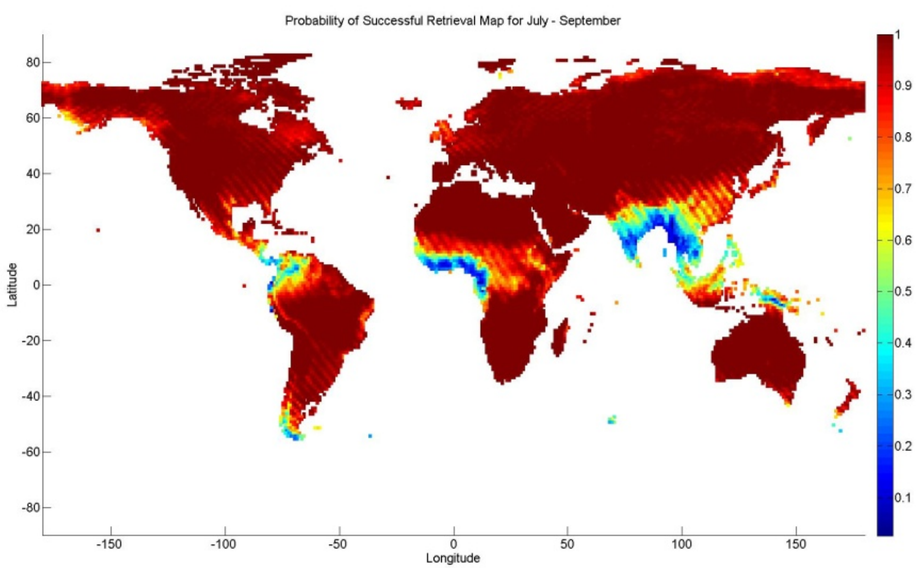

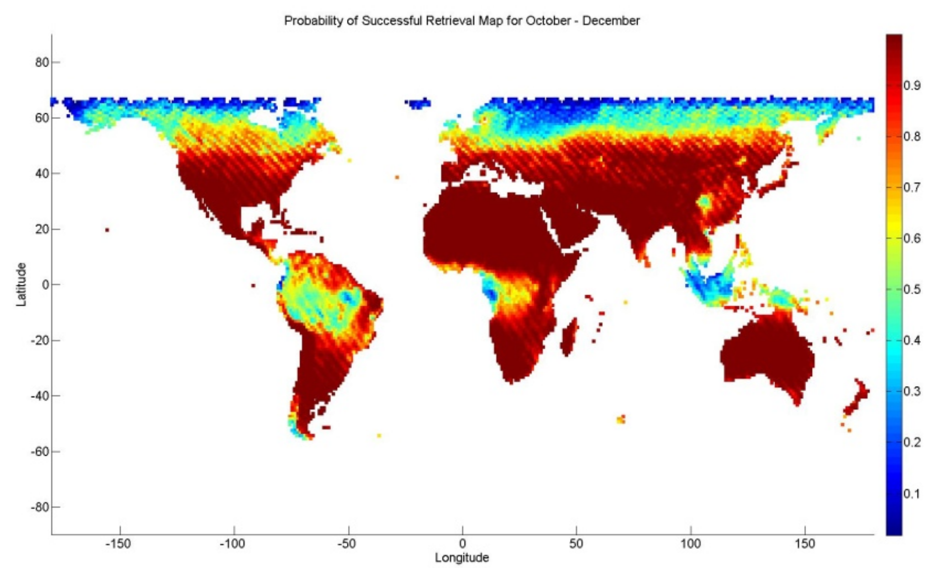

HyspIRI VSWIR SNR and Uniformity Characteristics

Benchmark Radiances

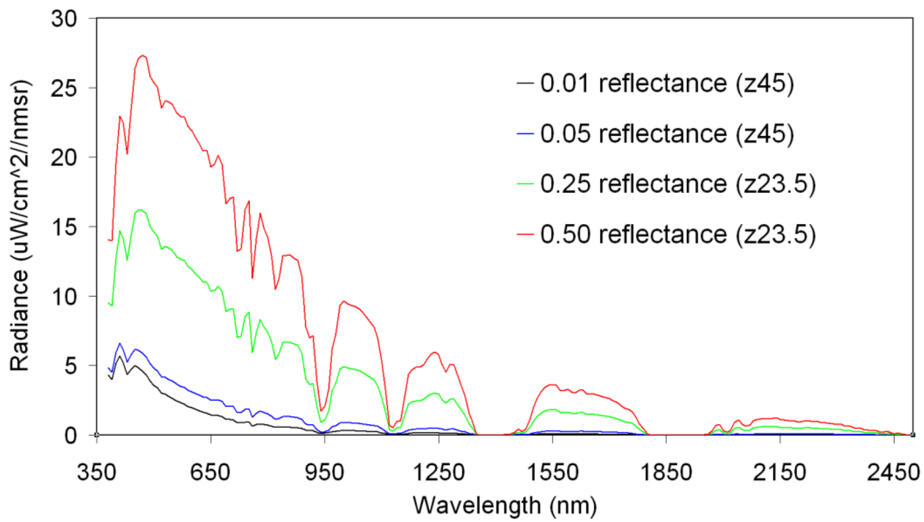

Signal-to-Noise Ratio

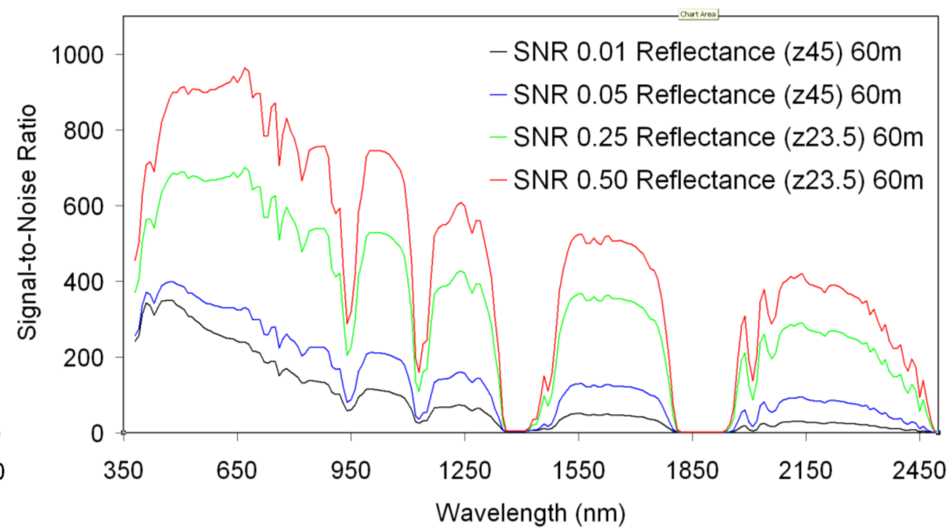

Uniformity Requirement

Cross Track Sample

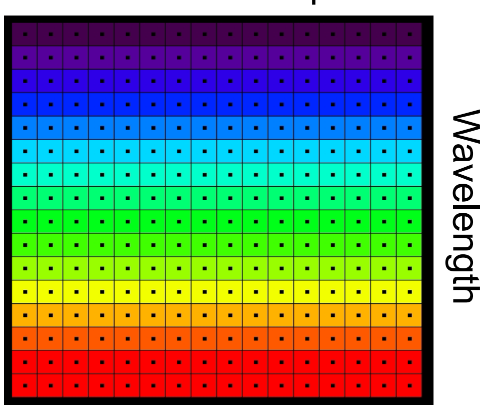

Depiction

-Grids are the detectors

-Dots are the IFOV centers

-Colors are the wavelengths

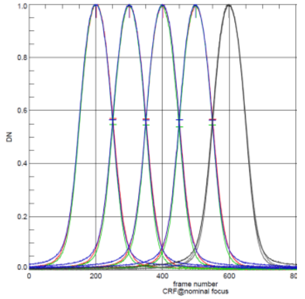

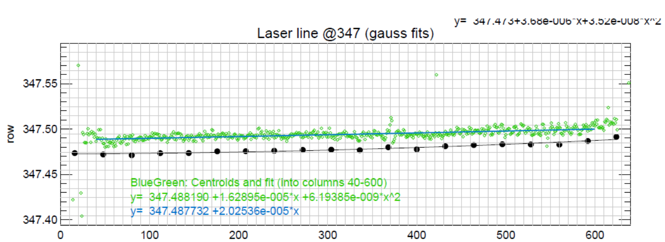

Requirement

Spectral Cross-Track	>95% cross-track uniformity {<0.5 nm min-max over swath}
Spectral-IFOV-Variation	>95% spectral IFOV uniformity {<5% variation over spectral range}

VSWIR - Instrument Concept

Spectral	Requirement	Status
Range	380 to 2500 nm (solar reflected spectrum)	Demonstrated – AVRIS, MaRS, M3
Sampling	<= 10 nm {uniform over range}	Demonstrated – MaRS, M3
Response	<= 13 nm (FWHM) {uniform over range}	Demonstrated – MaRS, M3
Accuracy	<0.5 nm	Demonstrated – MaRS, M3, CAO-VSWIR

Radiometric	Requirement	Status
Range & Sampling	0 to 1.5 x benchmark radiance, 14 bits	Demonstrated via analysis and 14 bit ADC bread board electronics
Accuracy	>95% absolute radiometric, 98% on-orbit reflectance, 99.5% stability	Demonstrated – AVIRIS, MaRS
Linearity	>99% characterized to 0.1 %	Demonstrated via test, MaRS and CAO-VSWIR
Polarization	<2% sensitivity, characterized to 0.5 %	Demonstrated via analysis of design and test data on the grating

HyspIRI – VSWIR

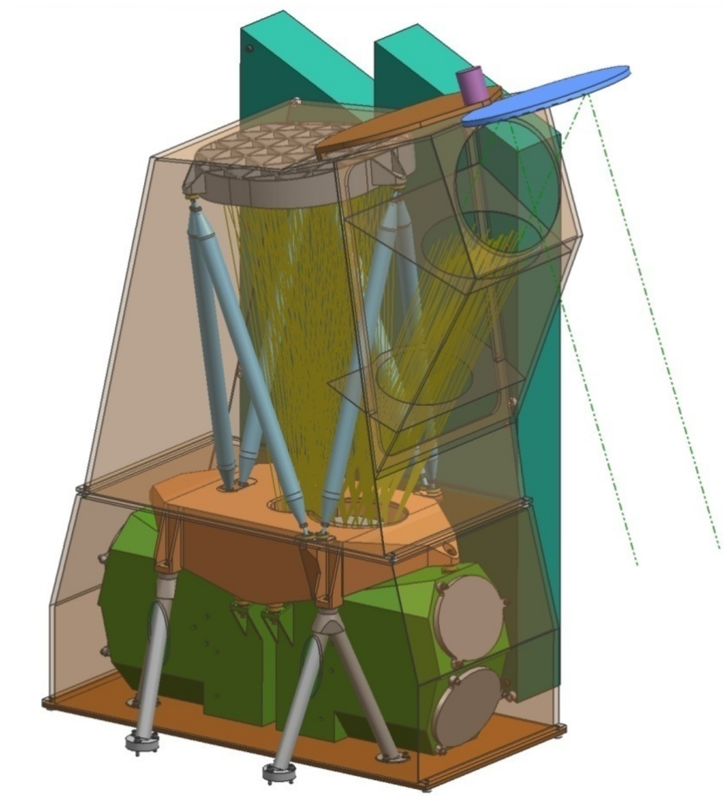

Mass (CBE) ***55Kg***
Power (Ave.) ***41Watts***

HyspIRI VSWIR Concept

Optics

- Front End Telescope consists of a primary spherical mirror and a secondary aspherical mirror
- Back End Spectrometers consist of 2 optimized Offner spectrometers

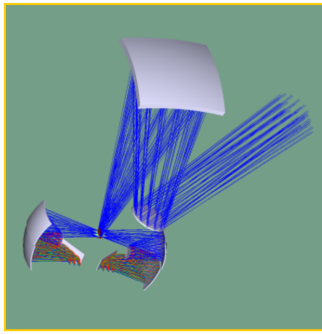

Spectrometers (2x)

- 2 identical Offner spectrometers
- Each contains:
  - E-Beam grating
  - Si air slits
  - FPA assembly

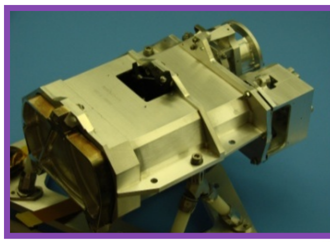

FP A (2x)

- Mount is adjustable in 6 DOF
- Thermal strap connects mount to radiator
- Includes integral OSF

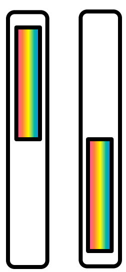

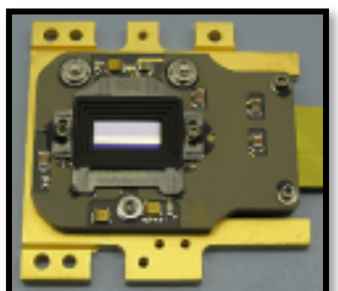

Radiator

- Area 0.6m^2
- M3 technology heritage

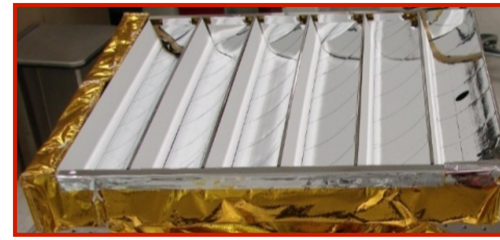

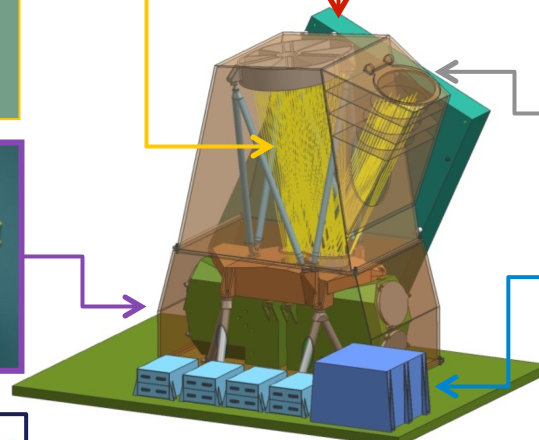

Baffle/Cover/Cal Panel

- *Launch cover*
- *Used as a solar reflectance calibration target*
- *Hyperion Heritage*

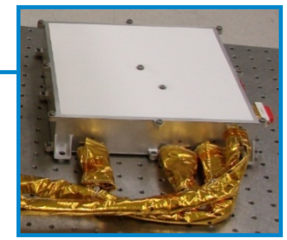

Electronics

- M3 Derivative 4x
- Electronic concept is based upon available flight approved parts
- Ins. control, Data Compression, mode control

Detectors

- Teledyne 6604b detectors, scaled from 6604a detectors flown on M3
- Analog output
- Each spectrum readout as snapshot, so that there is no time delay, yaw, or jitter impact to the spectral-IFOV-uniformity.

HyspIRI Thermal Infrared Multispectral (TIR) Science Measurements

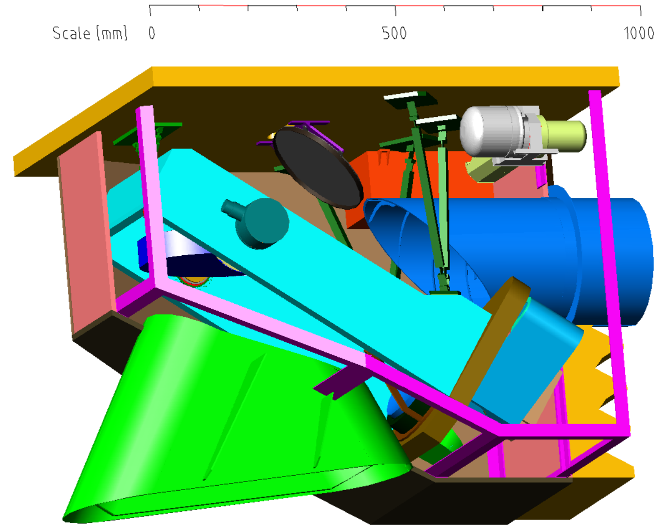

Measurement:

- 7 bands between 7.5-12 μm and 1 band at 4 μm
- 60 m resolution, 5 days revisit
- Global land and shallow water

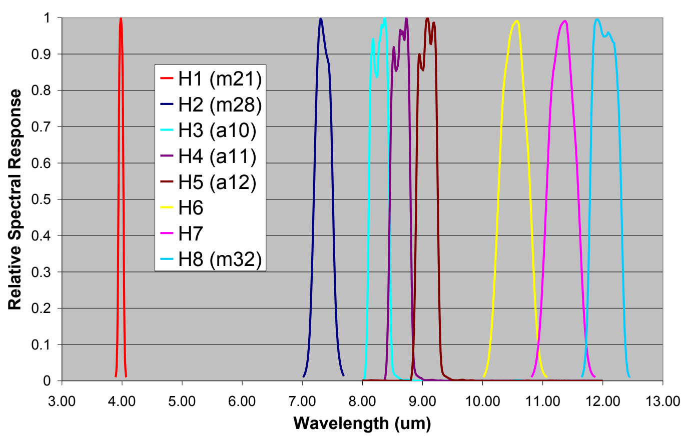

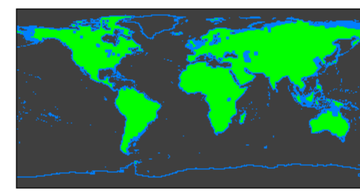

Key Measurement Parameters:

Overpass time: 10:30 am

Whisk-Push system

Day and night imaging

Compression: 2:1 lossless

Cross-Track Samples: 10,000

Down-Track Samples: 256

Swath Width: 600 km (±25.5° at 623 km altitude)

Swath Length: 15.4 km (+/- 0.7-degrees at 623km altitude)

Saturation: Bands 2-8= 200K – 500K; Band 1= 1200K

TIR Instrument Concept

Scanning and Data Rate

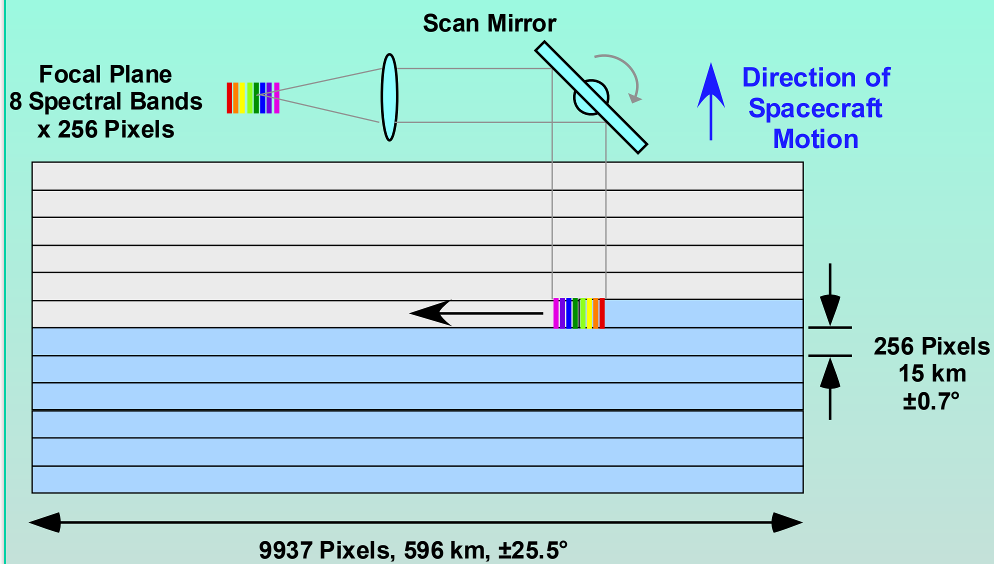

- 60 m Pixel Footprint
- Time-Averaged Science Data Rate 0.024 Gbps
- Assuming 14 bits, 2:1 Compression
- Scan Mirror Rotation Rate 13 RPM
- Pixel Dwell Time 32 microseconds

Mass and Power (JPL Team X)

- Mass CBE 60 kg
- Power CBE 109 W

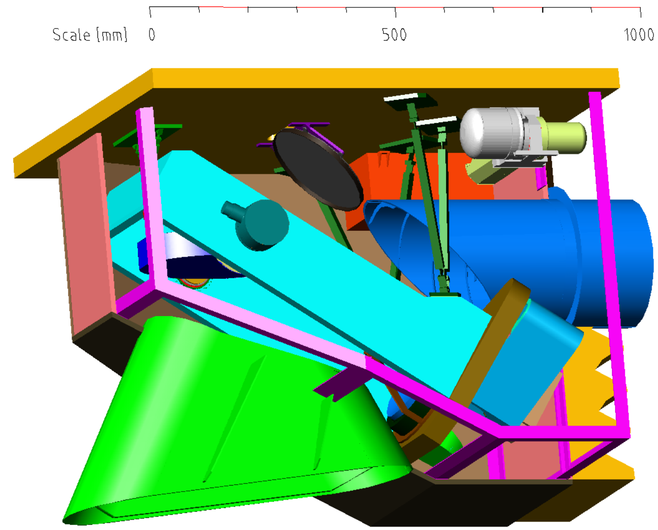

Spectral Bands

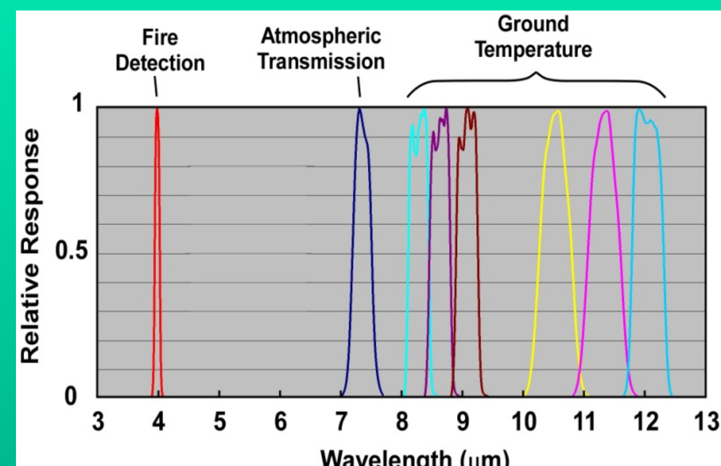

Risk Reduction

AVIRIS-NG
HyTES
PHyTIR

AVIRIS Next Generation First Spectra 20120422

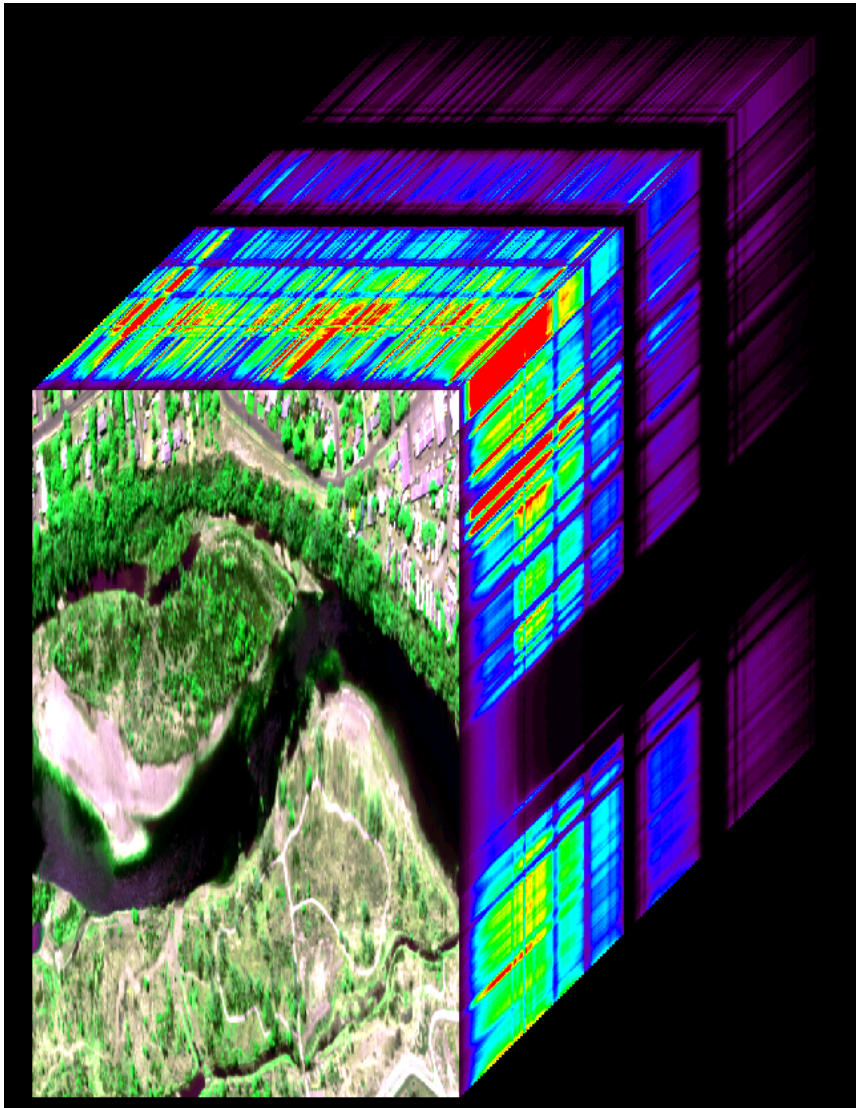

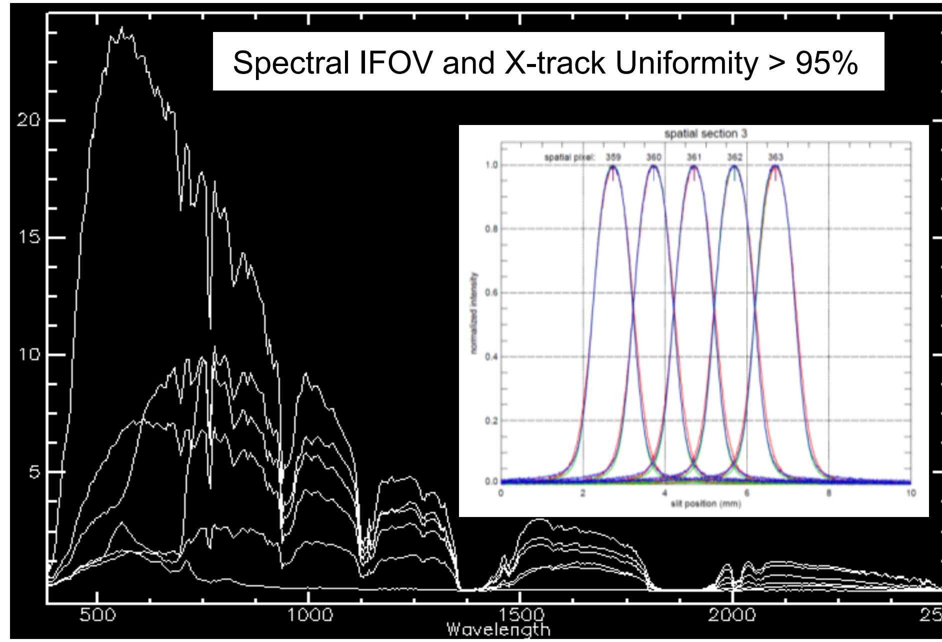

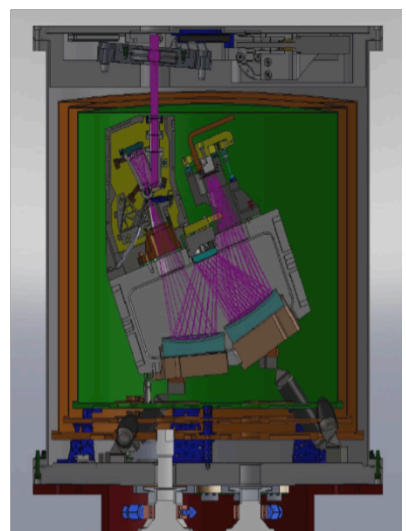

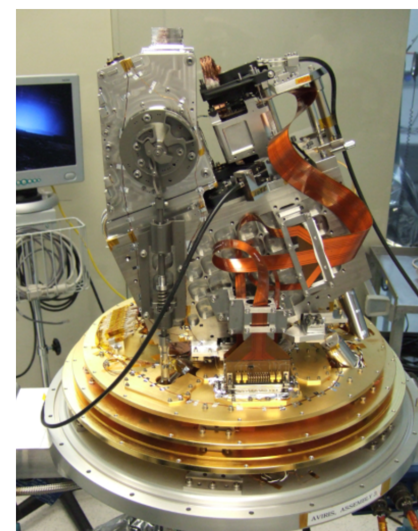

AVIRIS-NG First Flight 22 April 2012

- Photo of the scrolling quicklook. Spectra to follow.

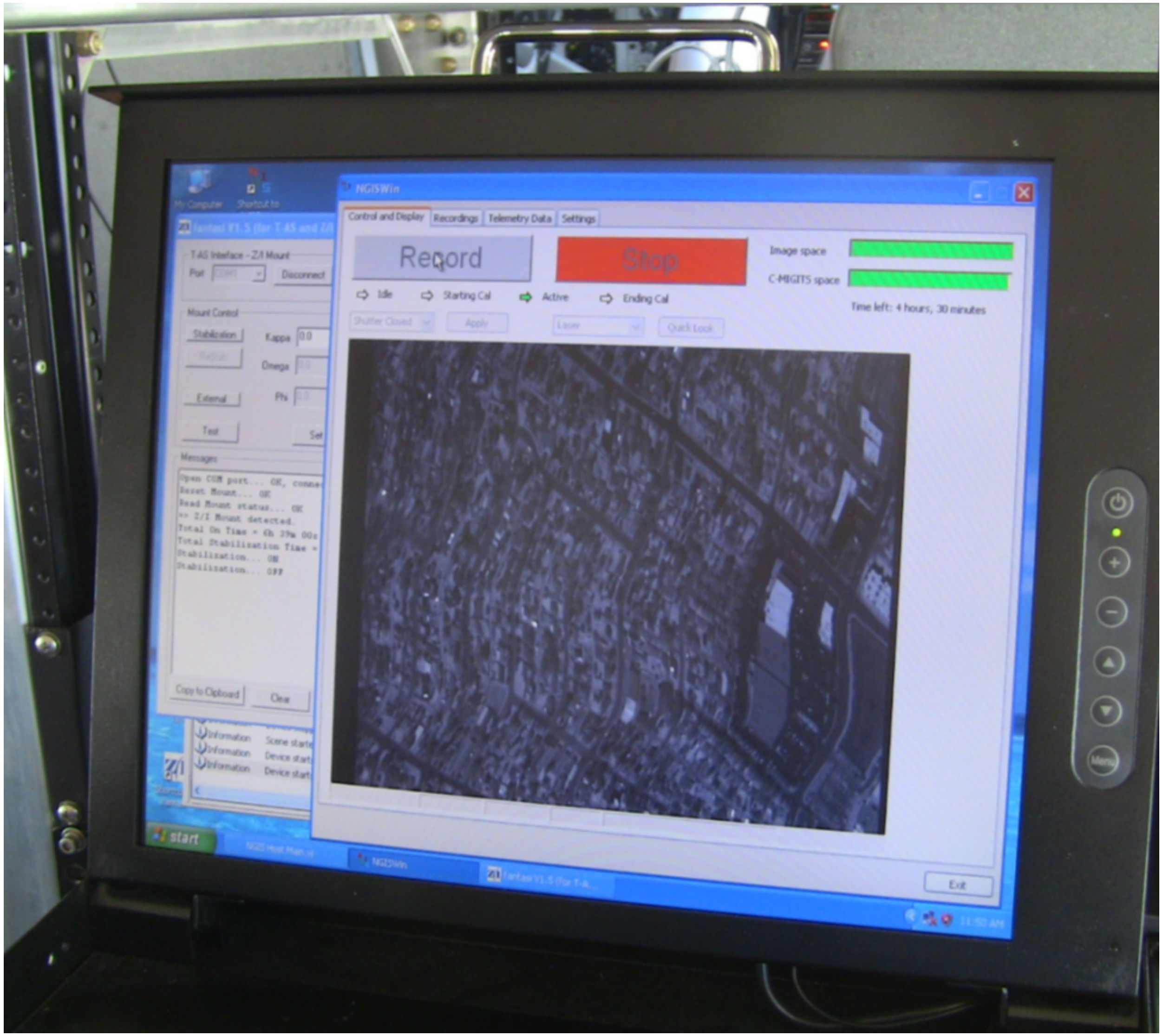

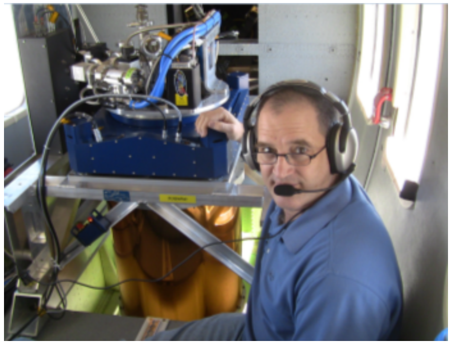

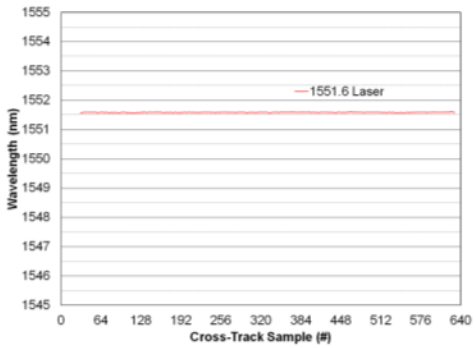

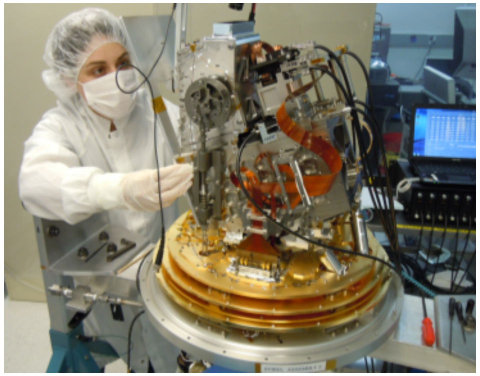

AVIRIS Next Generation

NASA Earth Science and Science Applications

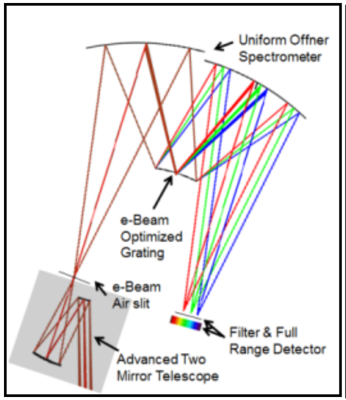

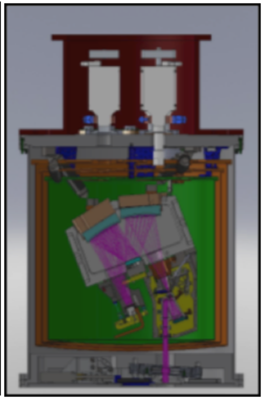

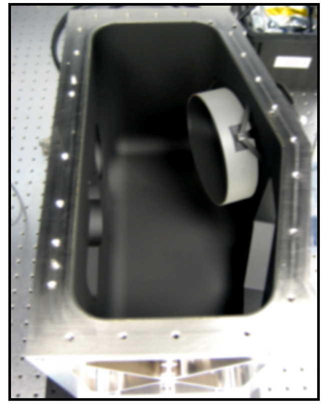

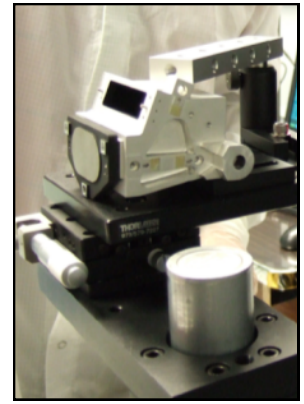

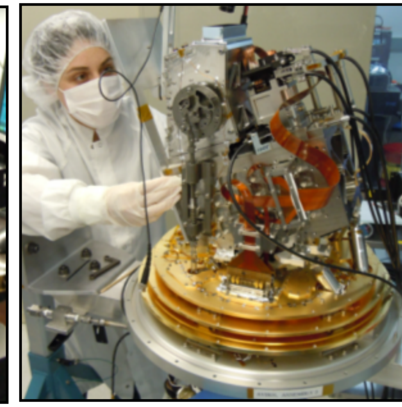

- Designed to exceed AVIRIS-Classic in the spectral, spatial, radiometric and uniformity domains
- Uses 21st century elements: design, grating, slit, mounts, alignment/calibration (many HyspIRI concept VSWIR elements)
- Completed cold alignment on the 30th of March 2012
- Completed calibration on the 6th of April 2012
- All requirements are met
- Test flights planned the week of the 23rd of April 2012

Spectral X-track Uniformity > 95%

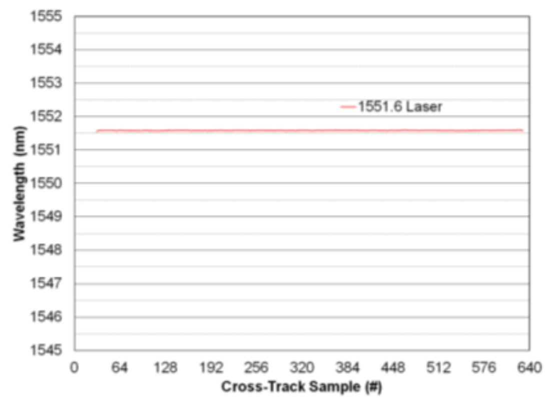

Spectral IFOV Uniformity > 95%

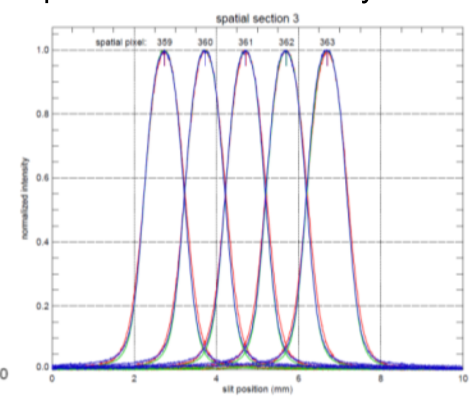

Alignment complete

Initial flights on a Twin Otter aircraft

Hyperspectral Thermal Emission Spectrometer (HyTES)

Flights in July 2012

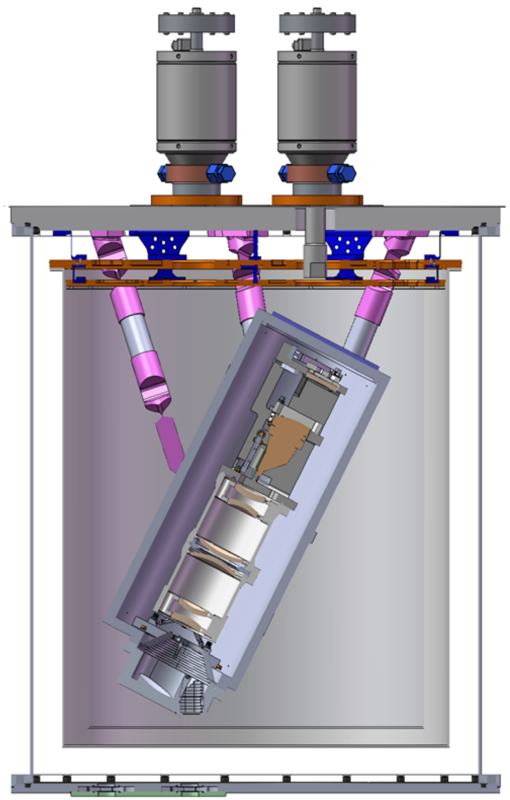

Instrument Characteristic	HyTES
Mass (Scanhead)[1]	12kg
Power	400W
Volume	1m x 0.5m (Cylinder)
Number of pixels x track	512
Number of bands	256
Spectral Range	7.5-12 um
Integration time (1 scanline)	30 ms
Total Field of View	50 degrees
Calibration (preflight)	Full aperture blackbody
QWIP Array Size	1024x512
QWIP Pitch *	19.5um
QWIP Temperature	40K
Spectrometer Temperature	100K
Slit Width	39 μm
Pixel size at 2000 m flight altitude	3.64m
Pixel size at 20,000 m flight altitude	36.4m

1. Does not include 1 rack of electronics to operate instruments

HyTES Recent Gas Measurements in Lab

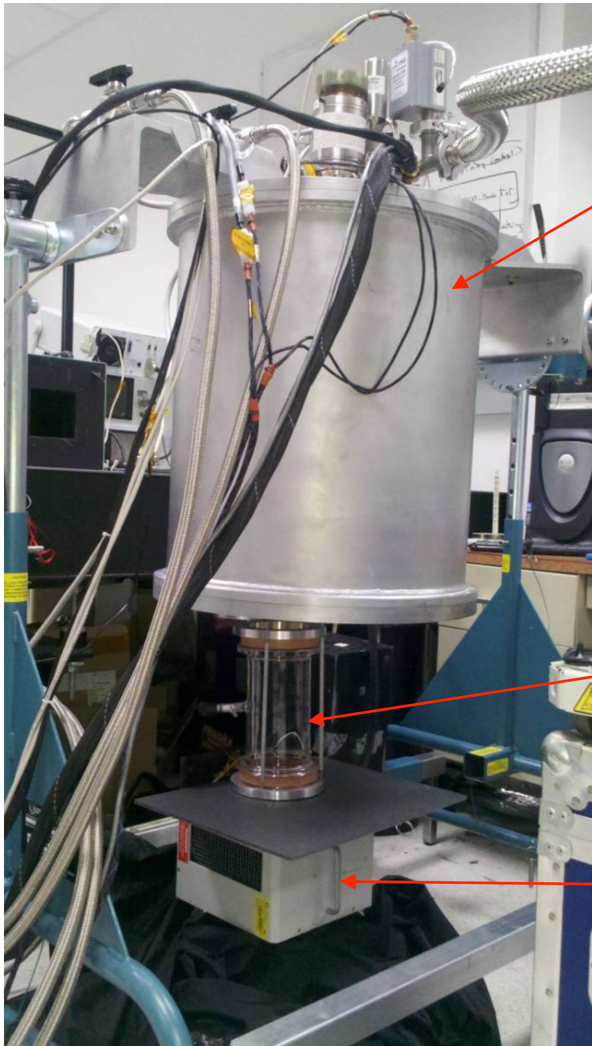

HyTES Scan head

Gas cell housing

Blackbody transmission source

Custom cell housing

- **200mm cell length**
- **ZnSe transmission optics with anti-reflection coatings for maximum transmission.**
- **All gas species are held at 50torr pressure**

HyTES Sulfur Dioxide (SO_2) measurement

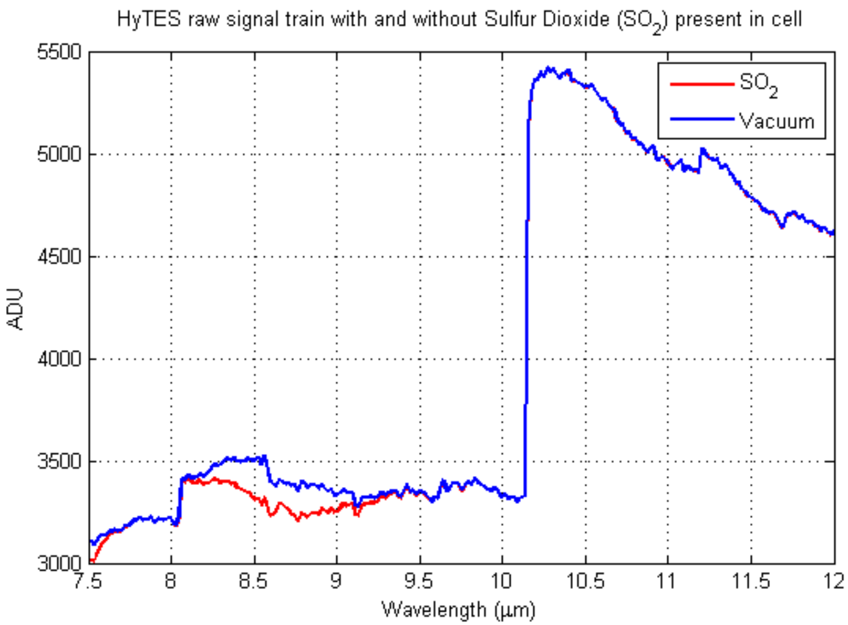

Difference in raw signal between having Sulfur Dioxide present in cell and not.

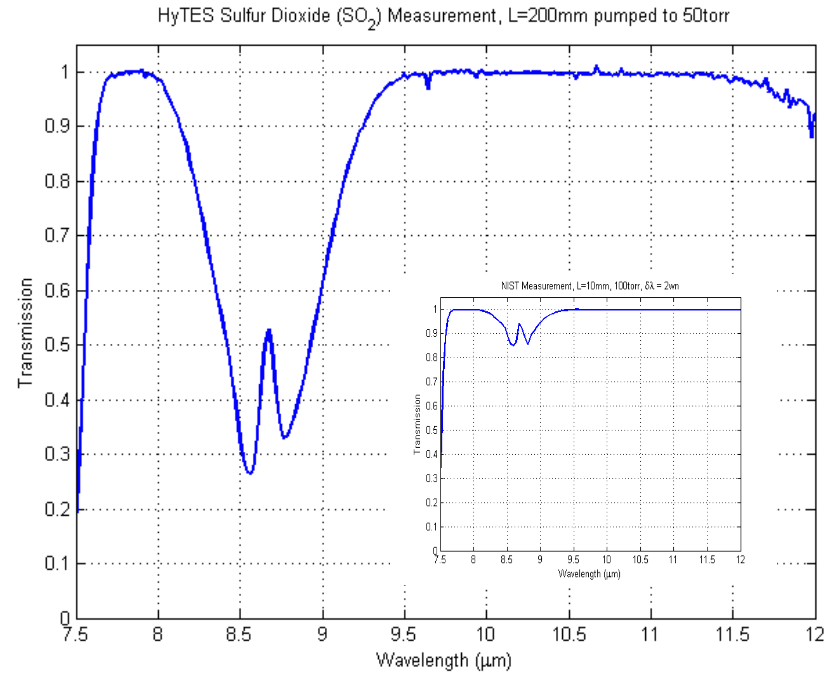

Pixel 256 of HyTES. HyTES ultimate spectral resolution is about 17.6nm.

Inset: SO2 gas data from NIST Standard Reference Database 69: *NIST Chemistry WebBook. $4cm^{-1}$ resolution.*

The HyspIRI Concept Enables the Full Set of Decadal Survey Science and Science Applications and Climate Science

- Key HyspIRI climate objectives from the Decadal Survey and IPCC
  - Ecosystem Measurement for Climate Feedback
  - Black Carbon/Dust Effects on Snow and Ice
  - Carbon Release from Biomass Burning
  - Evapotranspiration and Water Use and Availability
  - Critical Volcanic Eruption Parameters

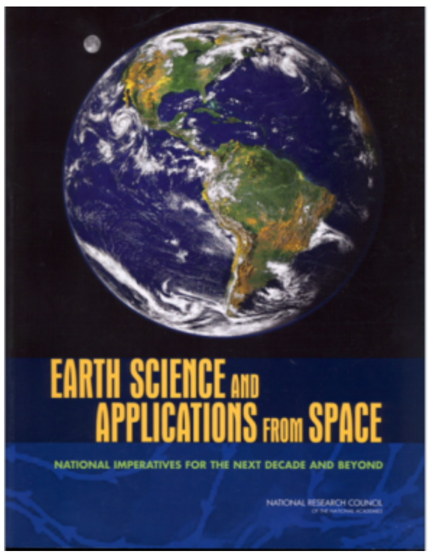

Imaging Spectrometer (VSWIR)

- Pattern and Spatial Distribution of Ecosystems and their Components
- Ecosystem Function, Physiology and Seasonal Activity
- Biogeochemical Cycles
- Changes in Disturbance Activity
- Ecosystem and Human Health
- Earth Surface and Shallow Water Substrate Composition

Combined Imaging Spectrometer and Multi-Spectral Thermal Science

- Coastal habitats, and inland aquatic environments
- Wildfires
- Volcanoes
- Ecosystem Function and Diversity
- Land surface composition and change
- Human Health and Urbanization

Questions?

HyspIRI Products Symposium on Identifying Priority Products to Support HyspIRI's Science Questions

NASA/GSFC, May 16 and 17, 2012
Building 34, Conference room W150

GSFC EO-1/HyspIRI Team

Betsy Middleton, NASA
Bob Knox, NASA
Steve Ungar, UMBC

Petya Campbell, UMBC
Qingyuan Zhang, USRA
Fred Huemmrich, UMBC
Ben Cheng, ERT
Larry Corp, Sigma Space
Lisa Henderson, Sigma Space
David Landis, Sigma Space
Lawrence Ong, SSAI
Dan Mandl, NASA
Pat Cappelaere, Vightel Corp

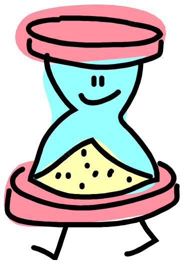

Wed/Thurs Lunches: Pay at Registration Desk
Wednesday Dinner: Sign up

HyspIRI Products Symposium on Identifying Priority Products for SQs

Focus: To Identify Priority Products to Support HyspIRI Science Questions

Objectives:

- Identify science/application data products to be derived from HyspIRI measurements;
- Discuss issues underlying data product processing/integration/fusion;
- Prioritize the development of product prototypes.

Science Discipline Areas to be addressed:

- Ecosystem Function and Composition
- Disturbance and Human Impacts
- Volcano, Natural Hazards and Mineral/Resources

Participants: 100+

Science Questions for the HyspIRI Mission

(http://hyspIRI.jpl.nasa.gov)

HyspIRI has three top-level science questions [identified in the NRC Decadal Survey] related to:

1) Ecosystem function and composition

What is the global distribution and status of terrestrial and coastal-aquatic ecosystems and how are they changing?

2) Volcanoes and natural hazards

How do volcanoes, fires and other natural hazards behave and do they provide precursor signals that can be used to predict future activity?

3) Surface composition and the sustainable management of natural resources.

What is the composition of the land surface and coastal shallow water regions and how can they be managed to support natural and human-induced change?

Topic 1. Ecosystem Function & Composition Questions

VQ1. Ecosystems Pattern and Spatial Distribution and Components

What is the global spatial pattern of ecosystem and diversity distributions and how do ecosystems differ in their composition or biodiversity?

VQ2. Ecosystem Function, Physiology and Seasonal Activity

What are the seasonal expressions and cycles for terrestrial and aquatic ecosystems, functional groups, and diagnostic species? How are these being altered by changes in climate, land use, and disturbance?

VQ3. Biogeochemical Cycles

How are the biogeochemical cycles that sustain life on Earth being altered/disrupted by natural and human-induced environmental change? How do these changes affect the composition and health of ecosystems and what are the feedbacks with other components of the Earth system?

VQ5. Ecosystems and Human Well-being

How do changes in ecosystem composition and function affect human health, resource use, and resource management?

CQ1. Coastal, ocean, and inland aquatic environments

How are local and landscape-scale changes in inland, coastal, and open ocean aquatic ecosystems related to changes in variability in regional and global climate?

CQ4. Ecosystem Function and Diversity

How do species, functional type, and biodiversity composition within ecosystems influence the energy, water and biogeochemical cycles under varying climatic conditions?

Topic 2. Disturbances & Human Impact Questions

VQ4. Ecosystem Response to Disturbance

How are disturbance regimes changing and how do these changes affect the ecosystem processes that support life on Earth?

TQ3. Water Use and Availability

How is consumptive use of global freshwater supplies responding to changes in climate and demand, and what are the implications for sustainable management of water resources?

TQ5. Earth surface composition and Change

What is the composition and temperature of the exposed surface of the Earth? How do these factors change over time and affect land use and habitability?

CQ2. Wildfires

How are fires and vegetation composition coupled?

CQ6. Human Health and Urbanization

How do patterns of human environmental and infectious diseases respond to leading environmental changes, particularly to urban growth and change and associated impacts of urbanization?

Topic 3. Volcano, Natural Hazard & Mineral/Resource Questions

TQ1. Volcanoes

How can we help predict and mitigate earthquake and volcanic hazards through detection of transient thermal phenomena?

CQ3. Volcanoes

Do volcanoes signal impending eruptions through changes in the temperature of the ground, rates of gas and aerosol emission, temperature and composition of crater lakes, or health and extent of vegetation cover?

TQ2. Wildfires

What is the impact of global biomass burning on the terrestrial biosphere and atmosphere, and how is this impact changing over time?

CQ5. Land Surface Composition and Change

What is the composition of exposed terrestrial surface of the Earth and how does it respond to anthropogenic and non anthropogenic drivers?

Expected Outcomes of Symposium

Goal: To Identify and Evaluate Potential Products to Support HyspIRI Science Questions

Objectives/Outcomes:

1] Identify science/application data products that could be derived from HyspIRI measurements.

2] Prioritize the development of product prototypes.

3] Address the geo-location challenges.

4] Discover issues underlying data product processing and related to data integration/fusion.

5] Develop a report on the community consensus for **1-4** above.

2011 NASA Senior Review

Earth Observing-1 (EO-1)

Mission Scientist, Dr. Elizabeth Middleton (NASA/GSFC Code 614.4)
Mission Manager, Mr. Daniel Mandl (NASA/GSFC Code 581.0)

May 3, 2011

Toxic Red Flood in Hungary (2010), ALI True-Color

Gulf Oil Spill (2010), ALI Oil Product

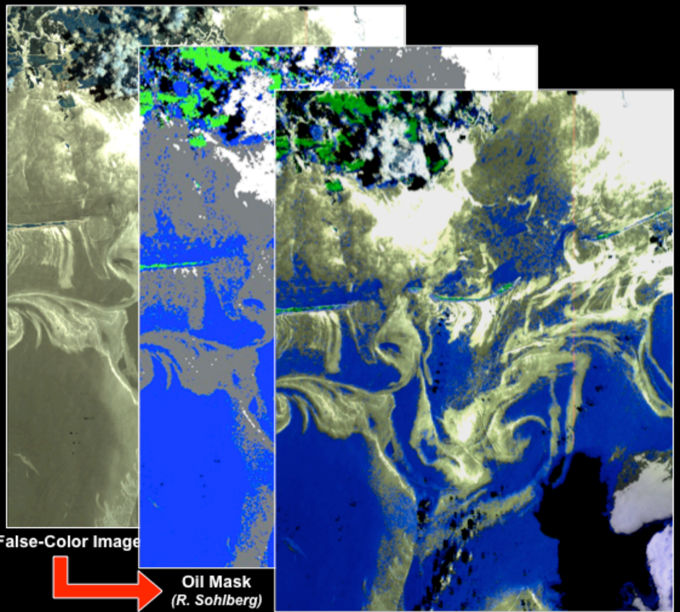

Hyperion Spectral Response

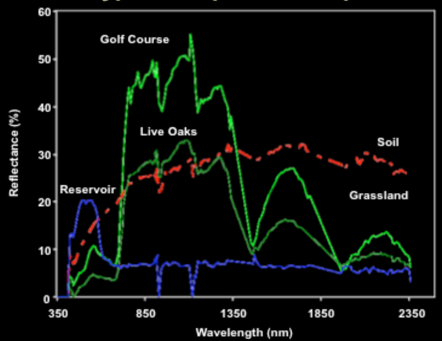

Hyperion Timeseries of Cornfield 2008

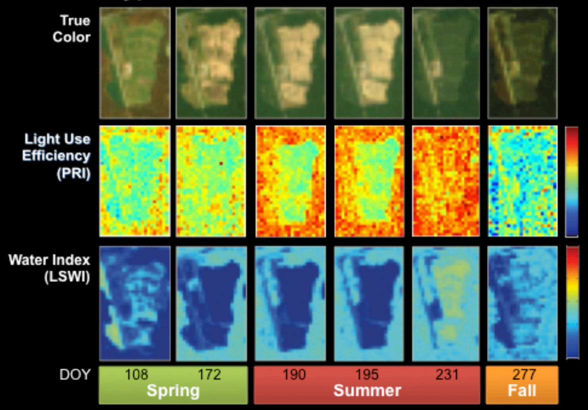

Hyperion Images of Cornfield Area

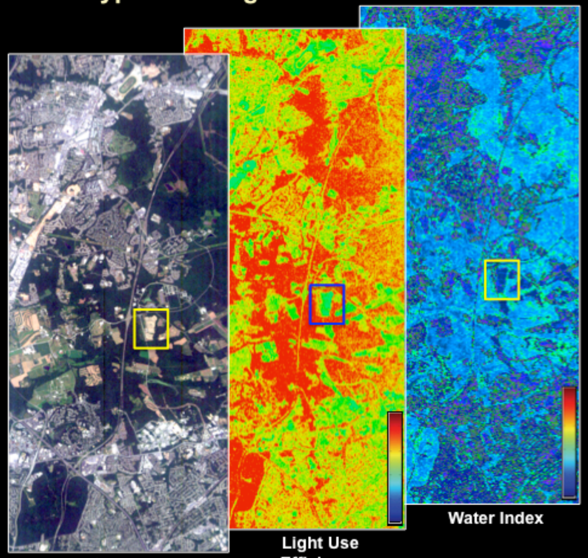

Fire SensorWeb Experiments with U.S. Forest Service

From 2003 to 2009, SensorWeb team conducted a variety of experiments to identify how best to inject SensorWeb technology into assisting Forest Service to manage large wildfires and assist decision makers. This involved interoperating satellite sensors and an Unmanned Aerial System sensors to produce useful data products to assist U.S Forest Service emergency managers.

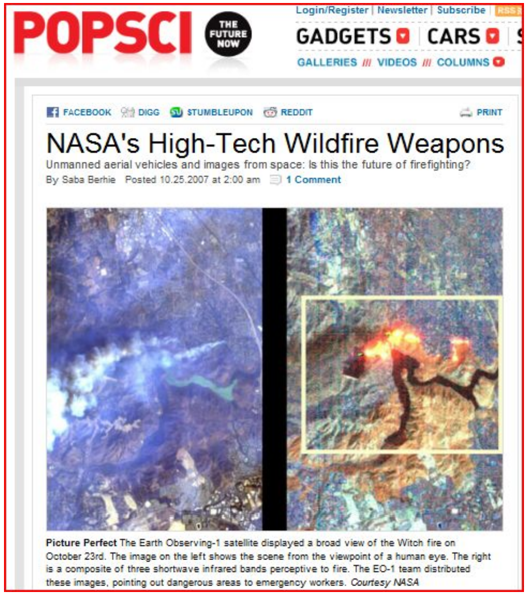
POPSCI THE FUTURE NOW

Login/Register | Newsletter | Subscribe

GADGETS CARS

GALLERIES /// VIDEOS /// COLUMNS

FACEBOOK DIGG STUMBLEUPON REDDIT PRINT

NASA's High-Tech Wildfire Weapons

Unmanned aerial vehicles and images from space: Is this the future of firefighting?

By Saba Berhie Posted 10.25.2007 at 2:00 am 1 Comment

Picture Perfect The Earth Observing-1 satellite displayed a broad view of the Witch fire on October 23rd. The image on the left shows the scene from the viewpoint of a human eye. The right is a composite of three shortwave infrared bands perceptive to fire. The EO-1 team distributed these images, pointing out dangerous areas to emergency workers. *Courtesy NASA*

Detect: National Fire Interagency Center (NIFC) large fire map and MODIS daily hot pixel maps acted as triggers
Respond: Trigger EO-1 and Unmanned Aerial System (UAS) images automatically to take a detailed look
Product Generation: Active fire maps, burn scar maps
Delivery: Experimented with various web based delivery such as mash up displays and RSS feeds

"An exciting aspect of the SensorWeb capability is the ability to automatically image, process and deliver higher resolution satellite imagery products online with little effort."
Everett Hinkley
National Remote Sensing Program Manager

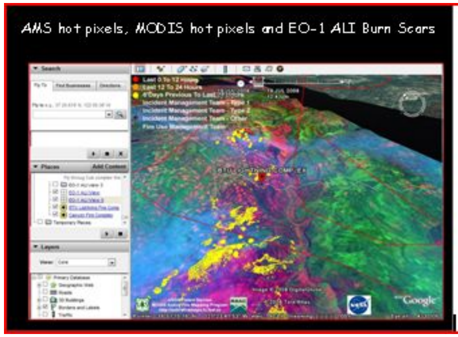

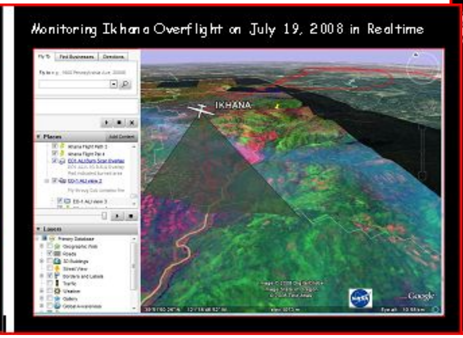

Transformation to On-Demand Product Cloud Part 1
EO-1 Data Product Pipeline

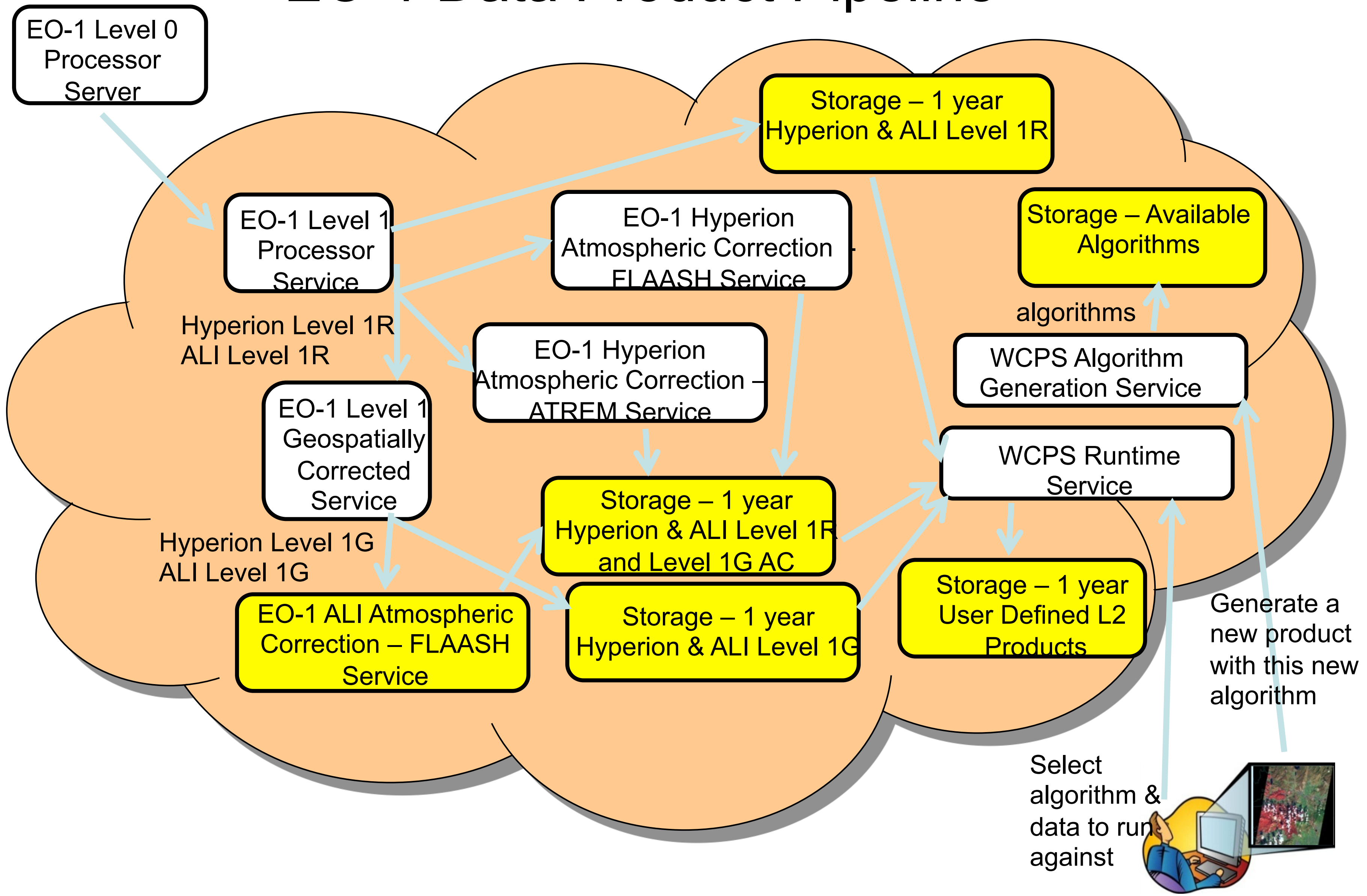

Phase 3 Add Elastic Cloud Ongoing Feb 2011

Ecosystem Measurements for Climate Feedbacks

Ecosystem Species-type, Chemistry & Condition

Invasive Species in the Hawaiian Rainforest from Airborne Imaging Spectrometer data: Patterns of Invasion and Biogeochemical Consequences

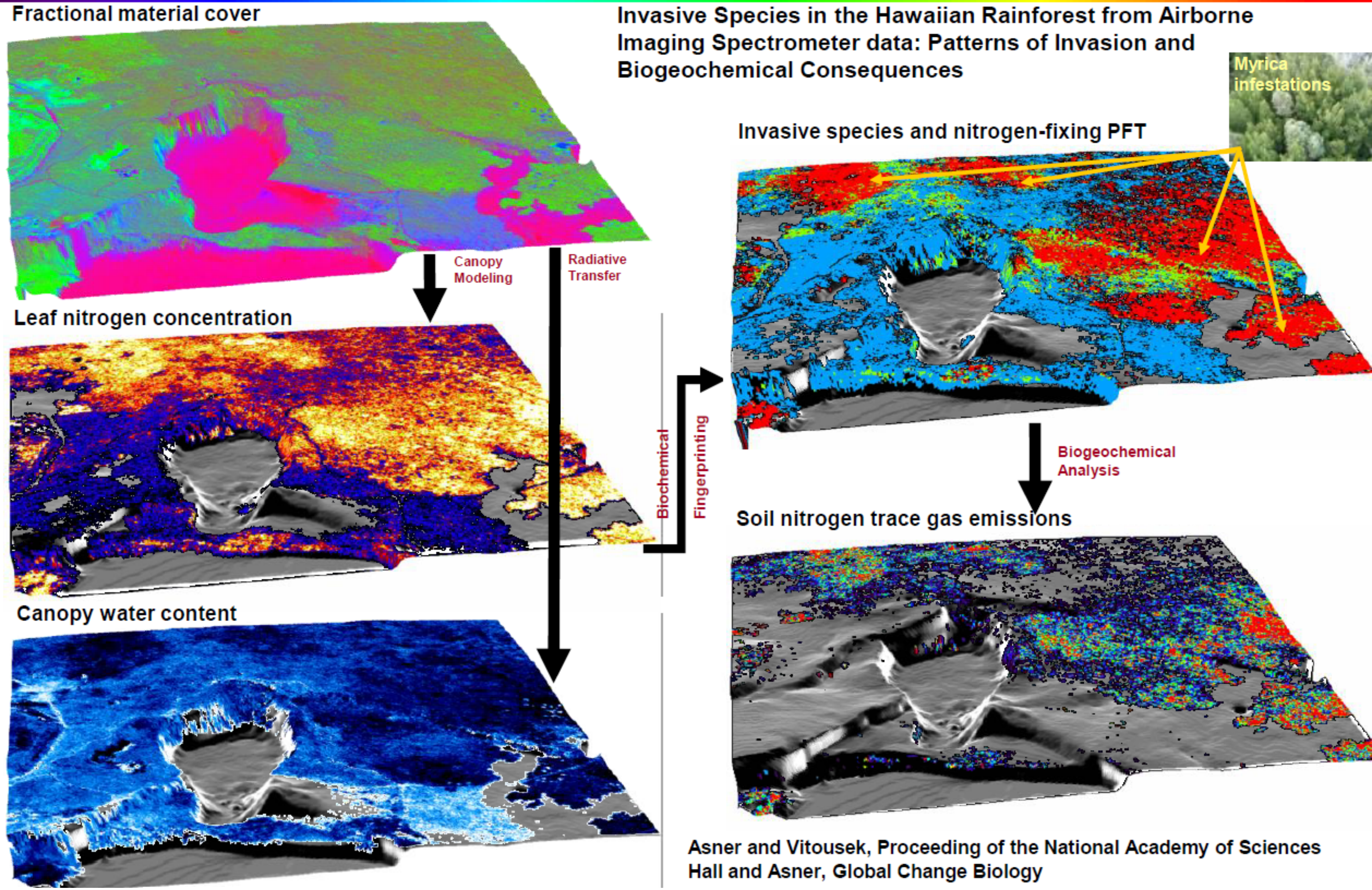

Asner and Vitousek, Proceeding of the National Academy of Sciences
Hall and Asner, Global Change Biology

HyspIRI Global Coverage

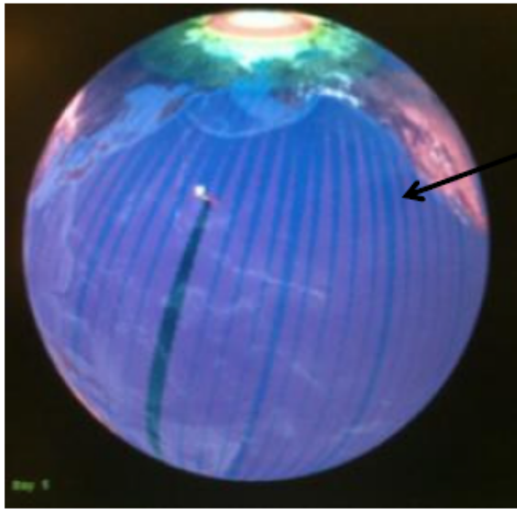

TIR Coverage after 5 days

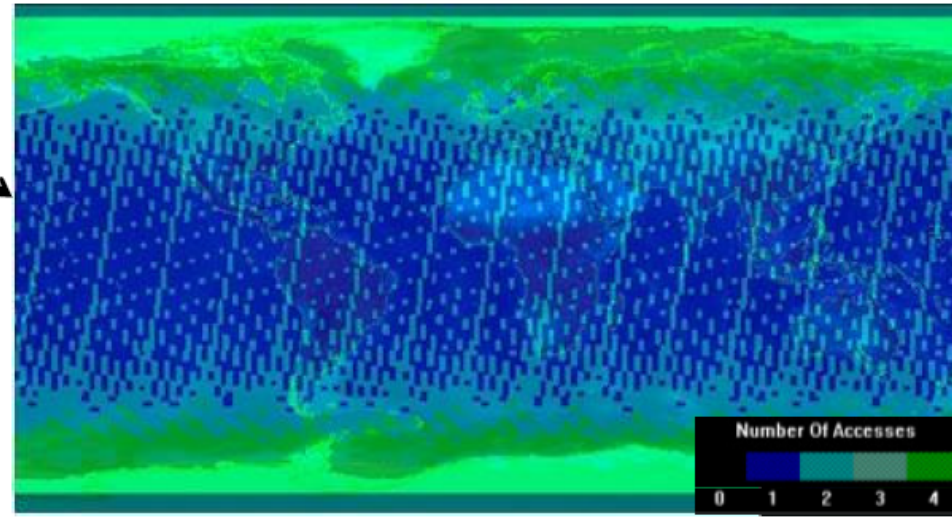

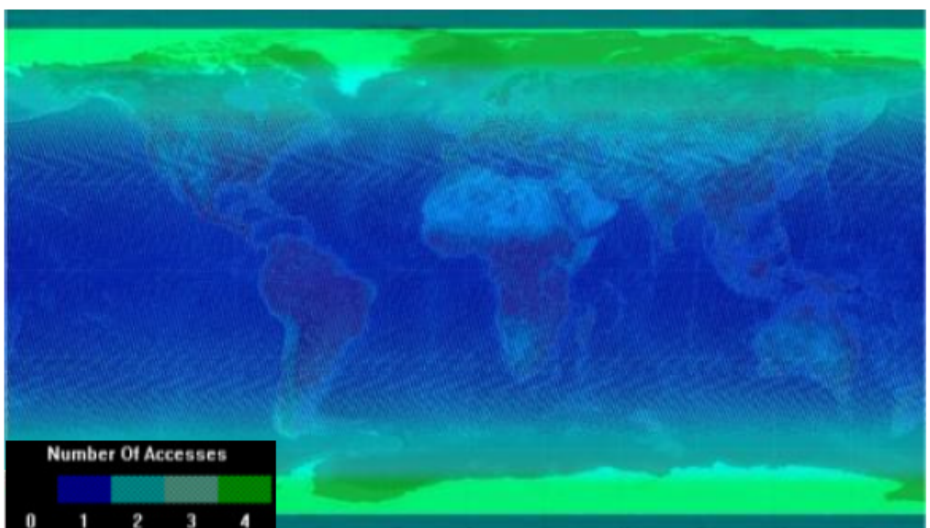

VSWIR Coverage after 19 days

Due to the min 20 deg Sun elevation angle constraint on the VSWIR acquisition, the latitudes covered change with the seasons

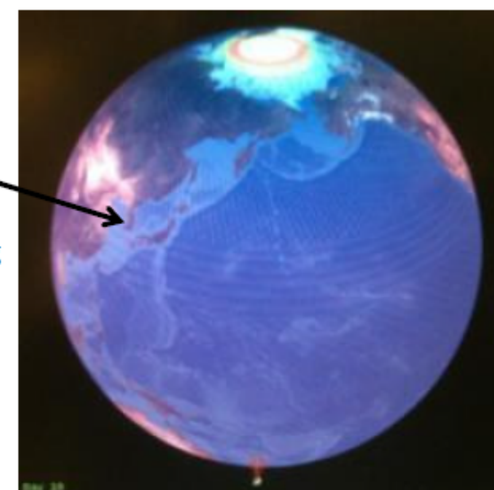

HyspIRI Science Symposium on Ecosystem Data Products

NASA/GSFC, May 4 and 5, 2010
Building 33, Room H114

Mature & Ready: *Proposed HyspIRI Terrestrial Ecology Products*

(* = Climate Variable; ** = Essential Climate Variables defined by CEOS/GEO)

(Green text items show significant enhancement over existing multi-spectral observations)

VSWIR Imaging Spectrometer ALONE

Level 4 Biophysical & Physiological Products

1 **Directional Canopy Albedo [**]**
2 Fractional Cover: Snow, Water and Ice [**]
3 Leaf Area Index, LAI [**]
4 Canopy fAPAR (PAR absorbed by vegetation) [**]
5 Canopy fAPARchl (PAR absorbed by chlorophyll-containing canopy only) [*]
6 **Total Canopy Chlorophyll Content [*]**
7 **Fractional Cover: Green Vegetation, Non-Photosynthetic Vegetation, impervious surfaces, soil [*]**
8 **Fractional Cover for Vegetation Classes: Coniferous, Deciduous, and Mixed Forests; Grasslands; Wetlands; Crops [*]**

Multi-Spectral TIR Imagery ALONE

Level 2 & 3 Products [Day or Night swath & gridded data] (Terrain corrected; Day/Night Seasonal Composites)

1 Soil Moisture [**]
2 Fire Severity & Direction & Fire Radiative Power [**]
3 Distribution and variation in land surface temperature [*]
4 Water Stress Indicators [*]
5 Emissivity-Based Land Surface Classification (e.g., pervious vs. impervious) [*]
6 Cloud Mask [*]

VSWIR + TIR Combined

Level 4 Combined Products

1 **Biomass for Grasslands [**]**
2 **Diversity, Coastal Habitats [**]**
3 **ET by Land Cover Type [*]**
4 **Functional Types/Species Composition [*]**
5 **Ecological Disturbance Area (logging, natural disasters) [*]**
6 **Drought Index (PET/AET) by Land Cover Type [*]**

Proposed Terrestrial Ecology Products from HyspIRI

Potential Products Needing Further Validation (* = Climate Variable; ** = ECV defined by CEOS)

(Green text items show significant enhancement over existing multi-spectral observations)

VSWIR Imaging Spectrometer ALONE

Level 4 Biophysical & Physiological Products

1. **Photosynthetic Parameters (LUE, Jmax, Vcmax) [*]**
2. **Environmental Stress Measurements (response variables) [*]**
3. **Canopy N content (mass/area) [*]**
4. **Canopy Water Content [*]**
5. **Vegetation Pigment Content (Chl a, Chl b, Carotenoids, Anthocyanins)**
6. **Canopy Lignin and Cellulose**

Multi-Spectral TIR Imagery ALONE

L3 Products [Day or Night swath & gridded data]

1. Burn Area (experimental as TIR only)
2. Burn Severity (experimental as TIR only)

VSWIR + TIR Combined

L4 Products – Regional

1. **Surface Energy Flux [**]**
2. **Combusted Biomass [**]**
3. **Sensible Heat due to Urban Heat Islands (Anthropogenic Heat) [*]**
4. **LST: Day/Night Differences for Ecosystems & Urban Areas [*]**
5. **LST Urban/Suburban [*]**
6. **LST by Functional Groups and Ecosystem Types [*]**
7. **Surface Topographic Temperature Mapping [*]**

L4 Products – Global

1. **LST & Emissions by Fractional Land Cover (Vegetation, Soil, Water, Snow, Ice, etc.) [**]**
2. **Ecosystem/Crop Phenology with Fusion Approaches [*]**

HyspIRI Science Symposium on Ecosystem & Environmental Global/Regional Data Products

NASA/GSFC, May 17 and 18, 2011
GSFC Visitor Center

Higher Level Products for HyspIRI – Discussion Summary

#	Product	Level (L2/3/4)	Maturity	MODIS	Landsat	Models	Notes
Reflectance & TIR Products							
A.	***Global Products for Data Continuity***						
1	Convolved Reflectance to other sensors (long term data recors; narrowband/broadband)	3	yes	yes	progress	yes	R(%), LEDAPS, WELD algorithms
2	Symulated LST for other sensors (e.g. MODIS, LDCM/TIRS)	2	yes	yes	yes	yes	LST (T C°)
3	Fractional land cover type (FLC) [continuous fields, % of land cover: soil, water, vegetation, ice&snow]	3	yes	yes	yes	yes	for long term records continue MODIS product, test f(PV, NPV) for vegetation cover
4	Thermal Anomalies	4	yes		yes/limited	yes	
B.	***Terrestrial (veg. & soil)***						
I.	**Spectral End-member Abundance**	3	in progress	no	no	no	Local Spectral libraries (cal/val) needed
	- mineral maps, veg type maps						
II.	**Vegetation Spectral Bio-indicators (VIs)**	3/4	in progress	EVI, NDVI	TM 5/4, 4/3 etc.	progress	
	- water, cellulose, chlorophyll, general stress	3	in progress	yes/limited	no	no	
	- nitrogen	4	in progress	no	no	yes	Local Spectral libraries and chemistry (cal/val)
	- hot spots	4	in progress	yes/limited	yes	no	
	- LST per VFC and LC	4	in progress	yes/limited	in progress	no	
III.	**Canopy function Yield (CO2 sequestration, GPP, NEP)**						
	- LUE, WUE	4	in progress		no	yes	
	- ET	4	in progress		no	yes	
IV.	**Classifications**						
1	**Fractional vegetation cover (FVC)** *[photosynthetic vegetation [PV] or non-photosynthetic vegetation [NPV], Soil]*	3	yes	no	limited		AutoMCU or equivalent (SWIR and red-edge with tied spectra)
2	**Fractional cover by plant functional type (PFTs)**	4	in progress	see below	no	yes	Required by DVGM (dynamic global vegetation models) end ESM (Earth system models); At launch 2-6 types/km^2, goal 6-10 resolved
V.	**Terrestrial Products Supporting Long Term Data Records**						For HyspIRI products context, and for long term records continuity
1	**MODIS Vegetation Continuous Fields (VCF - cotext &**	4	yes	yes			
	- life form (proportion of woody vegetation, herbaceous	4	yes			yes	
	- leaf type (proportion of woody vegetation that is needle	4	yes			no	
	- leaf longevity (proportion of woody vegetation that is	4	yes			no	
2	**Ecological disturbance (NPV increase)**	4	yes, global on progress	Fire product	LEDAPS		Based on PV, spectral change diagnosing disturbance type; decline/recoveery; for land history
	- Land cover conversions	4	yes, global in progress	yes	yes/limited	yes	Terrestrial ECVs: LC, permafrost, glaciers/ice, LAI, fire
	- Severe wind, deought, insect, etc.	4	in progress	yes	yes/limited	yes	False alarm a possibility
	- Fires (VISWIR detection, severity)	4	in progress	yes	yes/limited		
VI.	**Biodiversity**						
	- Optical types diversity	4	initialized	no	no	yes	see publication on the topic by Usting and Gammon
	- Plant functional diversity	4	initialized	no	no	yes	see publication on the topic by Asner, Wright, et al.
	- Biodiversity indicators	4	in progress	no	no	yes	Spectral corelation with bio-diversity

Higher Level Products for HyspIRI – Discussion Summary *(continued)*

#	Product	Level (L2/3/4)	Maturity	MODIS	Landsat	Models	Notes
C.	***Aquatic [shallow water, rivers, lakes]***						
1	Remote Sensing Reflectance (Rrs)	2 or 3	yes, operational	yes	no		Remote Sensing Reflectance = water-leaving radiance (Lw) / downwelling irradiance (Ed); (Rrs, units sr-1, 400–800 nm) ; This is the result
2	Sea Surface Temperature	2-Jan	yes, operational	yes	no		Routine product from many satellites.
3	Seafloor Spectral Reflectance (units %, 400–??? nm)	3	in progress	no	no		Combined results from aquatic retrieval
4	Water Depth	3	in progress	no	no		There are several candidate algorithms in
5	Water Optical Properties	3	in progress	yes	no		-"-
6	Retrieval Quality Flags	3	in progress	na	no		-"-
7	Fractional Cover	3	in progress	na	no		Derived from Rrs, mixture decomposition methods need scaling to HyspIRI data
8	Pigments (e.g. chlorophyll)	3	mature, work in progress to separate aquatic sources	yes	no		Derived from Rrs, work in progress to separate contributions of planktonic, submerged and emerged aquatic sources
9	Light-Use Efficiencies (for (1) Productivity and (2) Calcif	3	in progress	yes	no		There are few investigations for shallow
	- Productivity (Gross/Net)	4	in progress	yes	no		Investigations for fresh water bodies, needs synthesis of fresh, coastal and deep ocean
	- Calcification	4	not initialized	na	no		There are no existing algorithms, and there have been (virtually) no investigations
10	Water content Dissolved Organic Mater (DOM)	4	in progress	yes	no		Investigations for fresh water bodies, needs synthesis of fresh, coastal and ocean methods
11	Degree Heating Weeks	3	mature	yes	no		Routine product from many satellites.
D.	***Snow/Ice [high latitudes, high***						**Input to be obtained from:**
	Snow cover, Ice caps, Glaciers	3/4	no experts present				**Dorothy Hall, Jeff Dozier, Thomas Painter**
Top of Atmosphere and Localized Products, and By-products of Level 2 Processing							
1	TOA Optical and TIR Radiance (bands)	1B	yes	yes/limited	yes/limited		
2	Volcanoes eruption, size, prognosis	4	yes	yes/limited	yes/limited	yes	
3	Clouds (masks)	3	yes	yes	yes/limited		
4	Incident PAR (direct, diffuse PAR)	3				yes	
5	Water vapor product	3	yes			yes	
6	Aerosol optical depth product	3	yes	no	no	no	
7	Albedo	4	in progress	yes	no		

DAY 1 (May 16): Morning Agenda

8:00-8:30am: Registration, Coffee, Posters Up (W150)

***8:30-9:30am (W150)* HyspIRI Mission Update**

Status of HyspIRI Mission ***[Woody Turner, NASA/HQ, 10 min]***

HyspIRI Plans & Perspectives ***[Jack Kaye, NASA/HQ, 10 min]***

Summary of HyspIRI Mission & Instruments ***[Rob Green & Simon Hook, NASA/JPL, 30 min]***

Review of Symposia 1 & 2, HyspIRI Science Questions and Symposium 3 Objectives
[Betsy Middleton, NASA/GSFC, 15 min]

***9:50-10:20am (W150)* Topic 1. Ecosystem Function & Composition Questions (VQ1-3, 5; CQ1, 4)**

Examples of existing higher level products: ***[Fred Huemmrich, UMBC, 15 min]***

Desired New HyspIRI Products ***[Petya Campbell, UMBC, 15 min]***

10:20-10:30am: Coffee Break & Posters

10:30am-11:45am (W150)* Contributed Talks *[20 min each]

1] Daily ET Products at Landsat/HyspIRI Scale from MODIS- & Landsat/HyspIRI-like Data
[Carmelo Cammalleri, USDA]

2] Evapotranspiration Using Remote Sensing & Weather Data in Mesoscale/local Scale Physically Based Models ***[Susan Ustin, UCD]***

3] Tower Flux Estimates at Validation Sites with EO-1 Hyperion ***[Fred Huemmrich & Petya Campbell, UMBC]***

4] 3 years, 150 AVIRIS images: Practical considerations for analyses of large hyperspectral data sets for ecosystem studies ***[Aditya Singh & Phil Townsend, UW]***

11:45am-1:00pm: Lunch

DAY 1 (May 16): Afternoon Agenda

1:00-2:05pm* Discussion of Topic 1 - Higher Level Ecosystem Products: Prioritize desired products; Discuss methods, tools and resources required *[Susan Ustin, UCD & Fred Huemmrich, UMBC]

Discussions by Breakout Groups *[2-3 Groups, 45 min, W120A, W120B, W150]*

Summary of Discussions *[Everyone, 20 min, W150]*

***2:10-2:30pm (W150)* Contributed Talk**

5] Extracting Temperature and Emissivity from High Spatial Resolution Multispectral Thermal Infrared Data ***[Simon Hook & Glynn Hulley, JPL]***

***2:30-3:00pm (W150)* Topic 2. Disturbances & Human Impact Questions (VQ4, TQ3, 5; CQ2, CQ6)**

Examples of existing higher level products: ***[Dale Quattrochi & Jeff Luvall, NASA/MSFC, 15 min]***

3:00pm-3:25pm: Coffee Break & Posters

3:25-4:25pm (W150)* Contributed Talks *[20 min each]

6] Synergies between VSWIR and TIR data for the urban environment: An evaluation of the potential for the Hyperspectral Infrared Imager (HyspIRI) Decadal Survey mission ***[Dar Roberts, UCSB, Dale Quattrochi, NASA/MSFC; Glynn Hulley, Simon Hook & Rob Green, JPL]***

7] Estimating Agricultural Crop Residue: Opportunities for HyspIRI ***[Melba Crawford, Purdue]***

8] Values and Advantages of HyspIRI for Remote Sensing of Aquatic Environments ***[ZhongPing Lee, UMASS]***

4:25-5:30pm* Discussion of Topic 2 - Disturbances & Human Impact: Prioritize desired products; Discuss methods, tools and resources required *[Dale Quattrochi, NASA/MSFC & Melba Crawford, Purdue]

Discussions by Breakout Groups *[2-3 Groups, 45 min, W120A, W120B, W150]*

Summary of Discussions *[Everyone, 20 min, W150]*

5:30-6:00pm *(W150)* General Discussion ***[Leaders: Woody Turner, NASA/HQ & Petya Campbell, UMBC]***

6:00pm Adjourn for Dinner

6:30pm Happy Hour & Dinner [at Ruby Tuesday]

DAY 2 (May 17): Morning Agenda

8:00-8:30am: Coffee & Posters

8:30-9:30am *(W150)* IPM & Cloud Data Distribution, Low Latency Tools & Products; ESTO activities

[Demo & Examples: Dan Mandl, NASA GSFC, & Robert Sohlberg, UMBC, 75 min]

9:30-10:30am (W150) **Topic 3. Volcano, Natural Hazard & Mineral/Resource Questions (TQ1-2, 4; CQ3, 5)**

Examples of Higher level Products Possible from Existing Assets: Landsat, MODIS, ASTER, MASTER, AVIRIS, Hyperion, ALI ***[John "Lyle" Mars, USGS, HyspIRI staff-15 min]***

Identify desired new HyspIRI products ***[Rob Wright, UH, 15 min]***

10:30-10:45am **Contributed Talk**

9] Atmospheric Correction Tools/Application for HyspIRI: Onboard & on the Cloud

[Tim Perkins, Spectral Sciences, Inc.]

10:45-11:00am: Coffee Break & Posters

11:00-11:45am (W150) **Contributed Talks from SSG** ***[15 min each]***

10] ASTER Standard TIR Data Products ***[Mike Abrams, NASA/JPL]***

11] Results of increased spatial and spectral observations of volcanic activity: Implications for HyspIRI TIR data

[Michael Ramsey, Univ. Pittsburgh]

12] Quantifying global volcanic unrest with HyspIRI: near-real-time algorithms and products ***[Rob Wright, UH]***

11:45am-12:50pm Lunch & Demo

Atmospheric Correction Tools and Application Needs, Using EO-1 Hyperion Images

[Pat Cappelaere, NASA GSFC & Steve Adler-Golden, Spectral Sciences,, Inc.]

DAY 2 (May 17): Afternoon Agenda

12:50-2:05pm **Discussion of Topic 3 - Volcanoes, Natural Hazards & Mineral/Resources: Prioritize desired products; Discuss methods, tools and resources required**
[Mike Abrams, NASA/JPL & Rob Wright, UH]

Discussions by Breakout Groups *[2-3 Groups, 45 min, W120A, W120B, W150]*

Summary of Discussions *[Everyone, 20 min, W150]*

2:10-2:40pm (W150) **Contributed Talk from SSG, Introduction to Geolocation Challeng**es

13] Geo-location knowledge requirements for HyspIRI products & science questions

[Steve Ungar & Pat Cappelaere, NASA/GSFC, 30 min]

2:40-3:10pm: Coffee Break, Posters & AC Demo

3:10-4:10pm *(W120A, W120B, W150)* **Interactive Discussion on Geolocation Challenges** (60 min)

W120A Group 1**:** Geolocation Challenges & Topic 1 (Ecosystems)

[Leaders: Susan Ustin, UCD & Fred Huemmrich, UMBC]

W120B Group 2**:** Geolocation Challenges & Topics 2 (Disturbance/Human Impacts) and 3 (Volcanoes & Disasters) ***[Leaders: Dale Quattrochi, NASA/MFSC & Rob Wright, UH]***

4:15-4:30pm *(W150)* **Open Discussion on General Needs & Issues for Higher Level HyspIRI Products**

[Leader: Betsy Middleton, NASA GSFC & Yen-Ben Cheng, ERT]

4:30-5:30pm *(W150)* **Reports to Full Meeting from Each Discussion**

[Discussion Leaders: Betsy Middleton, NASA GSFC & Woody Turner, NASA/HQ]

Generate list of Recommendations from Discussions (by Topic 1-3)

Summary of Meeting

5:30pm **Adjourn**

NASA Decadal Survey HyspIRI

Determine the global distribution, composition, and condition of ecosystems, including agricultural lands

Tree species mapping, Bartlett Forest, NH

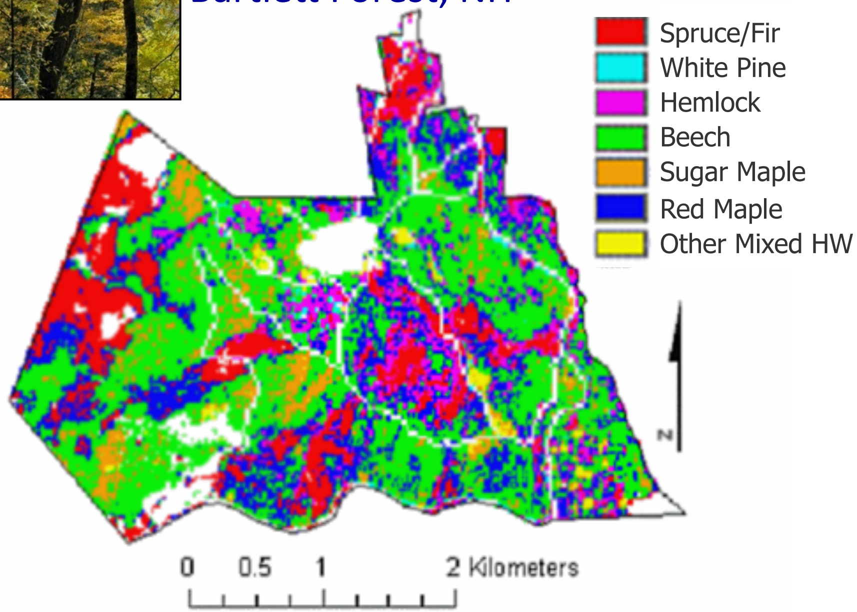

Societal Issue:

- Forests, farmlands and a variety of other ecosystems are critical to life on the Earth. Many ecosystems are changing in ways that are poorly understood.

Scientific Issue:

- Understanding the distribution, diversity and status of ecosystems is necessary for understanding how they function and for predicting future changes.

Approach (Why we need HyspIRI):

- HyspIRI will provide an important new capability to detect & monitor ecosystem composition and condition globally, with spectroscopic and thermal measurements.

HyspIRI Airborne Simulator Data Set

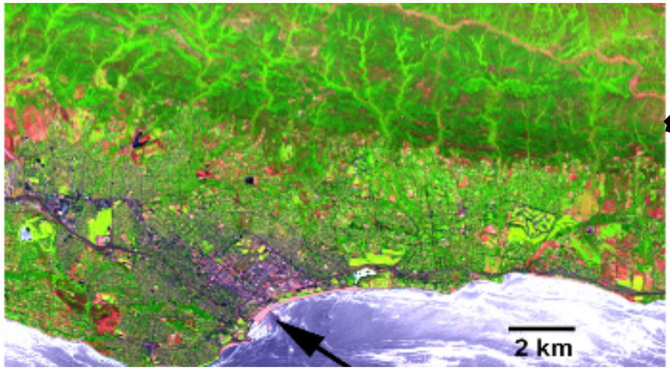

Species Type Determination

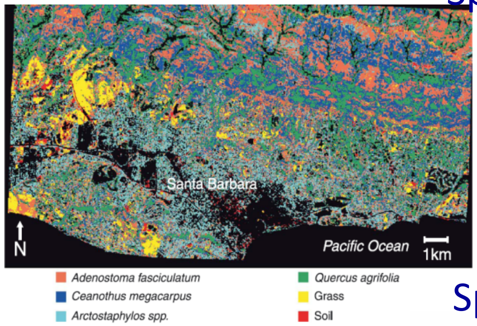

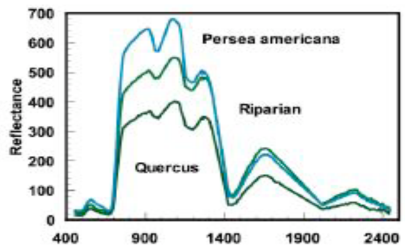

Species Fractional Cover

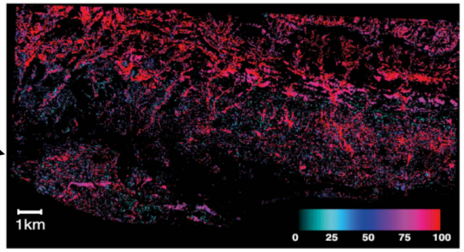

Existing Satellite Land Data Products

a non-comprehensive review

NASA
Goddard
SPACE FLIGHT CENTER

K. Fred Huemmrich
University of Maryland Baltimore County
May 16, 2012

UMBC JCET NASA-GSFC

Introduction

We want to look at some existing satellite land products to highlight issues for HyspIRI products

- How do data products relate to each other?
- How are data organized spatially?
- How are data grouped temporally?
- What are approaches are used to calculate data products?
- How are data distributed?

Overview of MODIS Processing Levels

- Level 0 data - raw satellite feeds
- Level 1 data - radiometrically calibrated, but not otherwise altered
- Level 2 data - atmospherically corrected to yield a surface reflectance product
- Level 3 data - level 2 data gridded into a map projection
  - usually have also been temporally composited or averaged
  - The advantage of level 3 data is that each pixel of L3 data is precisely geolocated
  - a disadvantage is that the process of compositing may compromise data
- Level 4 data - products that have been put through additional processing

MODIS Surface Reflectance

The MODIS Surface Reflectance products provide an estimate of the surface spectral reflectance as it would be measured at ground level in the absence of atmospheric scattering or absorption.

- level-2 and -3 data
- gridded 250 m (Bands 1 & 2), 500 m, 5600 m (climate grid)
- Daily, 8-day
- Utilizes 6S atmosphere radiative transfer model

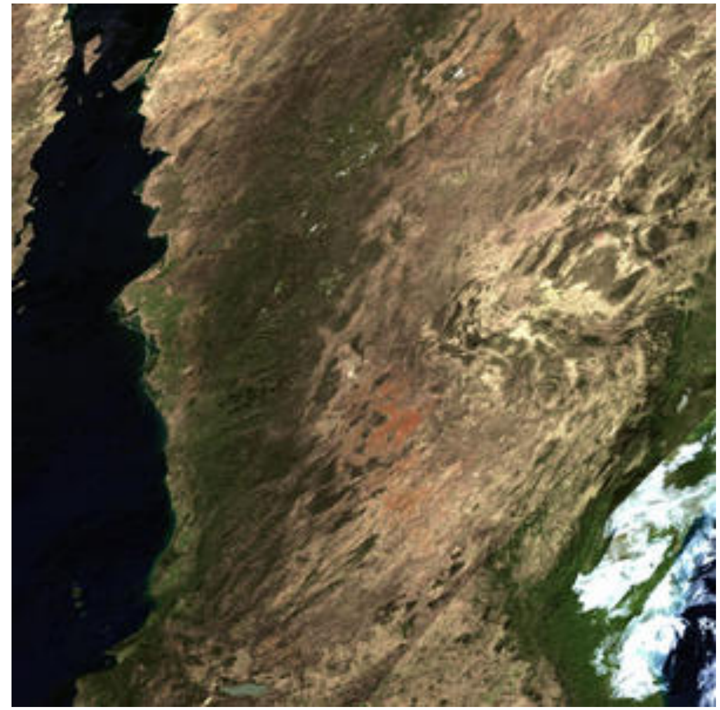

A combination of Bands 1, 4, 3 displays an R, G, B Surface Reflectance image using 500-m data acquired between January 1 - 8, 2007 over much of Mexico (h08v06), giving a clear view of the pine-oak forests defining the Sierra Madre Occidental in the west, across the altiplano region occupying much of the Mexican interior.

https://lpdaac.usgs.gov/products/modis_products_table/surface_reflectance/8_day_l3_global_500m/mod09a1

MODIS Land Surface Temperature & Emissivity

The MODIS Land Surface Temperature and Emissivity (LST/E) products provide per-pixel temperature and emissivity values

- level-2 and -3 data
- gridded 1000 m, 6000 m, 5600 m (climate grid)
- Daily, 8-day, monthly
- Utilizes generalized split-window algorithm at 1 km and day/night algorithm at 6 km

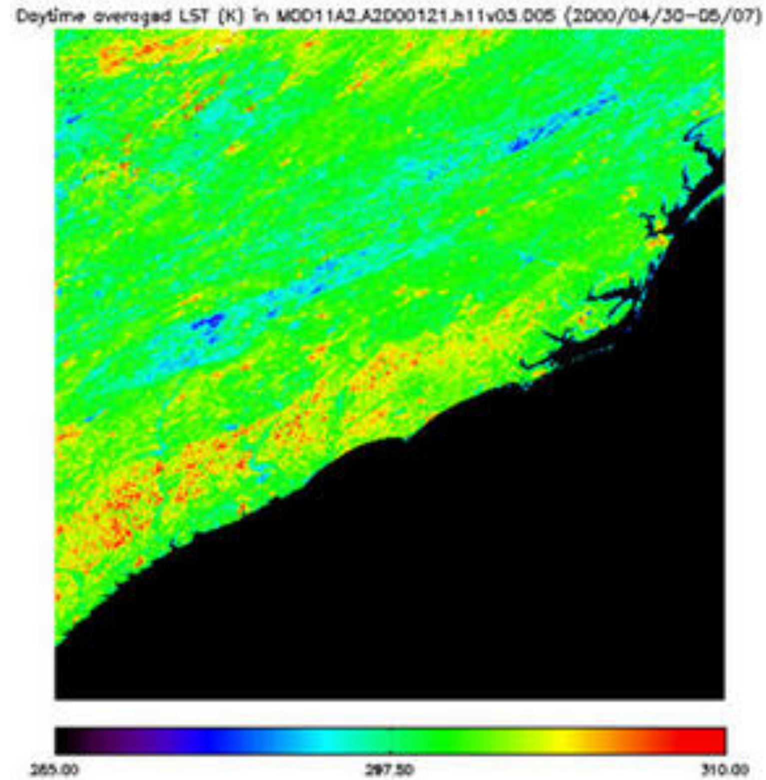

This false-colored MOD11A2 image shows the 8-day average values of daytime clear-sky LSTs retrieved from MODIS data in the period of April 30 May 7, 2000 over the eastern coast of the United States.

https://lpdaac.usgs.gov/products/modis_products_table/land_surface_temperature_emissivity/8_day_l3_global_1km/mod11a2

MODIS Land Cover Type and Dynamics

MODIS Land Cover product porvides five different land cover classification schemes and the Land Cover Dynamics product includes layers on the timing of vegetation growth, maturity, and senescence that mark the seasonal cycles

- level-3 data
- gridded 500 m, 1000 m, 5600 m (climate grid)
- yearly
- uses supervised decision-tree classification
- uses vegetation indices for dynamics

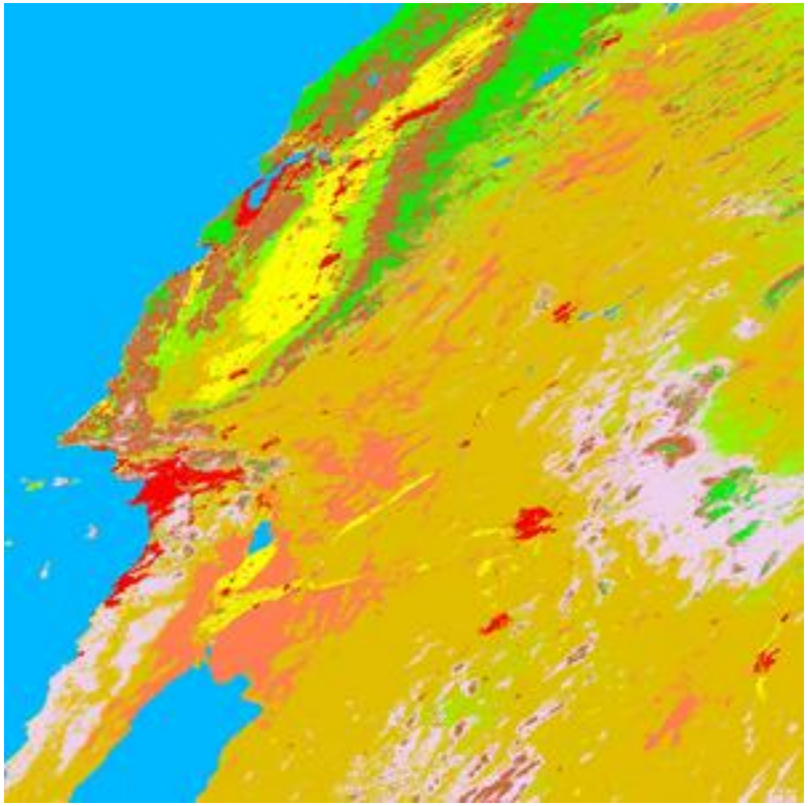

This image represents the 2005 land cover types for the western United States (h08/v05). This first SDS layer depicts the IGBP classification. The predominant light brown color represents the open shrublands. Varying shades of green portray the evergreen and deciduous forests. Sienna shades are areas of woody savannas, and savannas. Closed shrublands are characterized in thistle, and yellow indicates croplands. Red represents urban and built-up areas, while coral indicates barren and sparse vegetation.

https://lpdaac.usgs.gov/products/modis_products_table/land_cover/yearly_l3_global_500_m/mcd12q1

MODIS Land Bidirectional Reflectance Distribution Function (BRDF) and Albedo

The MODIS Albedo product describes both directional hemispherical reflectance (black-sky albedo) and bihemispherical reflectance (white-sky albedo), model weighting parameters (fiso, fvol, fgeo), and modeled nadir view reflectance

- level-3 data
- gridded 500 m, 1000 m, 5600 m (climate grid)
- 16-day sampled at 8-days
- Combines both Aqua and Terra data
- Uses RossThick-LiSparseReciprocal kernel semiempirical model

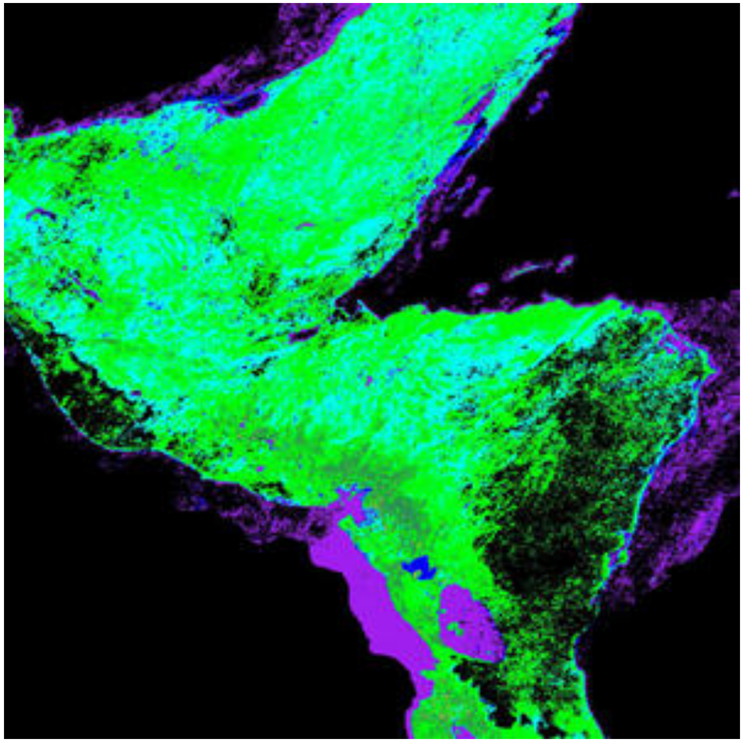

This is a representation of the first of the three model parameters used to reconstruct surface anisotropic effects and thus correct directional reflectences to a common view geometry, or to compute integrated albedos. The colors describe isotropic weighting parameters for data acquired between February 26 and March 13, 2001 over Central America including the Yucatan Peninsula, El Salvador, Honduras, Nicaragua, and some of Costa Rica (h09v07).

https://lpdaac.usgs.gov/products/modis_products_table/albedo/16_day_l3_global_500m/mcd43a3

MODIS Vegetation Indices

The MODIS Vegetation Indices product provides Normalized Difference Vegetation Index (NDVI) and Enhanced Vegetation Index (EVI)

- level-3 data
- gridded 250 m, 500 m, 1000 m, 5600 m (climate grid)
- 16-day, monthly
- Vegetation index

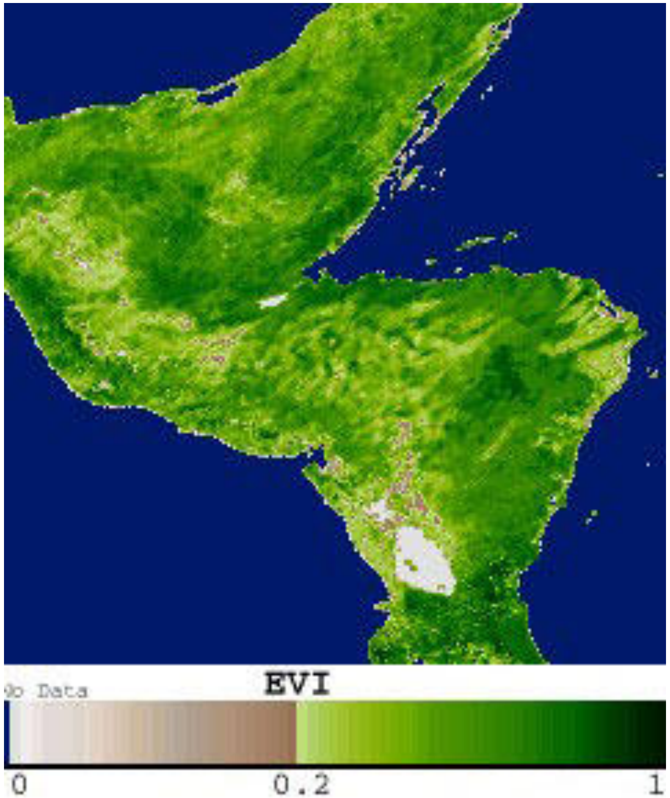

The MYD13A2 images shown are samples of the MODIS/ Aqua Vegetation Indices 16-Day L3 Global 1km SIN Grid. EVI has been pseudo-colored to represent the biomass health of the Yucatan Peninsula using tile h09v07 from May 1 16, 2007.

https://lpdaac.usgs.gov/content/view/full/6657

MODIS Thermal Anomalies/Fire Products

MODIS Thermal Anomalies/Fire products include fire occurrence (day/night), fire location, the criteria used for the fire selection, detection confidence, and a calculation of Fire Radiative Power. It distinguishes between fire, no fire and no observation.

- level-3 data
- gridded 1000 m
- daily, 8-day
- Derived from MODIS 4- and 11-micrometer radiances.
- The fire detection strategy is based on both absolute detection and on detection relative to its background

Using the MOD14A2 Fire Mask a color code was applied to highlight fires in yellow, water bodies in blue, and leaving land area in black. Each yellow pixel is 1km2.

https://lpdaac.usgs.gov/products/modis_products_table/thermal_anomalies_fire/8_day_l3_global_1km/mod14a2

MODIS Vegetation Continuous Fields

MODIS Vegetation Continuous Fields (VCF) product is a sub-pixel-level description of surface vegetation cover as proportions of: tree cover, non-tree cover, and bare.

- level-3 data
- gridded 250 m
- yearly
- uses a semi-automated process to generate regression trees with machine learning software
- uses surface reflectance and surface temperature

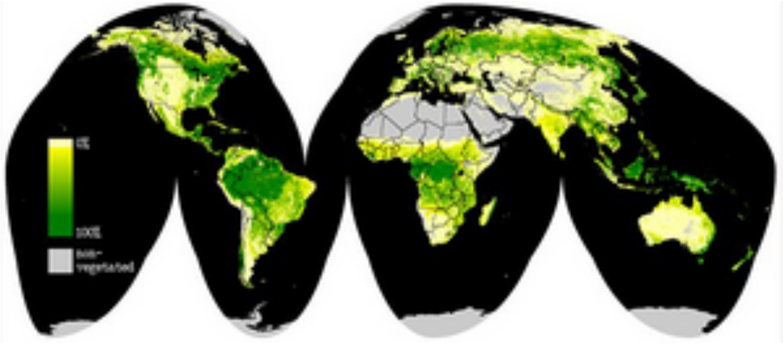

Global Vegetation Continuous Fields percent tree cover for 2001. Darker greens indicate denser tree cover, pale colors indicate light tree cover, and gray indicates completely bare.

https://lpdaac.usgs.gov/products/modis_products_table/vegetation_continuous_fields/yearly_l3_global_500m/mod44b

MODIS Leaf Area Index and *f*PAR

The MODIS leaf area index (LAI) and fraction of absorbed photosynthetically active radiation (*f*PAR) provides LAI, the number of equivalent layers of leaves relative to a unit of ground area, and *f*PAR, the photosynthetically active radiation absorbed by a canopy

- level-4 data
- gridded 1000 m
- 8-day
- uses MODIS surface reflectance data and land cover inputs
- Uses canopy reflectance model inversion with vegetation indices as a backup

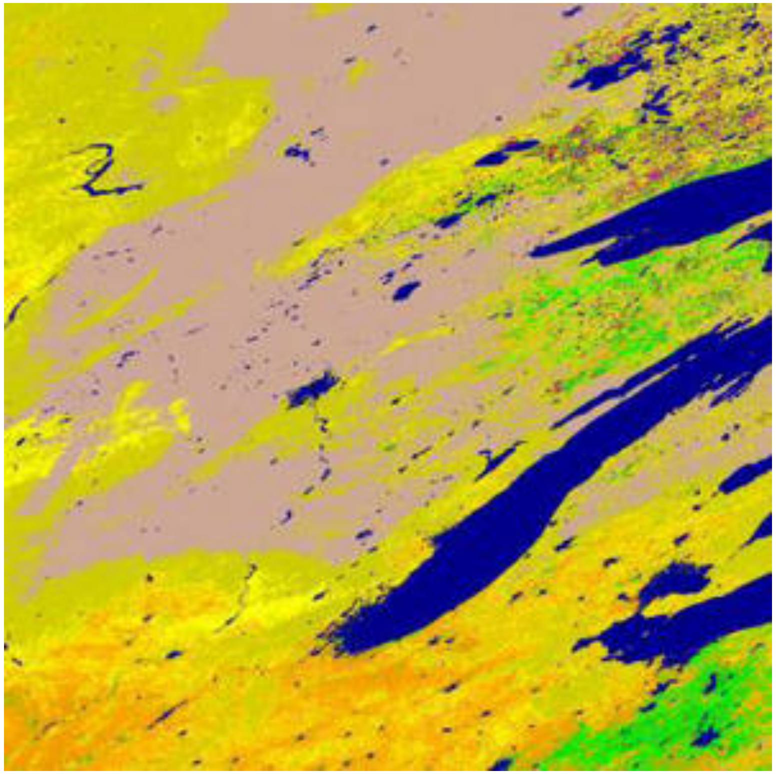

This image is pseudo-colored to display the Fraction of Photosynthetically Active Radiation (FPAR) calculated over north-central U.S., from the Great Lakes westward across the Northern Great Plains. These data collected between March 6 13, 2007 indicate more vegetation growing furthest to the East, as expected during this time of the year.

https://lpdaac.usgs.gov/products/modis_products_table/leaf_area_index_fraction_of_photosynthetically_active_radiation/8_day_l4_global_1km/mod15a2

MODIS Gross Primary Productivity and Net Primary Productivity

The MODIS Gross Primary Productivity (GPP) product uses a radiation-use efficiency model. Net Primary Productivity (NPP) is the rate plants in an ecosystem produce net useful chemical energy. NPP is equal to the difference between the rate plants in an ecosystem produce useful chemical energy (or GPP), and the rate they expend energy for respiration.

- level-4 data
- gridded 1000 m
- 8-day GPP, annual NPP
- Uses MODIS fPAR, MODIS land cover, and meterological data inputs
- Uses ecosystem process model

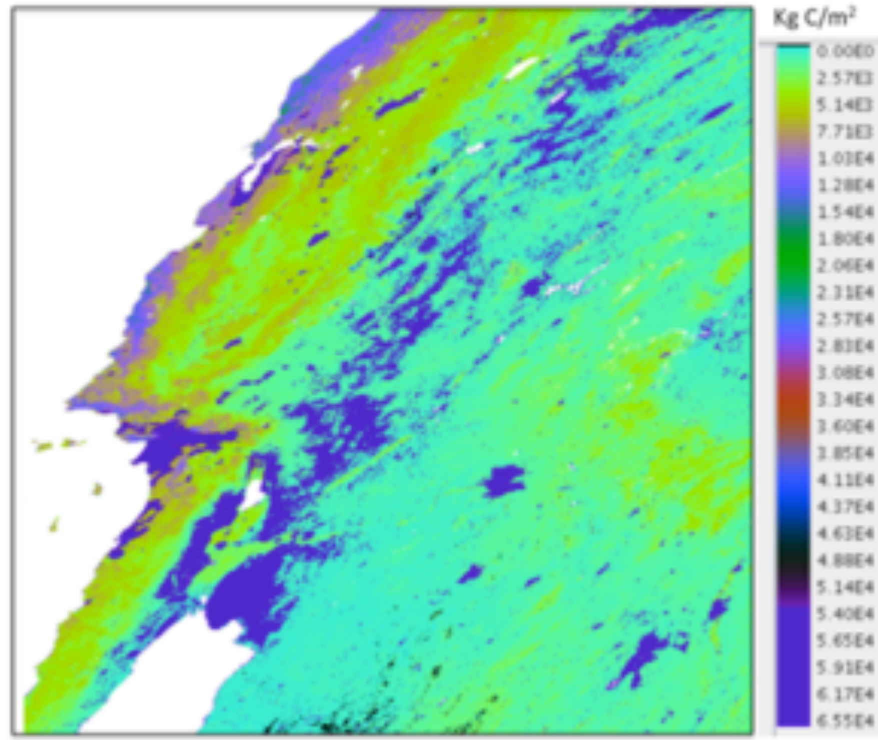

This image depicts the 2010 Terra MODIS 1-km annual Net Primary Productivity (in Kg C/m2) over the H08/V05 tile that covers much of the western/southwestern US.

https://lpdaac.usgs.gov/products/modis_products_table/gross_primary_productivity/8_day_l4_global_1km/mod17a2

ASTER Surface Emissivity

The ASTER Surface Emissivity is generated using the five thermal infrared (TIR) bands (acquired either during the day or night time). The Temperature/Emissivity Separation (TES) algorithm derives both E (emissivity) and T (surface temperature) taking into account the land-leaving radiance and down-welling irradiance vectors for each pixel

- 90 m resolution
- 5 thermal IR bands
- uses ASTER Level-2 Surface Radiance (TIR)
- Emissivity is estimated using the Normalized Emissivity Method (NEM),
- On-demand product

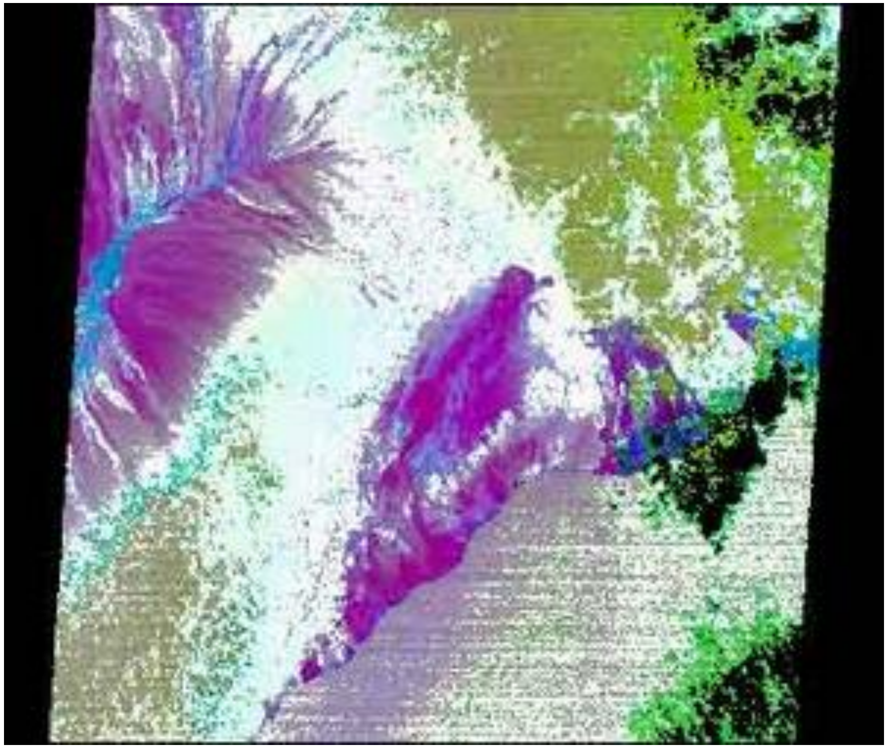

Sample ASTER surface emissivity scene.

https://lpdaac.usgs.gov/products/aster_products_table/on_demand/surface_emissivity/v1/ast_05

ASTER Digital Elevation Model

ASTER stereo pairs from nadir and backward views are used to produce single-scene (60x60 km) digital elevation models (DEM) having vertical (RMSE) accuracies between 10- and 25-m. Data from multiple scenes are grouped to make global DEM. Global data partitioning into 1° x 1° tiles.

- 30 m resolution
- automated stereo-correlation method
- cloud masked

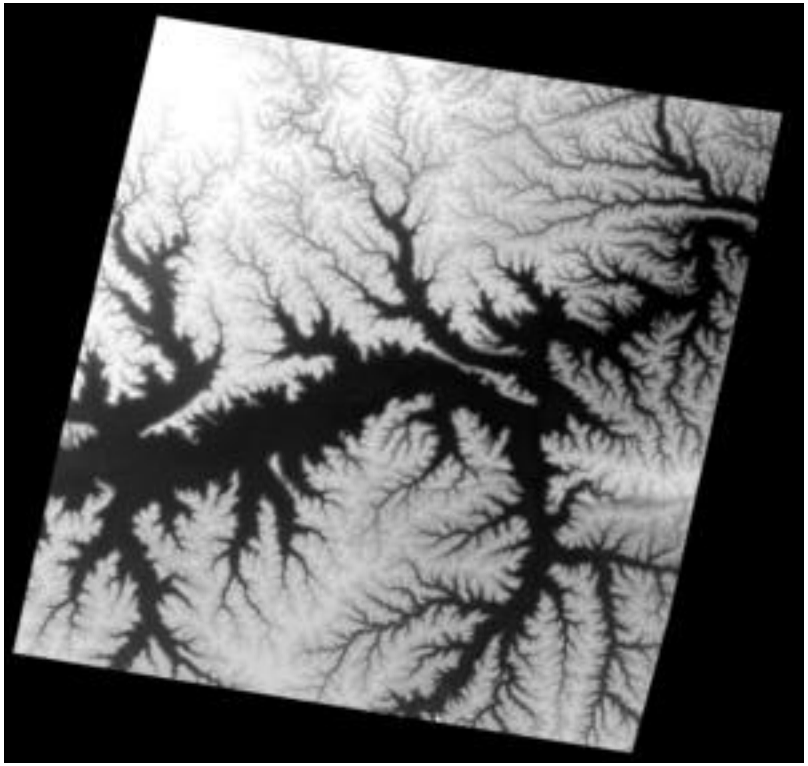

Sample ASTER DEM scene.

https://lpdaac.usgs.gov/content/view/full/11033

Landsat Ecosystem Disturbance Adaptive Processing System

The LEDAPS project processes Landsat data to surface reflectance and uses change-detection techniques to map disturbance, regrowth, and permanent forest conversion across the continent.

- –Scene based
- –Starts with global calibrated TOA reflectance from Global Land Survey dataset
  - Orthorectified, low cloud cover, during leaf-on conditions
- – Processed to surface reflectance using MODIS algorithm
  - Also does cloud and cloud shadow masking
- –Disturbance Index calculated from Kauth-Thomas tassled-cap transform
- –Uses land cover map to identify forest pixels

Landsat-5 image of Eastern Virginia, showing "patchwork" of land-cover types

http://ledaps.nascom.nasa.gov/overview/overview.html

Web Enabled Landsat Data (WELD) Products

WELD creates reflectance composites of TOA reflectance. Brightness temperature are resampled to 30 m.

- Uses NDVI compositing and cloud and cloud shadow masking
- Annual, seasonal (3-month), monthly, weekly
- 30 m pixels
- Broken into 5000x5000 tiles

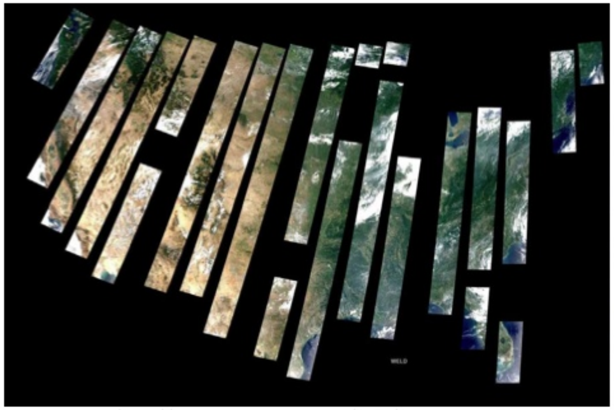

Figure 4 Example weekly WELD CONUS composite (July 15 - 21, 2008)

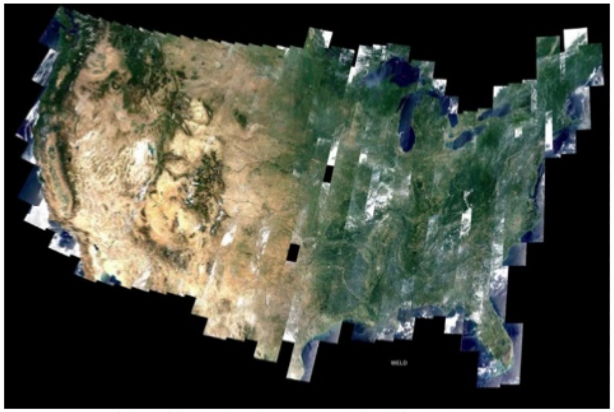

Figure 5 Example monthly WELD CONUS composite (July 2008)

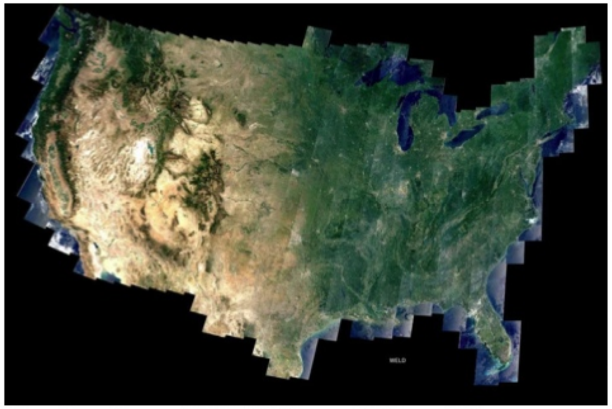

Figure 6 Example seasonal WELD CONUS composite (Summer 2008)

http://globalmonitoring.sdstate.edu/projects/weld/

Prototype USGS Essential Climate Variables from Landsat

- Based on MODIS product concepts
- WELD/LEDAPS Surface Reflectance
- Land Surface Temperature
- Land Cover
  - Uses surface reflectance
  - for end-users and for modeling/algorithm stratification
  - Global land cover – annual continuous fields and 5-year thematic classifications
- LAI / fPAR
  - Uses surface reflectance and land cover
  - Based on Landsat scenes
    - Must consider phenology when using composites
- On demand processing?

Conclusions

There are a number of issues for HyspIRI products

- Data products are connected
  - Multiple levels of processing
  - Data from lower levels are inputs to higher level products
- Swath or Scene vs. Gridded Data
  - How to scale to climate grids?
  - What approach best suits applications?
- Temporal compositing approaches
  - Frequent views vs. data quality
- How to merge VSWIR and Thermal Data?

Conclusions

- Data products may be produced using a number of different approaches
  - Simple calculations (e.g. vegetation indices)
  - Empirical relationships (e.g. regression trees)
  - Models and model inversions
- Data archive vs. on-demand processing?

MODIS	Surface Reflectance	8-day surface reflectance for land bands	500 m
MODIS	Snow Cover/Sea Ice	daily/8-day/monthly Normalized Difference Snow Index	500 m
		Sea ice from NDSI	1km/4km
MODIS	Land Surface Temperature (LST) and Emissivity	Daytime and nighttime LST/emissivity	1km/6km
MODIS	Landcover	Landcover type	500 m
		Landcover dynamics	1 km
		Onset_Greenness_Increase	
		Onset_Greenness_Maximum	
		Onset_Greenness_Decrease	
		Onset_Greenness_Minimum	
		NBAR_EVI_Onset_Greenness_Min	
		NBAR_EVI_Onset_Greenness_Max	
		NBAR_EVI_Area	
MODIS	Vegetation Indices	16 day NDVI, EVI	250 m/500 m
MODIS	Thermal Anomalies/Fire	Daily/8-day fire products	1 km
		fire occurrence (day/night)	
		fire location	
		fire radiative power	
MODIS	LAI/fPAR	8 day LAI/fPAR	1 km
MODIS	Gross Primary Production	8 day GPP	1 km
		annual NPP	
		8-day ET (prototype)	
MODIS	BRDF/Albedo	16 day Albedo	500 m/1 km
		BRDF adjusted reflectance	
		Albedo model parameters	
MODIS	Vegetation Continuous Fields	Tree Cover	500 m
MODIS	Burned Area	Burn date/burned area	500 m

Landsat	Orthorectified at-sensor radiance		30 m
Landsat	TOA reflectance		30 m
Landsat	Surface reflectance		30 m
Landsat	Surface temperature		60 m
Landsat	global land cover		30 m
Landsat	LAI/fPAR		30 m
Landsat	MRLC National Land Cover Dataset	roughly every 5 years	30 m
Landsat	Landfire US forest disturbance		30 m
Landsat	MTBS burn severity history for the US		30 m
Landsat	USDA National Cropland Data Layer (crop type for the US)		30 m
Landsat	NGA/MDA-Federal "cultural (ie. urban)" growth monitoring		30 m

Anticipated New HyspIRI Products
Examples for Ecological Applications

Petya Campbell, UMBC

2012 HyspIRI Products Symposium

New & Improved Ecosystem Products

1) Ecosystem nutrients and chemistry (nitrogen, water‡, etc.)

2) Biodiversity (improved species‡ and functional-type†)

3) Ecosystem health (physiological condition)
   - *Canopy structure (improved LAI, fraction of green biomass‡)*
   - *Canopy pigments (e.g. chlorophyll‡, carotenoids†, anthocyanins†)*
   - *Canopy water‡*
   - *Lignin & cellulose‡, crop residue cover**
   - *Nitrogen‡*
   - *General stress†*

4) Temperature and emissivity estimates by vegetation components (species, functional groups, vegetation health class)

5) Relationships and feedbacks between canopy composition/function and canopy temperatures; predictive relationships between **VSWIR** and **TIR** indicators

----

**application ready*　　*‡advanced*　　*†researched*

Spectroscopic Measurements are Required for Global Ecosystem Assessments

Multi-Spectral Measurements

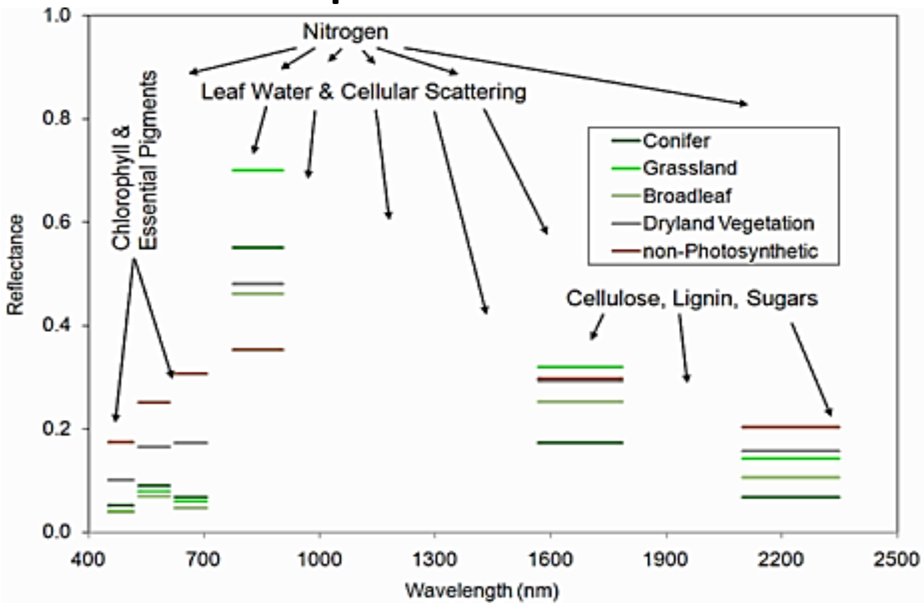

Multi-spectral imaging is insufficient to derive the required terrestrial surface compositional parameters accurately.

Spectroscopic Measurement

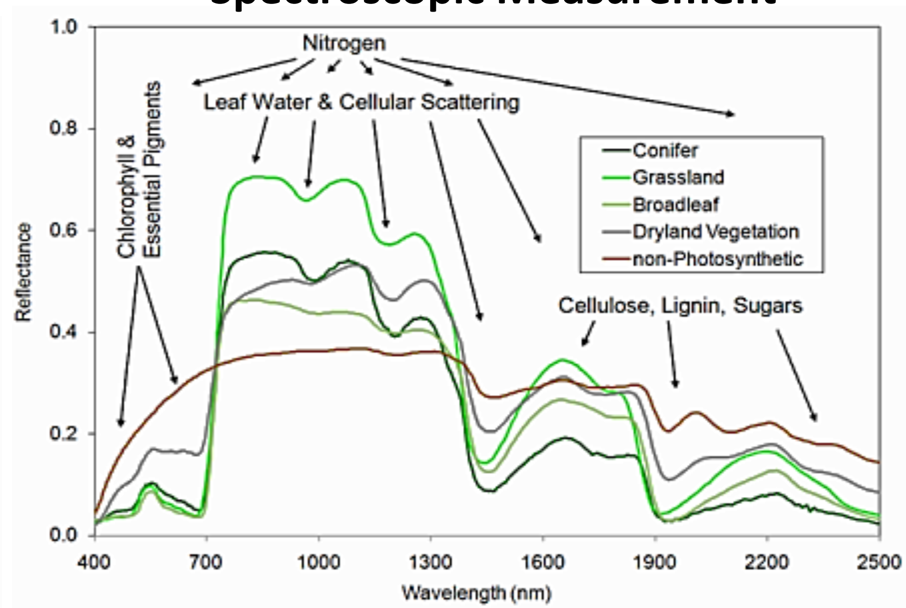

Full range imaging spectroscopy is required to measure composition, chemistry, health and change of ecosystems.

- *Plant species and functional types have biochemical and biophysical properties that are expressed as **reflectance, absorption and scattering features** spanning the spectral region from 380 to 2500 nm.*
- *Individual bands do not capture the **diversity of biochemical and biophysical signatures** of plant functional types, species or physiological condition.*
- *Changes in the chemical and physical configuration of ecosystems are expressed as **changes in the contiguous spectral signatures** related to plant functional types, physiological condition, vegetation health, and species distribution.*

Green et al.

Spectral Time Series - *Phenology of Summer Wheat*

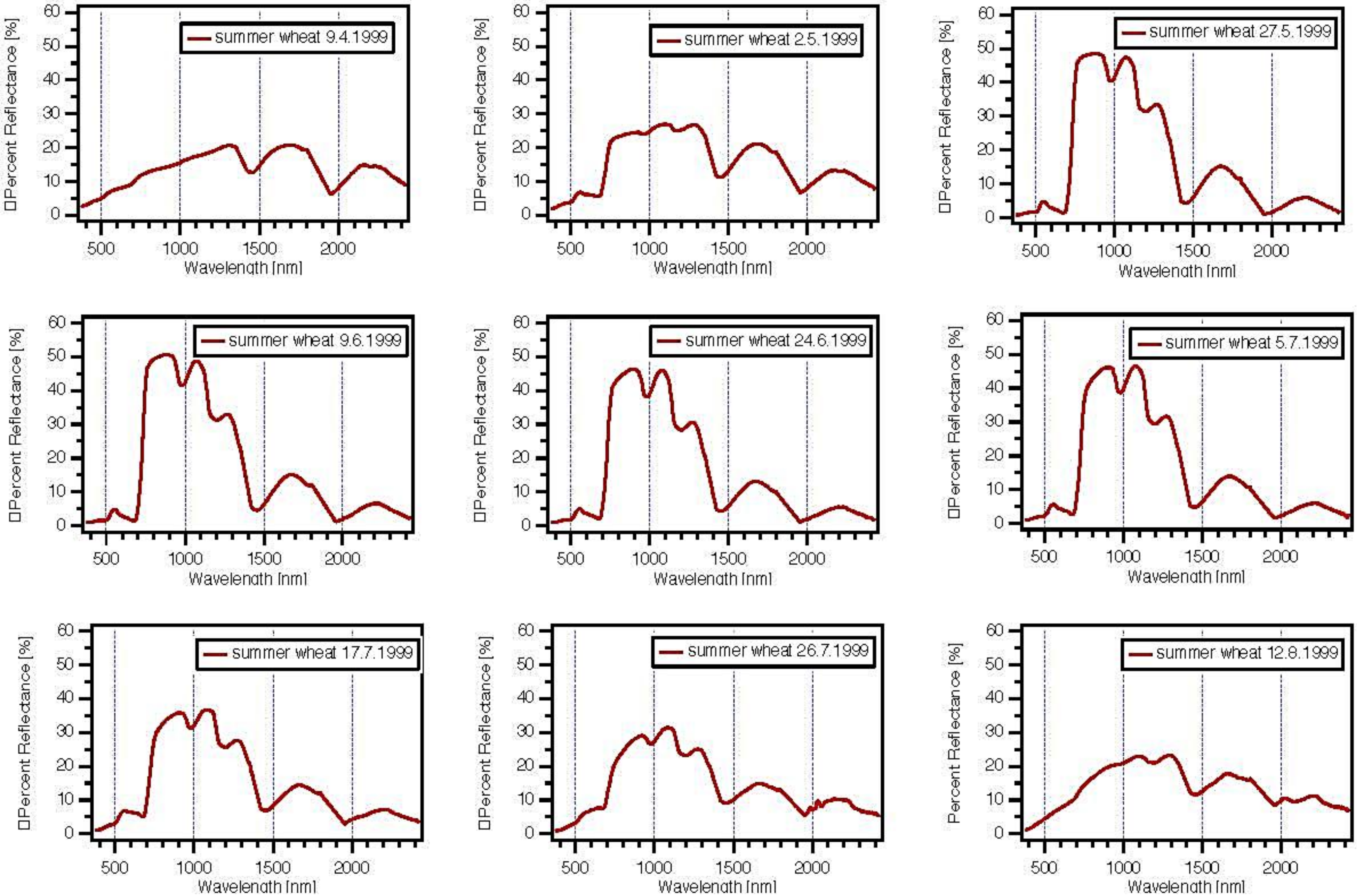

Kneubuhler , 2002

Methods For Hyperspectral Analysis

	Acronyms	VSWIR Methods	Objective / Use	Required
1	ACORN	Atmospheric CORrection Now	radiometric calibration and atmospheric correction	Spectral Hypercubes
2	FLAASH	Fast Line-of-sight Atmospheric Analysis of Spectral Hypercubes	radiometric calibration and atmospheric correction	Spectral Hypercubes
3	SS&R	Spectral sensitivity & relationship to *in situ* measurements	knowledge of important spectral information	contiguous spectra
4	CR &FD	Continuum Removal & Feature Depth	analysis on specific absorption features	contiguous spectra
5	SI, P-VI	Physiological Vegetation Indexes (P-VI)	reduce the number of bands but retain the most important spectral information	Spectral Hypercubes, SS&R
6	MNF	Minimum noise fraction (two-stage PCA)	reduce wavelength specific noise and dimensionality of data	Spectral Hypercubes
7	SAM	Spectral Angle Mapper of spectral cubes	comparing spectra of image pixels to the spectra of reference endmembers	Spectral Hypercubes
8	SMA, SUM, MESMA	Spectral Mixture Analysis and Unmixing Methods	derive apparent fractional abundance of specific endmember in a pixel	a priori known endmembers (b-1)
9	MF	Matched Filters	maximizes target-to-background contrast	Spectral Hypercubes, known signatures to match
10	MTMF	Mixture Tuned Matched Filtering	combines the strength of MF with physical constraints imposed by mixing theory	Knowledge of the target species endmembers
11	MLc of MNF	Maximum Likelihood classification of MNF transformed images	species identification	MNF
12	MLc of P-VI	MLc of P_VI Images	identification of physiological state	Physiological Vegetation Index Images

Continuum Removal & Feature Depth Analysis

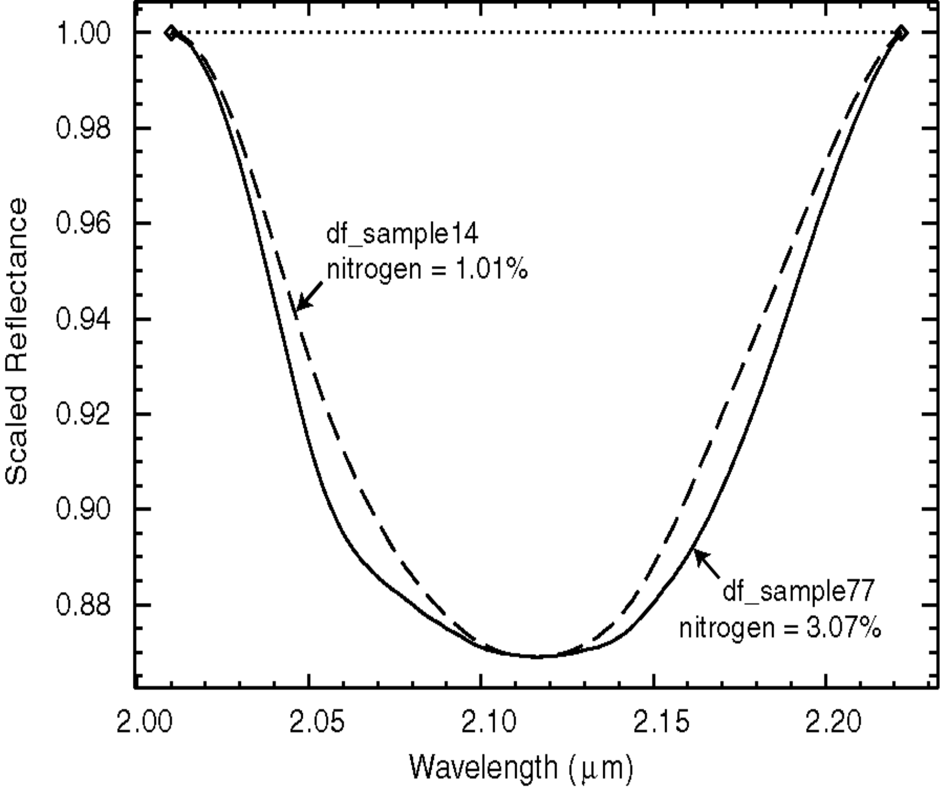

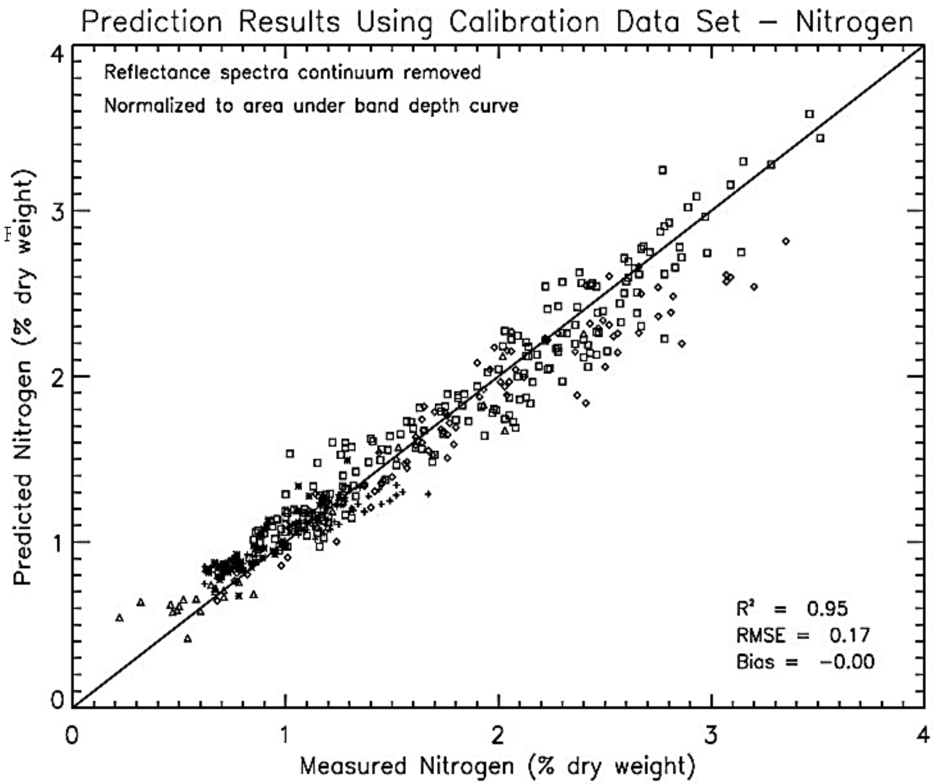

- *N determination*

Kokaly, REMOTE SENS. ENVIRON. 75:153–161 (2001)

Cover Fractions in Transition from Live/Green to Dry/Dead

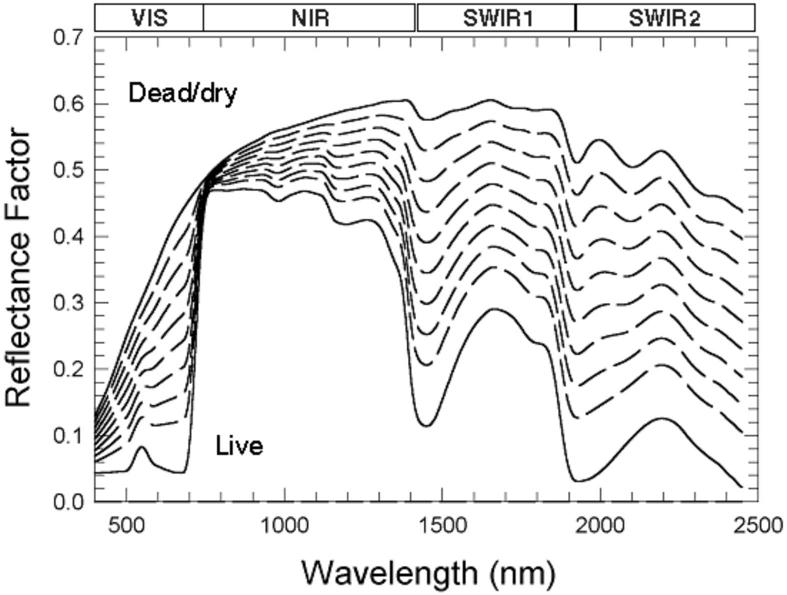

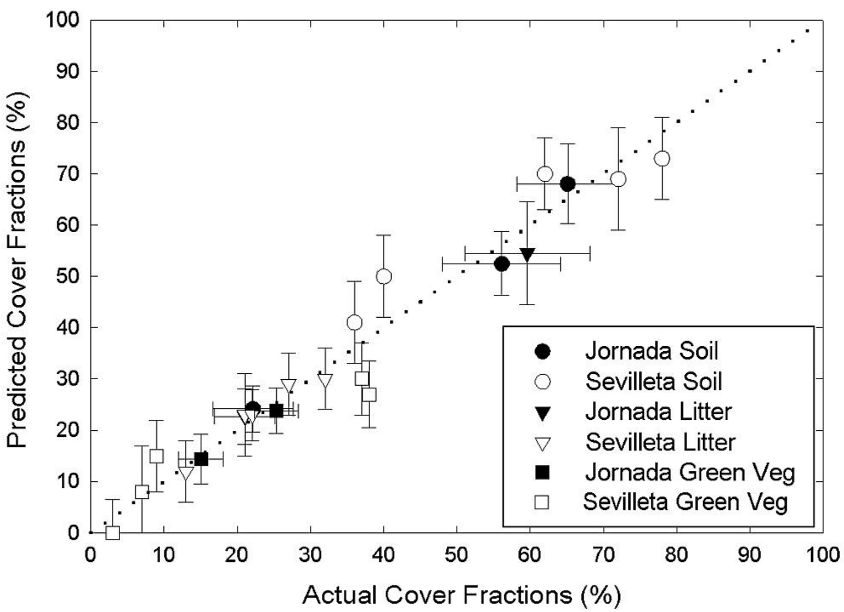

Sevilleta LTER Site, N.M.

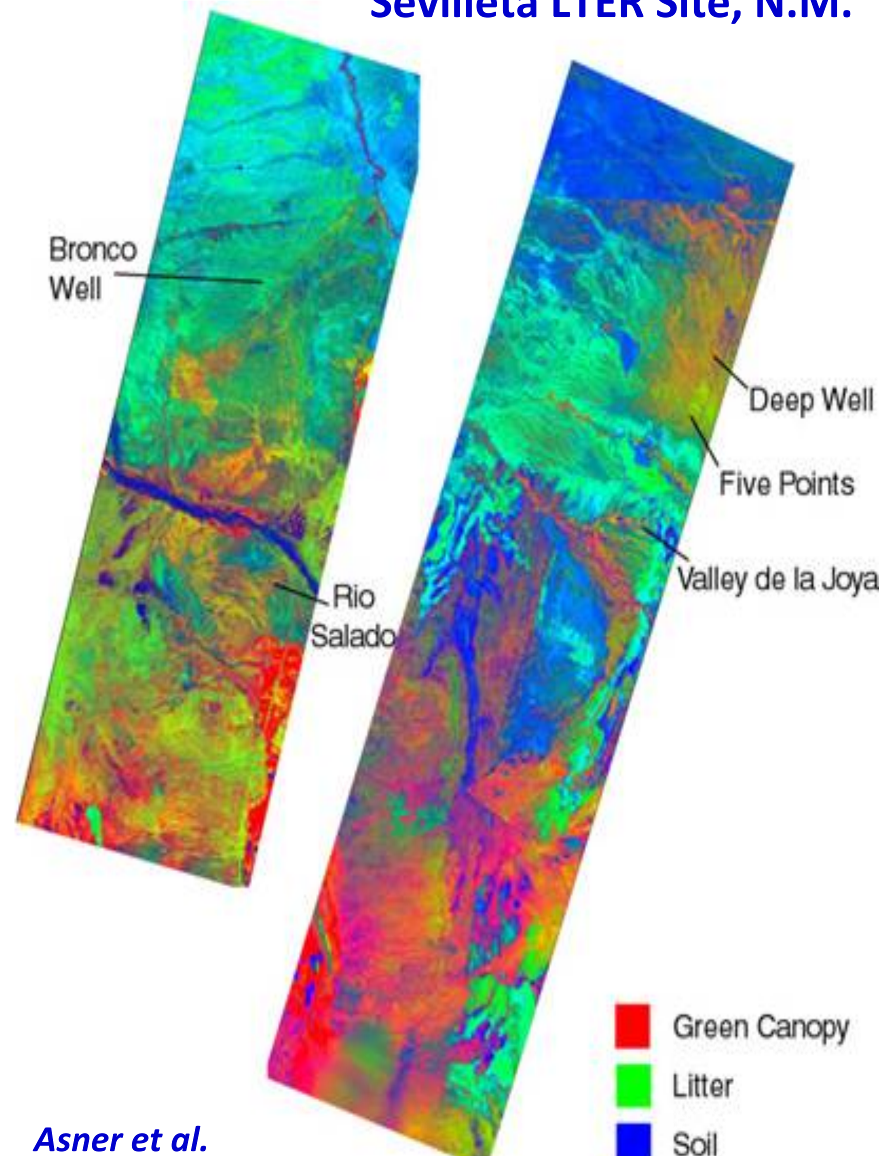

Asner et al.

Reflectance and Derivative Analysis

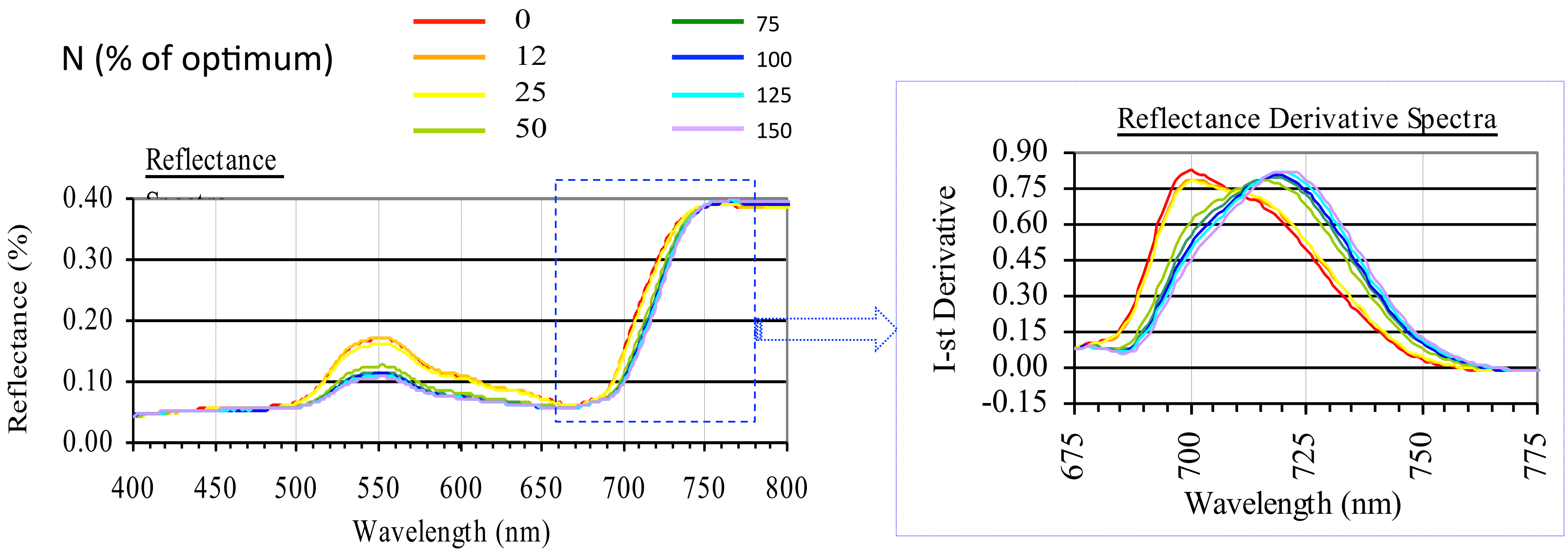

Vegetation Indices of function, structure and foliar chemistry

- **REIP** = wavelength (in nanometers) of the maximum slope **Dmax** of the reflectance spectrum at wavelengths between 690 and 740 nm; $D = (R_n - R_{n-1})/(w_n - w_{n-1})$; in the 690-740nm range
- Chlorophyll (Gitelson) = $(R_{NIR}/ R^{-1}_{720\text{-}730}) - 1$; Function, *PRI = (R531 - R570)/(R531 + R570); NDWI=(Rnir-R1240)/(Rnir+R1240), etc.*
- *TVDI = (Ts – Ts_min)/(a + bNDVI – Ts_min); WSVI=NDVI/Ts, where Ts is the brightness temperature at ~11 µm*

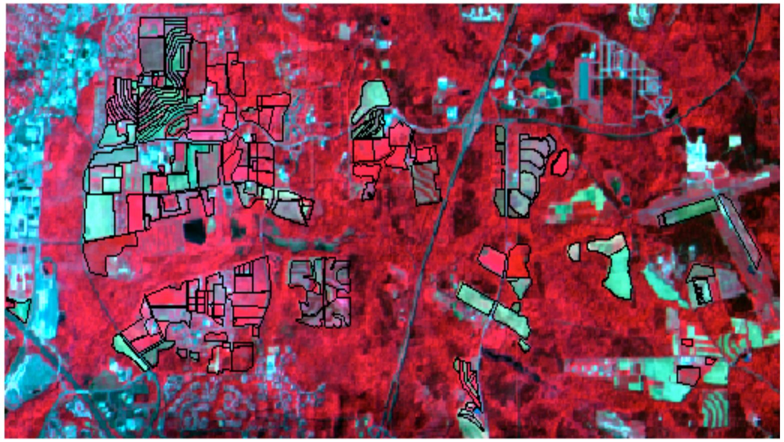

Color Infrared composite AVIRIS image with field boundaries.
549 nm -- blue
646 nm – green
827 nm – red

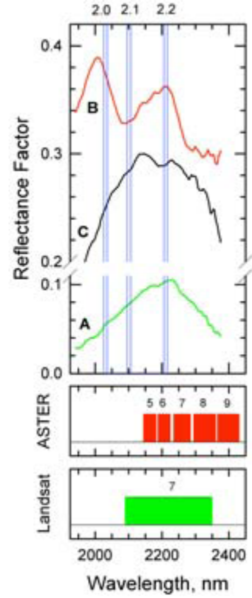

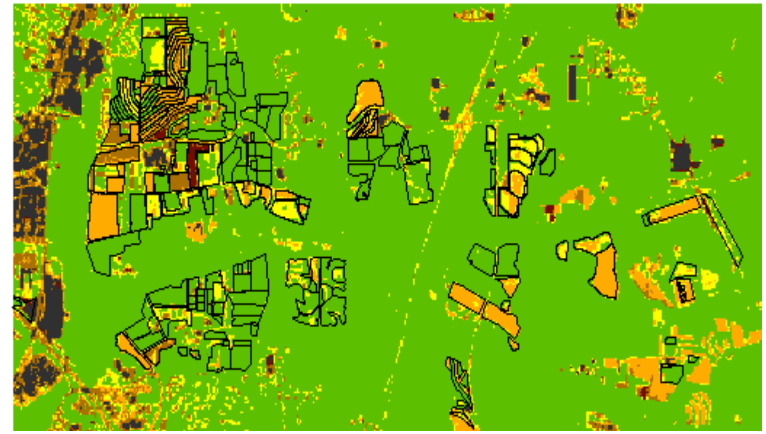

Tillage intensity classification using CAI and NDVI (overall classification accuracy = 92%).

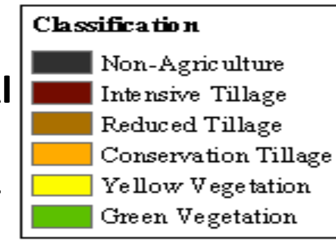

$$CAI = 0.5(R_{2000} + R_{2200}) - R_{2100}$$

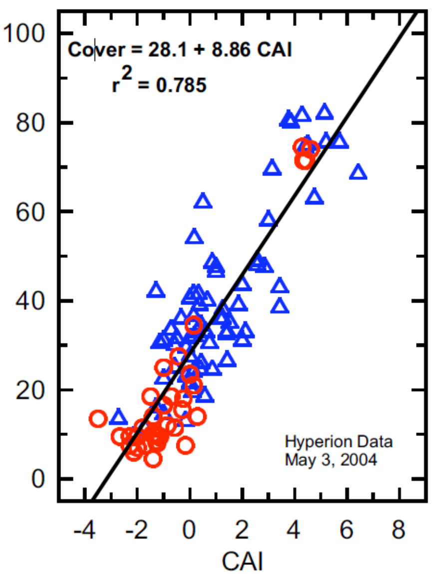

Crop Residue Cover vs. CAI for Hyperion Image Iowa – May 3, 2004

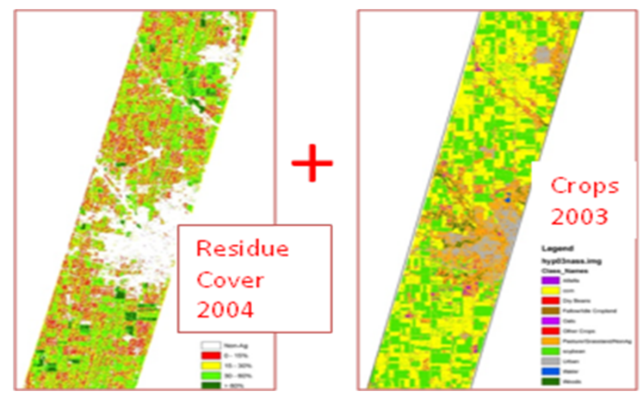

For dry and moist conditions CAI is adequate for assessing crop residue cover.

(Daughtry et al. 2001, 2006 and 2010)

Bio-indicators of Photosynthetic Function

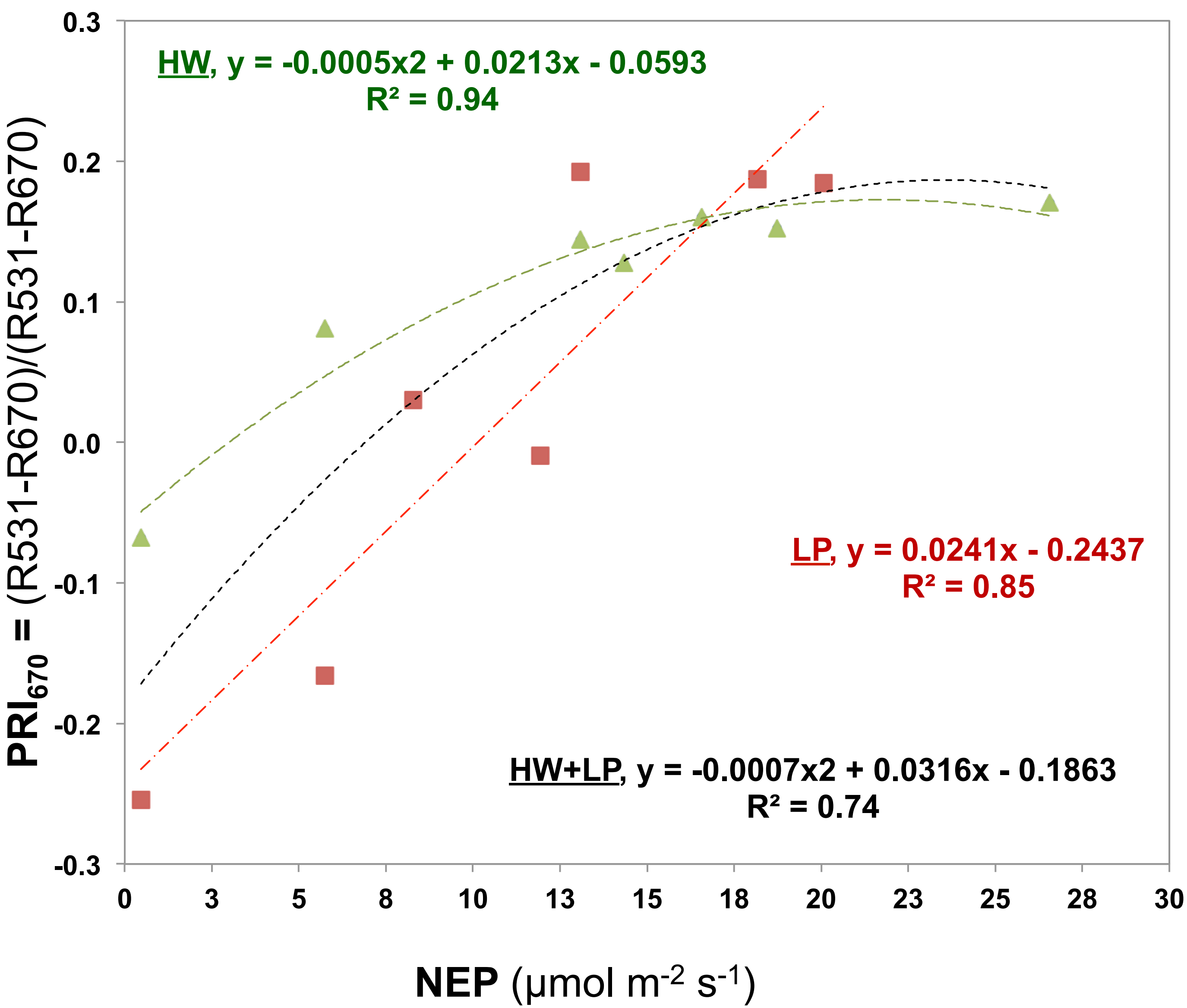

Duke Forest : PRI_{670} & NEP

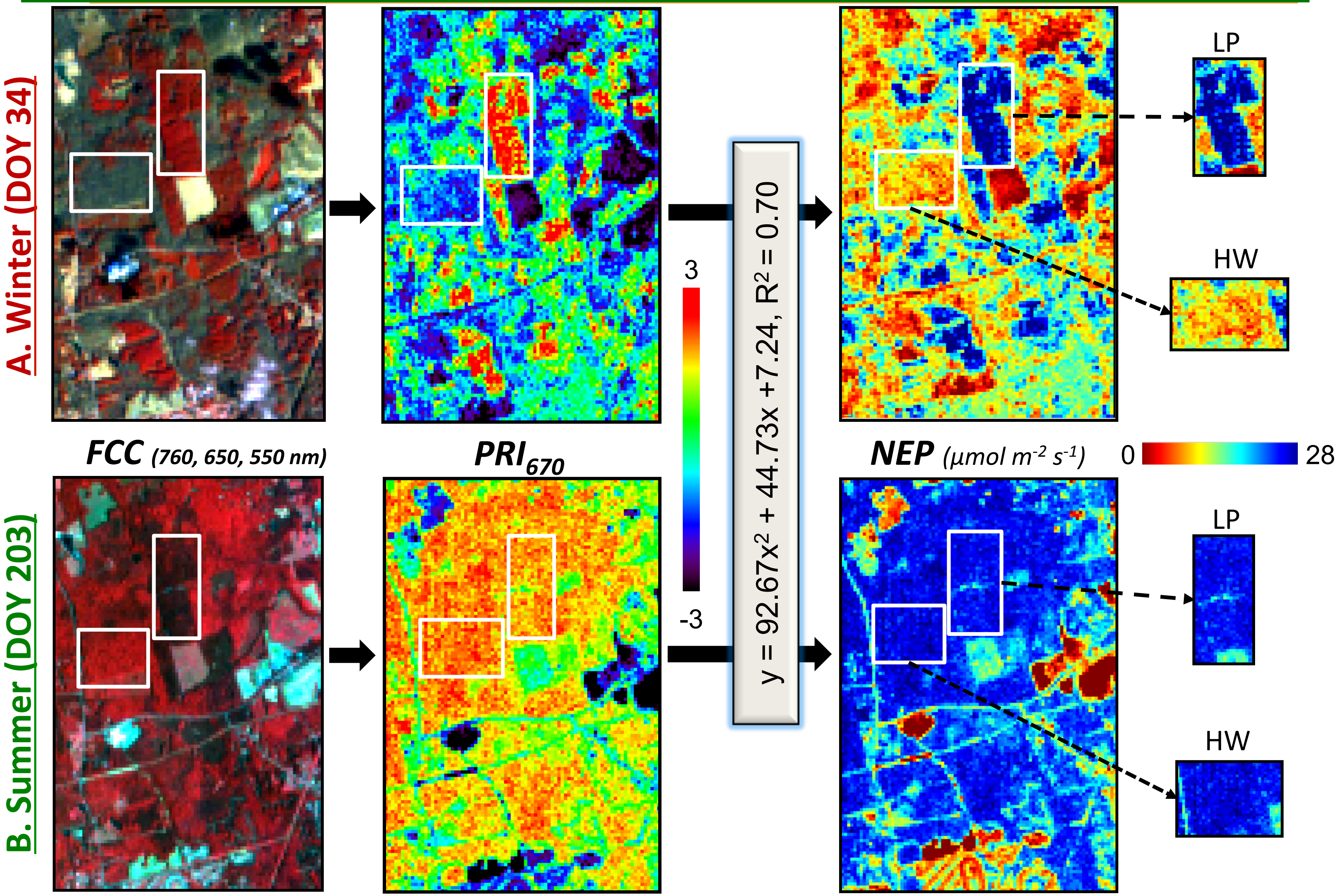

Forage & Fiber Distribution in African Savanna

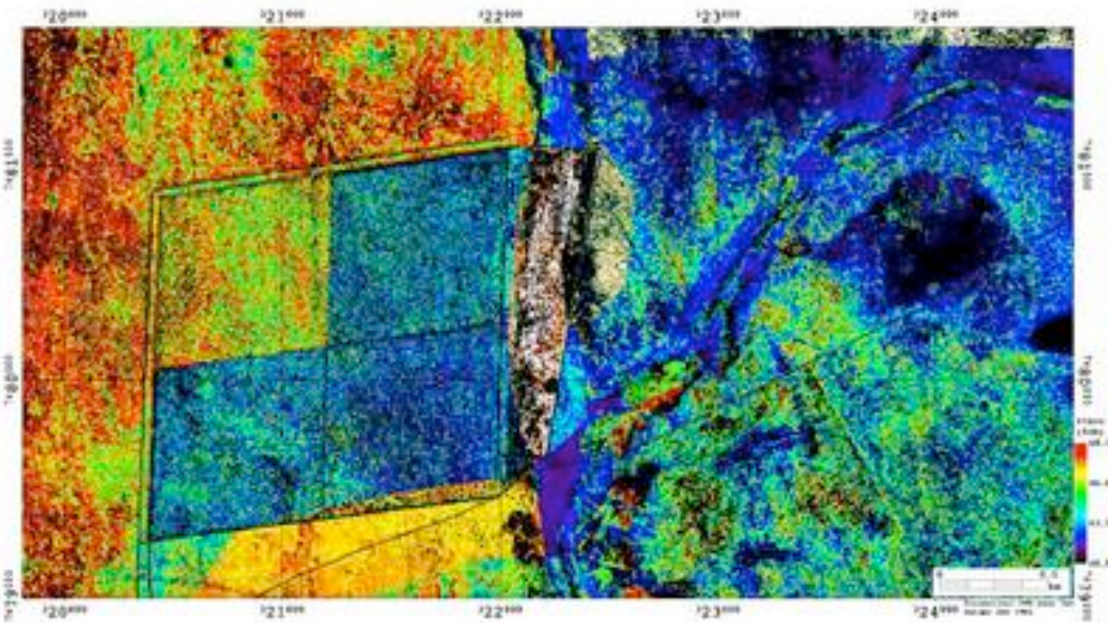

Airborne mapping of dry season forage and fiber distribution across the N'washitsumbe roan enclosure and surrounds on the Northern Plains of the Kruger National Park, South Africa.

Carnegie Airborne Observatory

Forage quality in African savannas can be described in terms of nutrients that are limiting (nitrogen and phosphorus) and constrain the rate at which herbivores take in fiber. These forage quality nutrients are particularly crucial in the African dry season when their concentrations decline.

Using the Carnegie Airborne Observatory (CAO) Alpha sensor, in combination with ancillary data, researchers from ITC-University of Twente and the Carnegie Institution mapped **grass forage nutrients** in the early dry season within an African savanna.

Respectively, 65%, 57% and 41% of the variance in fiber, phosphorus and nitrogen concentrations could be explained.

In addition, for the first time, a landscape map of grassland fiber was created from CAO imagery.

Species Recognition

Landsat 7 | **Hyperion** | **AVIRIS**

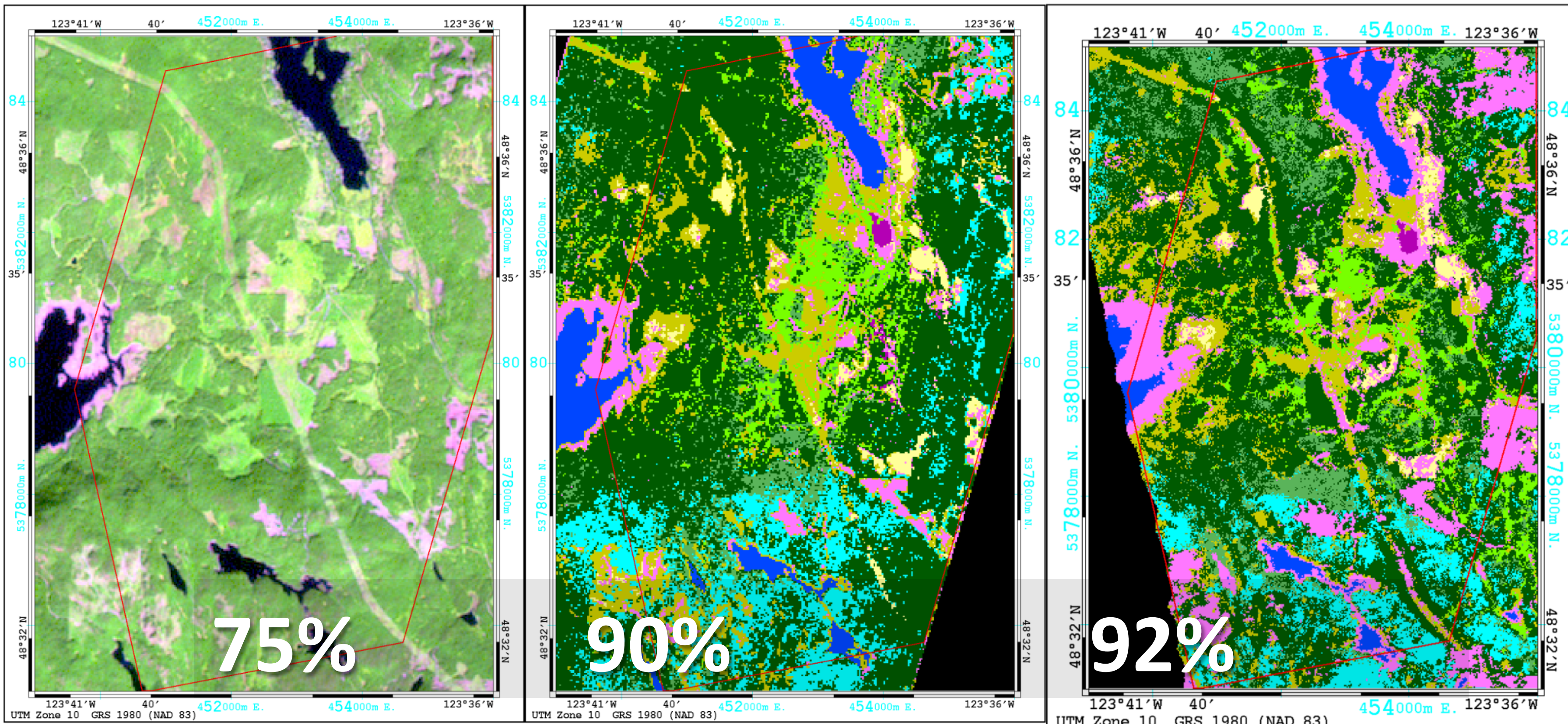

Landsat-7 ETM+ Image
September 10, 2001

Hyperion Classification
September 10, 2001

AVIRIS MNF Classification
August 10, 2001

Kilometres 1 0 1 2 3
Miles 1 0 1 2

- Exposed land
- Water body
- Shrub, low
- Herb graminoids
- Swamp area
- Red alder, dominant
- Hemlock, dominant
- Lodgepole pine dominant
- Western redcedar
- Douglas-fir, dominant
- Unclassified

Pacific Forestry
Natural Resources Canada

Goodenough et al. 2003

Reflectance & Temperature for Common Cover Types

Indicators of plant function (60 m)

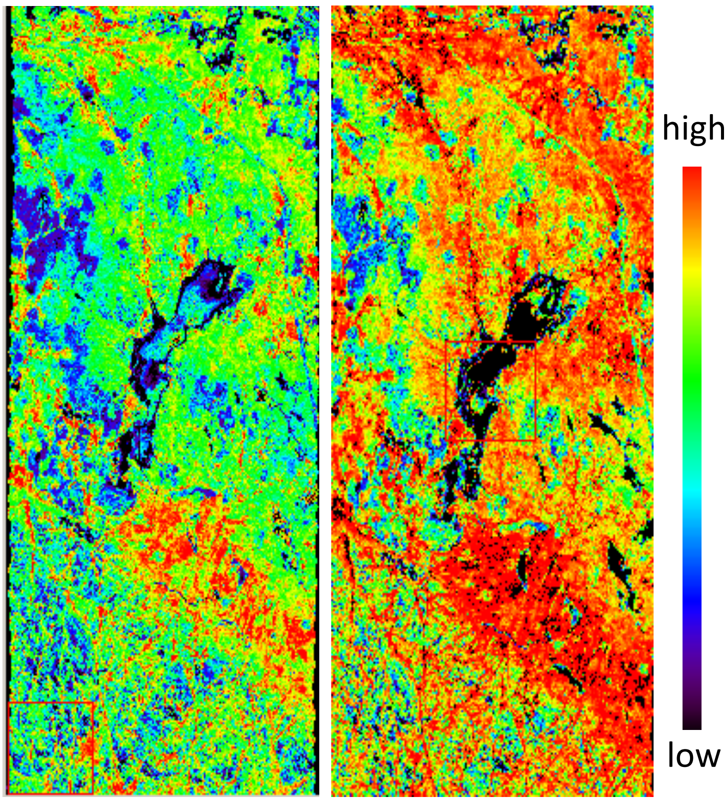

V1 - chlorophyll ***Dmax - stress***

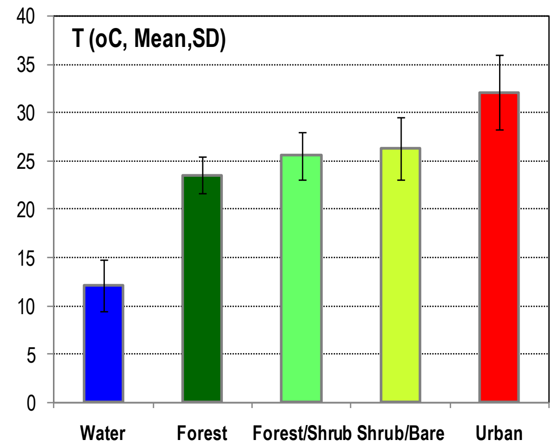

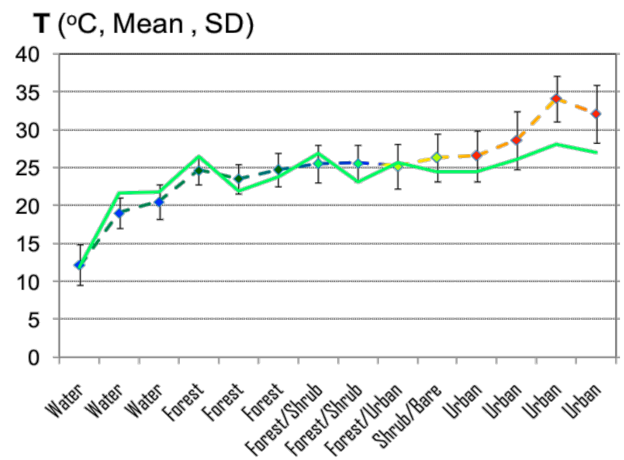

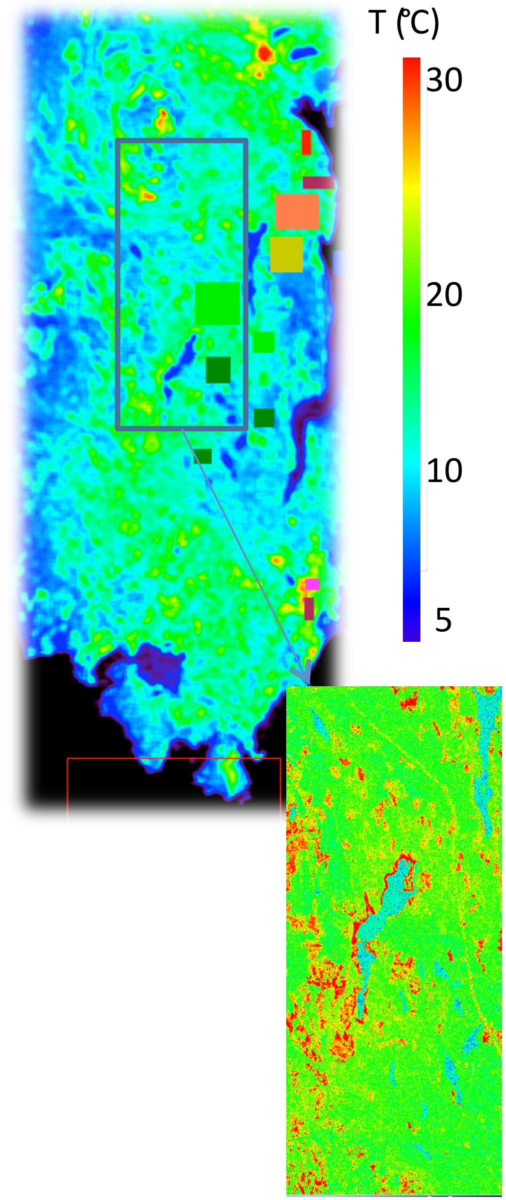

HyspIRI-like data provided range of indicators of plant function and showed temperature gradient of ~ 15° C between rural and urban areas in British Columbia.

Canopy Moisture & Temperature

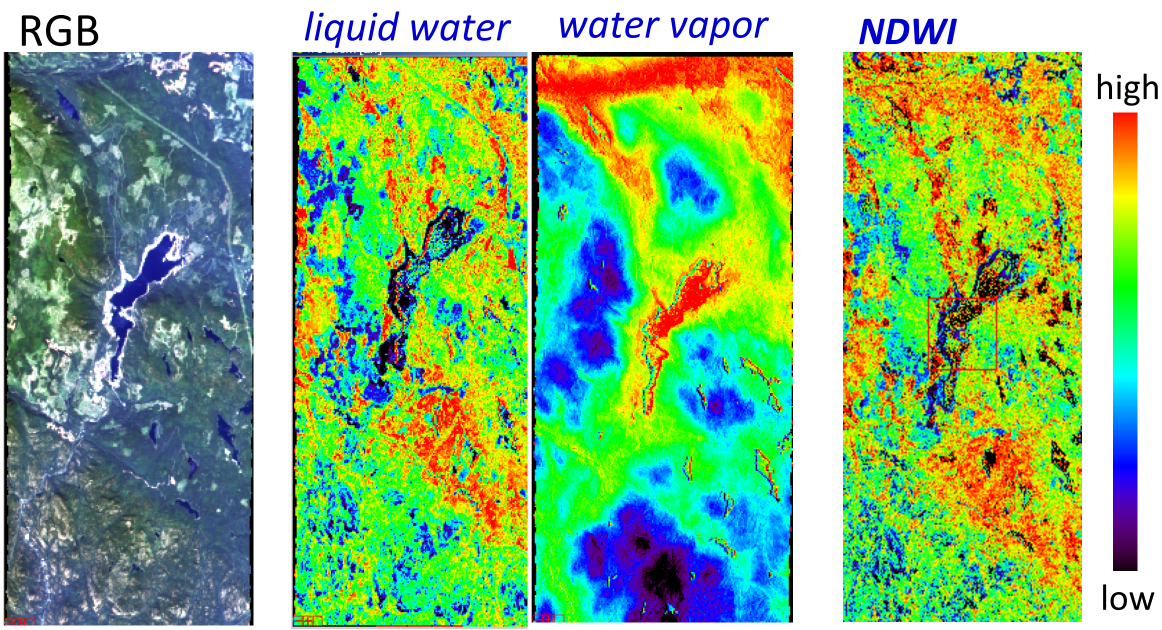

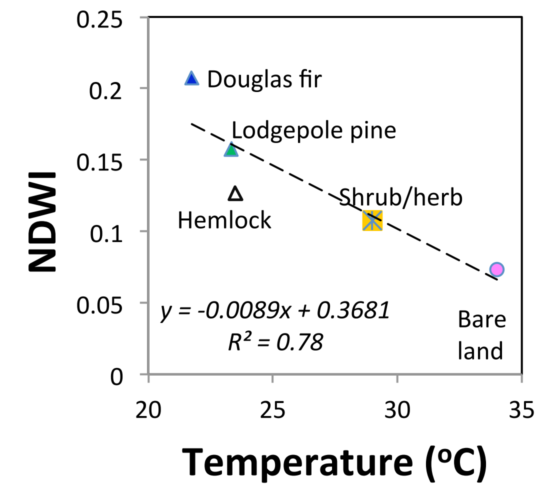

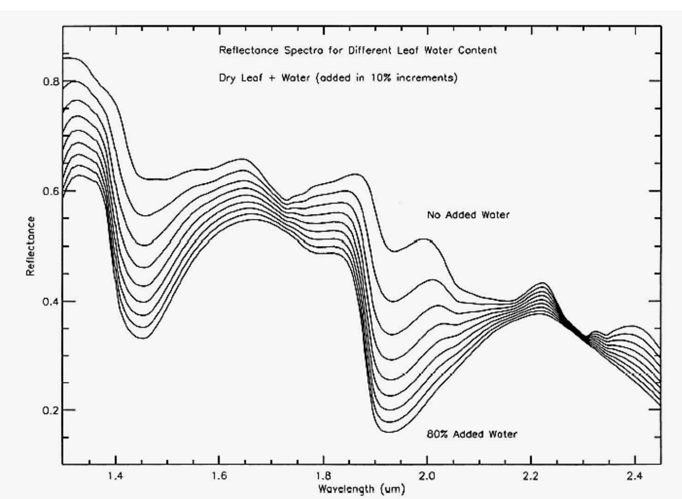

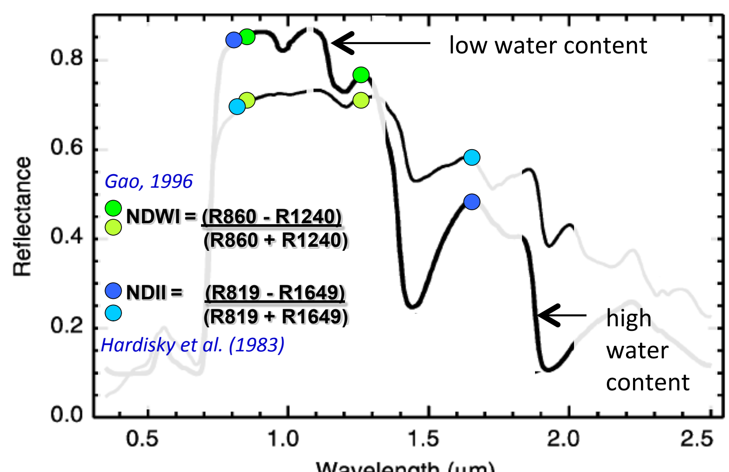

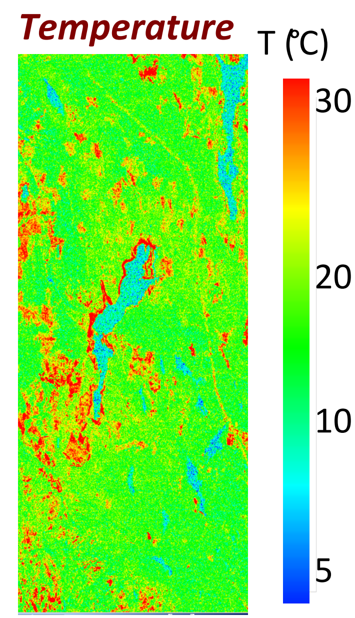

Kokaly and Clark, REMOTE SENS. ENVIRON. 67:267–287 (1999)

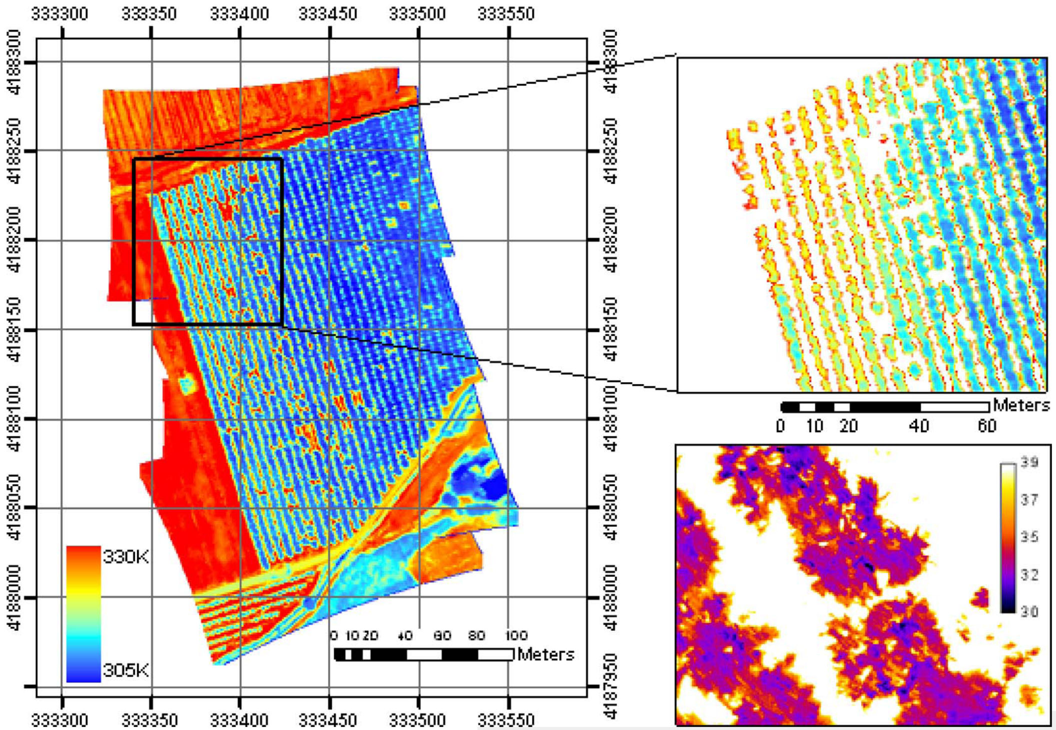

Canopy Structure, Function & Temperature

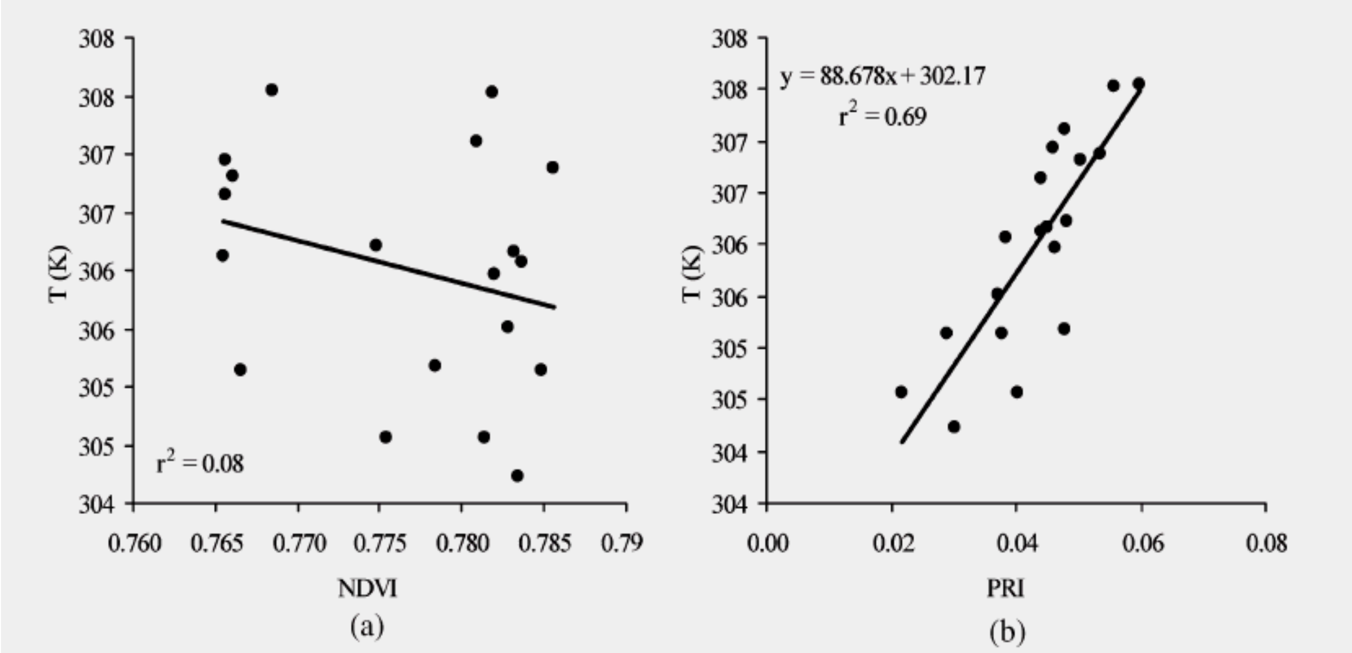

Zarco-Tejada et al. 2012

Surface temperature distribution for Nagoya, Japan on (a) July 10, 2000 1055 JST

Artificial (UHI) increase in sensible heat flux for Nagoya, Japan on July 10, 2000.

Kato et al. 2005

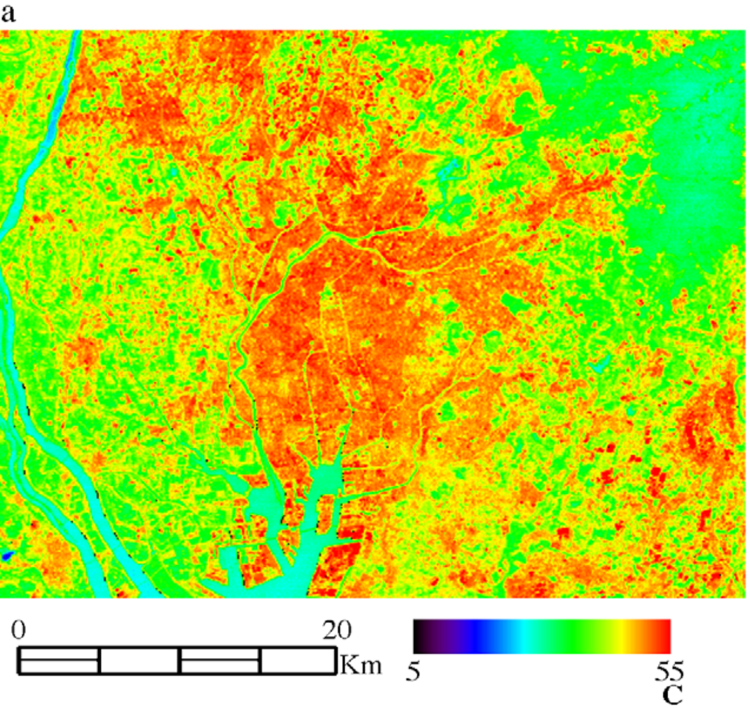

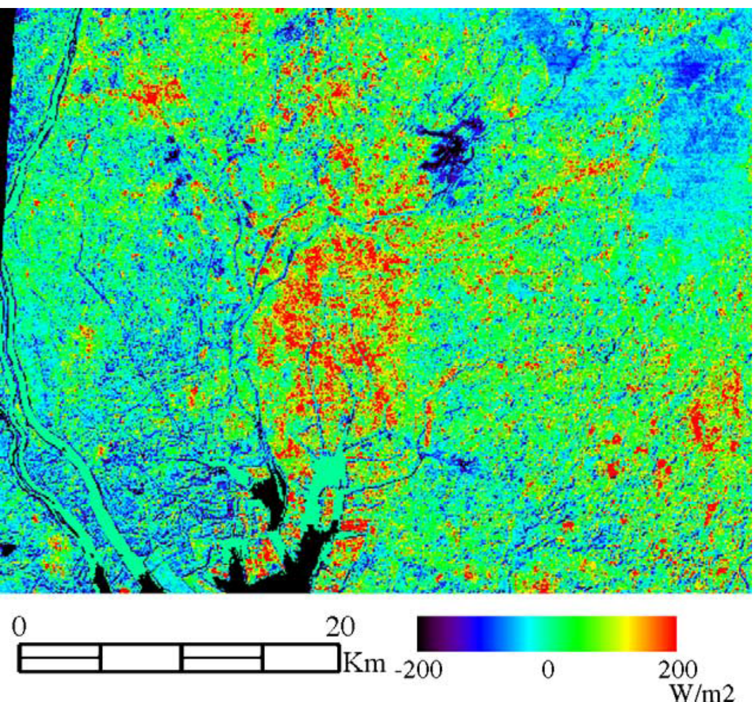

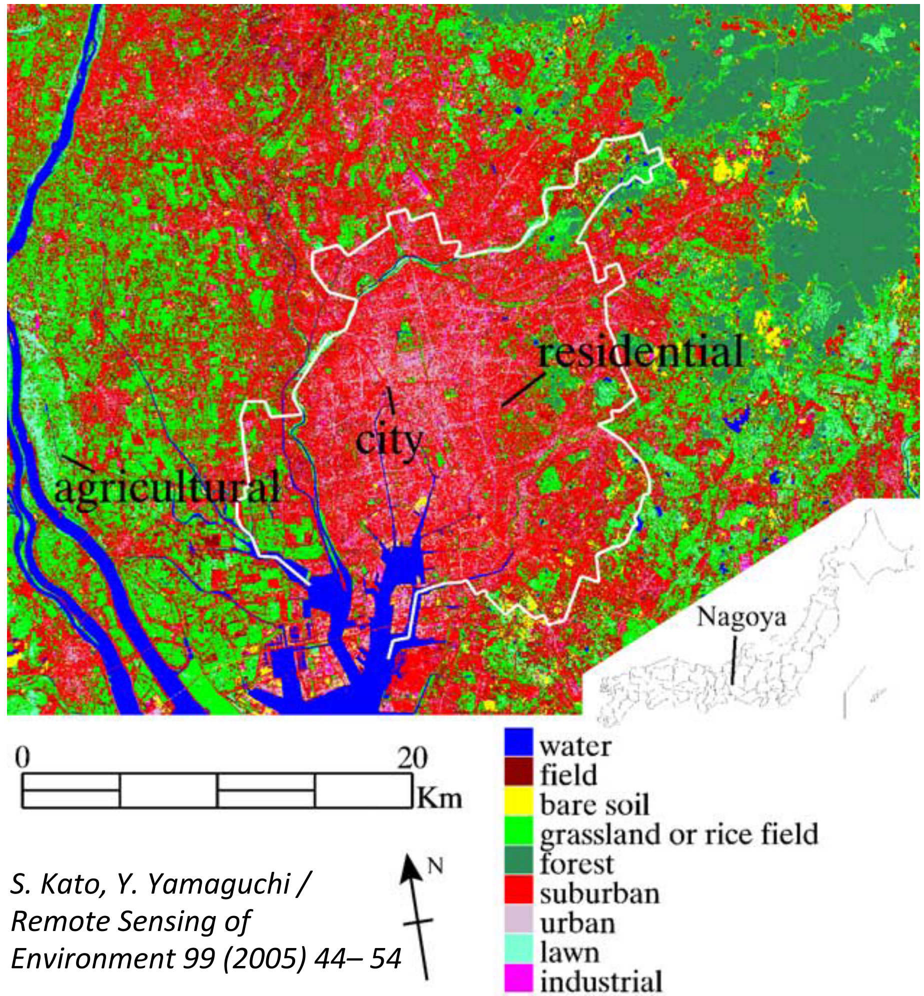

S. Kato, Y. Yamaguchi / Remote Sensing of Environment 99 (2005) 44– 54

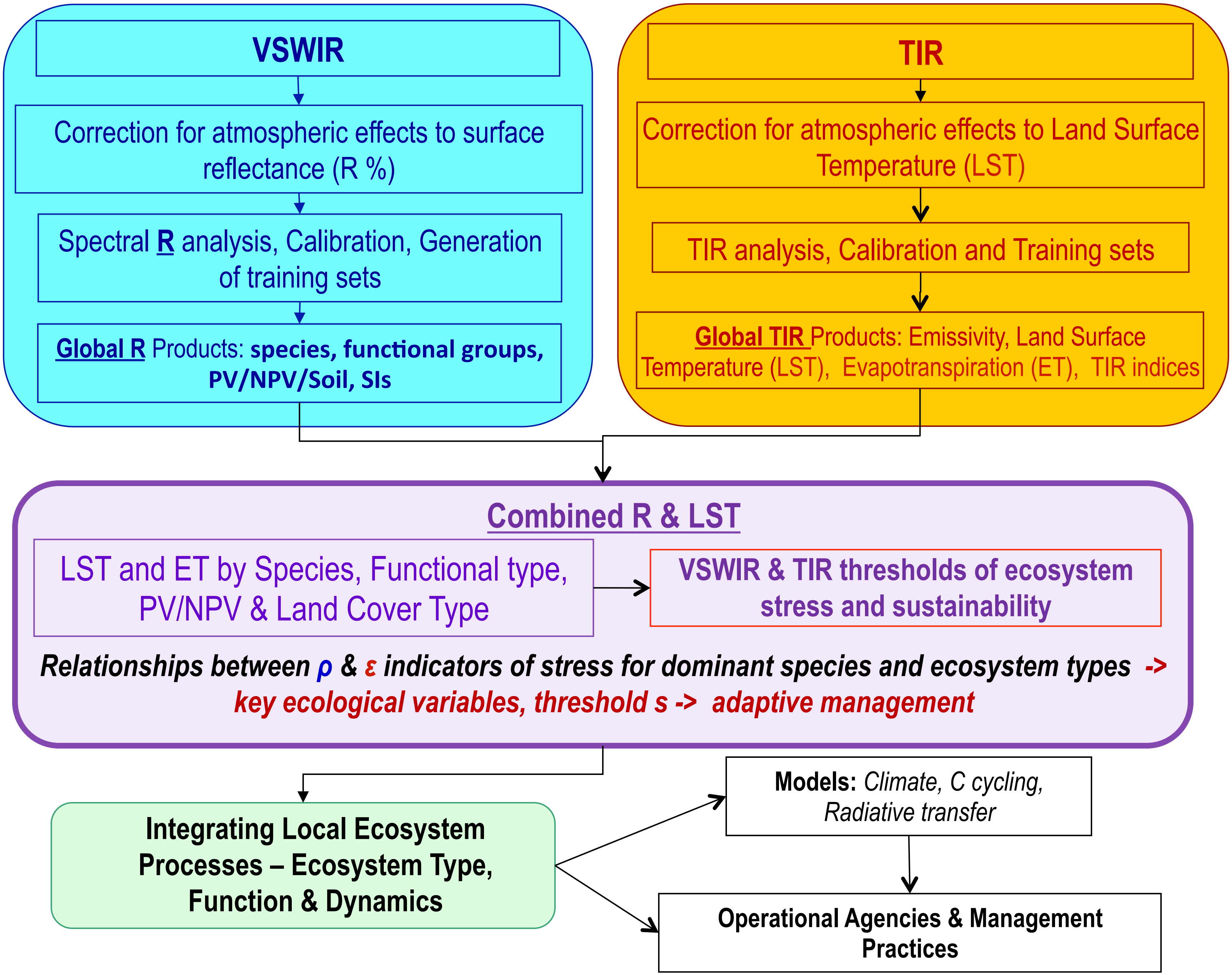
VSWIR
Correction for atmospheric effects to surface reflectance (R %)
Spectral R analysis, Calibration, Generation of training sets
Global R Products: species, functional groups, PV/NPV/Soil, SIs
TIR
Correction for atmospheric effects to Land Surface Temperature (LST)
TIR analysis, Calibration and Training sets
Global TIR Products: Emissivity, Land Surface Temperature (LST), Evapotranspiration (ET), TIR indices
Combined R & LST
LST and ET by Species, Functional type, PV/NPV & Land Cover Type
VSWIR & TIR thresholds of ecosystem stress and sustainability
Relationships between ρ & ε indicators of stress for dominant species and ecosystem types -> key ecological variables, threshold s -> adaptive management
Integrating Local Ecosystem Processes – Ecosystem Type, Function & Dynamics
Models: Climate, C cycling, Radiative transfer
Operational Agencies & Management Practices

LPV Focu	SWIR / TIR
LAND CO	
Fractional	
Disturban	
SURFACE	
Surface R	
Surface Al	
BIOPHYS	
Gross / Ne	
fPAR	
LAI	
Water con	
FIRE	
Detection	
Fire fuel lo	
LAND SU	
LST	
Emissivity	
Evapotranspiration	

Existing Val Methods | Research Required

J. Nightingale, 2011

HyspIRI Products for LPV

LPV Focus Group / Product	VSWIR L 2/ 3	VSWIR L4	VSWIR Global	TIR L4	SWIR / TIR
LAND COVER					
Fractional land cover / veg. cover		Existing Val Methods	Existing Val Methods		
Disturbance, PFT, hazard susceptibility		Research Required			
SURFACE RADIATION					
Surface Reflectance	Existing Val Methods				
Surface Albedo	Existing Val Methods				
BIOPHYSICAL					
Gross / Net Primary Production		Existing Val Methods	Existing Val Methods		
fPAR		Existing Val Methods	Existing Val Methods		
LAI		Existing Val Methods	Existing Val Methods		
Water content, LUE, Pigments		Research Required			
FIRE					
Detection of Fire events				Existing Val Methods	Existing Val Methods
Fire fuel loads		Research Required			
LAND SURFACE TEMPERATURE					
LST				Existing Val Methods	Existing Val Methods
Emissivity				Existing Val Methods	Existing Val Methods
Evapotranspiration				Research Required	

Existing Val Methods

Research Required

J. Nightingale, 2011

Summary

Existing:

1) Many approaches / tools / applications
2) Local to regional studies & pilot projects
3) Application demand for new ecosystem products

Needed:

1) To determine their sensitivity and application extend of the existing approaches we need large scale VSWIR/TIR data-sets for variety of ecosystems
2) Calibrated spectral products (establish a network producing *in-situ* bio-physical measurements)
3) Establish seasonal VSWIR/TIR relationships for major species, functional groups, etc.
4) Long term VSWIR/TIR spectral time series to reveal normal & divergent ecosystem patterns

HyspIRI Ecosystem Products

1. Seamless global bi-directional reflectance, surface emissivity and temperature products

2. Global discrimination of species through phenology

3. Sub-pixel fractions of functional groups, species, photosynthetic & non-photosynthetic vegetation and bare soil, incl. detection thresholds

4. Seamless VSWIR suites of established stress indices (SI) - Estimations of bio-physical variables

5. Temperature and emissivity estimates by vegetation components (species, functional groups)

6. Feedbacks between changes in canopy composition and canopy temperatures –

7. Complementary T, ET and VSWIR spectral indictors as measures of function, phenology and water use

HyspIRI Ecosystem Science Questions

- *Vq1. What is the global spatial pattern of ecosystem and diversity distributions and how do ecosystems differ in their composition or biodiversity?*
- *Vq2. What are the seasonal expressions and cycles for terrestrial and aquatic ecosystems, functional groups, and diagnostic species? How are these being altered by changes in climate, land use, and disturbance?*
- *Vq3. How are the biogeochemical cycles that sustain life on Earth being altered/disrupted by natural and human-induced environmental change? How do these changes affect the composition and health of ecosystems and what are the feedbacks with other components of the Earth system?*
- *Vq5. How do changes in ecosystem composition and function affect human health, resource use, and resource management?*

- *Cq1. How do Inland, Coastal, And Open Ocean Aquatic Ecosystems Change Due To Local and Regional Thermal Climate, Land-Use Change, And Other Factors?*
- *Cq4. How do species, functional type, and biodiversity composition within ecosystems influence the energy, water and biogeochemical cycles under varying climatic conditions?*

2012 HyspIRI Symposium

May 16-17, NASA/GSFC Greenbelt (MD)

Identifying Priority Products to Support HyspIRI's Science Questions

Carmelo CAMMALLERI[1]
M.C. Anderson[1]
F. Gao[1]
M.A. Schull[1]
R. Houborg[2]
W.P. Kustas[1]

1 USDA-ARS, Hydrology & Remote Sensing Lab, Beltsville, MD

2 European Commission, JRC, Ispra, Italy

Daily ET products at Landsat/HyspIRI scale from MODIS & Landsat Data

May 16, 2012

RESEARCH GOAL

- Water demand has doubled in the last 50 years.
- A large fraction of water resource (about 60%) is used for agricultural irrigation but with efficiencies often less than 50% (ga.water.usgs.gov/edu/wuir.html).
- Climate forecasts of precipitation suggest a future reduction in water availability.
- Quantification of crop water loss (mainly through evapotranspiration) assumes a key role in agricultural water management.

Cost effective estimates of actual evapotranspiration (**ET**) on large areas (~ 10^2-10^4 km^2) can be obtained only through the use of thermal infrared (**TIR**) satellite data.

Practical applications require ET estimates at:

→ Daily and Season time-scales

→ Field or finer spatial-scales

CURRENT AND FUTURE MISSIONS

Currently, TIR satellite sensors are characterized by low spatial resolution (1-10 km) and high frequency (day to 15 min) or high spatial resolution (30-m) but low repeatability (2 weeks). **Multi-sensor technique have to be developed** to fuse the best qualities of the datasets.

Landsat-5
120 m
16 days

Landsat-7
60 m
16 days

HyspIRI
60 m
5 days

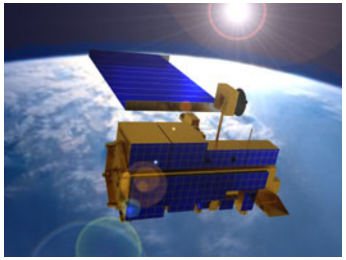

MODIS/Terra
1 km
1 days

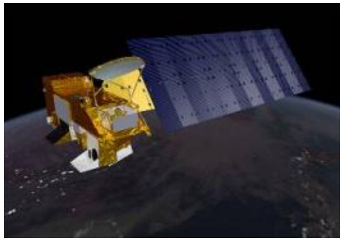

MODIS/Aqua
1 km
1 days

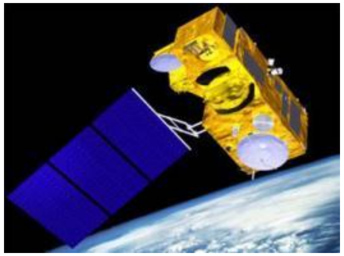

Sentinel-3
1 km
1 days

Cloud cover often reduces actual TIR data frequency from the nominal value, especially during winter period [Ju & Roy, RSE112: 2008].

During SMEX02:

- Summer period (June-August 2002)
- Both Landsat 5 and 7.

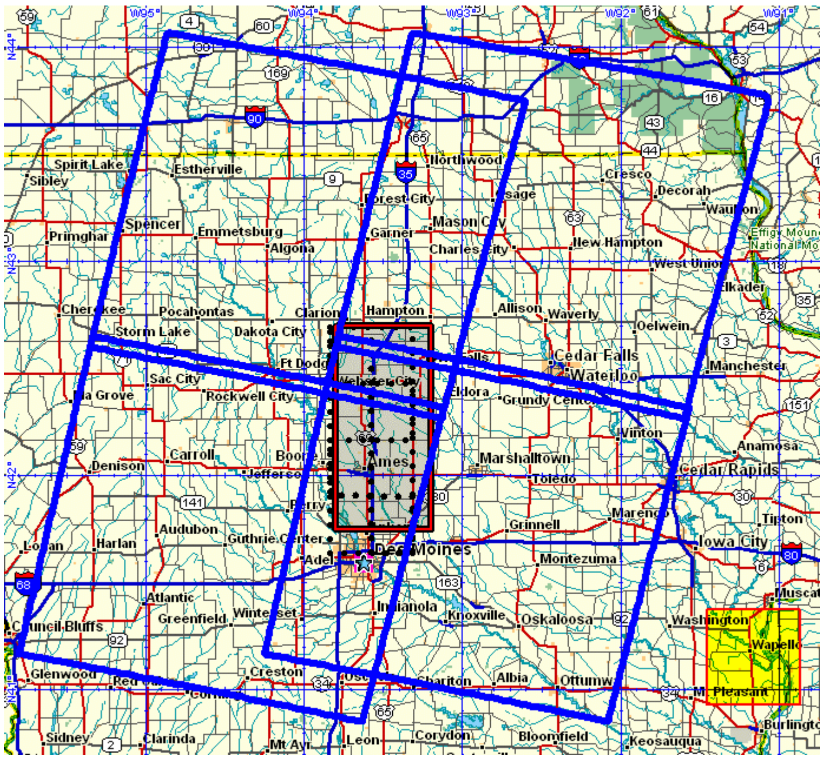

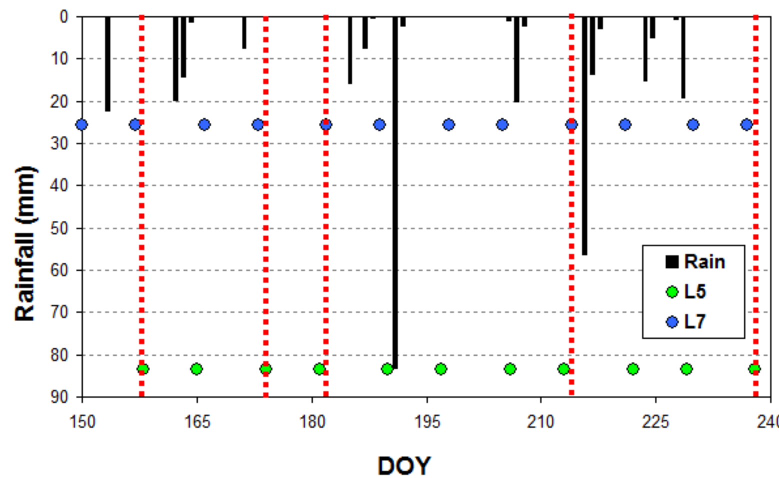

- Only **5 scenes** were clear.
- Average frequency of 21 days.
- Maximum gap of 32 days.

METHODOLOGY (1/2)

GOES

MODIS
Landsat

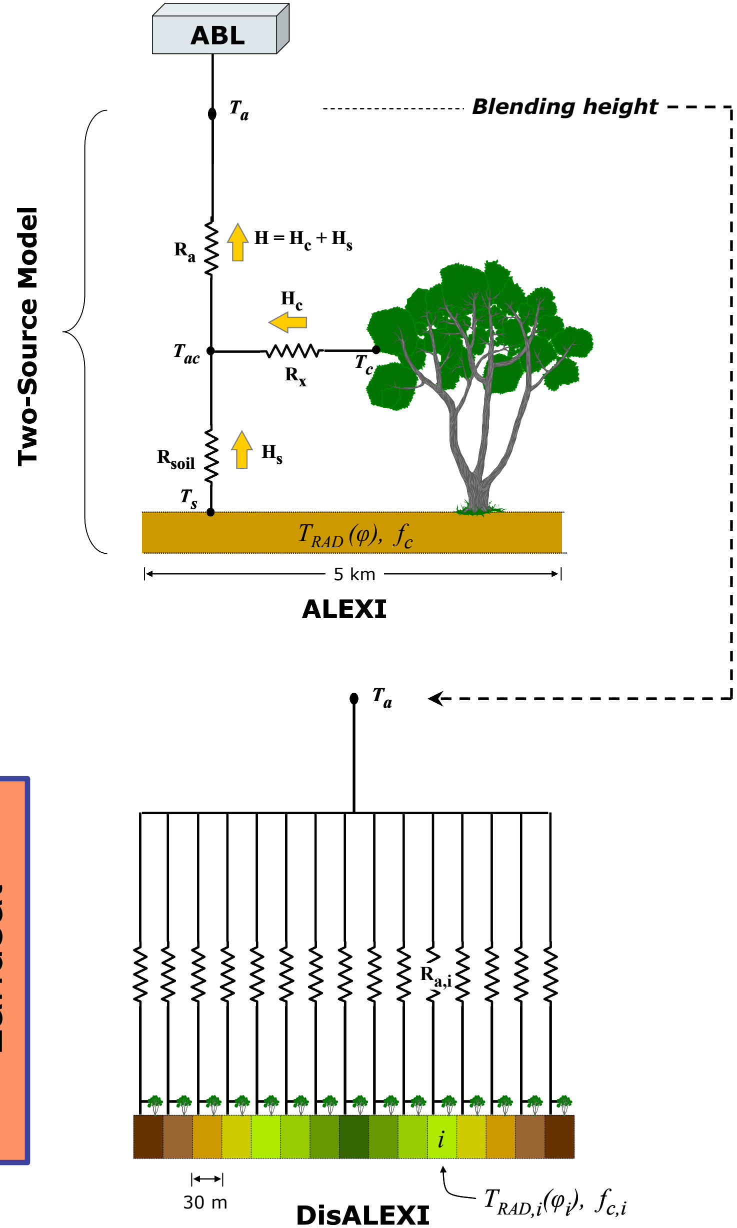

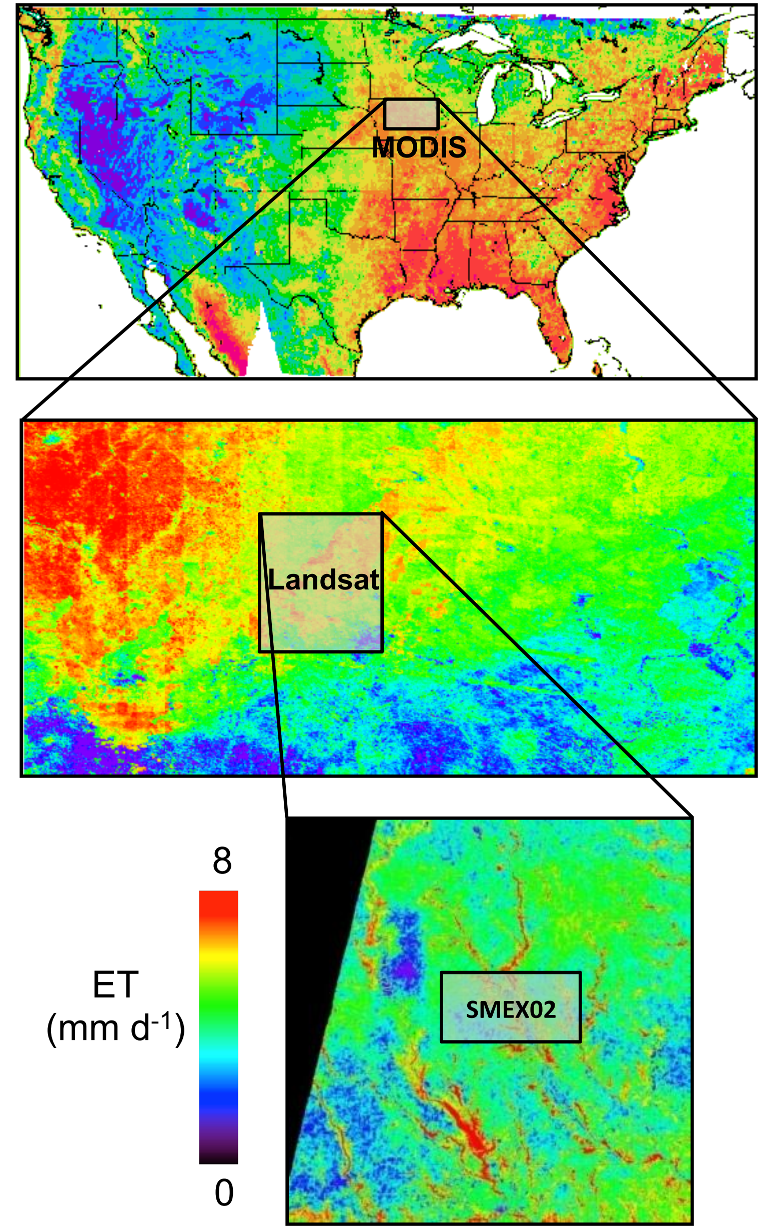

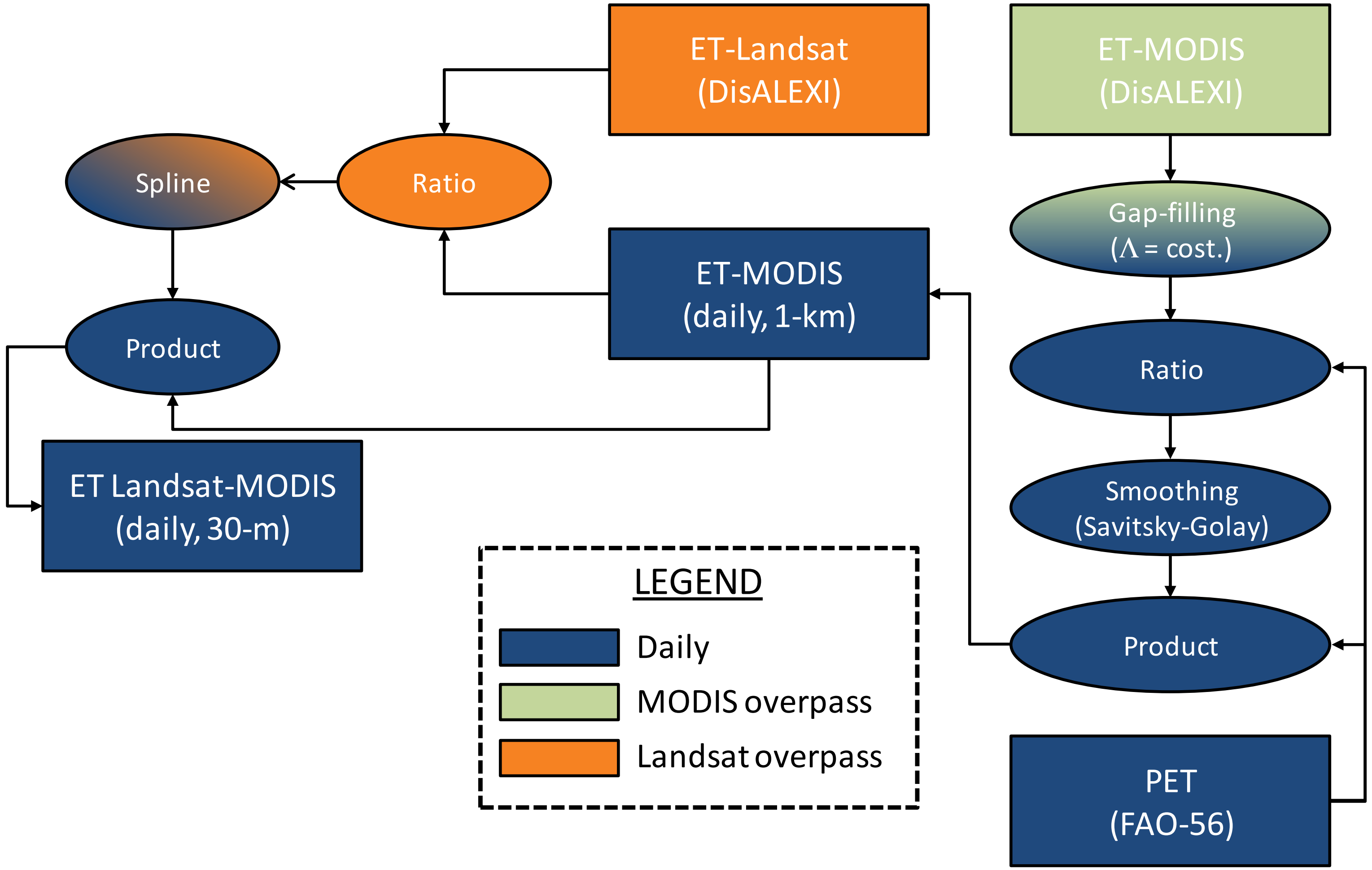

- A change at MODIS scale have equal effects on all the Landsat pixels.
- Landsat and MODIS estimates are consistent at MODIS resolution.

METHODOLOGY (2/2)

METHODOLOGY (2/2)

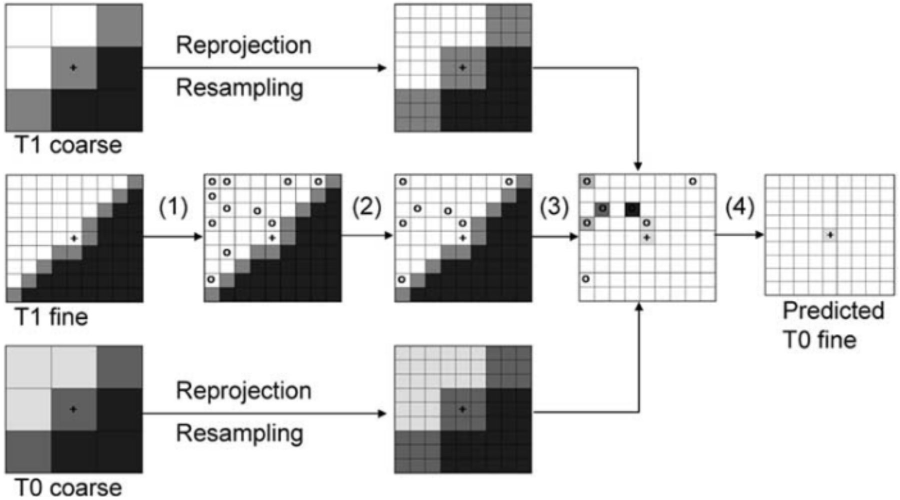

- A pair coarse/fine resolution is required.
- Similarities are detected at high resolution.
- Prediction determined using a weighting function.

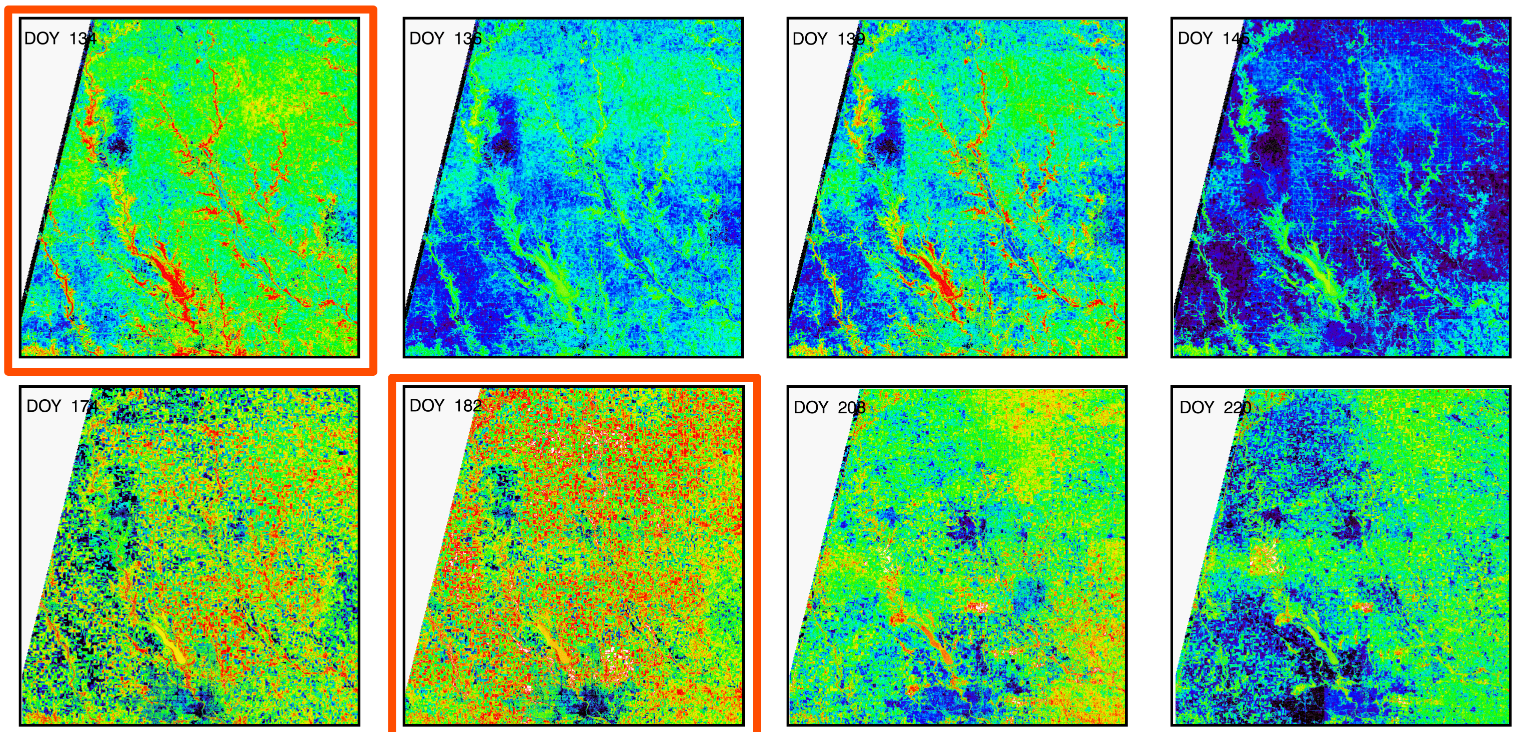

STUDY CASE

- Soil Moisture EXperiment (**SMEX02**), **June-August** 2002.
- Walnut Creek watershed (5,100-ha), **central Iowa**.
- ET monitoring by means of **8** micrometeorological **flux towers** (red dots in figure) on **corn** and **soybean** fields during a period of rapid crop development.

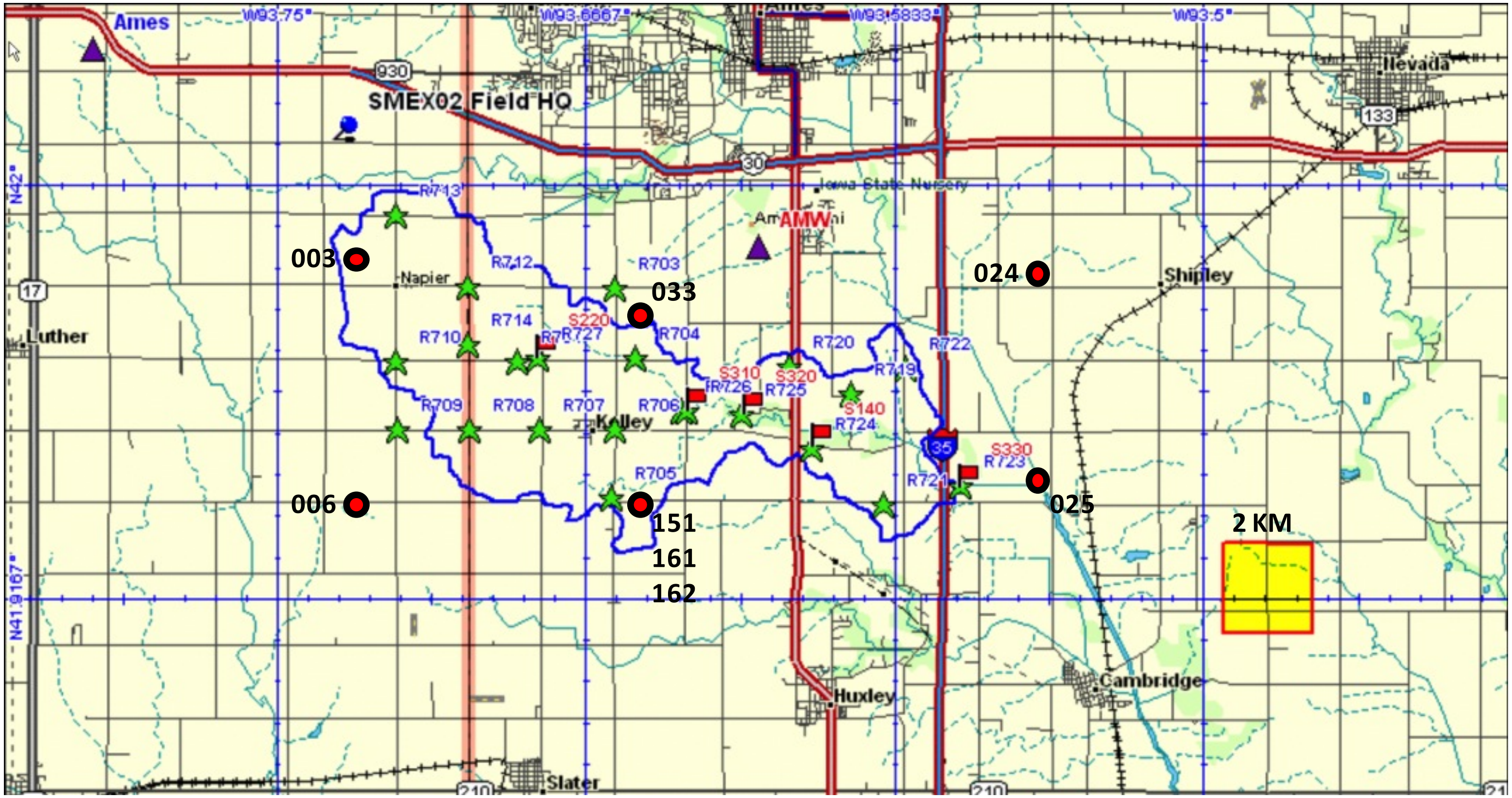

RESULTS (1/4)

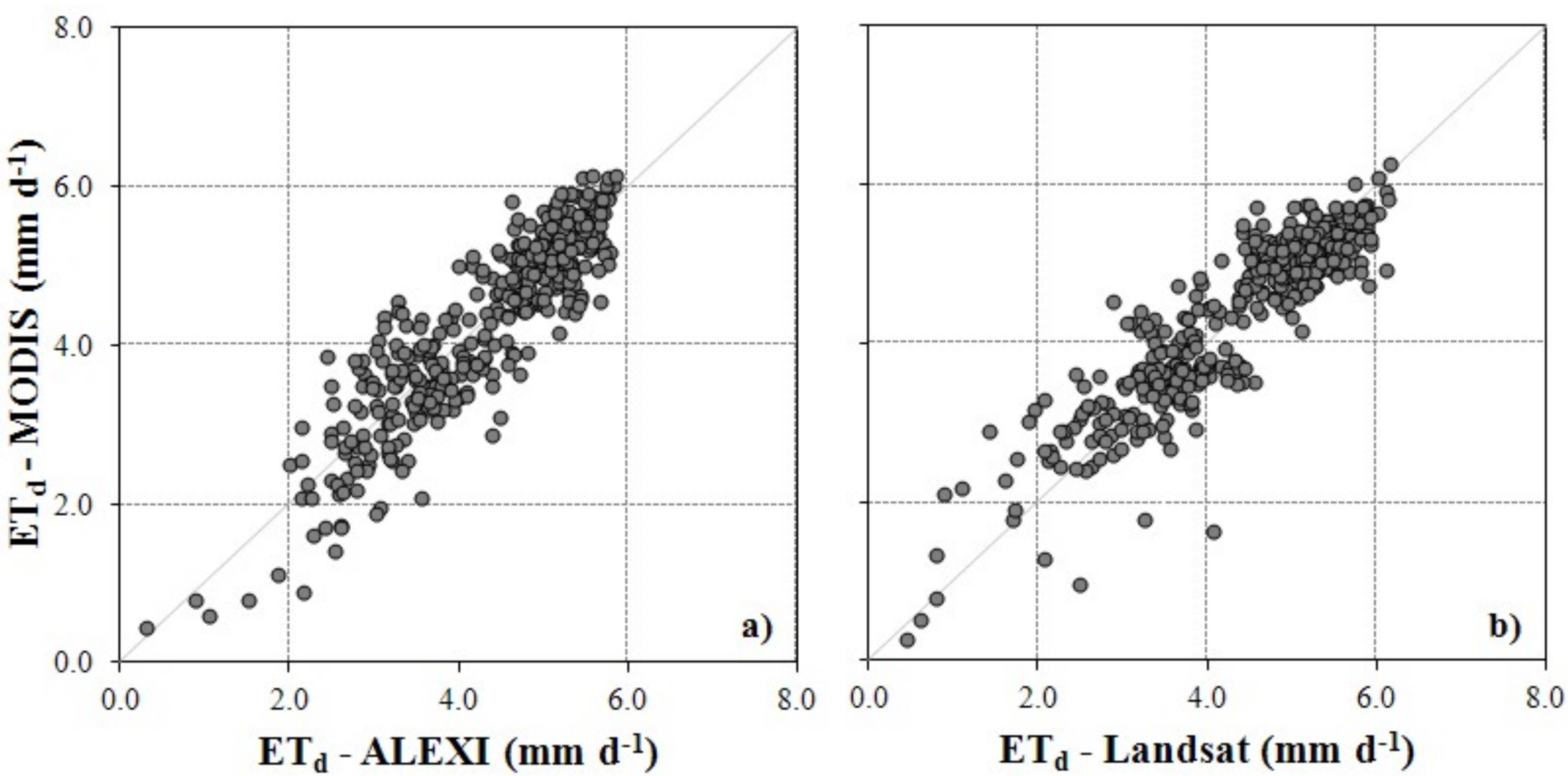

- Absence of biases among the three maps at ALEXI resolution.
- Some dispersion is present in both data due to the smoothing procedure.
- Slopes practically equal to 1, R^2 of 0.82 (Landsat) and 0.80 (MODIS).
- Agreement in the order of 0.3 mm d^{-1}.

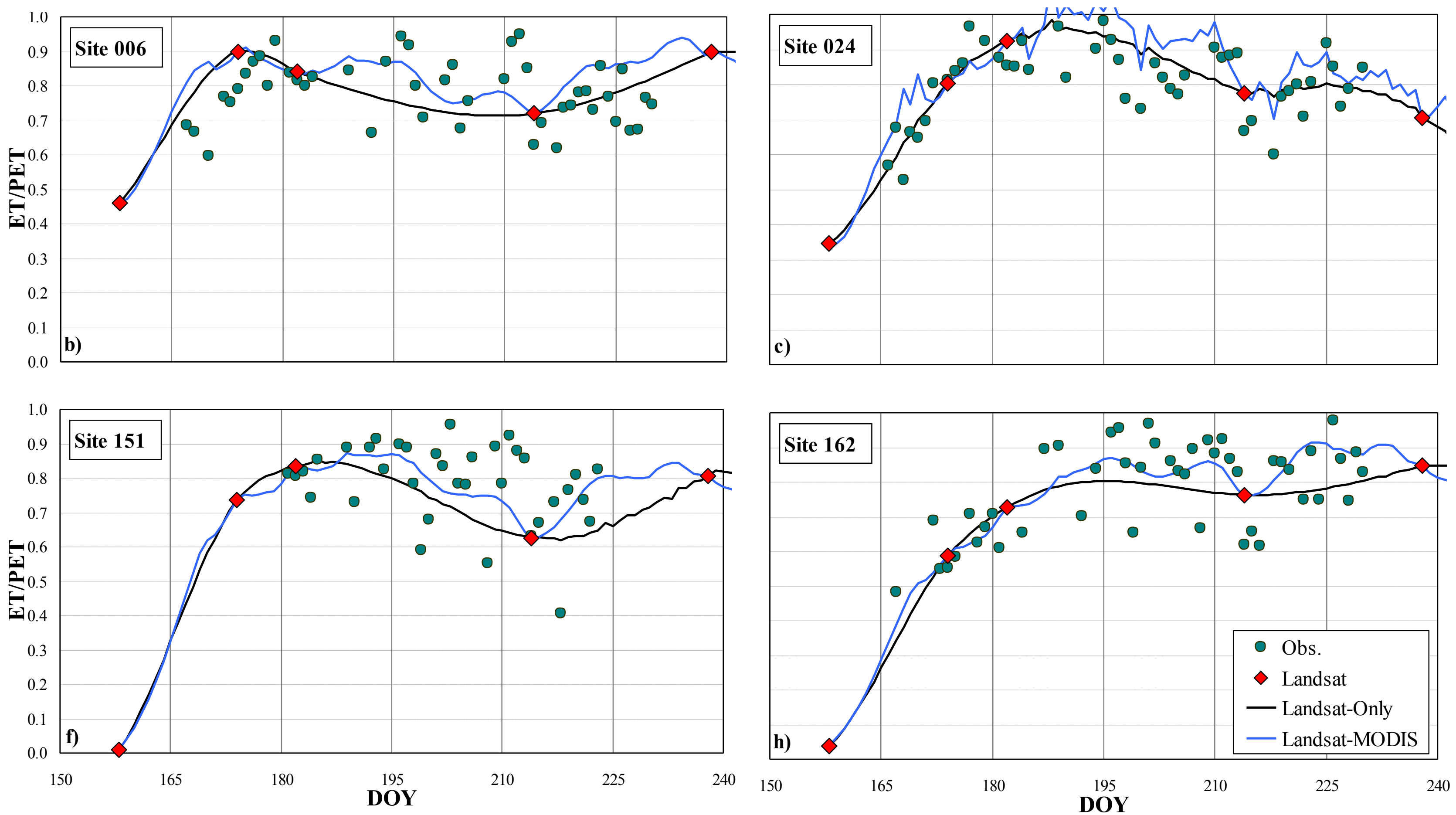

RESULTS (2/4)

- Good performance of Landsat-Only model.
- Increasing trend until DOY 185 and a successive stable stage around 0.8.
- Rainfall events seem to do not cause significant changes in water stress.

RESULTS (3/4)

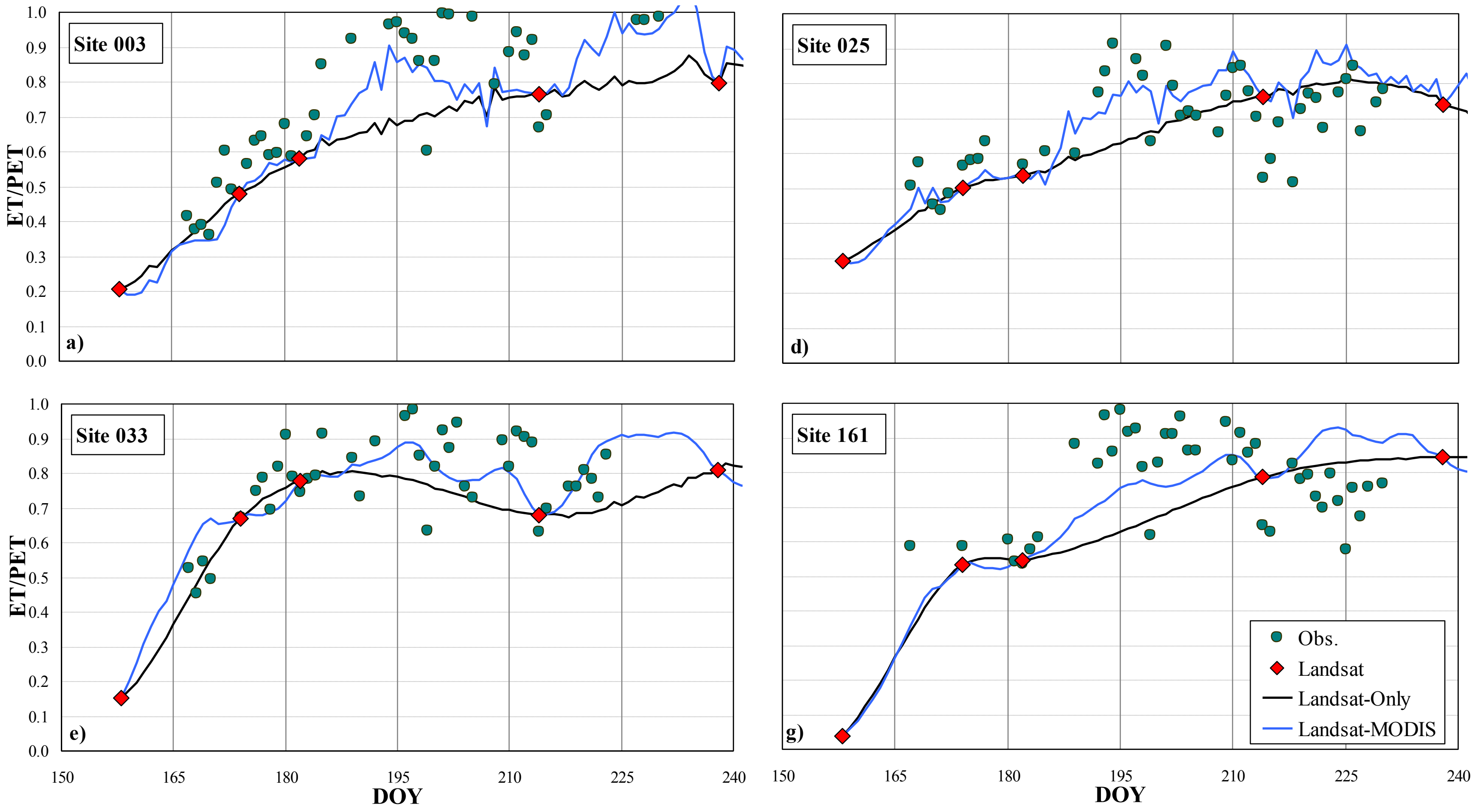

- Significant leap in the ratio ET/PET after the first rainfall event (DOY 185).
- Landsat-Only seems to underestimate the observations in DOY 185-210.
- Fused Landsat-MODIS partially overcomes the underestimates.

Site	Crop Type	Obs. Cum. (mm)	Landsat-only MAD (mm d^{-1})	Landsat-only RE (%)	Landsat-only Slope	Landsat-only ΔCum. (mm)	Landsat-MODIS MAD (mm d^{-1})	Landsat-MODIS RE (%)	Landsat-MODIS Slope	Landsat-MODIS ΔCum. (mm)
003	Soybean	237	1.02	19.4	0.81	-41.0	0.78	14.9	0.87	-28.5
006	Corn	292	0.82	14.6	0.90	-17.4	0.79	14.1	0.95	-1.9
024	Corn	270	0.45	8.2	1.02	6.8	0.55	9.9	1.06	17.6
025	Corn	210	0.67	14.4	0.93	-10.9	0.61	13.1	1.01	5.0
033	Corn	230	0.66	12.1	0.89	-21.8	0.54	9.9	0.96	-4.6
151	Corn	212	0.81	15.0	0.89	-21.0	0.65	11.9	0.94	-8.2
161	Soybean	210	0.92	17.8	0.88	-21.0	0.78	15.2	0.98	0.5
162	Soybean	258	0.65	12.3	0.92	-15.8	0.52	9.9	0.99	-2.6
Average		240	0.75	14.2	0.90	-17.8	0.65	12.3	0.98	-2.8

- Both **MAD** and **RE** (errors) are in average **reduced** of about **10%**.
- The systematic **bias** (underestimation) of Landsat-only model (slope = 0.90) is **significantly reduced** (slope = 0.97) by introducing MODIS data.
- The **total difference** on seasonal cumulative ET is **reduced of ≈ 50%**.
- Almost all the sites show improvements by introducing MODIS data.

RESULTS (2/4)

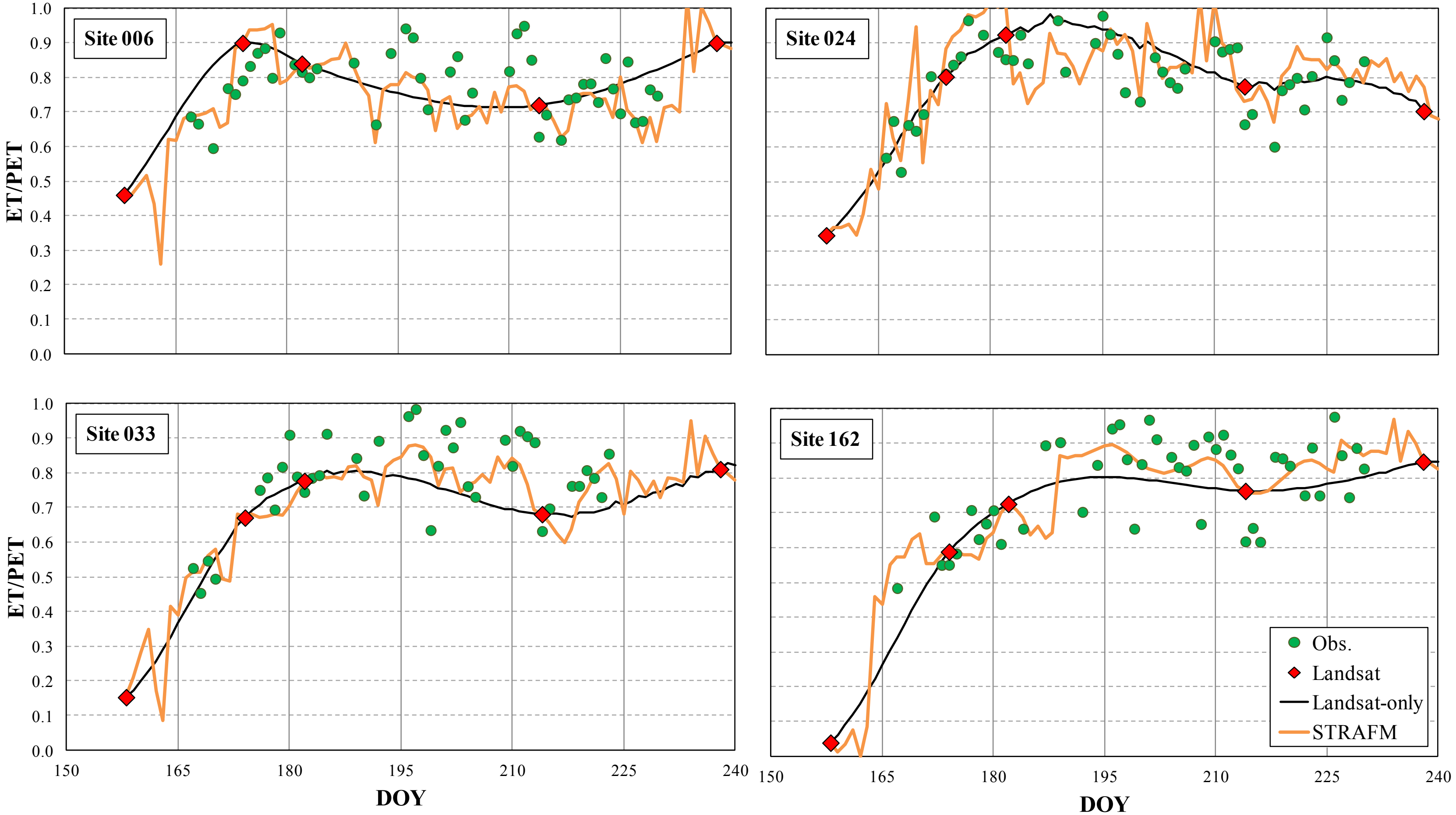

- Good performance of Landsat-Only model.
- Increasing trend until DOY 185 and a successive stable stage around 0.8.
- Rainfall events seem to do not cause significant changes in water stress.

RESULTS (3/4)

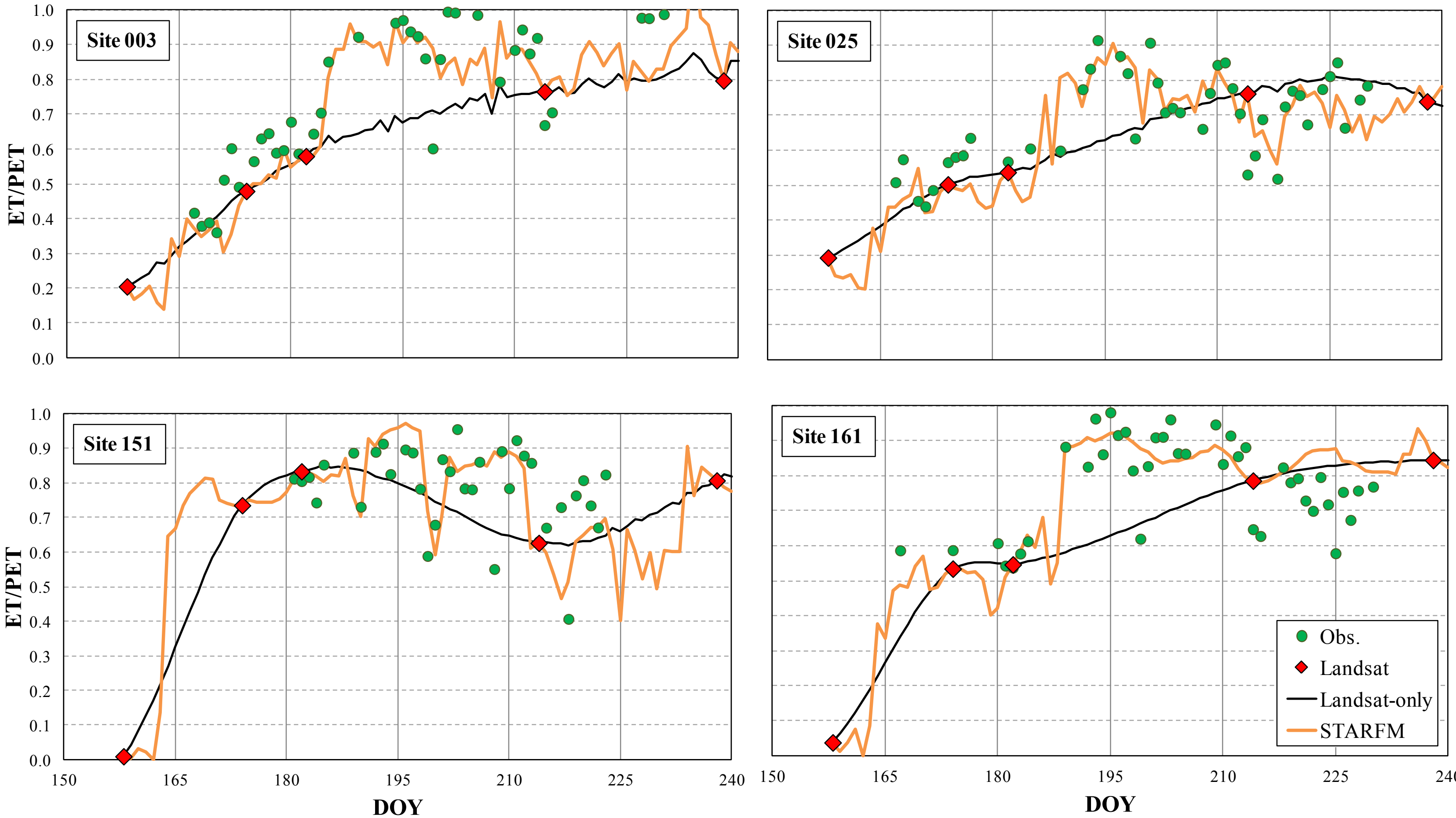

- Significant leap in the ratio ET/PET after the first rainfall event (DOY 185).
- Landsat-Only seems to underestimate the observations in DOY 185-210.
- Fused Landsat-MODIS partially overcomes the underestimates.

RESULTS (4/4)

Site	Crop Type	Obs. Cum. (mm)	Landsat-only MAD (mm d^{-1})	Landsat-only RE (%)	Landsat-only Slope	Landsat-only ΔCum. (mm)	STARM MAD (mm d^{-1})	STARM RE (%)	STARM Slope	STARM ΔCum. (mm)
003	Soybean	237	1.02	19.4	0.81	-41.0	0.64	12.3	0.92	-17.9
006	Corn	292	0.82	14.6	0.90	-17.4	0.78	14.0	0.90	-24.3
024	Corn	270	0.45	8.2	1.02	6.8	0.49	8.9	1.03	9.7
025	Corn	210	0.67	14.4	0.93	-10.9	0.54	11.5	0.97	-5.6
033	Corn	230	0.66	12.1	0.89	-21.8	0.52	9.6	0.94	-12.1
151	Corn	212	0.81	15.0	0.89	-21.0	0.65	12.0	0.97	-5.2
161	Soybean	210	0.92	17.8	0.88	-21.0	0.50	9.7	1.02	5.9
162	Soybean	258	0.65	12.3	0.92	-15.8	0.53	10.1	0.97	-4.3
Average		240	0.75	14.2	0.90	-17.8	0.58	11.1	0.98	-6.7

- Both **MAD** and **RE** (errors) are in average **reduced** of about **20%**.
- The systematic **bias** (underestimation) of Landsat-only model (slope = 0.90) is **significantly reduced** (slope = 0.98) by introducing MODIS data.
- The **total difference** on seasonal cumulative ET is **reduced of ≈ 60%**.
- Almost all the sites show improvements by introducing MODIS data.

SUMMARY AND CONCLUSIONS

- A **multi-scale** (from continental to field) and **multi-sensor** (geostationary and polar-orbit satellites) **modeling framework** was tested to derive **ET** maps at **high resolution** (≈ 10-100 m) and **daily** frequency.

- The proposed **methodology** is developed to be consistent at different scales and it is **suitable** (and transferable) for next generation sensors (as **HyspIRI**).

- A **general improvement** in the agreement with in-situ measurements was observed by **fusing MODIS** (daily, 1-km) data **with Landsat** (16 days, 30-m) maps if compared to Landsat-only case.

- The **gain** related to MODIS data is **higher** when **leaps** in water availability were observed **between** two **successive Landsat** acquisitions.

- The obtained **average errors** (10% on daily evapotranspiration and 5% on seasonal cumulative ET) are **appropriate** to provide a support tool in **practical management** of agricultural water resource.

Carmelo CAMMALLERI, PhD

U.S. Department of Agriculture (USDA)
Agricultural Research Service (ARS)
Animal and Natural Resources Institute (ANRI)
Hydrology and Remote Sensing Laboratory (HRSL)

Evapotranspiration using remote sensing and weather data in linked mesoscale and local scale physically base models

Susan L. Ustin
Matthias Falk, Dave Pyles, Shuhua Chen, Kyaw Tha Paw U

University of California Davis

Linked NCAR Weather Research Forecasting (WRF) and UCD Advanced Canopy-Soil Algorithm (ACASA) Model For Estimating And Predicting Fluxes

ACASA: An SVAT Flux Model that Accounts for Vertical and Spatial Heterogeneity at Local Scale (0.5km^2)

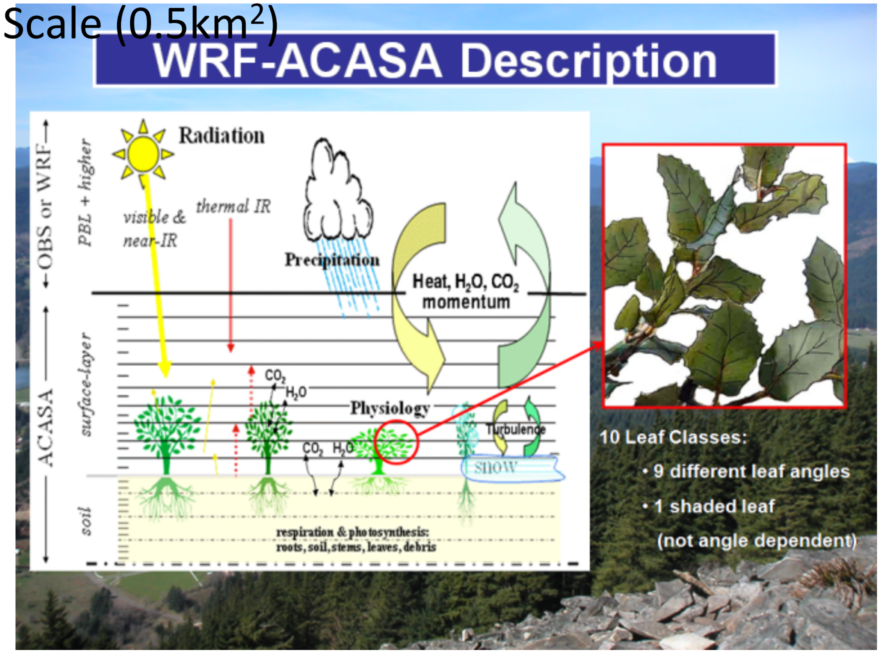

Schematic Overview of ACASA

WRF: Atmospheric Physics Model to Estimate Fluxes at Regional Scales (cells down to ~ 1km^2)

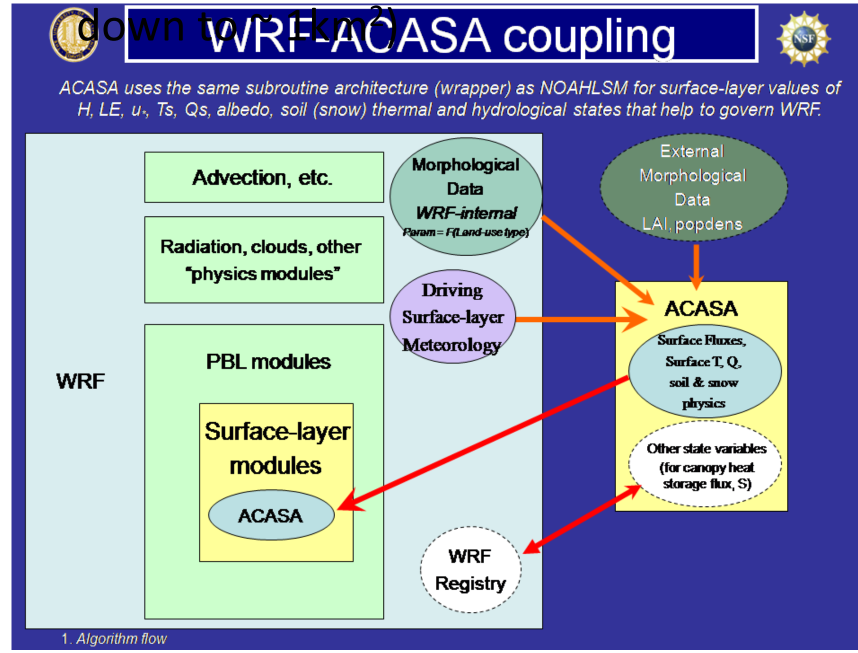

WRF with ACASA Surface Layer Scheme

ACASA is a type of Surface Vegetation Atmosphere Transfer (SVAT) model

Nested WRF-ACASA Domains with 16 km, 4 km, 1km, 0.5km Horizontal Resolution

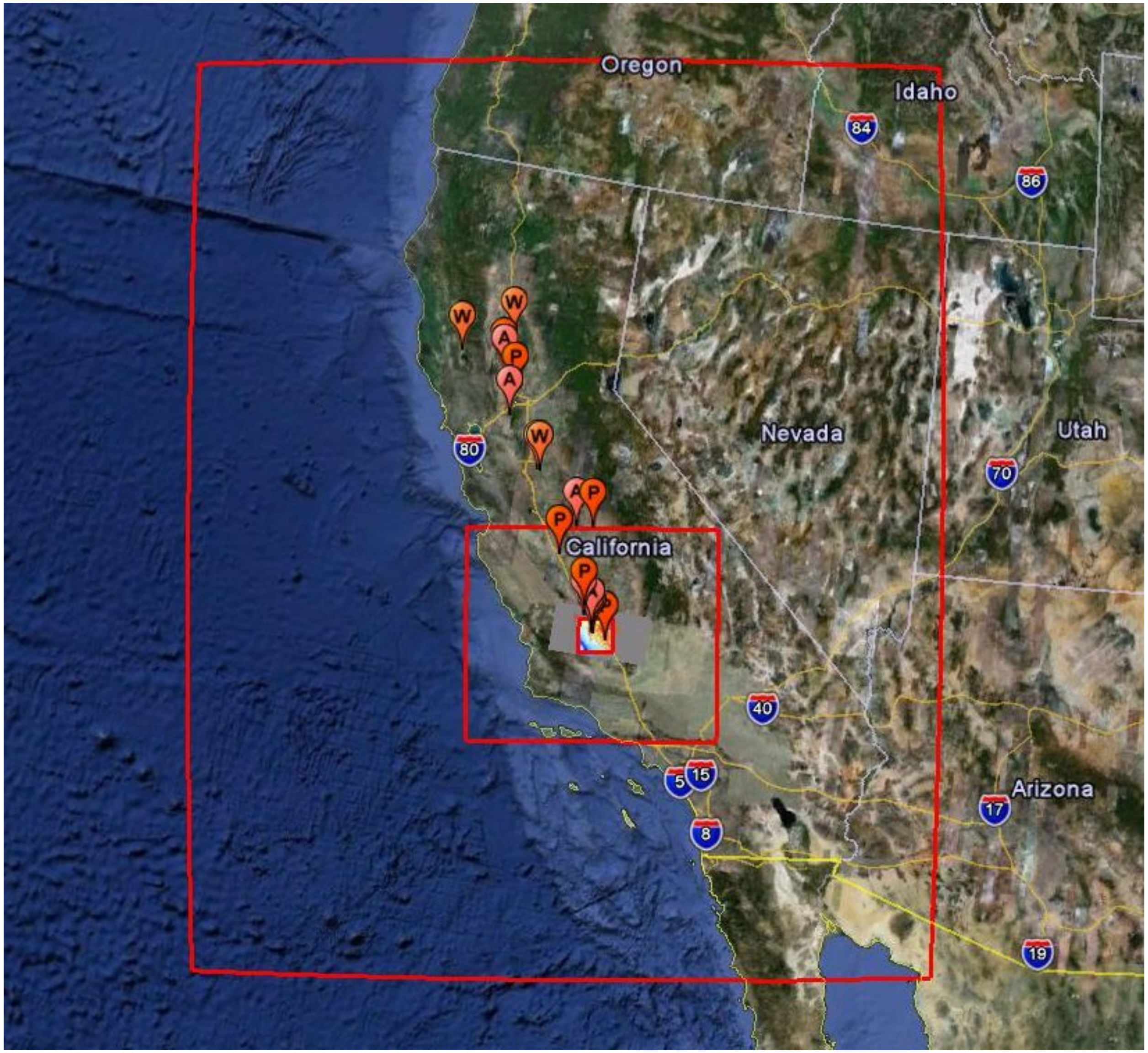

Typical sequence of nested WRF-ACASA Domains over California and the Central Valley (rectangles). Almond and pistachio orchard locations (balloons)

SCRI WRF-ACASA: Experimental Domain

California Augmented Multisource Landcover map

100 meter resolution

http://cain.ice.ucdavis.edu/caml

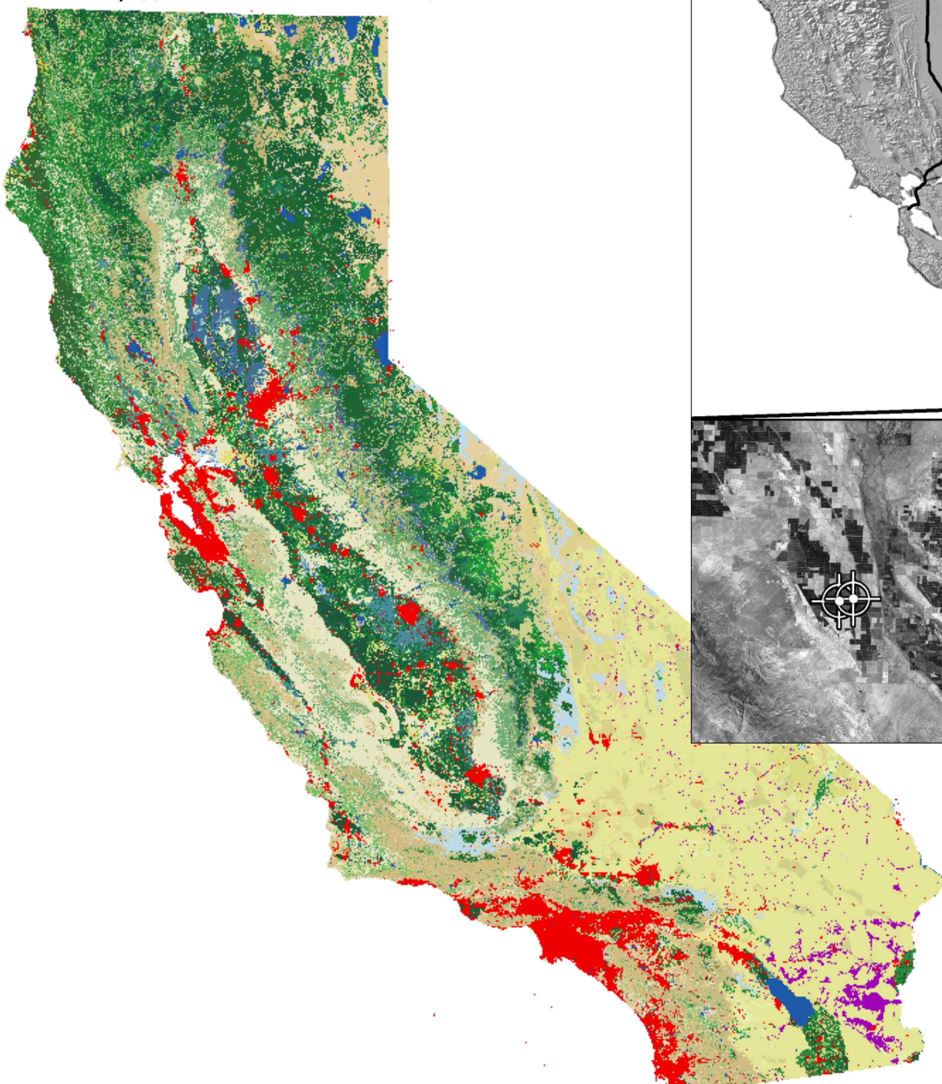

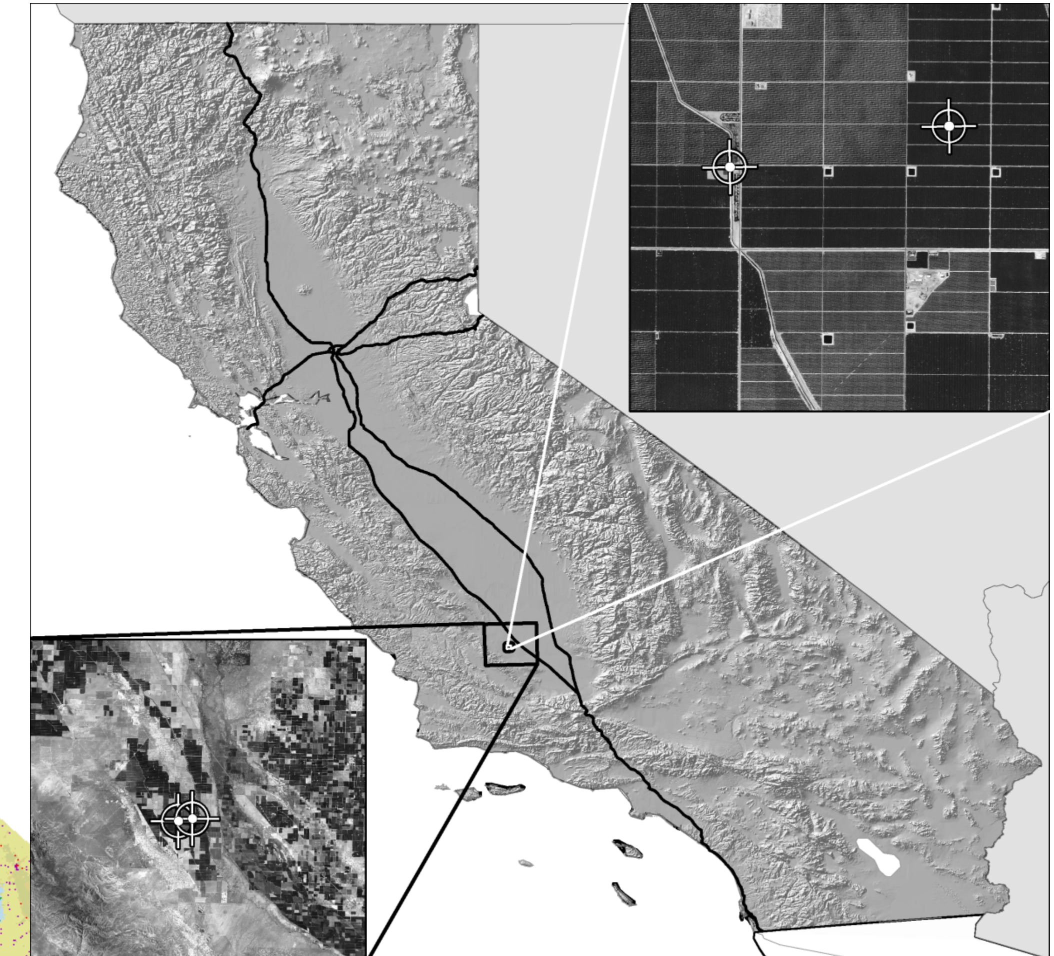

40 km x 40 km scene with 0.5 km pixels

SCRI WRF-ACASA: Experimental Domain

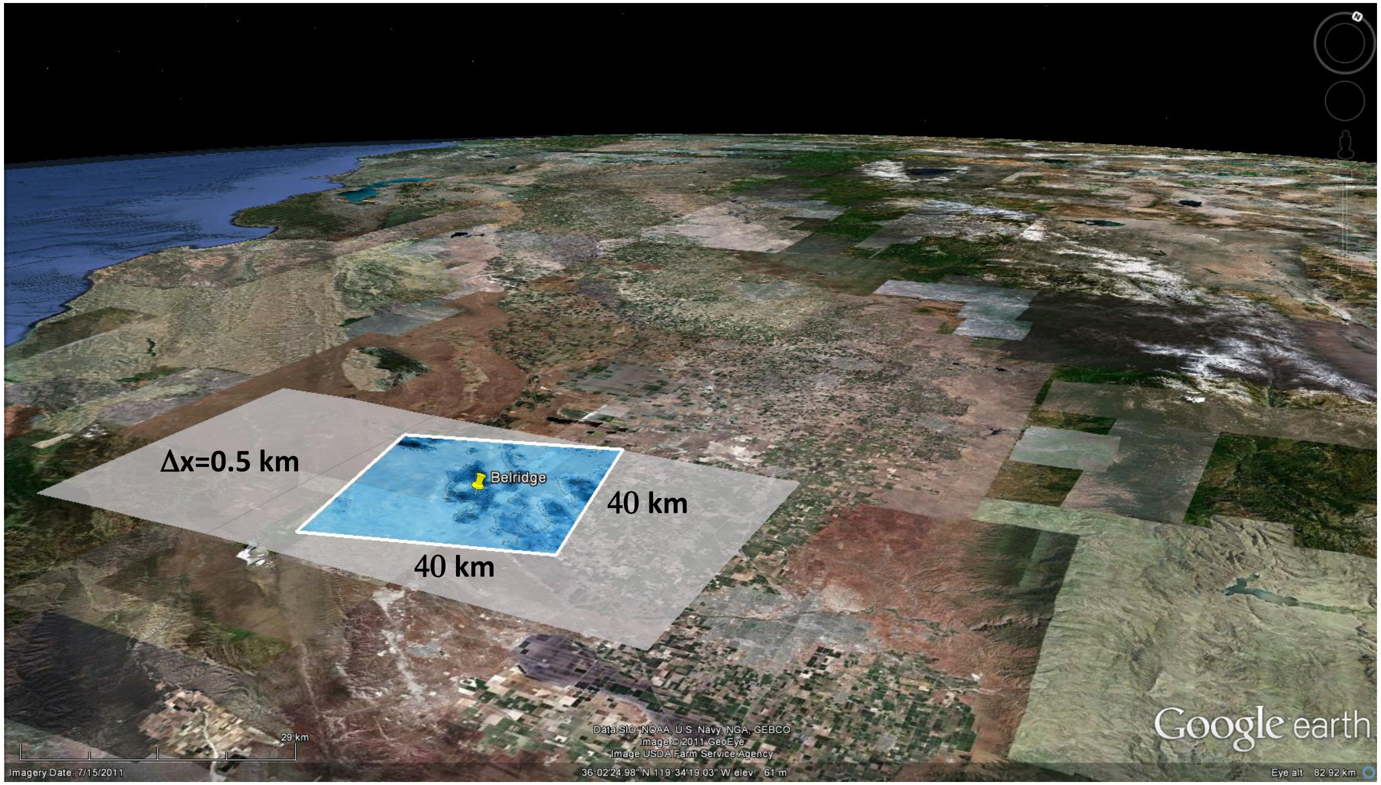

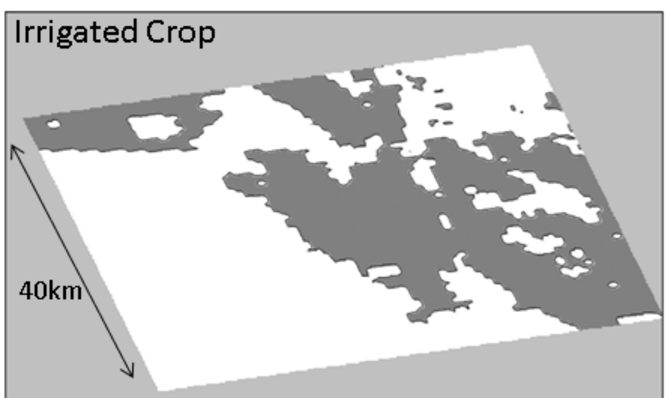

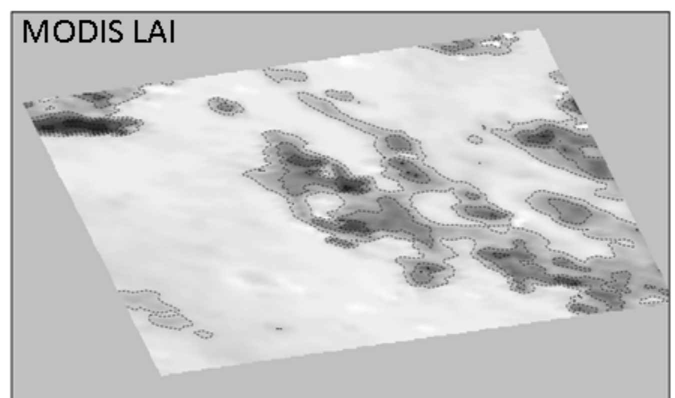

The spatial, spectral, and temporal resolutions of HyspIRI data can contribute to improved estimates of radiative and non-radiative (physiological) forcing:

partitioning the energy budget
emissivity
Evapotranspiration and other trace gas fluxes

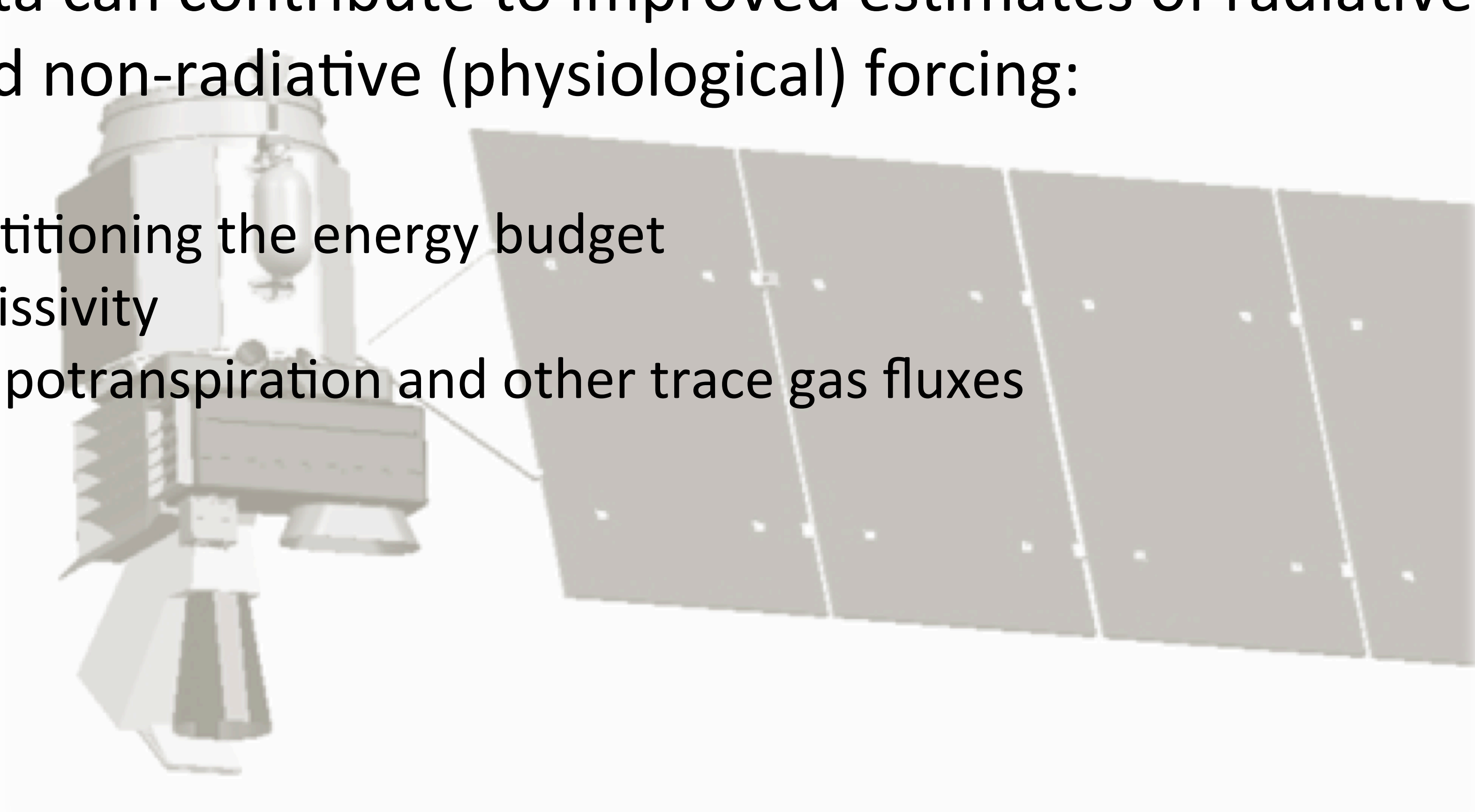

- 60m pixel resolution
- Imaging spectrometer + 8 TIR bands
- 19 day and 5 day repeat global coverage
- High SNR, Stability & uniformity

2008 ACASA vs. Flux Tower ETc Estimates

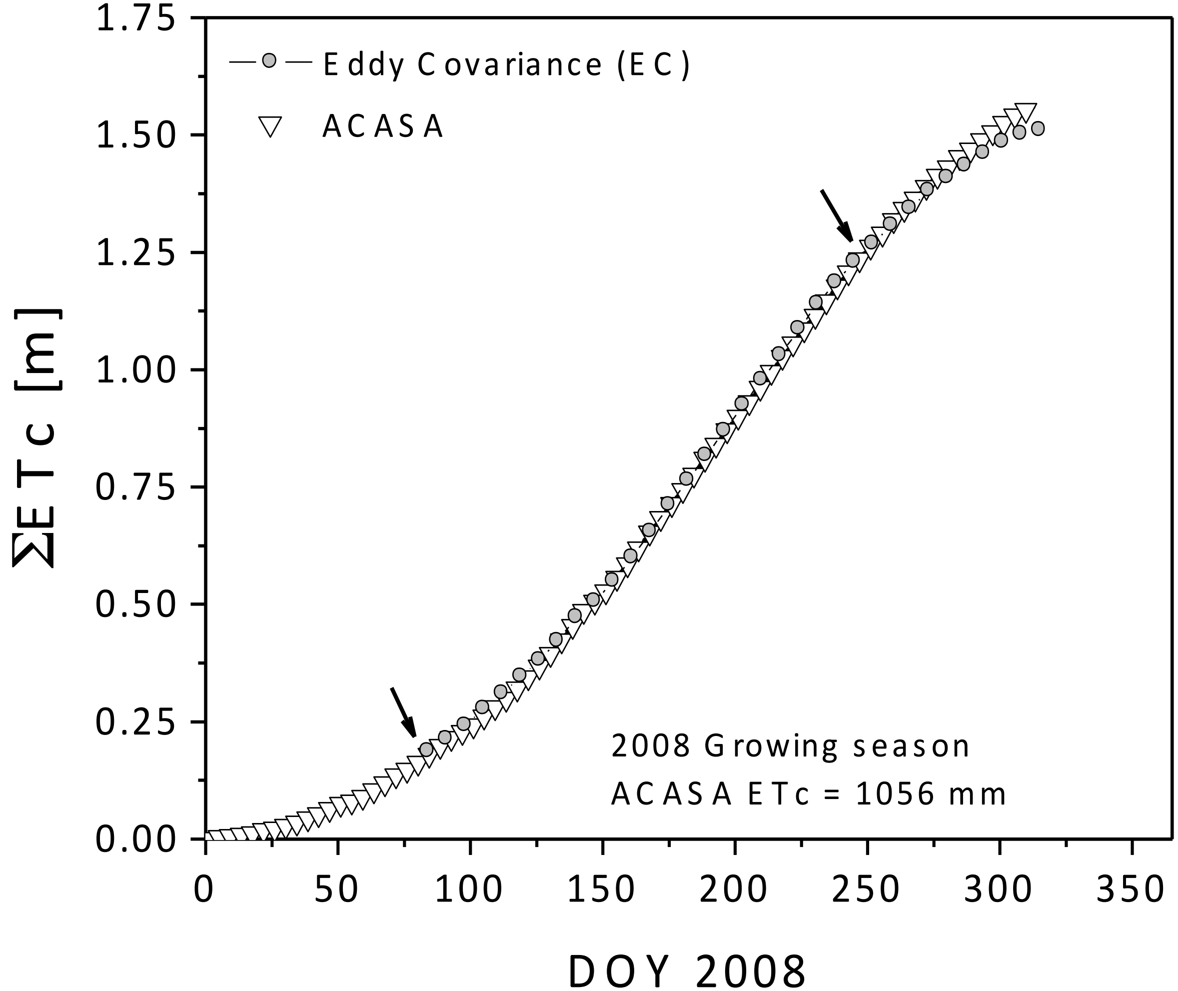

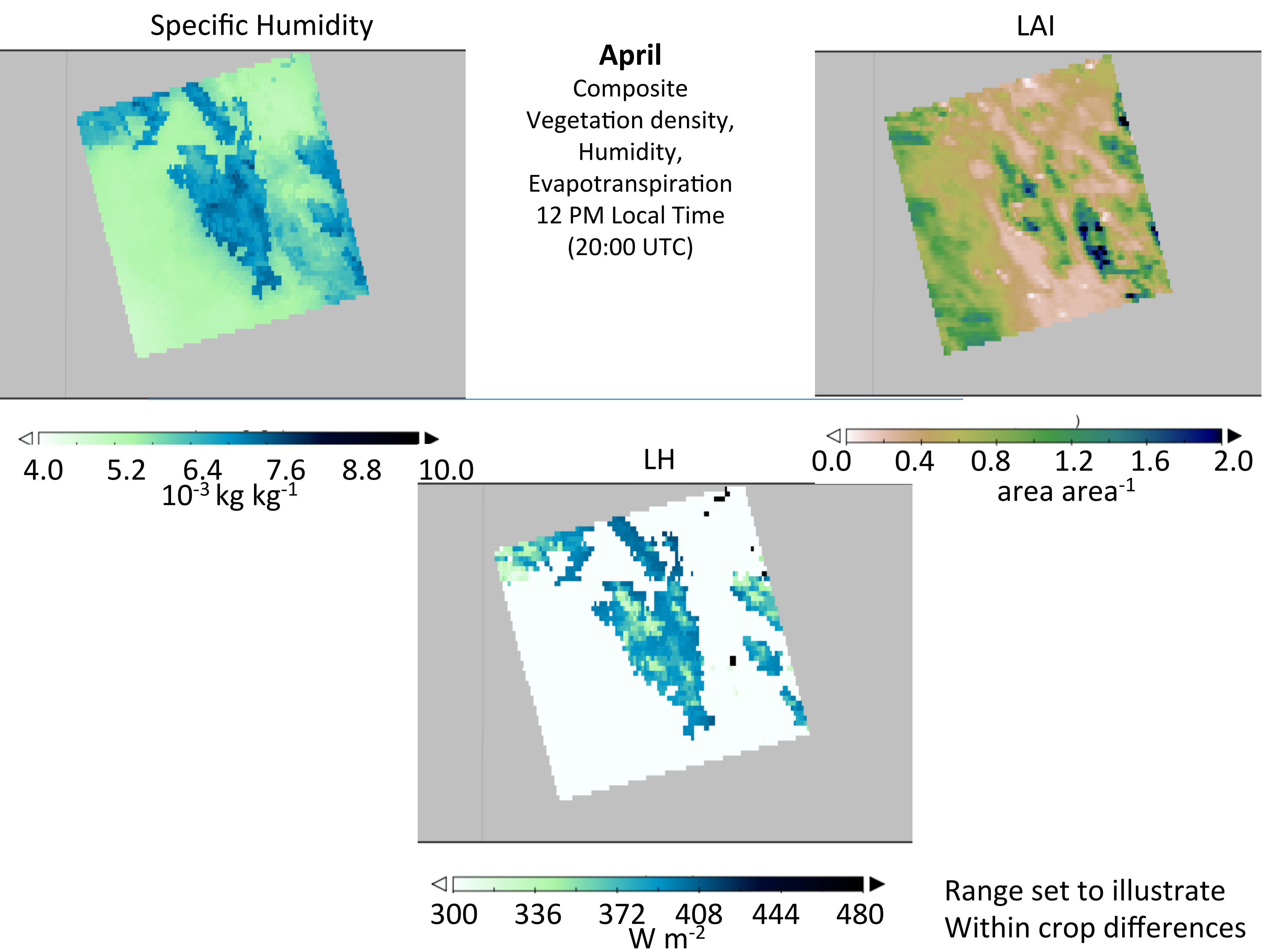
Specific Humidity
April
Composite
Vegetation density,
Humidity,
Evapotranspiration
12 PM Local Time
(20:00 UTC)
LAI
4.0 5.2 6.4 7.6 8.8 10.0
10^-3 kg kg^-1
0.0 0.4 0.8 1.2 1.6 2.0
area area^-1
LH
300 336 372 408 444 480
W m^-2
Range set to illustrate
Within crop differences

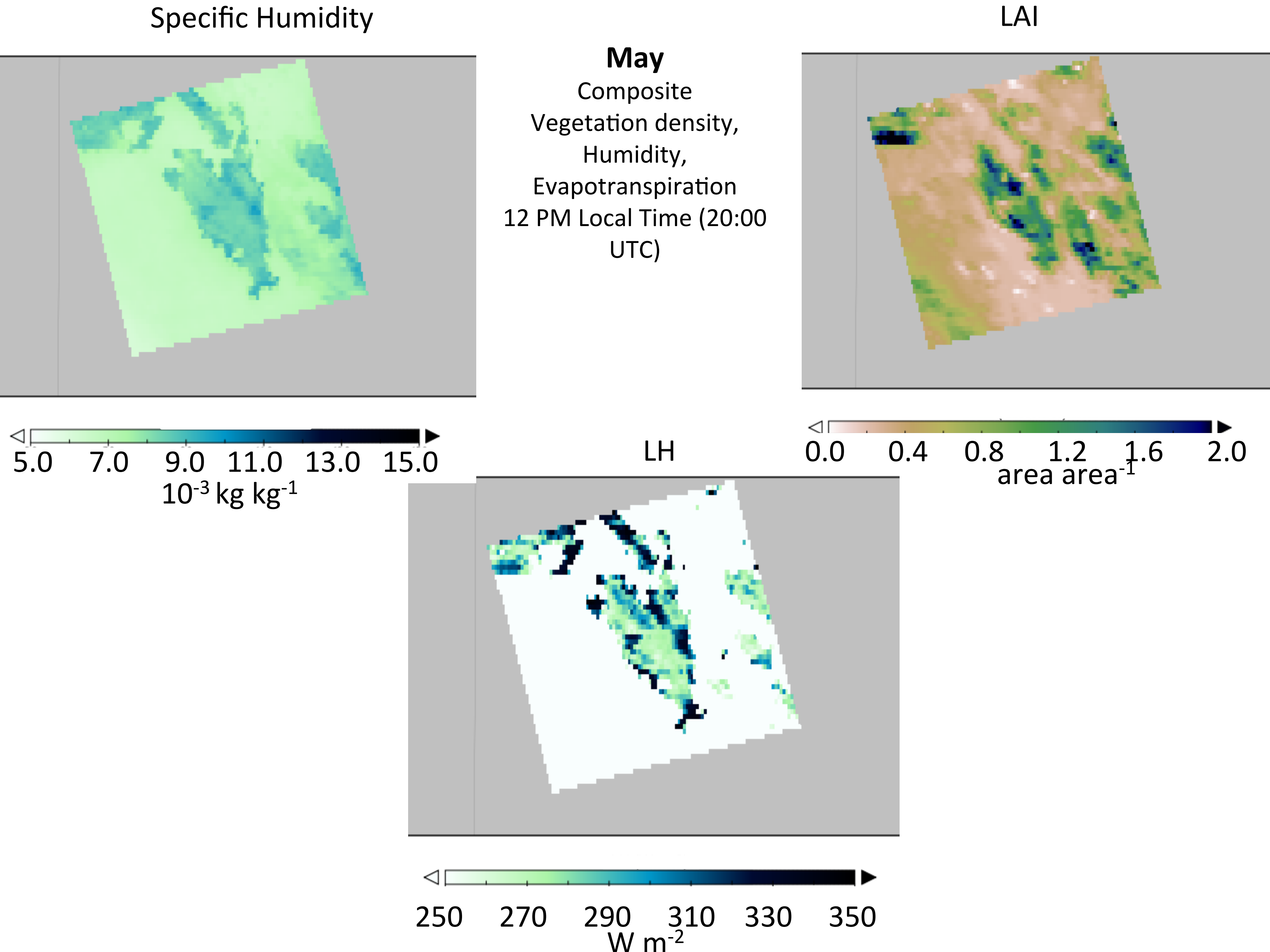
Specific Humidity
May
Composite
Vegetation density,
Humidity,
Evapotranspiration
12 PM Local Time (20:00 UTC)
LAI
5.0 7.0 9.0 11.0 13.0 15.0
10^-3 kg kg^-1
0.0 0.4 0.8 1.2 1.6 2.0
area area^-1
LH
250 270 290 310 330 350
W m^-2

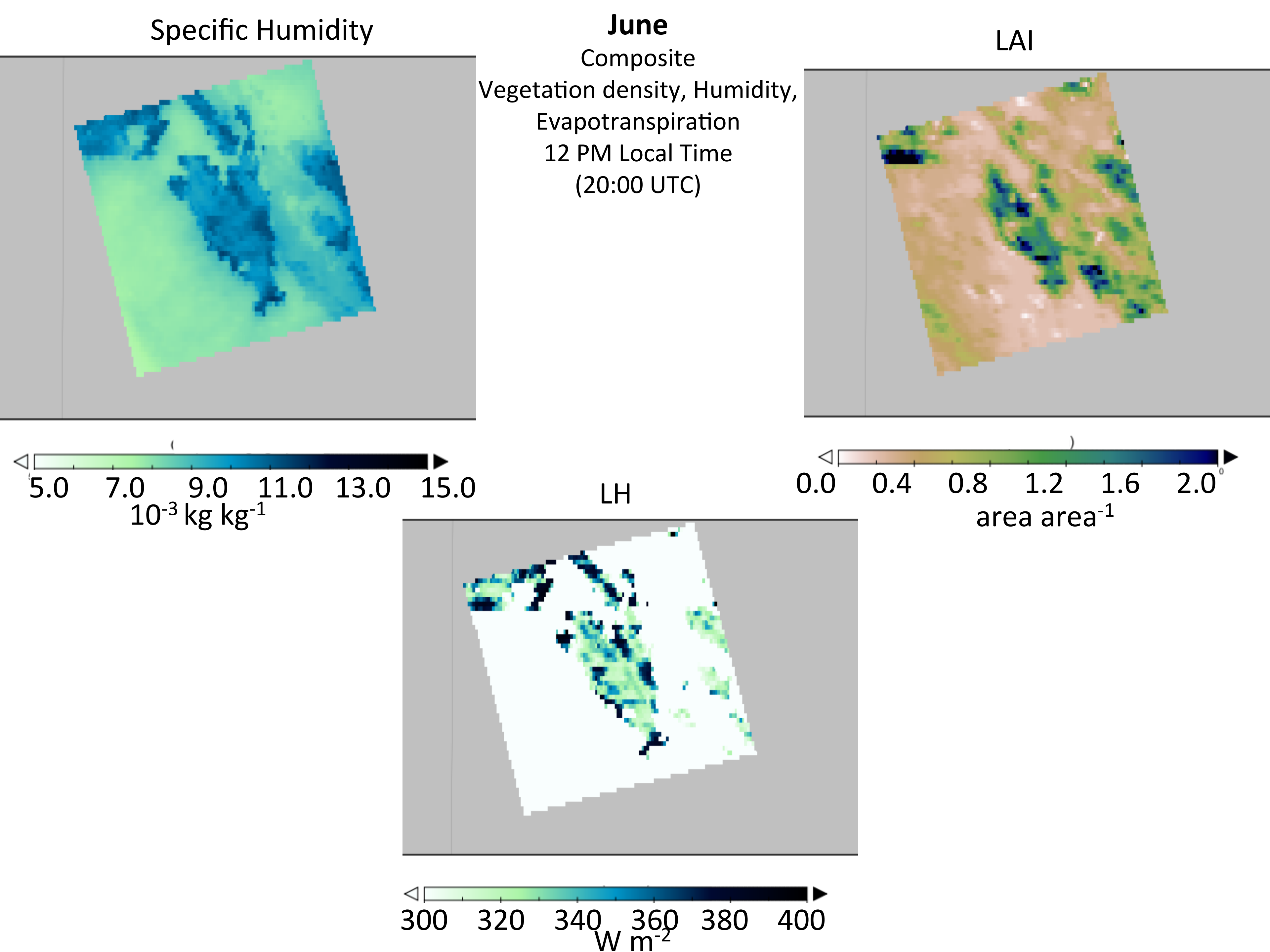

June
Composite
Vegetation density, Humidity, Evapotranspiration
12 PM Local Time
(20:00 UTC)
Specific Humidity
5.0 7.0 9.0 11.0 13.0 15.0
10-3 kg kg-1
LAI
0.0 0.4 0.8 1.2 1.6 2.0
area area-1
LH
300 320 340 360 380 400
W m-2

April: composite-averaged diurnal cycle for Latent Heat

Note: similar curves for May, June, Jul…but maxima are ~100 Wm^{-2} greater

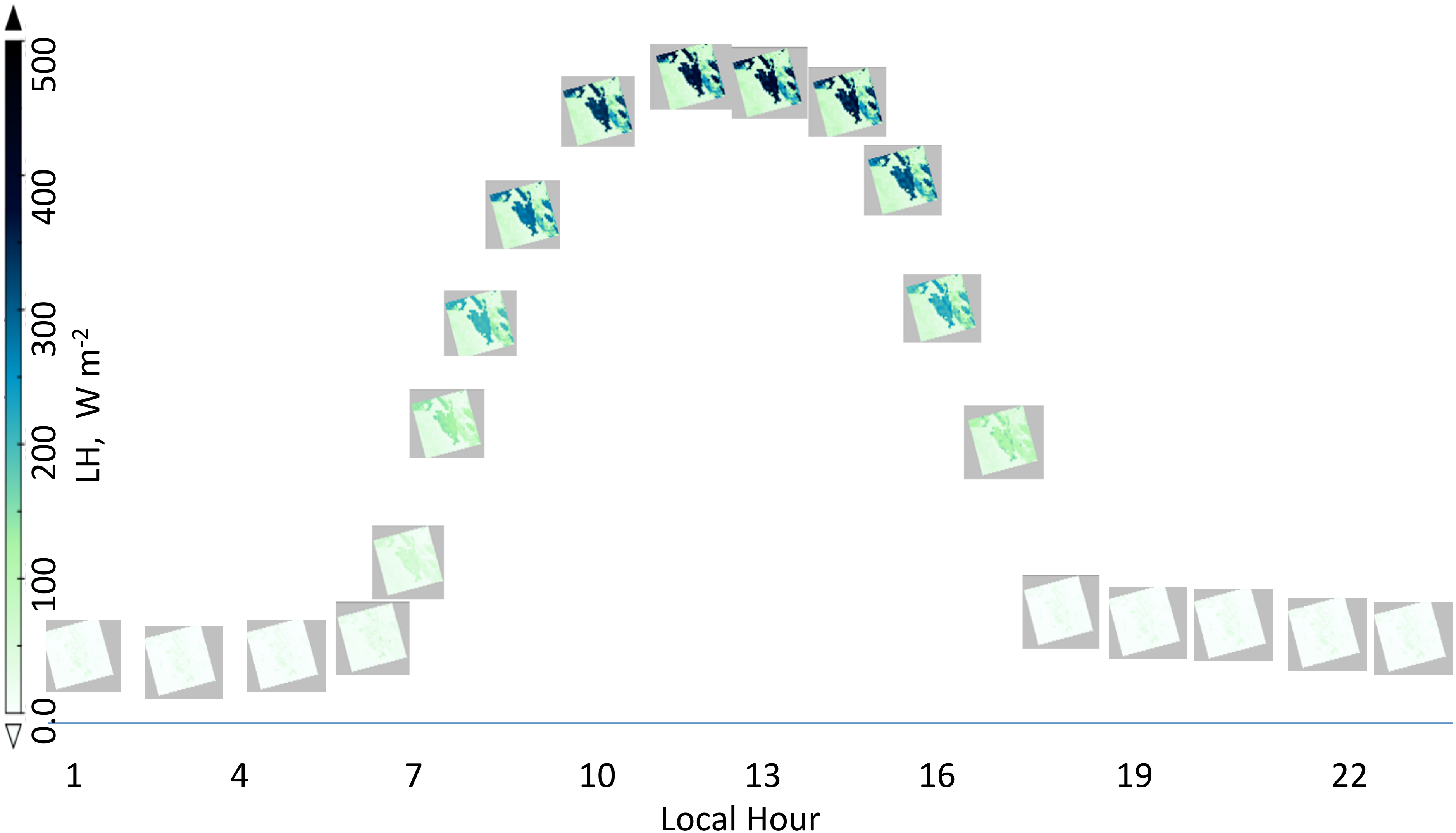

Note: y-axis indicates value of maximum LH for each plot & color scale

Total Seasonal Crop Evapotranspiration (ETc) for Almond Orchards in the San Joaquin Valley

April 1st through August 31st 2008

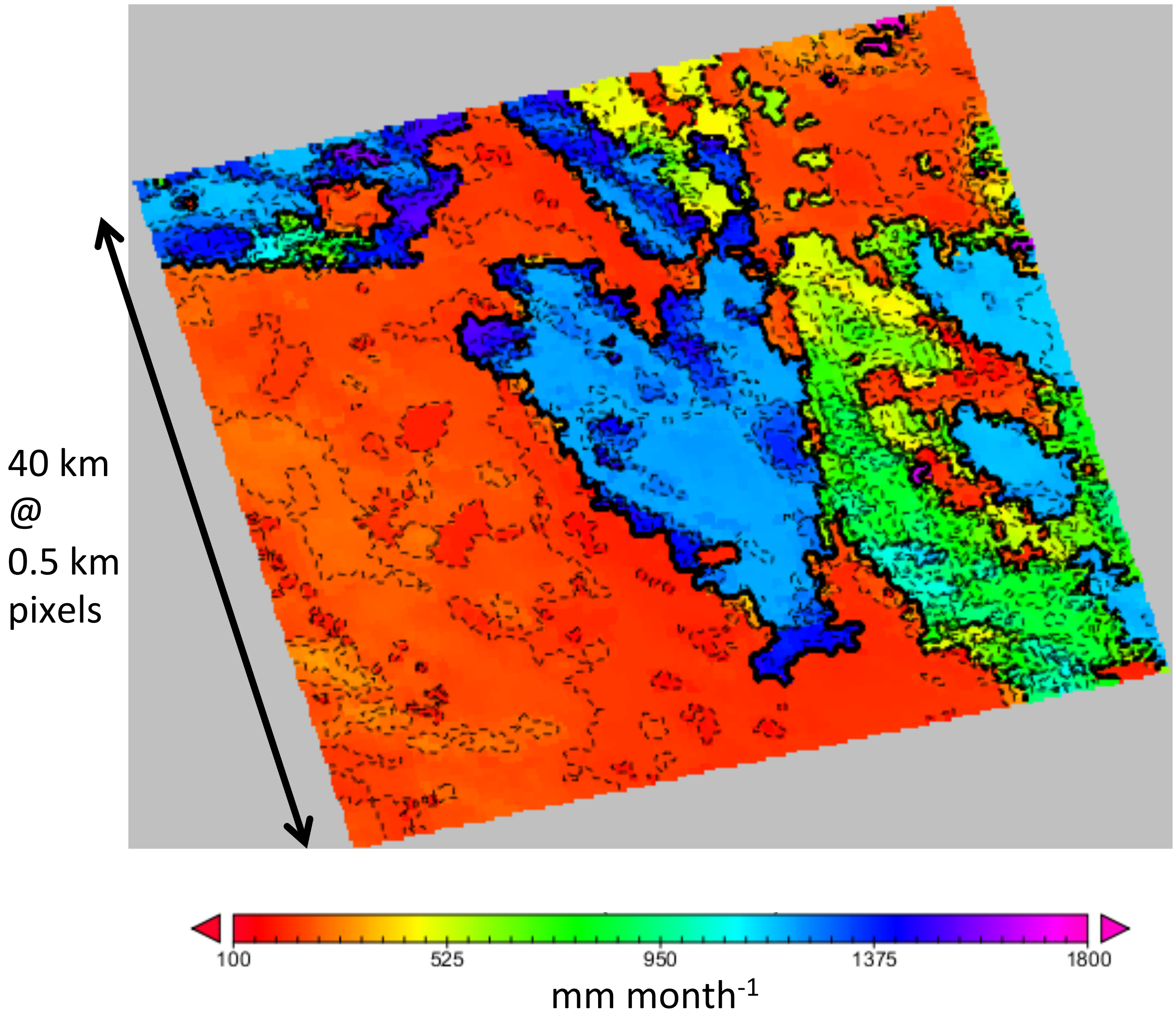

Monthly Evapotranspiration (ET) for Almonds in the San Joaquin Valley

April through August 2008

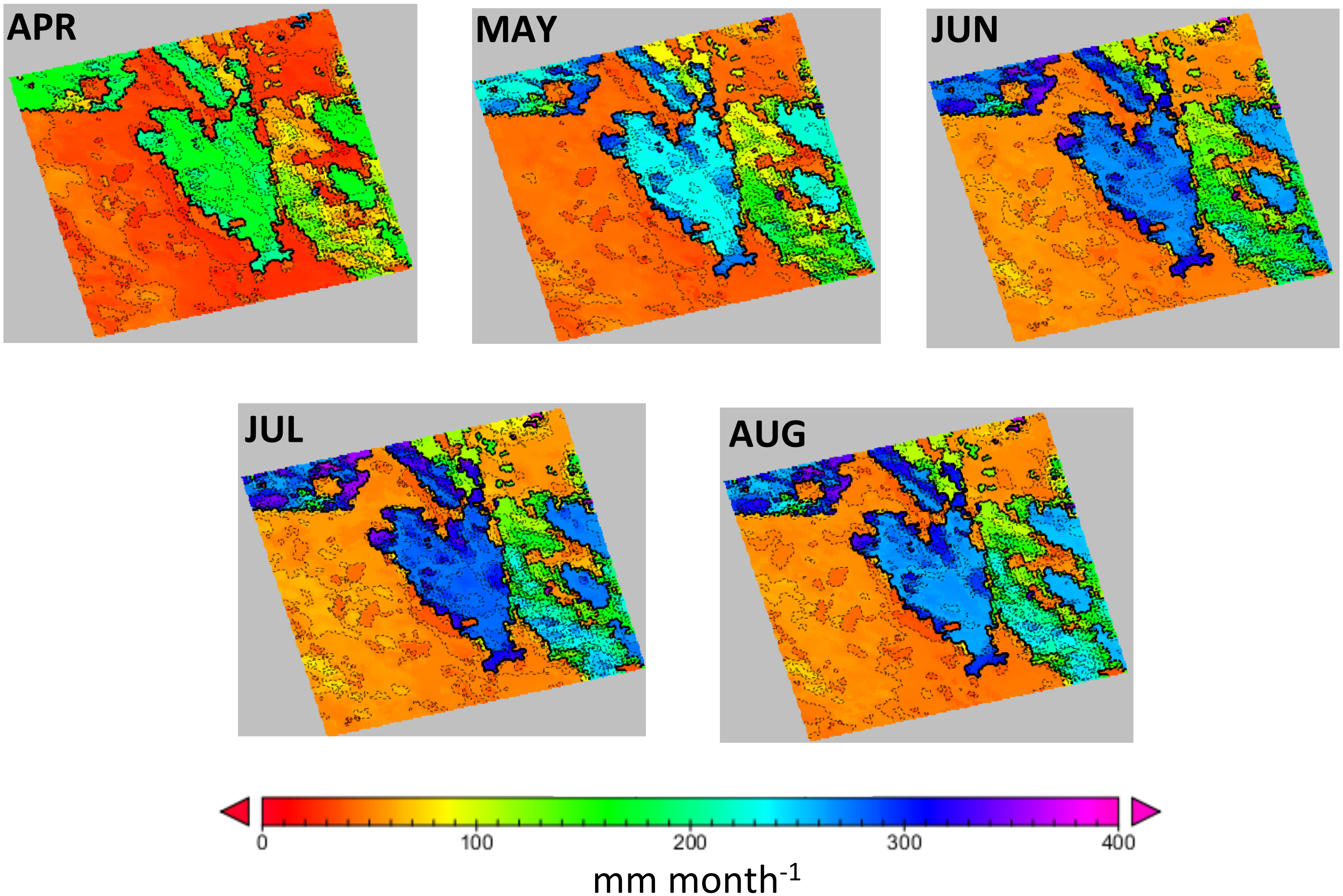

WRF-ACASA Model Inputs Improved by HyspIRI

- Updated vegetation map/ crop type*
  - ACASA can differentiate more plant communities and canopy types
- Leaf Area Index* (LAIgreen) (m^2 m^{-2} 1-sided)

- Leaf PAR reflectivity (0.3-0.7 micron wavelength)
- Leaf NIR reflectivity (0.7-2.0 micron wavelength)
- Soil bkg. PAR reflectivity (0.3-0.7 micron wavelength)
- Soil bkg. NIR reflectivity (0.7-2.0 micron wavelength)
- Vcmax (maximum RuBisCO) (µmol $m^{-2}s^{-1}$) and Jmax
  - Total chlorophylls, carotenoids, xanthophyll cycle, water, Nitrogen, dry matter;

- Distributed skin temperature and emissivity
- Fractional cover

* WRF-ACASA now uses MODIS LAI product, California Augmented Multisource Landcover map

other parameters are assigned via WRF parameter table for each landuse type

April Composite-averaged Plots; 17:00 LT (00:00 UTC)

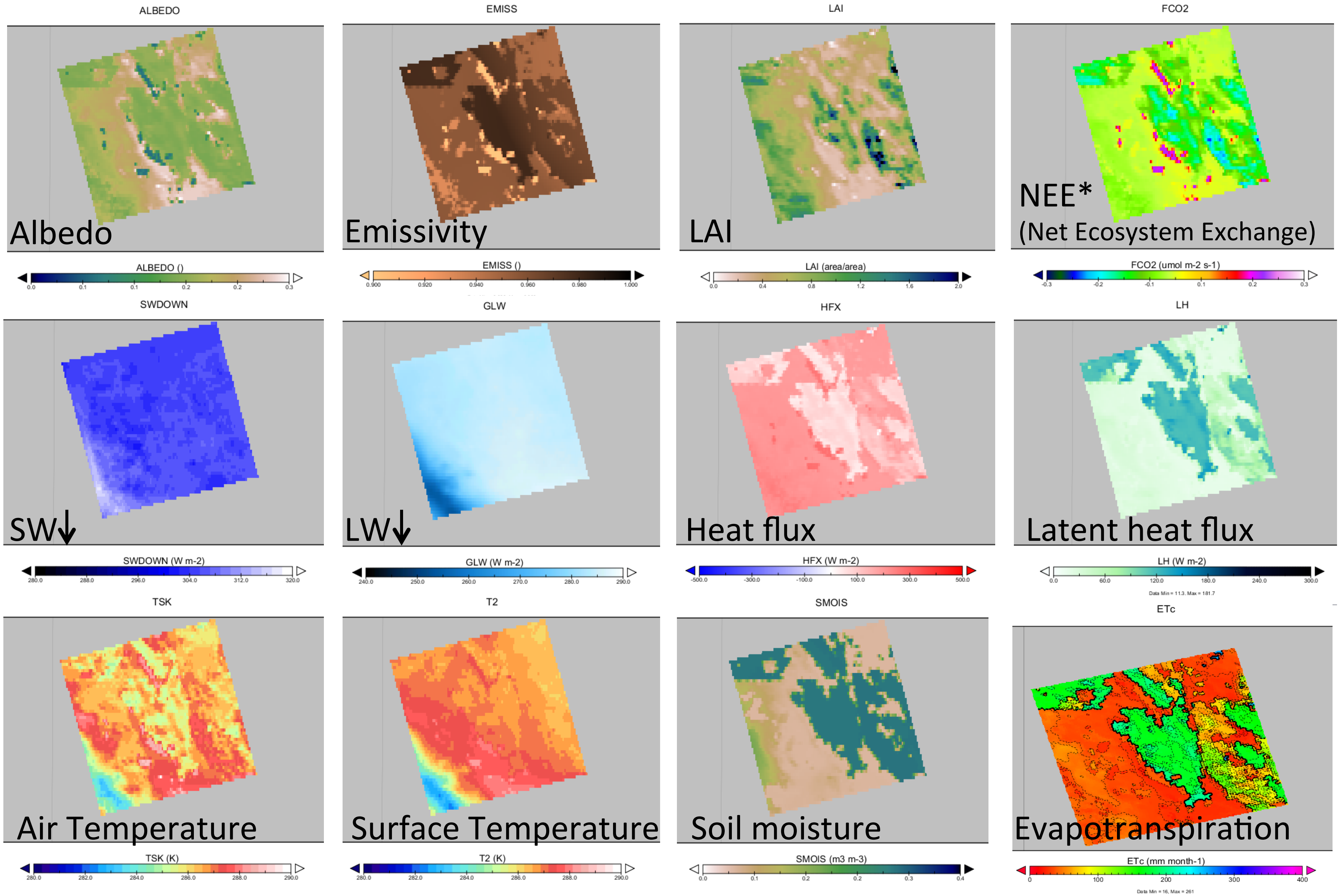

* Can output GPP, NPP, heterotrophic respiration

May Composite-averaged Plots; 17:00 LT (00:00 UTC)

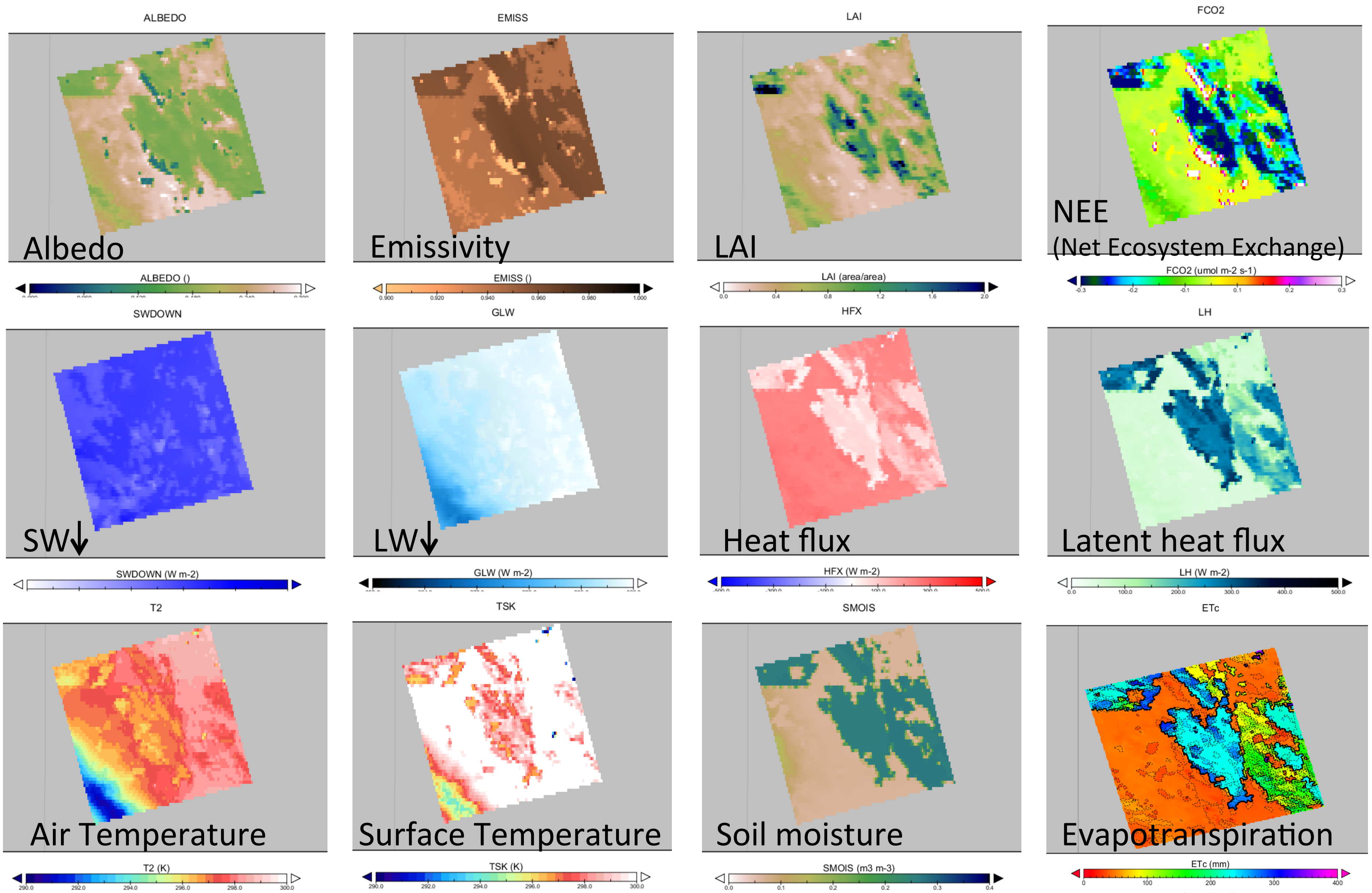

June Composite-averaged Plots; 17:00 LT (00:00 UTC)

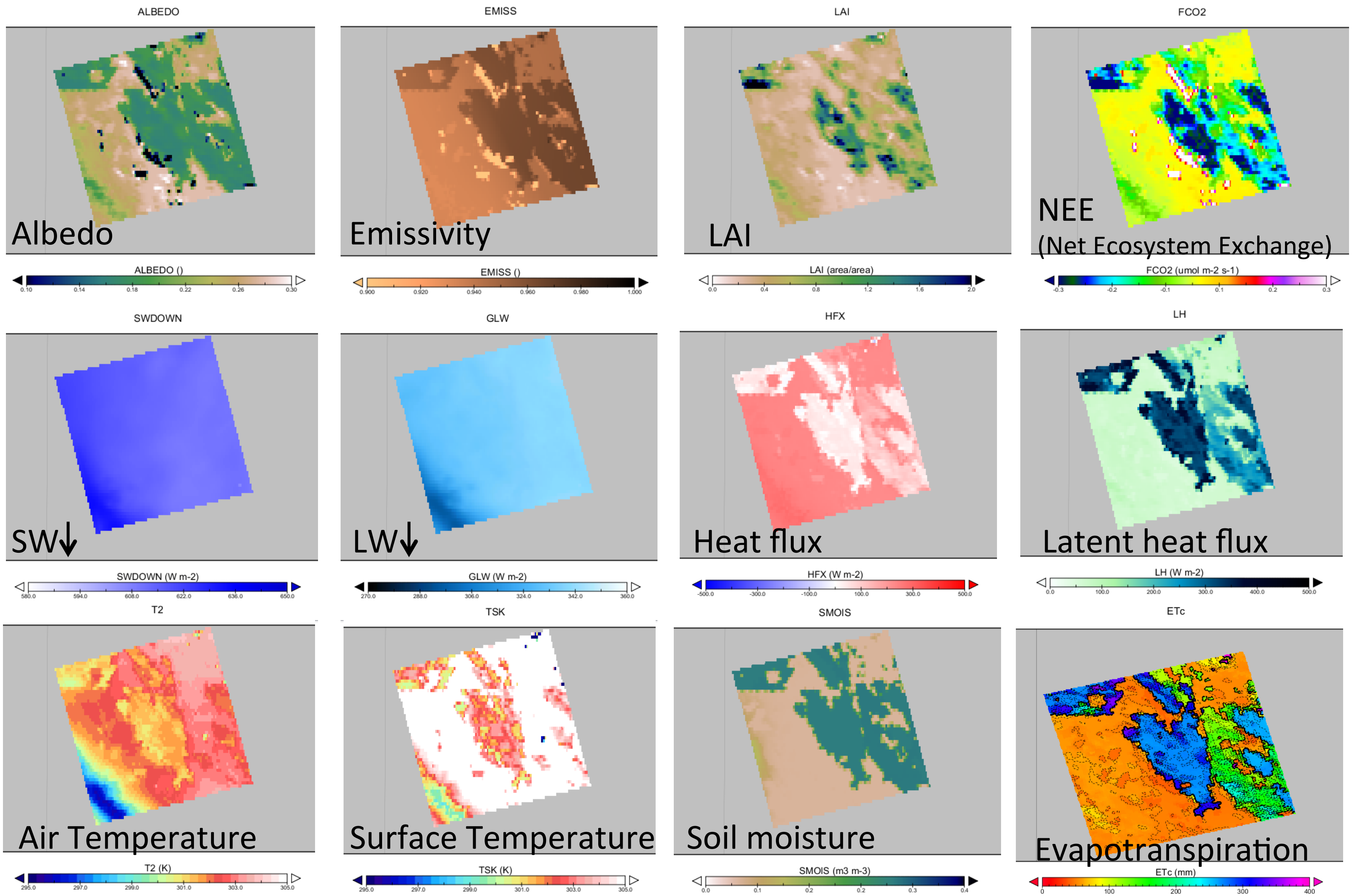

Remote Sensing of Fluxes: *EO-1 Hyperion and Flux Towers*

Question: *Can we demonstrate robust algorithms driven by hyperspectral satellite data that can estimate carbon flux variables through the seasons and over a wide range of sites?*

- *How do spectral properties and temporal dynamics of different ecosystems compare?*
- *Are there common (global) spectral approaches to trace vegetation function?*

Petya Campbell
K. Fred Huemmrich
University of Maryland Baltimore County
May 16, 2012

Data Summary

Preliminary results from studies matching Hyperion imagery to flux towers

Multi-site Historical study

- Match flux data from LaThuile Fluxnet Synthesis with Hyperion
  - 33 different flux tower sites during mid-growing season from 2001 to 2007

Time Series study

- Ongoing observations of 90 tower sites
  - Started 2008
  - Capture seasonal change
  - 20 sites processed

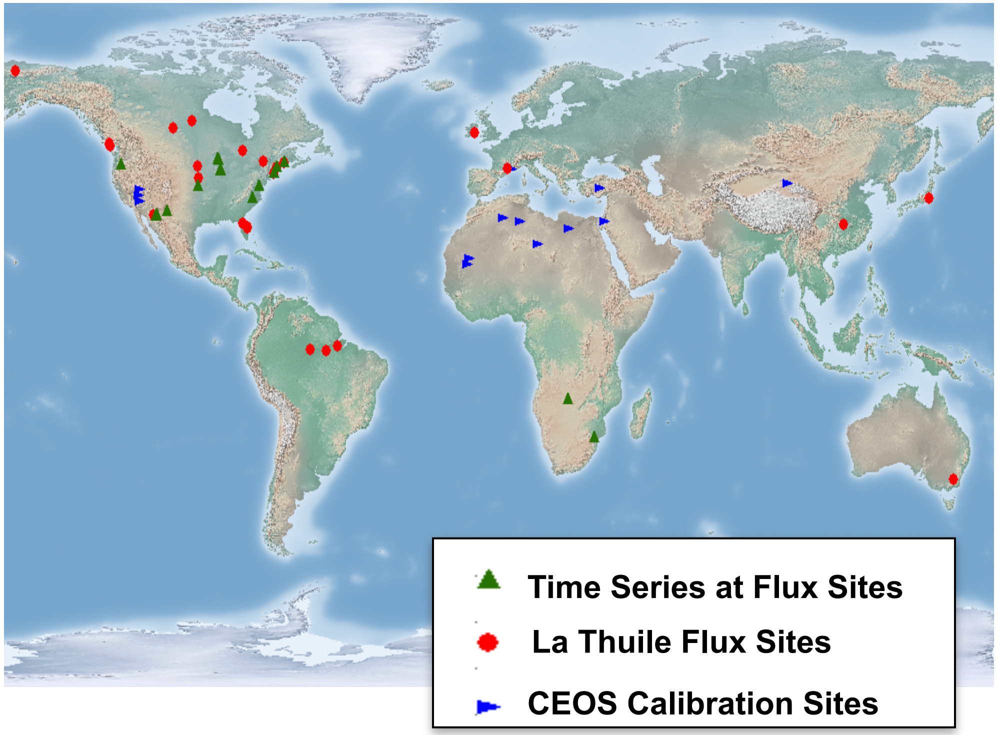

CO_2 Flux Data

Existing global network of flux towers measuring CO_2 flux using eddy covariance techniques provide a consistent ground dataset to work with

- Net Ecosystem Production (NEP, $\mu mol\ m^{-2}\ s^{-1}$) is the total CO_2 flux measured by flux towers.
- Ecosystem Respiration (Reco), the CO_2 flux from the ecosystem to the atmosphere, is calculated from relationships developed between nighttime NEP and temperature.
- Gross Ecosystem Production (GEP), the CO_2 uptake by vegetation, was calculated from the observed NEP and Reco.
- Light Use Efficiency (LUE), the ratio of GEP to photosynthetically active radiation absorbed by vegetation

Time Series at Flux Sites
(examples from 3, 20 being processed)

FLUX Site Name	Location	Climate	Vegetation
1. Mongu lat: -15.4377778, lon: 23.252778 25 images	Zambia, Africa	Tropical/ dry vs. wet seasons/ hot	Kalahari/ Miombo woodland
2. Duke Loblolly Pine, lat: 35.977130, lon: -79.095240 7 images	North Carolina, US	Temperate/ no dry season/ hot summer	Mixed forest/ Hardwoods/ Evergreen
3. Konza Prairie lat: 39.0823925 lon: -96.560277 7 images	Kansas, US	Continental/ cold winter/ hot summer	Grassland/ C4 tall grass prairie

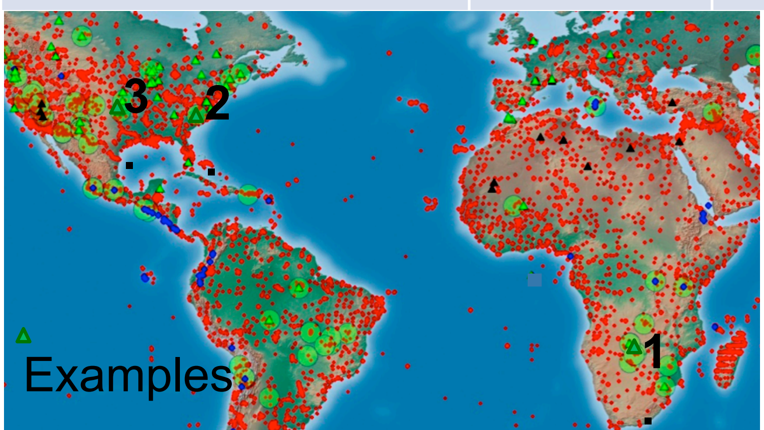

Mongu, Zambia

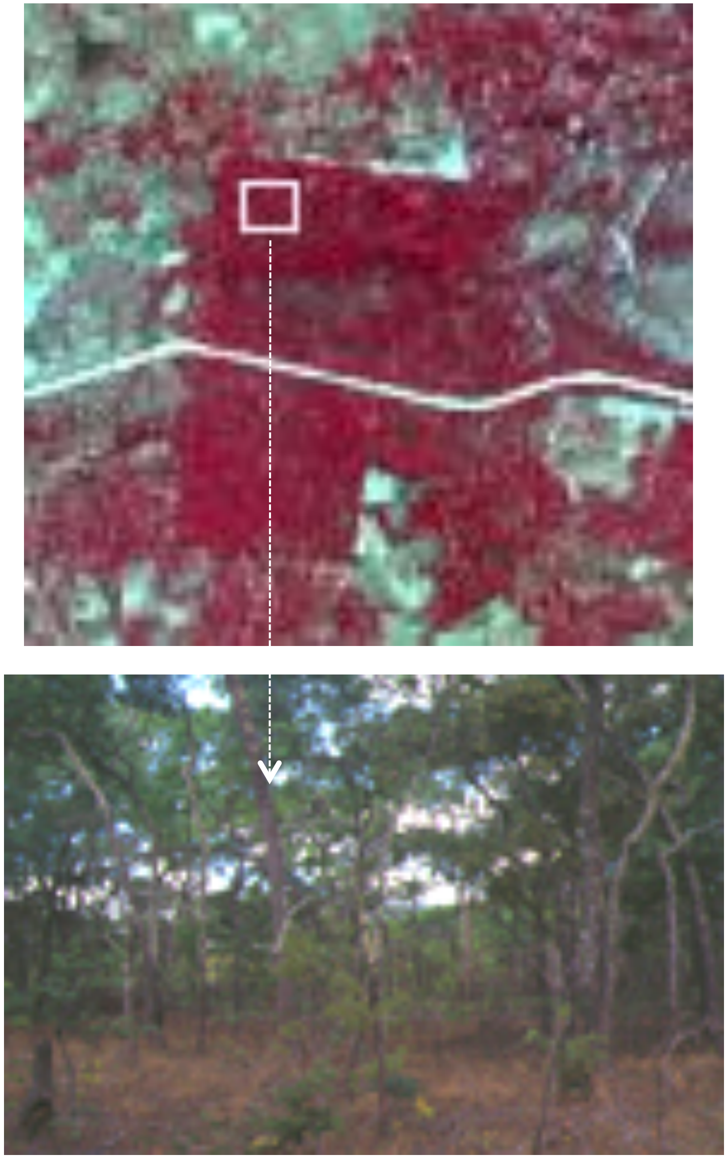

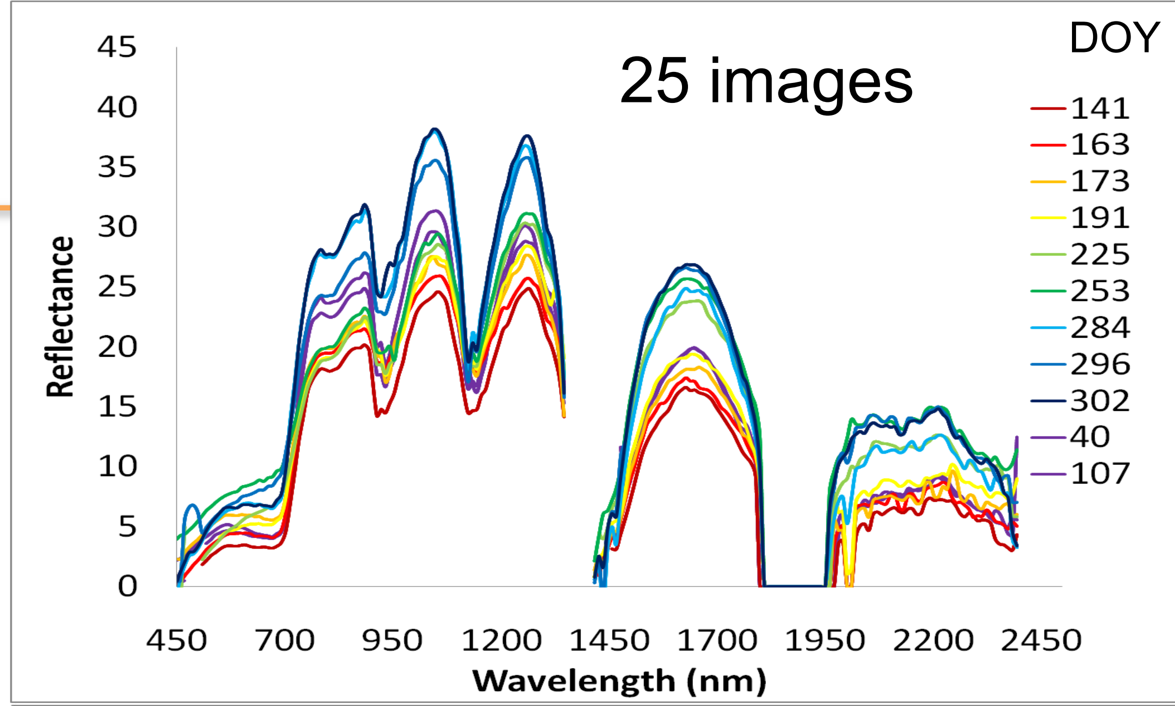

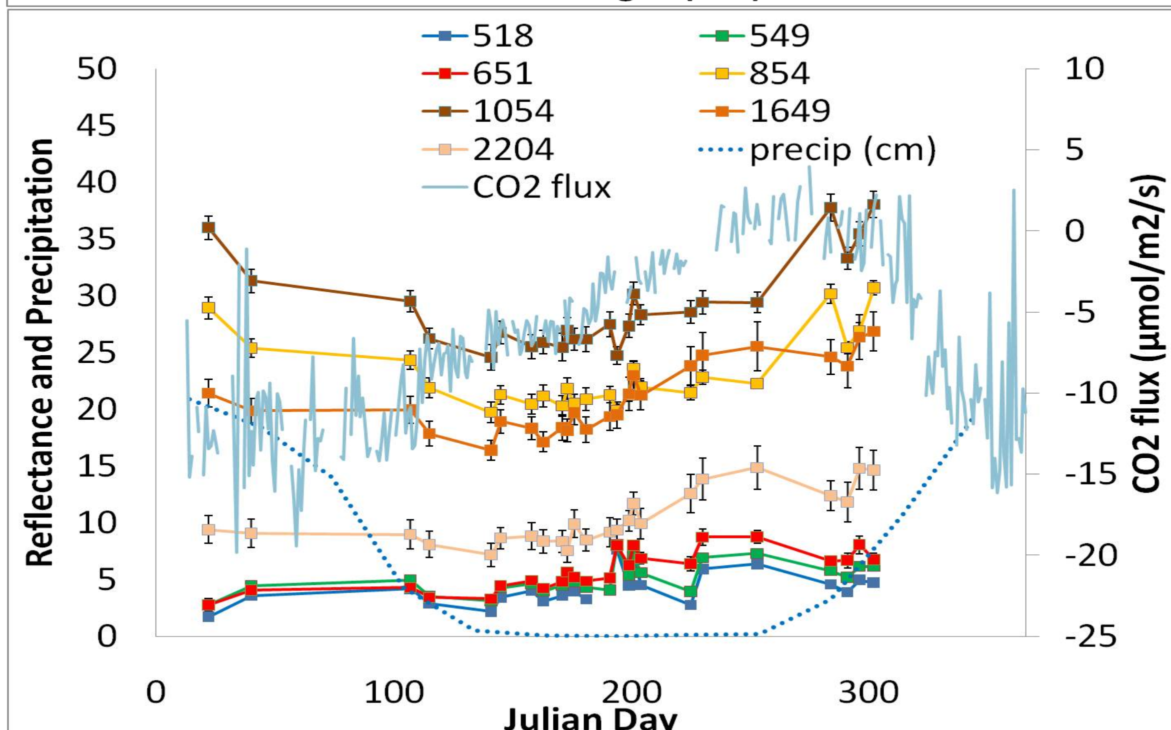

Bio-indicator	Bands (nm)	R^2 [NEP (GEP)]
G32	R750, 700, 450	0.83 (0.81) NL
Dmax	D max (650…750 nm)	0.77 (0.87) NL
Dmax / D704	D(690-730)	0.79 (0.80) NL
mND705	R750, 704, 450	0.75 (0.79) NL
RE1	Av. R 675…705	0.71 (0.56) NL
EVI	R (NIR, Red, Blue)	0.73 (0.88) L
NDVI	Av. R760-900, R620-690	0.52 (0.60) NL

Examined multiple Spectral Indices at each site

- Best for NEP at Mongu was G32
- Associated with Chlorophyll

(Gitelson et al. 2003)

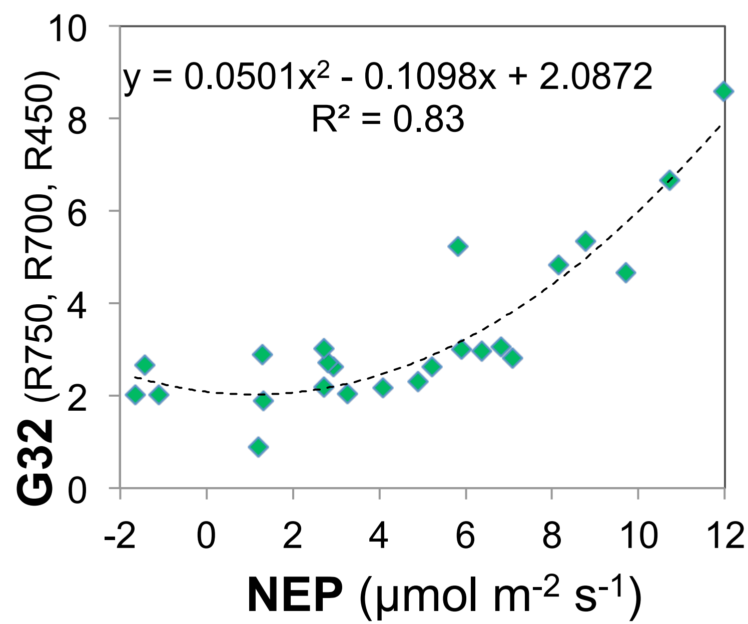

Campbell et al. 2012

Mongu – Hyperion Spectral Indices and NEP

Campbell et al. 2012

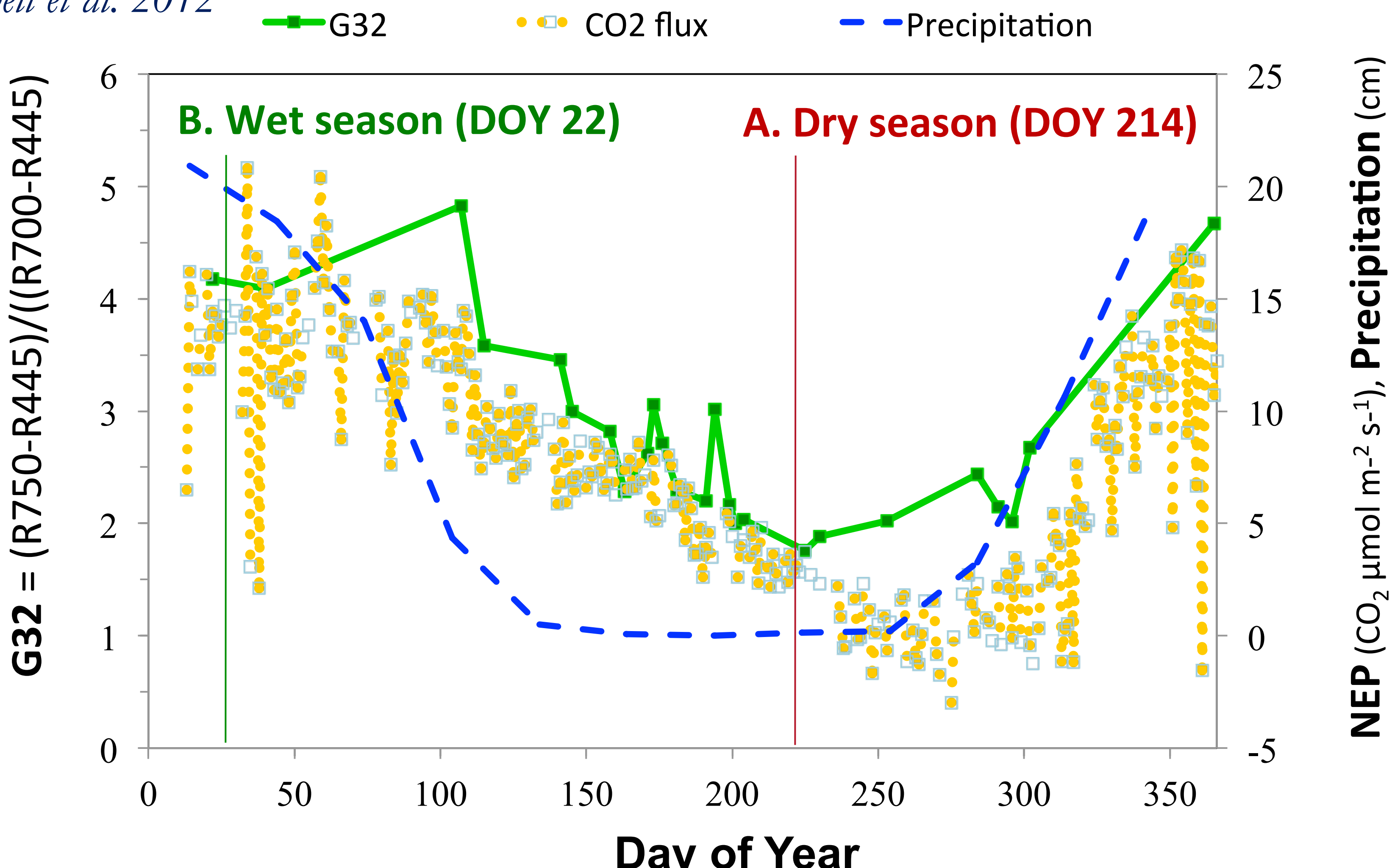

The spectral bio-indicator associated with chlorophyll content (G32, green line) best captured the CO_2 dynamics related to vegetation phenology.

Mongu – Mapping Seasonal Change in NEP

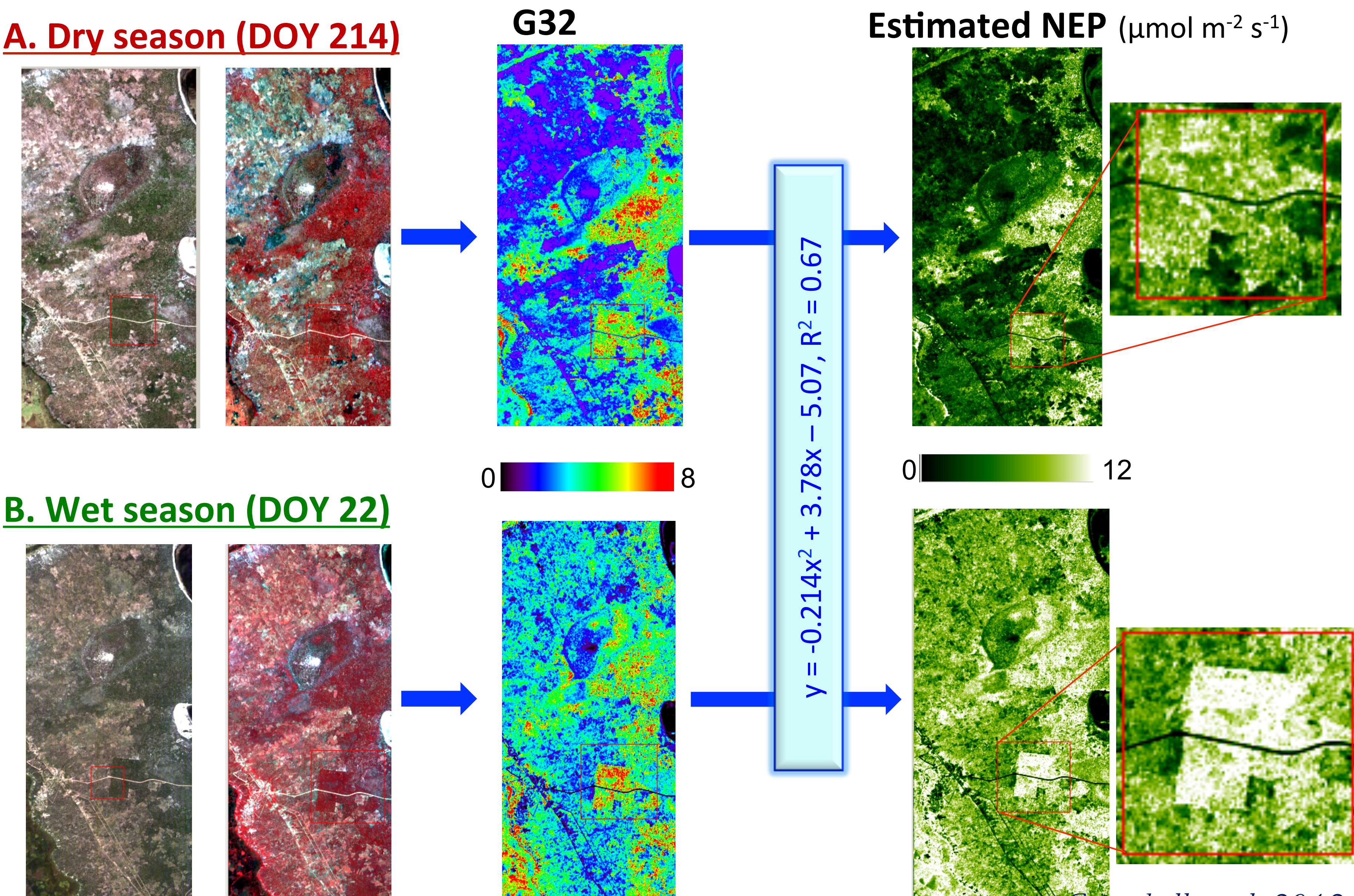

Campbell et al. 2012

Top Performing Vegetation Indices (R^2 values) – Three Seasonal Sites Combined

Spectral indicator	Formula	NEP	GEP	LUE
Dmax	Max D in the 650-750 nm	**0.73 L+**	**<u>0.77</u>** L+	0.75 L+
DP22	Dmax/D(max + 12)	0.65 L+	0.74 NL+	0.71 L+
NDWI	R(870-1240)/R(870-1240)	**<u>0.74</u>** NL +	0.67 NL+	0.63 L+
MCARIa	Chlorophyll, R bands at 700, 670, and 550	0.41 L+	0.75 L+	**<u>0.77</u>** L+
PRI4	(R531-R670)/(R531-R670)	0.66 NL+	0.62 NL+	0.49 NL+
NDVI	(NIR-R)/(NIR+R) NIR= Av. 760..900, R=Av. 620..690	0.56 NL+	0.59 NL+	0.44 NL+

Campbell et al. 2012

39 images

Combined Seasonal Sites – Derivative Maximum

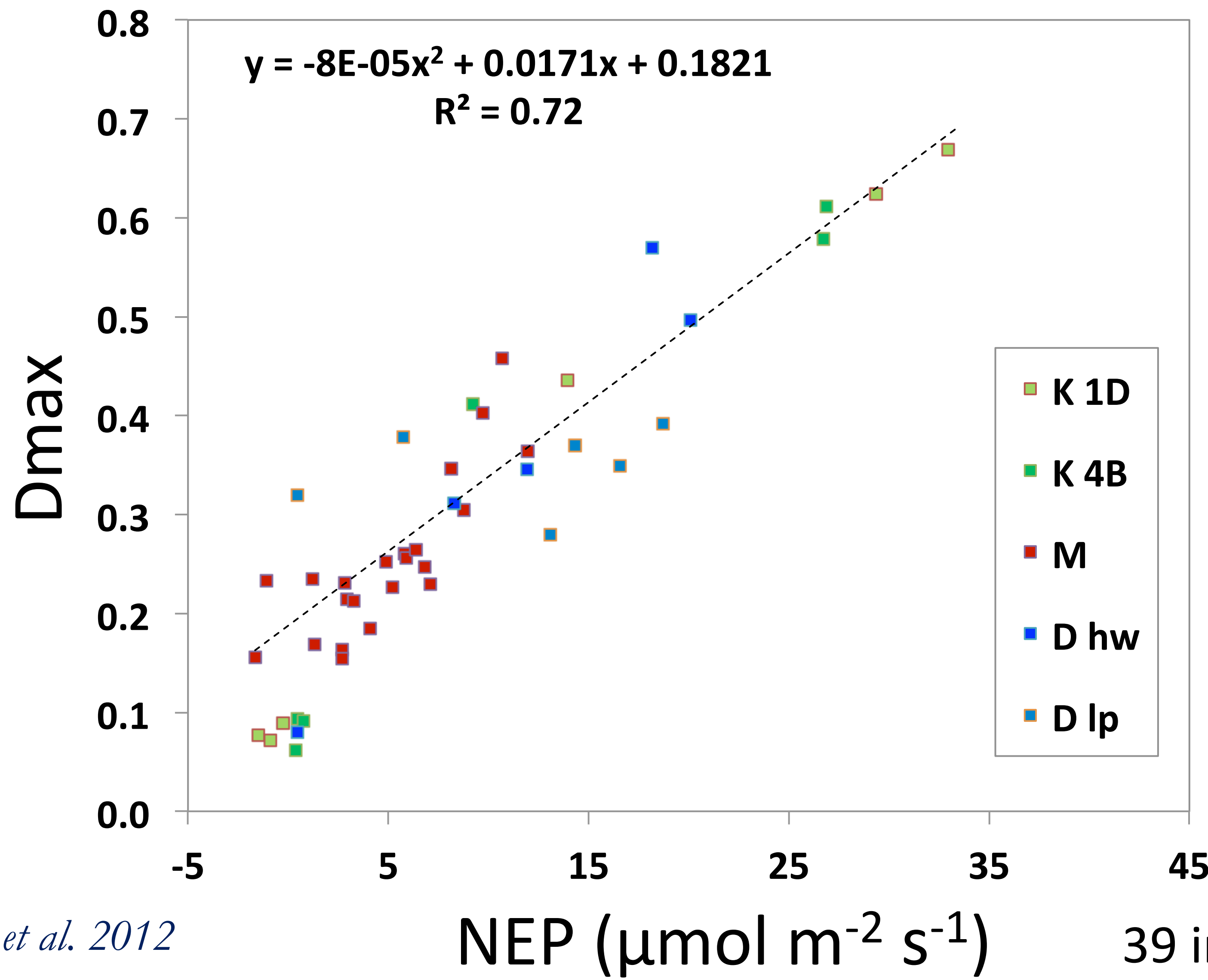

Campbell et al. 2012

39 images

Multi-site – Vegetation Index and LUE

- Best index (out of 107 tried) for LUE at overpass time for 33 different sites was the first derivative at 732 nm divided by the derivative at 712 nm

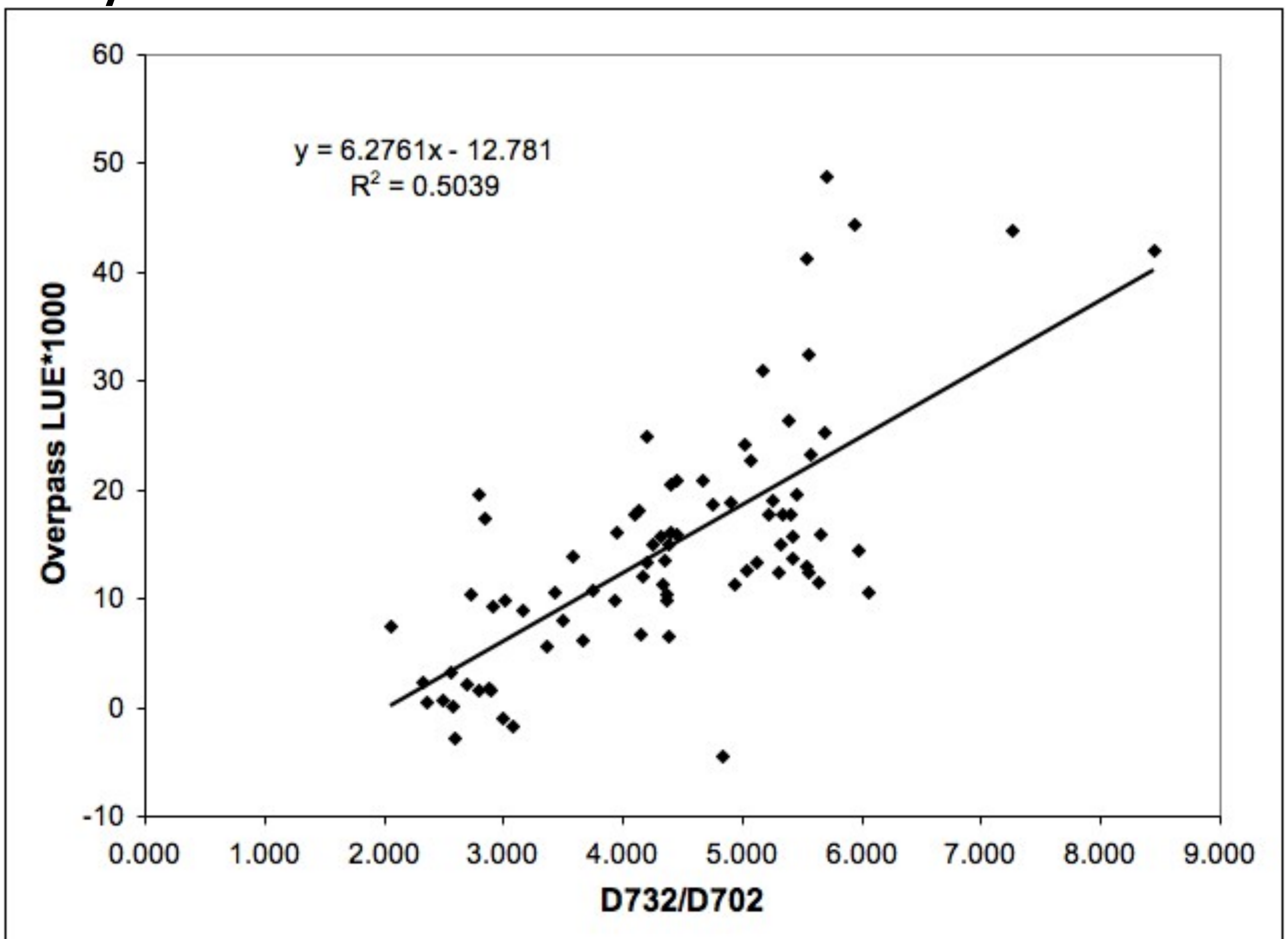

79 Points

Multi-site – Vegetation Index and Reco

- Best index (out of 107 tried) for Reco at overpass time was the Normalized Difference Water Index (NDWI), using reflectances at 876 and 1245 nm

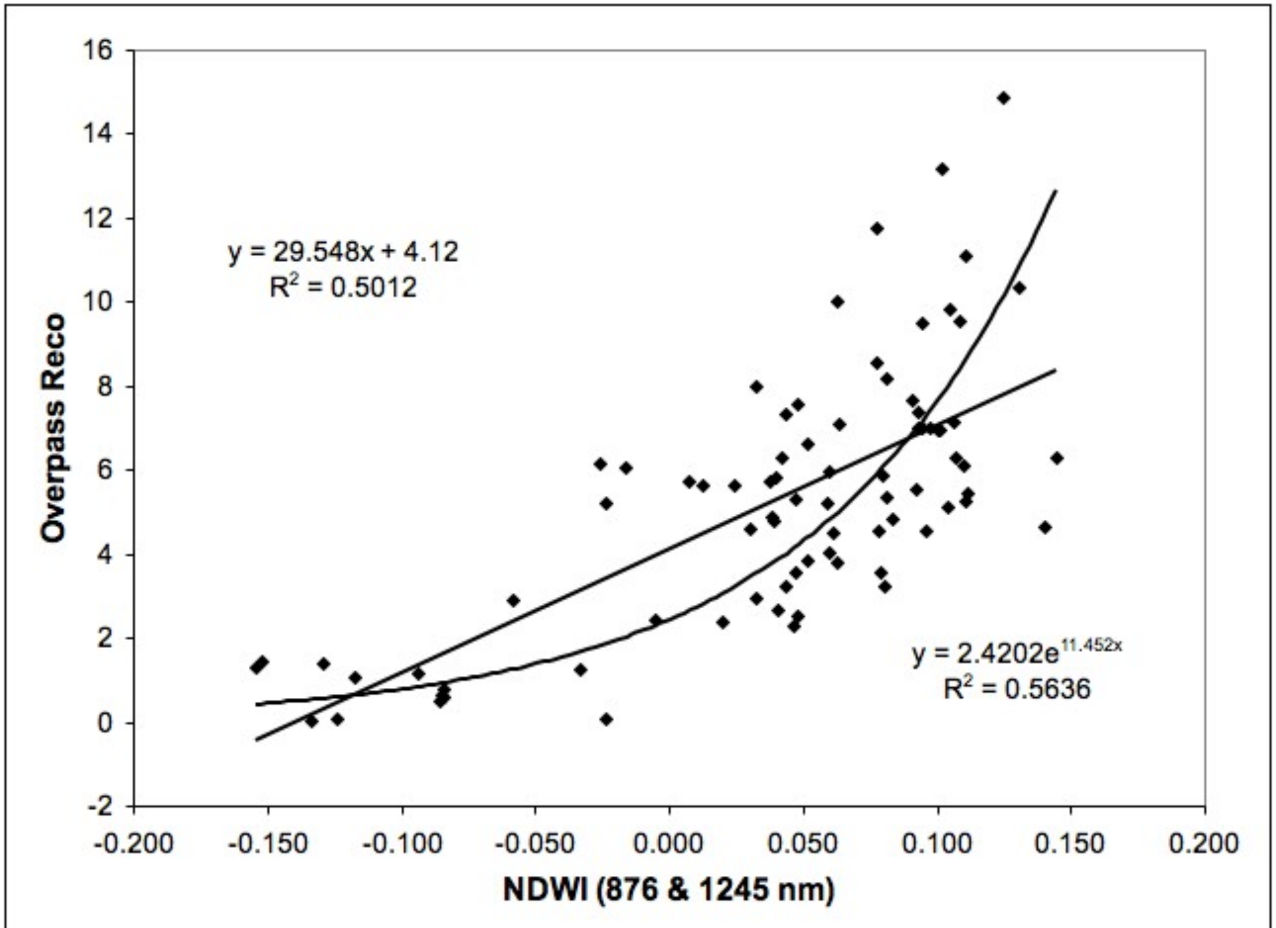

80 Points

Multi-site – Partial Least Squares Overpass LUE

- An example of an approach that utilizes all of the spectral information

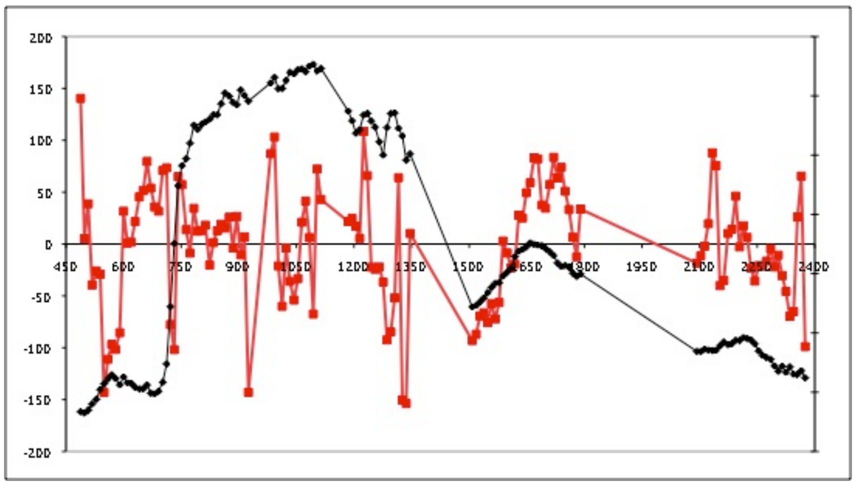

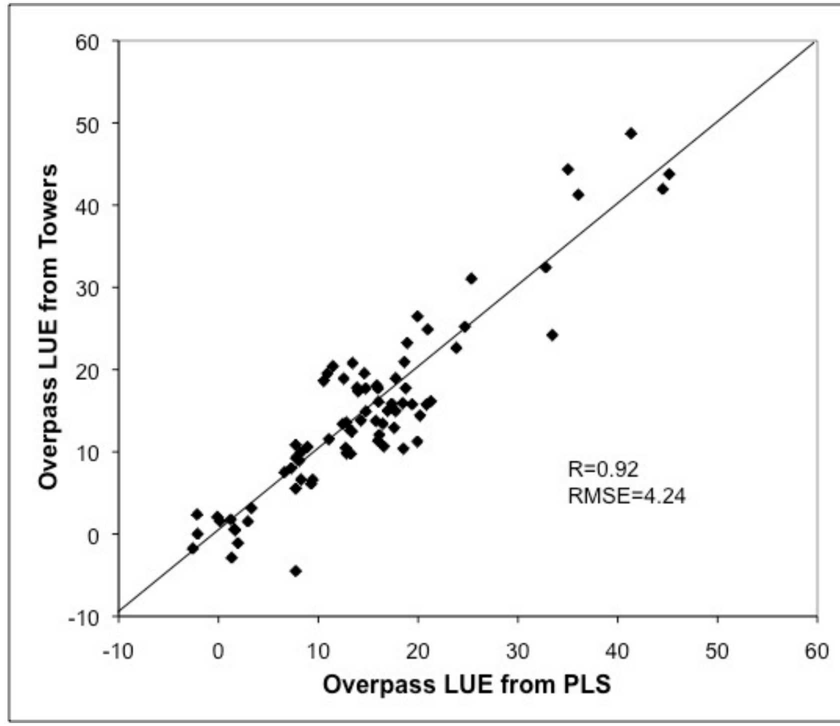

red - PLS coefficients
black - sample reflectance spectra

79 Points

Multi-site – Partial Least Squares Overpass Reco

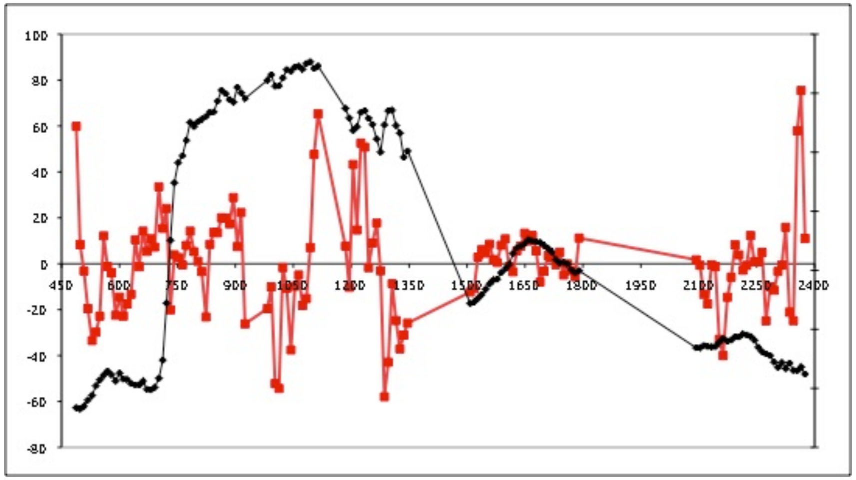

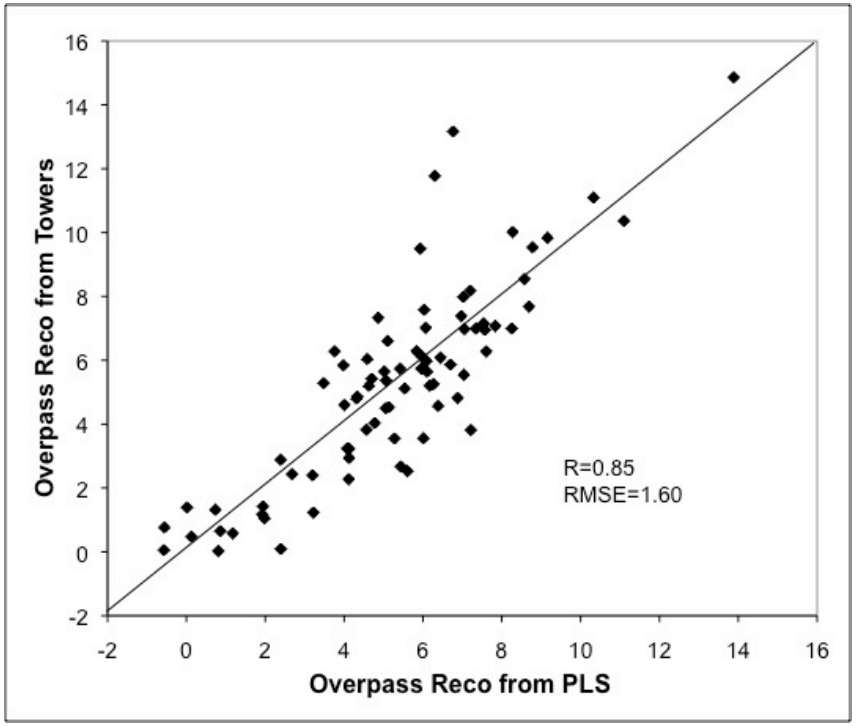

red - PLS coefficients

black - sample reflectance spectra

79 Points

Remote Sensing of Fluxes
Hyperion and Flux Towers

- Hyperion on EO-1 provides us with two important capabilities:
  - the capability of collecting hyperspectral observations of globally-distributed sites, and
  - the ability to make repeated measurements of a site
- Provides a dataset for testing and developing algorithms for global data products
- The strongest relationships with carbon uptake parameters used continuous spectra, numerous wavelengths associated with chlorophyll content, and/or derivative parameters.
- A common (global) spectral approach appears feasible. To derive it will require:
  - Diverse coverage, representing major ecosystem types, and
  - time series, to cover the dynamics within a cover type.

Recommendations

These studies utilize data from the existing flux tower network

For many HyspIRI products we will need more studies applying algorithms for a number of different landcover types

- Use ground, aircraft, and satellite spectral reflectance data
- Need to develop protocols for ground measurements of potential HyspIRI products
- Need to establish network of sites measuring these products
- These sites can grow into a HyspIRI cal/val network

Three years, 150 AVIRIS images

Practical considerations for analyses of large imaging spectroscopy data sets for ecosystem studies

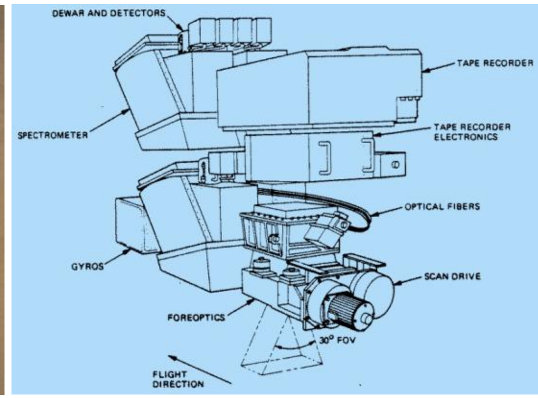

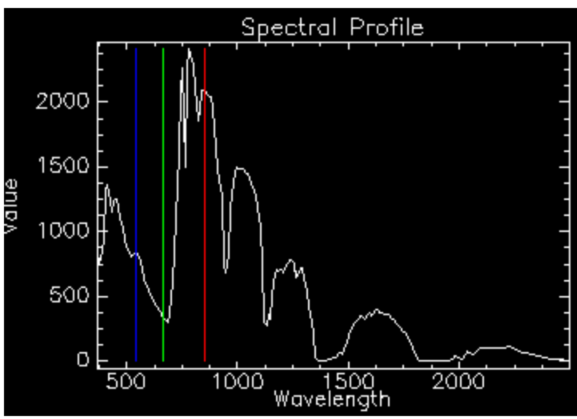

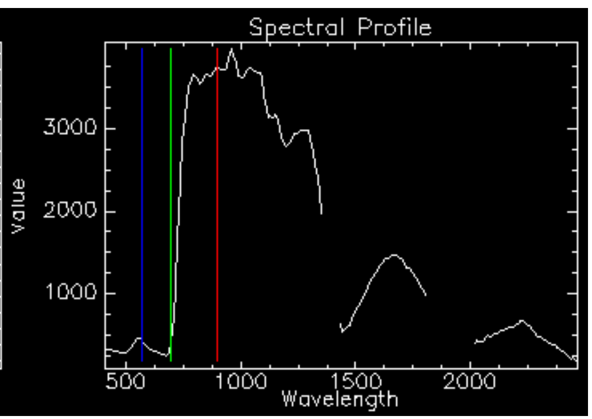

Aditya Singh
Philip A. Townsend

FERST
Forest Ecosystem Remote Sensing Team
Department of Forest and Wildlife Ecology
University of Wisconsin - Madison

The University of Wisconsin Madison

Why does AVIRIS processing matter for HyspIRI?

- Imaging spectroscopy has enabled the retrieval of key canopy foliar biochemical and structural attributes over large scales.
- With the great volume of images that will come from HyspIRI, we will need to ensure that retrievals are consistent across time and space.
- Our biggest worry is having retrieval algorithms that can be applied "globally."
- AVIRIS imagery (and similar airborne data) will be critical to scaling and validation of canopy level estimates from HyspIRI.
- Multi-date, multi-location AVIRIS images are currently our best analogue for HyspIRI.

In order to apply algorithms "globally"….

- **We' ve been trying to figure out what steps in the processing stream are critical to ensuring consistent retrievals.**
- **At UW-Madison, we have worked with >150 AVIRIS scenes from WI, MD, WV, UT, CO, NY, MN and MI spanning 2008-2011.**
- **The scenes are not comparable off the shelf, even if the biological/physical attributes of the ecosystems in them are similar.**
- **All imagery has issues with:**
  - Occlusion by clouds, cloud-shadows,
  - Terrain effects,
- **Airborne images may have particular issues with:**
  - Along and across-track illumination gradients
  - Possible geo-location errors

Example: Baraboo Hills WI, 2008 AVIRIS campaign

The "best-case" scenario: Scenes from the same location, taken a short time interval apart, same flight geometry.

- Hypothesis: retrievals should match **exactly.**

The data:

- Baraboo Hills, WI; Two images, acquired 13th July 2008.
- ~20min apart (UTC 16.099 – UTC 16.426)
- Same general coverage and flight orientation (77.12°)
- ~3° difference in solar elevation (57.03° – 59.92°)
- ~6° difference in solar azimuth (122.07° – 128.75°)

Spectra extracted from 30 forested sites

- Averaged in a 3X3 window to simulate a ~50m. Plot (17.8*3m.)
- Martin et al. (RSE 2008) coefficients applied to get canopy N%.
- Gitelson & Merzlyak (JPP 1996) for Chlorophyll-a.

Example: Comparison of reflectance, no other corrections applied

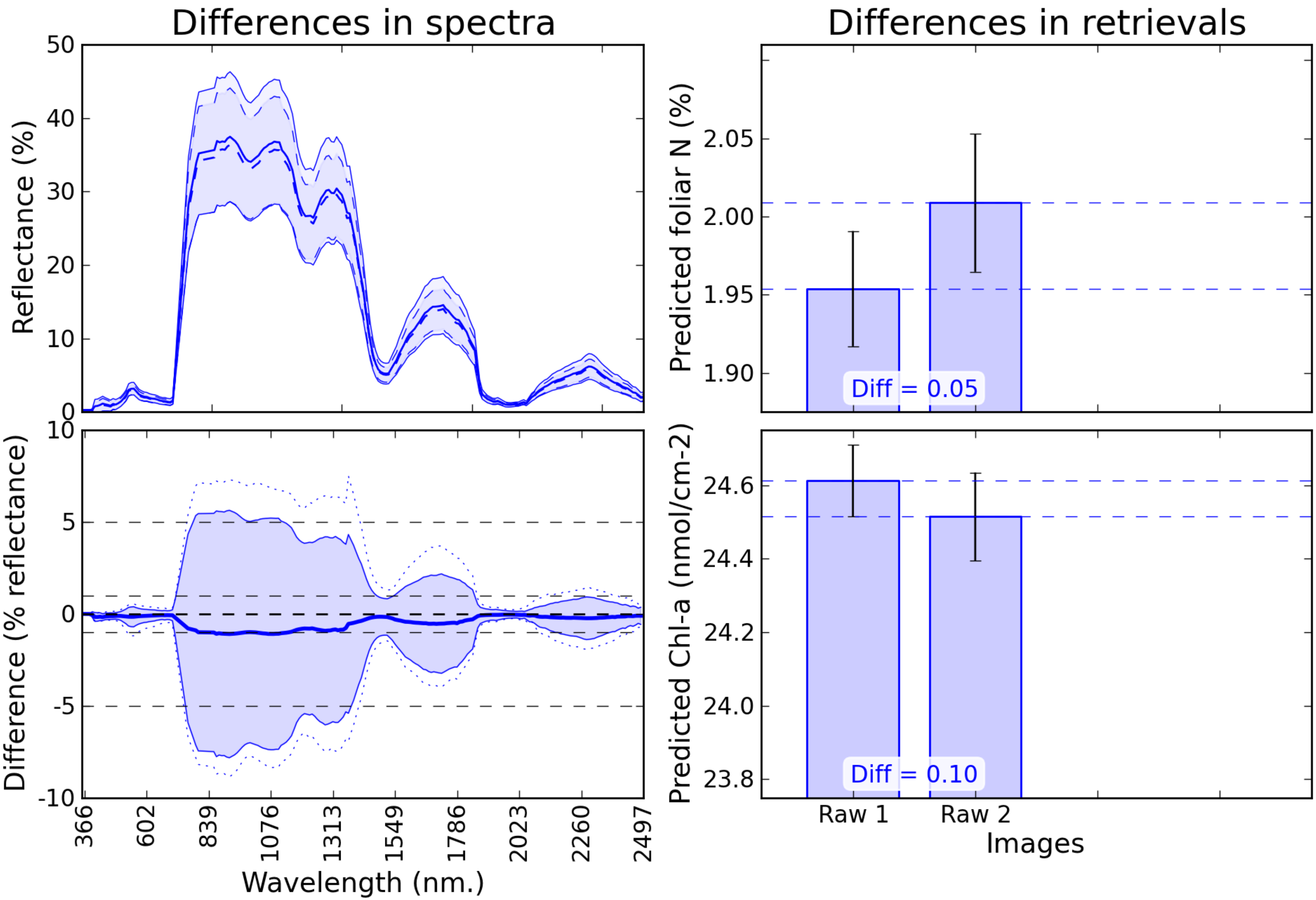

AVIRIS Pre-processing: Steps

Raw image

Cloud, shadow, water mask

Atmospheric correction

Cross-track correction

Terrain normalization

Precision georeferencing

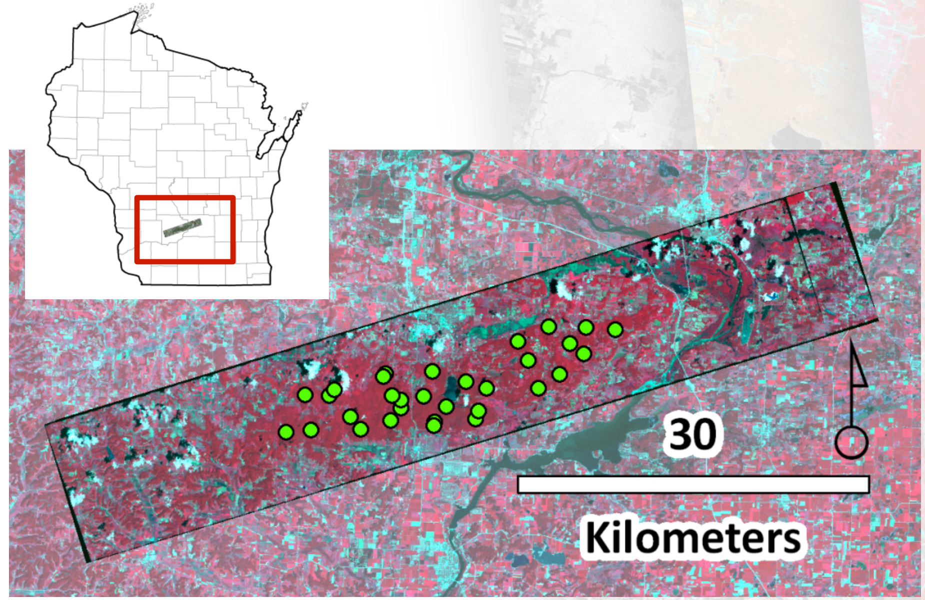

AVIRIS Pre-processing: Atmospheric correction

1. Atmospheric correction: one of the following…
   - ACORN5b
   - ATREM (TAFKAA)
   - ATCOR4 (explicit scan line geometry)

AVIRIS Pre-processing: Cloud/Shadow mask development

2. **Cloud/Shadow mask development**
   - Important because other corrections depend on it

- **Band thresholding does not always work!**
  - All images need to have the exact radiometric behavior (… same for Image indices)

- **Gaussian mixture modeling** (of bands, indices, histograms)

$$DN = \sum_{i=1}^{n} \pi_i \left(N(\mu_i, \sigma_i) \right) \quad \textbf{and...} \quad \sum_{i=1}^{n} \pi_i = 1$$

  - **Works as long as histograms have same number of peaks**
    - 2 peaks if bright clouds and dark background
    - 1 peak if only background (or no clouds, or all haze)
    - >2 peaks if clouds and haze (…etc.)
  - **…still need to find breakpoint to threshold**

AVIRIS Pre-processing: Cloud mask development

…Problems with Gaussian mixture modeling when number of histogram peaks indeterminate

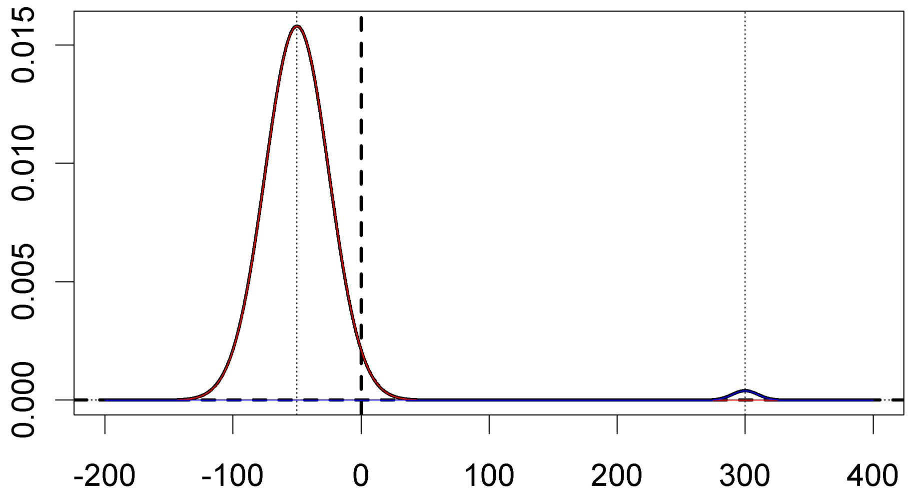

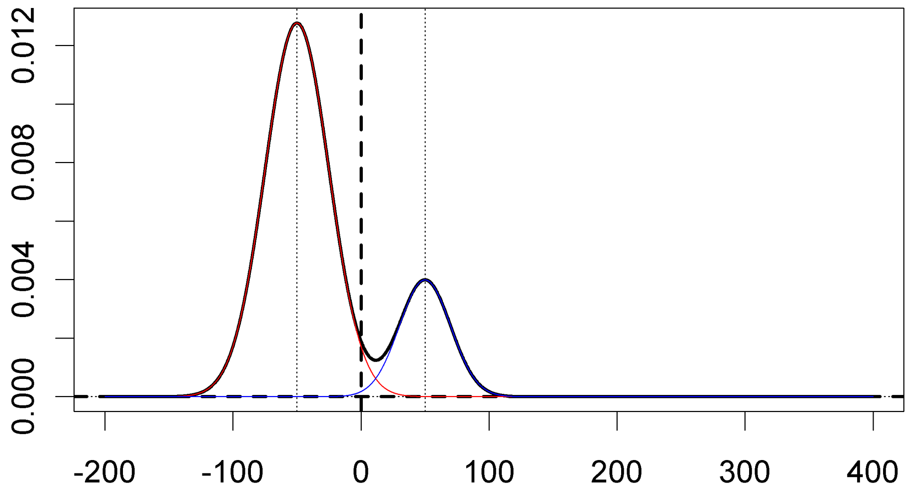

AVIRIS Pre-processing: Cloud mask development

Mixture modeling needs predetermined number of peaks to estimate parameters.

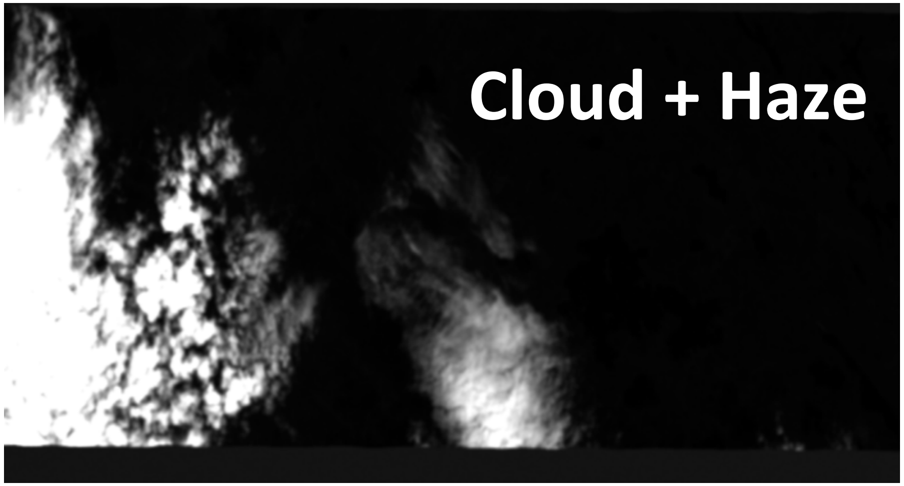

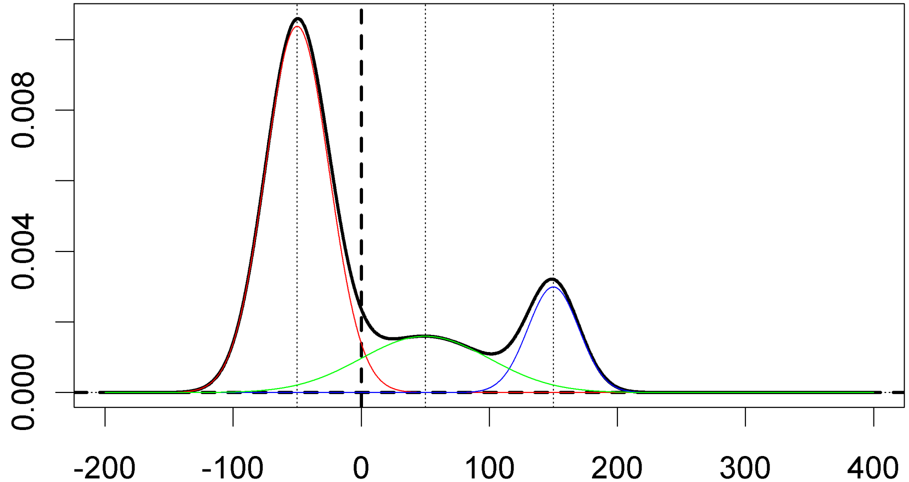

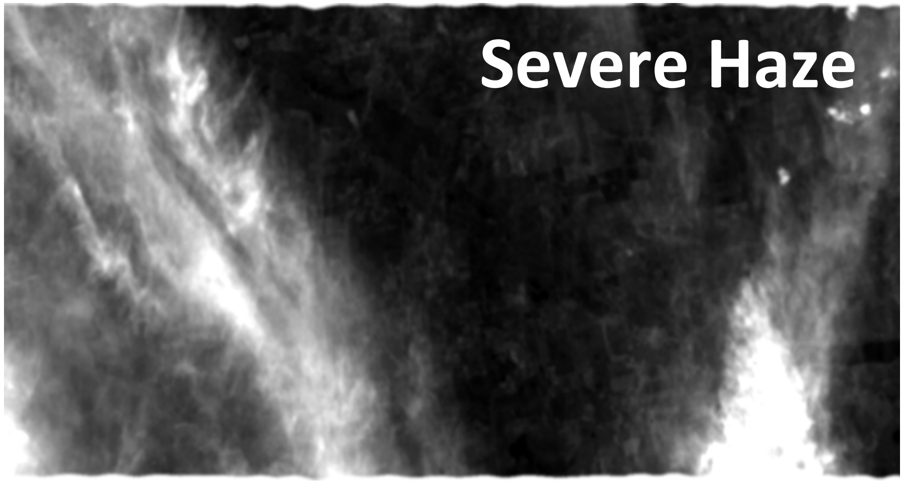

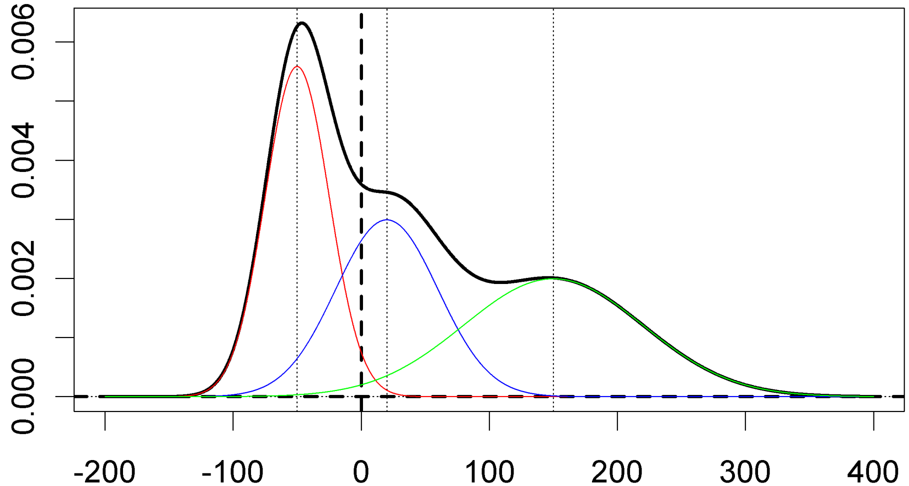

AVIRIS Pre-processing: Cloud mask development

Approach: Reflected Histogram Thresholding (RHT)

- **First, get "best estimate" of bright pixels:**
- Use a Mixture Tuned Match Filter (MTMF) to generate "abundance" images:
  - **Clouds:** 1.33nm^{B106}-1.38nm^{B110} and 1.77nm^{B149}-1.81nm^{B153} using *band maximum as target spectra.*
  - **Shadows:** 1.17nm^{B87}-1.30nm^{B102} *array of zeros as target spectra.*

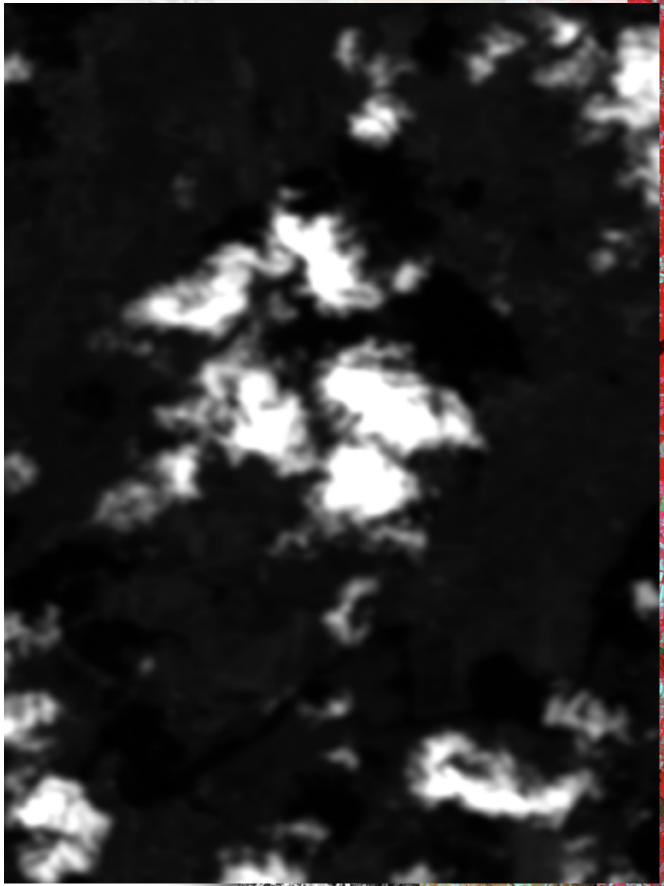

AVIRIS Pre-processing: Cloud mask development

Reflected Histogram Thresholding:

1. Build histogram of MTMF abundance
2. Find peak of histogram in negative region (= background)
3. Get histogram to the ‘left’ of peak (this is the leading edge of the ideal ‘background’ histogram)
4. ‘Reflect’ it onto the other side to complete distribution

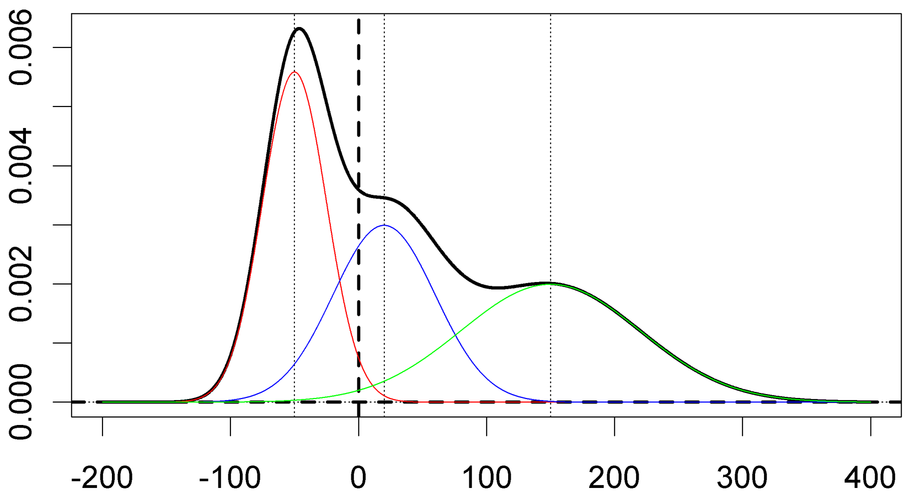

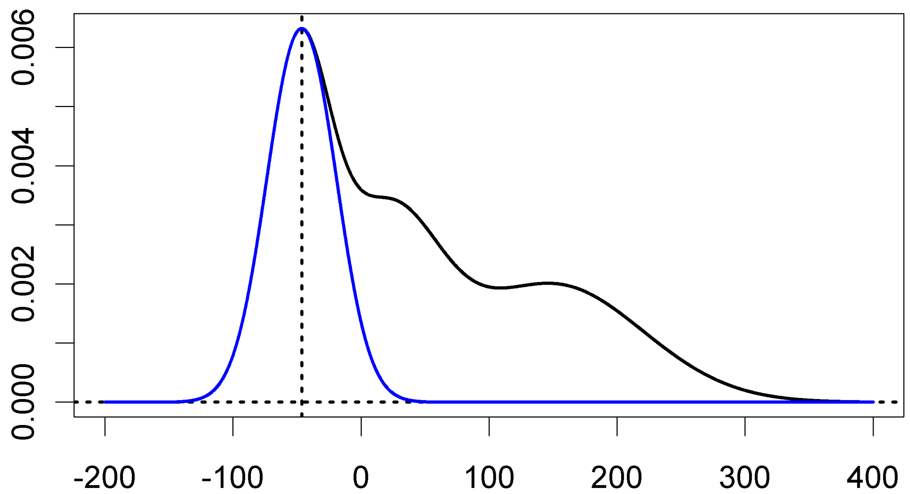

5. Calculate mean, stdev. from constructed histogram
6. Calculate Z-score of image, invert PDF, threshold by *P* ~> 0.95

AVIRIS Pre-processing: Shadow mask development

Shadow masking:

- Same as clouds, but easier because shadows are consistently dark:
  - Do MTMF using vector of zeros as reference spectrum.
  - Threshold resulting ‘shadow fraction’ image by 400.

Effect of modulating *P* cutoff, or shadow threshold

- Low *P* misses clouds.
- High *P* includes most Urban areas, bright soil, some bright Veg.
- Low shadow threshold includes deeply shaded terrain.

“Features” not “Problems”

- Rather than clouds or shadows, we are more interested in anomalously bright or dark objects that may affect overall image radiometry.

AVIRIS Pre-processing: Cloud/Shadow mask development

RHT results: Combined cloud/haze + shadow/water masks

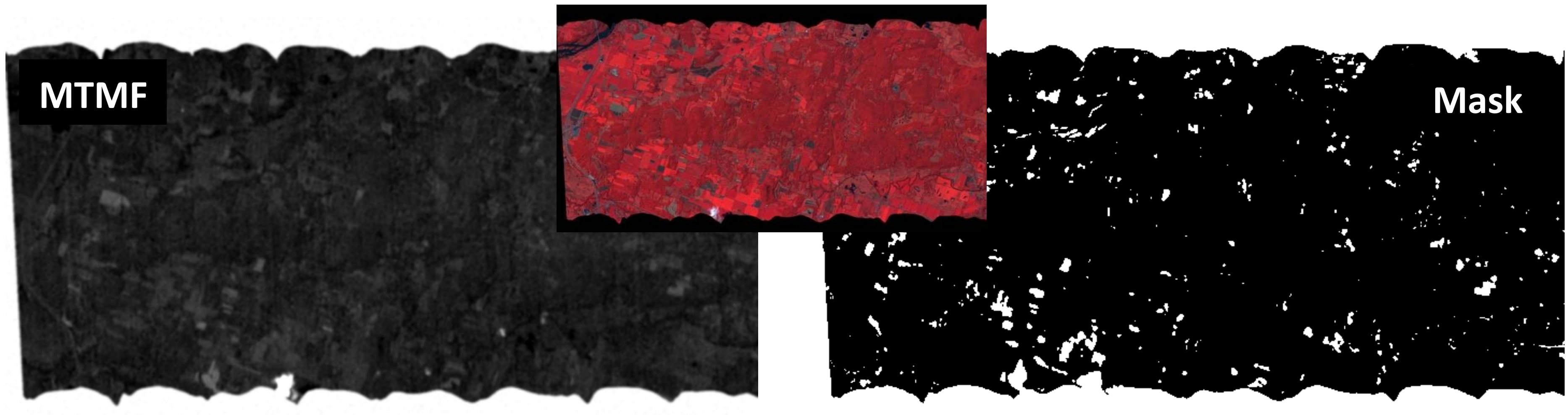

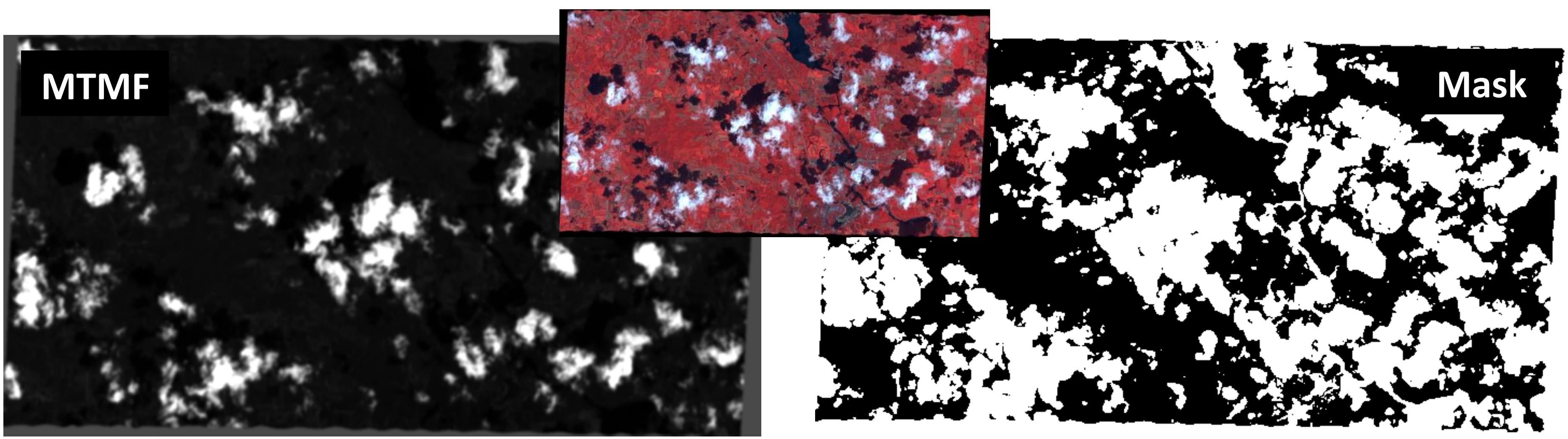

AVIRIS Pre-processing: Cloud/Shadow mask development

RHT results: Combined cloud/haze + shadow/water masks

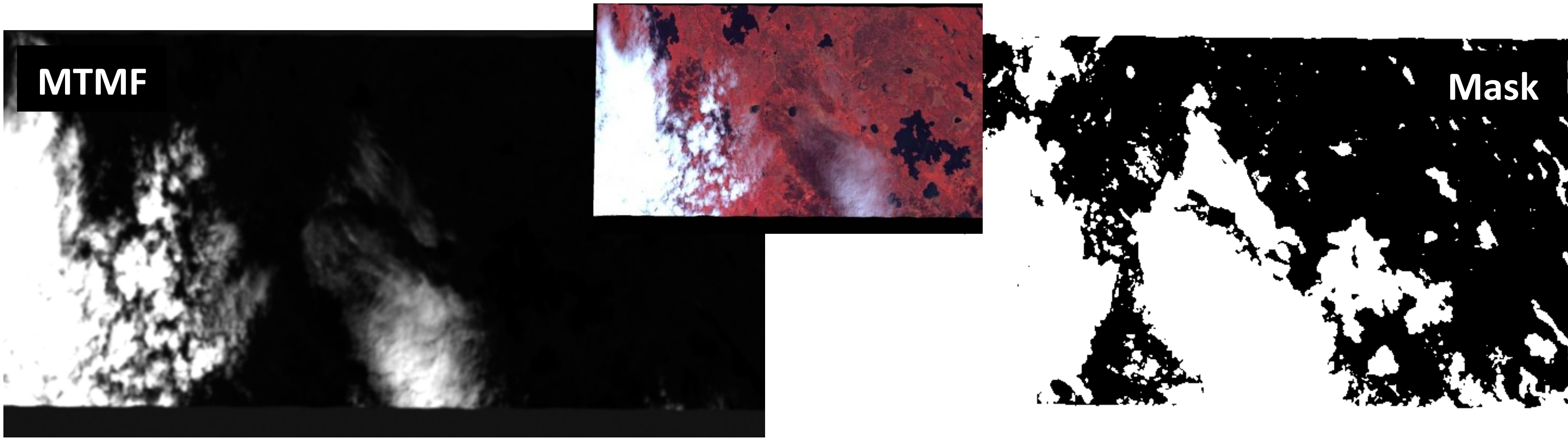

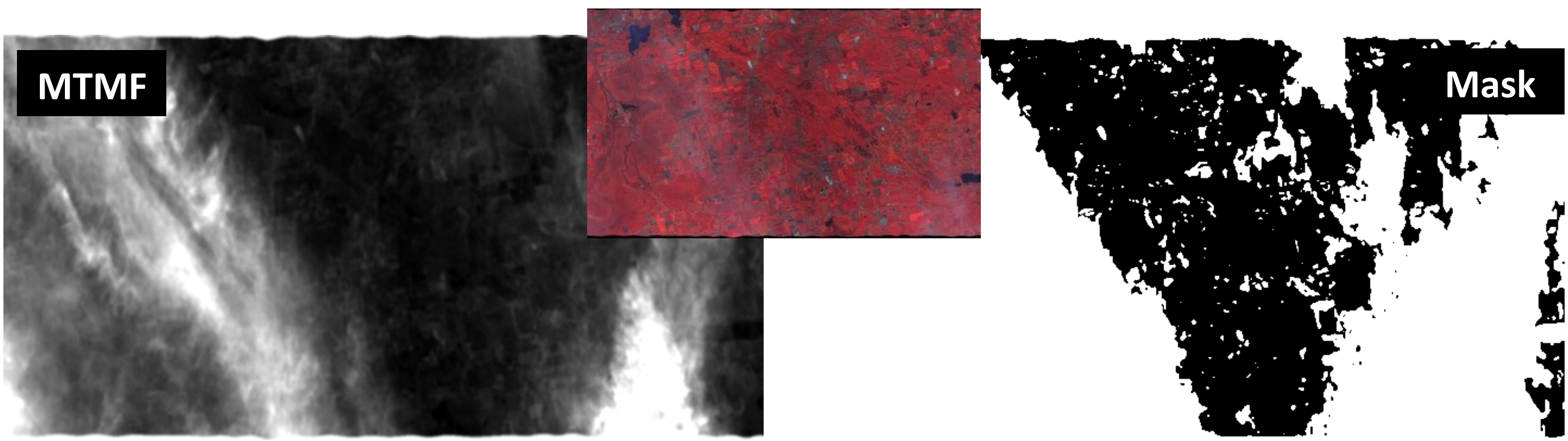

AVIRIS Pre-processing: Cross-track illumination correction

3. **Bilinear cross-track illumination correction:**
   …because images can have brightness gradients in any direction

- **For each band…**

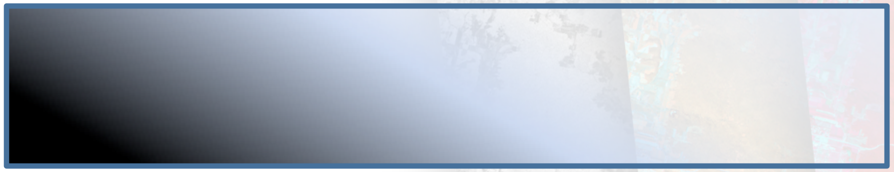

1. **Regress (masked) pixel DNs against pixel locations**

$$DN_{\lambda m} = \beta 0_\lambda + (x_m \cdot \beta 1_\lambda) + (y_m \cdot \beta 2_\lambda) + (y_m \cdot x_m \cdot \beta 3_\lambda)$$

2. **Estimate the brightness 'plane'** (gradients in ***x, y, x*y*** directions)

$$IL_\lambda = \beta 0_\lambda + (x \cdot \beta 1_\lambda) + (y \cdot \beta 2_\lambda) + (y \cdot x \cdot \beta 3_\lambda)$$

3. **…ness plane**

$$DN_{c\lambda} = DN_\lambda - IL_\lambda + (\overline{DN_{\lambda m}})$$

AVIRIS Pre-processing: Cross-track illumination correction

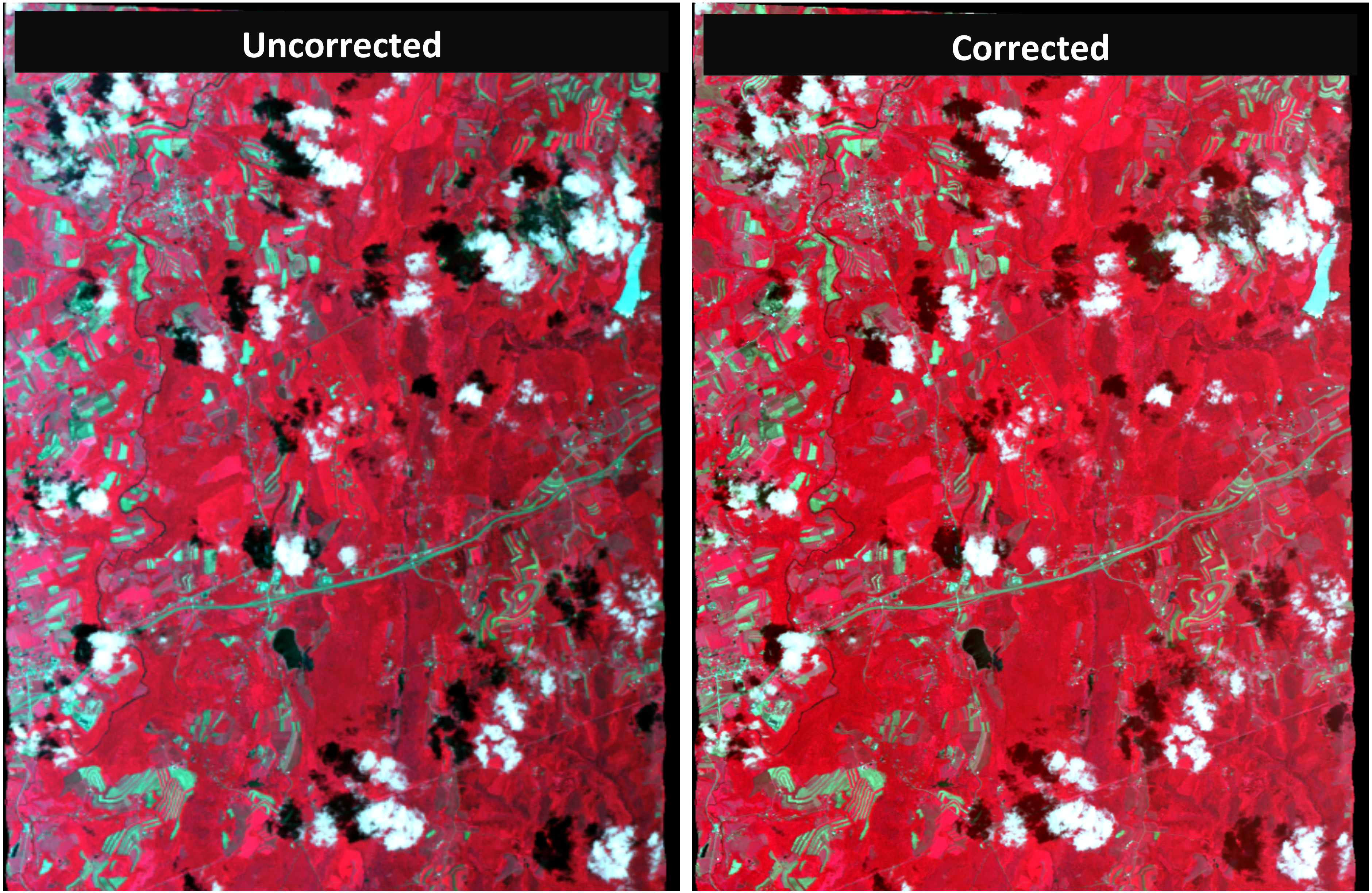

AVIRIS Pre-processing: C-factor terrain normalization

4. Terrain normalization: C-Factor correction (Teillet et al. 1982)

$$L_H = L_T \left(\frac{cos(z) + c}{cos(i) + c} \right)$$

Where: L_H = Reflectance from horizontal surface; L_T uncorrected reflectance

$$c = b/m$$

b and *m* determined by regressing each band with the *cos(i)* image

$$L_T = m \cdot cos(i) + b$$

$$cos(i) = cos(e) \cdot cos(\Phi_z) + sin(e) \cdot sin(\Phi_z) \cdot cos(\theta - \theta')$$

Where: *e* = terrain slope, ϕ_z solar zenith angle, θ = solar azimuth, θ’ = terrain aspect

•**Note**: *cos(i), z,* images included with AVIRIS data product.

AVIRIS Pre-processing: Radiometric corrections

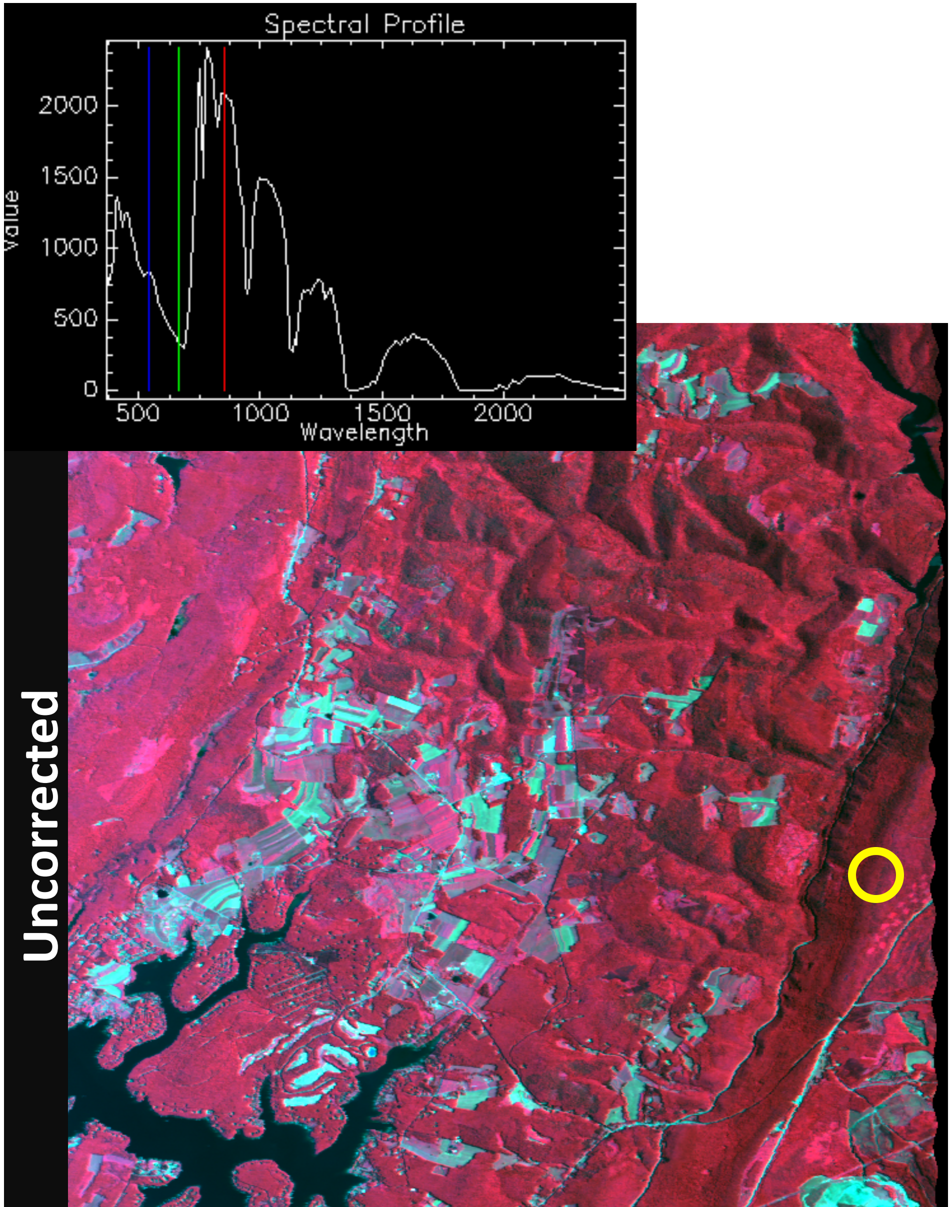

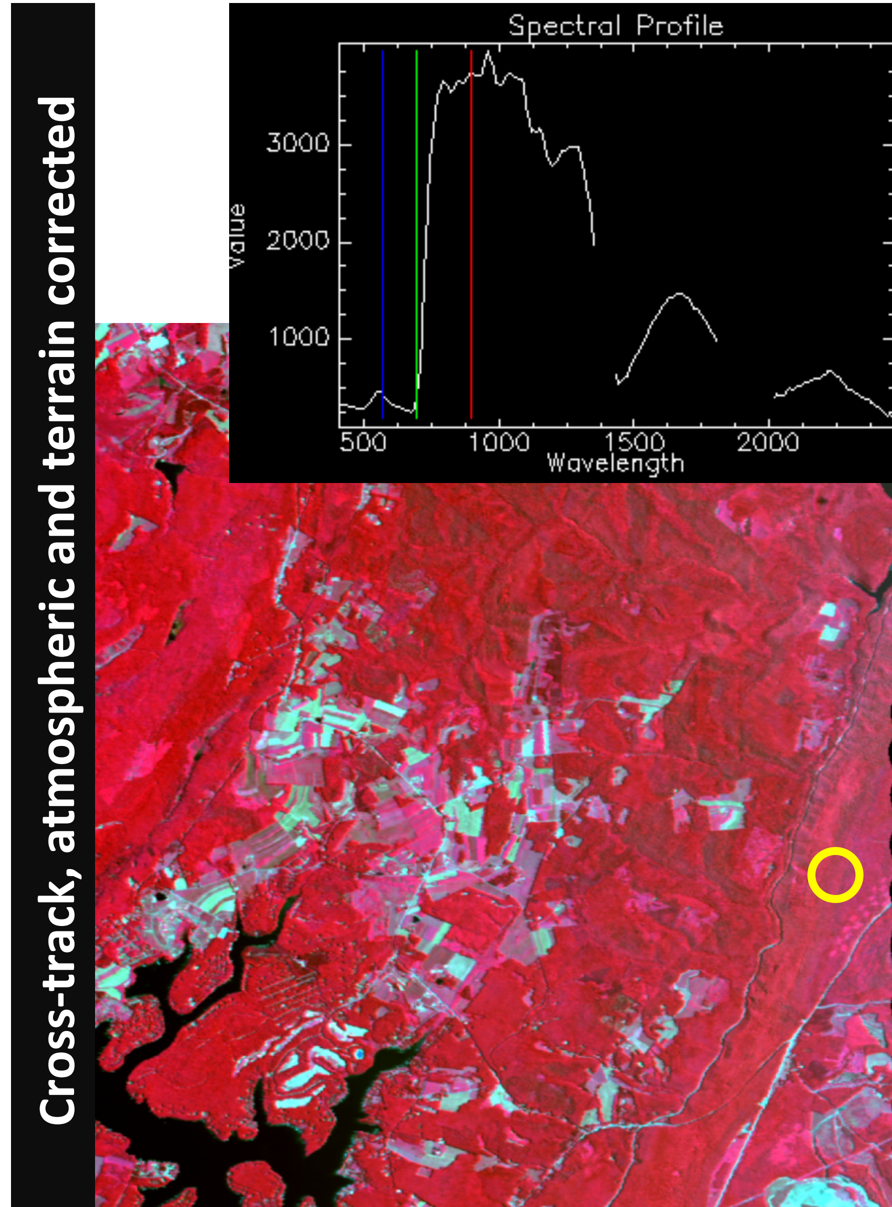

AVIRIS Pre-processing: Precision georeferencing

- **Some (orthorectified) AVIRIS images can be off by 1-5 pixels!**
  - Will cause errors when extracting spectra.
  - …pixels should be locatable to within Landsat resolution (ultimately HyspIRI), the usual reference for our plot sizes
- **Manual georeferencing possible,** time consuming, error-prone;
  - Need for a fast, automated technique (>150 images!)
- **Approach:** Use **Landsat Geocover** imagery as reference, use capabilities of the open computer vision (**OpenCV**) library to automate feature finding.

AVIRIS Pre-processing: Precision georeferencing

5. Precision georeferencing:

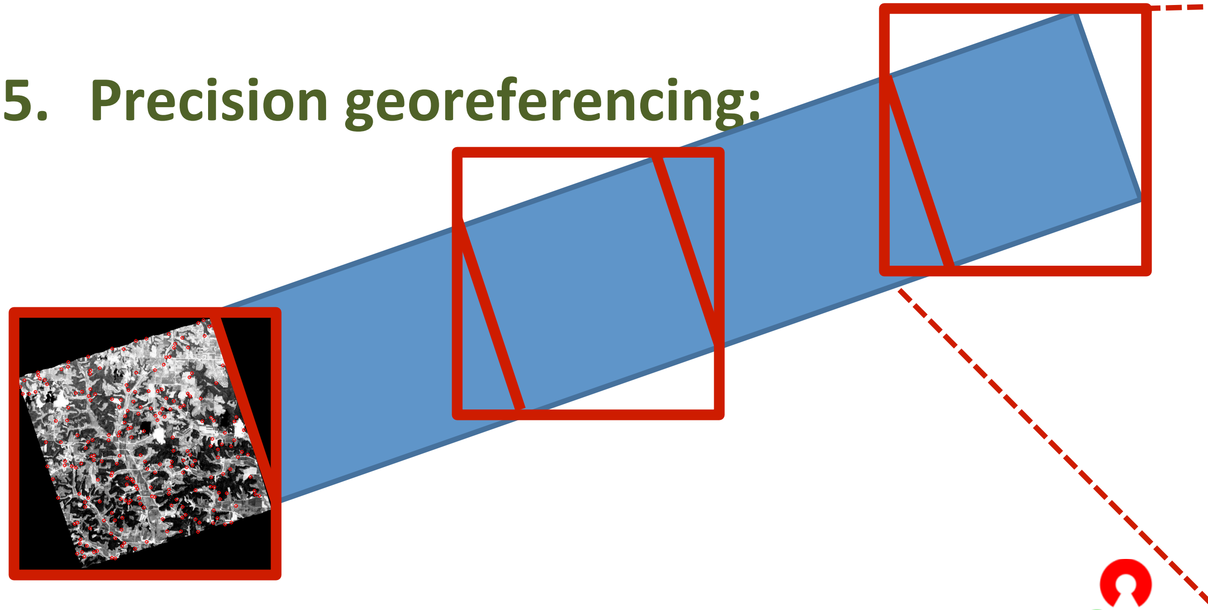

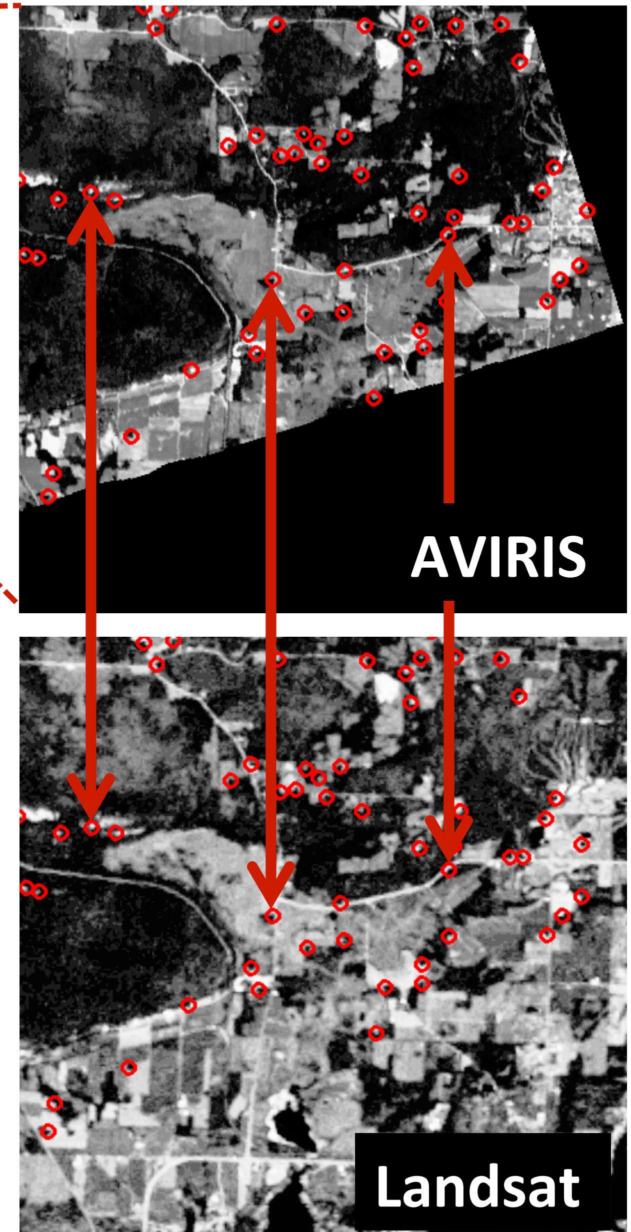

1. Get 3 chunks from AVIRIS imagery,
2. …same coverage from resampled Landsat,
3. Use **OpenCV** to find locations, match,
4. Store forward and inverse affine matrices.

RMSE <~13.0m, accuracy (R^2) > 0.99999

Test data: Comparisons with pre-processed imagery

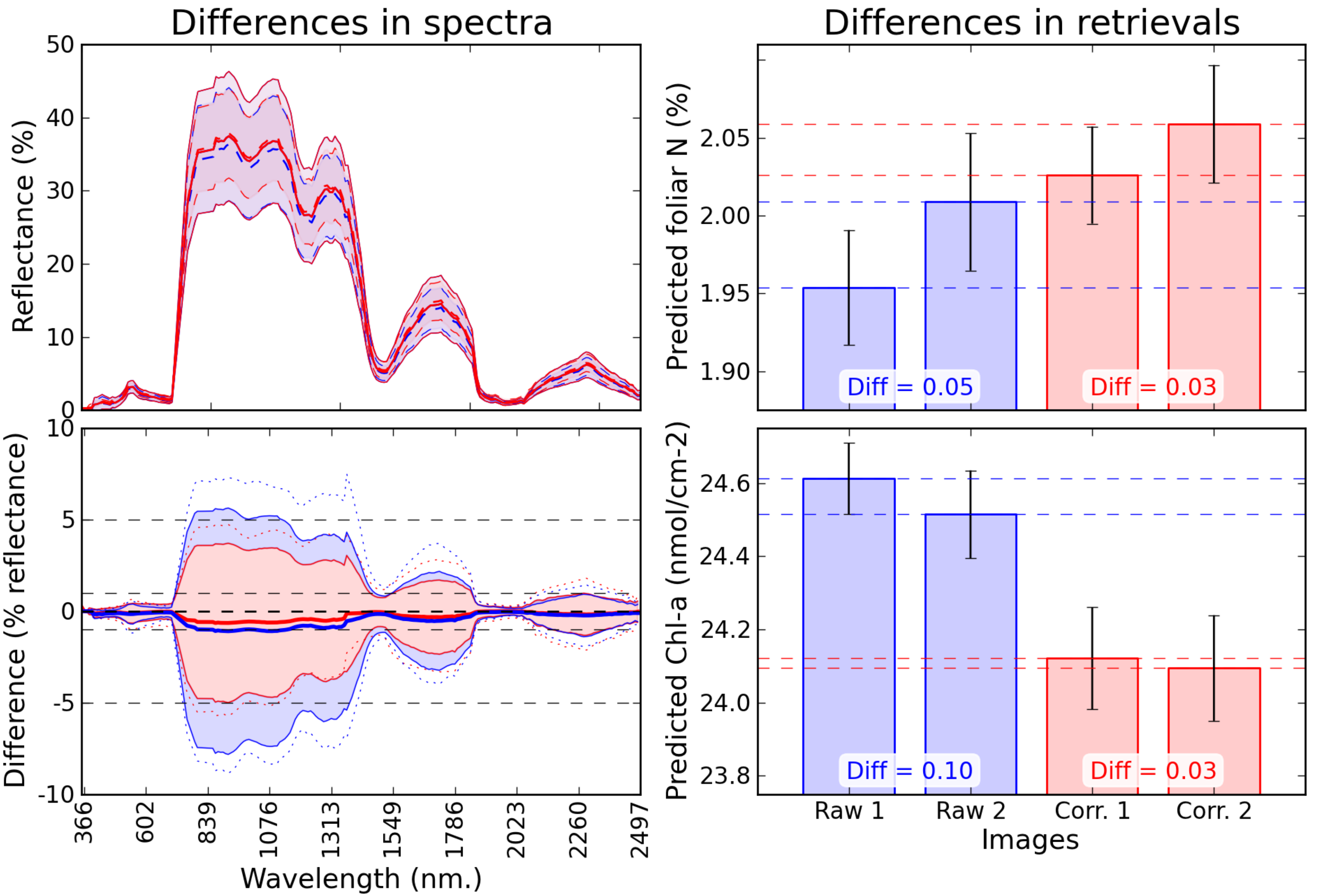

In conclusion:

- Evidence that following a consistent pre-processing protocol may be instrumental in making ecosystem-scale predictions comparable across space and time.

- The tool-chain is mostly automated (using Python/IDL)

- We will present results comparing retrievals of key foliar biochemical and structural traits (%N, %C, %Lignin, %Cellulose, LMA, $\delta^{15}N$) from physically-based and statistical models at the upcoming HyspIRI workshop.

Thank you. Questions?

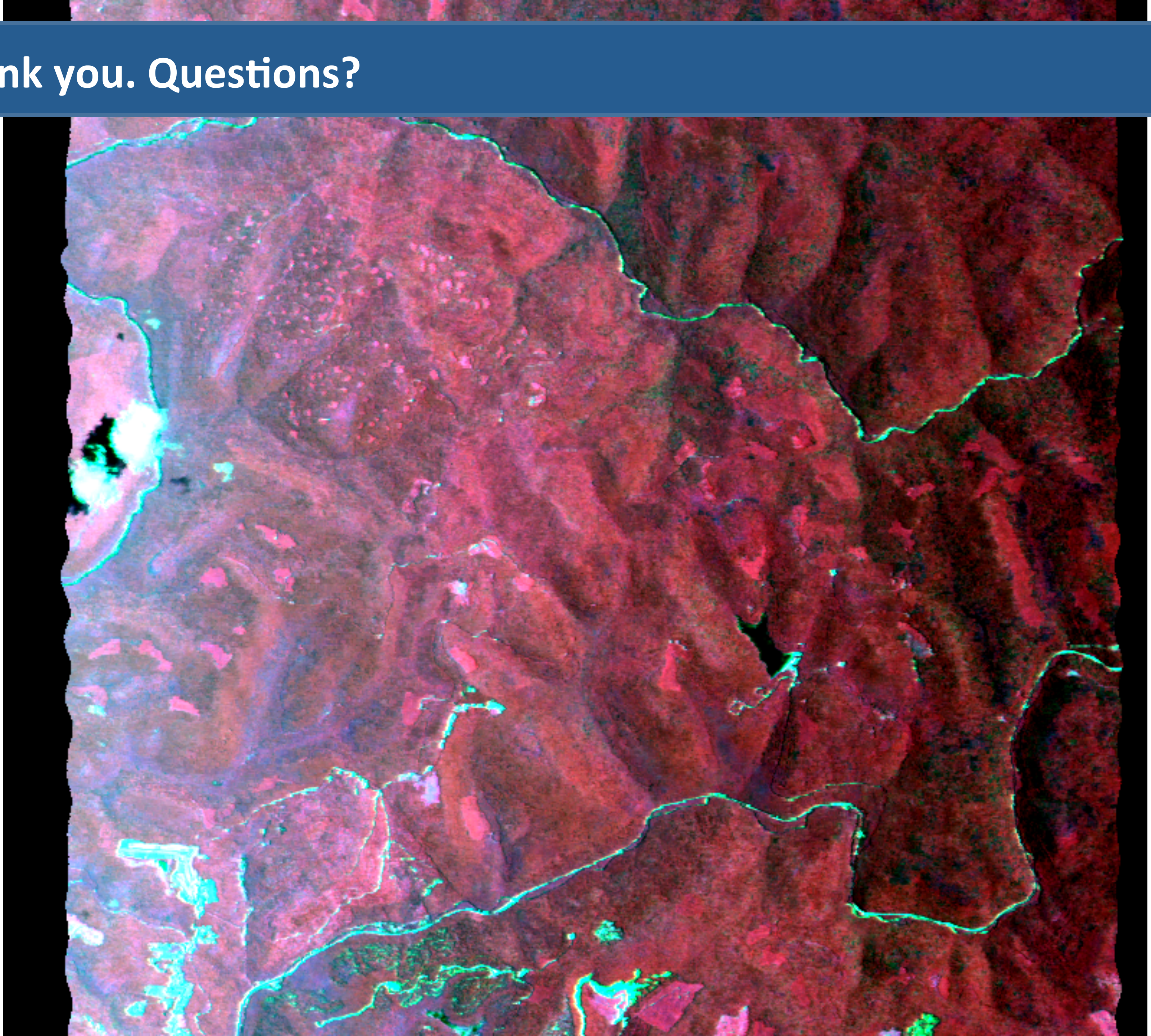

Acknowledgements

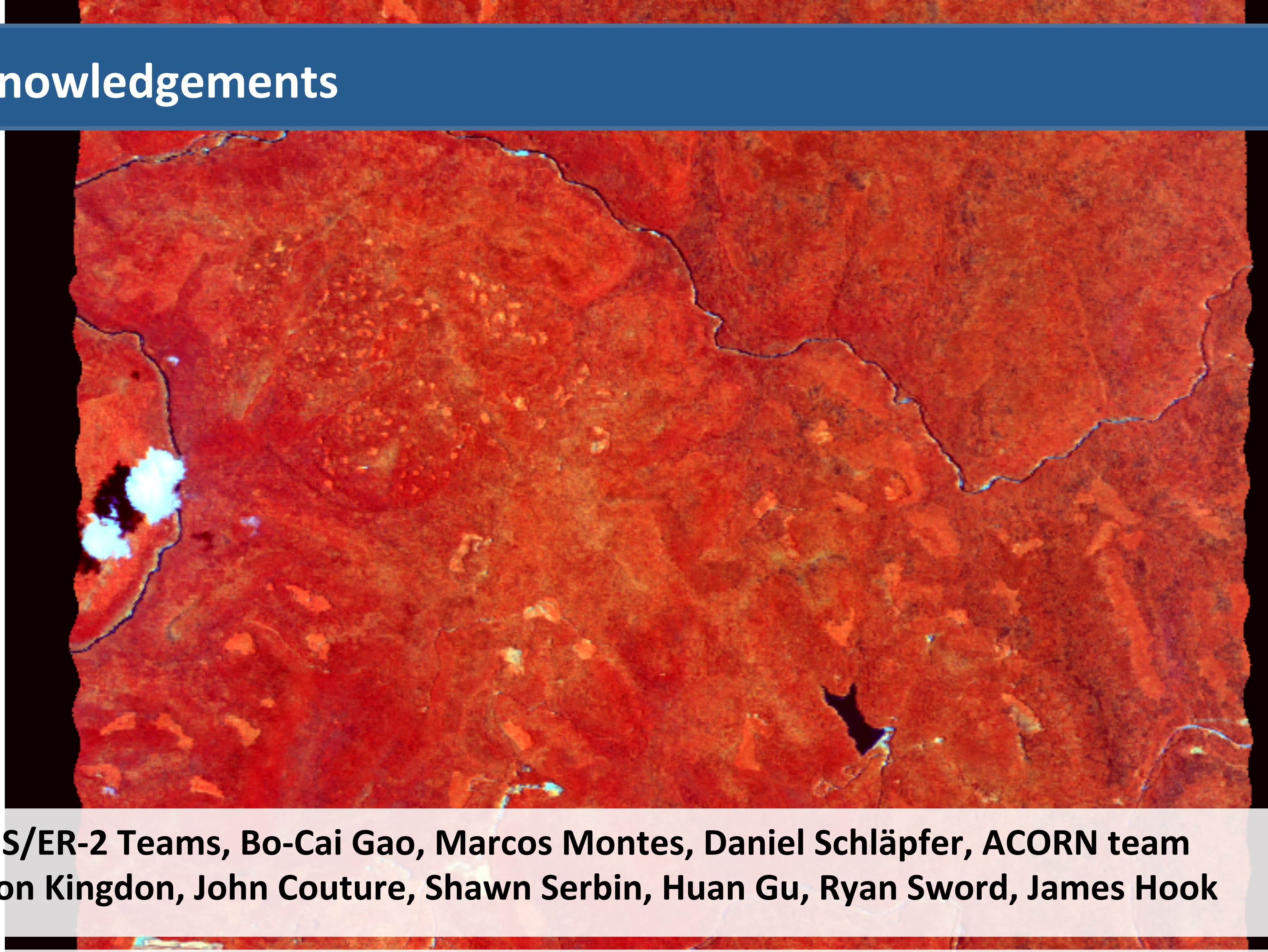

AVIRIS/ER-2 Teams, Bo-Cai Gao, Marcos Montes, Daniel Schläpfer, ACORN team
Clayton Kingdon, John Couture, Shawn Serbin, Huan Gu, Ryan Sword, James Hook

Extracting Temperature and Emissivity from High Spatial Resolution Multispectral Thermal Infrared Data

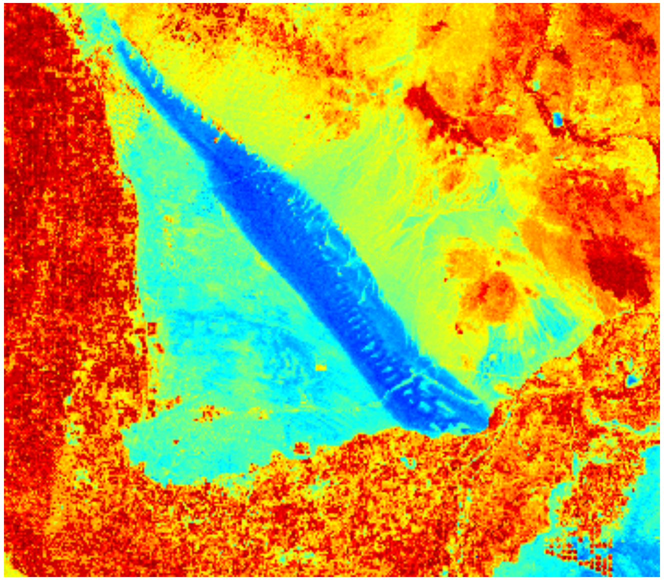

Simon Hook, Glynn Hulley

Jet Propulsion Laboratory, California Institute of Technology, Pasadena, CA

Outline

- Introduction
- Thermal Infrared Remote Sensing
- Atmospheric Correction
- Temperature Emissivity Separation
- ASTER-GEM
- MODIS LST&E (MOD21)
- Validation

Introduction

- **<u>Land Surface Emissivity:</u>** ratio between actual emitted radiation, and radiation emitted by a blackbody at the same temperature (typically varies from 0.6 – 0.99)

$$\epsilon_\lambda = \frac{L_\lambda}{L_\lambda(BB)}$$

- **<u>Land Surface Temperature (LST)</u>:** how 'hot' the skin surface of the Earth feels at any given time

- LST and emissivity closely coupled variables, both determine amount of thermal radiation emitted by the Earth's surface, BUT are independent measurements!
  - Emissivity is intrinsic property of the Earth's surface
  - LST varies with local atmospheric conditions and irradiance history
  - Emissivity error of 0.015 = ~1 K LST error

Motivation:

Why is Land Surface Temperature/Emissivity (LST&E) Important?

- Climate and Hydrological Modeling
  - LST is a critical component for evapotranspiration modeling (e.g. ALEXI)
  - Emissivity set to constant value (eg. 0.96) with simple parameterizations in land models, e.g. NCAR Community Land Model (CLM3)
  - Simulations by Zhou et al. (2003) showed emissivity decrease of 0.1 resulted in 7 W/m^2 underestimation longwave radiation estimates (greenhouse gases, ~2 W/m^2)
- Atmospheric Retrievals
  - Boundary layer temperature and water vapor over land are heavily dependent on accurate LST&E, eg. Emissivity error of 0.15 leads to more than 3 K error in temperature retrievals in boundary layer (Kornfield and Susskind, 1977)
- Land use, Land cover change (LCLUC)
  - Increased demand for agricultural land, and significant land cover changes from extreme climatic events => increased demand for LST&E products for monitoring these events
- Soil Moisture Mapping
  - Evapotranspiration models require LST&E to characterize surface energy balance
  - LST will be critical input for NASA's future Soil Moisture Active & Passive (SMAP) mission

NASA LST&E Product Characteristics

	ASTER (Advanced Spaceborne Thermal Emission and Reflection Radiometer)	**HyspIRI (Hyperspectral Infrared Imager)**	**MODIS (Moderate Resolution Imaging Spectroradiometer)**	**AIRS (Atmospheric Infrared Sounder)**
Satellite	Terra (2000)	Expected launch: 2020+	Terra/Aqua (2000/2002)	Aqua (2002)
Calibration	<0.3 K	<0.2 K	<0.2 K	<0.2 K
LST&E Algorithm	TES Calibration Curve	TES Calibration Curve	1. Day-Night 2. Split-Window	Regression plus simultaneous retrieval
LST&E Product	AST05/08	tbd	MOD11A1/B1/C3	AIRSX2RET
ATBD LST Product Accuracy	1K	1K	1K	2-3 K
Product versions	Version 3	n/a	C4.1, 4.0 and 5.0	Version 4 and 5
Temporal sampling	16 day repeat (1030 AM/PM)	5 day repeat (1030 AM/PM)	Twice-daily (10:30/1:30 AM/PM)	Twice-daily (10:30 AM/PM)
Spatial resolution	90 m	60 m	5 km (c4), 6 km (c5)	45 km
Spectral resolution	5 TIR bands (8-12 µm)	8 TIR bands (4-12 µm)	7 MIR/TIR bands (3.7-14 µm)	39 'hinge-points' (3.7-15.4 µm)
Swath Width	60 km	600 km	2330 km	1650 km

Sensor Spatial Resolution Differences

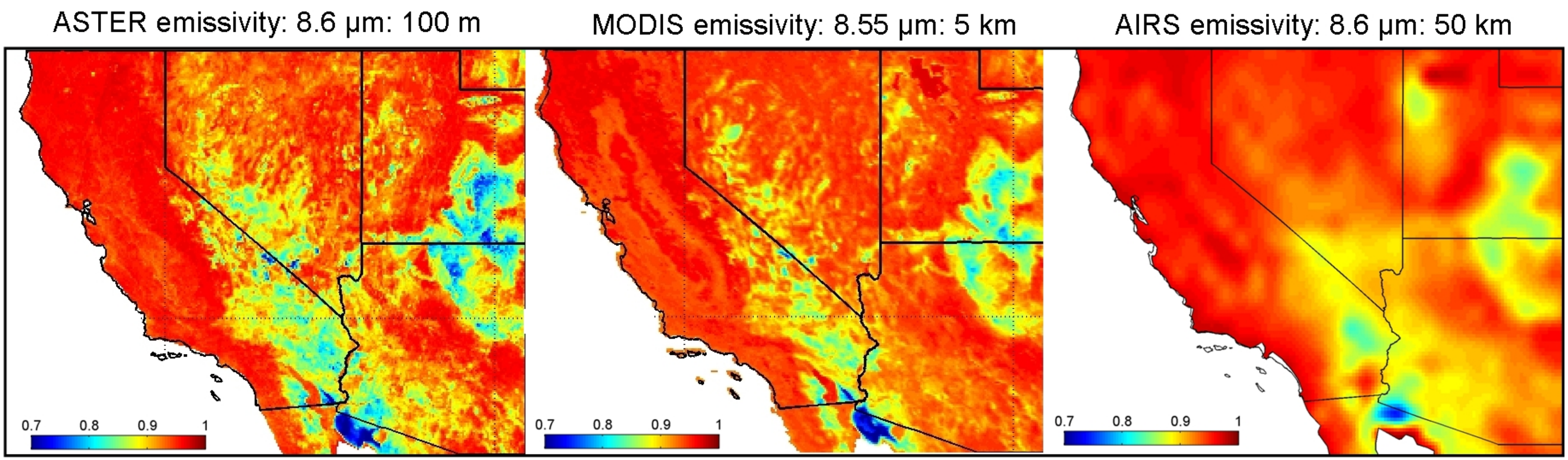

At spatial resolutions < 100m capture variation at the field scale

Thermal Infrared Radiative Transfer

Surface Radiance

TOA Radiance

$$L_i(\theta) = \underbrace{\tau_i(\theta)\cdot e_i \cdot B_i(T_S)}_{\text{Surface Emission}} + \underbrace{\tau_i(\theta)\cdot(1-e_i)\cdot \overline{L}_i^{\downarrow}}_{\text{Surface Reflection}} + \underbrace{\int B_i(T(P))\,d\tau_i}_{\text{Atmospheric Emission}}$$

Surface Emission

Surface Reflection

Atmospheric Emission

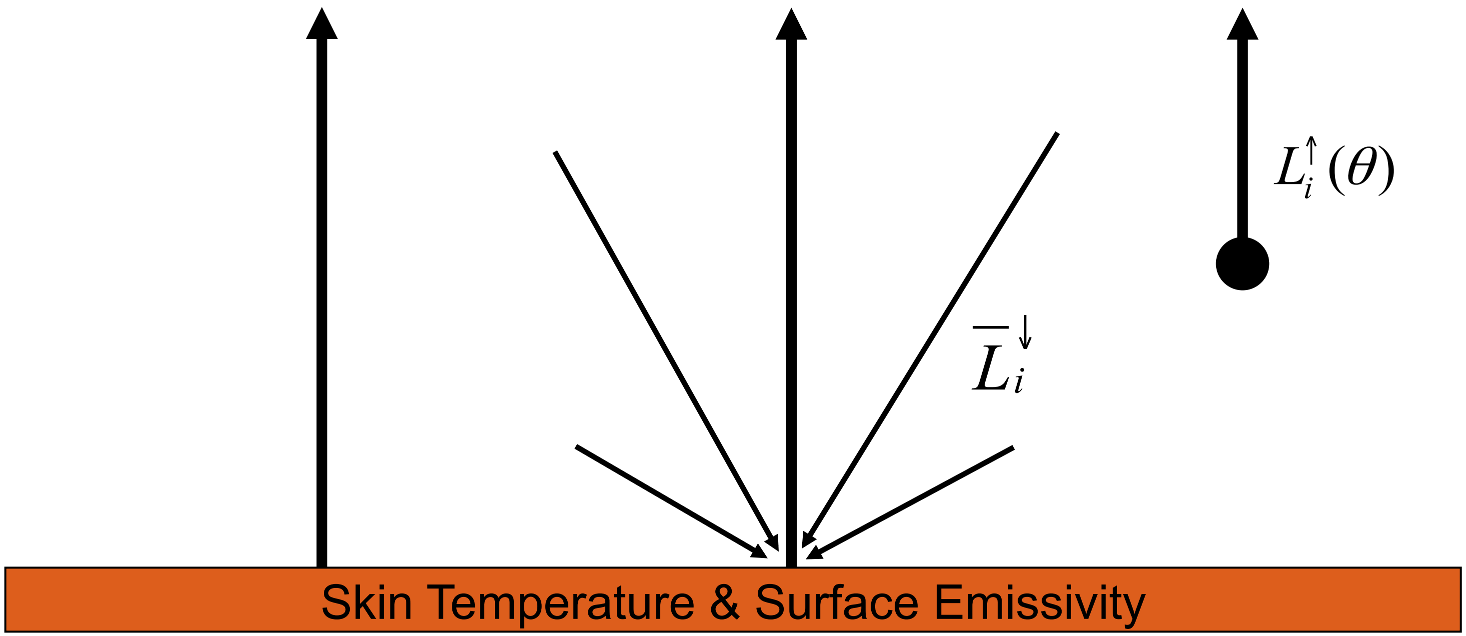

HyspIRI Response Functions

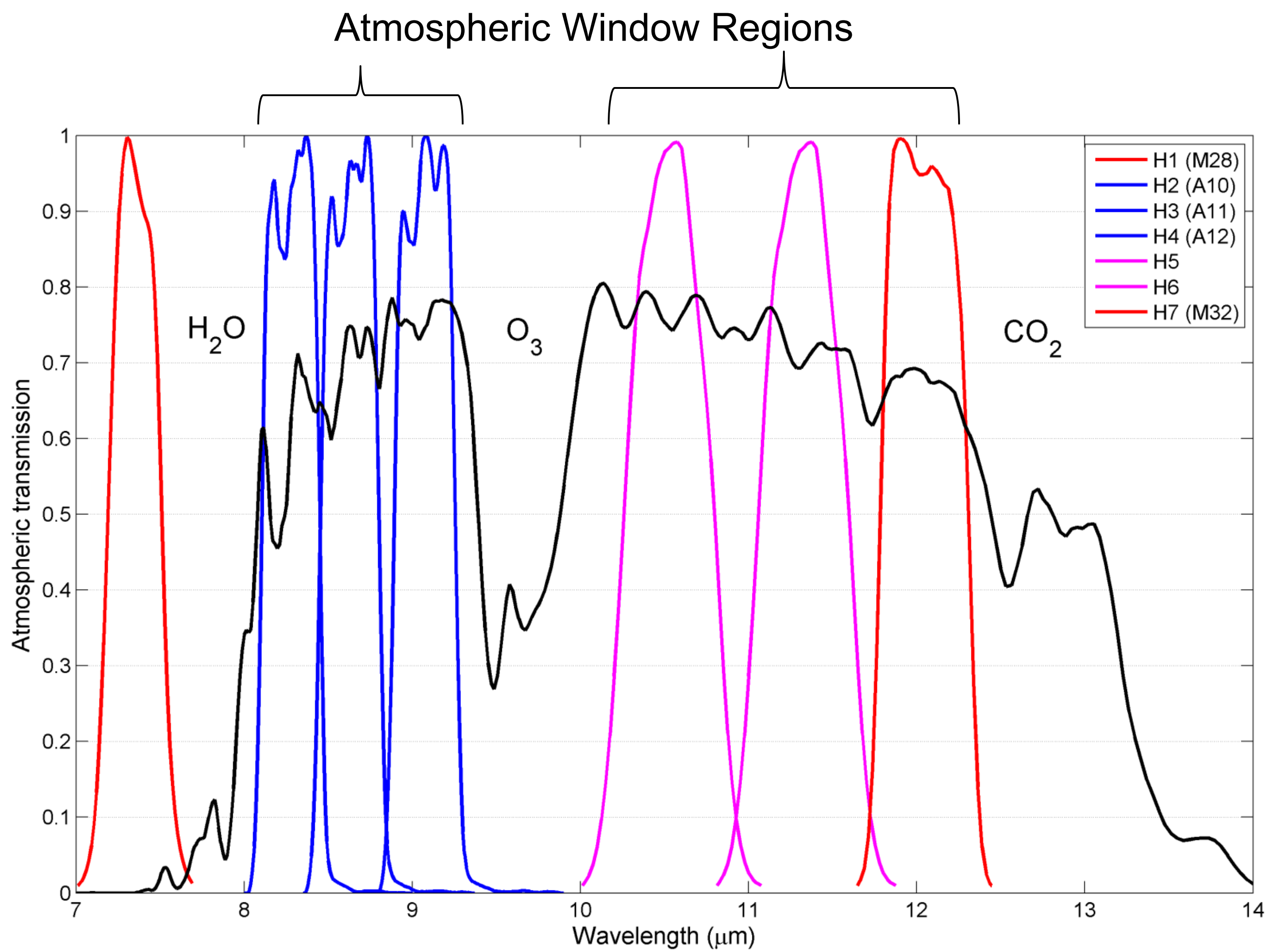

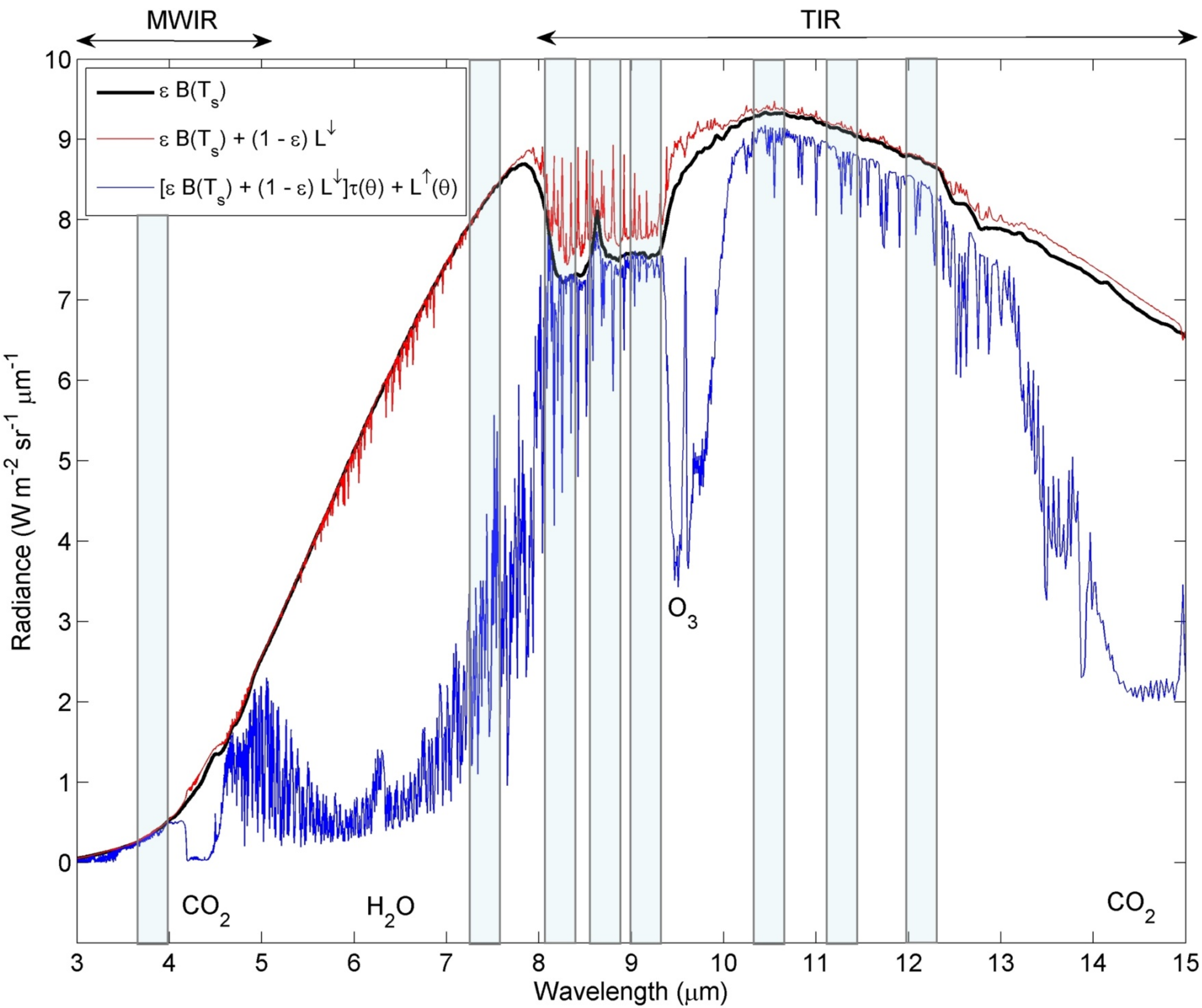

MWIR
TIR
ε B(T_s)
ε B(T_s) + (1 - ε) L↓
[ε B(T_s) + (1 - ε) L↓]τ(θ) + L↑(θ)
Radiance (W m^-2 sr^-1 μm^-1)
Wavelength (μm)
O_3
CO_2
H_2O
CO_2
0
1
2
3
4
5
6
7
8
9
10
3
4
5
6
7
8
9
10
11
12
13
14
15

Atmospheric Correction

Observed Radiance

Surface Radiance:

$$L_{surf,i} = e_i \cdot B_i(T_S) + (1 - e_i) \cdot \overline{L}_i^{\downarrow} = \frac{L_i(\theta) - L_i^{\uparrow}(\theta)}{\tau_i(\theta)}$$

- **Atmospheric Parameters:** $\tau_i(\theta)$, $L_i^{\uparrow}(\theta)$, $L_i^{\downarrow}(\theta)$

  Estimated using radiative transfer code such as MODTRAN with Atmospheric profiles and elevation data

- Derivation of e_i and T_s is an undetermined problem

  The number of parameters (T_s, e_i in N channels) is always greater than the number of simultaneous equations needed to solve the problem (N)

  =>Additional, independent constraint is needed

Temperature/Emissivity Separation (TES)

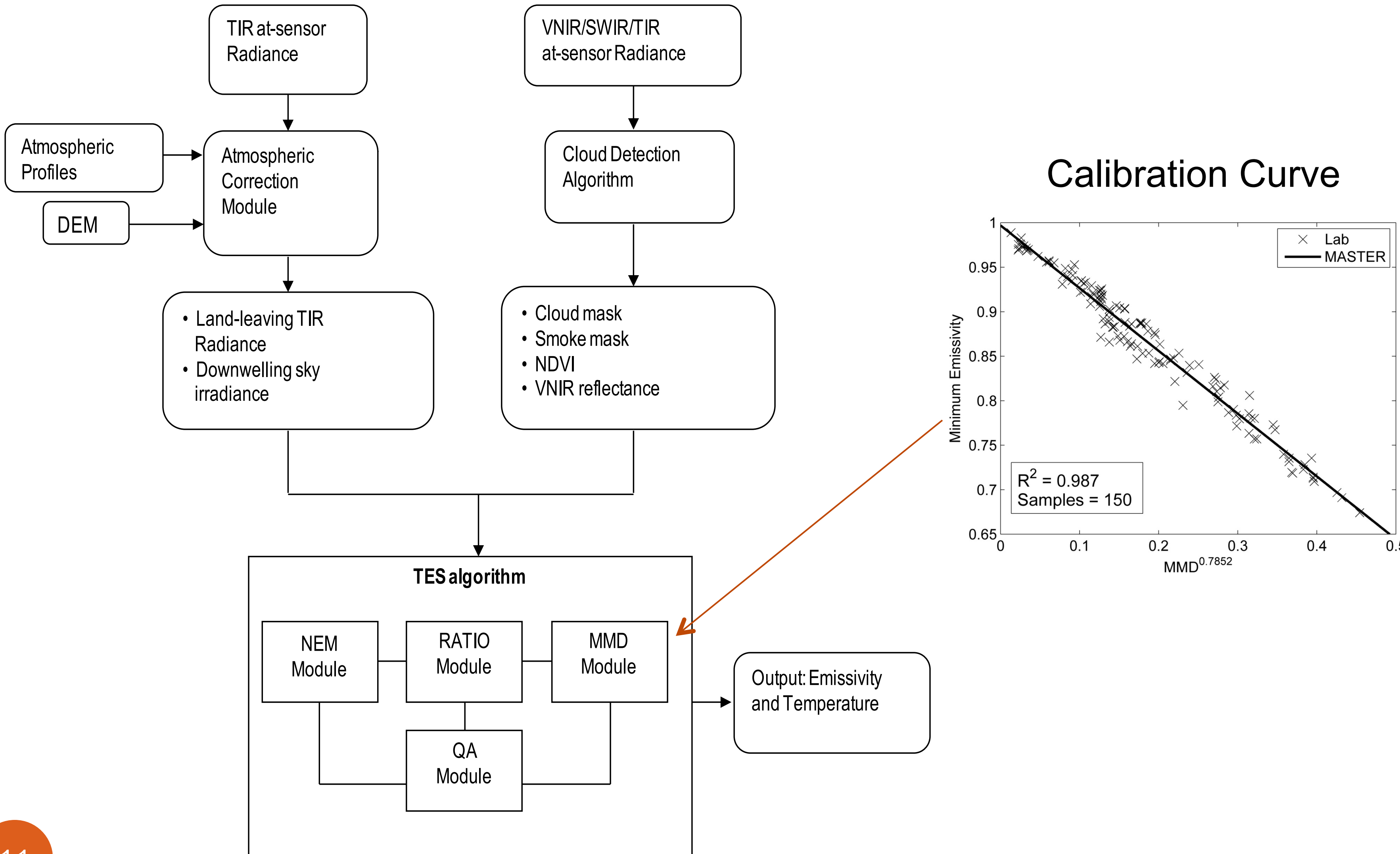

ASTER & MODIS Emissivity spectra for the Salton Sea showing effects of water vapor scaling (wvs)

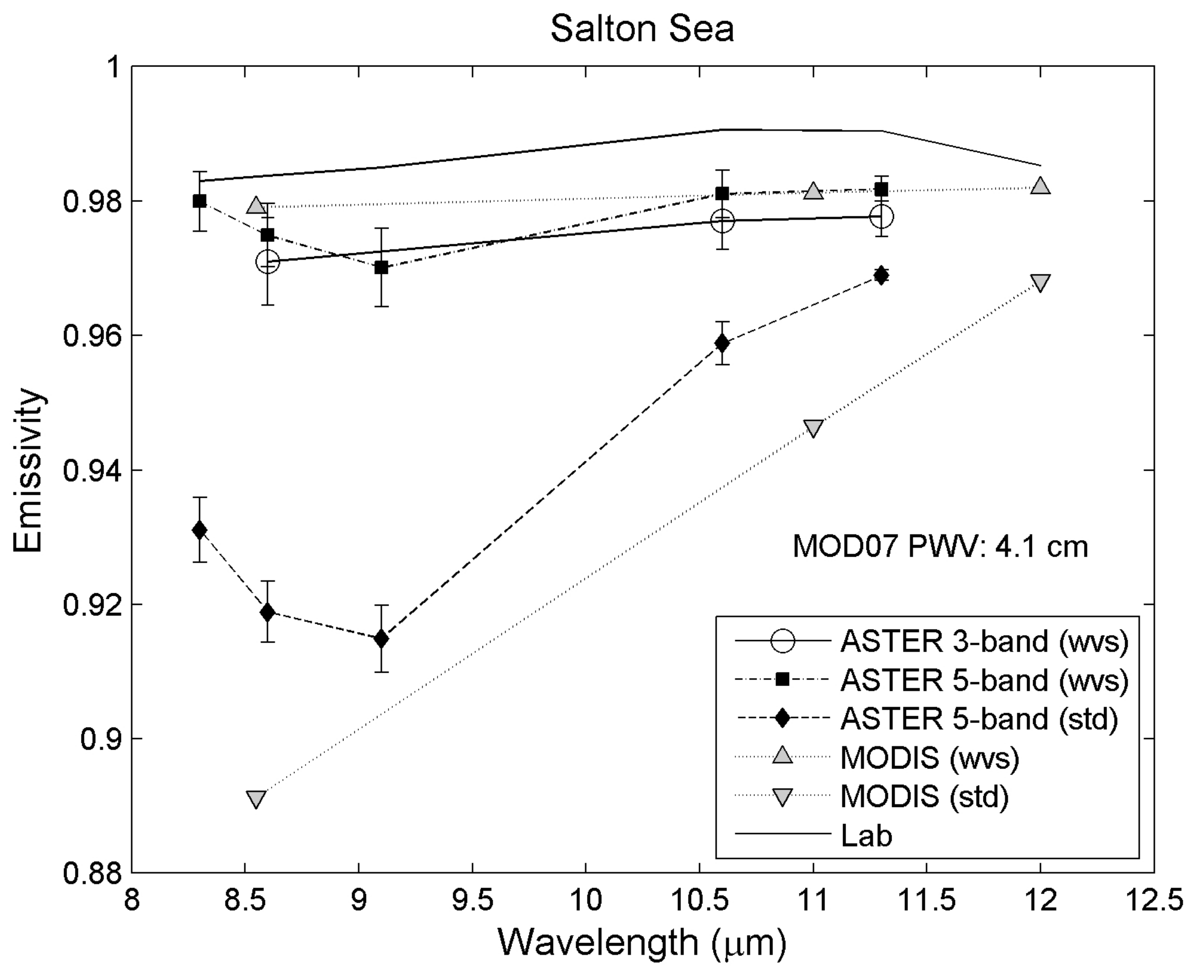

Now lets look at some products!

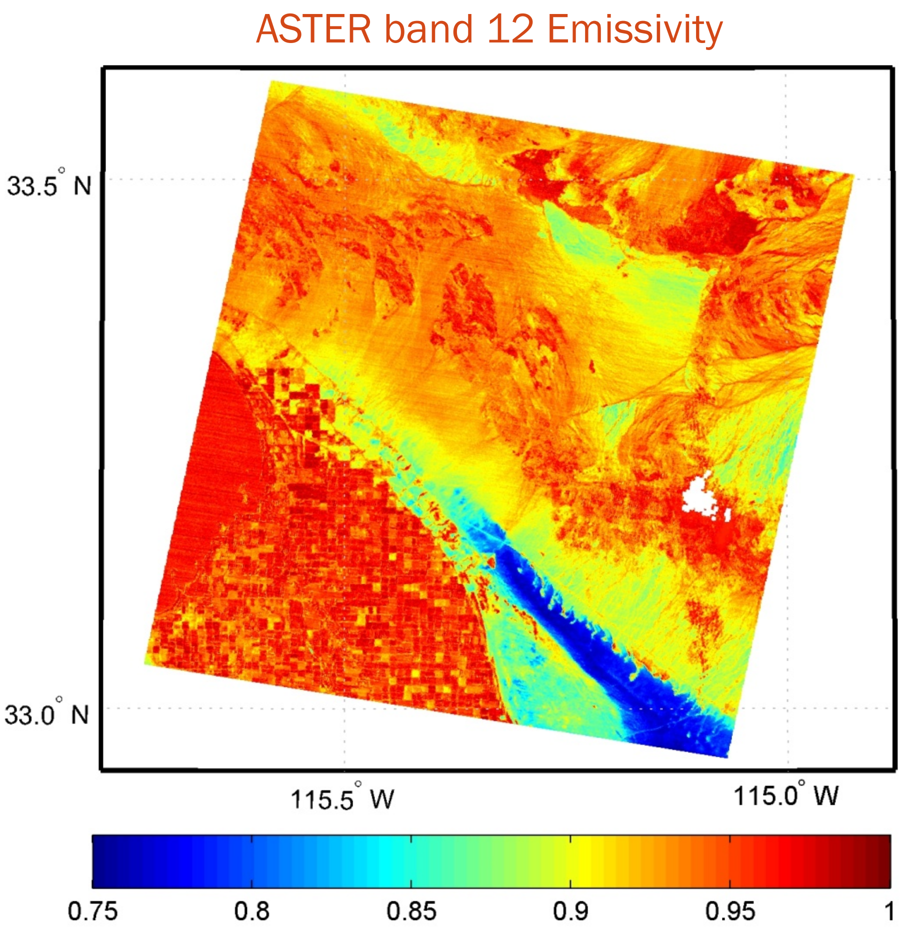

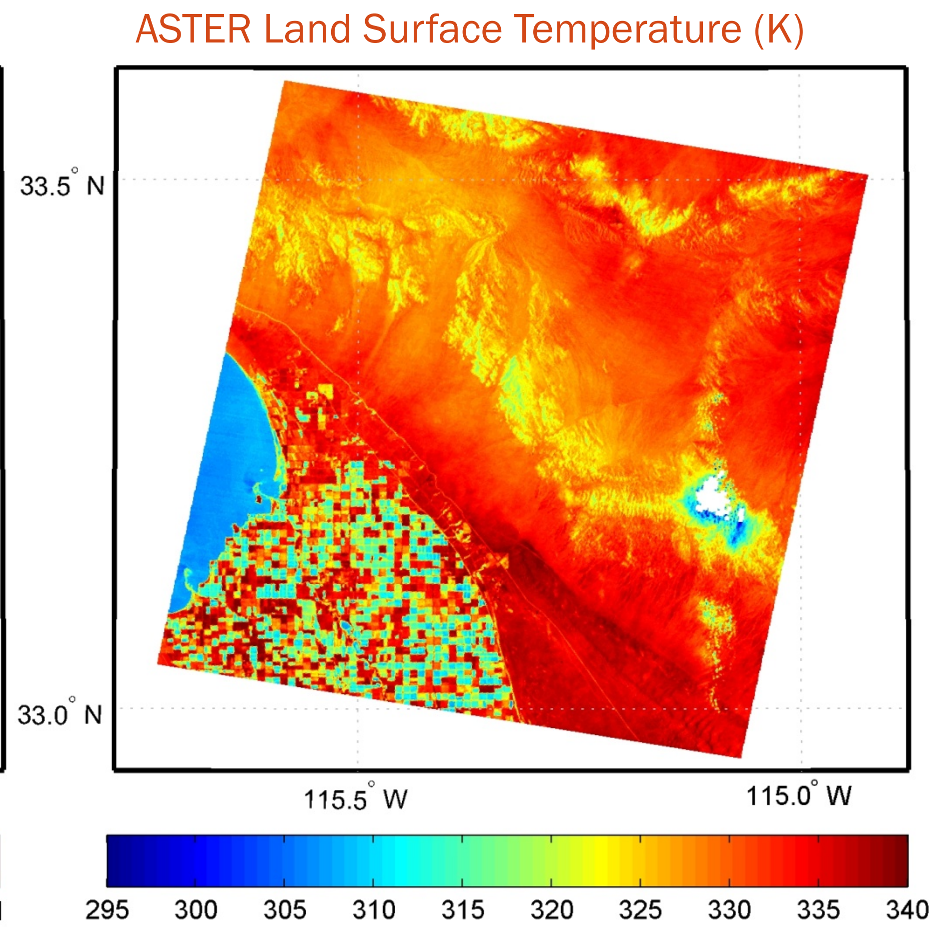

The ASTER Global Emissivity Map (GEM)

- ASTER produces Level-2 LST&E products at 90m
- Scenes (60 x 60 km) produced on demand, limited repeat (16 days) with no L-3 gridded data
- ASTER-GEM: Long-term mean gridded composite of all ASTER scenes acquired since 2000 at 100m, 1km, 5km, 50km resolution
  - Summertime (Jul-Sep), 2000-present
  - Wintertime (Jan-Mar), 2000-present
- Progress:
  - North America (JPL)
  - Africa & Arabian Peninsula (JPL, Tonooka)
  - Australia (JPL)
  - Asia and Europe (Tonooka)

NAALSED Summertime Emissivity (Jul-Sep 2000-2010), Band 12 (9.1 µm), 5km

Lowest emissivity over southwest

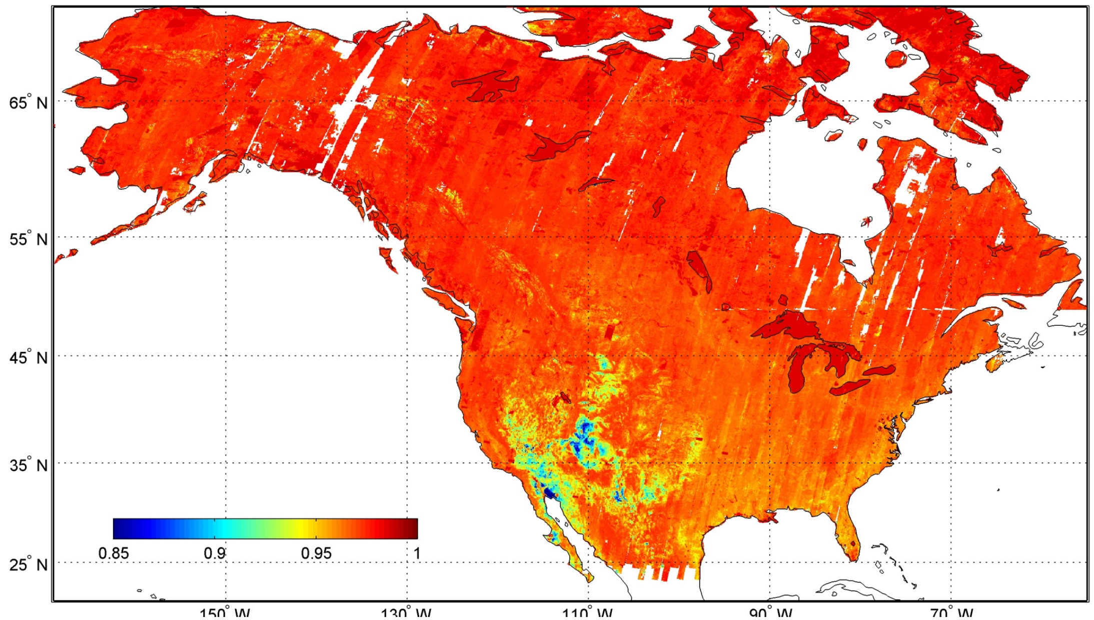

Number of pixels averaged for a given location ->

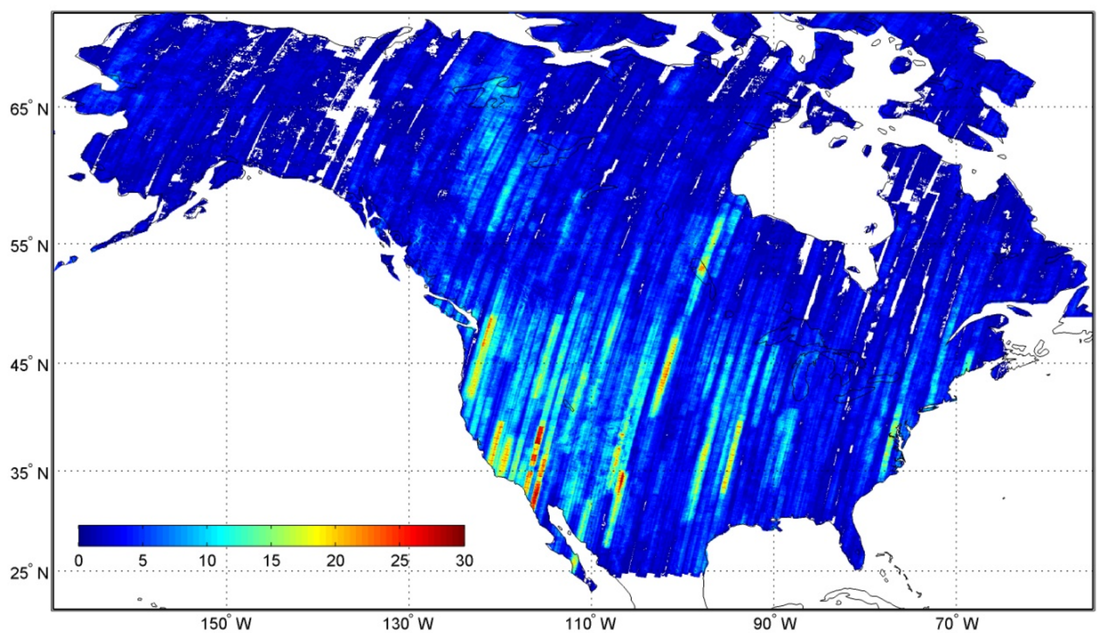

ASTER-GEM Band 12 emissivity (9.1 µm)
5km resolution: 2000-2010 (~112,000 scenes)

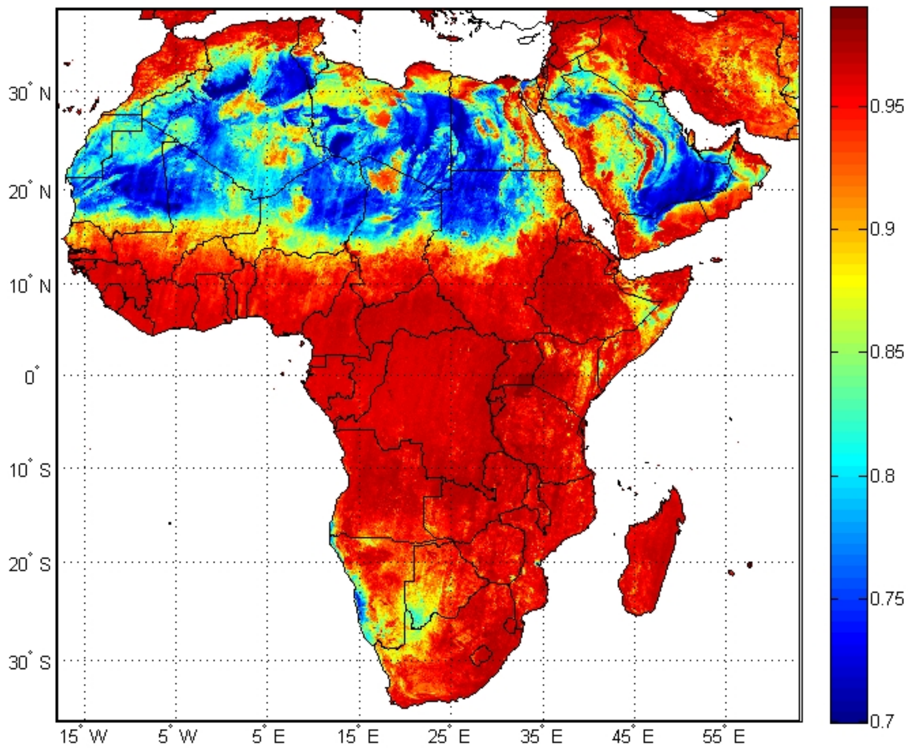

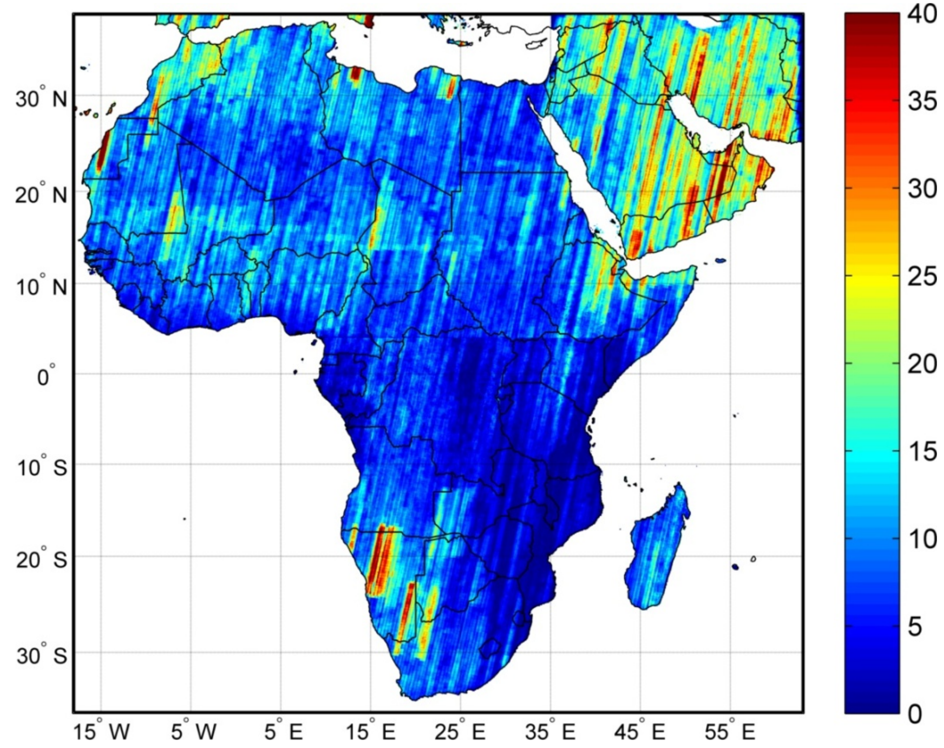

Certain regions have far more coverage than others!

ASTER-GEM Band 12 emissivity (9.1 μm)
5km resolution: 2000-2010

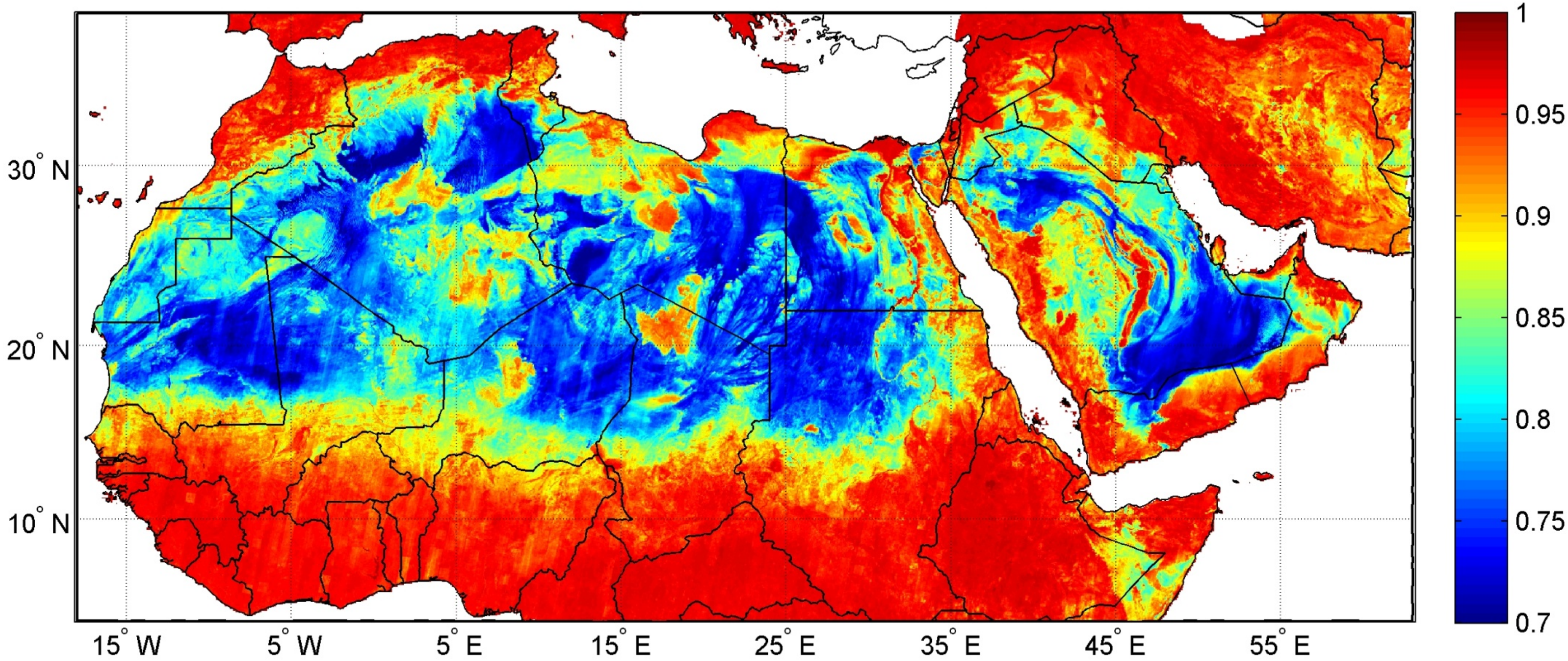

At 100 m spatial resolution see tremendous variation in emissivity (see next slide from Nambia)

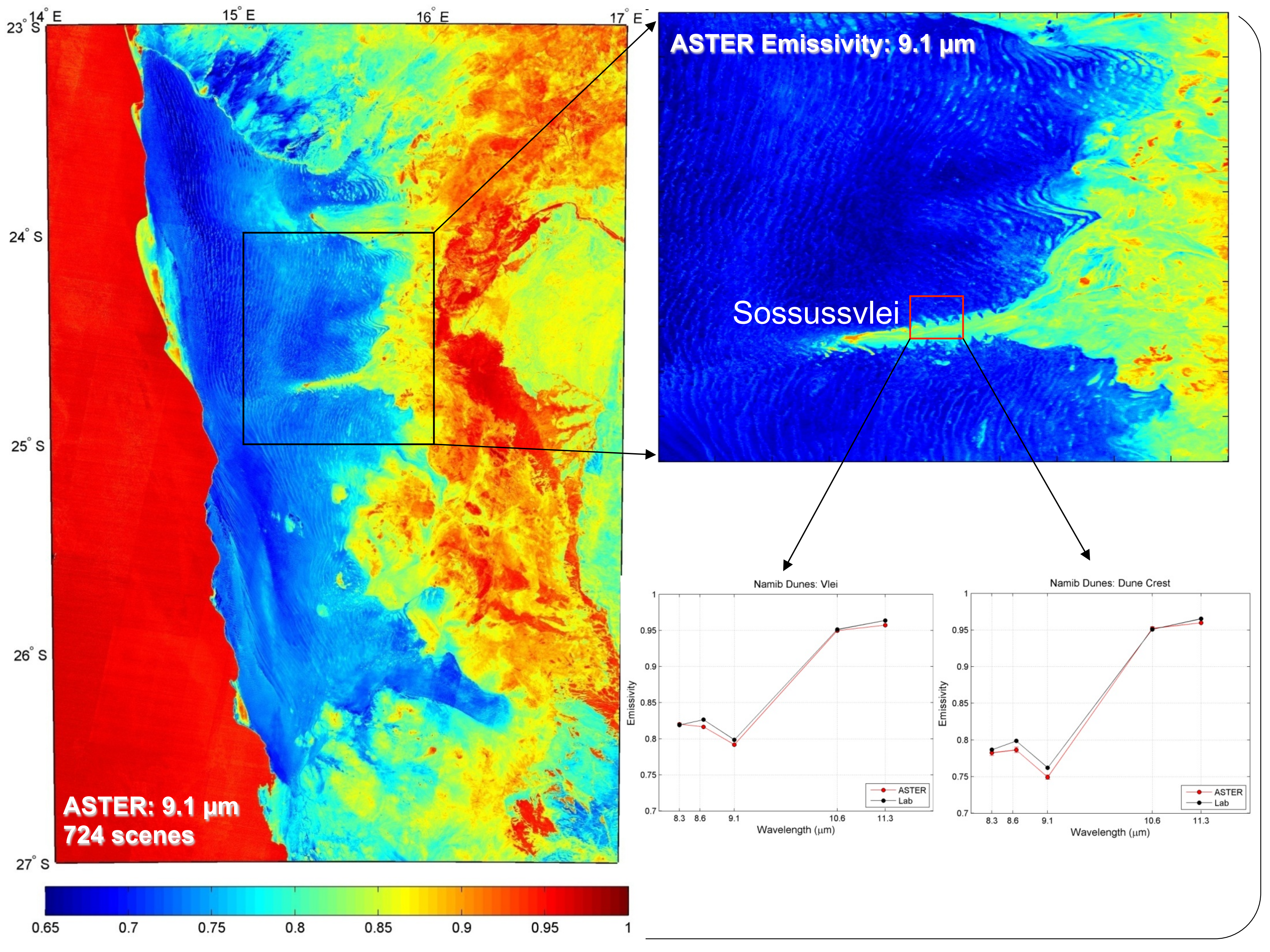

ASTER Emissivity: 9.1 μm
Sosussvlei
ASTER: 9.1 μm
724 scenes
14° E
15° E
16° E
17° E
23° S
24° S
25° S
26° S
27° S
0.65
0.7
0.75
0.8
0.85
0.9
0.95
1
Namib Dunes: Vlei
Namib Dunes: Dune Crest
Emissivity
Wavelength (μm)
ASTER
Lab

ASTER Global Emissivity Map (GEM): Death Valley

Death Valley - Mean Summer Emissivity - Band 10 (8.3μm)

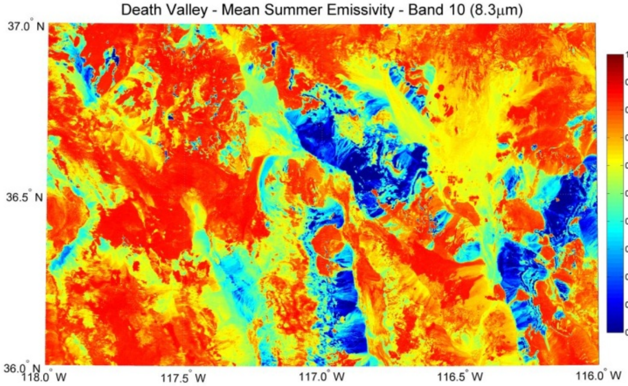

Death Valley - Mean Summer Emissivity - Band 11 (8.65μm)

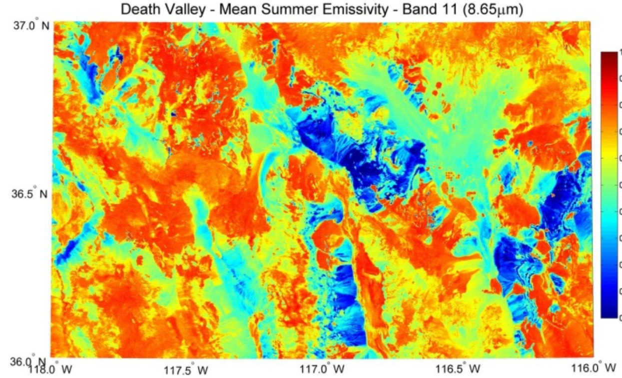

Death Valley - Mean Summer Emissivity - Band 12 (9.1μm)

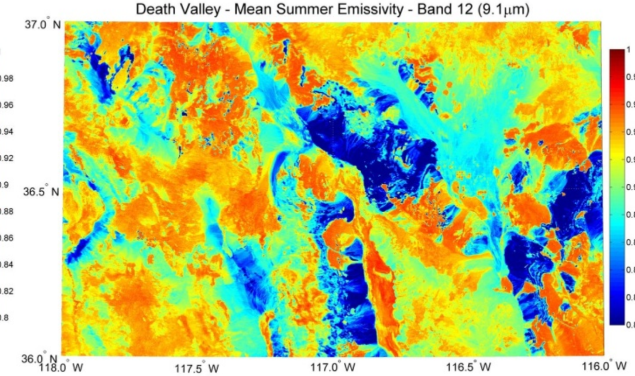

With HyspIRI we will produce similar products!

Death Valley - Mean Summer Emissivity - Band 13 (10.6μm)

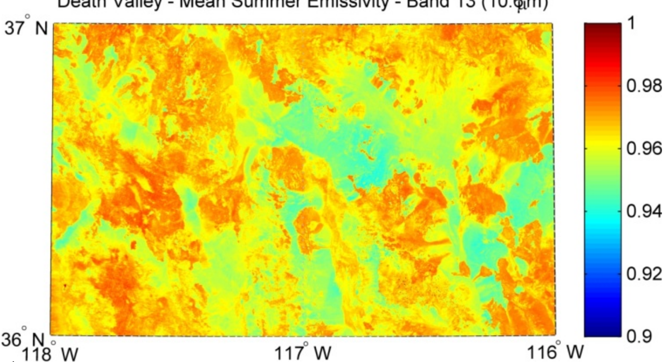

Death Valley - Mean Summer Emissivity - Band 14 (11.3μm)

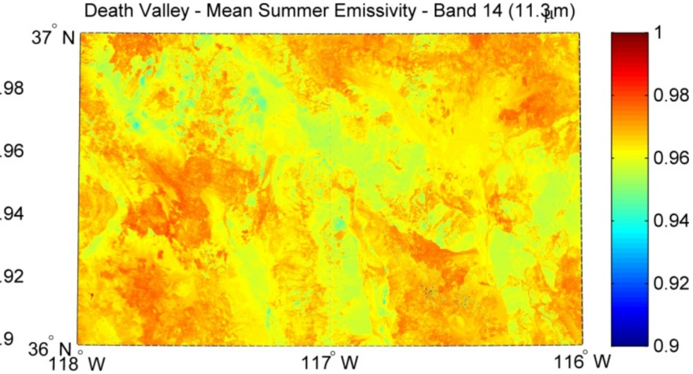

Death Valley - Mean Summer Temperature (K)

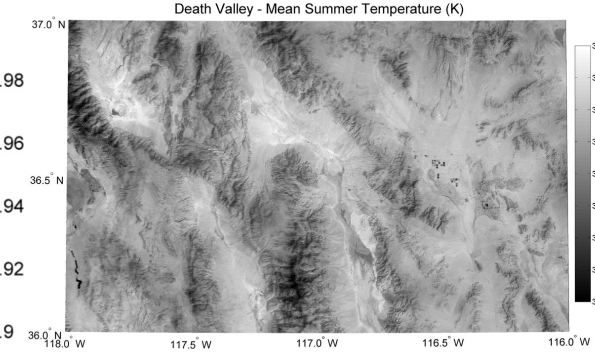

Less variation at longer wavelengths, hence the use of long wave IR Bands in split-window algorithms

Death Valley - Decorrelation Stretch - RGB (Band 14,12,10)

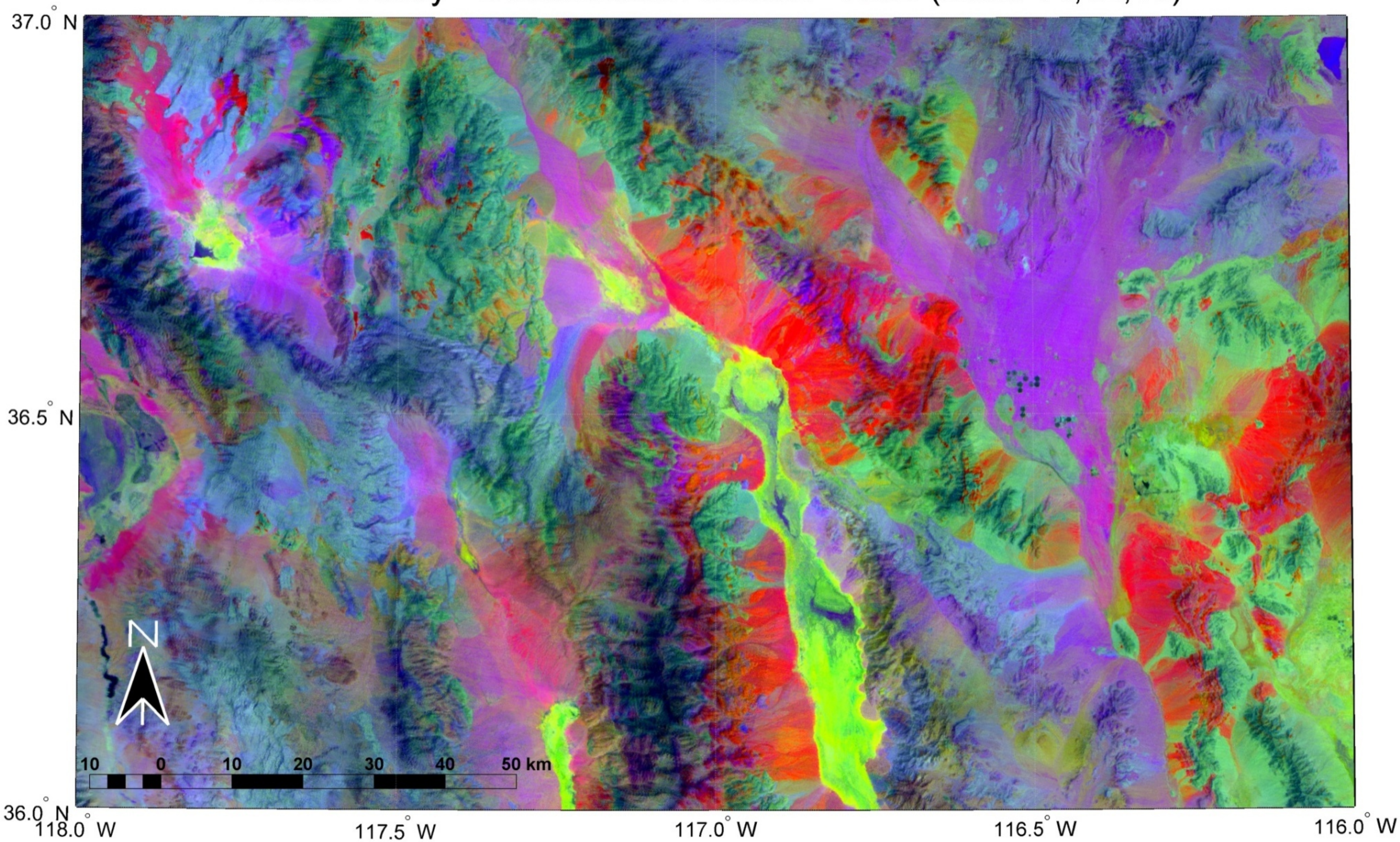

- Quartz-rich
- Carbonates
- Quartz-poor

Can use average temperature and emissivites to reconstruct a destretch without noise!

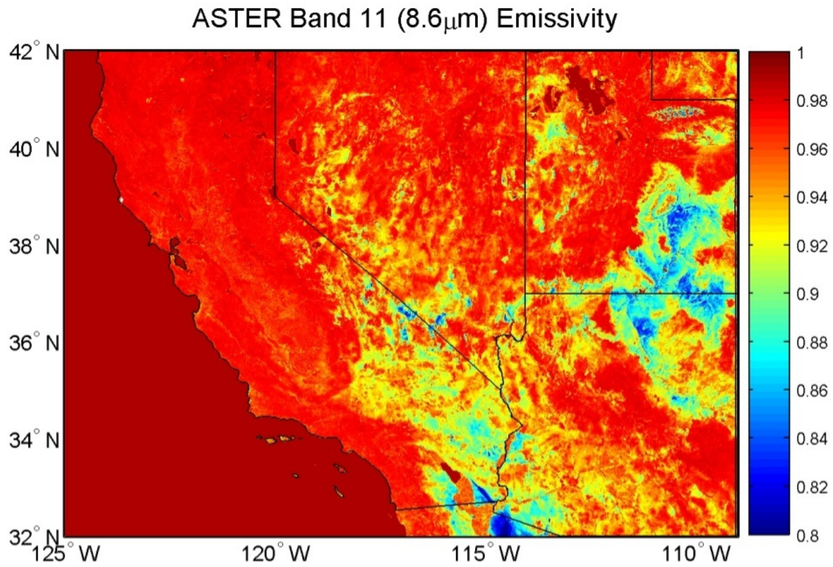

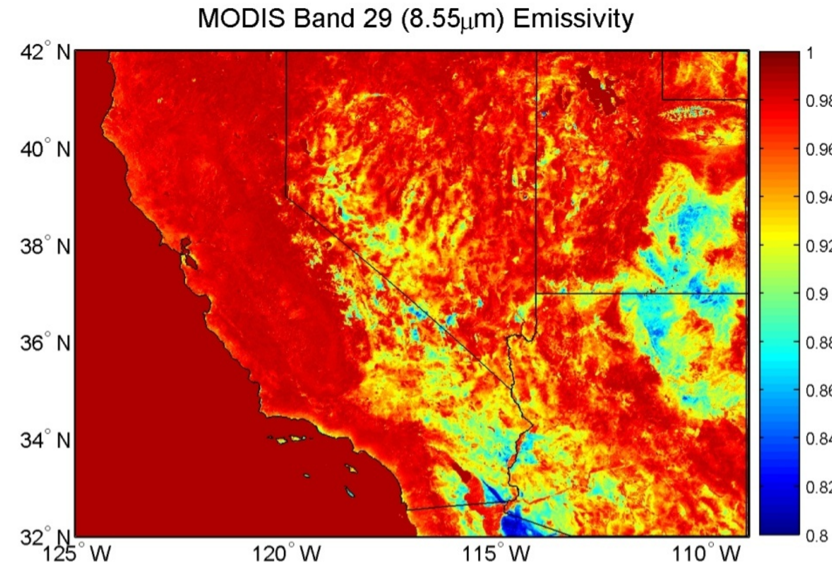

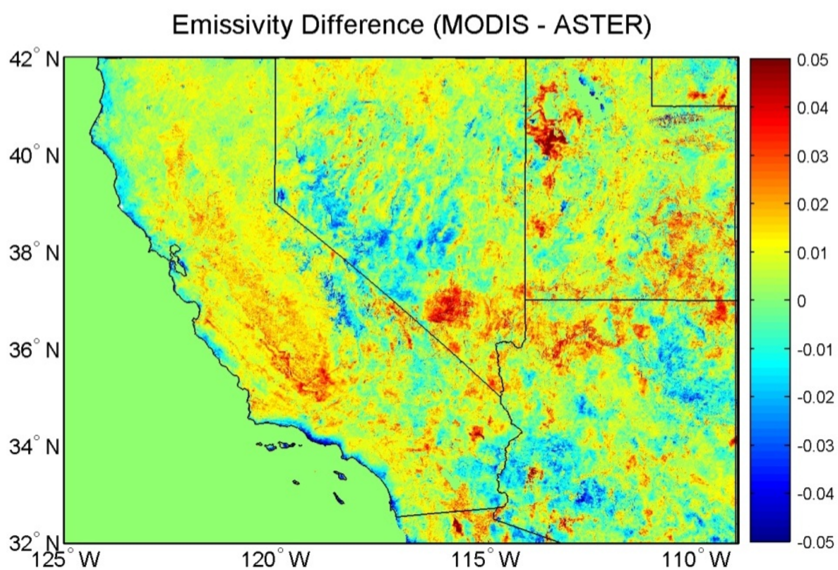

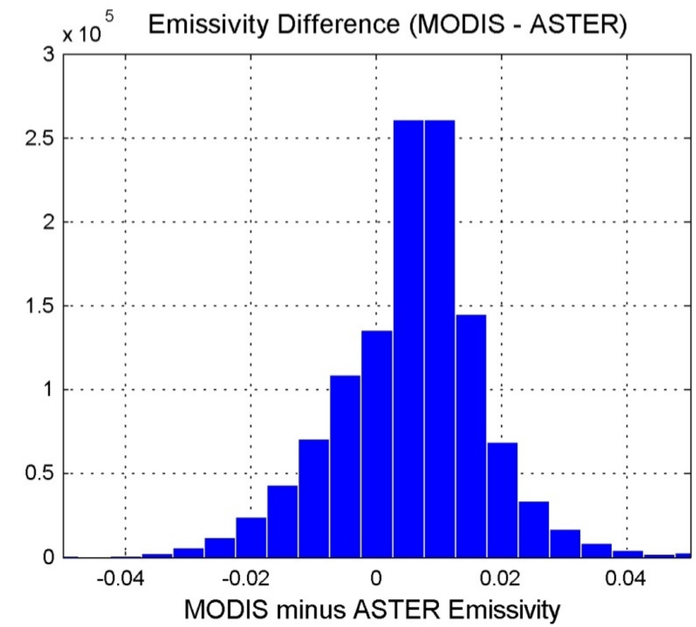

MOD21 product uses same algorithm as ASTER and provides 1km resolution emissivity

MODIS Temperature Emissivity Separation (MODTES) – MOD21_L2

- A new MODIS LST&E Product
- Generated using the ASTER Temperature/Emissivity Separation (TES) Algorithm with WVS
- Output: LST and emissivity for MODIS bands 29, 31, 32 at 1km spatial resolution
- Currently undergoing testing at MODAPS
- Future work:
  - Product testing and inter-comparisons
  - Validation (Radiance-based, Temperature-based)
  - Product ATBD

MOD21 Land Surface Temperature [K], 8-day mean, August 2004

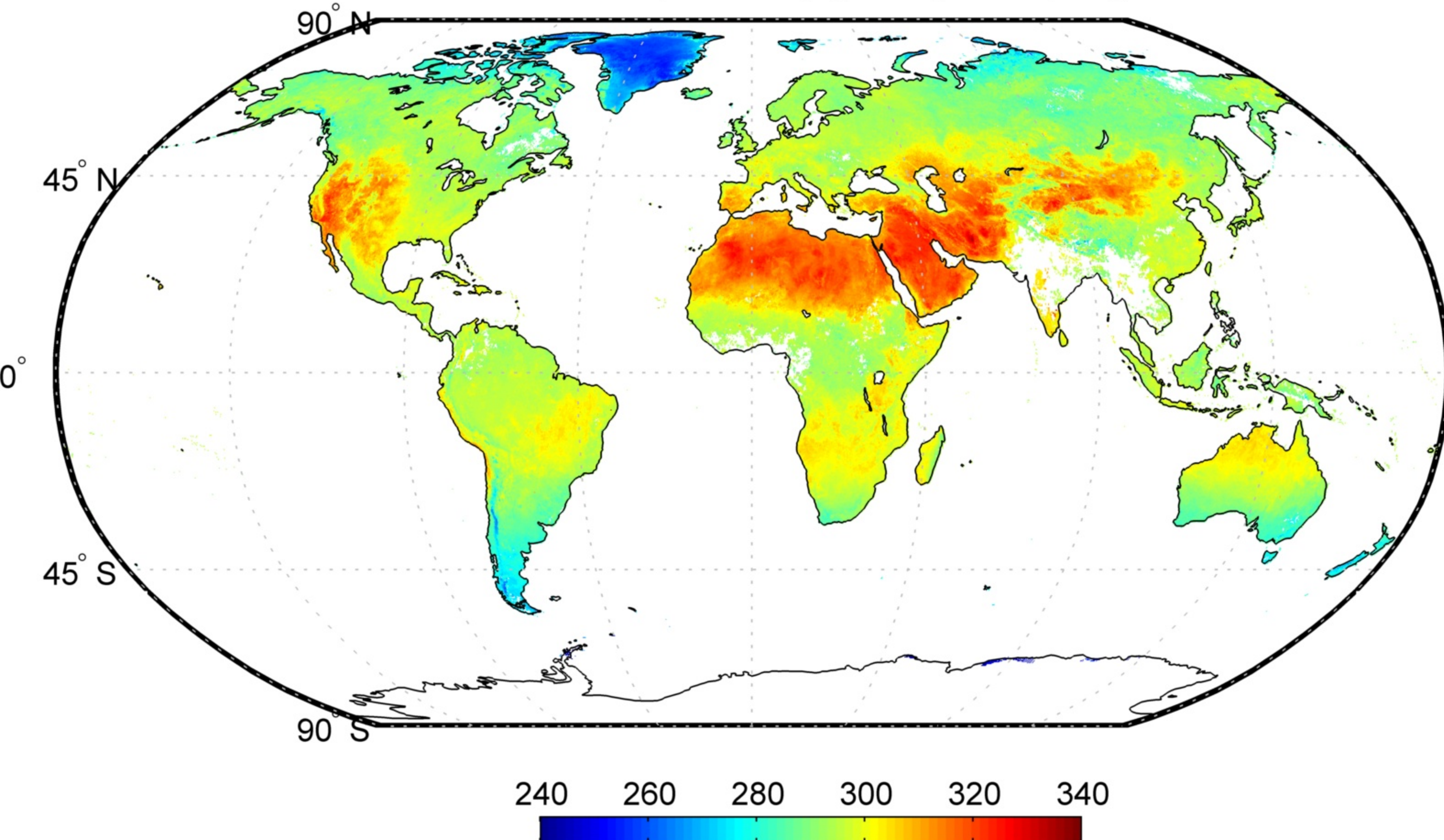

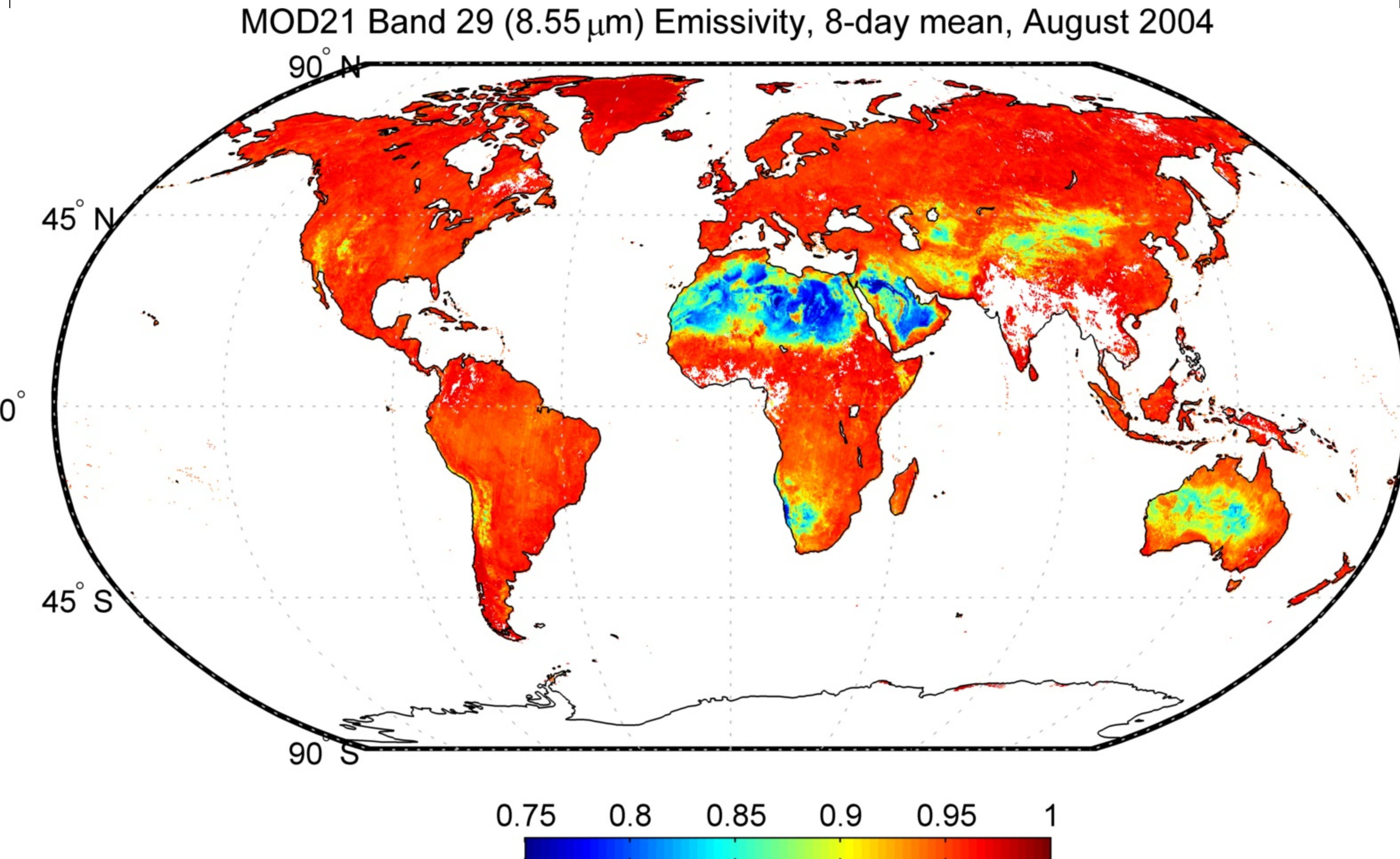

Great variation globally associated with reststrahlen band (Si-O stretching region)

MOD21 Band 31 (11 μm) Emissivity, 8-day mean, August 2004

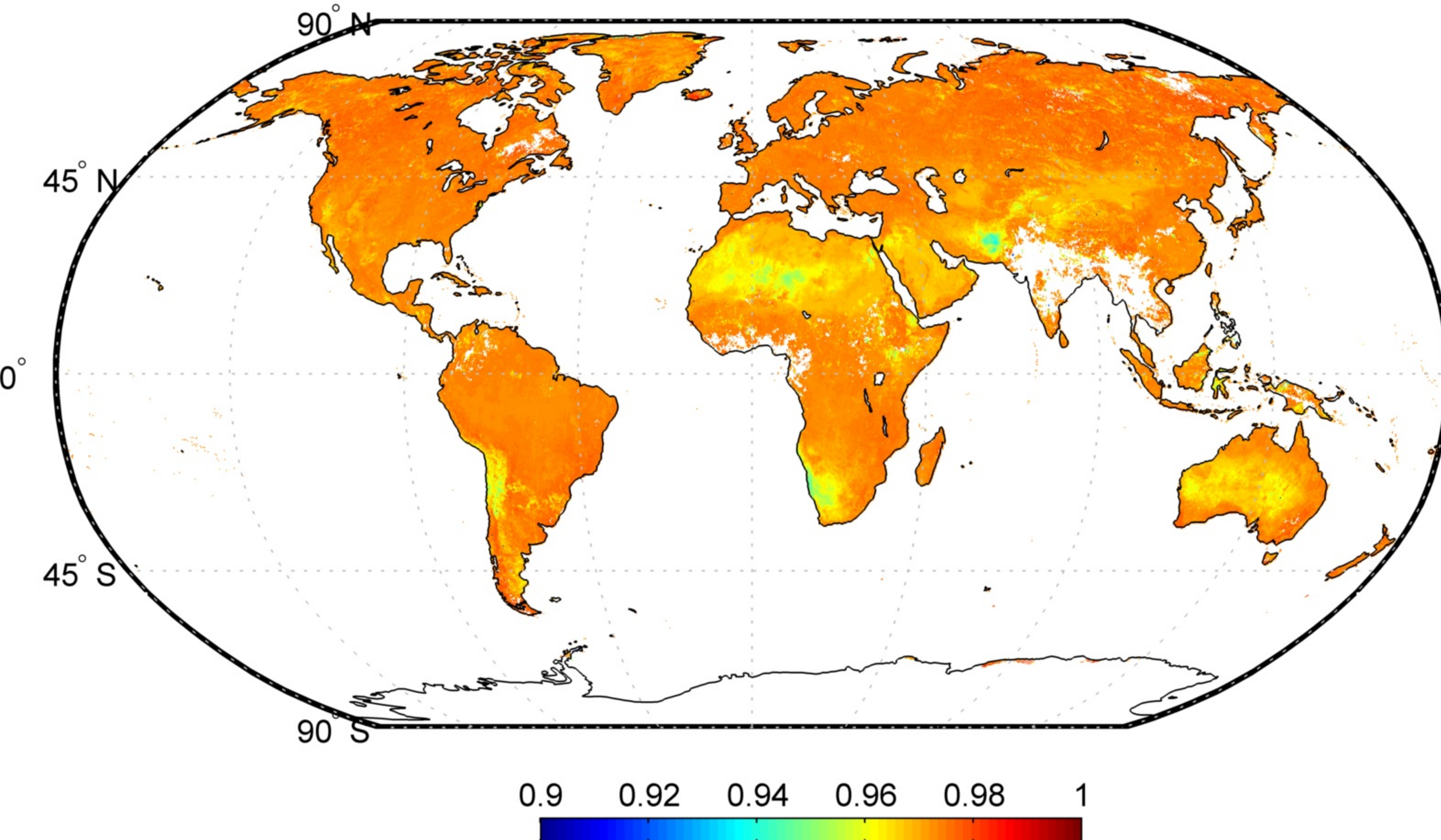

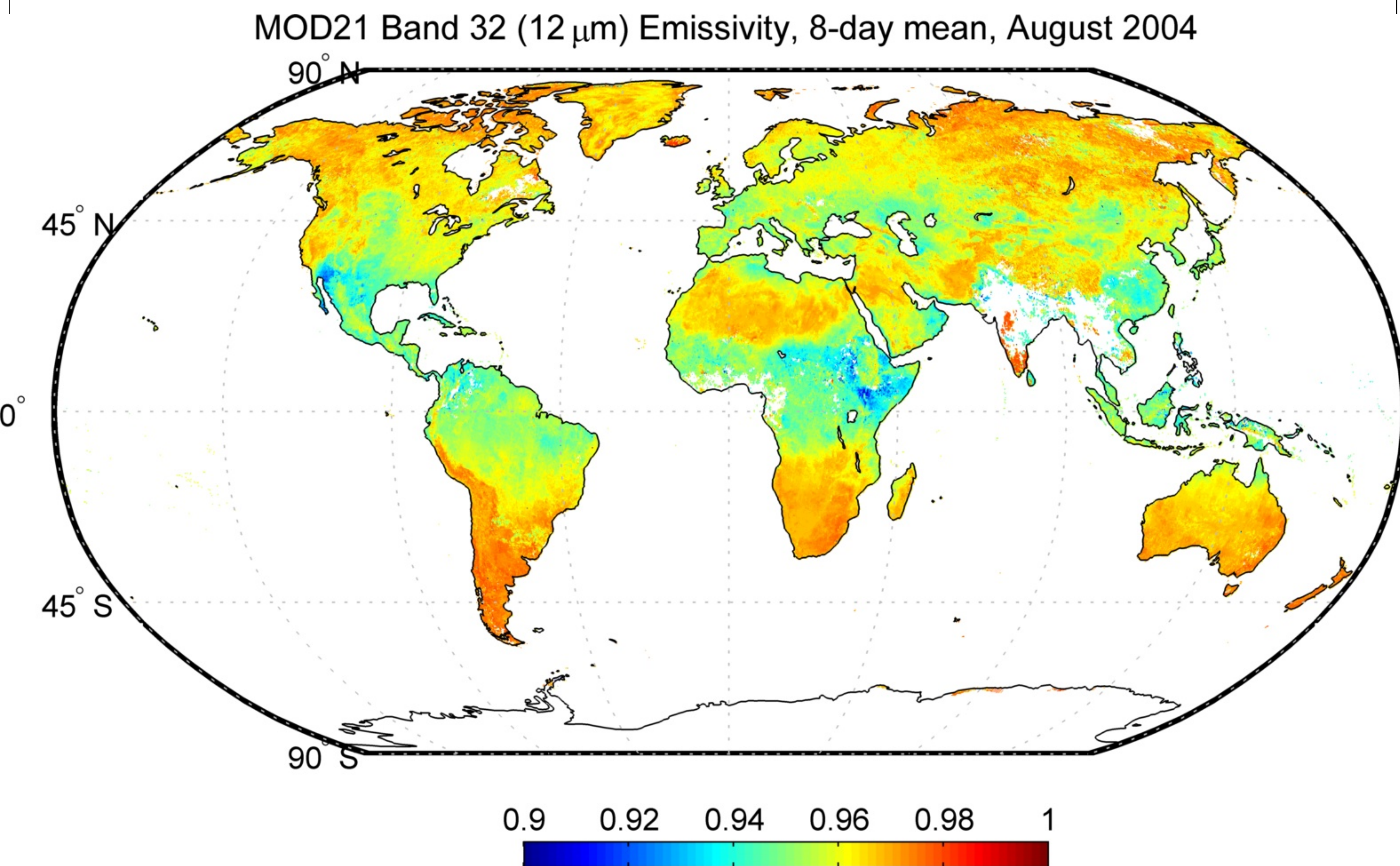

Variation in Band 32 highlights problems with split window algorithms which assume emissivity is constant

Emissivity Validation: Pseudo-Invariant sand dune sites

- Emissivity is notoriously difficult to validate. Typically large homogeneous areas with known composition are required (possible with ASTER – 90m)
- Large Sand-dune sites consistent mineralogy and physical properties over long time periods
- Rapid infiltration after rains, and drying of surface does not lead to cracks
- Mineralogy and composition can be accurately determined using lab reflectance and X-ray diffraction measurements at JPL
- **Sand-dune validation sites:**

Algodones dunes, El Centro, California

White Sands National Monument, New Mexico

Stovepipe Wells Dunes, Death Valley, California

Kelso Dunes, Mojave Desert, California

Great Sands National Park, Colorado

Sand Hollow State Park, Utah

Coral Pink Sand Dunes, Utah

Little Sahara, Utah

Killpecker Dunes, Wyoming

Moses Lake, Washington

ALGODONES DUNES, California

Sand Dune Validation Results

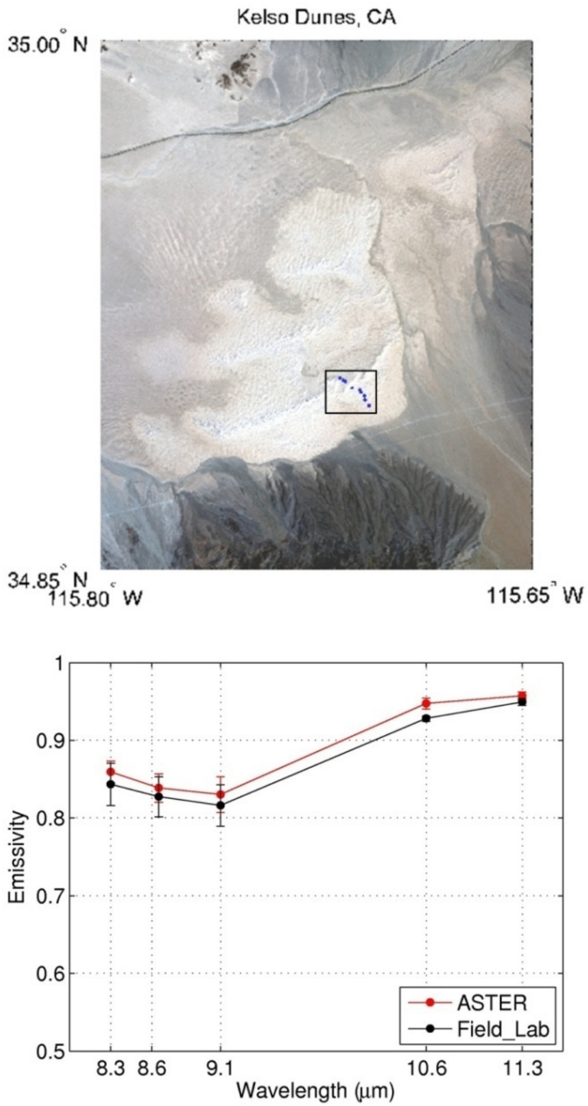

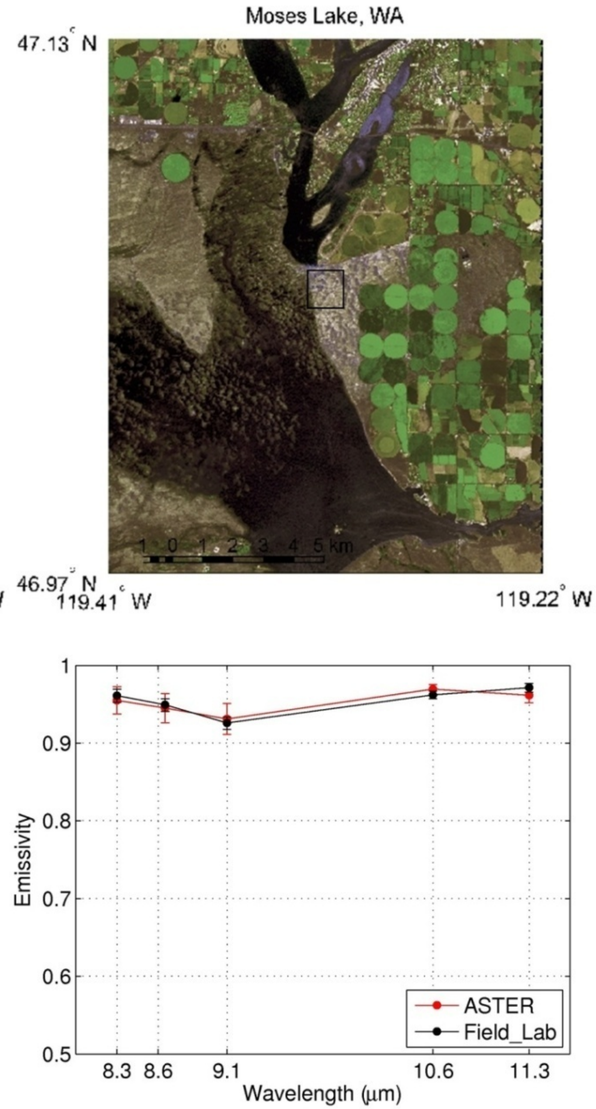

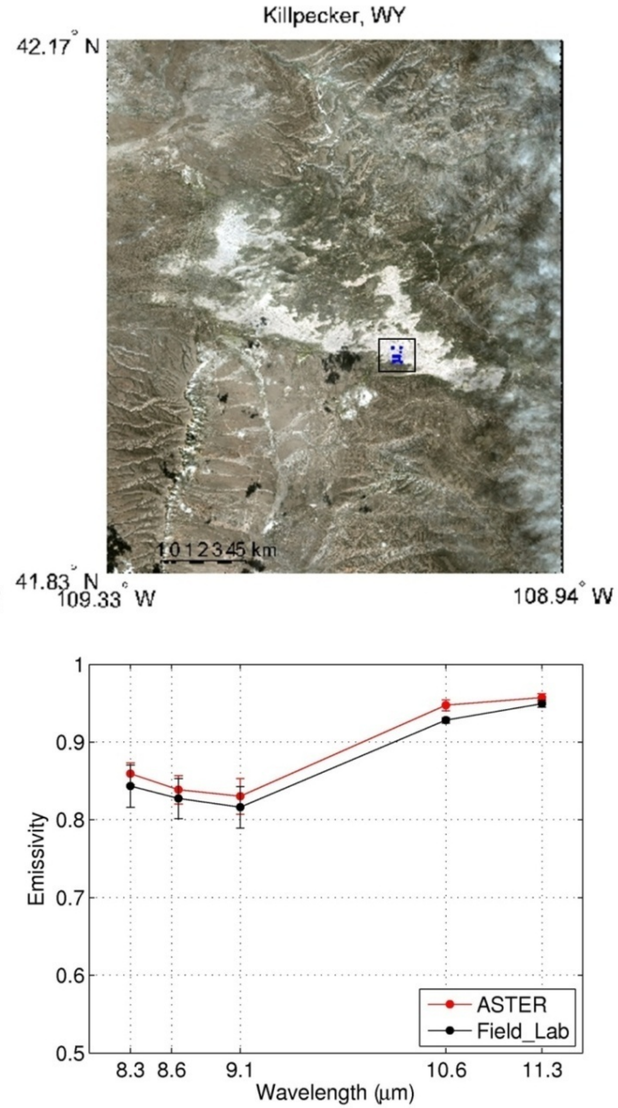

Hulley, G. C., Hook, S. J., and A.M. Baldridge, Validation of the North American ASTER Land Surface Emissivity Database (NAALSED) Version 2.0, *Remote Sensing of Environment* (2009), accepted

Sand Dune Emissivity Validation Results

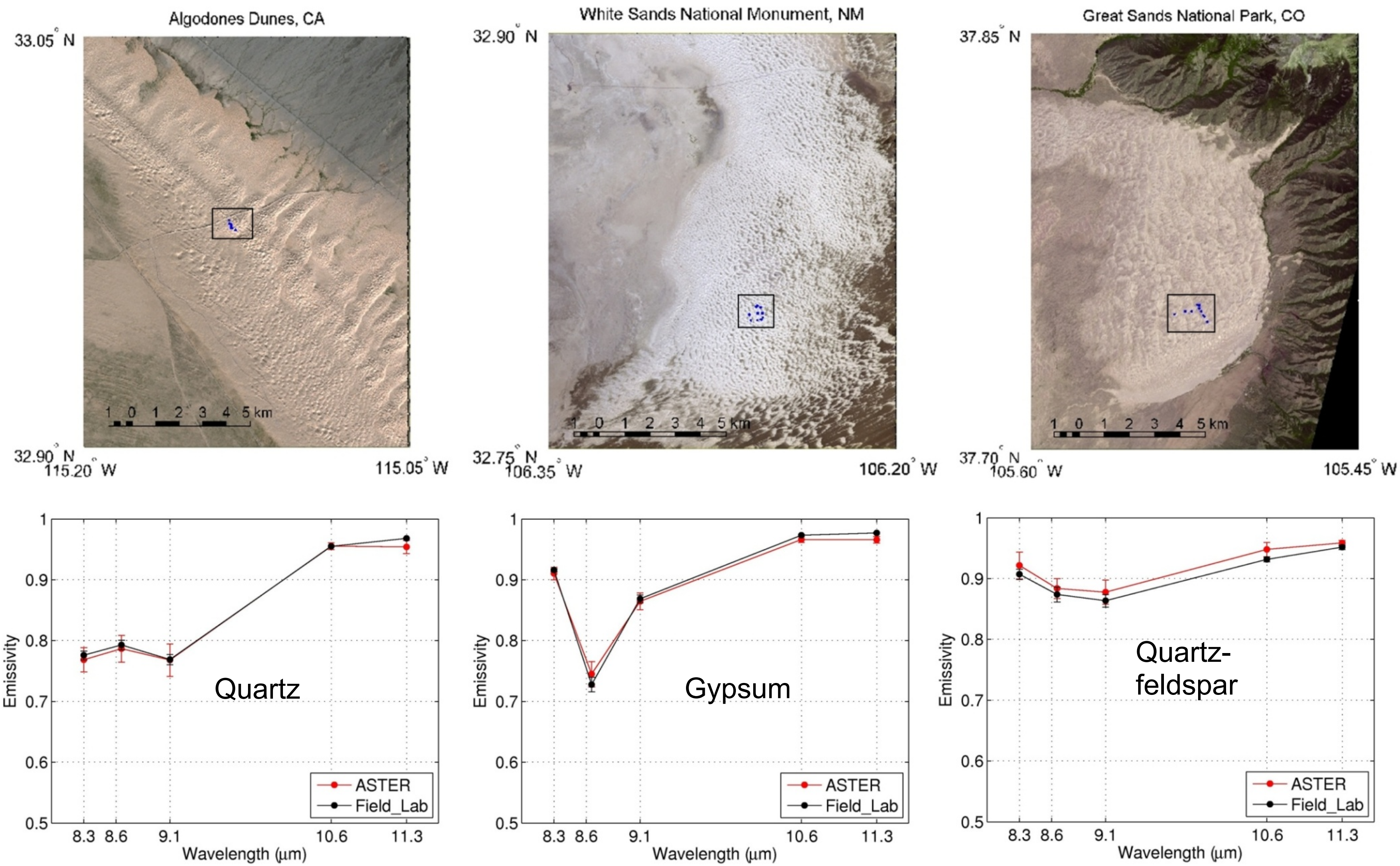

Hulley, G. C., Hook, S. J., and A.M. Baldridge, Validation of the North American ASTER Land Surface Emissivity Database (NAALSED) Version 2.0, *Remote Sensing of Environment* (2009), accepted

The End

National Aeronautics and Space Administration

Jet Propulsion Laboratory
California Institute of Technology
Pasadena, California

www.nasa.gov

JPL 400-1278 7/06

WVS Scaling Factor, γ

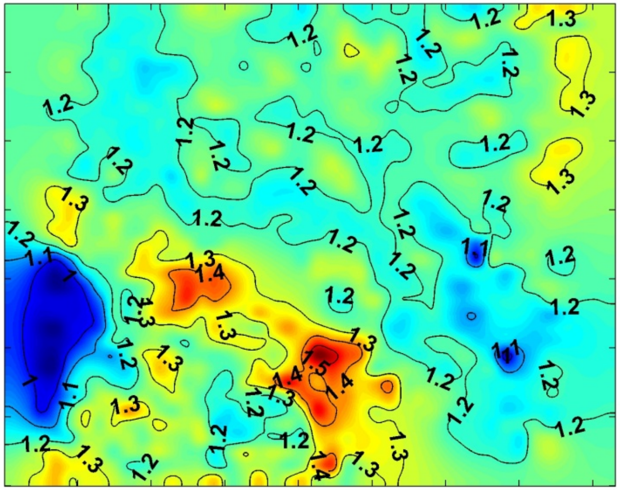

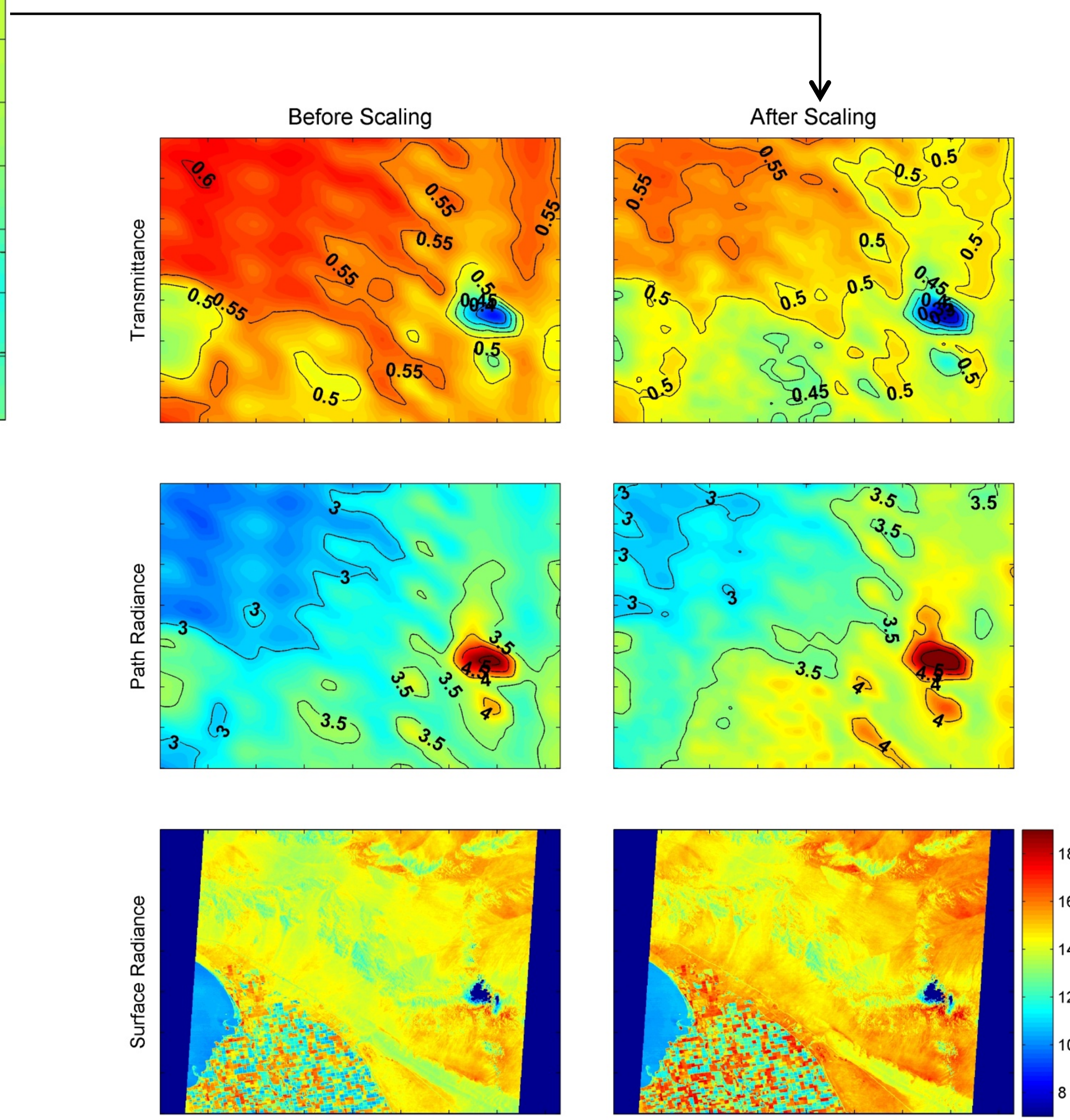


GREAT SANDS, Colorado
24 June, 2008
104 km²
Major: Quartz
Minor: Feldspar


WHITE SANDS, New Mexico
20 May, 2008
704 km^2
Major: Gypsum

Sand samples collected in field

Reflectance measured using Nicolet 520 FTIR spectrometer

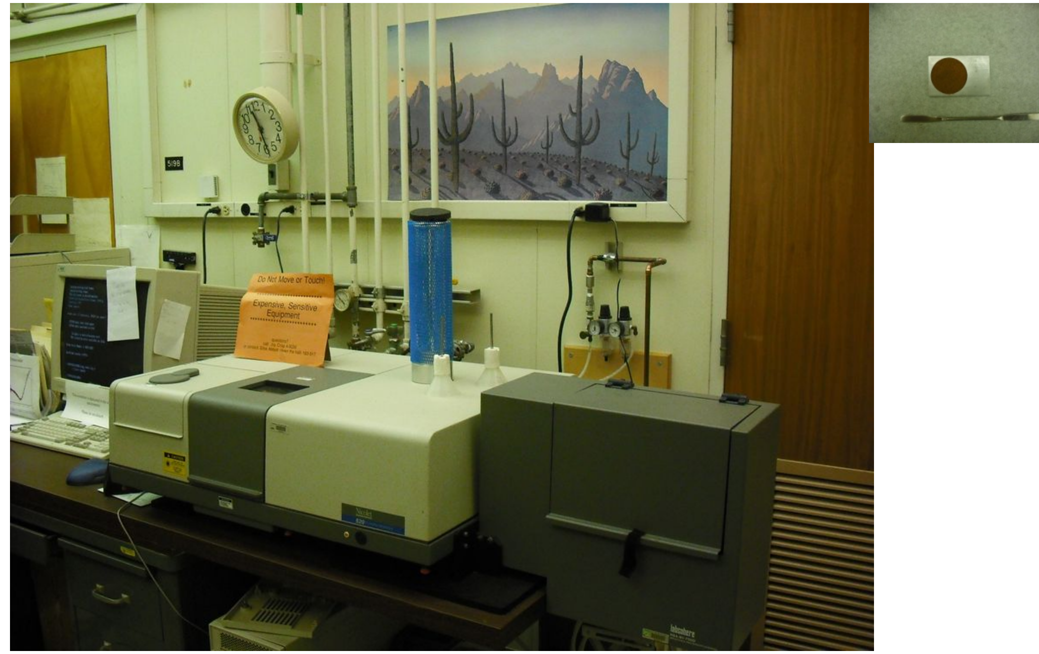

JPL

LAB MEASUREMENTS

$\varepsilon = 1 - r$

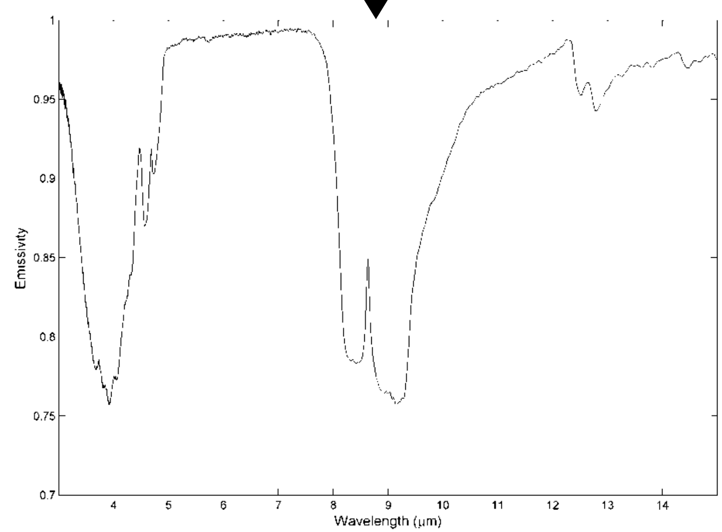

spectral range: 2.5 – 15 µm

spectral resolution: 4 cm^{-1}

1000 scans in 10 minutes

Pseudo-Invariant Sand Dune Sites

Table 1
Summary of the major characteristics of each dune site including locality, elevation, surface area, dune height, grain size, sand source and bulk mineralogy.

Dune site	Locality	Surface area (km^2)	Elevation/max dune height (m)	Grain size	Sand source	Mineralogy (XRD)
Algodones (32.95° N, 115.07° W)	Southeast CA, Eastern margin of the Salton Trough	720	94/80	Medium to coarse sand	Beach sand from Lake Cahuilla	Major: quartz
Coral Pink (37.04° N, 112.72° W)	Sand Valley, just north of UT–AZ border, west Kanab	13.6	1780/10	Medium sand	Navajo, Page and Estrada Jurassic sandstones of the Vermillion Cliffs	Major: quartz
Great Sands (37.77° N, 105.54° W)	San Luis Valley, CO, adjacent to Sangre de Cristo, NE of Alamosa	104	2560/230	Medium to coarse sand	Quartz and volcanic fragments derived from Santa Fe and Alamosa formations, recent fluvial (Rio Grande) deposits	Major: quartz Minor: potassium feldspar
Kelso (34.91° N 115.73° W)	Mojave Desert, CA, southeast of Baker	115	800/195	Medium sand	Derived from sedimentary, metamorphic, igneous terrains from Mojave River alluvial apron	Major: quartz Minor: potassium feldspar Trace: magnetite
Killpecker (41.98° N 109.10° W)	Southwest WY, from Eden across Rock Springs into Red Desert	550	2000/45	Medium sand	Sandstone and siltstone of the Laney member of the Green River Formation	Major: quartz Trace: magnetite Minor: plagioclase feldspar, epidote
Little Sahara/Lynndyl (39.7° N 112.39° W)	West-central UT, Sevier River drainage basin, west of Lynndyl	575	1560/200	Fine sand	Deltaic and shoreline sediments from the Provo shoreline of Lake Bonneville	Major: quartz Minor: plagioclase feldspar, pyroxene, carbonate, magnetite
Stovepipe Wells (36.62° N, 117.11° W)	Central Death Valley, CA, near Stovepipe Wells	7.7	−12/40	Medium sand	Mixed lithic fragments and quartz from Emigrant Pass to the west and Furnace Wash to the east	Major: quartz Minor: plagioclase feldspar, potassium feldspar
Moses Lake (47.05° N, 119.31° W)	Quincy Basin in central WA	40	345/18	Fine sand	Basaltic sand from the east bank of the Columbia River	Major: quartz, albite
White Sands (32.89° N, 106.33° W)	South-central NM, Tularosa Valley	704	1216/10	Fine sand	Paleo-lake Otero, present playa Lake Lucero to the southwest	Major: gypsum

Hulley, G. C., Hook, S. J., and A.M. Baldridge, (2009), Validation of the North American ASTER Land Surface Emissivity Database (NAALSED) Version 2.0, *Remote Sensing of Environment*, 113, 2224-2233

ASTER validation with pseudo-invariant sand dune sites

	ASTER MINUS LAB EMISSIVITY (%)					
Dune site	**Band 10**	**Band 11**	**Band 12**	**Band 13**	**Band 14**	**Mean**
Algodones	0.68	0.60	0.13	0.02	1.40	**0.57**
Stovepipe Wells	0.17	0.77	1.02	0.34	0.37	**0.53**
White Sands	0.34	2.76	0.16	0.92	1.08	**1.05**
Kelso Dunes	1.57	1.04	1.33	1.91	0.81	**1.33**
Great Sands	1.44	0.97	1.42	1.64	0.69	**1.23**
Moses Lake	0.69	0.52	0.42	0.61	1.01	**0.65**
~~Sand Mountain~~	~~7.74~~	~~6.47~~	~~9.01~~	~~1.82~~	~~1.10~~	~~**5.23**~~
Coral Pink	7.48	6.44	7.32	2.50	1.70	**4.90**
Little Sahara	3.55	2.39	2.60	0.96	0.19	**1.94**
Killpecker	2.34	1.99	2.26	1.33	0.81	**1.75**

< 1.6% (1 K)

Examples of Level Products Possible from Existing Assets

Dale A. Quattrochi
NASA
Earth Science Office
Marshall Space Flight Center
Huntsville, AL

HyspIRI Science Products Symposium – NASA/GSFC – May 16-17, 2012

Back to the Fundamentals: HyspIRI Science Questions

CQ6 Overarching Question: *How do patterns of human environmental and infectious diseases respond to leading environmental changes, particularly to urban growth and change and the associated impacts of urbanization?*

CQ6. HyspIRI Science Questions

Human Health and Heat Island

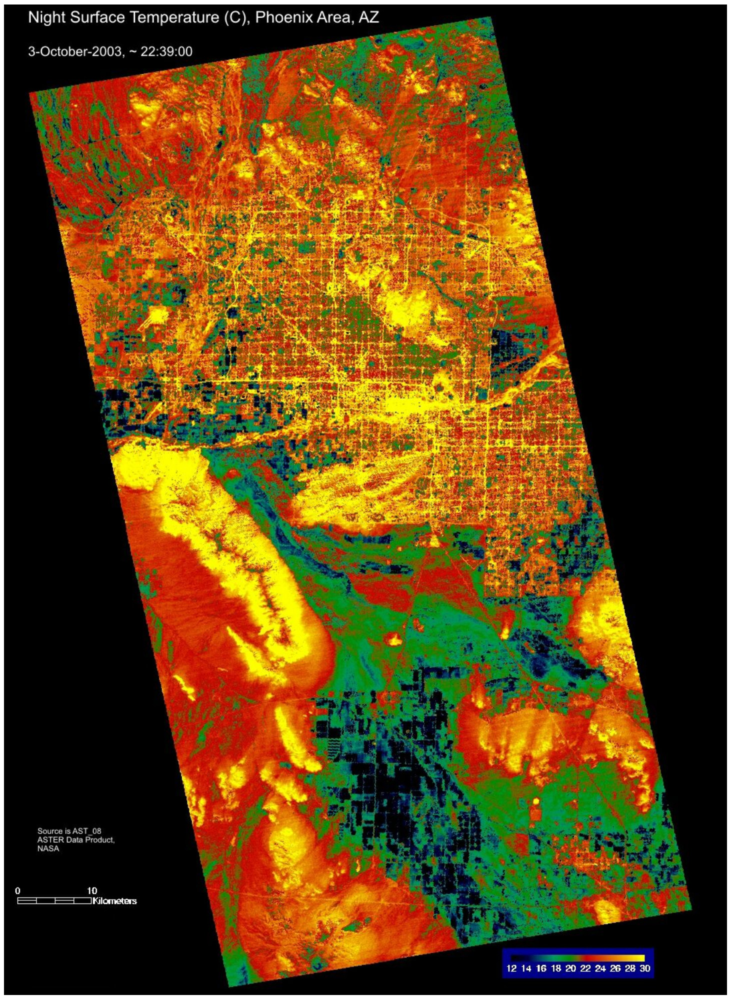

Heat Related Deaths - Chicago

Maximum Temperature and Heat Index

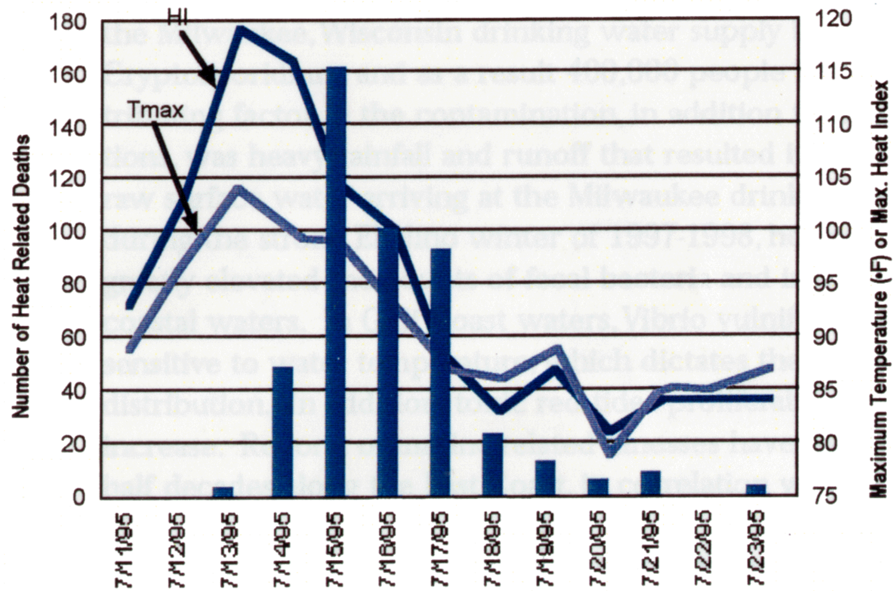

This graph tracks maximum temperature, heat index, and heat-related deaths in Chicago each day from July 11 to 23, 1995. The gray line shows maximum daily temperature, the blue line shows the heat index, and the bars indicate number of deaths for the day.

CQ6. HyspIRI Science Questions
Heat Stress & Drought

Chile 31 March 2001 Color Composite bands 3,5,4 (2.5% Saturation)

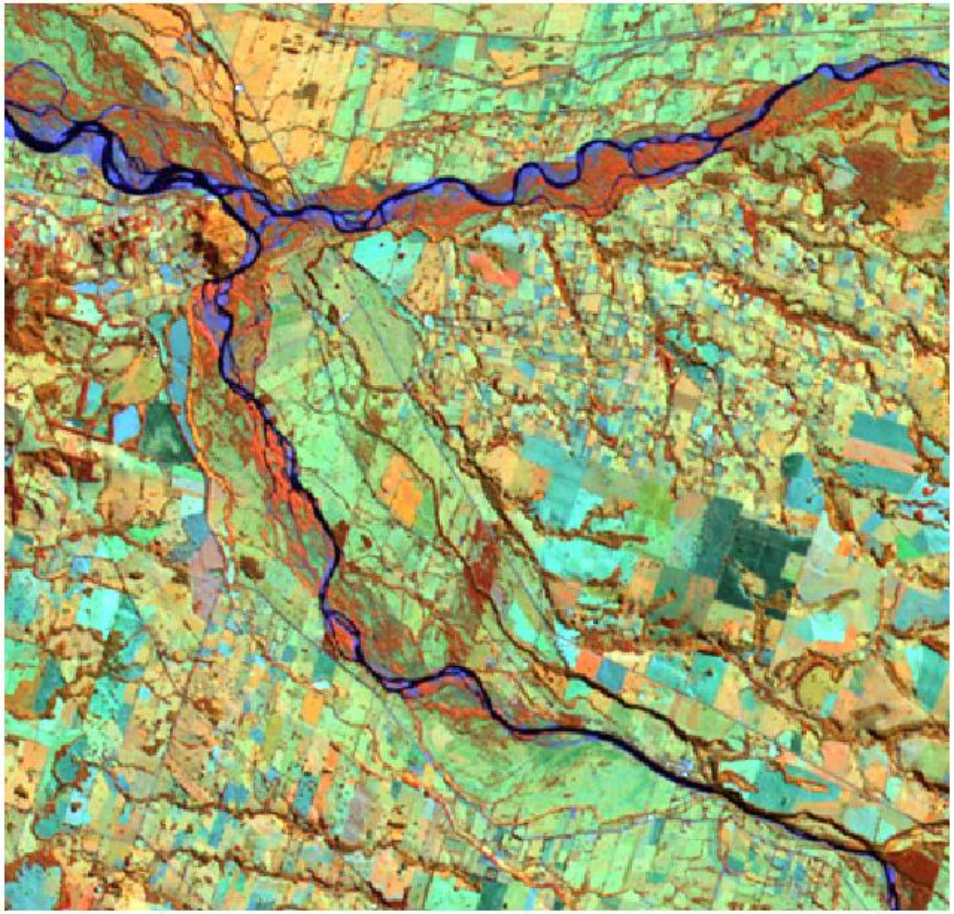

CQ6. HyspIRI Science Questions

Vector-borne Diseases (Malaria)
Heterogeneous Transmission with Landscape

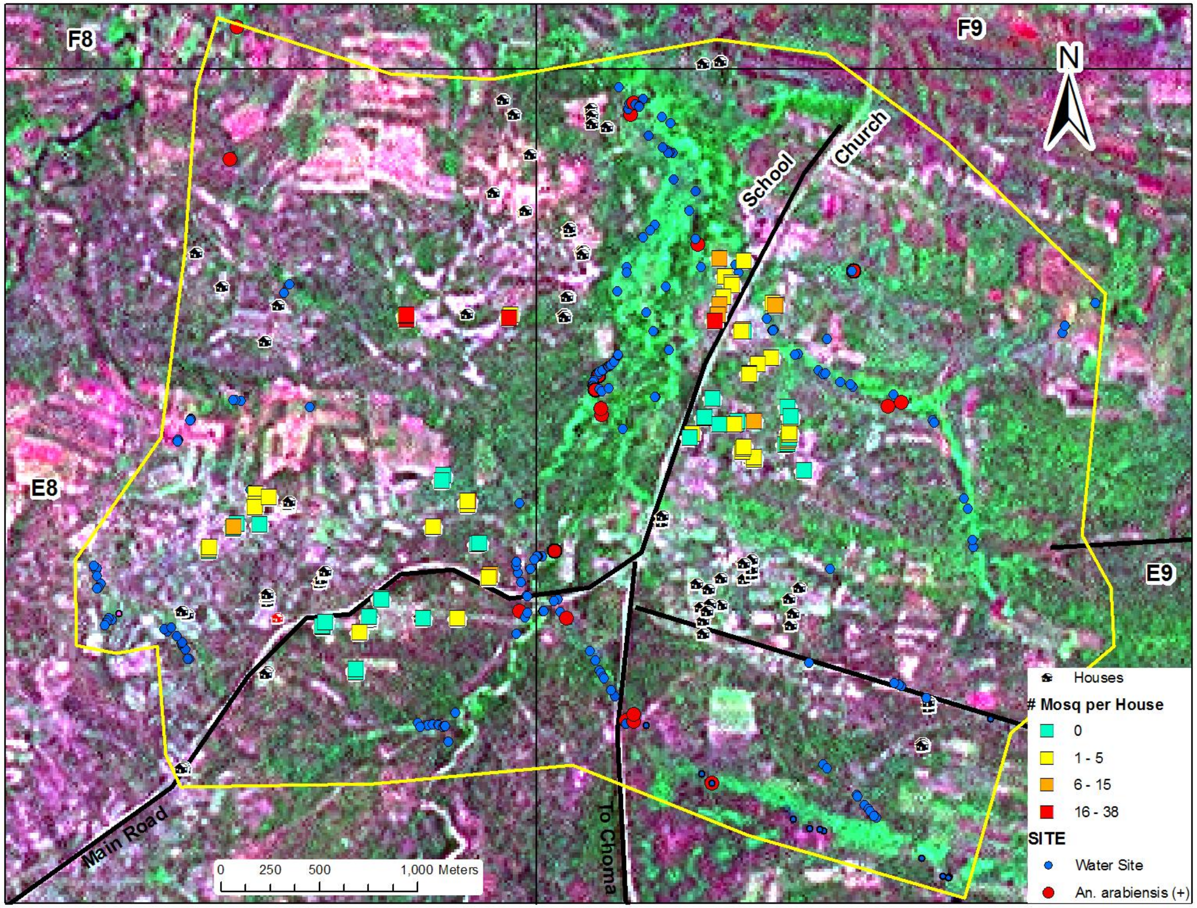

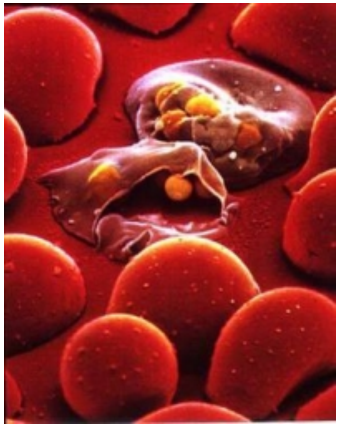

CQ6. HyspIRI Science Questions

Zoonotic Diseases

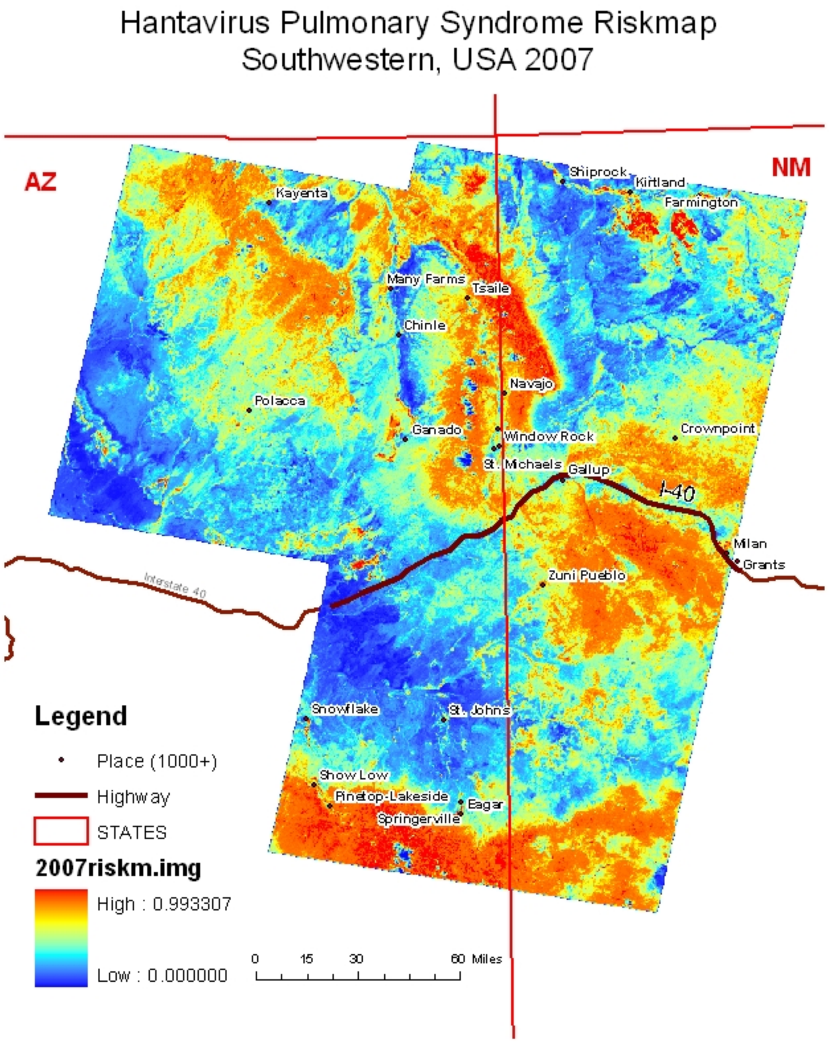

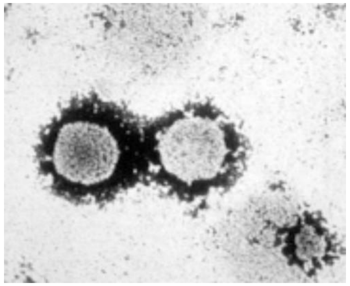

Back to the Fundamentals: HyspIRI Science Questions

TQ4 Overarching Question: *How does urbanization affect the local, regional, and global environment? Can we characterize this effect to help mitigate its impact and welfare?*

TQ4 HyspIRI Science Questions

Science Issue: How do changes in land cover and land use affect surface energy balance and the sustainability and productivity of natural and human ecosystems?

Potential Higher Level Products

- **Multispectral thermal IR land cover maps at a high spatial resolution (60m) on a weekly basis for long-term validation of surface energy responses and changes in emissivity**
- **Integration of HyspIRI TIR data with spatial modeling to assess changes in land cover/land use through time and subsequent changes in thermal energy responses**

Land Use Change around MSFC

Dramatic increase in urban-residential land use category from 1992-2001

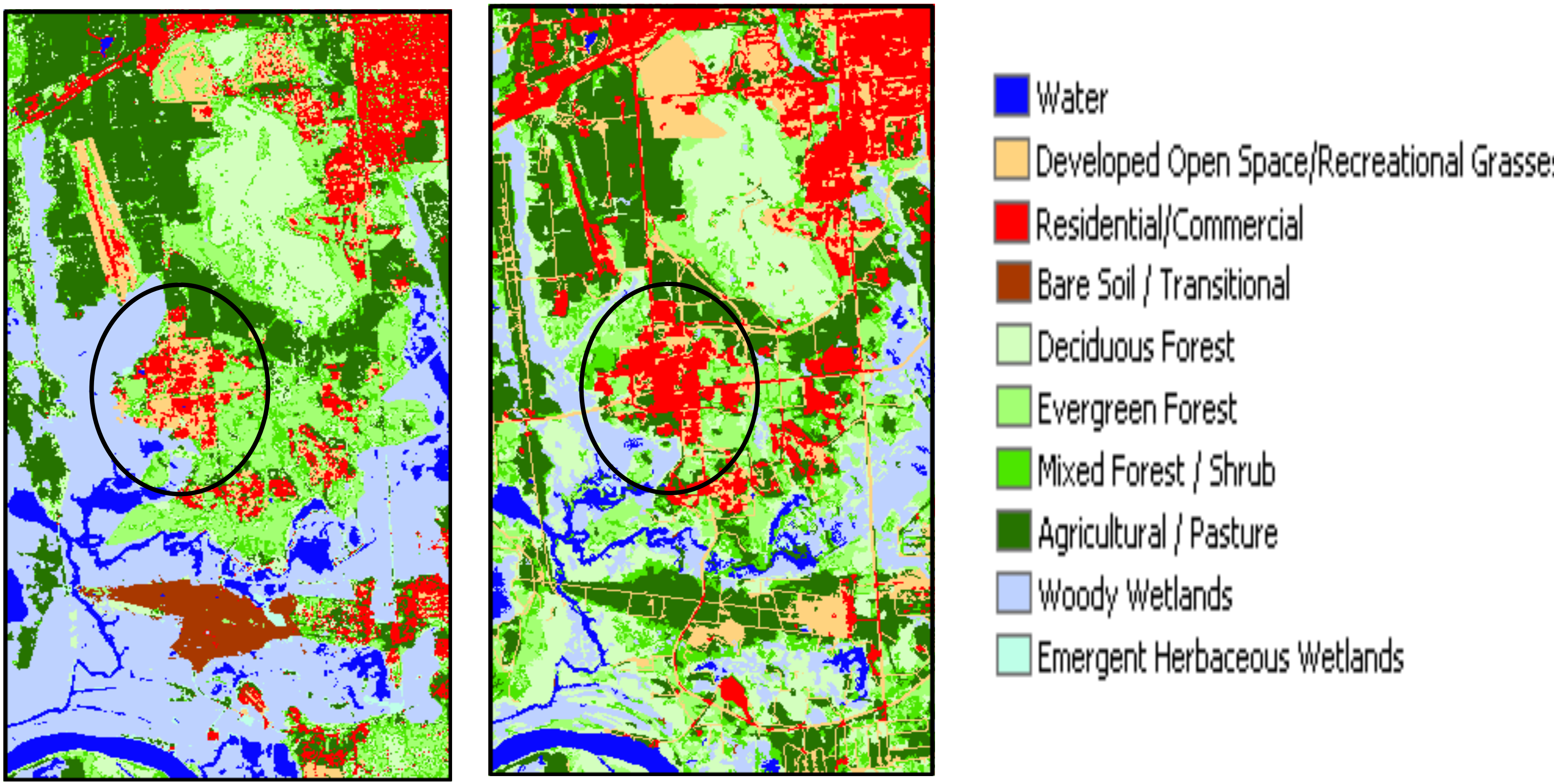

1992 2001

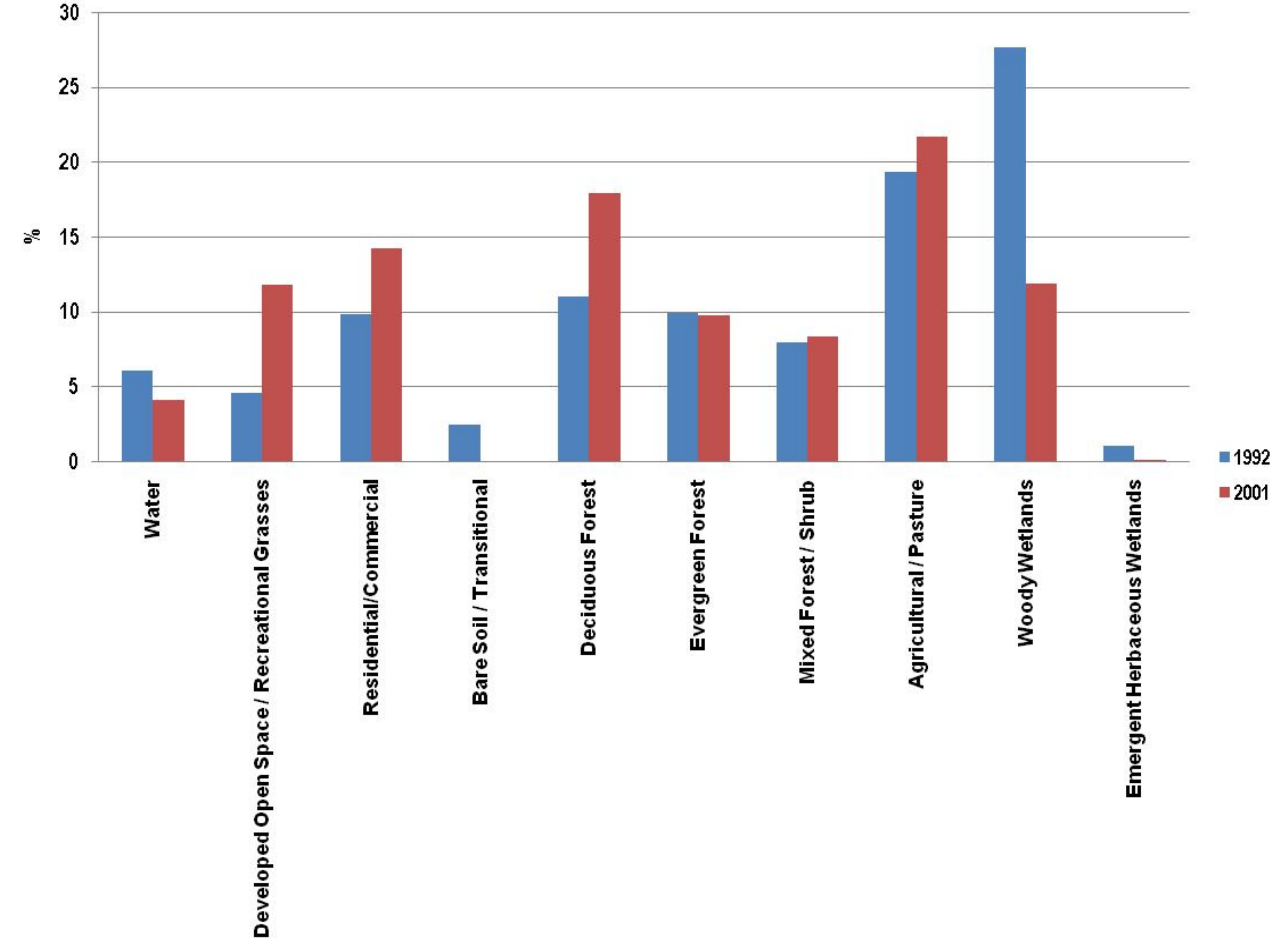
30
25
20
15
10
5
0
%
Water
Developed Open Space / Recreational Grasses
Residential/Commercial
Bare Soil / Transitional
Deciduous Forest
Evergreen Forest
Mixed Forest / Shrub
Agricultural / Pasture
Woody Wetlands
Emergent Herbaceous Wetlands
1992
2001

Land Use Change Drives Thermal Change

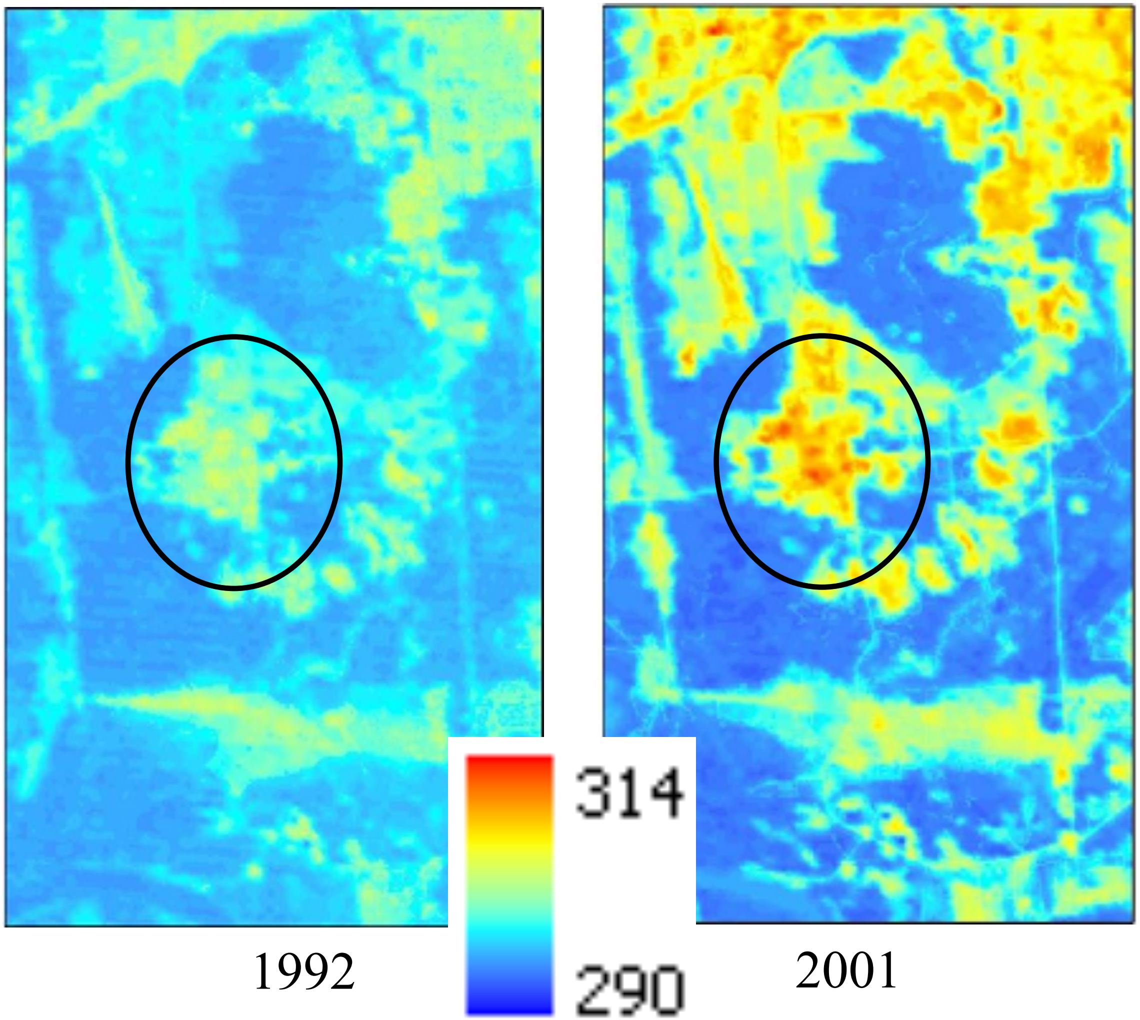

Conversion of forest, shrub, and agricultural land to MSFC infrastructure substantially changes surface thermal signatures

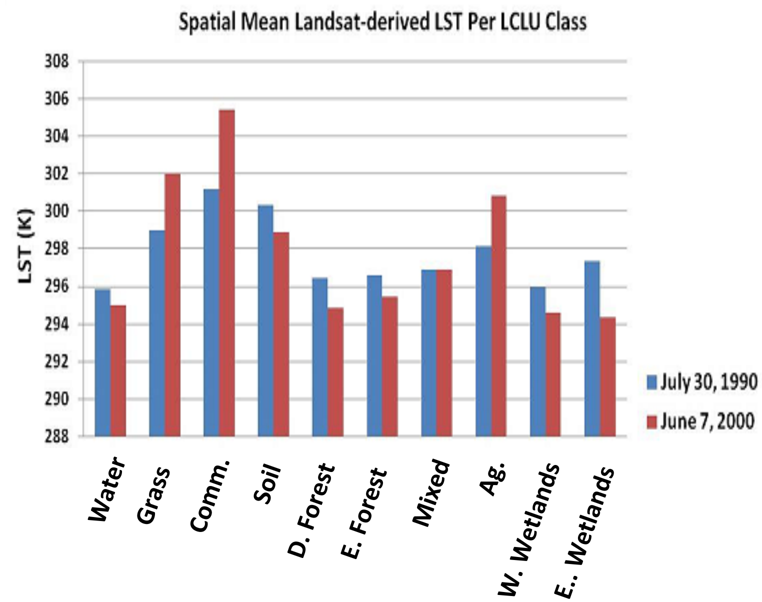

Need to determine impact on local temperatures

Emissivity 1992

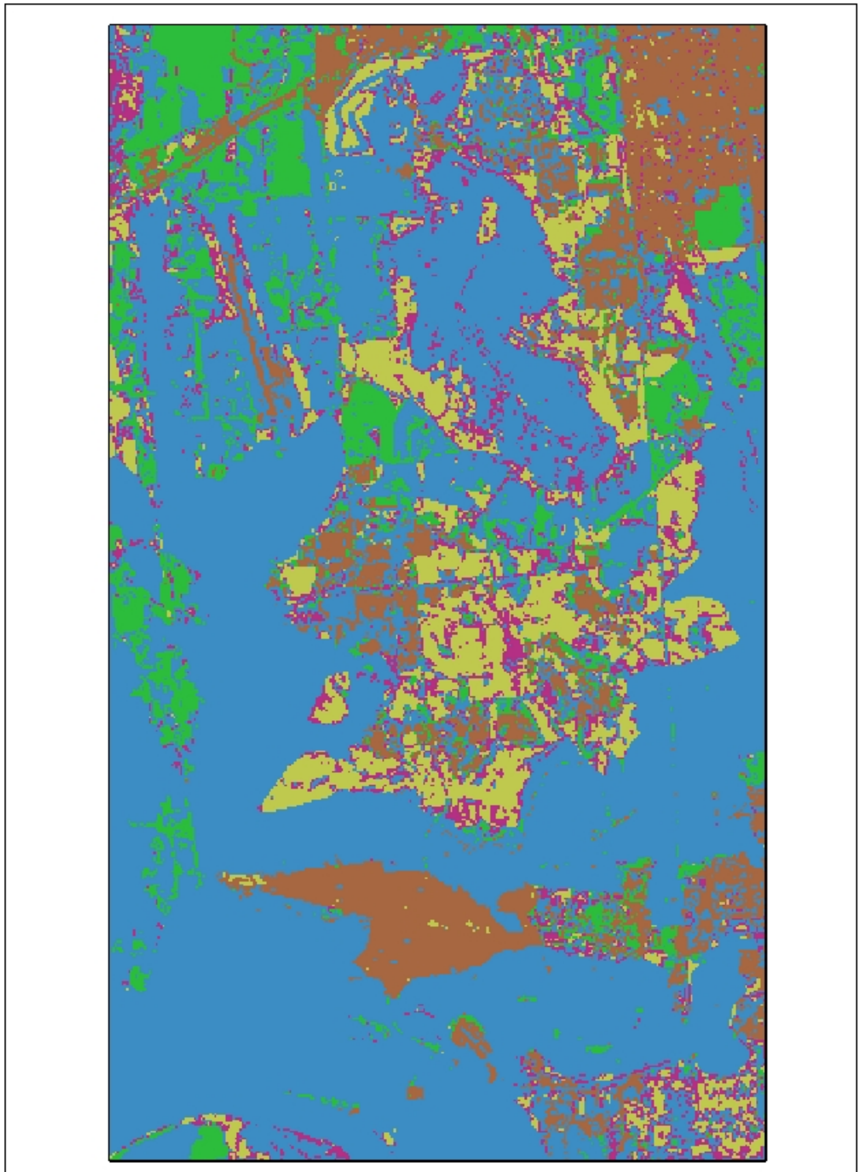

Emissivity

- 0.969 (Used for Bare Soil; and Developed Pixels)
- 0.974 (Used for Shrub Pixels)
- 0.980 (Used for Crops Pixels)
- 0.989 (Used for Deciduous Forests (assuming they're mostly Broadleaf); Wetlands, and Water Pixels)
- 0.9895 (Used for Mixed Forests Pixels)
- 0.990 (Used for Evergreen Pixels (assuming they're mostly Needle))

Based on a look-up table in Snyder et al. 1998 and given that our analysis is for a period when the vegetation is green.

Emissivity 2001

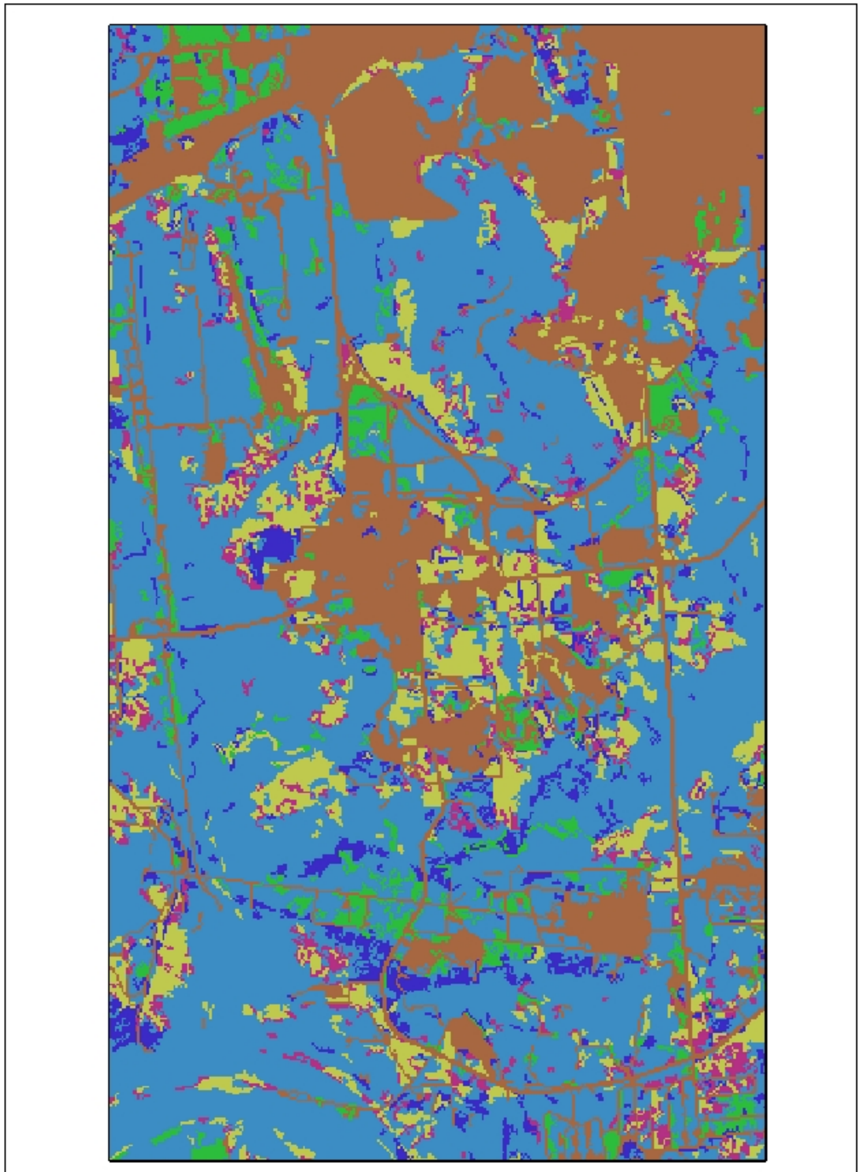

Emissivity

- 0.969 (Used for Bare Soil; and Developed Pixels)
- 0.974 (Used for Shrub Pixels)
- 0.980 (Used for Crops Pixels)
- 0.989 (Used for Deciduous Forests (assuming they're mostly Broadleaf); Wetlands, and Water Pixels)
- 0.9895 (Used for Mixed Forests Pixels)
- 0.990 (Used for Evergreen Pixels (assuming they're mostly Needle))

Based on a look-up table in Snyder et al. 1998 and given that our analysis is for a period when the vegetation is green.

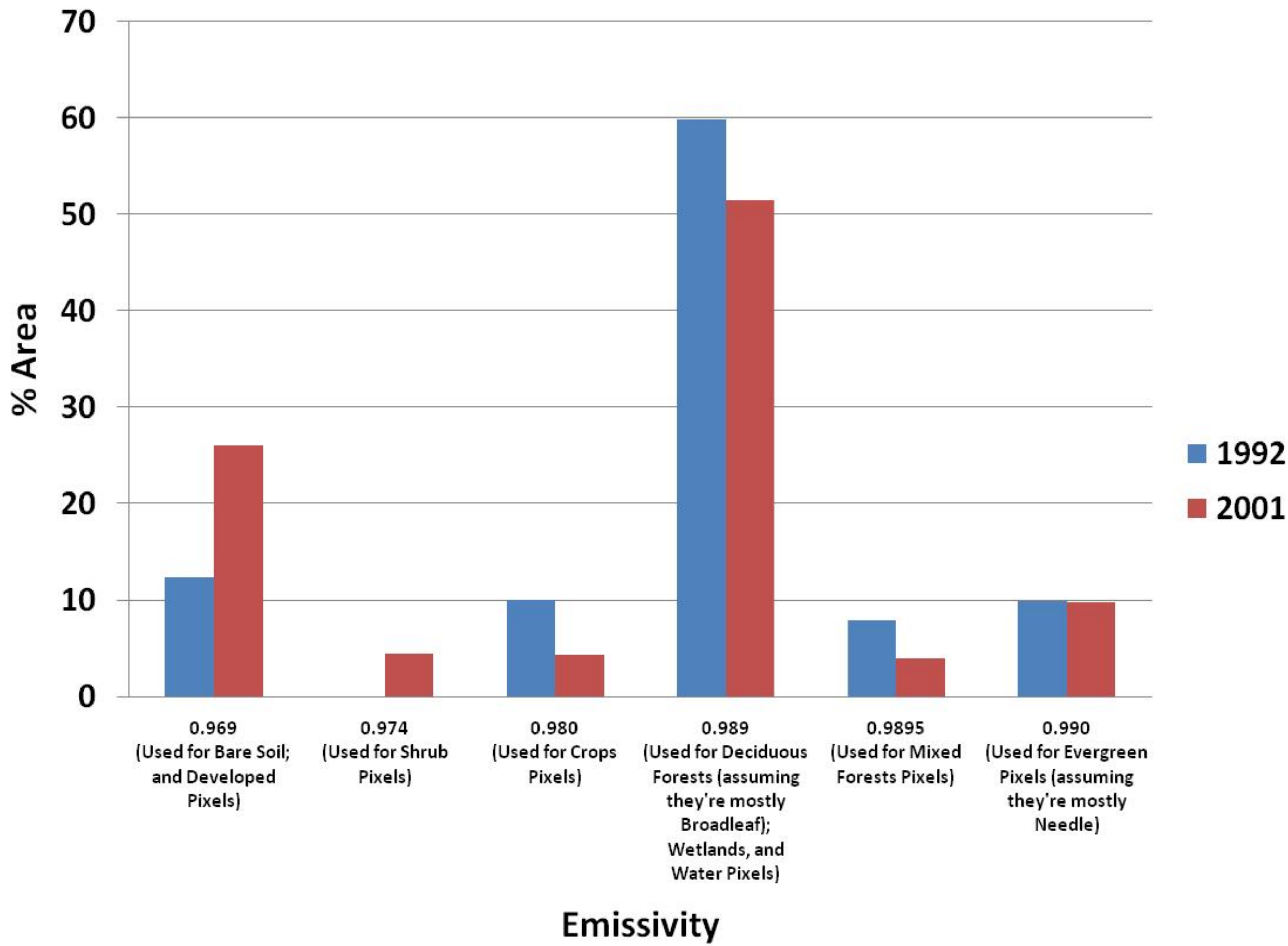
70
60
50
40
30
20
10
0
% Area
1992
2001
0.969
(Used for Bare Soil; and Developed Pixels)
0.974
(Used for Shrub Pixels)
0.980
(Used for Crops Pixels)
0.989
(Used for Deciduous Forests (assuming they're mostly Broadleaf); Wetlands, and Water Pixels)
0.9895
(Used for Mixed Forests Pixels)
0.990
(Used for Evergreen Pixels (assuming they're mostly Needle)
Emissivity

TQ4 HyspIRI Science Questions

Science Issue: What are the dynamics, magnitude, and spatial form of the UHI? How can it best be characterized?

Potential Higher Level Products

- **Maps of UHI development, extent and dynamics for various cities around the world using HyspIRI high spatial resolution (60m) data**
- **Multitemporal (weekly, seasonal) maps of UHI dynamics**
- **Day/Night maps of UHI dynamics**

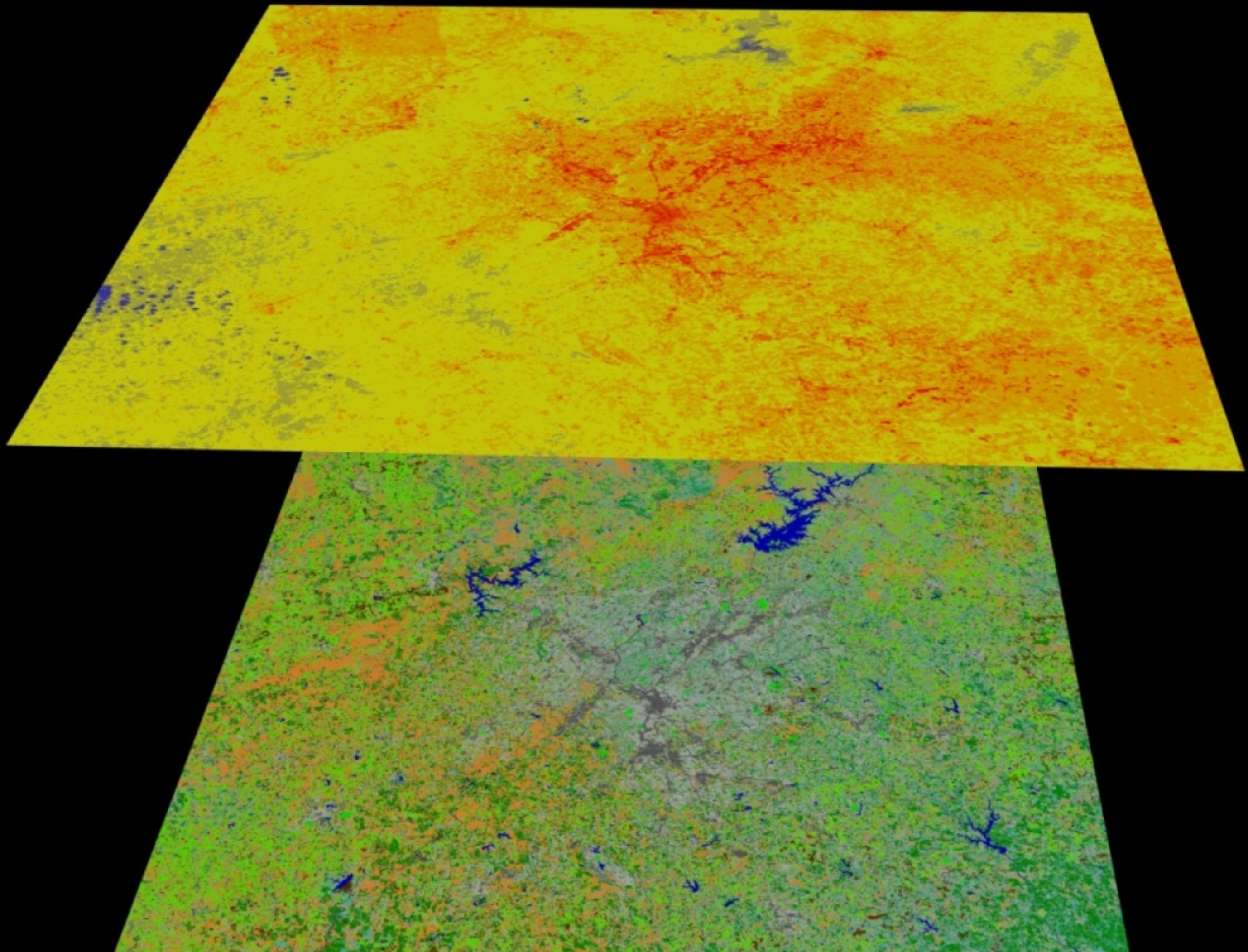

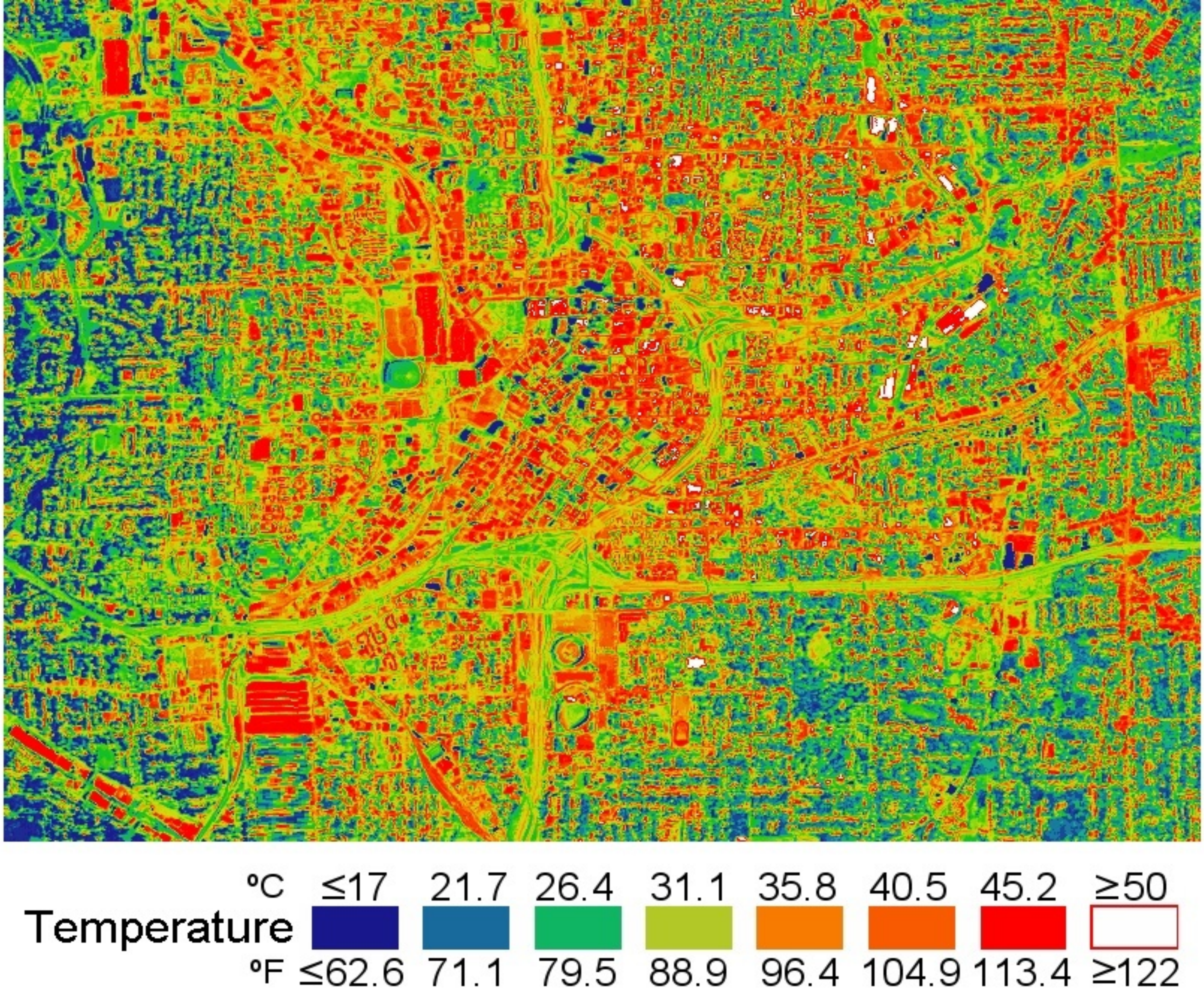

ºC ≤17 21.7 26.4 31.1 35.8 40.5 45.2 ≥50
Temperature
ºF ≤62.6 71.1 79.5 88.9 96.4 104.9 113.4 ≥122

Atlanta
Central Business District
Night Data – May 1997

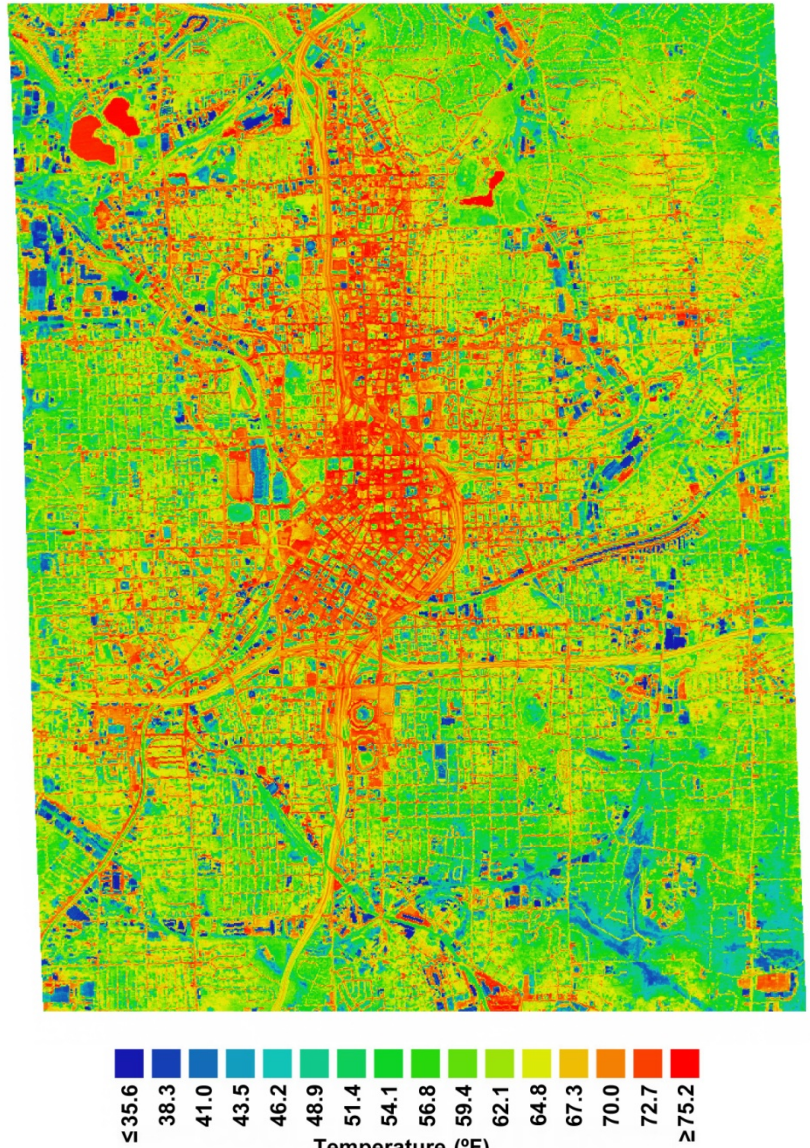

Source: NASA / EPA

TQ4 HyspIRI Science Questions

Science Issue: How can factors affecting heat stress on humans be better resolved and measured?

Potential Higher Level Products

- Heat stress maps as derived from HyspIRI thermal IR data for cities known to have morbidity/mortality cases during times of excess heat events
- HyspIRI modeled data to develop risk assessment maps for people who are at high health risk from heat-related events

TQ4 HyspIRI Science Questions

Science Issue: How can factors affecting heat stress on humans be better resolved and measured?

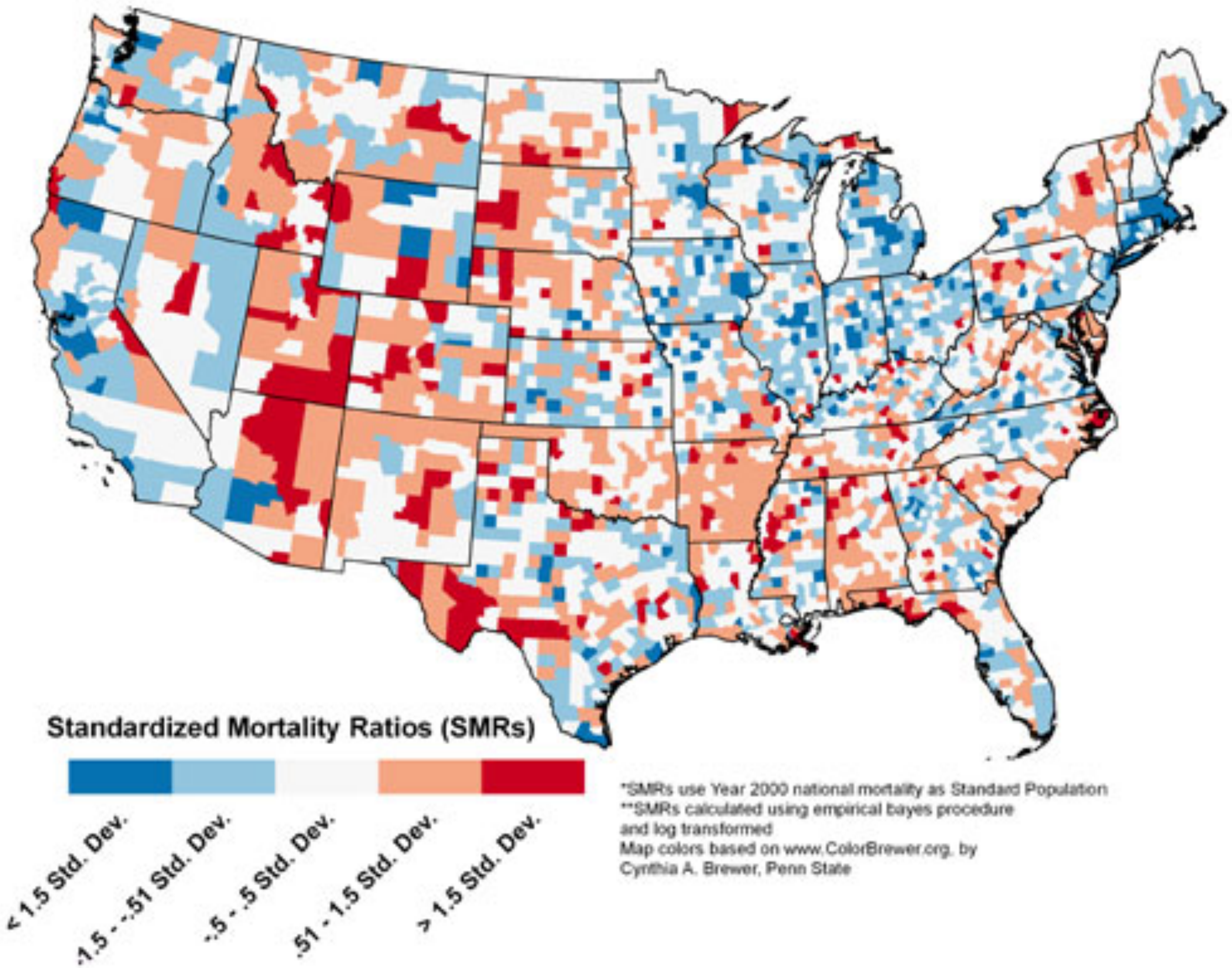

TQ4 HyspIRI Science Questions

Science Issue: How can factors affecting heat stress on humans be better resolved and measured?

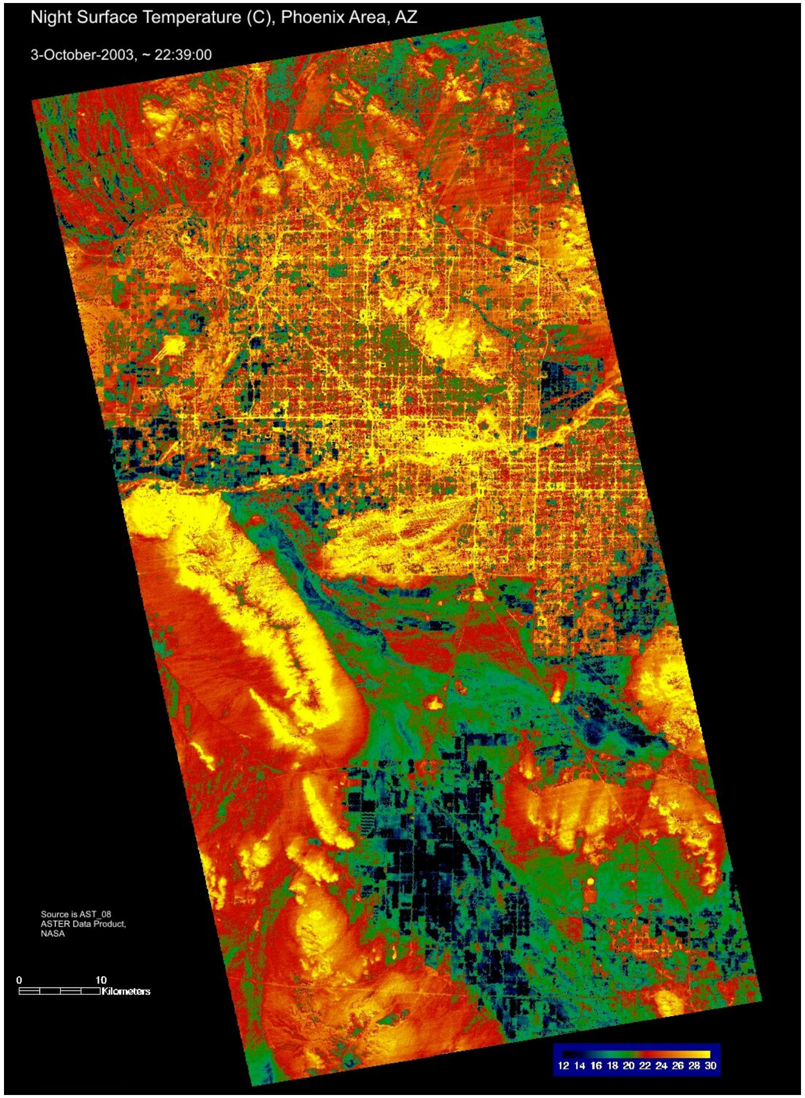

TQ4 HyspIRI Science Questions

Science Issue: How can characteristics associated with environmentally-related health effects that affect vector-borne and animal-borne diseases be better measured and resolved?

Potential Higher Level Products

- **Use HyspIRI TIR data to obtain observations and measurements of surface temperature and surface wetness as indicators of regions for possible disease transmission**
- **Use high spatial/temporal resolution, multispectral thermal HyspIRI data as inputs to disease models to produce risk maps for vector- and animal-borne disease persistence and expansion globally**

TQ4 HyspIRI Science Questions

Science Issue: How can characteristics associated with environmentally-related health effects that affect vector-borne and animal-borne diseases be better measured and resolved?

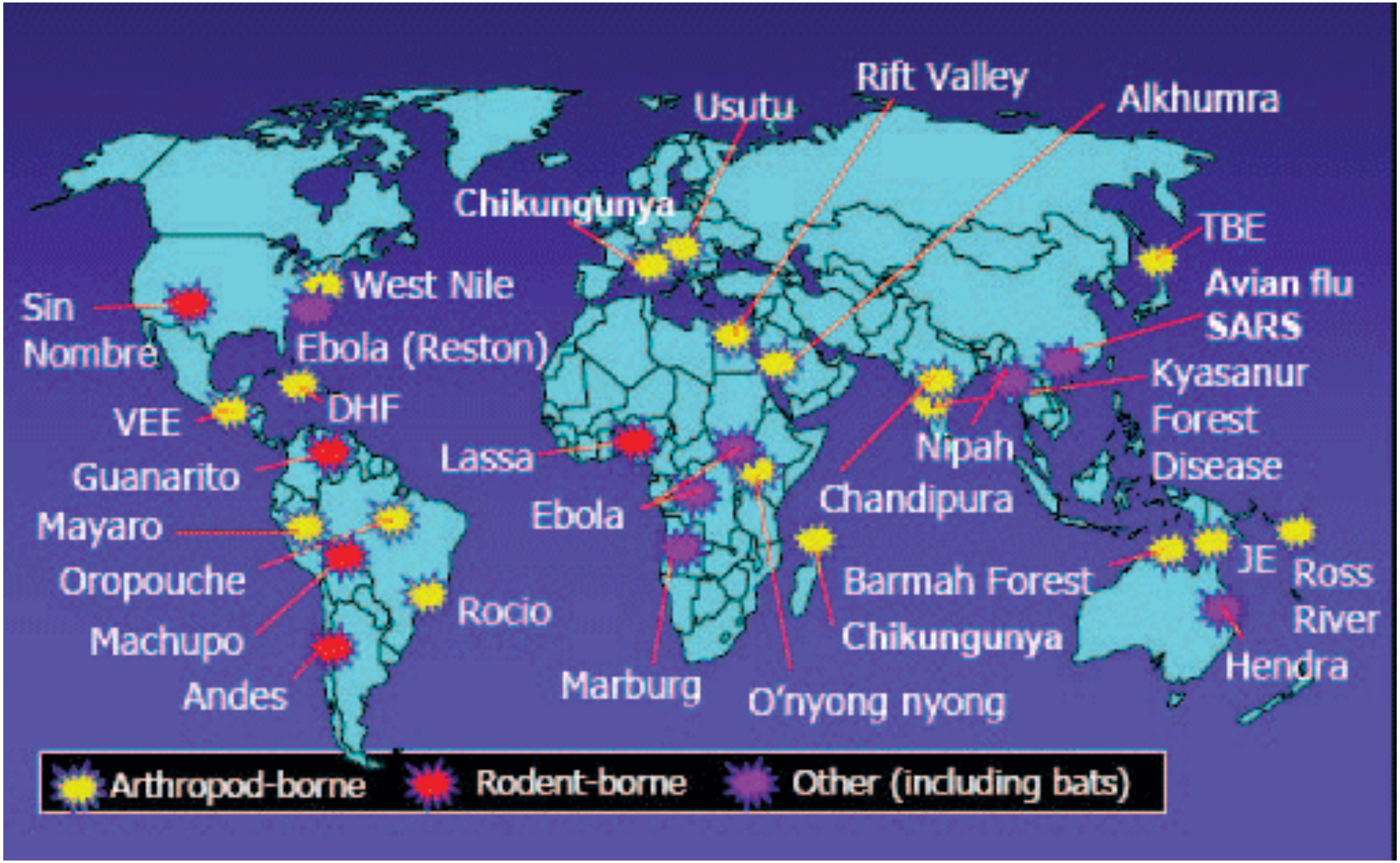

TQ4 HyspIRI Science Questions

Science Issue: How can characteristics associated with environmentally-related health effects that affect vector-borne and animal-borne diseases be better measured and resolved? human ecosystems and urbanization?

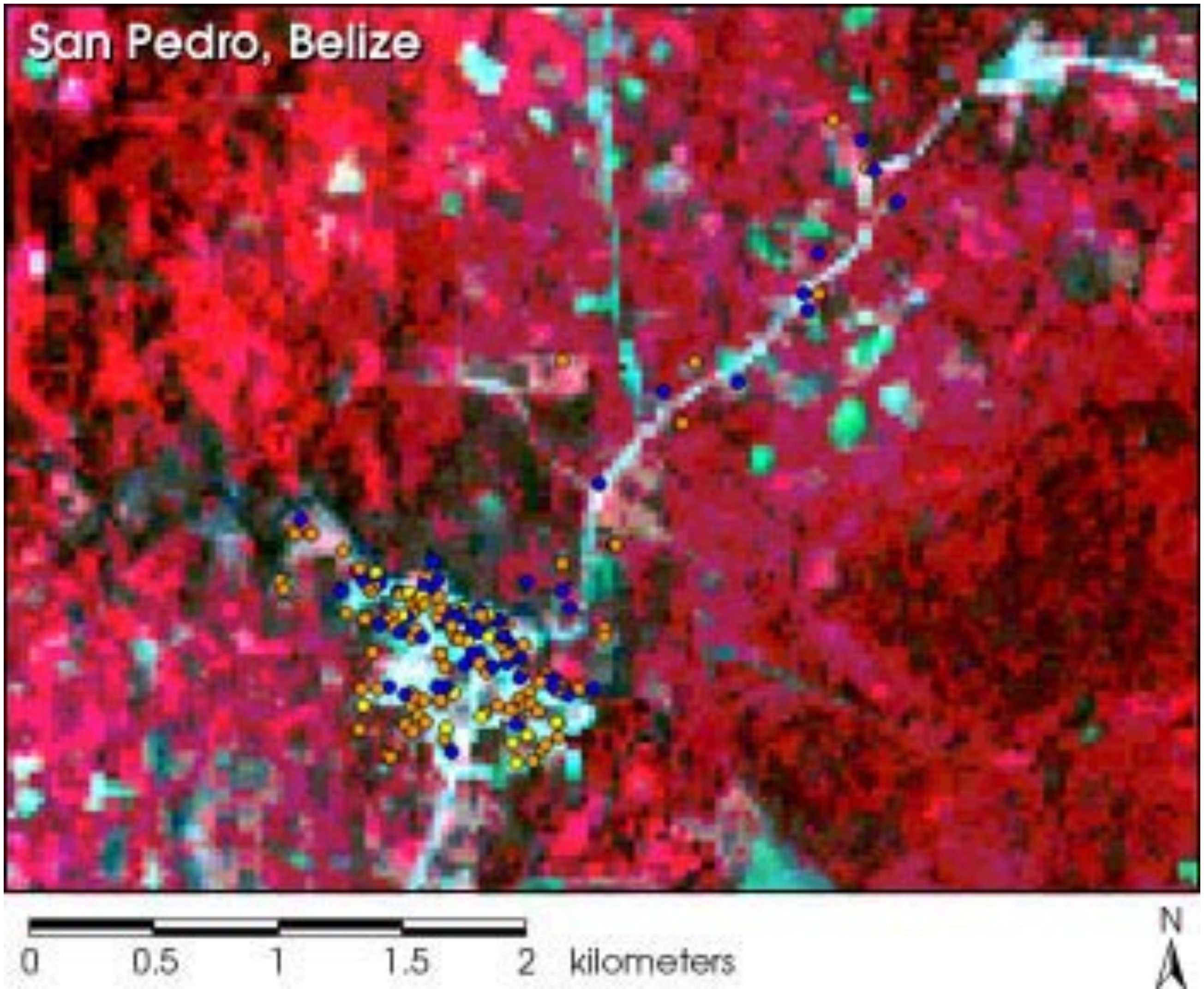

TQ4 HyspIRI Science Questions

Science Issue: How can characteristics associated with environmentally-related health effects that affect vector-borne and animal-borne diseases be better measured and resolved?

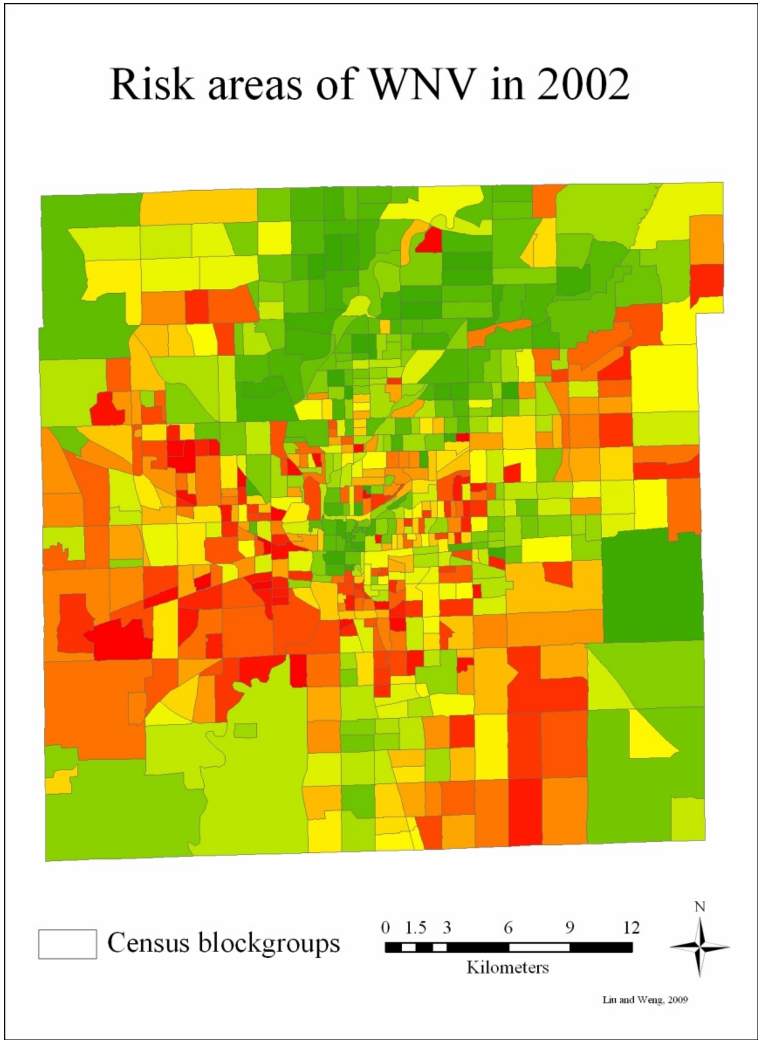

TQ4 HyspIRI Science Questions

Science Issue: How do horizontal and temporal scales of variation in heat flux and mixing relate to human health, human ecosystems and urbanization?

Potential Higher Level Products

- Maps of heat flux dynamics for various natural (e.g., forest, desert, mountain) and human (e.g., agriculture) derived from high spatial/multitemporal resolution HyspIRI data over multiple time periods
- Maps of emissivity for various land covers around the globe using HyspIRI thermal IR data
- Maps of vertical dynamics of heat flux derived from HyspIRI thermal IR data (i.e., overlain on 3-D topographic perspective)

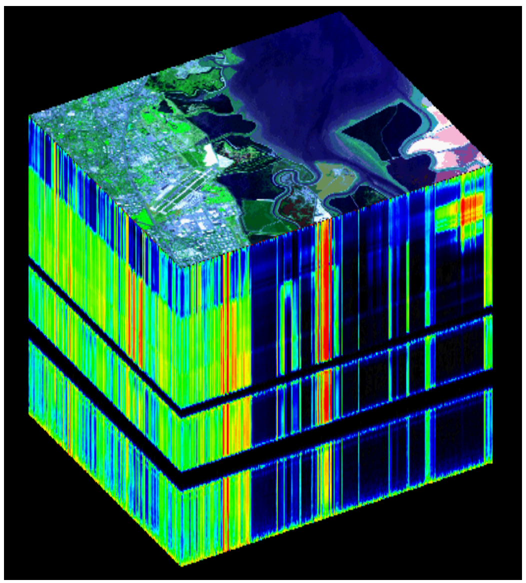

HyspIRI Hyperspectral VSWIR Level II Product
(NDVI, fPAR, surface reflectance characteristics)

+

HyspIRI TIR multispectral Level II product (8 TIR Bands)
(surface temperature, radiance, [day/night], emissivity)

=

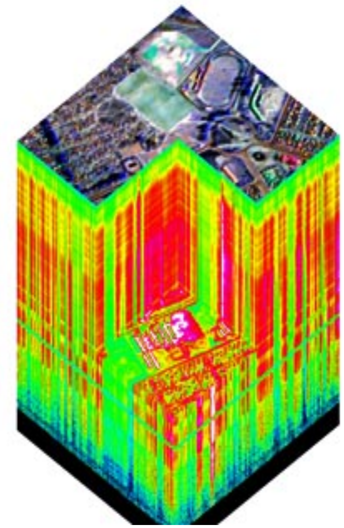

HyspIRI VSWIR/TIR composite data set
(quantitative integrative measurement of urban surface reflectances, temperatures, and emissivity across the urban ecosystem)

Through Time

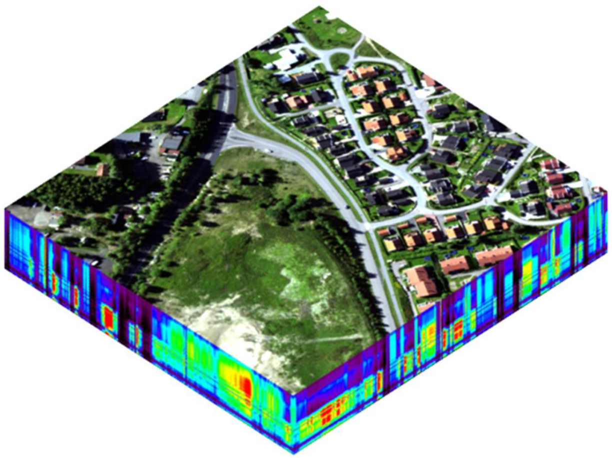

+

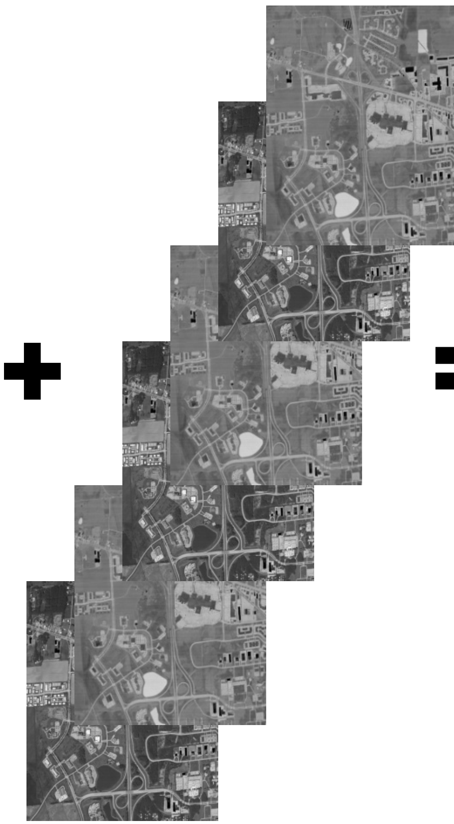

=

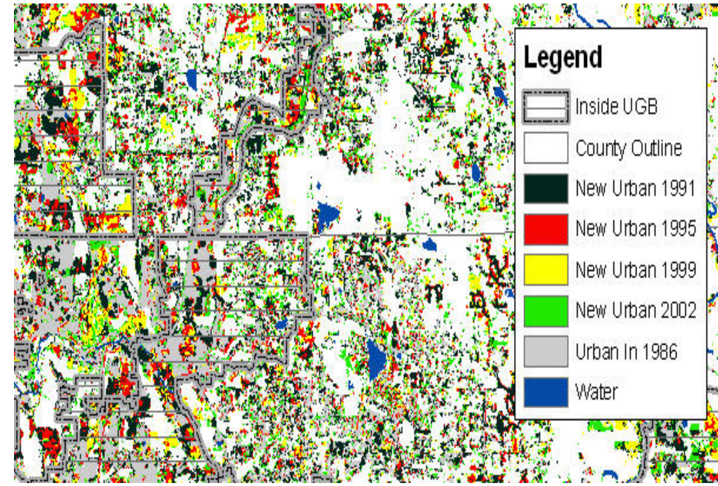

HyspIRI Hyperspectral VSWIR Level II Product
(NDVI, fPAR, surface reflectance characteristics)

HyspIRI TIR multispectral Level II product (8 TIR Bands)
(surface temperature, radiance, [day/night], emissivity)

HyspIRI VSWIR/TIR composite land cover change data set
(quantitative integrative measurement of urban surface reflectances, temperatures, and emissivity across the urban ecosystem as they change through time)

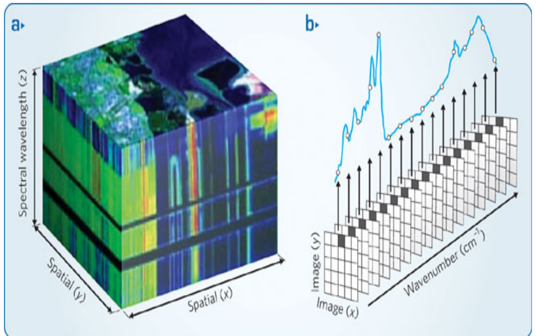

HyspIRI Hyperspectral VSWIR Level II Product (NDVI, fPAR, surface reflectance characteristics)

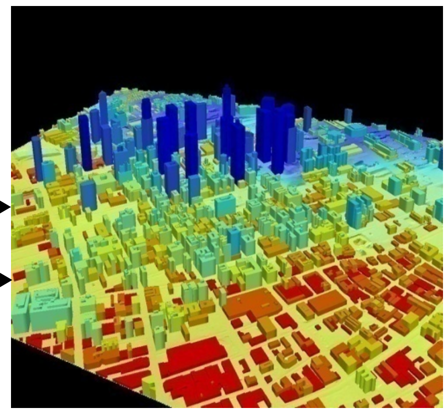

Lidar Data

=

HyspIRI VSWIR/TIR and Lidarcomposite data set

(X, y, z surface reflectance/ thermal interactions of urban ecosystem processes)

HyspIRI TIR multispectral Level II product (8 TIR Bands) (surface temperature, radiance, [day/night], emissivity)

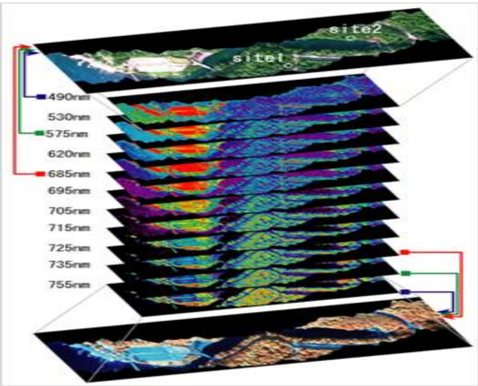

Hyperspectral VSWIR Level II Product (NDVI, fPAR, surface reflectance characteristics)

Digital Topographic Data (DEM)

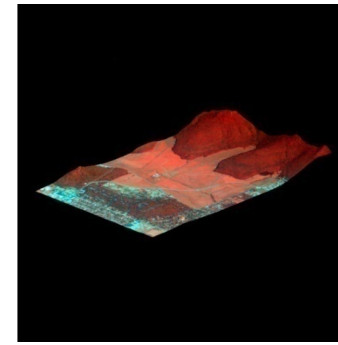

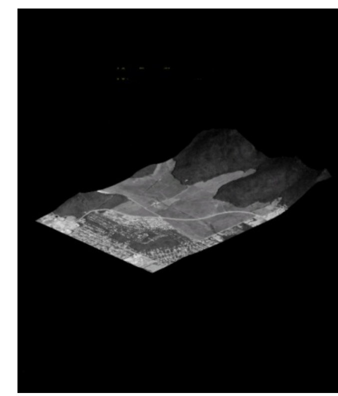

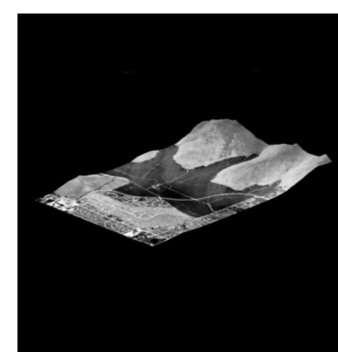

HyspIRI VSWIR/TIR and DEM composite data set

(hyperspctral/day/night TIR digital elevation model data sets))

HyspIRI TIR multispectral Level II product (8 TIR Bands) (surface temperature, radiance, [day/night], emissivity)

2012 HYSPIRI PRODUCTS SYMPOSIUM POLLEN ECOLOGY/PHENOLOGY

VQ5. Ecosystem and Human Health

Jeff Luvall
Marshall Space Flight Center

Integration of Airborne Aerosol Prediction Systems and Vegetation Phenology to Track Pollen for Asthma Alerts in Public Health Decision Support Systems

Jeffrey C Luvall Marshall Space Flight Center

William A. Sprigg, Goran Pejanovic, & Slobodan Nickovic,
Anup Prasad, Chapman University

Alfredo Huete, University of Technology Sydney

Heide Krapfl
Environmental Health Epidemiology Bureau, NM Department of Health

Amy Budge Earth Data Analysis Center, Margaret Menache, University of New Mexico

Alan Zelicoff, St. Louis University & ARES Corporation

Peter K. Van de water California State University, Fresno

Estelle Levetin & Landon Bunderson Dept. Biology University of Tulsa

Theresa Crimmins & *Jake Weltzin USGS National Phenology Network*

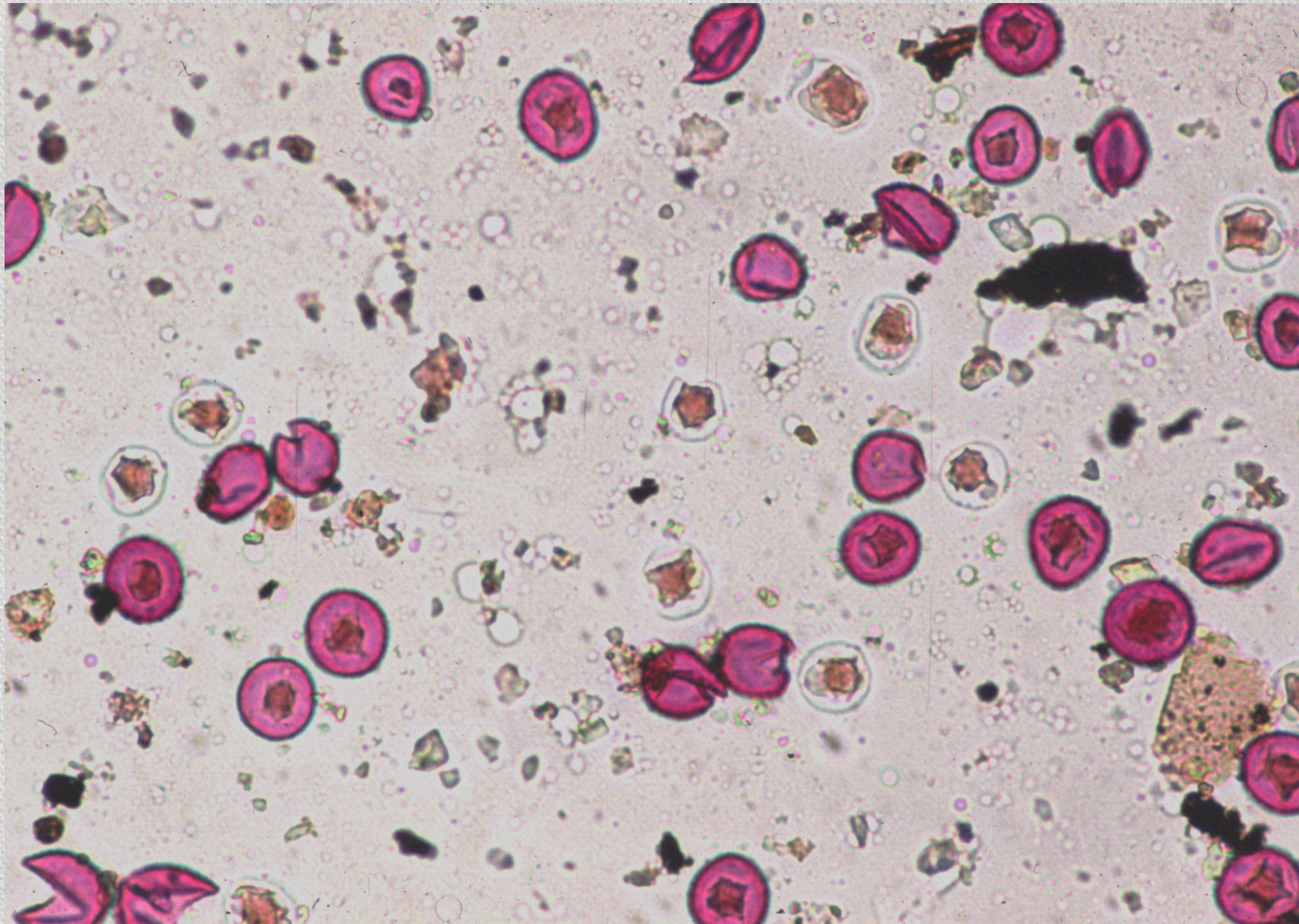

Continental Transport

- Our Jan 26, 1999 our forecast indicated that the "pollen has the potential to travel very long distances."
- 27 Jan 99, Jim Anderson in London, Ontario reported atmospheric *Juniperus* pollen - 58 pollen grains/m^3
- Trajectories show that the source of this pollen was Texas population of *Juniperus ashei*

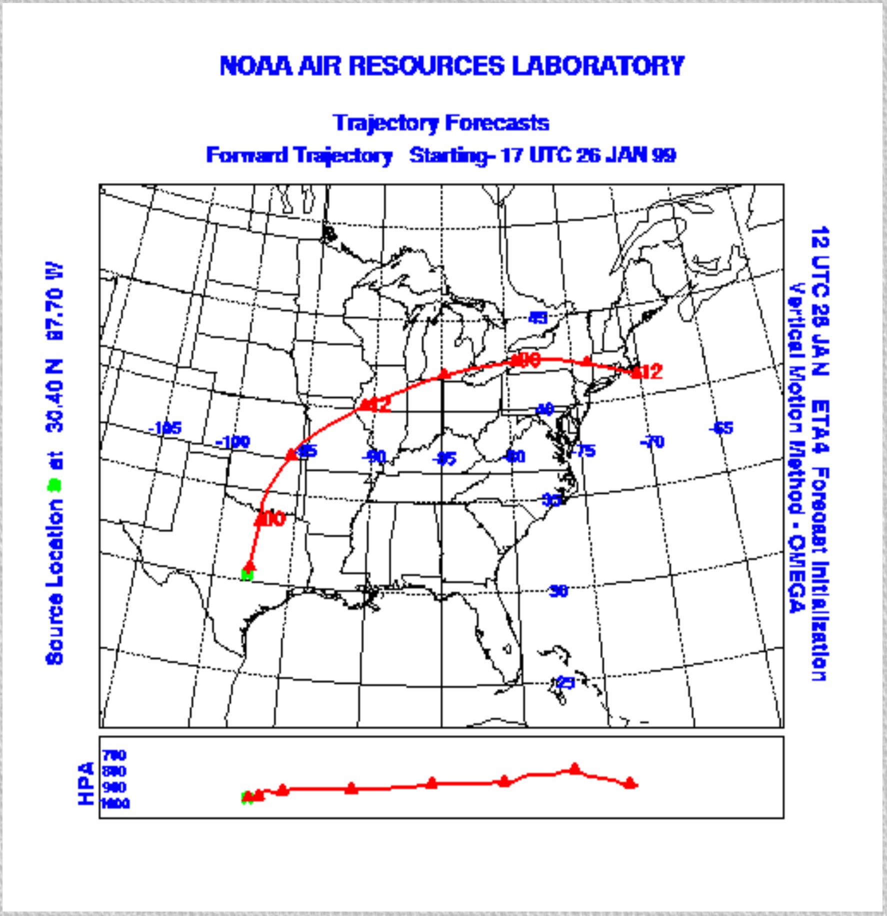

Red Cedar Encroachment

- Oklahoma has 17 million acres of prairie, shrub land, cross timbers forests and other forests
- 1950: 1.5 million acres with cedar problems
- 1985: 3.5 million acres with cedar problems
- 1994: 6.3 million acres with 50 trees/acre and 2.5 million acres with 250 trees/acre - 37% loss of native ecosystems
- 2001: 8.0 million acres with 50 trees/acre and 5.0 million acres with 250 trees/acre - this represented a 47% loss of native ecosystems
- 2013 projection: 12.6 million acres with 50 trees/acre and 8.00 million with 250 trees/acre

Air Sampling

- 6 Burkard samplers
- *Juniperus ashei*: OK and TX - Nov 2009 to Jan 2010
- *J. monosperma* and *J. scopulorum*: New Mexico – Feb to May 2010
- *J. pinchotii*: West Texas (& SW OK) Aug to Nov 2010
- *J. ashei*: TX & OK – Dec 2010 to Feb 2011
- *J. monosperma* and *J. scopulorum*: New Mexico – Feb

Report on Mapping /Phenology of Pollen Sources (Juniper)

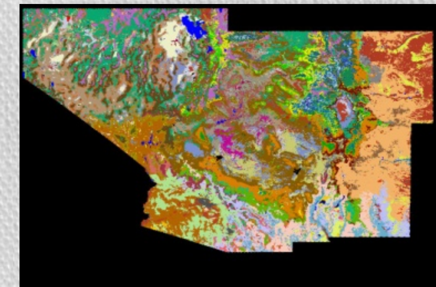

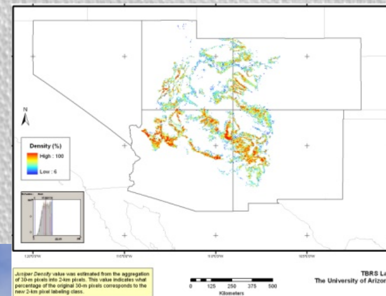

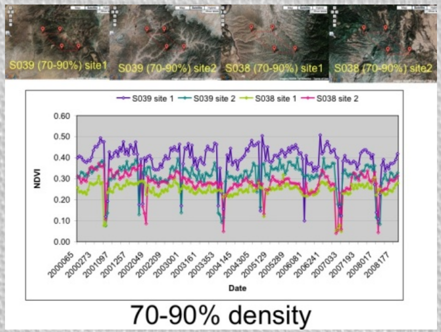

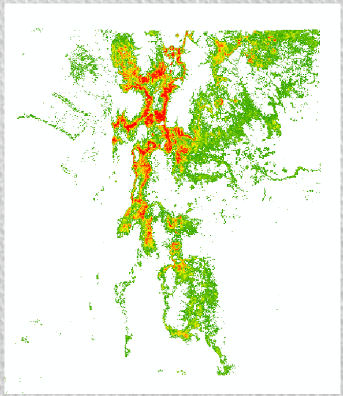

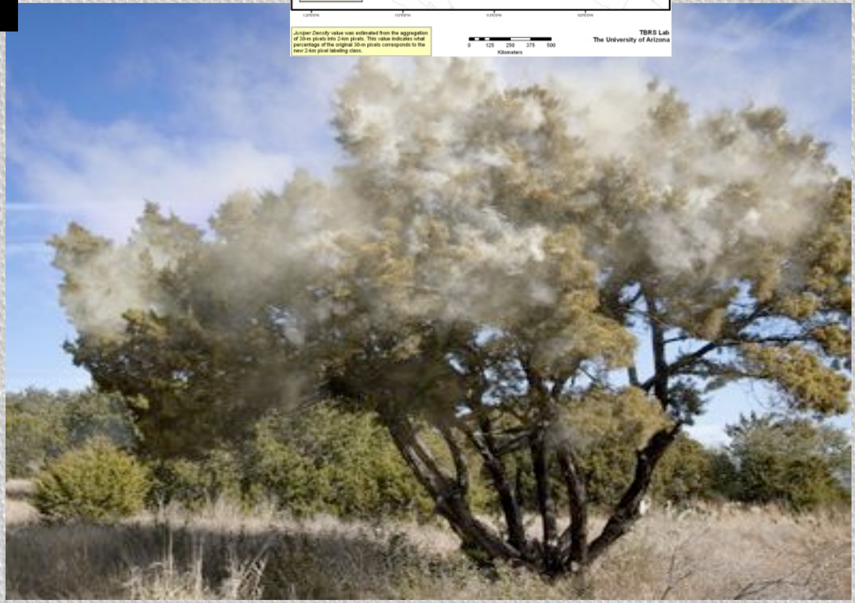

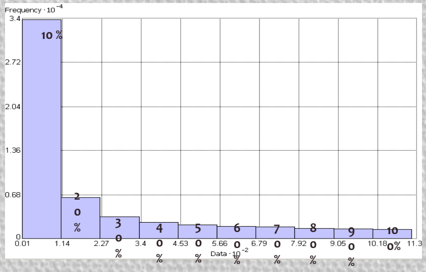

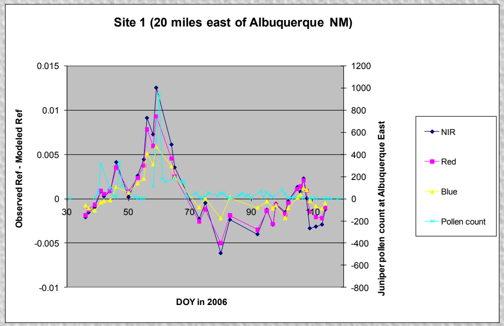

Guillermo Ponce
Alfredo Huete
Zhangyan Jiang
Ramon Solano
*University of Arizona

EDAC, Albuquerque, NM, February 20-21, 2011

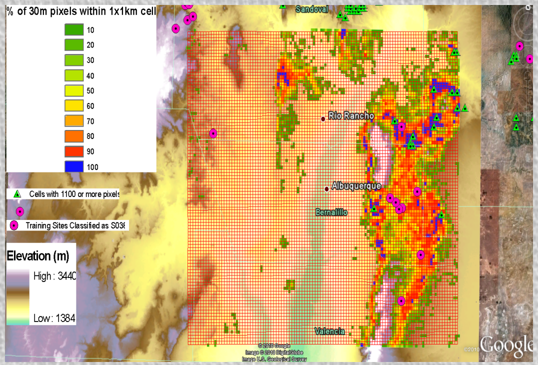

Spectral characteristics of male juniper canopies at different bud density levels

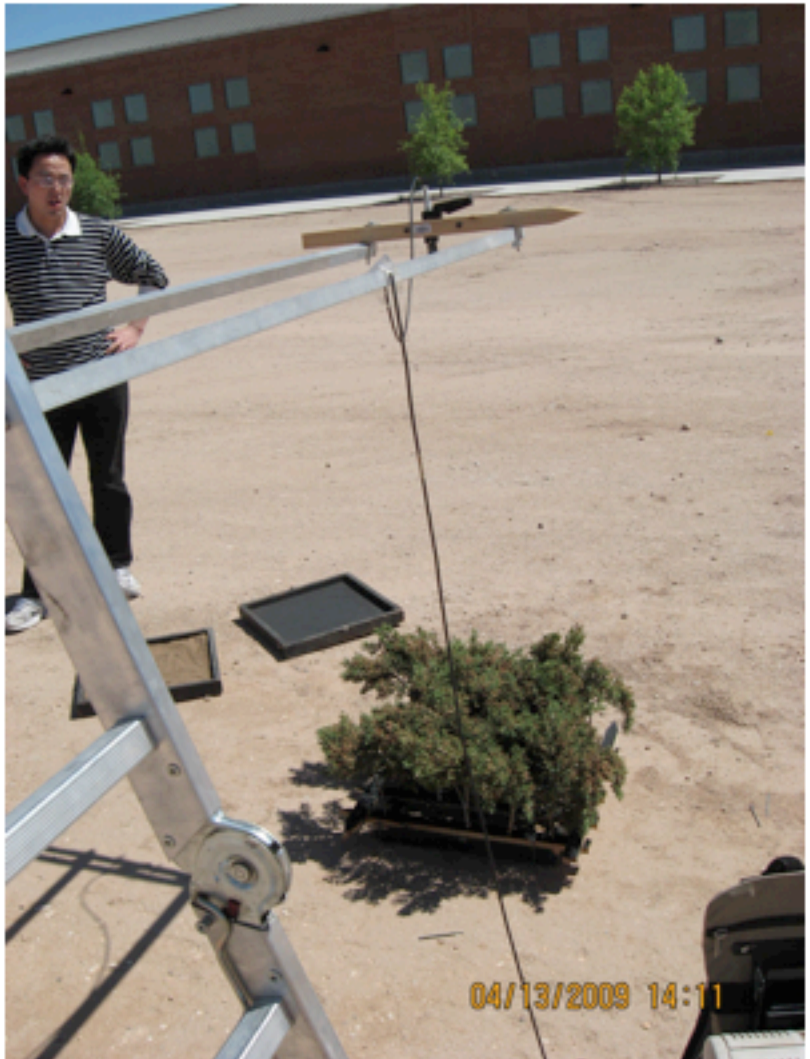

Spectral characteristics of male juniper canopies at different bud density levels

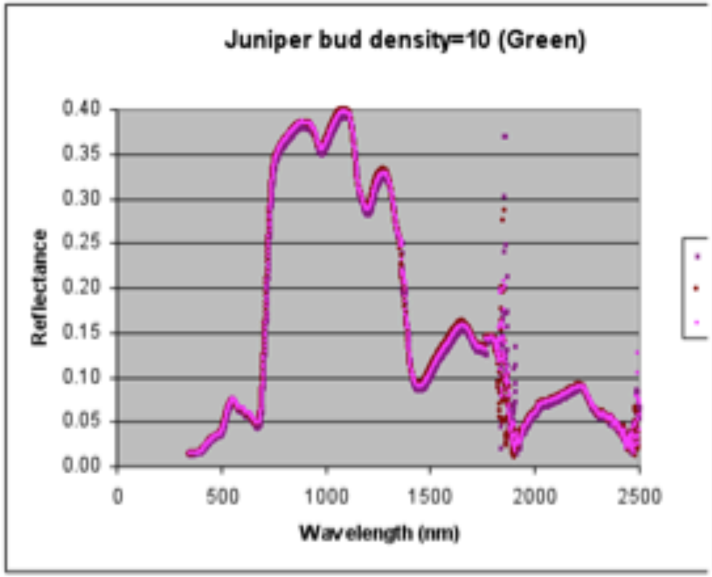

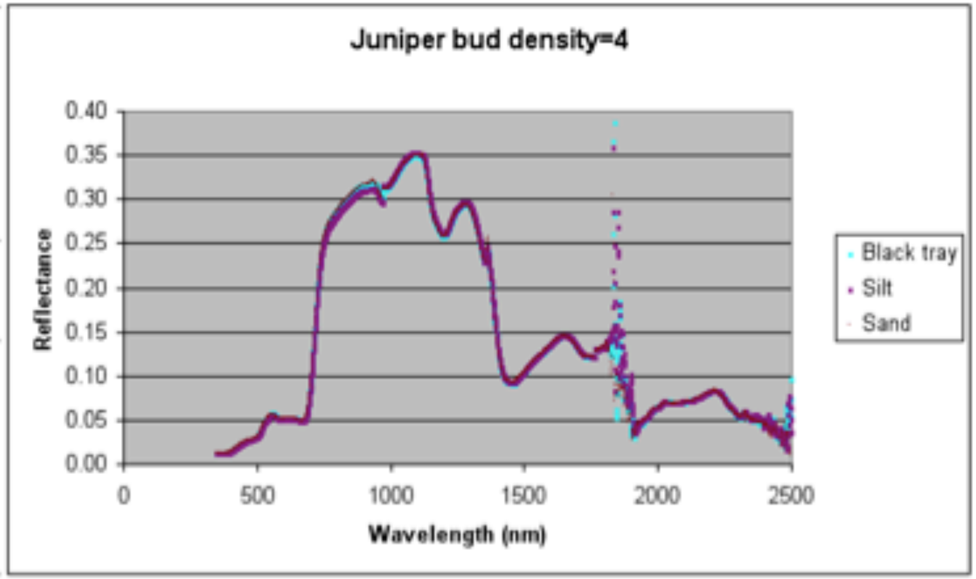

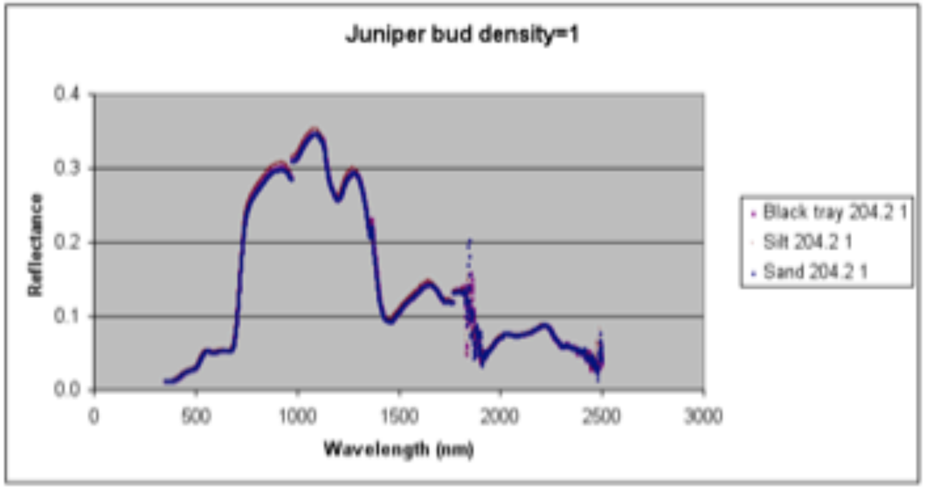

Density level	Bud density (g/m^2)
1	204.2
2	190.0
3	176.9
4	164.9
5	151.1
6	136.2
7	115.8
8	92.9
9	45.9
10	0.0

Convolve to the hyperspectral data to MODIS sensor broad bandpasses

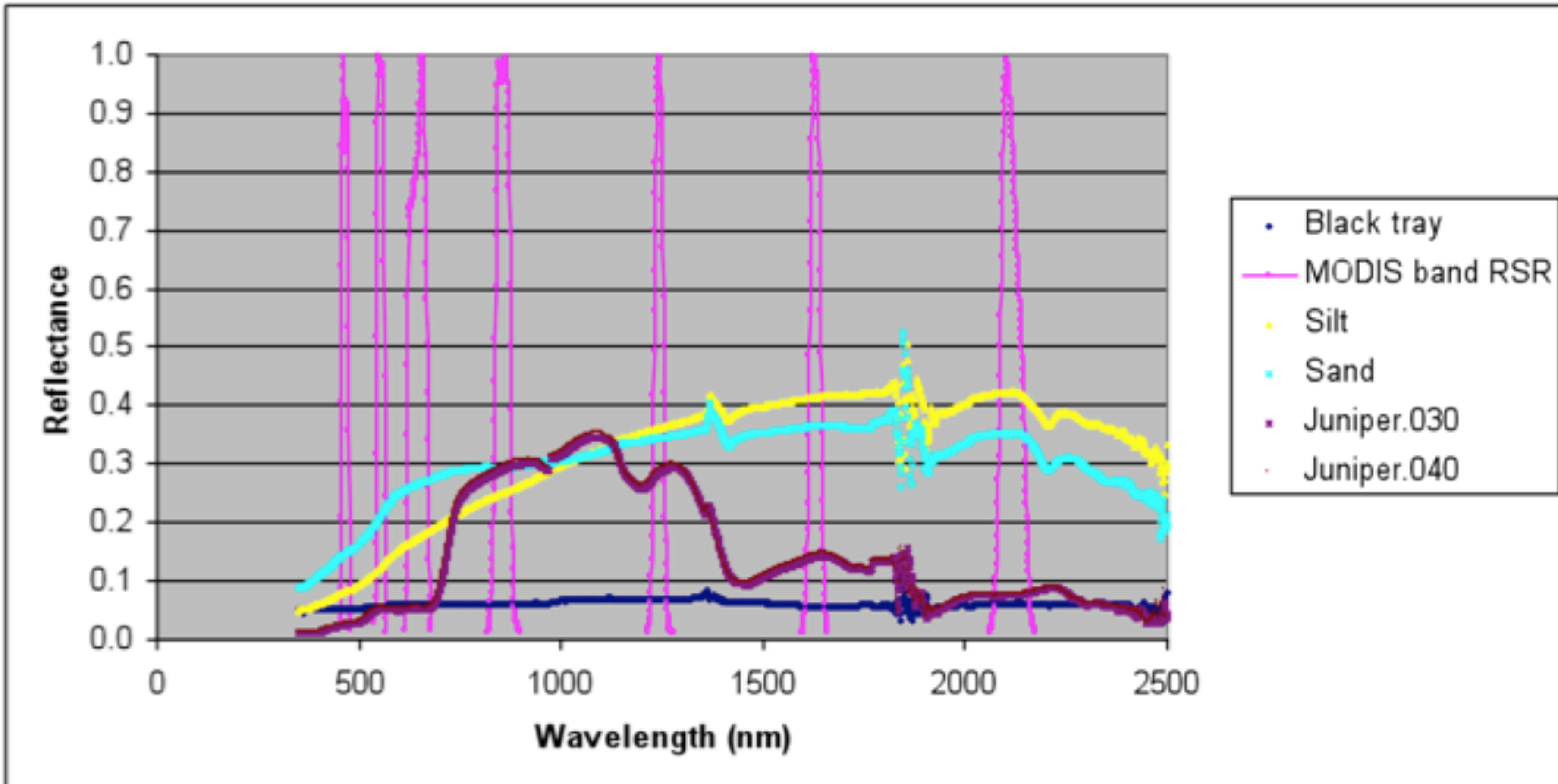

Relationships between spectral indices and juniper bud density levels

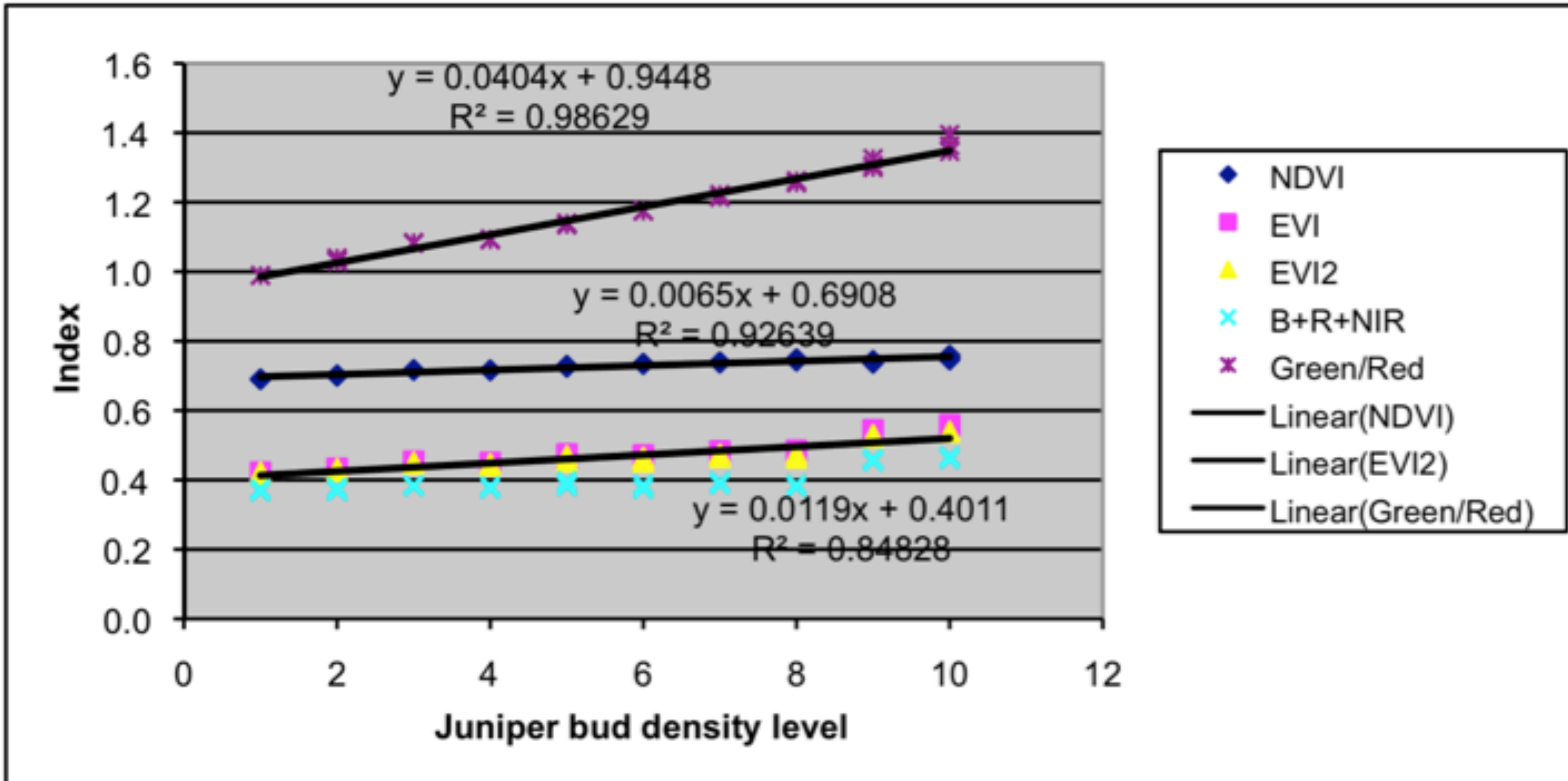

Juniper Ashei

Juniper Pinchotii

Juniper Monosperma & Scopulorum

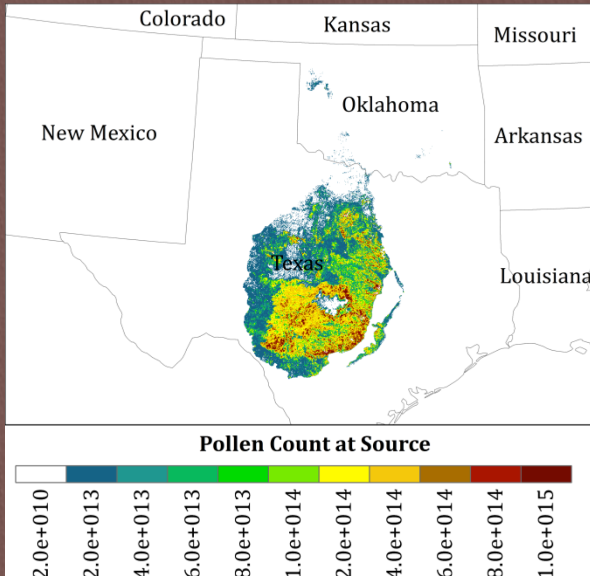

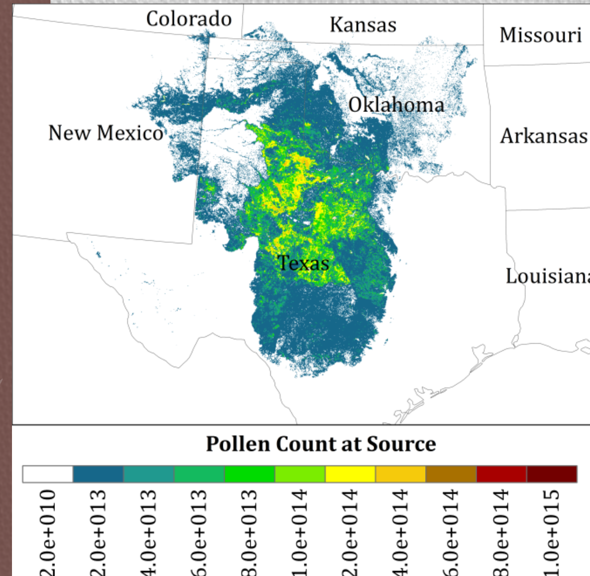

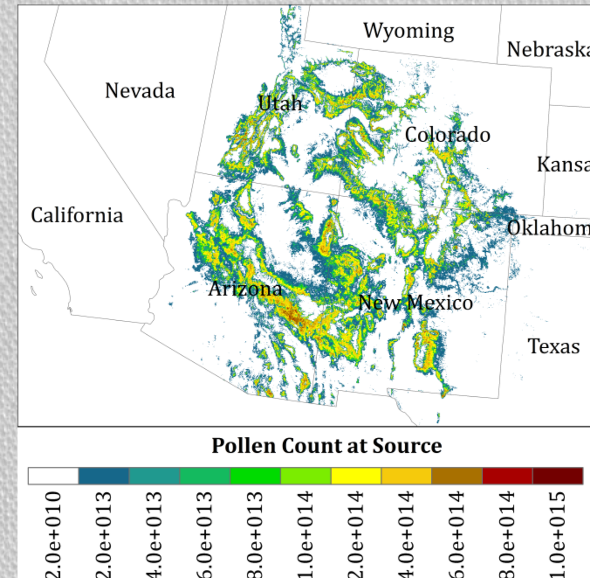

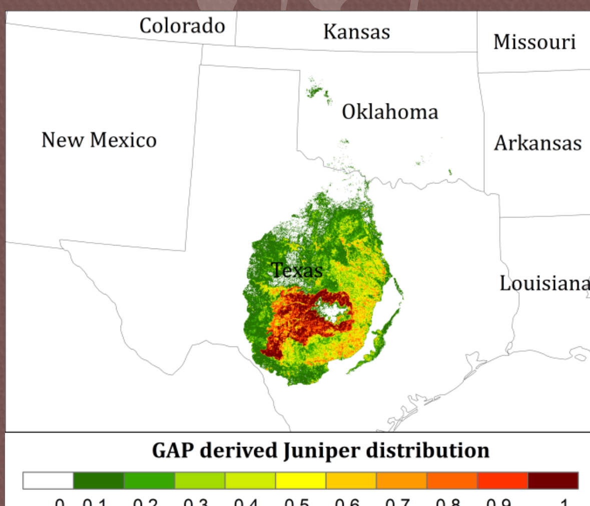

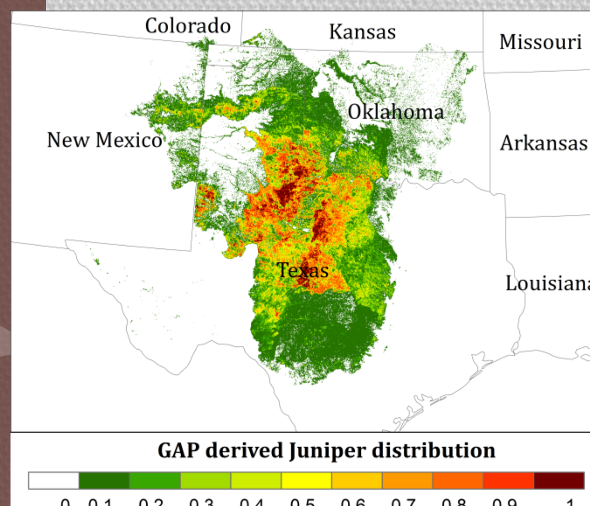

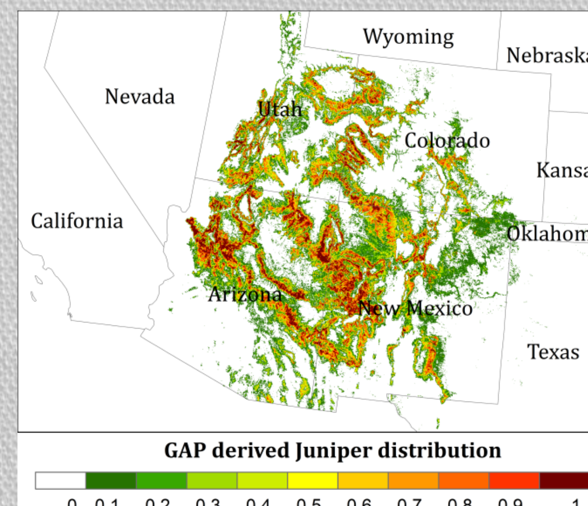

Spatial resolution: ~1 km (990 m)

USA npn National Phenology Network

A new data resource—*a national network of integrated phenological observations across space and time*

Key Goal

Understand how plants, animals and landscapes respond to environmental variation and climate change

USA npn National Phenology Network

Taking the Pulse of Our Planet

Log In

western columbine

View All Species

Join Us!

We are looking for volunteers to help us monitor plant and animal species found across the United States. Click "Observe" to join us!

Observe

Featured Projects

1 of 2 ››

Sponsors

USA National Phenology Network

The USA National Phenology Network brings together citizen scientists, government agencies, non-profit groups, educators and students of all ages to monitor the impacts of climate change on plants and animals in the United States. The network harnesses the power of people and the Internet to collect and share information, providing researchers with far more data than they could collect alone.

Learn more about us

What is phenology?

Phenology refers to recurring plant and animal life cycle stages, or phenophases, such as leafing and flowering, maturation of agricultural plants, emergence of insects, and migration of birds. Many of these events are sensitive to climatic variation and change, and are simple to observe and record. As an USA-NPN observer, you can help scientists identify and understand environmental trends so we can better adapt to climate change.

Why is phenology important?

USA-NPN News | **Phenology Feed** | **Join the Conversation**

- Phenoclimatology Position at UA
- Introducing the USA-NPN Video
- ***Nature's Notebook:*** "How to Observe" Handbook and Training Videos
- Phenology Special Issue in the Philosophical Transactions of the Royal Society
- USA-NPN Reports (including Strategic Plan and 2009 Annual Report)
- Call for Papers: 4th Annual PROSE in Tucson, AZ, October 2010

- Recent Media Reports
- Newsletter Archive

Are you...?

New to phenology?

Ready to start observing?

One of our partners?

Interested in creating a partnership?

An educator?

Interested in finding data to use?

A media outlet?

USA National Phenology Network, National Coordinating Office
1955 E. Sixth St., Tucson, AZ 85721

Land-surface Phenology Program

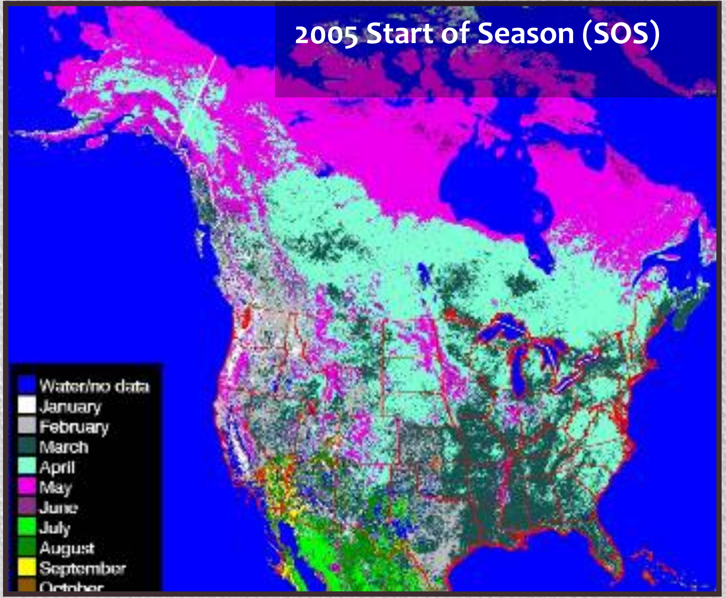

- Scaling of in-situ observations
- Validation of remote imagery
- Development of standards
- Information & data clearinghouse
- Research directions and priorities

Synergies between VSWIR and TIR data for the urban environment: An evaluation of the potential for the Hyperspectral Infrared Imager (HyspIRI)

- Dar A. Roberts[1], Dale A. Quattrochi[2], Glynn C. Hulley[3], Simon J. Hook[3], and Robert O. Green[3]
- 1 UC Santa Barbara Dept. of Geography
- 2 NASA Marshall Space Flight Center
- 3 NASA Jet Propulsion Laboratory

Acknowledgements: NASA HyspIRI Preparatory Program

HyspIRI Science Products Symposium – NASA/GSFC – May 16-17, 2012

Remote Sensing of Environment 117 (2012) 83–101

Contents lists available at ScienceDirect

Remote Sensing of Environment

journal homepage: www.elsevier.com/locate/rse

Synergies between VSWIR and TIR data for the urban environment: An evaluation of the potential for the Hyperspectral Infrared Imager (HyspIRI) Decadal Survey mission

Dar A. Roberts [a,*], Dale A. Quattrochi [b], Glynn C. Hulley [c], Simon J. Hook [c], Robert O. Green [c]

[a] Department of Geography, University of California Santa Barbara, CA, 93106, USA
[b] NASA, Earth Science Office, Marshall Space Flight Center, Huntsville, AL, 35812, USA
[c] Jet Propulsion Laboratory, California Institute of Technology, Pasadena, CA, 91109, USA

ARTICLE INFO

Article history:
Received 3 March 2011
Received in revised form 13 June 2011
Accepted 12 July 2011
Available online 8 September 2011

Keywords:
HyspIRI
Urban remote sensing
Spectral Mixture Analysis
Land surface temperature
Spectroscopy

ABSTRACT

This study provides an introduction to the HyspIRI mission a National Research Council "Decadal Survey" mission that combines a 213 channel visible, near—infrared and shortwave infrared (VSWIR) imaging spectrometer with an 8 channel multispectral thermal infrared (TIR) instrument and evaluates some of its potential in urban science. Potential synergies between VSWIR and TIR data are explored using analogous airborne data acquired over the Santa Barbara metropolitan region in June, 2008. These data were analyzed at both their native spatial resolutions (7.5 m VSWIR and 15 m TIR), and aggregated 60 m spatial resolution similar to HyspIRI. A spectral library of dominant urban materials (e.g., grass, trees, soil, roof types, roads) was developed from field and airborne-measured spectra using Multiple-Endmember Spectral Mixture Analysis (MESMA) and used to map fractions of impervious, soil, green vegetation (GV, e.g., trees, lawn) and non-photosynthetic vegetation (NPV). Land Surface Temperature (LST) and emissivity were also retrieved from the airborne data. Co-located pixels from the VSWIR and TIR airborne data were used to generate reflectance/emissivity spectra for a subset of urban materials. MESMA was used to map GV, NPV, soil and impervious fractions at the different spatial resolutions and compare the fractional estimates across spatial scales. Important surface energy parameters, including albedo, vegetation cover fraction, broadband emissivity and surface temperature were also determined for and evaluated for 14 urban and natural land-cover classes in the region. Fractions were validated using 1 m digital photography.

Fractions for GV and NPV were highly correlated with validation fractions at all spatial scales, producing a near 1:1 relationship but with a <10% overestimate of GV from MESMA. Similar, high correlations were observed for impervious surfaces, although impervious was significantly underestimated in most urban areas and soil overestimated. Comparison of fractions across scales showed high correlation between GV and NPV at 7.5 and 60 m resolution, suggesting that HyspIRI will provide accurate measures of these two measures in urban areas. An inverse relationship between vegetation cover and LST was observed. Albedo proved to be highly variable and poorly correlated with LST. Broadband emissivity was far less variable with high emissivity surfaces (~0.95) including vegetation, water and asphalt, and low emissivity surfaces (<0.95) including selected roof types, beach sands and senesced grasslands. Residential and commercial areas showed a general pattern of increasing LST with increasing impervious fraction with the highest impervious fractions mapped in commercial areas, roads and roofs. Fine scale spatial structure in cover fractions and LST demonstrated important departures from a simple inverse relationship between GV and LST, even at 60 m. The results demonstrate the utility of HyspIRI data for urban studies and provide an insight of what will be possible on a global scale when HyspIRI data become available.

1. Introduction

The 21st century can be characterized as the first "urban century", in which a majority of people live in cities. This great urban explosion is projected to continue with the United Nations estimating global urban population to reach 81% by 2015. There are currently 21 so-called "mega-cities" with populations exceeding 10 million, and it is projected that they will significantly increase in

* Corresponding author. Tel.: +1 805 880 2531; fax: +1 805 893 3146.
E-mail address: dar@geog.ucsb.edu (D.A. Roberts).

doi:10.1016/j.rse.2011.07.021

Outline

- Why Urban?
- Potential HyspIRI Synergies
- Santa Barbara Study Design
- Research Results
- What’s next?
- Summary

Why Urban? (Vol 1)

- **A majority of the human population lives in urban and sub-urban areas**
  - **How does urbanization and urban composition modify urban environments and human habitat?**
  - **How might this change in a warmer world?**
    - **1995 Chicago Heat Wave (750 heat related deaths)**
    - **2003 European Heat Wave (>40,000, heat related Deaths)**
    - **2010 Great Russian Heat Wave (11,000 heat related deaths in Moscow)**

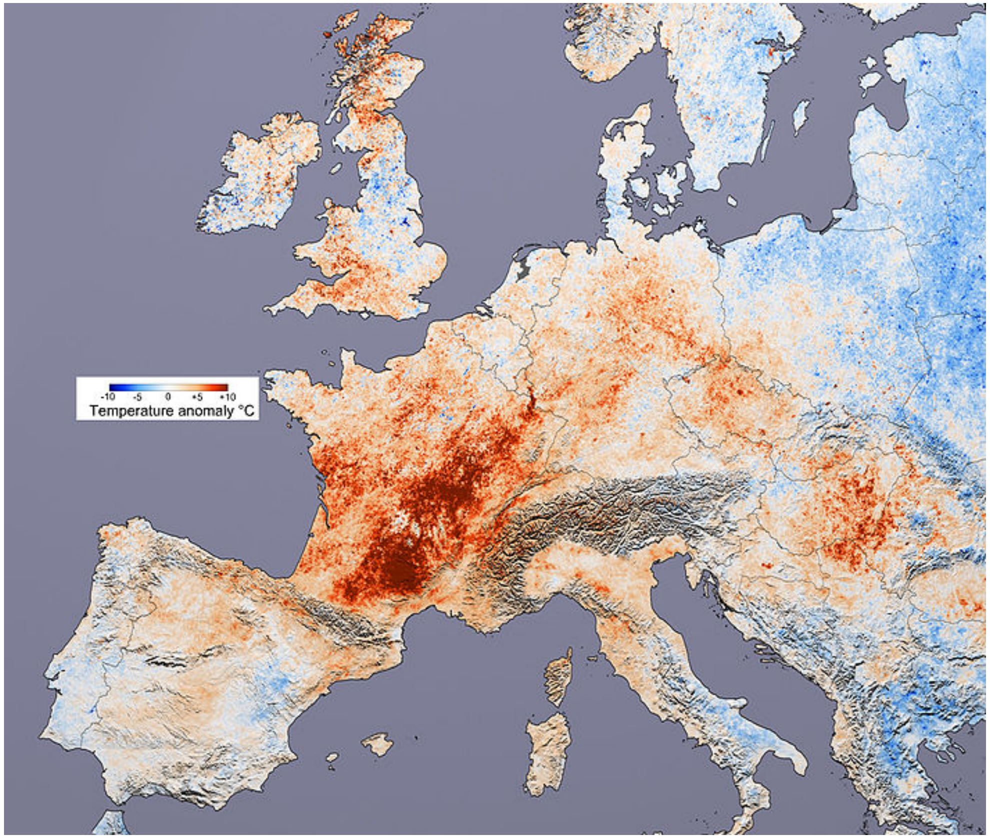

Image: http://en.wikipedia.org/wiki/File:Canicule_Europe_2003.jpg

Why Urban? (Vol 2)

- **Urban areas are major sources of airborne and waterborne pollutants and major sinks for materials and energy**
  - **How do the properties of urban environments modify the flow of water borne pollutants, urban water use and urban energy use?**

Image Source: http://www.guardian.co.uk/politics/2007/mar/06/greenpolitics.uknews

Urban Heat Islands

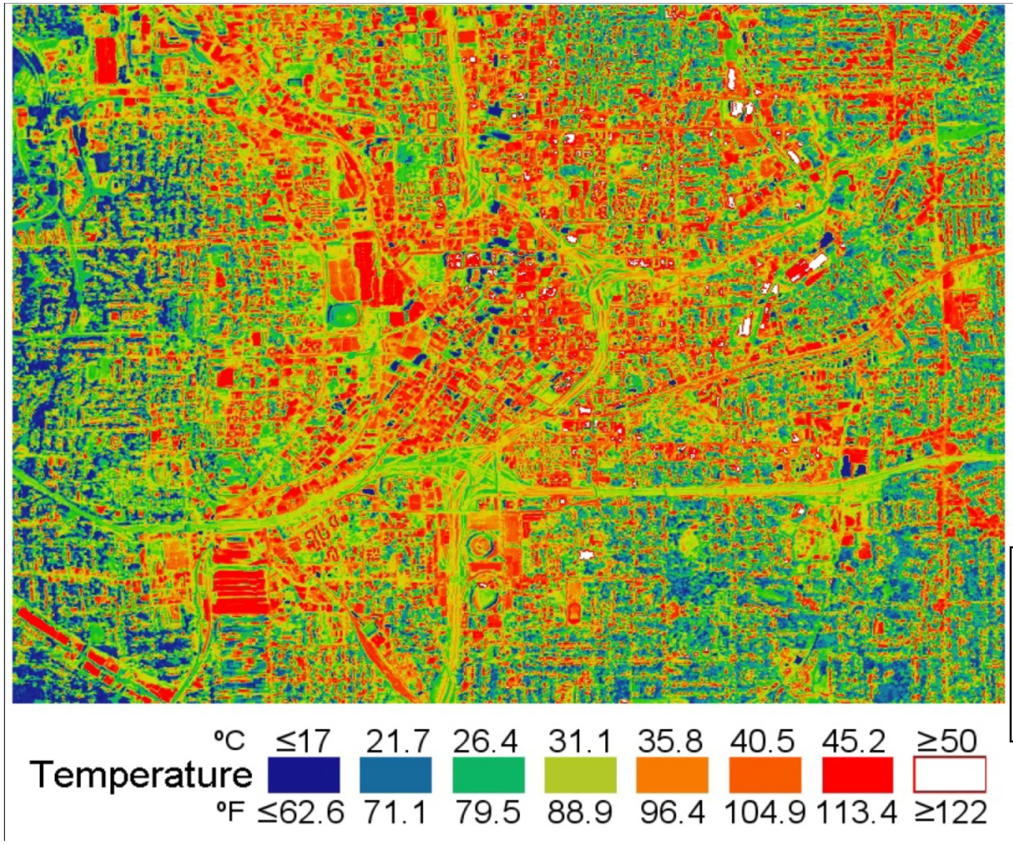

1997 Day time TIR image of Atlanta Georgia
Source: Quattrochi, "HyspIRI Thermal IR (TQ4) Science Questions …."
Image source: Atlas, May 1997

Atlas: 15 channel system
6 TIR, 1 MIR, 8 VNIR-SWIR
http://www.ghcc.msfc.nasa.gov/atlanta/

- **Urban areas are warmer than natural areas**
  - **Low albedo surfaces**
  - **Lack of vegetation cover and shading**
- **Urban areas can create their own weather**

Potential HyspIRI Synergies

- **Improved Temperature Emissivity Separation**
  - **Water vapor largest error source**
  - **Replace regional column water vapor with VSWIR water vapor**
- **Full characterization of surface energy properties**
  - **Surface albedo, vegetation cover, impervious cover, emissivity, Land Surface Temperature (LST)**
- **Improved discrimination of materials**
- **Multi-wavelength measures of plant stress**
  - **VSWIR biochemistry, physiology**
  - **TIR canopy temperature**

Synopsis

- This study provides an introduction to the HyspIRI mission that combines a 213 channel visible, near-infrared and shortwave infrared (VSWIR) imaging spectrometer with an 8 channel multispectral thermal infrared (TIR) instrument and evaluates some of its potential in urban science.
- Potential synergies between VSWIR and TIR data are explored using analogous airborne data acquired over the Santa Barbara metropolitan region in June, 2008.
- These data were analyzed at both their native spatial resolutions (7.5 m VSWIR and 15 m TIR), and aggregated 60 m spatial resolution similar to HyspIRI.
- A spectral library of dominant urban materials (e.g., grass, trees, soil, roof types, roads) was developed from field and airborne-measured spectra using Multiple-Endmember Spectral Mixture Analysis (MESMA) and used to map fractions of impervious, soil, green vegetation (GV, e.g., trees, lawn) and non-photosynthetic vegetation (NPV).

Synopsis

- **Land Surface Temperature (LST) and emissivity were also retrieved from the airborne data. Co-located pixels from the VSWIR and TIR airborne data were used to generate reflectance/emissivity spectra for a subset of urban materials.**
- **MESMA was used to map GV, NPV, soil and impervious fractions at the different spatial resolutions and compare the fractional estimates across spatial scales.**
- **Important surface energy parameters, including albedo, vegetation cover fraction, broadband emissivity and surface temperature were also determined for and evaluated for 14 urban and natural land-cover classes in the region.**
- **Fractions were validated using 1 m digital photography.**

Study Site: Santa Barbara

1650, 831, 684 nm: RGB

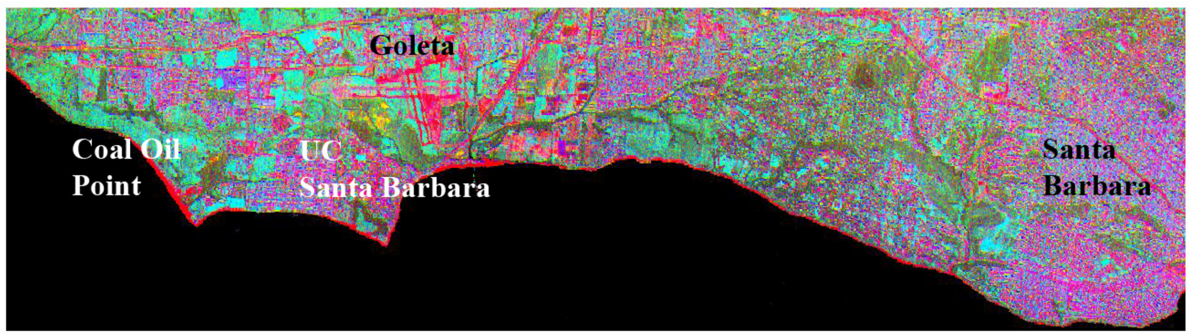

11.35, 9.1, 8.6 um: RGB

2 km

- Mixed urban-natural systems, ~ 150,000 people
- AVIRIS-MASTER pair, June 19, 2008
  - 7.5 m AVIRIS, 15 m MASTER
  - Spatial degradation, 15 m AVIRIS, 60 m AVIRIS/MASTER

Methods

- **AVIRIS Analysis**
  - **Atmospheric CORrection Now (ACORN 5), applied to 7.5, 15 and 60 m radiance data**
    - **ACORN software package provides an atmospheric correction of hyperspectral and multispectral data measured n the spectral range from 350 to 2500 nm**
    - **ACORN is designed to work with all airborne and spaceborne calibrated data**
    - **Reflectance, water vapor, liquid water, albedo (Modo 4.3 Irradiance)**
  - **Surface Composition**
    - **VIS Model (Vegetation, Impervious, Soil expanded to include NPV)**
    - **Multiple Endmember Spectral Mixture Analysis**
      - **Fused field and AVIRIS-derived spectral library (7.5 m)**
      - **Count-based Endmember Selection, cover class (i.e., bark, composite shingle, oak)**
      - **Multi-level fusion (2, 3, 4 em models, selected based on 0.007 RMS threshold)**
    - **Water screened by LST (< 297.15K)**
- **MASTER Analysis**
  - **Temperature Emissivity Separation (TES)**
    - **Modtran 5.2 derived atmospheric correction**
    - **NCEP column water vapor, iteratively adjusted for water over Laguna Blanca**
    - **TES, using ASTER algorithm (Gillespie et al.)**
  - **Spectral emissivity, broad band emissivity, LST**

Land-Cover Analysis/Mixture Validation

- **Defined 14 dominant land-cover classes on Google Earth Imagery**
  - Residential (high, medium, low), Commercial, Transportation, Roofs
  - Closed canopy forest, Forested park, Golf courses, Grass sports fields, Orchards, Annual crop
  - Bare soil, crop
- **Extracted GV, NPV, Impervious, Soil fractions and land surface energy properties**
- **Developed Mixture Validation Data Sets from National Agricultural Imagery Program (NAIP)**
  - 120x120 m polygons (ranges in surface fractions)
  - Large, mixed land-cover polygons

Land-Cover Analysis: Examples


Closed Canopy Forest


Low Density Residential


High Density Residential


Commercial/Transportation

Mixture Validation

- **Utilized 85 polygons**
  - 64 land-cover
  - 21 designed
- **Calculated fractions from high-res imagery**
  - Manually delineated polygons for GV, NPV, Soil and Impervious
  - Determination aided by AVIRIS

Figure showing three validation polygons
A: 44% NPV, 11.3% GV, 44.7% Soil
B: 50.45%NPV, 1.5% GV, 48%Soil
C: 4.8% NPV, 57.4% GV, 34.5% Soil, 3.3% Imp

Results
AVIRIS-MASTER Products

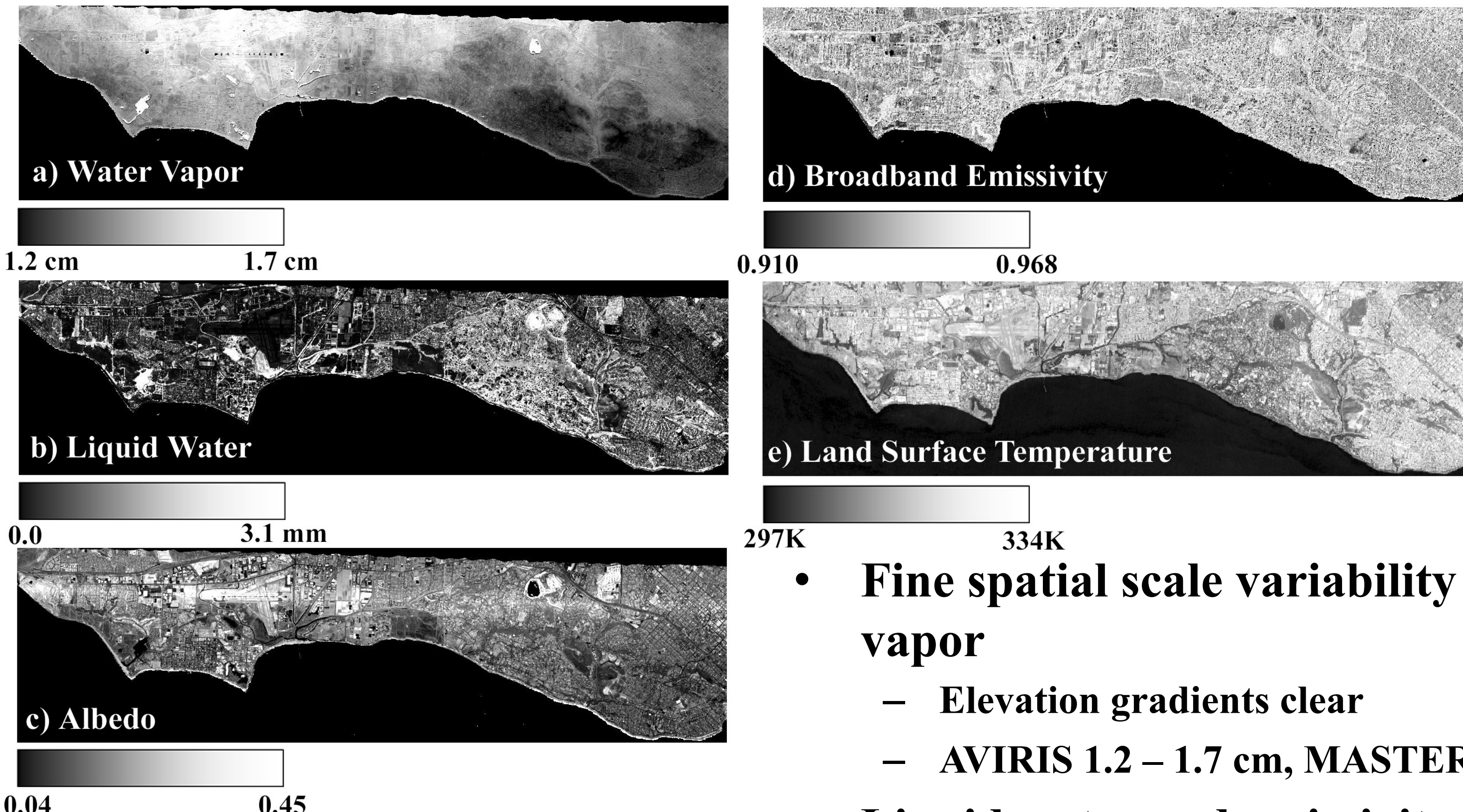

- **Fine spatial scale variability in water vapor**
  - Elevation gradients clear
  - AVIRIS 1.2 – 1.7 cm, MASTER 0.78 cm
- **Liquid water and emissivity positively correlated**
  - Asphalt also high emissiivty
- **Albedo and LST poorly correlated**

Reflectance and Emissivity Spectra

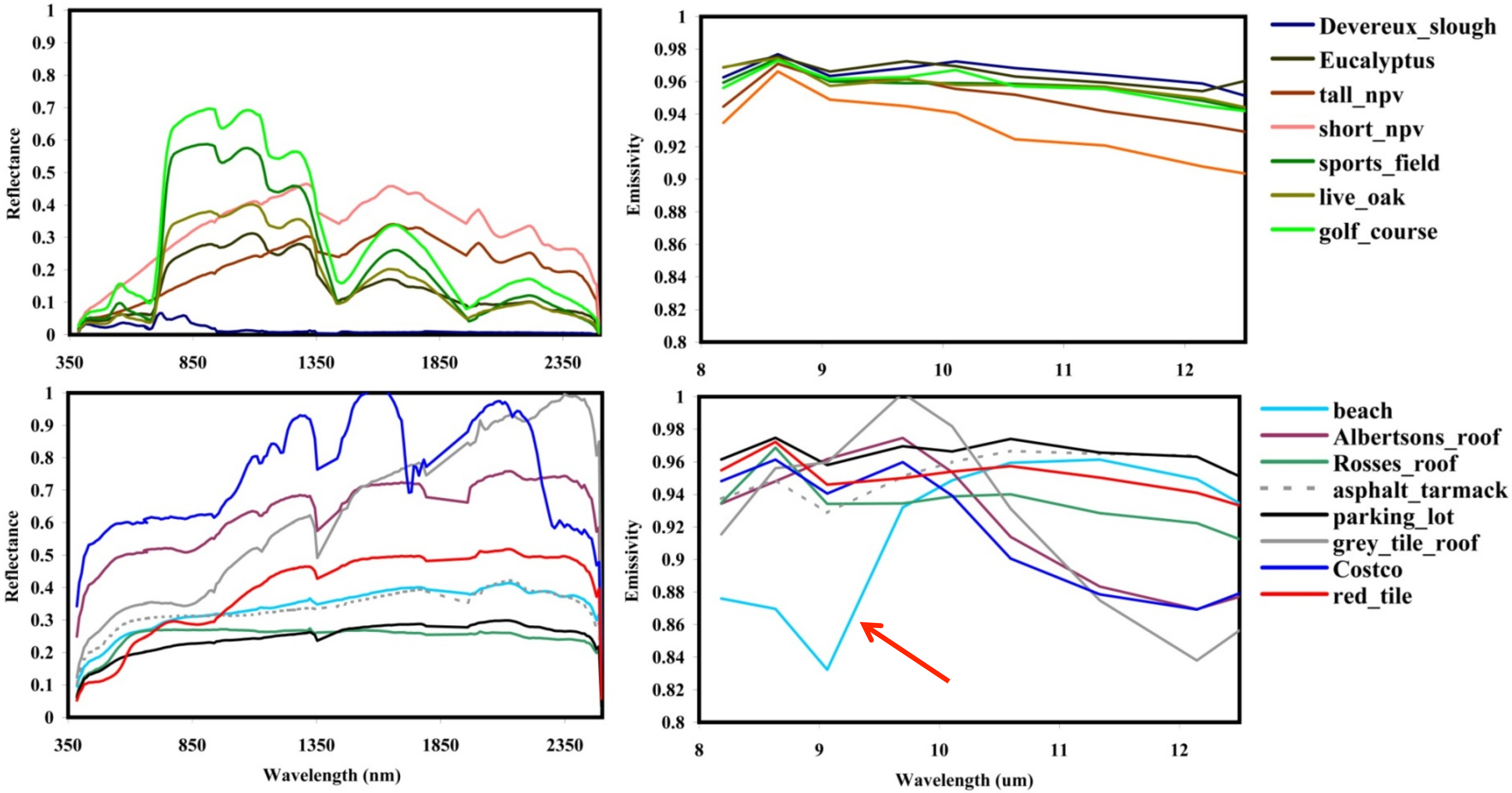

- Biotic Materials – Most Distinct in VSWIR (all unique)
  - NPV low emissivity in TIR (Differs by stature)
- Abiotic Materials – Varies
  - AVIRIS: Painted roofs, red tile
    - Soils and some road surfaces are not distinct*
  - MASTER: Quartz beach sands, various roof types
    - Asphalt surfaces are near black bodies

VSWIR-TIR improves discrimination of abiotic materials

MESMA: Endmember Selections

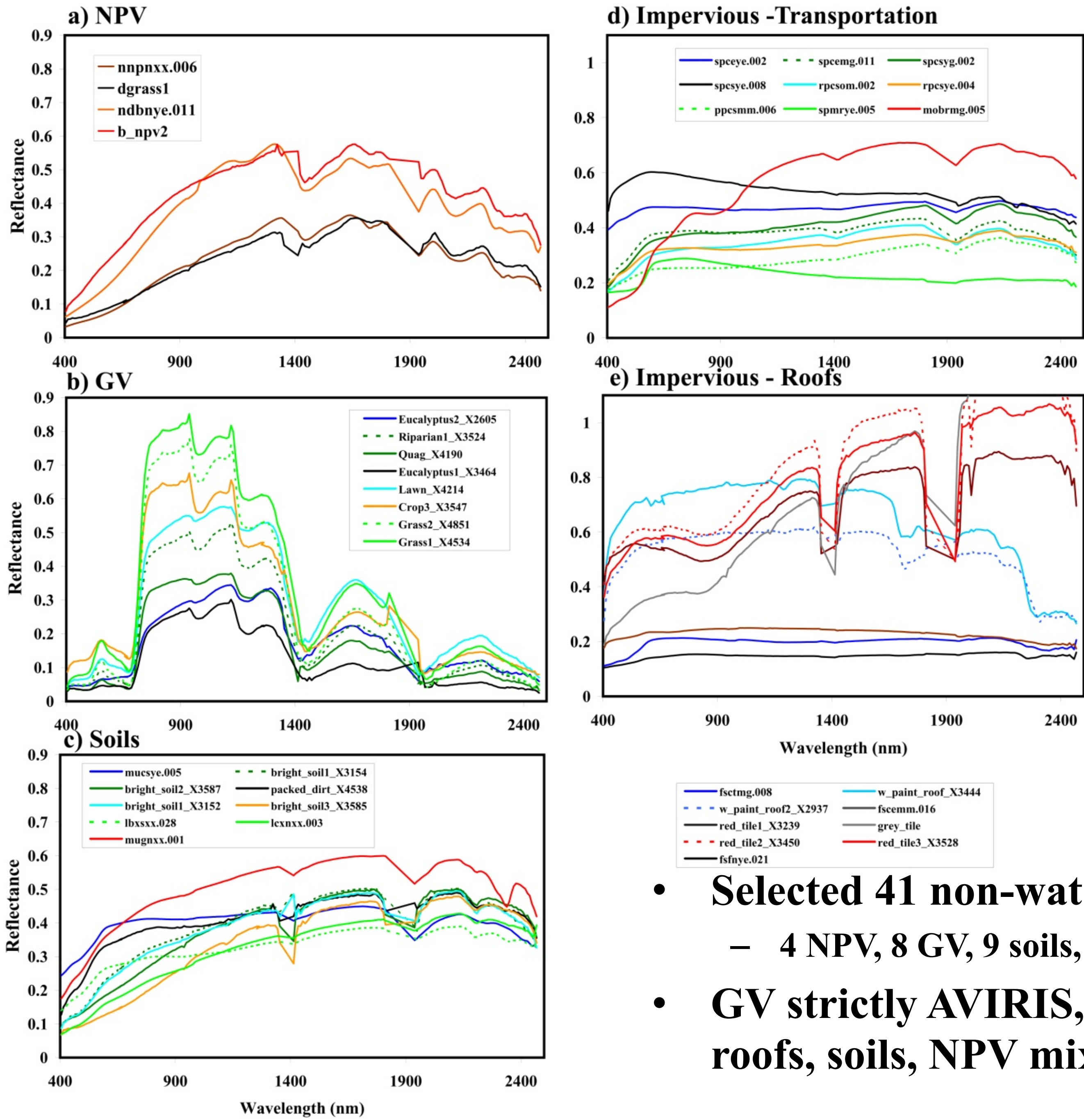

- Selected 41 non-water endmembers
  - 4 NPV, 8 GV, 9 soils, 20 Impervious
- GV strictly AVIRIS, transportation field, roofs, soils, NPV mixed

VIS-NPV Fractions: 15 and 60 m

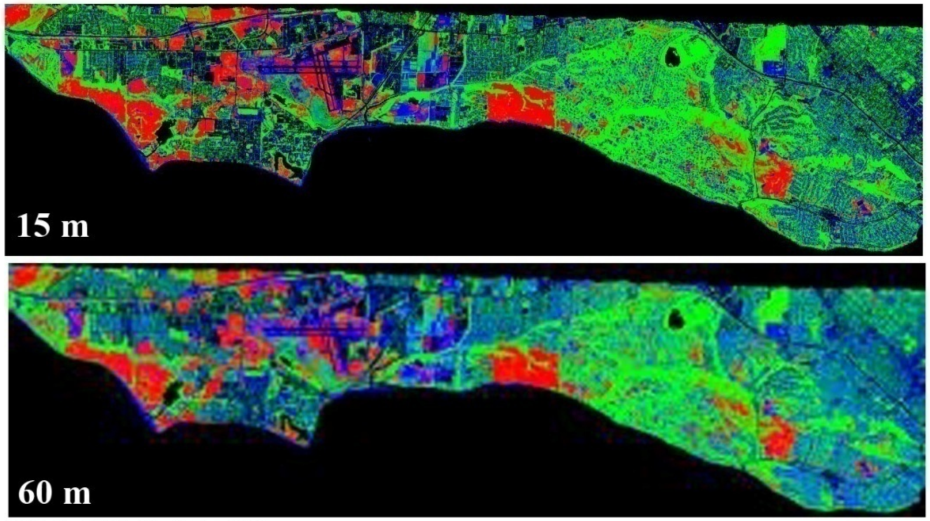

NPV, GV, Soil :RGB

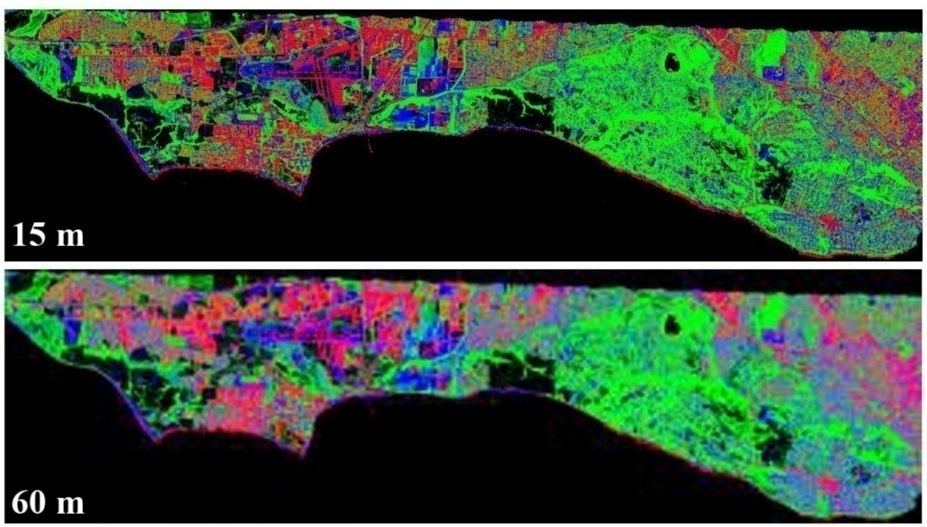

Impervious, GV, Soil: RGB

- **GV and NPV fractions scaled well between all spatial resolutions**
  - **7.5, 15 and 60 m**
- **Soil tended to be overmapped at the expense of Impervious at coarser scales**

Two error sources
Asphalt – soil
Red Tile Roof (so variable requires 3 ems)

Fraction Validation: 60 m

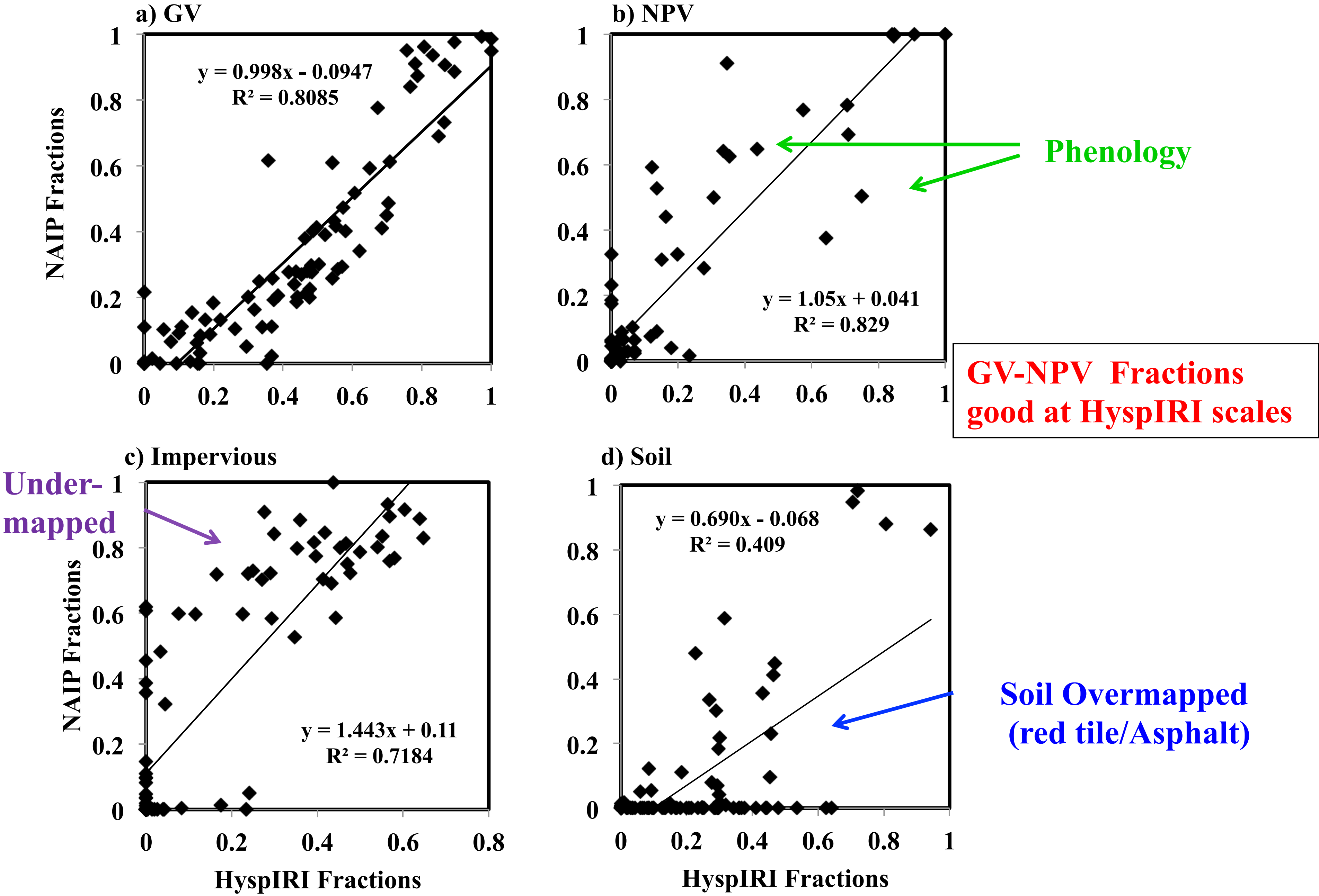

Land-cover Composition

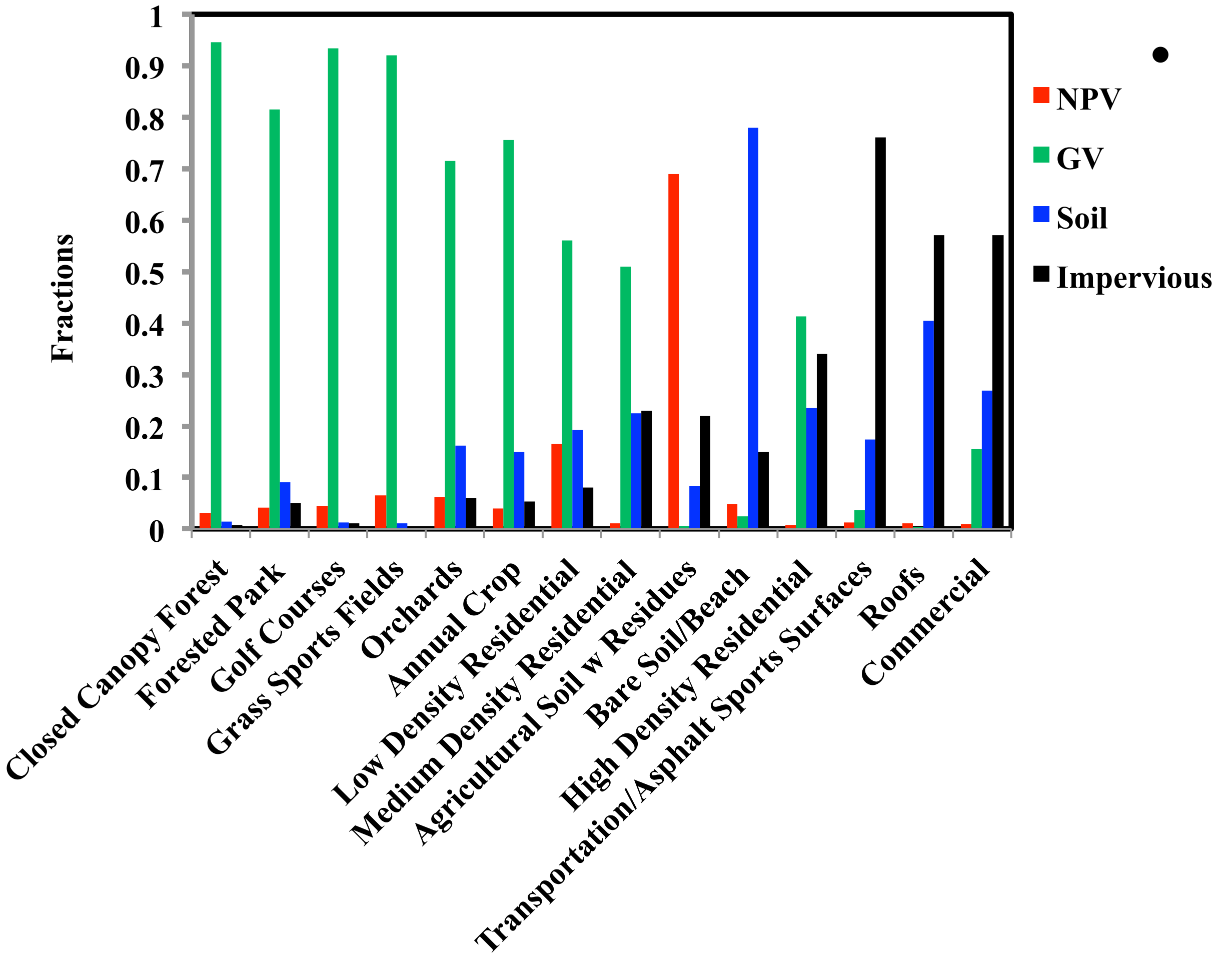

- **Cover fractions follow the expected pattern**
  - **High GV, low Temperature**
  - **High Impervious, high Temperature**
  - **Residential**
    - **Low density, high GV, Low T, low Imp**
    - **High density, low GV, High T, High Imp**

Green Cover and LST

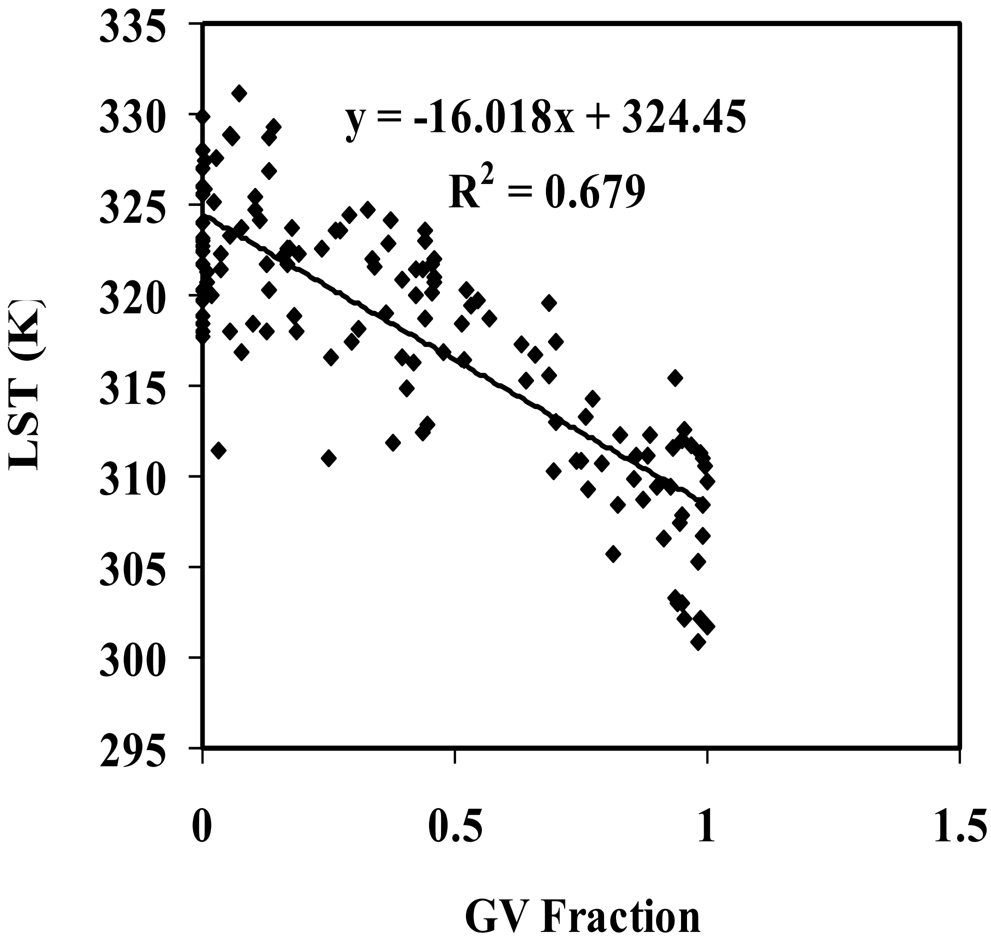

- Standard inverse relationship between GV Cover and LST
- Considerable scatter
  - The scatter is likely to be the most interesting part
  - Moist soils evapotranspiring
  - Closed canopies with variable ET

What's Next?

- **TES with AVIRIS derived column water vapor**
- **Spatial variation in LST in closed canopies**
  - **VSWIR stress measures**
- **Analysis of new AVIRIS-MASTER pair, 2011**
  - **Greater areal coverage, including greater elevation range, Gap, Tea and Jesusita Fire scars and a wide diversity of natural vegetation**
- **Seasonal VSWIR-TIR spectroscopy**
  - **JPL Perkin Elmer, ASD and Nicolet**
  - **17 tree species, chlorophyll water**
  - **First measures late July 2011**
    - **Follow up, Nov/Dec 2011, Mar 2012, June 2012**

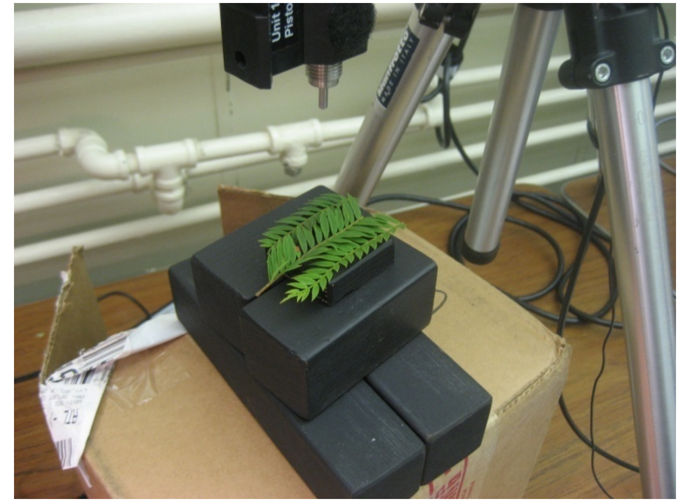

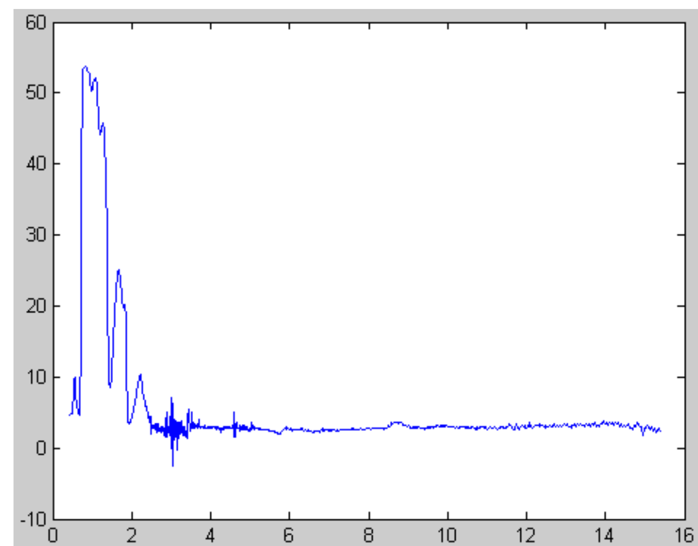

Source: Mike Alonzo, Keely Roth

Summary

- **Urban material Identification will be difficult with HyspIRI**
  - **Variation too fine scale**
- **GV-NPV cover stable at multiple scales**
  - **Impervious can be improved**
    - **Improved Red Tile Roofs**
  - **Potential for VSWIR-TIR unmixing for abiotic materials**
    - **Improved soil-impervious discrimination**
- **Energy patterns reasonable**
  - **GV-LST inversely correlated**
  - **Impervious-LST positively correlated**
  - **Considerable scatter – which is the interesting part**

Exploiting Multisensor Spectral Data to Improve Estimates of Agricultural Crop Residue Cover

Magda S. Galloza[1], Melba M. Crawford[2]

Laboratory for Applications of Remote Sensing
Purdue University

2012 NASA HyspIRI Products Symposium May 16-17, 2012

Outline

- Introduction
  - Estimation of Crop Residue
- Research Motivation
  - Evaluation of Hyperspectral / Multispectral Sensor data for residue estimation
  - Investigation of approaches for large scale applications
- Methodology
- Experimental Results
- Summary and Future Directions

PURDUE
UNIVERSITY

Introduction

- **<u>Residue Cover</u> (RC):** Plant material remaining in field after grain harvest and possible tillage

  - Nutrients

  - Organic material (soil)

  - Agricultural ecosystem stability
    - ↓ water evaporation
    - ↑ water infiltration
    - moderates soil temperature

  - Critical in sustaining soil quality
    - erosion
    - runoff rates

- **Ecosystem-based management approaches** (monitoring and impact assessments)

Introduction

- **Manual methods of analysis**
  - **Statistical sampling of fields via windshield surveys**
    - **Costly, requires trained personnel, subjective**
  - **Line transect method**
    - **Time and labor intensive**

- **Remote sensing based approaches**
  - **Detect within field variability**
  - **GREATER coverage area**
  - **Potentially reduce subjective errors**

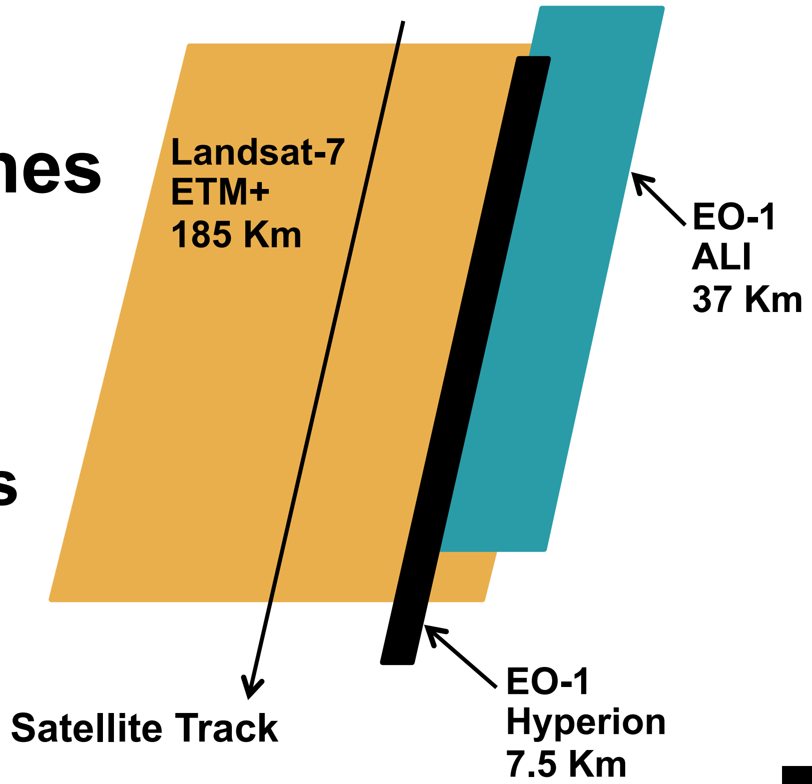

Research Motivation

- Evaluate performance of *Multispectral* and *Hyperspectral* data for estimating residue cover over local and extended areas
- Evaluate performance of next generation multispectral sensors
  - Landsat 8 Operational Land Imager (OLI)
- Investigate sensor fusion scenarios
  - Potential contribution of *Hyperspectral* data for improving (calibrating) residue cover estimates derived from wide coverage, *Multispectral* data
- Challenges
  - Residue cover can only be estimated between harvest and planting the following year
  - Vegetation in fence rows/waterways, weeks, etc
  - Cloud cover and limited extent of airborne/Hyperion data

Research Motivation

Transect Method vs. Remote Sensing based Method

Research Motivation

- **Land Cover Characteristics**
  - **Agricultural Cover Discrimination and Assessment**

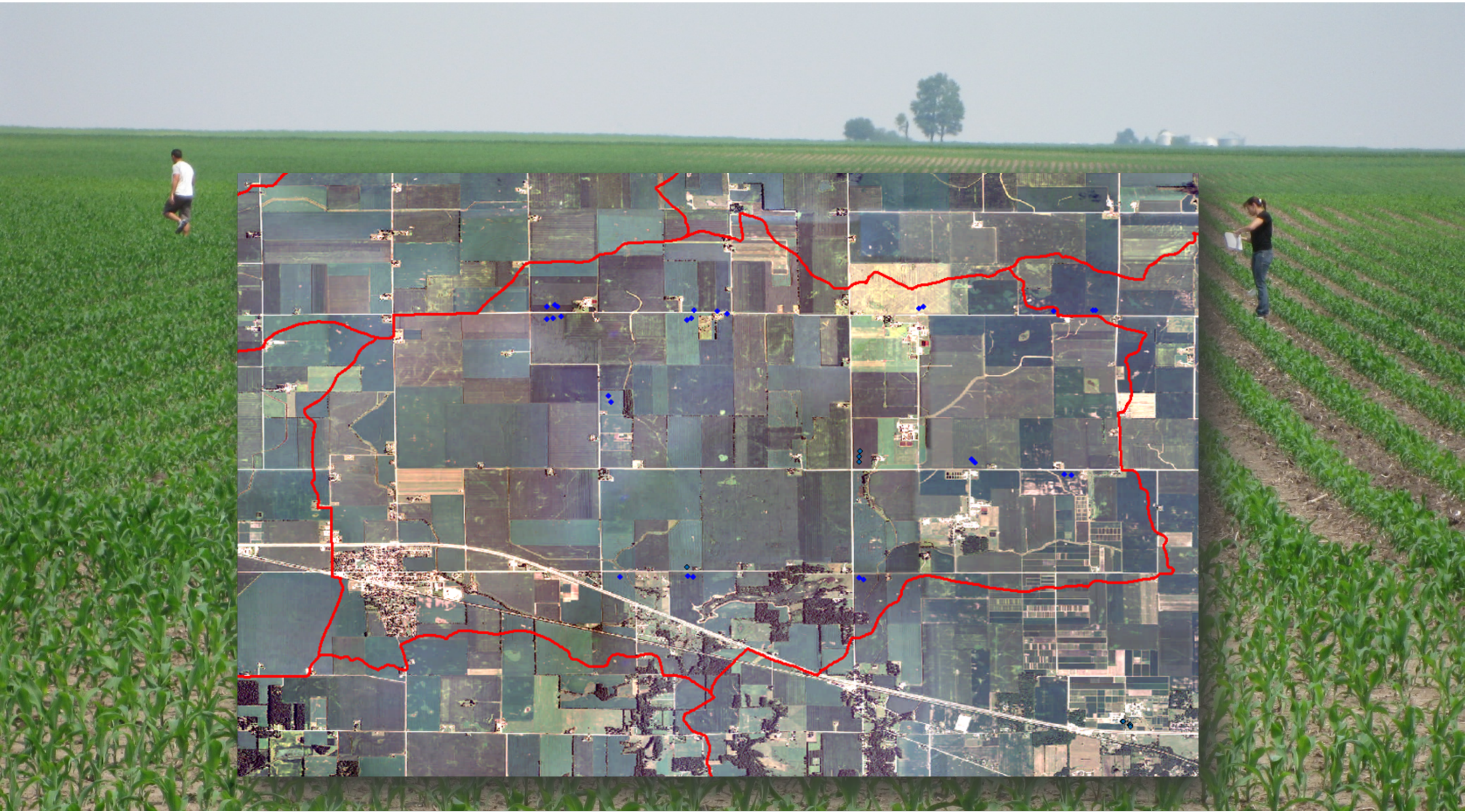

Proposed Approaches - NDTI

- **Classification or unmixing**
  - Discrete vs continuous estimates; extraneous endmembers
- **Band based Indices**
  - Based on the absorption characteristics (reflectance) of RC
  - Linear relationship between RC and indices exploited via regression models
- Multispectral **NDTI** (Normalized Difference Tillage Index)
  - Empirical models developed and validated locally
  - Applicable to multiple sensors: ASTER, Landsat, ALI (EO-1)

NDTI = (TM5 - TM7)/(TM5 + TM7)

Where:

- TM7: Landsat TM band 7 or equivalent
- TM5: Landsat TM band 5 or equivalent

Proposed Approaches - CAI

- Hyperspectral **CAI -** (Cellulose Absorption Index)
  - Physically based
  - Demonstrated to accurately RC [Daughtry, 2008]
  - Robust to crop and soil types
  - Limited coverage and

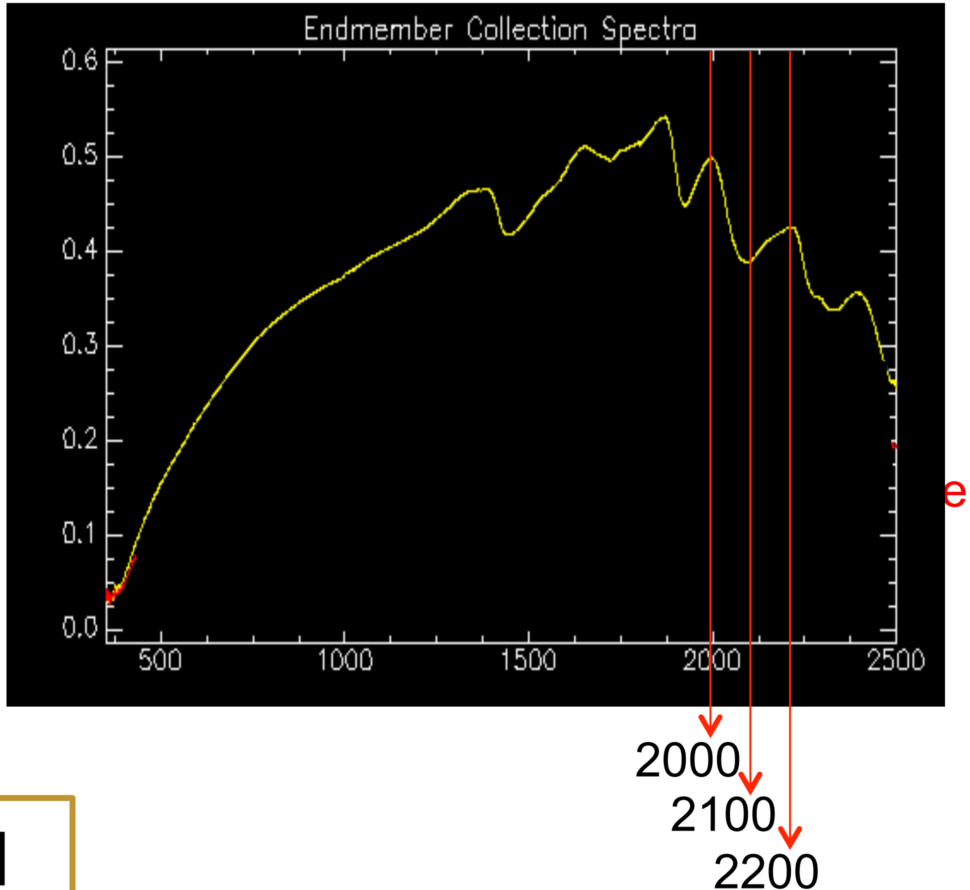

CAI = 0.5 * (R2.0 + R2.2) – R2.1

Where:

- R2.0, R2.1, R2.2: average response of 3 bands centered at 2000 nm, 2100 nm and 2200 nm respectively

Study Location / Field Data

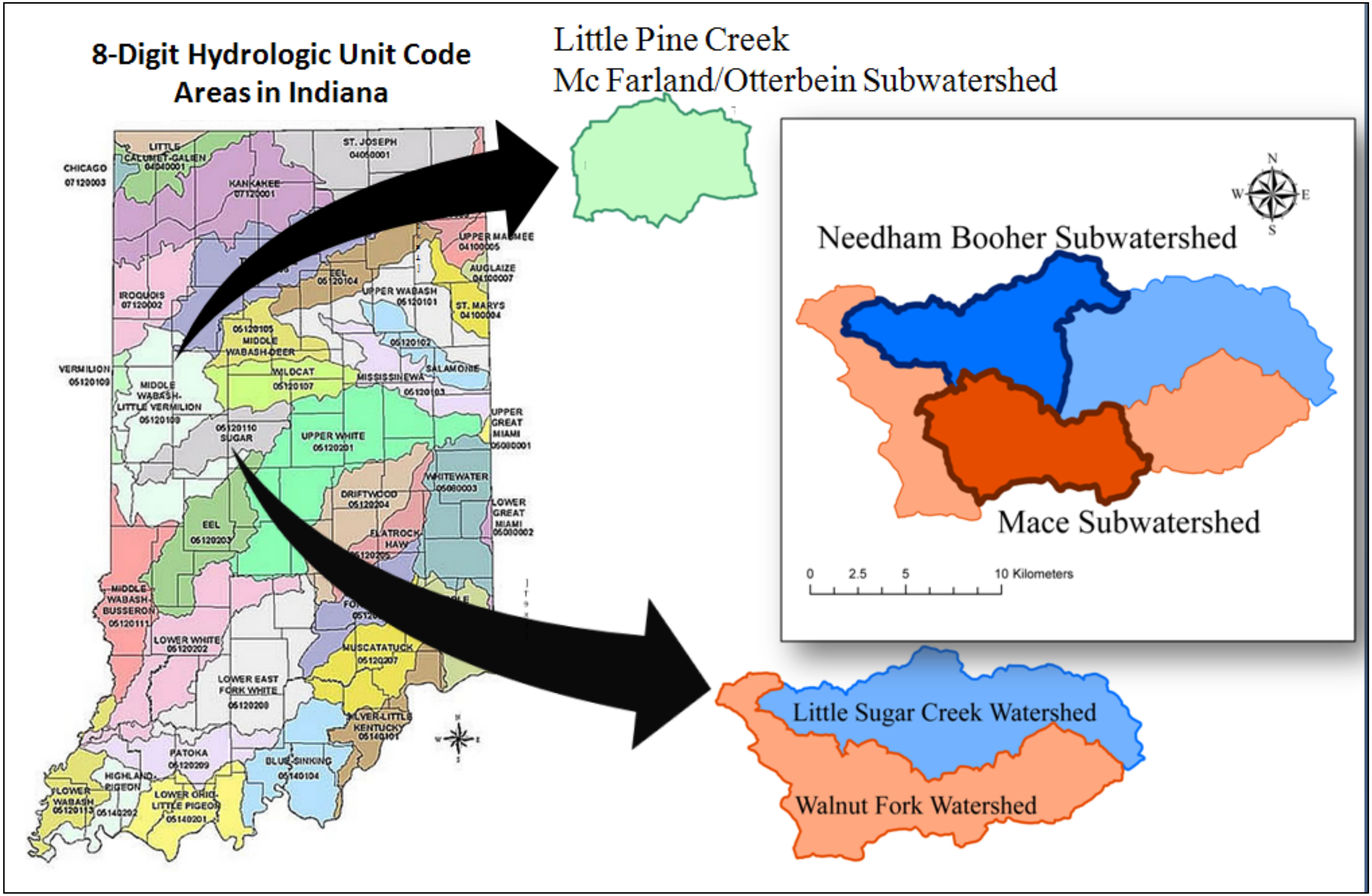

Remote Sensing Data (2008-2010)

Data Available	Spring 2008	Fall 2008	Spring 2009	Fall 2009	Spring 2010	Fall 2010
EO-1 ALI/Hyperion	May 6	Nov 1	No Data	Oct 11	May 23	Nov 2
Landsat TM	June 11	Nov 2	May 29	Oct 20	April 22	Nov 8
SpecTIR Airborne	No Data	Nov 3	June 5	No Data	May 24	No Data

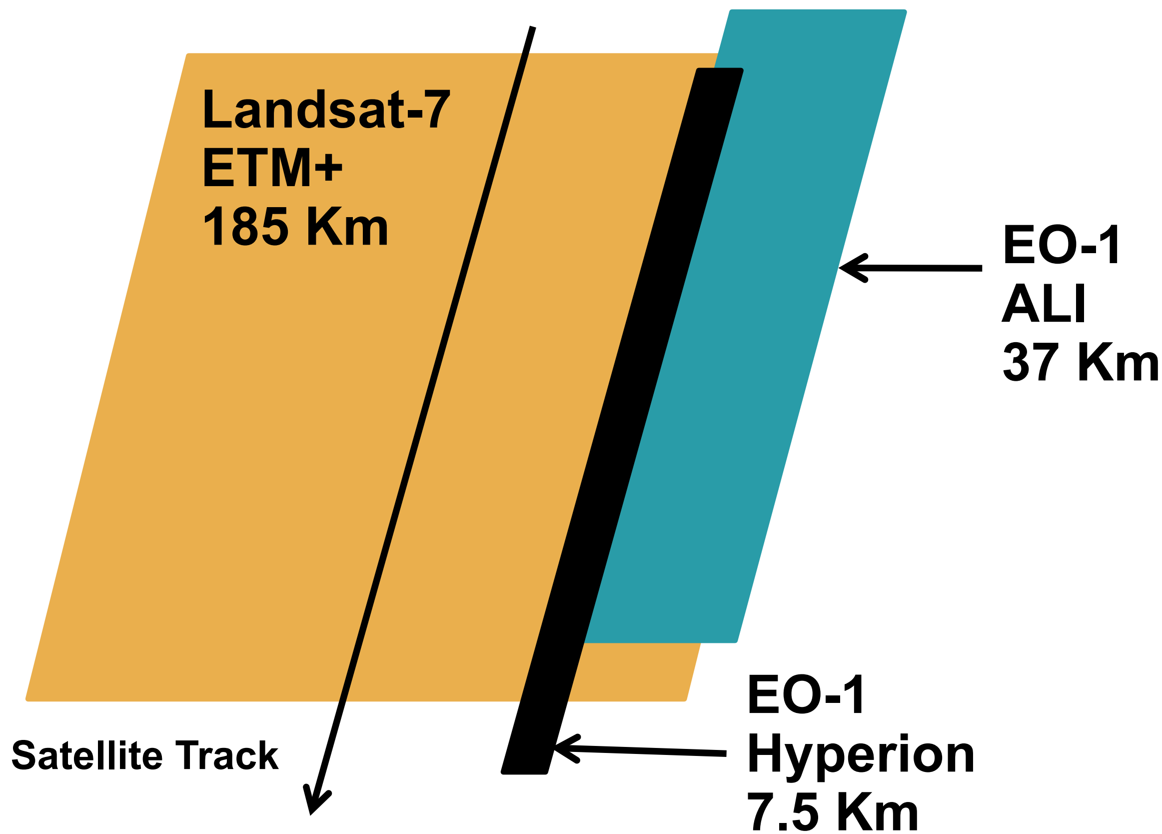

PURDUE UNIVERSITY

Linear Models

1- $y_i = \beta_0^1 + \beta_1^1 CAI_i + \varepsilon_i^1 \rightarrow \varepsilon_i^1 : \; N(0,\sigma_1^2)$

2- $y_i = \beta_0^2 + \beta_1^2 NDTI_i + \varepsilon_i^2 \rightarrow \varepsilon_i^2 : \; N(0,\sigma_2^2)$

3- $CAI_i = a_0 + a_1 NDTI_i + \varepsilon_i^3 \rightarrow \varepsilon_i^3 : \; N(0,\sigma_3^2)$

Substitute in Model 1

$$y_i = \beta_0^1 + \beta_1^1 (a_0 + a_1 NDTI_i) + \varepsilon_i^1$$

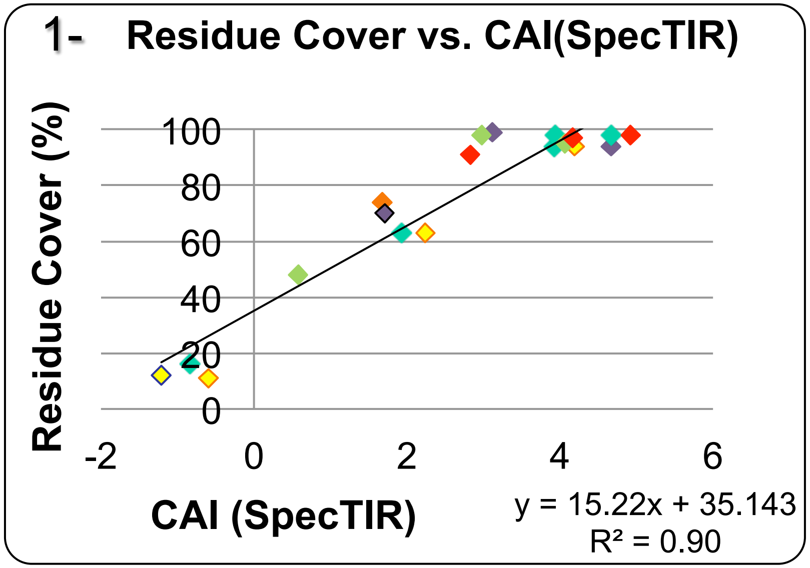

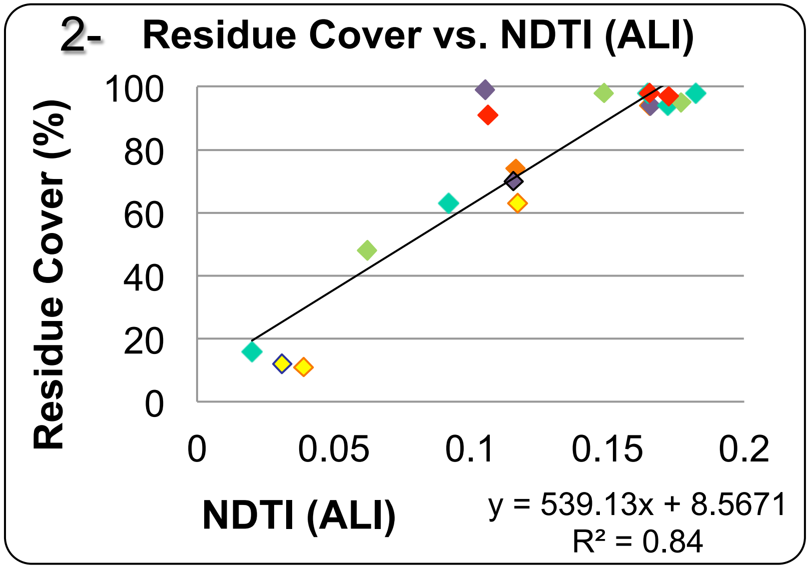

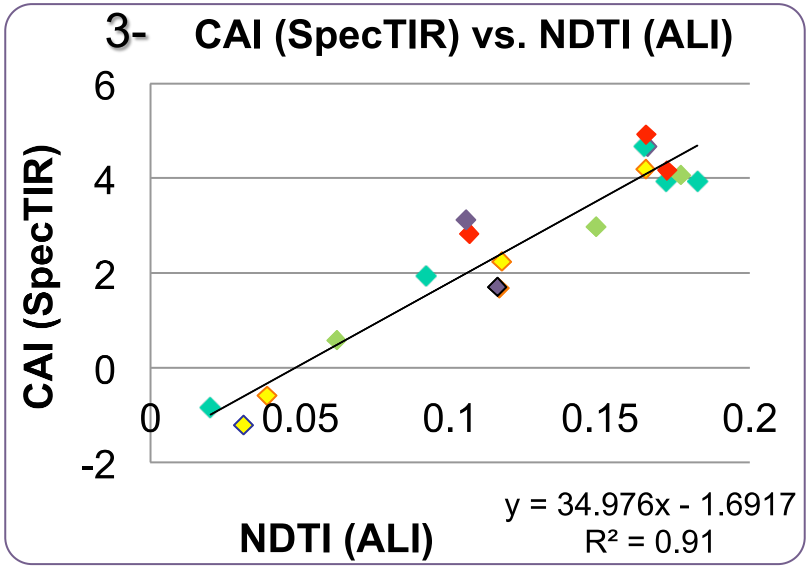

Linear Models

1- $y_i = \beta_0^1 + \beta_1^1 CAI_i + \varepsilon_i^1 \rightarrow \varepsilon_i^1 : \; N(0,\sigma_1^2)$

2- $y_i = \beta_0^2 + \beta_1^2 NDTI_i + \varepsilon_i^2 \rightarrow \varepsilon_i^2 : \; N(0,\sigma_2^2)$

3- $CAI_i = a_0 + a_1 NDTI_i + \varepsilon_i^3 \rightarrow \varepsilon_i^3 : \; N(0,\sigma_3^2)$

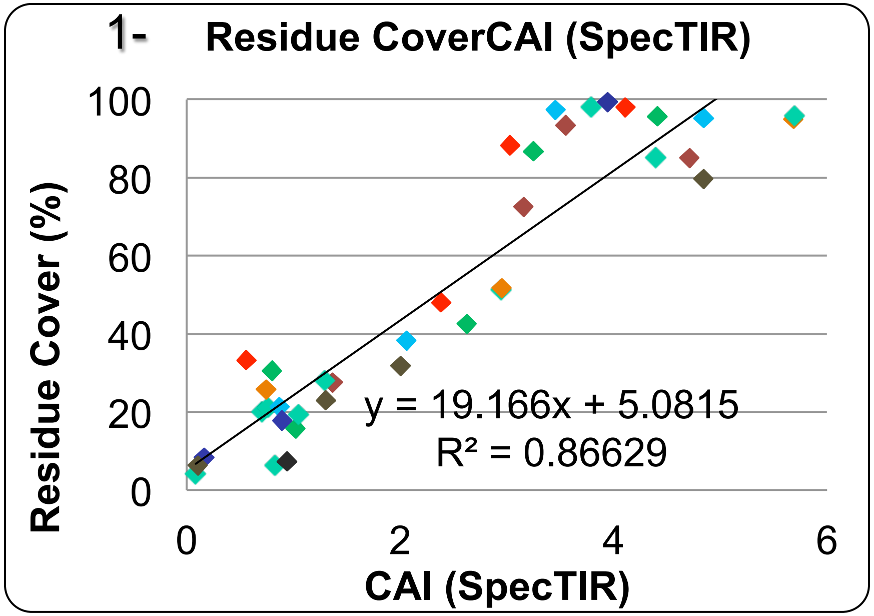

Substitute in Model 1

$$y_i = \beta_0^1 + \beta_1^1 (a_0 + a_1 NDTI_i) + \varepsilon_i^1$$

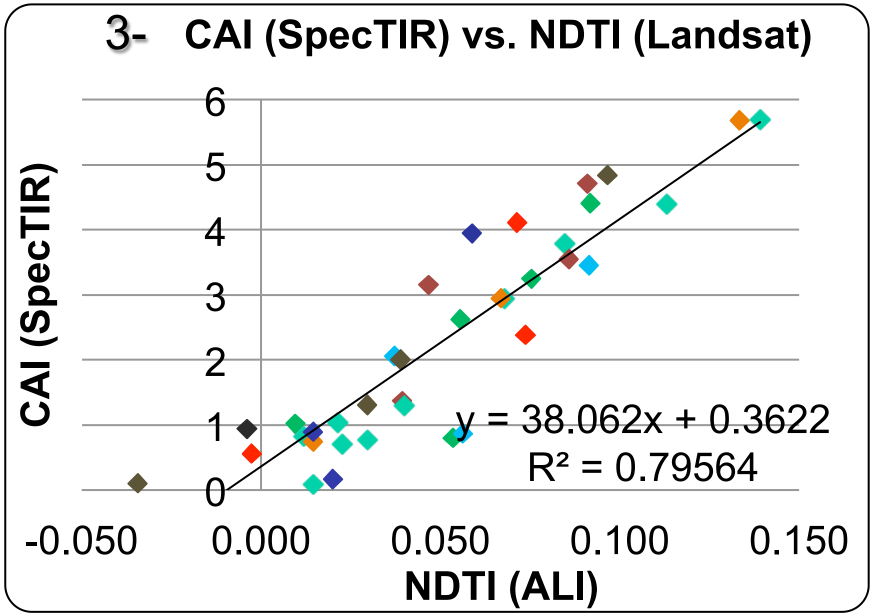

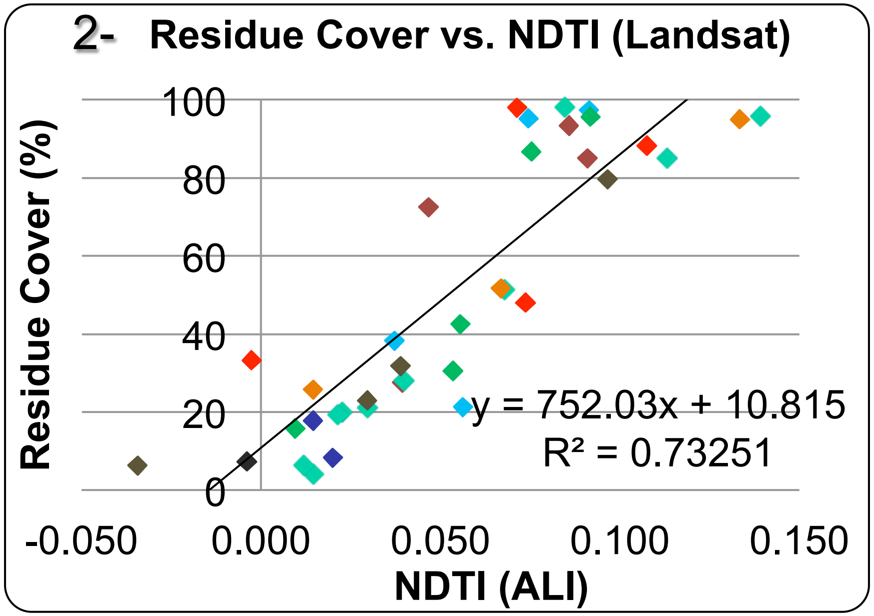

PURDUE UNIVERSITY

Model 1 - CAI Index

$$y_i = \beta_0 + \beta_1 CAI_i + \varepsilon_i^1 \rightarrow \varepsilon_i^1 : \; N(0, \sigma_1^2)$$

Legend:
- 0% - 25%
- 26% - 50%
- 51% - 75%
- 76% - 100%

Watershed Scale Evaluation

Residue Cover (%)	SpecTIR 4m (hec)	SpecTIR 30m (hec)	Hyperion (hec)
0% - 25%	34.97	26.49	4.87
26% - 50%	138.37	157.82	124.02
51% - 75%	498.19	464.81	525.65
76% - 100%	738.02	768.55	774.59

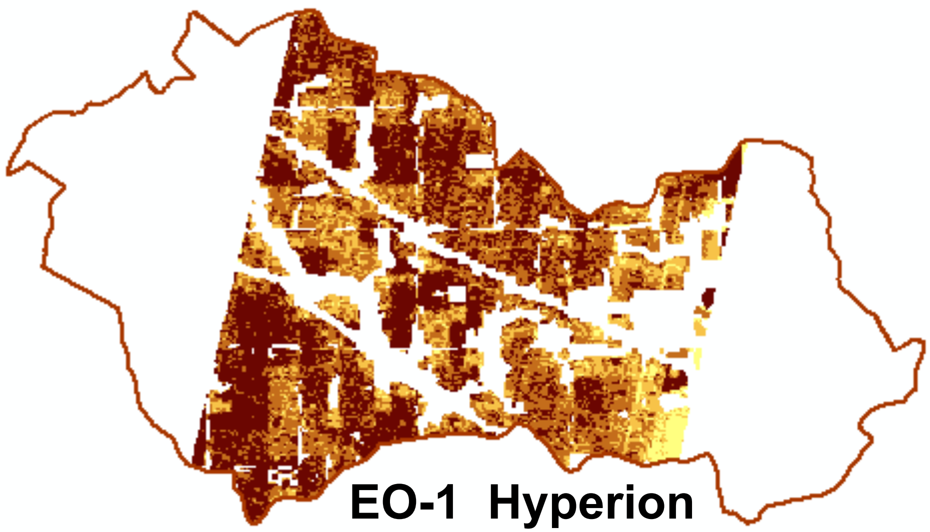

EO-1 Hyperion

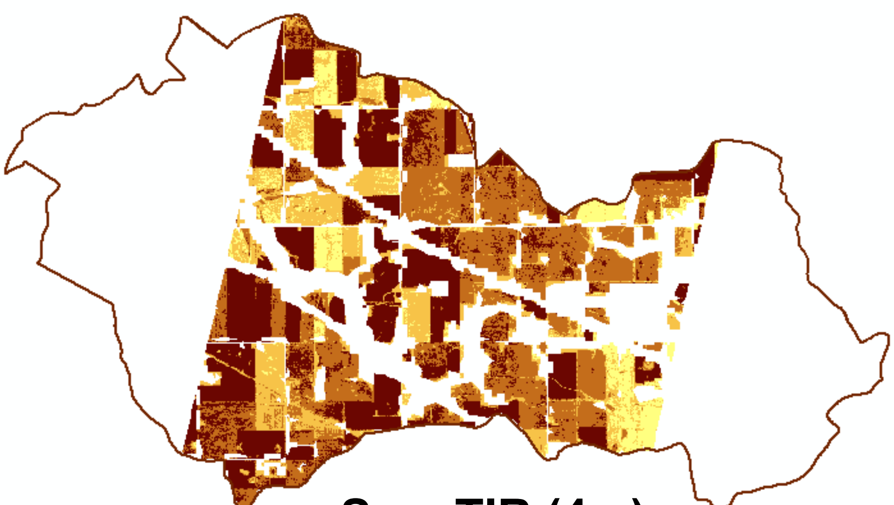

SpecTIR (4m)

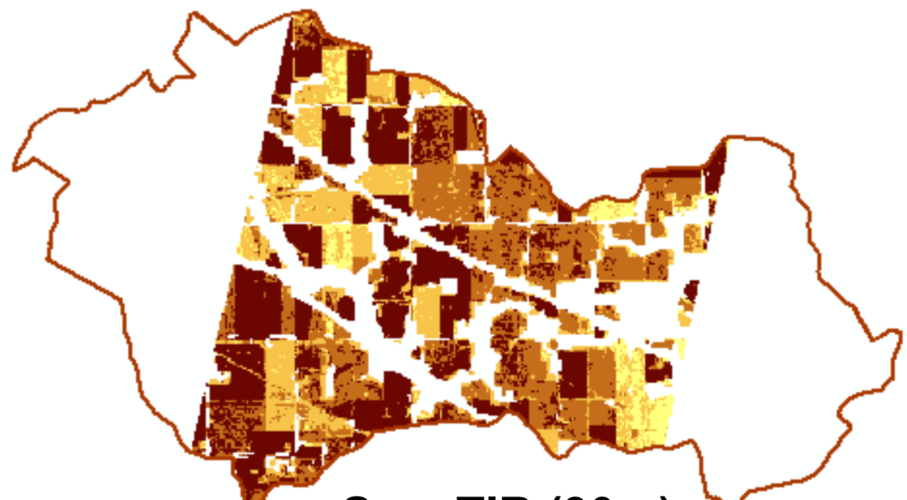

SpecTIR (30m)

Model 2 – NDTI Index

$$y_i = \beta_0 + \beta_2 NDTI_i + \varepsilon_i^2 \rightarrow \varepsilon_i^2 : \; N(0,\sigma_2^2)$$

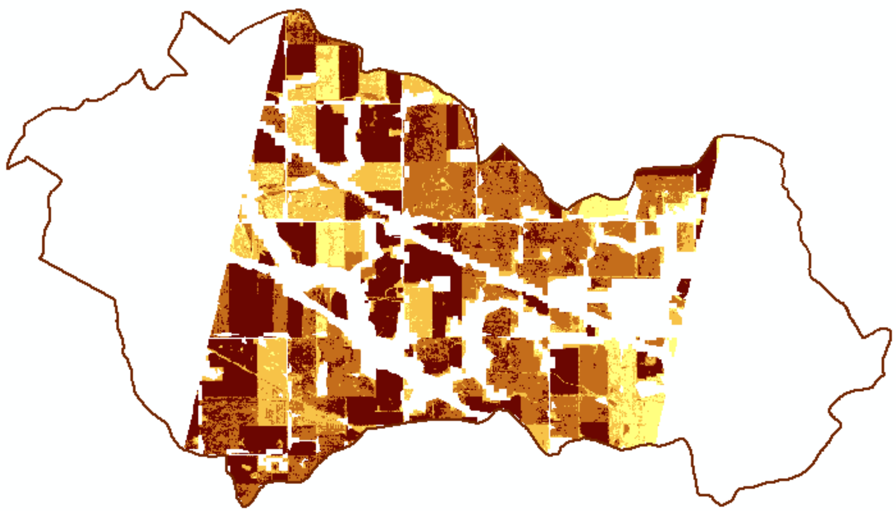

CAI Model – SpecTIR (4m)

0% - 25%
26% - 50%
51% - 75%
76% - 100%

Watershed Scale Evaluation

Residue Cover (%)	Landsat (hec)	ALI (hec)	SpecTIR 4m (hec)
0% - 25%	12.03	14.31	34.97
26% - 50%	99.91	97.41	138.37
51% - 75%	405.14	550.35	498.19
76% - 100%	1061.03	835.68	738.02

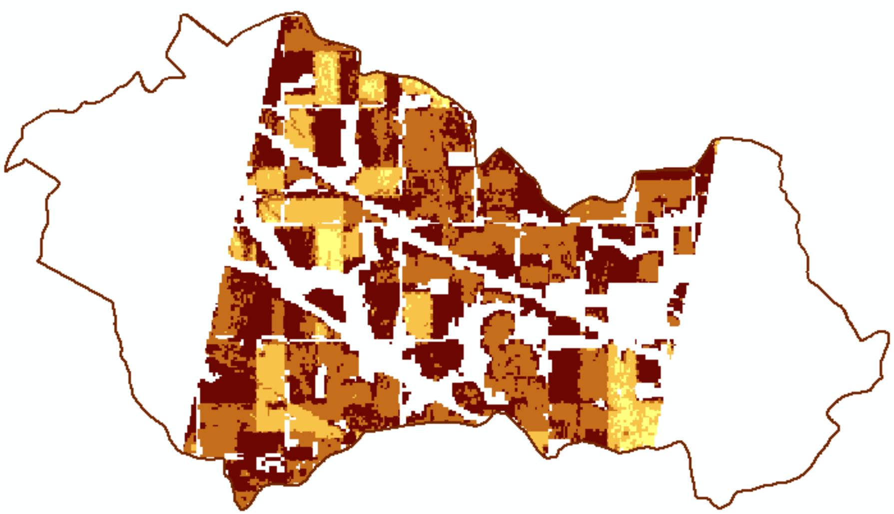

NDTI Model - ALI

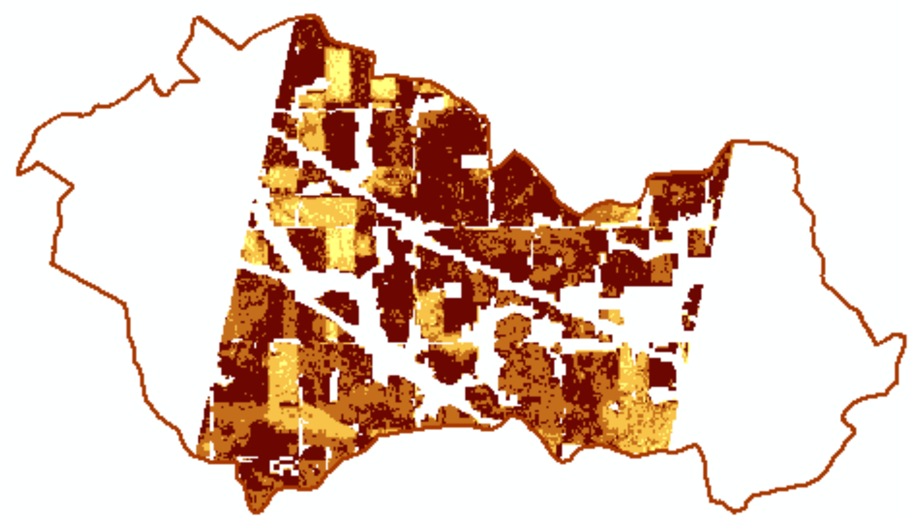

NDTI Model – Landsat TM

PURDUE UNIVERSITY

Generalization: Little Pine Creek Model Applied to Darlington Region

Model 2

$$y_i = \beta_0 + \beta_2 NDTI_i + \varepsilon_i^2$$

- 0% - 25%
- 26% - 50%
- 51% - 75%
- 76% - 100%

Watershed Scale Evaluation

Residue Cover (%)	ALI (hec)	ACRE Model (hec)
0% - 25%	62.82	0.63
26% - 50%	276.48	195.12
51% - 75%	808.47	149.13
76% - 100%	961.83	1766.16

Little Pine Creek Model Applied to Darlington

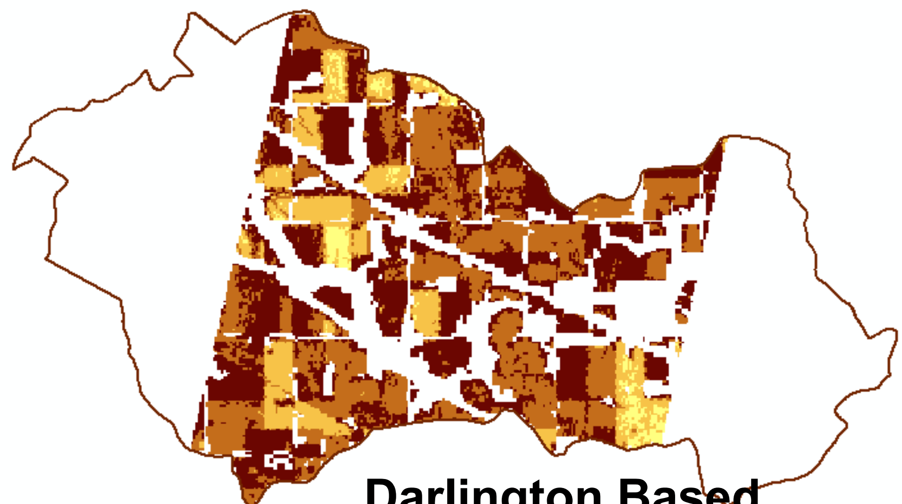

Darlington Based Model (ALI)

PURDUE UNIVERSITY

Model 3 – NDTI Substition in CAI Model

$$CAI_i = a_0 + a_1 NDTI_i + \varepsilon_i^3 \rightarrow \varepsilon_i^3 : \; N(0, \sigma_3^2)$$

Substitute in Model 1

$$y_i = \beta_0 + \beta_1(a_0 + a_1 NDTI_i) + \varepsilon_i^1$$

(light yellow)	0% - 25%
(yellow-orange)	26% - 50%
(orange)	51% - 75%
(dark red)	76% - 100%

Watershed Scale Evaluation

Residue Cover (%)	Model 3 (hec)	SpecTIR (hec)
0% - 25%	38.43	131.49
26% - 50%	297.36	441.27
51% - 75%	825.75	693.81
76% - 100%	949.50	844.56

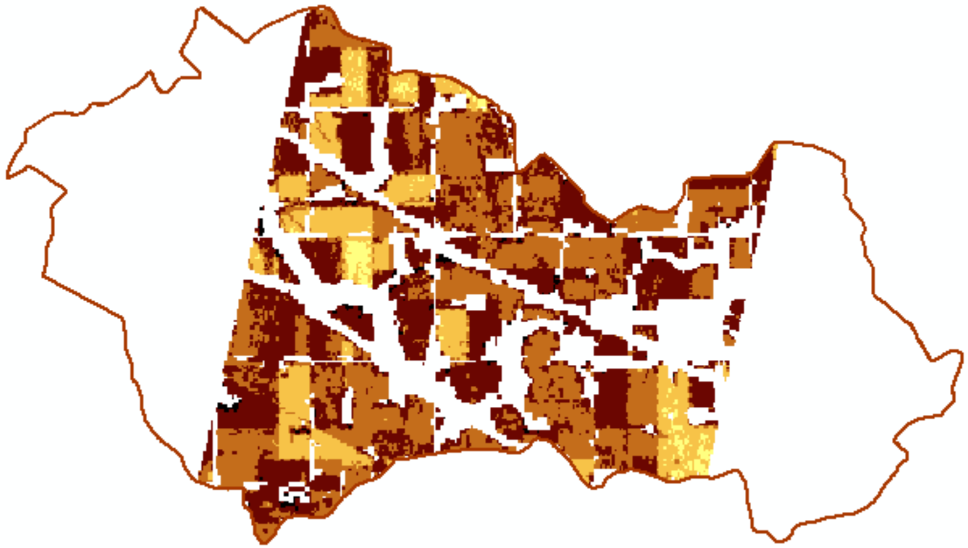

Model 3 - (Substitution Model)

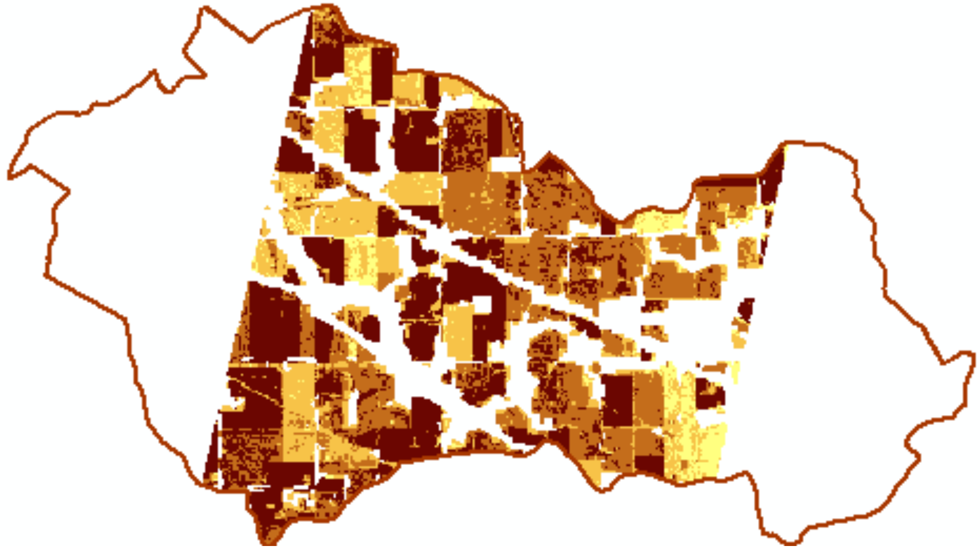

Model 1 – SpecTIR (30m)

Model 4 – CDF Based Rescaling

- **Matching Multi-source CDF**
  - Rank samples for the data sets CAI (I_h) and NDTI (I_m).
  - Compute differences between corresponding elements of the ranked data sets:
    - $I_{d,i} = I_{h,i} - I_{m,i}$

    where $I_{h,i}$ and $I_{m,i}$ are the ranked CAI and NDTI values for *i=1…n*;
    n = no. of samples.
  - Approximate the CDF using a global polynomial or piece-wise linear approaches

Knowledge Transfer via CDF Based Rescaling

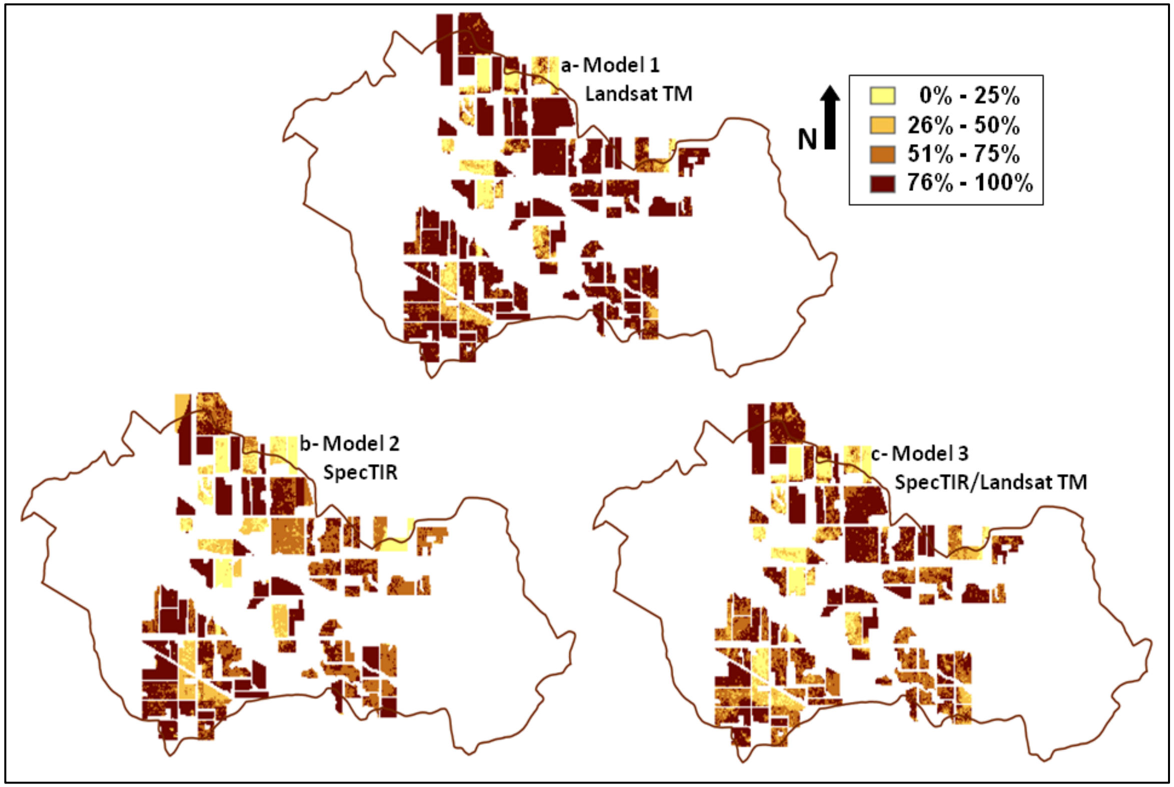

Field Residue Cover (%)	Residue Coverage				
	Model 1	Model 1	Model 2	Model 3	Model 3
	Landsat TM (ha)	ALI (ha)	SpecTIR (ha)	LandsatTM (ha)	ALI (ha)
0% - 25%	11.7	27.1	23.9	16.1	24.2
26% - 50%	35.2	47.5	48.5	52.6	49.6
51% - 75%	81.5	321.2	249.2	258.3	249.1
76% - 100%	883.3	485.1	556.0	541.1	554.7

Field Residue Cover (%)	Residue Coverage					
	MFOW in MW			MW		
	Model 1	Model 2	Model 3	Model 1	Model 2	Model 3
	Landsat TM (ha)	SpecTIR (ha)	Landsat TM (ha)	LandsatTM (ha)	SpecTIR (ha)	Landsat TM (ha)
0% - 25%	12.4	23.2	37.3	11.7	23.9	16.1
26% - 50%	31.5	56.6	50.7	35.2	48.5	52.6
51% - 75%	122.26	221.15	289.6	81.5	249.2	258.3
76% - 100%	863.6	647.0	592.6	883.3	556.0	541.1

Period	RMSE (Residue Cover Percent)				
	Model 1	Model 1	Model 2	Model 3	Model 3
	ALI	Landsat TM	Hyperion	ALI	Landsat TM
Fall 2008	12.9	19.7	18.9	16.1	19.8
Fall 2009	16.6	20.3	23.9	20.2	28.3
Fall 2010	12.2	13.8	17.1	12.3	14.5

Thank You

SpecTIR 30m vs. Hyperion 30m

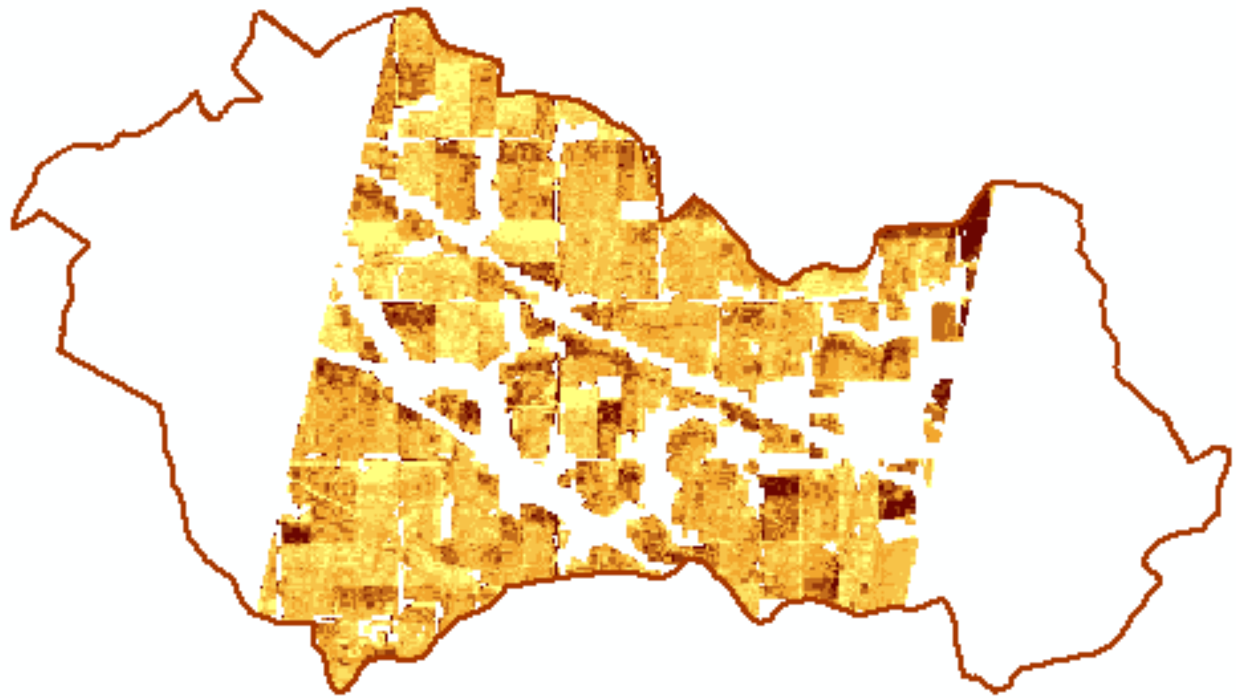

Residue Cover (%)	Difference (hec)
-60% - -40%	184.77
-39% - -20%	328.32
-19% - 0%	625.86
1% - 20%	564.93
21% - 40%	268.92
41% - 60%	99.36
61% - 70%	38.88

CAI (SpecTIR) vs. NDTI (Landsat/ALI)

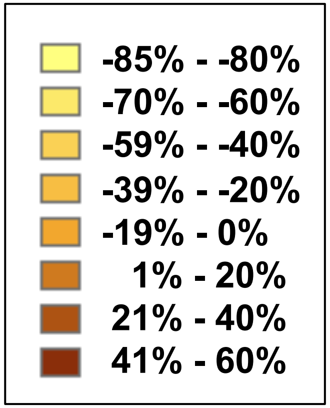

Residue Cover (%)	Landsat Difference (hec)	ALI Difference (hec)
-85% - -80%	67.41	34.2
-79% - -60%	69.21	65.52
-59% - -40%	146.52	92.45
-39% - -20%	**339.93**	**179.37**
-19% - 0%	**607.95**	**628.39**
1% - 20%	**925.75**	**682.47**
21% - 40%	177.66	174.79
41% - 60%	19.89	5.49

SpecTIR vs. ALI

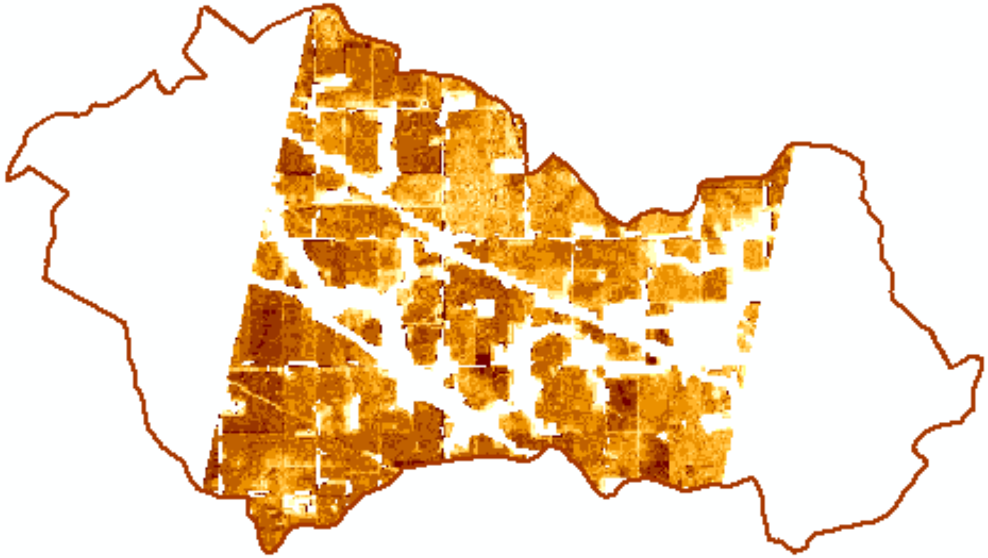

SpecTIR vs. Landsat TM

PURDUE UNIVERSITY

Model 1 vs. Model 3

Residue Cover (%)	Difference (hec)
-85% - -80%	49.14
-79% - -60%	49.77
-59% - -40%	90.9
-39% - -20%	180
-19% - 0%	653.94
1% - 20%	899.19
21% - 40%	183.06
41% - 60%	5.04

Little Pine Creek Model Applied to Darlington Region

Model 2

$$y_i = \beta_0 + \beta_1 CAI_i + \varepsilon_i^1 \rightarrow \varepsilon_i^1 : \; N(0, \sigma_1^2)$$

- 0% - 25%
- 26% - 50%
- 51% - 75%
- 76% - 100%

Watershed Scale Evaluation

Residue Cover (%)	SpecTIR (hec)	ACRE Model (hec)
0% - 25%	131.49	584.01
26% - 50%	441.27	491.85
51% - 75%	693.81	553.32
76% - 100%	848.56	481.86

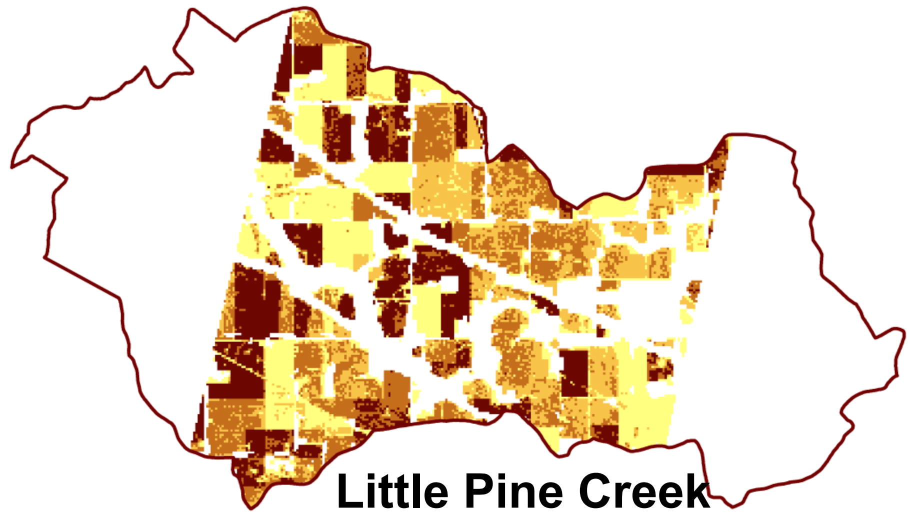

Little Pine Creek Data (Model 1)

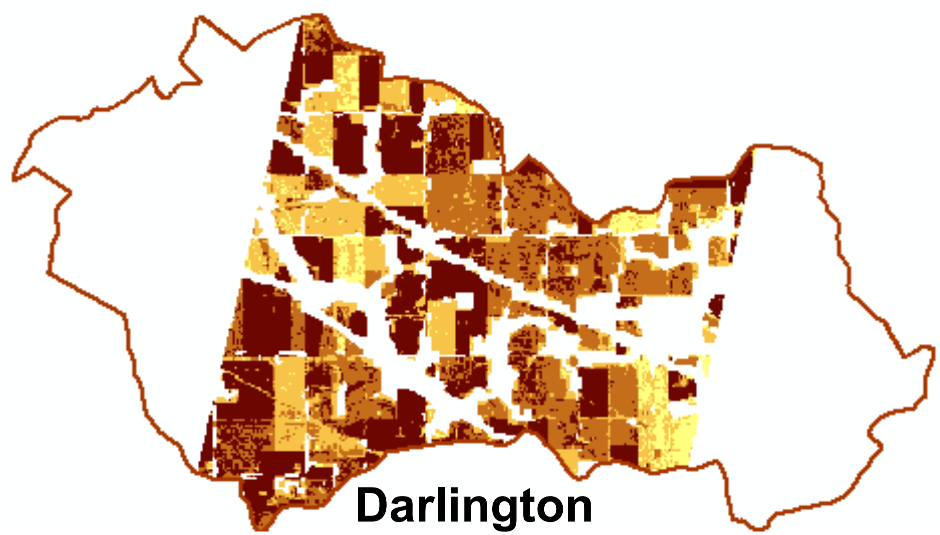

Darlington Data (SpecTIR)

Values and advantages of HyspIRI for remote sensing of aquatic environments

ZhongPing Lee

Environmental, Earth and Ocean Sciences
University of Massachusetts, Boston, MA

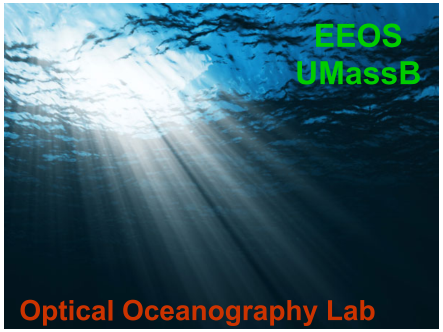

NASA HyspIRI Products Symposium, DC, May 16-17, 2012

Processes

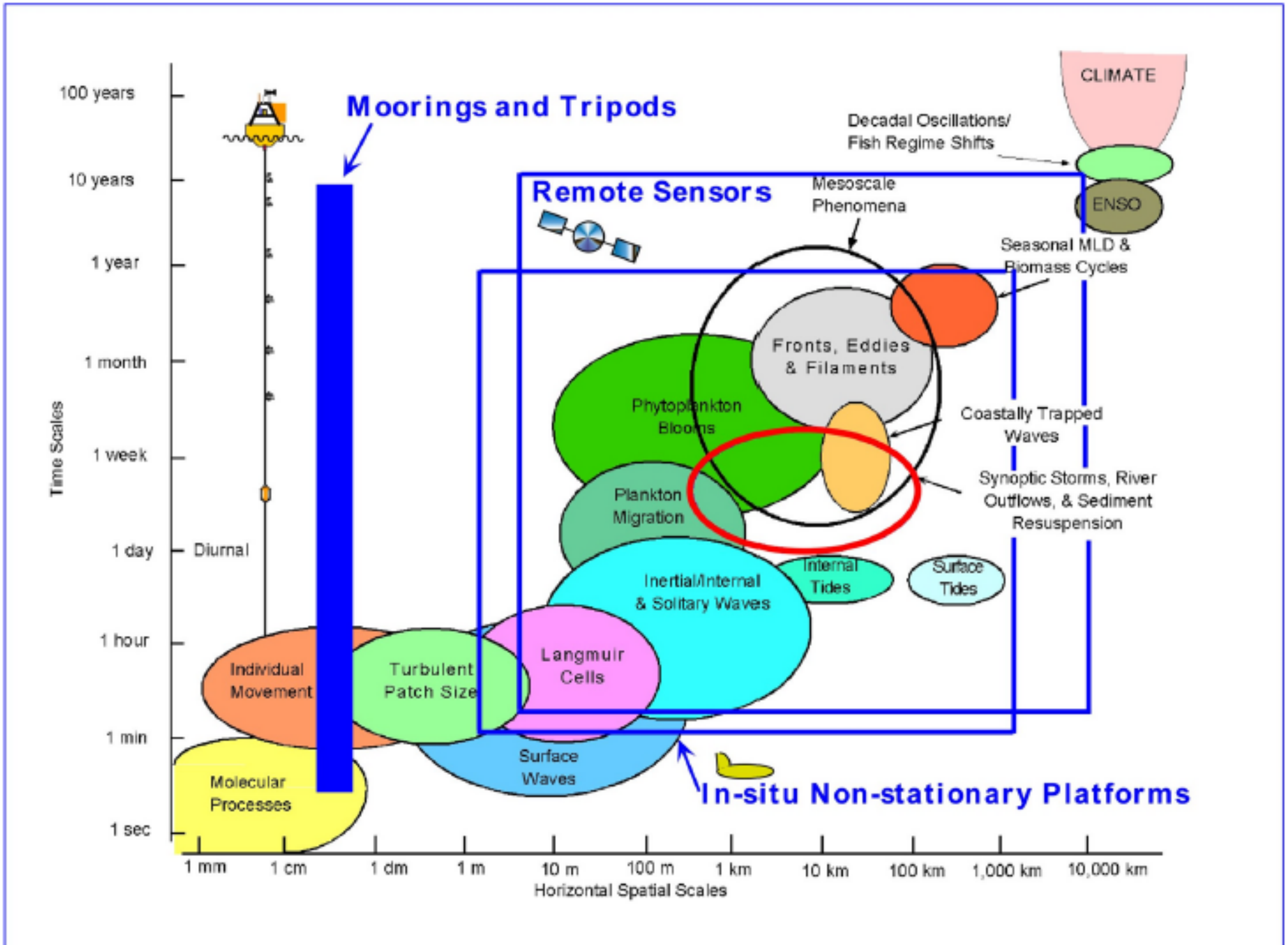

(Dickey et al 2006)

A dream remote sensor to study those processes:

High spatial resolution

High temporal resolution

High spectral resolution

High signal-to-noise ratio

Not feasible!

Some specs of HyspIRI

Name	Spectral bands (VISNIR)	Spatial Resolution (m)	Revisit time (day)
HyspIRI	hyperspectral	60	19

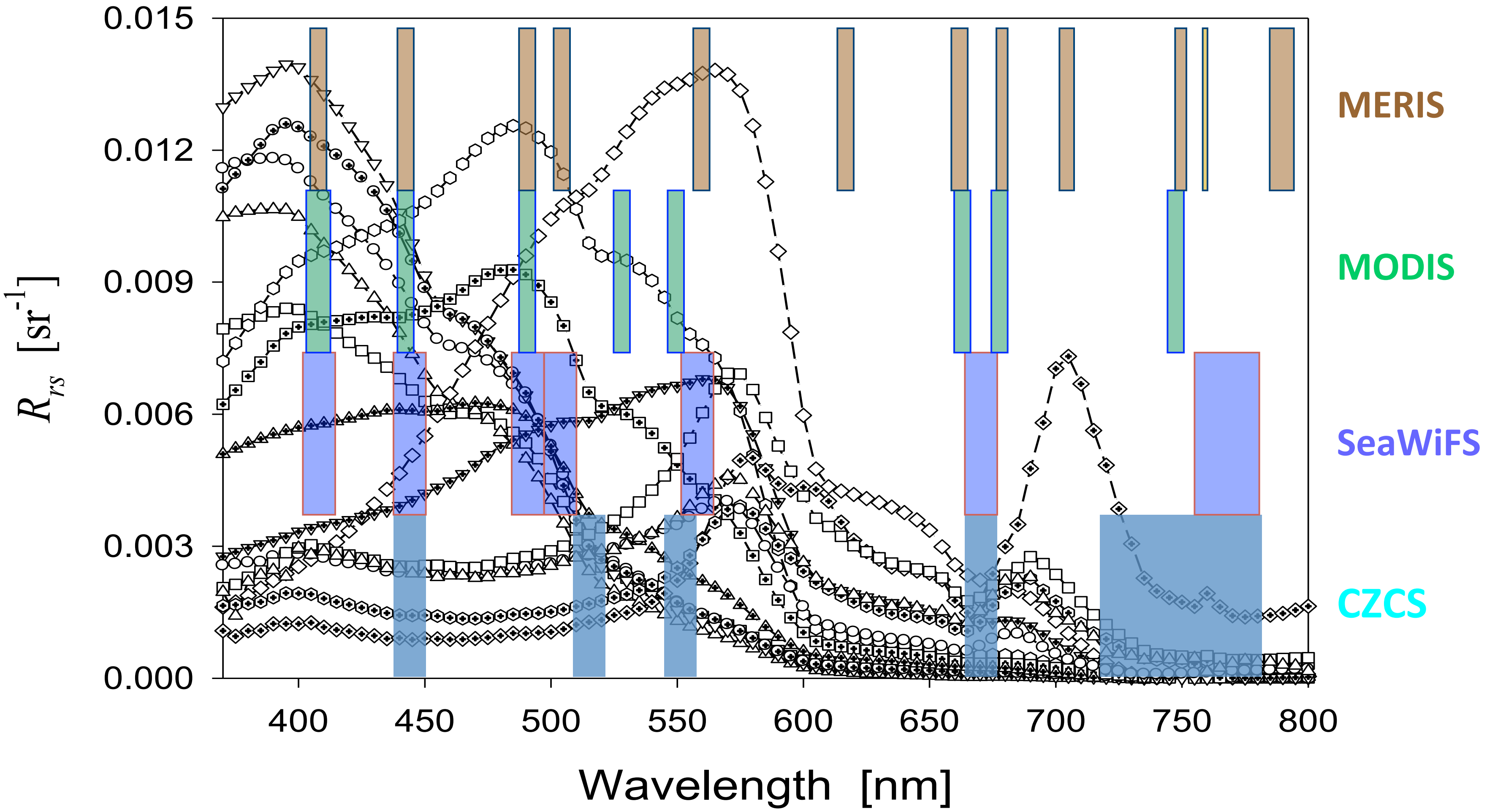

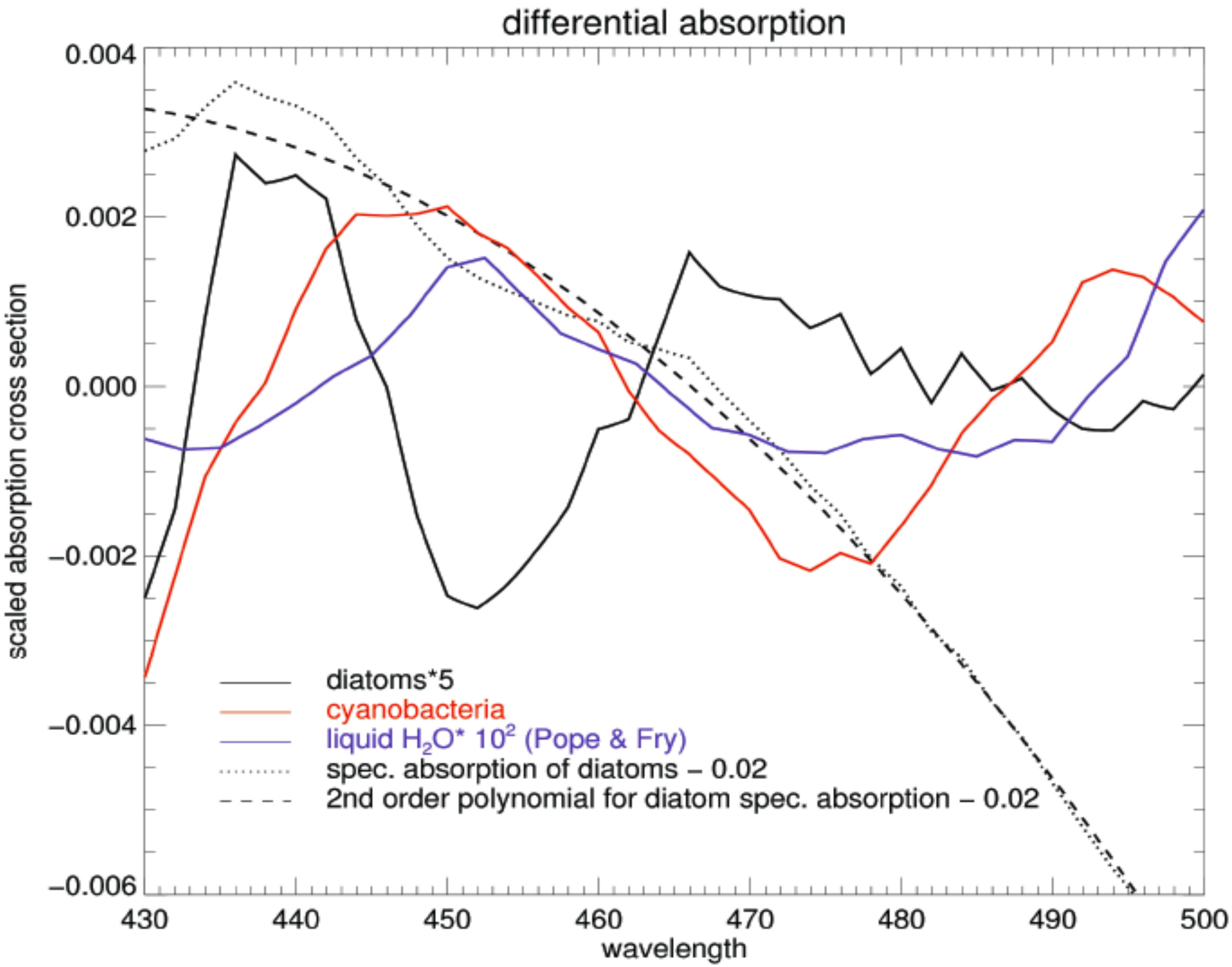

(Bracher et al 2009)

Derivative technique demands hyperspectral measurement.

Method to retrieve hyperspectral phytoplankton absorption is now available.

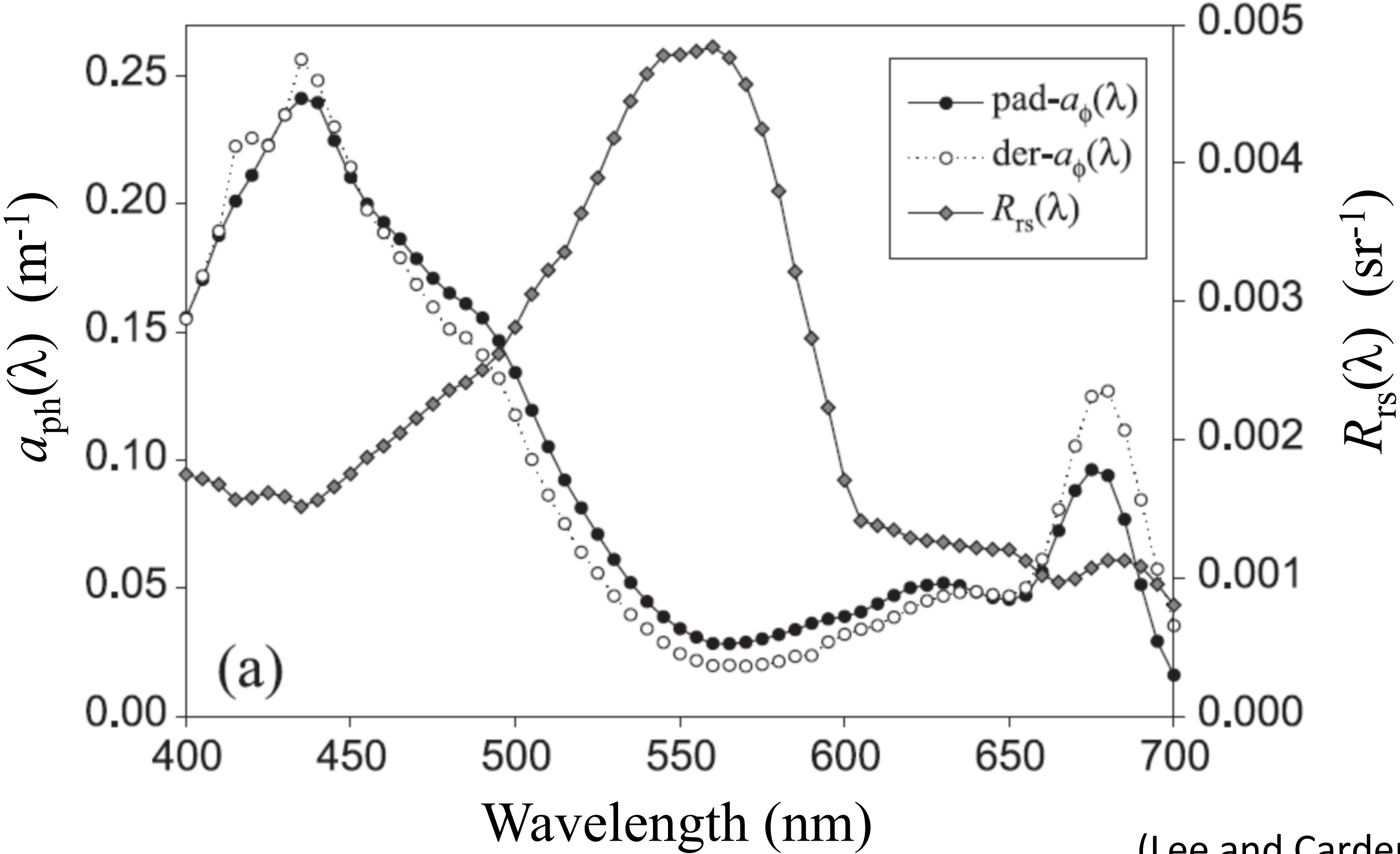

(Lee and Carder 2004)

Name	Spectral bands (VISNIR)	Spatial Resolution (m)	Revisit time (day)
HyspIRI	hyperspectral	60	19

100 m resolution (HICO)

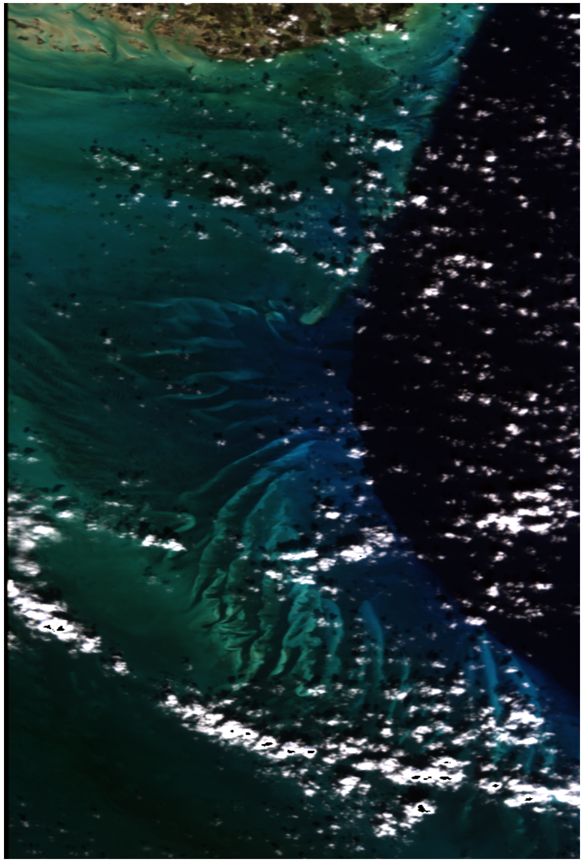

1000 m resolution (MODIS)

High spatial resolution is required to differentiate coastal/near-shore substrates!

Some specs of HyspIRI

Name	Spectral bands (VISNIR)	Spatial Resolution (m)	Revisit time (day)
HyspIRI	hyperspectral	60	19

Is a 19-day temporal resolution making data useful for studying aquatic environment?

aquatic environment

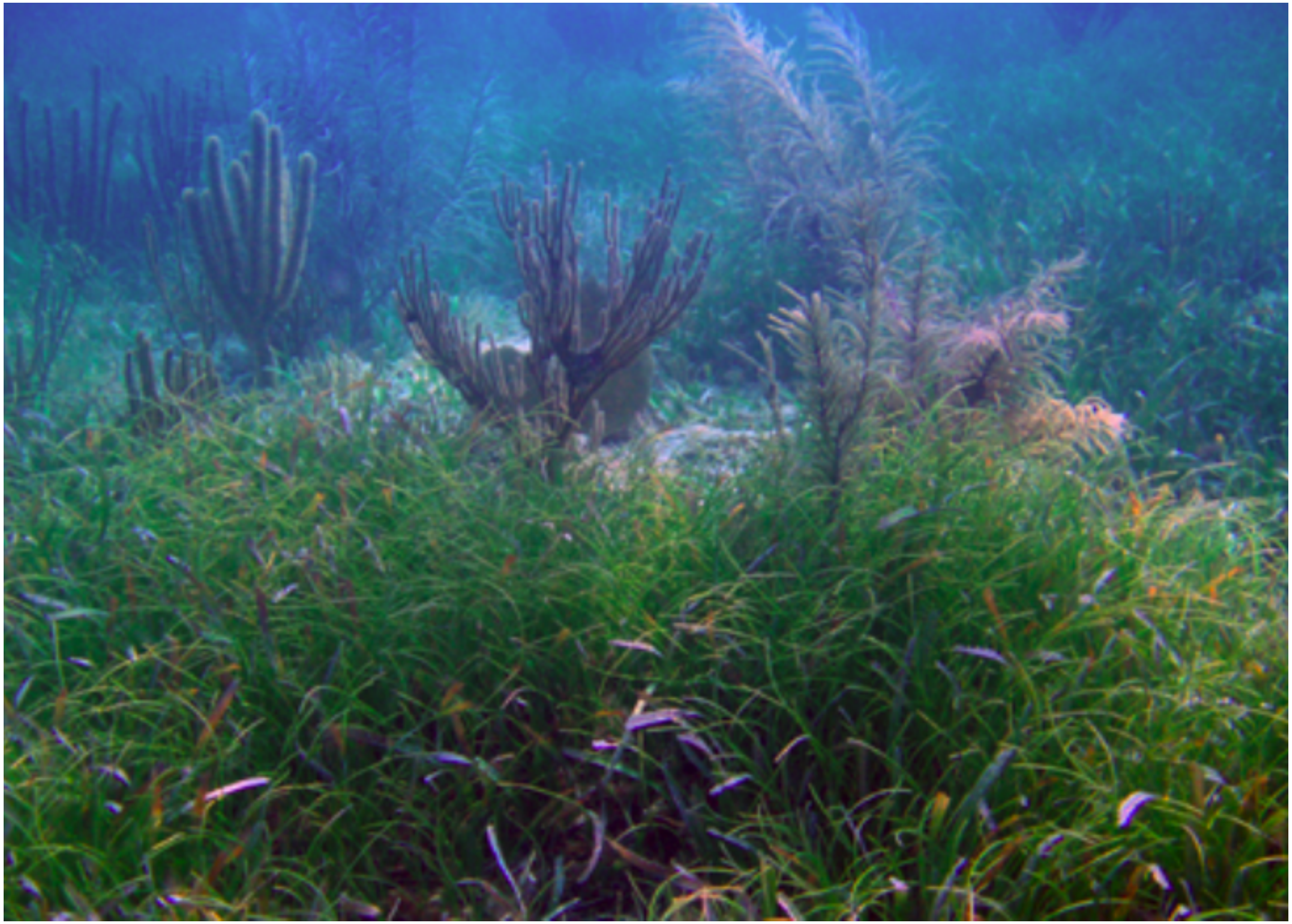

19 day revisit is still good for slowly changing environment.

Science questions:

Table 1: Overarching Thematic Science Questions

Question #	Area	Question	Lead and Co-Lead
VQ1	Pattern and Spatial Distribution of Ecosystems and their Components	What is the global spatial pattern of ecosystem and diversity distributions, and how do ecosystems differ in their composition or biodiversity?	Roberts, Middleton
VQ2	Ecosystem Function, Physiology, and Seasonal Activity	What are the seasonal expressions and cycles for terrestrial and aquatic ecosystems, functional groups, and diagnostic species? How are these being altered by changes in climate, land use, and disturbance?	Gamon
VQ3	Biogeochemical Cycles	How are the biogeochemical cycles that sustain life on Earth being altered/disrupted by natural and human-induced environmental change? How do these changes affect the composition and health of ecosystems, and what are the feedbacks with other components of the Earth system?	Ollinger
VQ4	Changes in and Responses to Disturbance	How are disturbance regimes changing, and how do these changes affect the ecosystem processes that support life on Earth?	Asner, Knox
VQ5	Ecosystem and Human Health	How do changes in ecosystem composition and function affect human health, resource use, and resource management?	Townsend, Glass
VQ6	Earth Surface and Shallow-Water Substrate Composition	What is the land surface soil/rock and shallow-water substrate composition?	Green, Dierssen
TQ1	Volcanoes and Earthquakes	How can we help predict and mitigate earthquake and volcanic hazards through detection of transient thermal	Abrams, Freund

In addition to substrate type …

Do we have adequate database of bottom topography in the littoral zone?

How bottom topography change due to drastic events?

Examples of inadequate topography information:

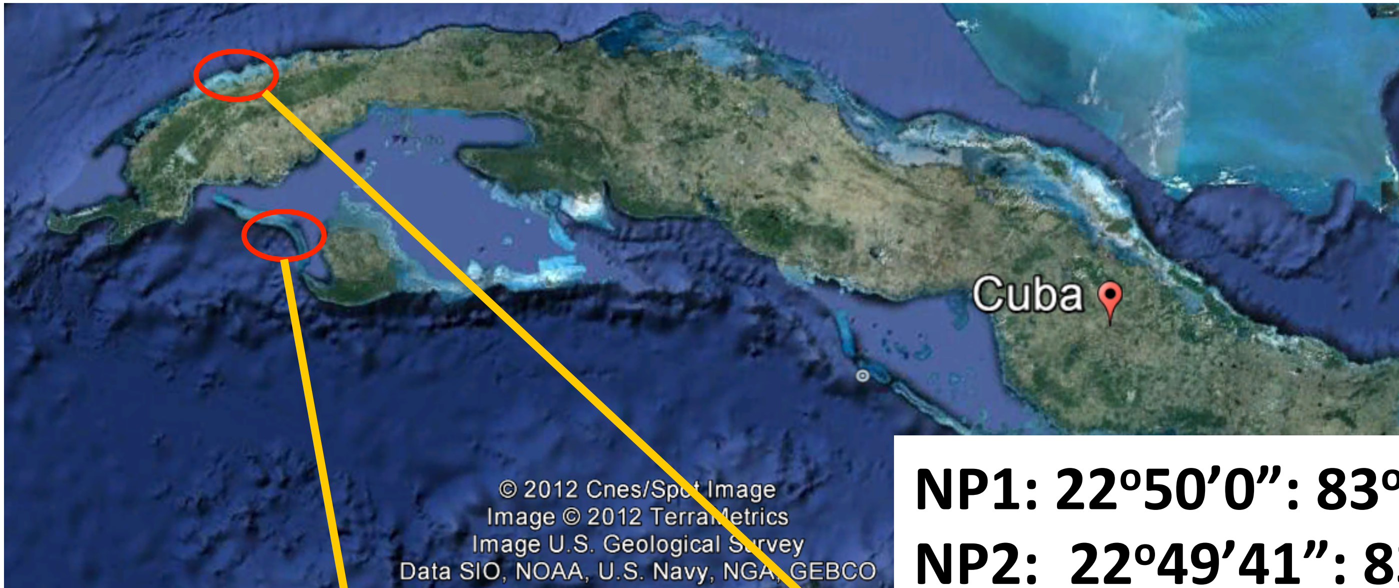

NP1: 22º50'0": 83º49'2"; 120 ft

NP2: 22º49'41": 83º49'23": 58 ft

SP1: 21º47'2": 83º13'37"; 110 ft

SP2: 21º47'6": 83º13'49" 220 ft

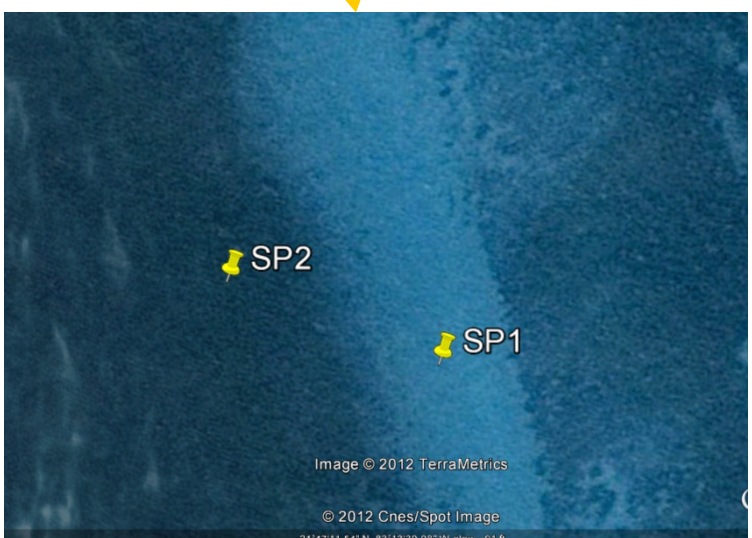

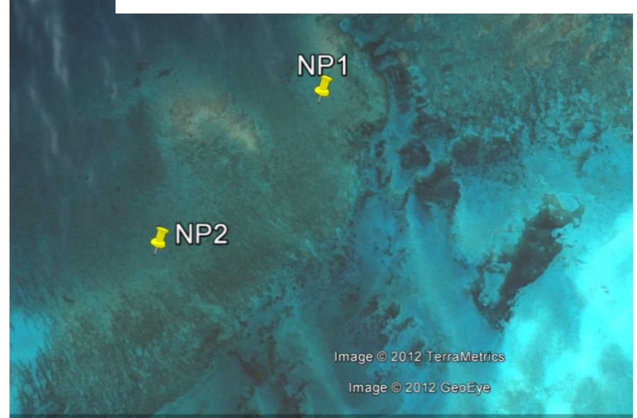

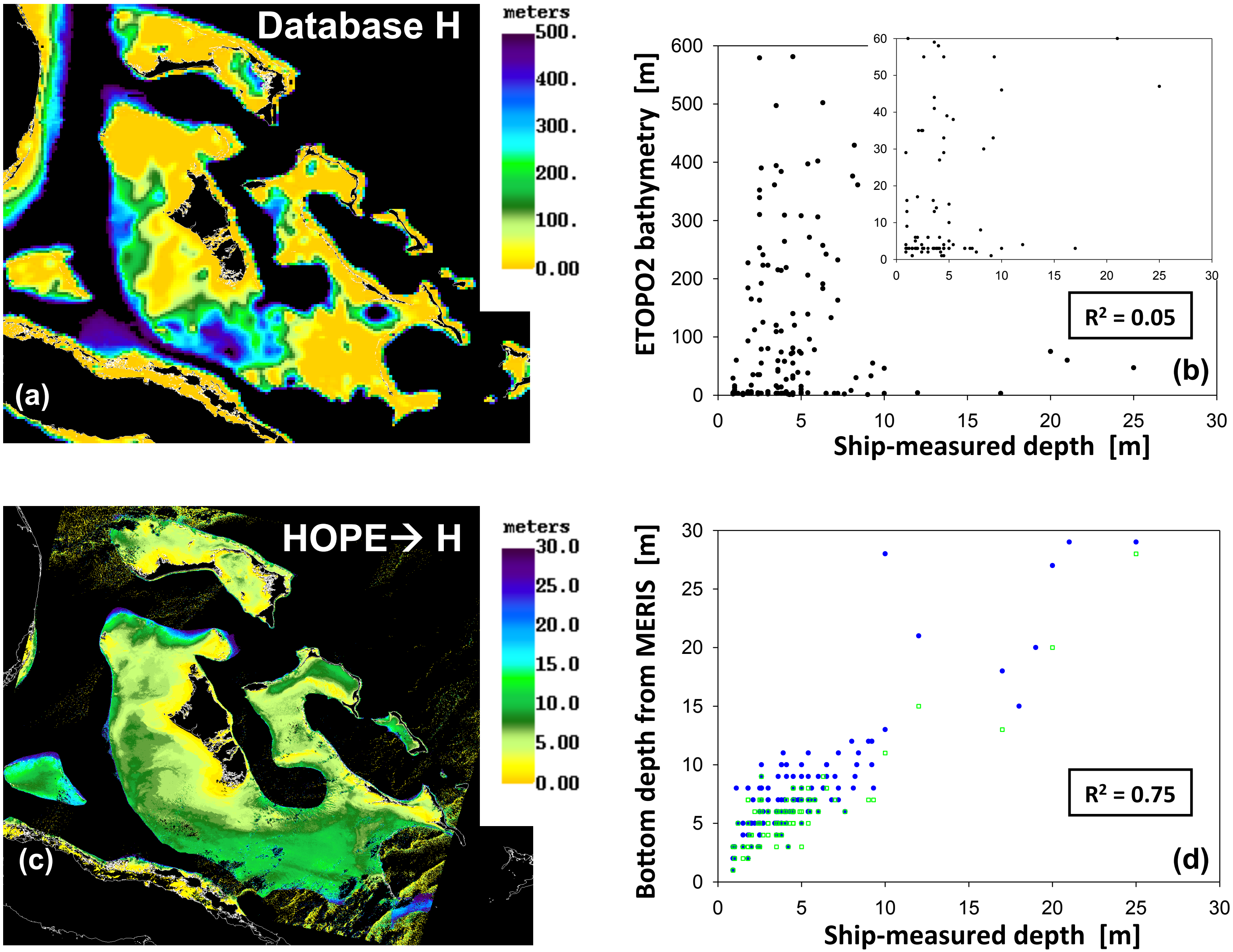

300 m spatial resolution is still very coarse …

(*Lee et al,* 2010, EOS)

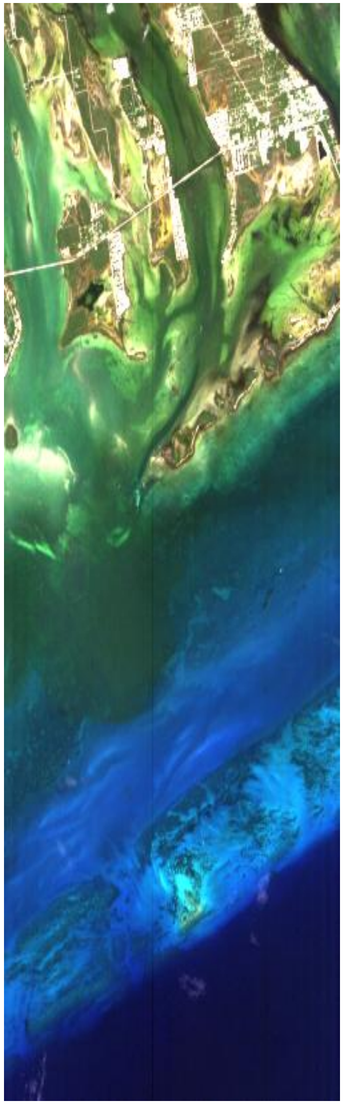

Hyperion image

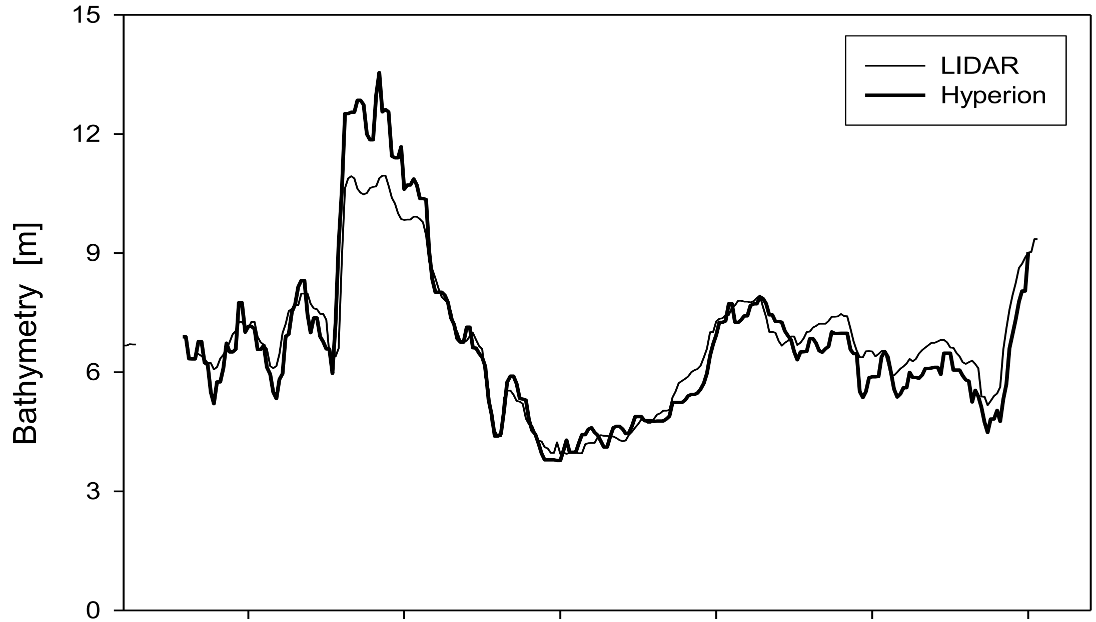

(*Lee et al*. JARS, 2007)

Some specs of ocean-targeting sensors

Name	Spectral bands (VISNIR)	Spatial Resolution (m)	Revisit time (day)
CZCS	4	900	~2
SeaWiFS	6	1100	~2
MODIS	8	250, 500, 1000	~2
MERIS	12	300, 1200	~2
OCM-2	9	360	~2
GEO-CAPE	hyper	375	0.12
ACE	Hyper+Lidar	250?	~xx
HyspIRI	**hyperspectral**	**60**	**19**

Only HyspIRI could resolve fine coastal/littoral zone variations!

Name	Spectral bands (VISNIR)	Spatial Resolution (m)	Revisit time (day)
HyspIRI	**hyperspectral**	**60**	**19**

VSWIR Coverage after 19 days

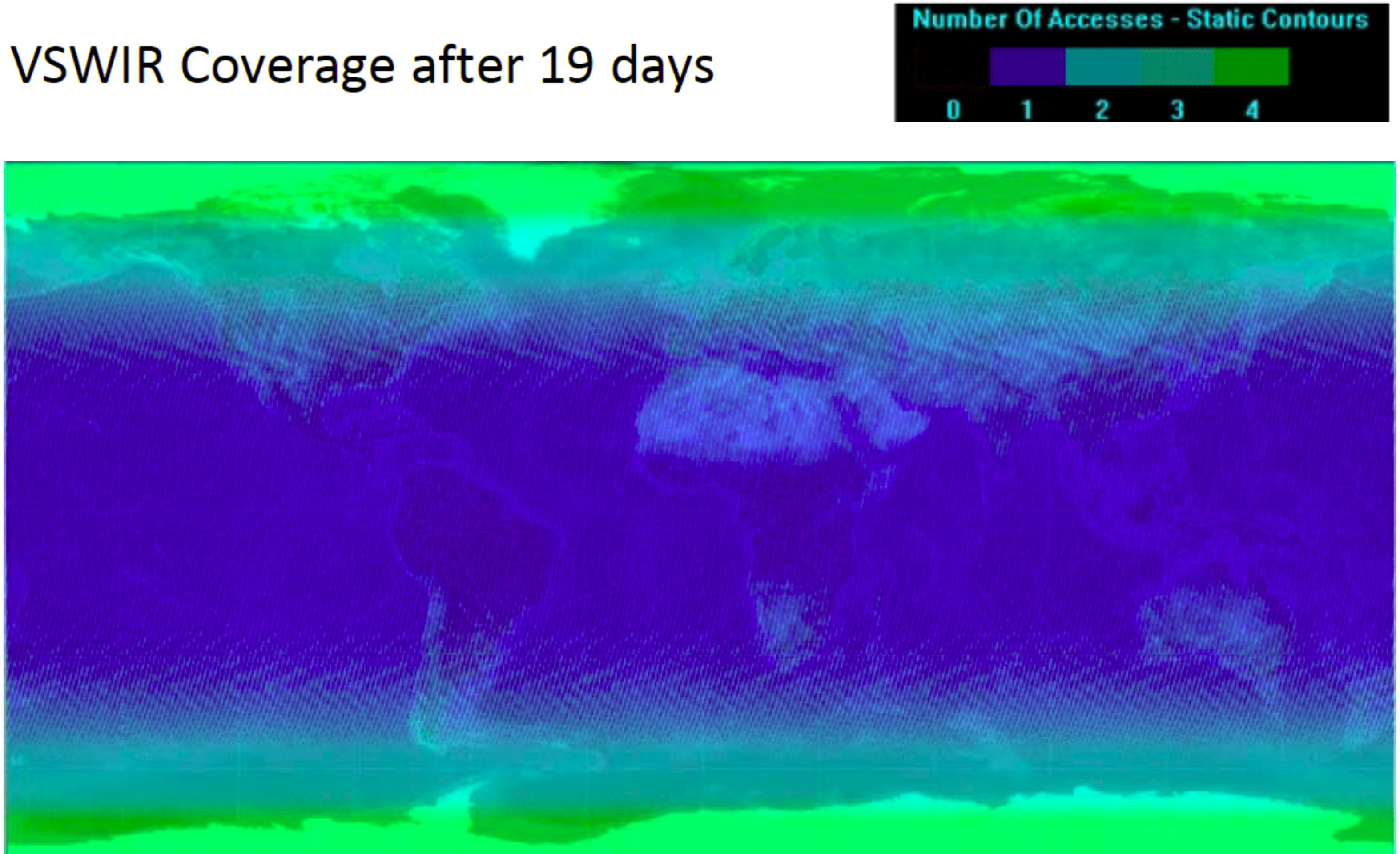

(Mercury 2010)

The current design (150 Km swath) has adequate temporal resolution (~6-7 visits/month) for high-latitude waters.

Temporal NOT an issue!

Importance of high-latitude waters

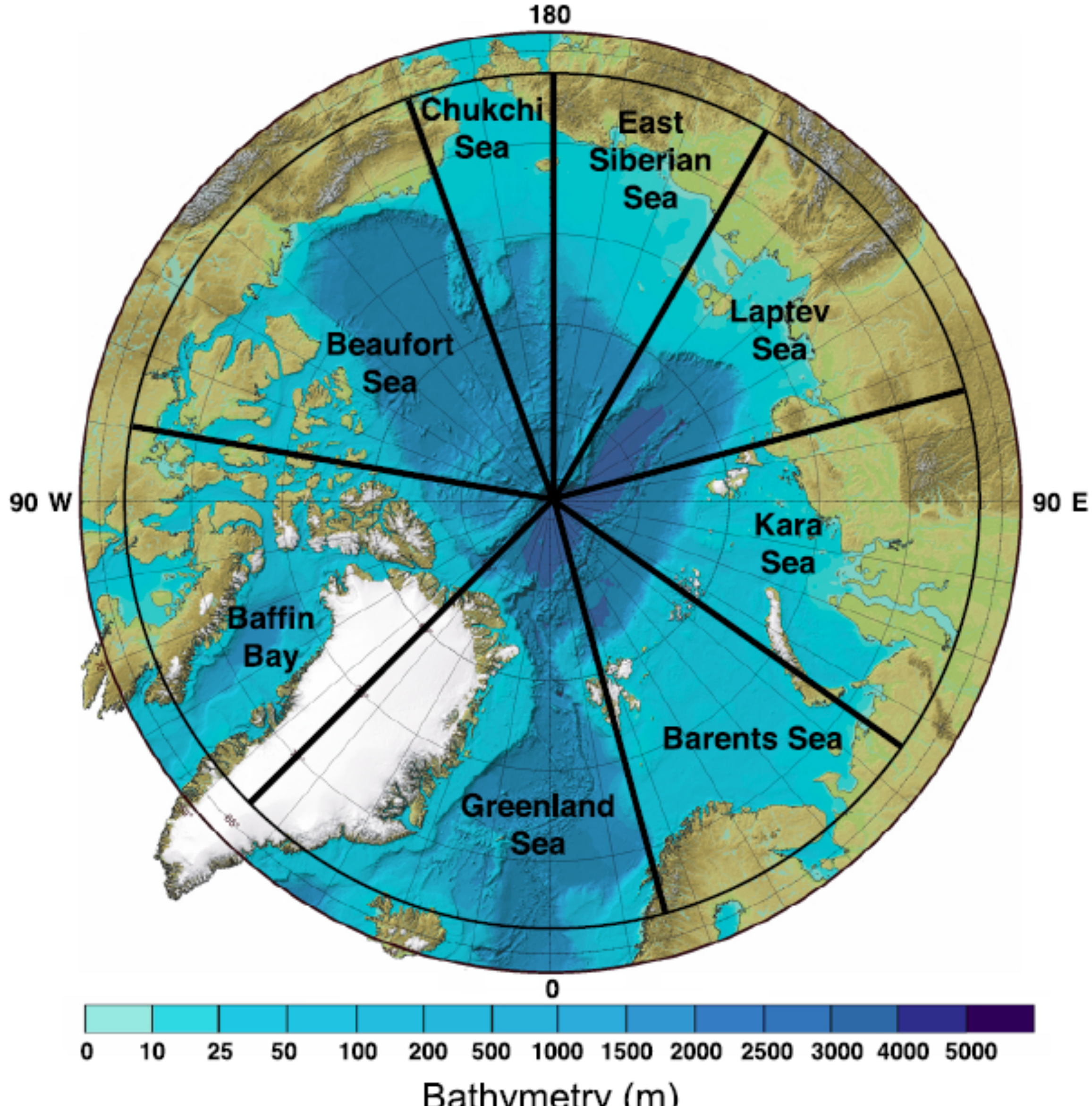

(Arrigo et al 2011)

Change of ice coverage

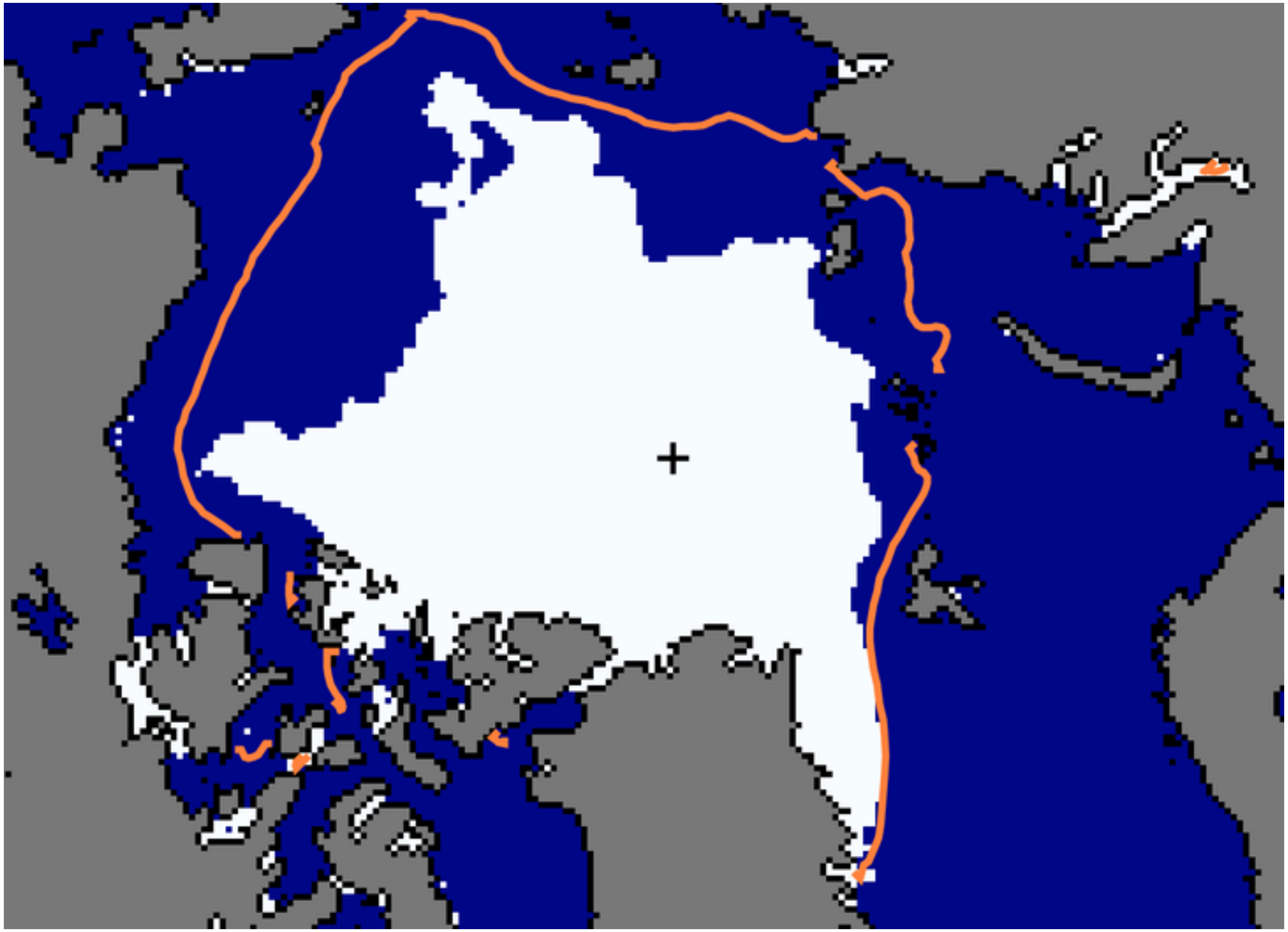

National Snow and Ice Data Center

(Cai et al, Science, 2010)

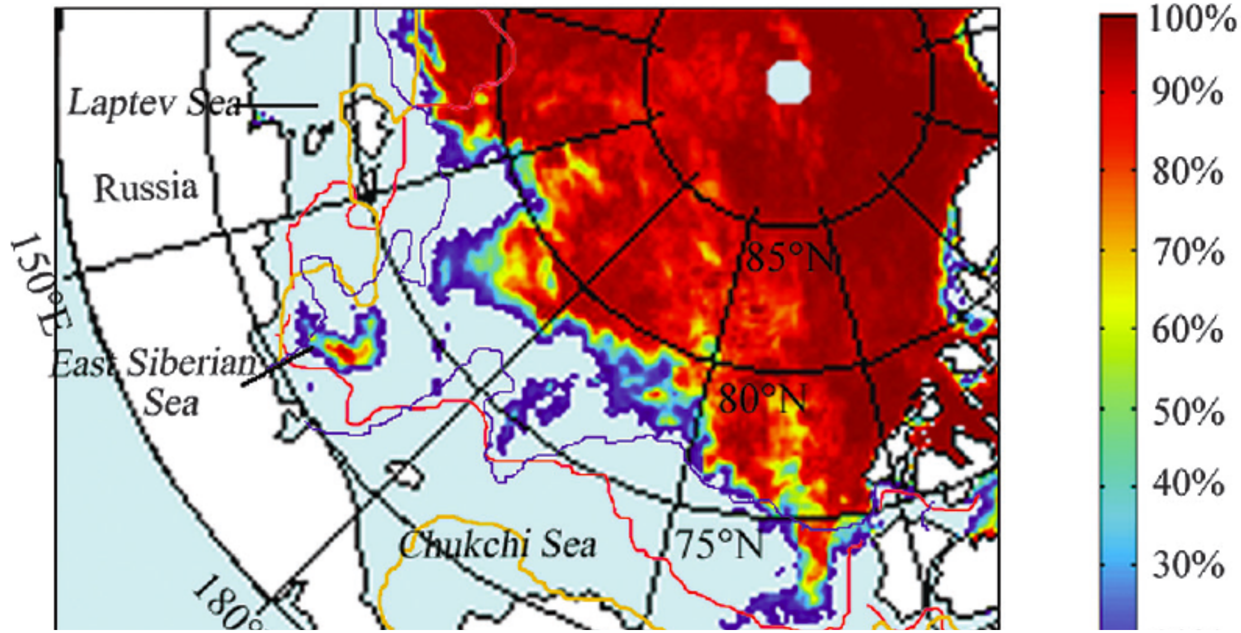

It has been predicted that the Arctic Ocean will sequester much greater amounts of carbon dioxide (CO_2) from the atmosphere as a result of sea ice melt and increasing primary productivity. However, this prediction was made on the basis of observations from either highly productive ocean margins or ice-covered basins before the recent major ice retreat. We report here a high-resolution survey of sea-surface CO_2 concentration across the Canada Basin, showing a great increase relative to earlier observations. Rapid CO_2 invasion from the atmosphere and low biological CO_2 drawdown are the main causes for the higher CO_2, which also acts as a barrier to further CO_2 invasion. Contrary to the current view, we predict that the Arctic Ocean basin will not become a large atmospheric CO_2 sink under ice-free conditions.

Conflicting views of the role of Arctic waters in the carbon cycle.

Sample science questions to waters in this “new frontier”:

Spatial distribution and temporal variations of phytoplankton?

Diversity of phytoplankton?

Messenger of climate change?

Contribution to the carbon cycle?

Need long term, large scale, observations: remote sensing!

Issues of sensing high-latitude waters with current ocean-color sensors:

1. software:
algorithm

Low/no high-latitude waters;
Large deviation from the regression line.

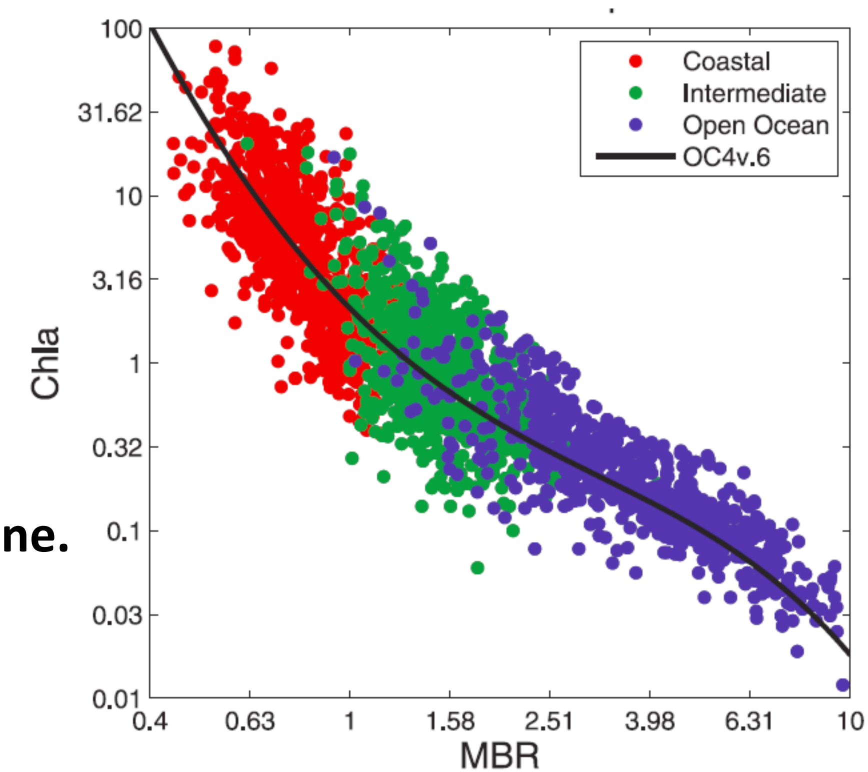

(Szeto et al 2011)

2. hardware:
spatial resolution

Only HyspIRI could resolve fine-scale variations!

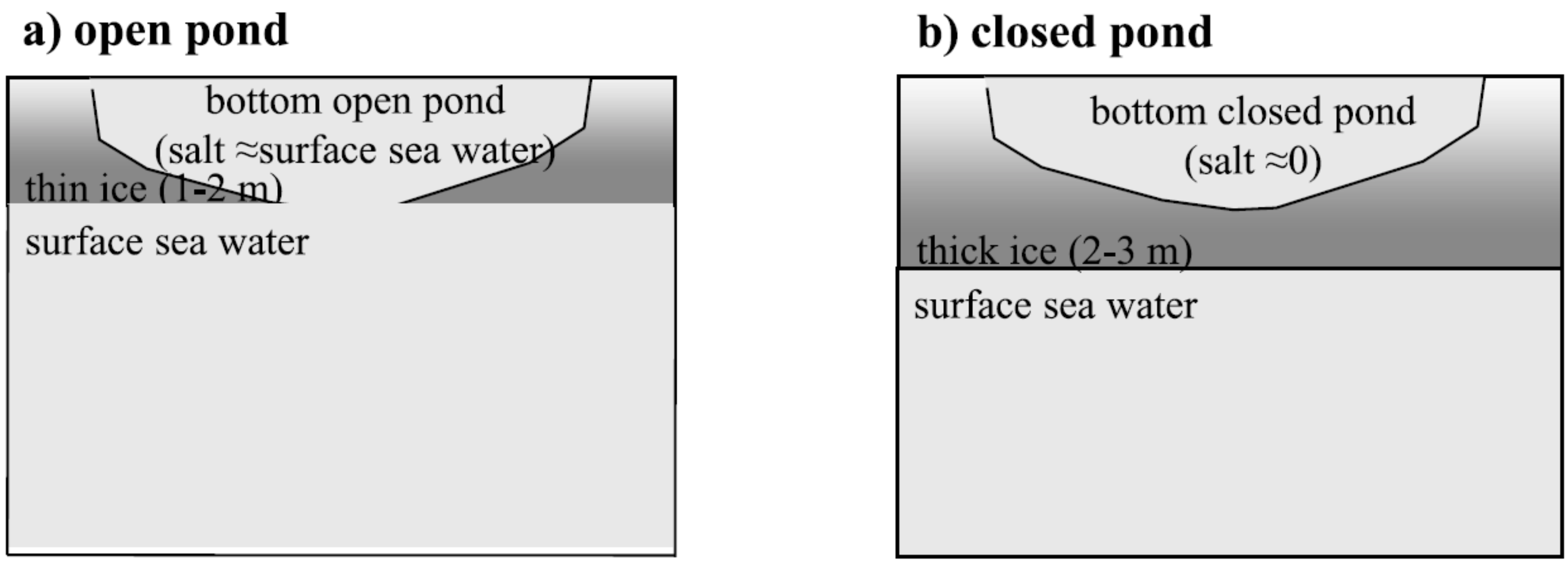

(Lee et al 2012)

Past and current ocean-color sensors are unable to sense water constituents in these "new" waters!

Requires a sensor like HyspIRI!

Summary:

The high-spatial resolution and hyperspectral sampling make HyspIRI

1. unique for near-shore/littoral zone
2. unique for high-latitude waters:
   aquatic environment of "new" frontier.

A tentative list of products for aquatic environment:

Shallow Bottom:

- Bathymetry
- Type of substrates (and status)

Water Column:

- Phytoplankton (Chl, functional types)
- Colored Dissolved Organic Matter (DOC)
- Suspended Particles (POC, Sediments)

Does it have enough SNR?

Thank you!

Prototyping Science As A Service with **Intelligent Payload Module**

Daniel Mandl - NASA\GSFC

May 17, 2012

Team

Daniel Mandl – NASA/GSFC - lead
Robert Sohlberg – Univ. of Maryland/Dept. of Geography – SensorWeb scientist
Pat Cappelaere – Vightel Corporation – SensorWeb architecture
Stuart Frye – NASA/GSFC – SGT Inc. – systems engineer
Vuong Ly – NASA/GSFC – system engineer, software developer
Matthew Handy – NASA/GSFC – software developer
Donald Sullivan – NASA/Ames – flight SW, ground SW for AMES based airborne flights
Geoff Bland – NASA/WFF – Cessna flights
Enric Pastor – Univ. of Cataluña, Barcelona, Spain – UAV Helicopter
Vince Ambrosia - NASA/Ames – AMS instrument, B200/B100 flights, Ikhana
Steve Crago – ISI – Univ. of Southern Cal/ISI – Maestro onboard computer arch
Steve Chien – NASA/JPL – onboard algorithms
Tawanda Jacobs – NASA/GSFC – flight SW
Tim Creech – Univ. of Maryland – NASA Science and Technology Research Fellow
Chris Flatley – NASA/GSFC summer intern
Neil Shaw – NASA/GSFC summer intern
Joshua Bronston – NASA/GSFC co-op

Objectives

- Develop methods to provide low latency users of HyspIRI with quick look data products
- Augment concept of Science As A Service by providing an interface for non-programmer users to define new algorithms and select data sets and data feeds to run the algorithms against
- Virtualize the interface to various environments with adapters that take into account the resources and methods to expose key data and data products
- Experiment with high performance multicore space computing architectures in order to meet the future significantly higher data rates.
- Develop increasingly realistic operational architectures that emulate the target satellite architecture for HyspIRI and other Decadal missions

Funding for IPM Effort

ESTO AIST-11 Award beginning May 2011

"A High Performance Onboard Multicore Intelligent Payload Module for Orbital and Suborbital Remote Sensing Missions"

GSFC IRAD FY 12:

"Optimization of Onboard Processing Using the Maestro Multicore Processor for Decadal Missions" (Stepping stone to AIST award)

Original HyspIRI Low Latency Data Flow Operations Concept

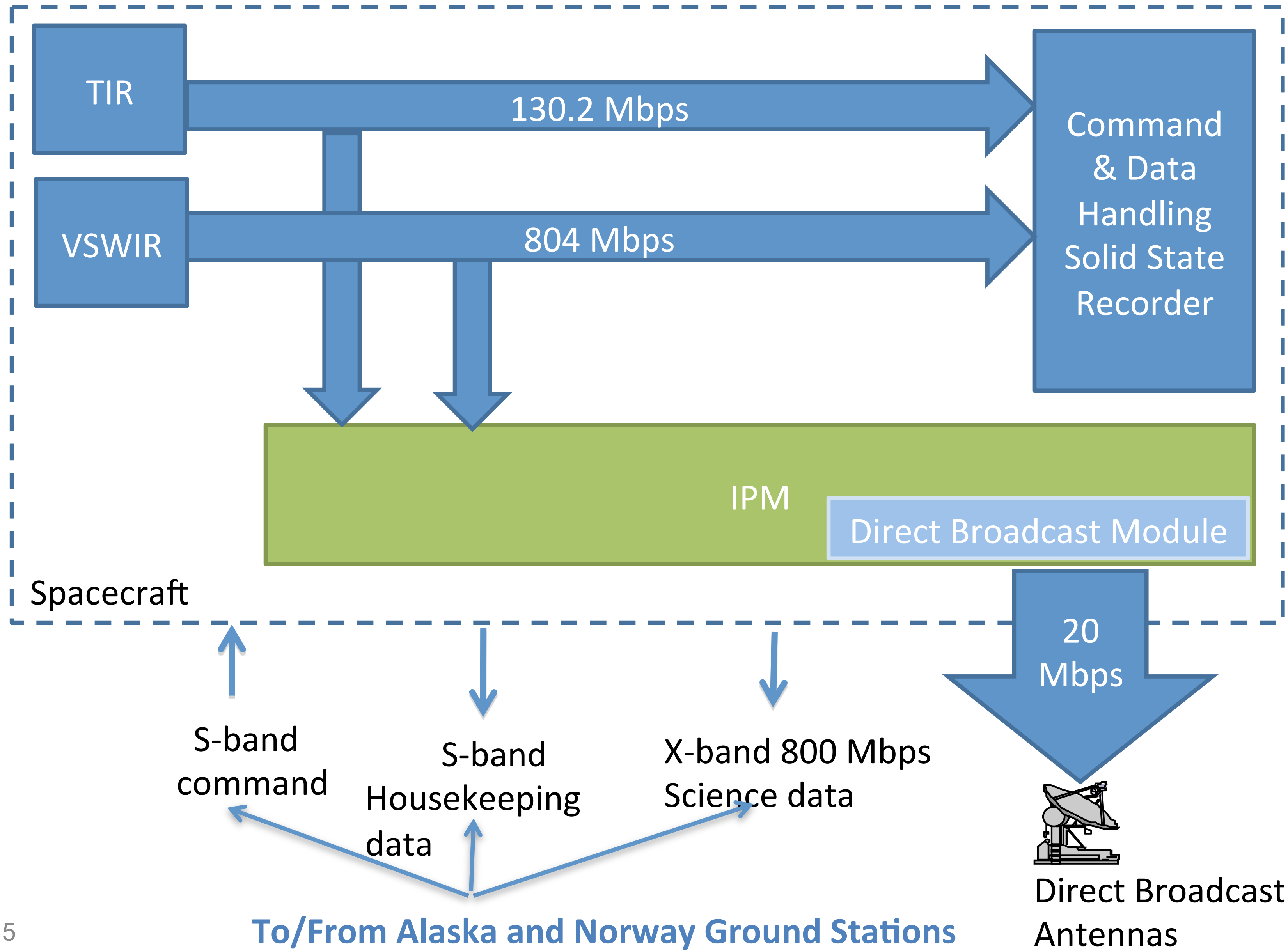

5

Experimental IPM Quick Load/Quick Look Ops Con

Enhanced Ops Con from Baseline IPM Ops Con

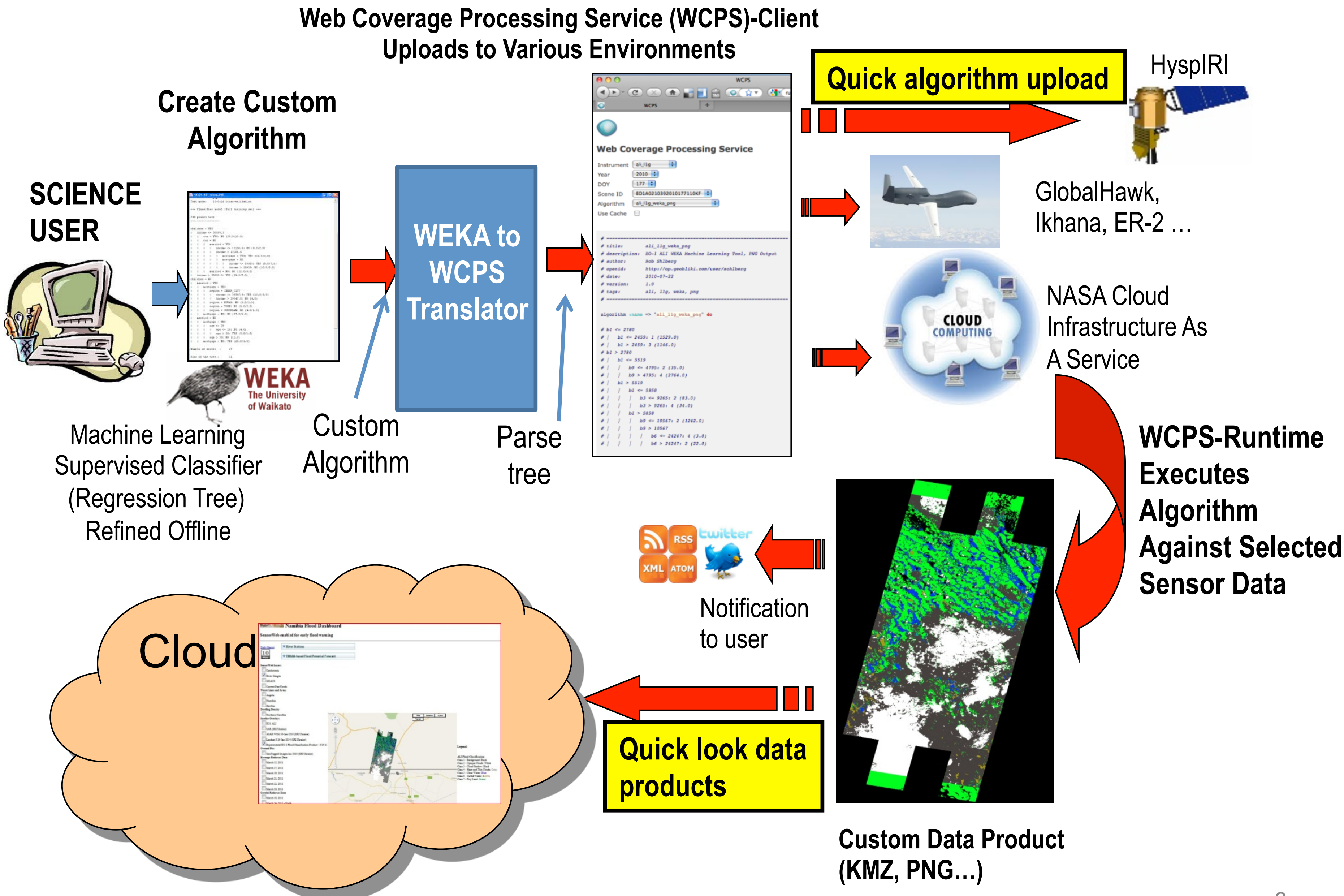

Roadmap for IPM Flight Opportunities

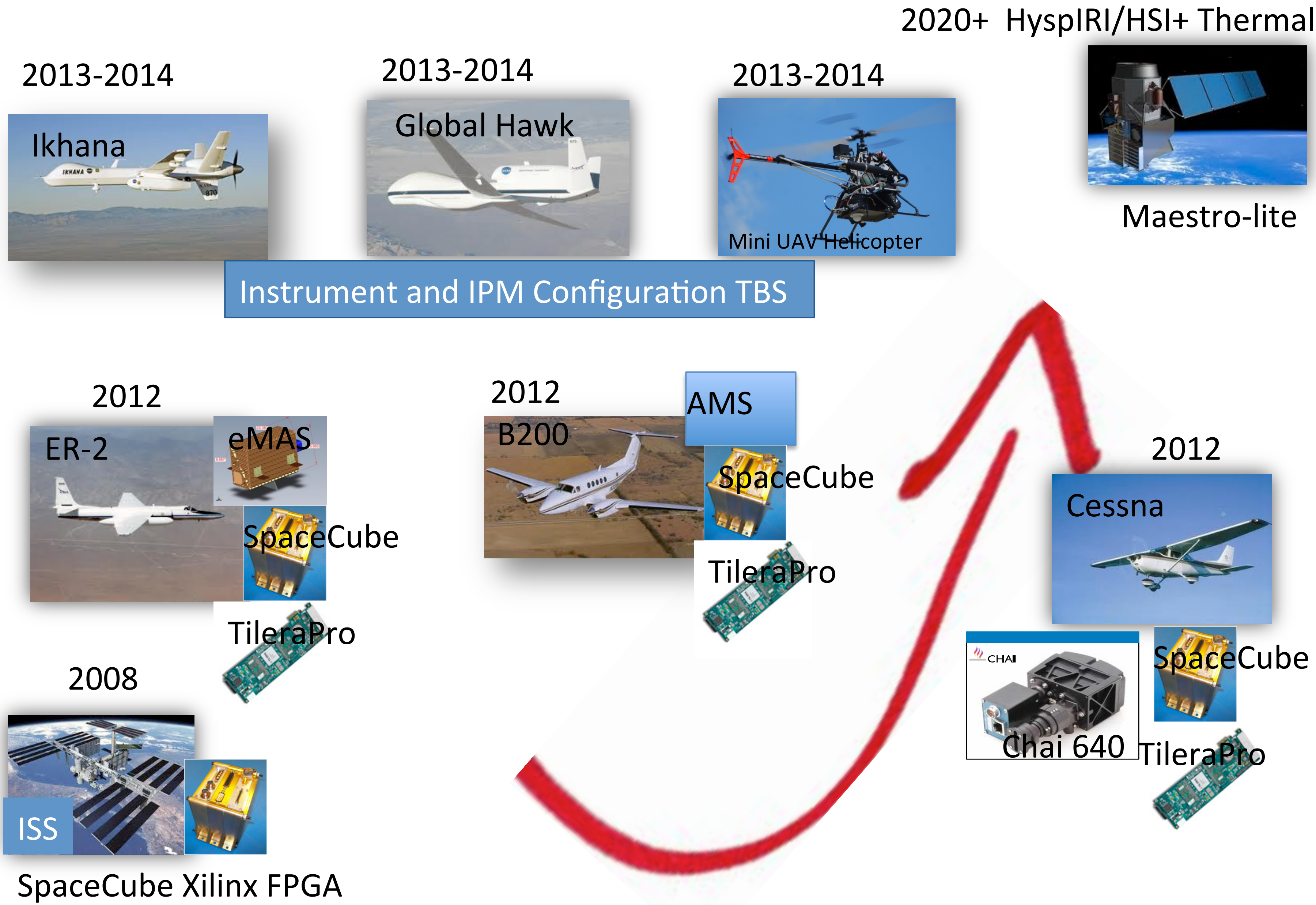

IPM Tilera Flight Testbed Ops Con
(Tilera board is proxy for Maestro and Maestro-lite)

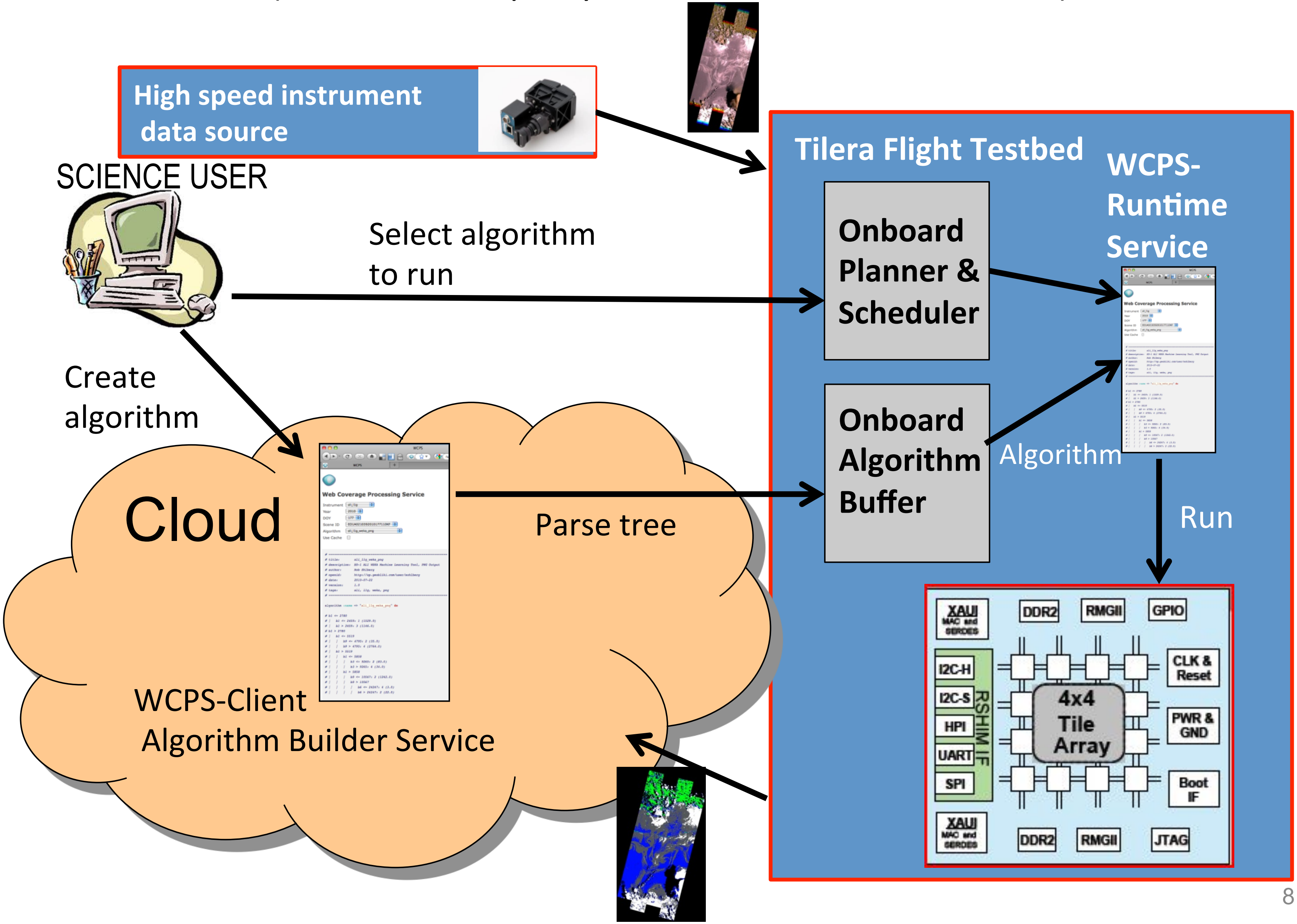

Chai640 Specs

Compact Hyperspectral Advanced Imager UV-VNIR

CHAI V-640

Compact and economical; ideal for UAV and field use.

BRANDYWINE PHOTONICS

CHAI V-640 Instrument* (prototype shown)

The CHAI V-640 is the instrument of choice for applications requiring a compact, low-cost, and high-performance hyperspectral imager. The V-640 integrates the most up-to-date Science CMOS image sensors with a powerful Offner spectrometer to achieve excellent image quality with high sensitivity. The V-640 form factor is suitable for multi-unit arrangements, including side-by-side, fore- and aft- viewing angles, and varying polarizations.

APPLICATIONS

Earth Science, Aerial Survey, Machine Vision, Medical Imaging, Microscopy

ADVANTAGES

High Sensitivity, Lower Cost, Compact, Low Power

MECHANICALS	ESTIMATE
Minimum Size	127 x 101 x 51 mm
Weight	1 kg sensor head 2 kg controller
Power	40 watts
Temperature Range	-20 to +50 C

Size does not include laptop, processor or INS.

OPTICS	SPECIFICATION
Spectrometer Type	Offner
Field of View	40 degrees (other upon request)
Cross Track Pixels	640 (with BIN x3)
F-Number	f/2.8
Data Rate	78 Mbps
Spectral Range	380-1000 nm
Smile	<0.1 pixels
Keystone	<0.1 pixels
Stray Light	<1e-4 Point Source Transmission
Spectral Bands	256
Spectral Sampling	2.5, 5, 10 nm
Peak Grating Efficiency	88%
Slit Size	9.6 x .015 mm
IMAGE SENSOR	
Image Sensor	1920 x 1080, 6.5 μm pixels
Well Depth	30,000 electrons
Read Noise	2 electrons
Maximum Frame Rate	60 frames/second
Quantum Efficiency	22% at 400 nm Peak 57% at 600 nm 15% at 900 nm
Camera Interface	CameraLink
Data Acquisition	500 MB Solid State Recorder Serial Interface for GPS/INS
CHAI SOFTWARE	
Trigger Modes	Pilot, GUI, electronic, and Lat/Long triggered acquisition
Visualization	3-band RGB waterfall display of real-time and recorded data
Metadata	Temperature, pressure, and humidity
Data Format	RAW, ENVI BIL, or Processed
Processing	EXPRESSO™

* *Final product may differ from image shown.*

Contact John Fisher | jfisher@brandywinephotonics.com | +1 (484) 459-9589 | www.brandywinephotonics.com

IPM Testbed with Tilera Acting as Proxy for Maestro & Maestro-lite Board (building 23)

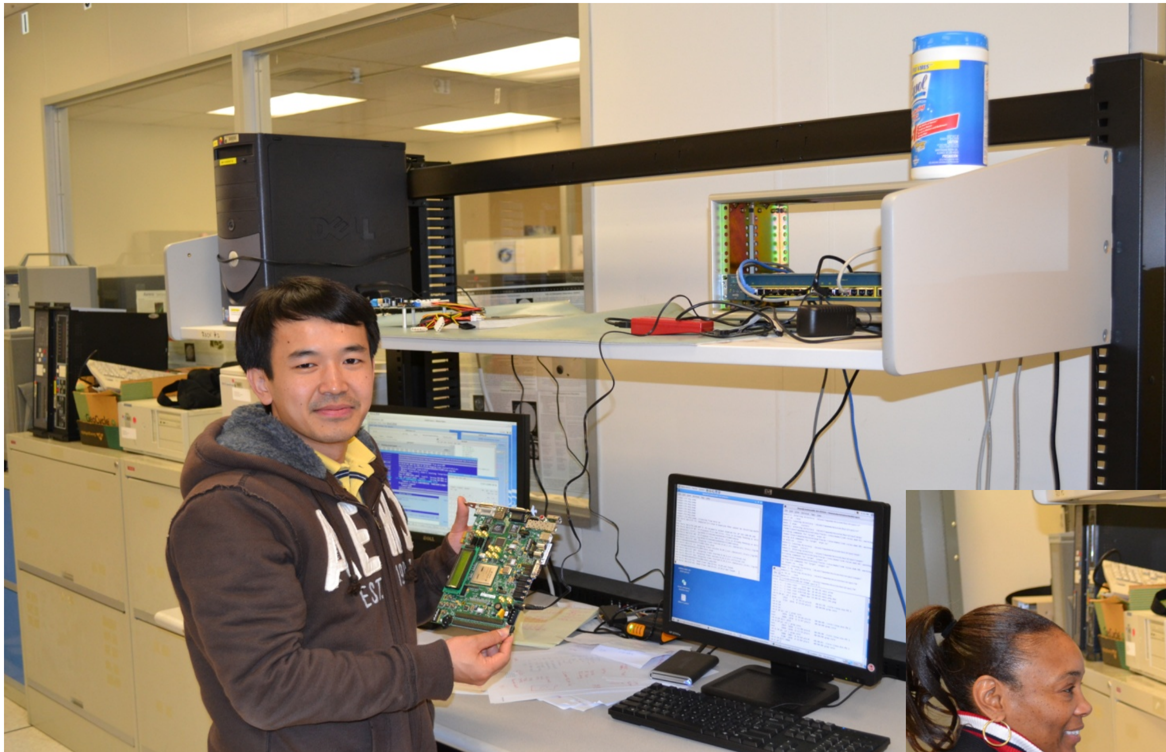

Above: Vuong Ly/583 (Ground System SW Branch) standing in front of IPM testbed holding a SpaceCube board.
Right: Tawanda Jacobs/582 (Flight SW Branch) working on integration of cFE onto IPM testbed.

First Flight Opportunity Summer 2012

- Use Skycomp helicopter originating out Clarksville Maryland
- Land at GSFC
- Mount IPM
- Test on ground
- Test at various altitudes

Hayesfield Airstrip in Clarksville, Md.

Target Hybrid Architecture

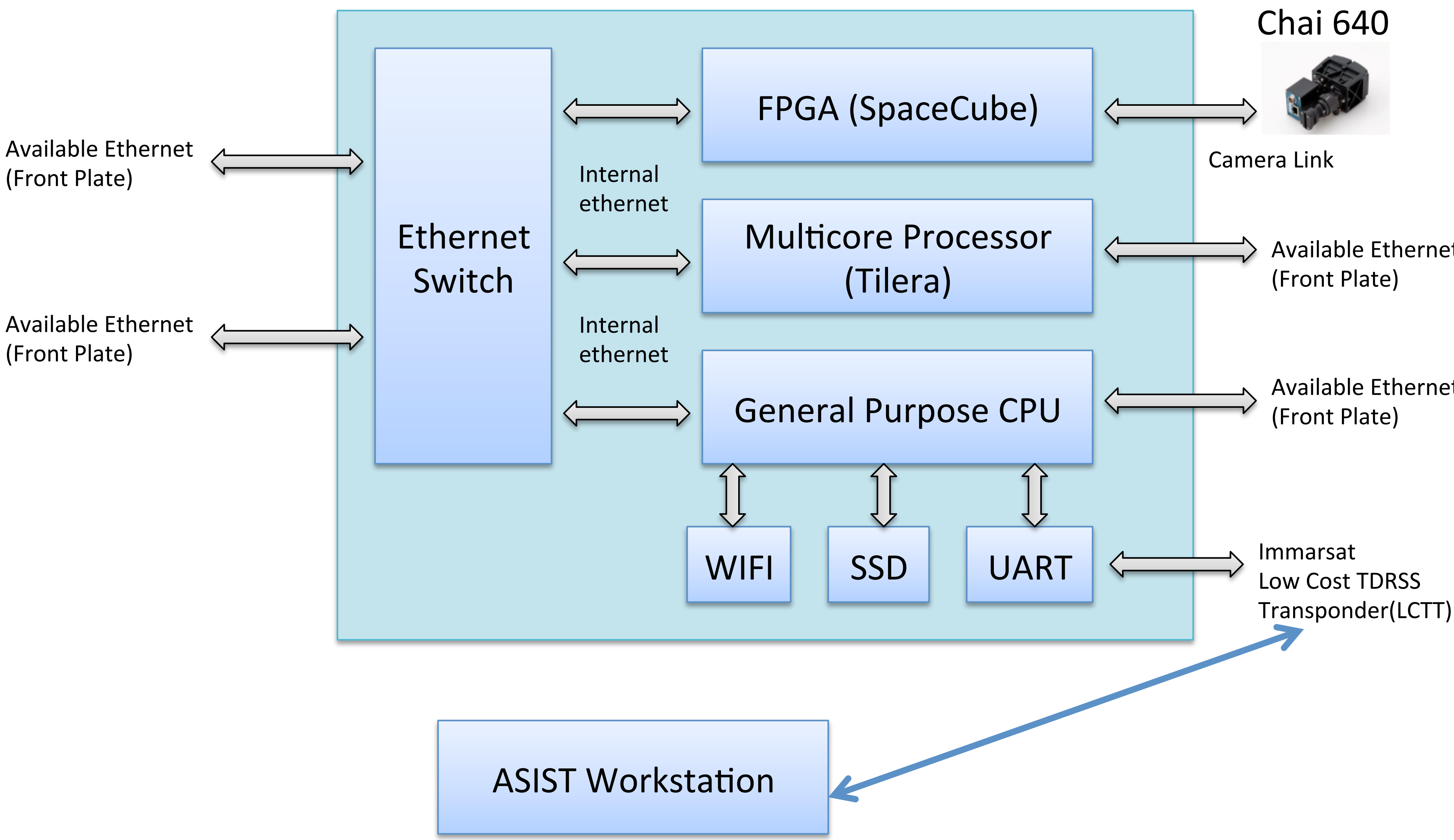

Preliminary Flight Architecture

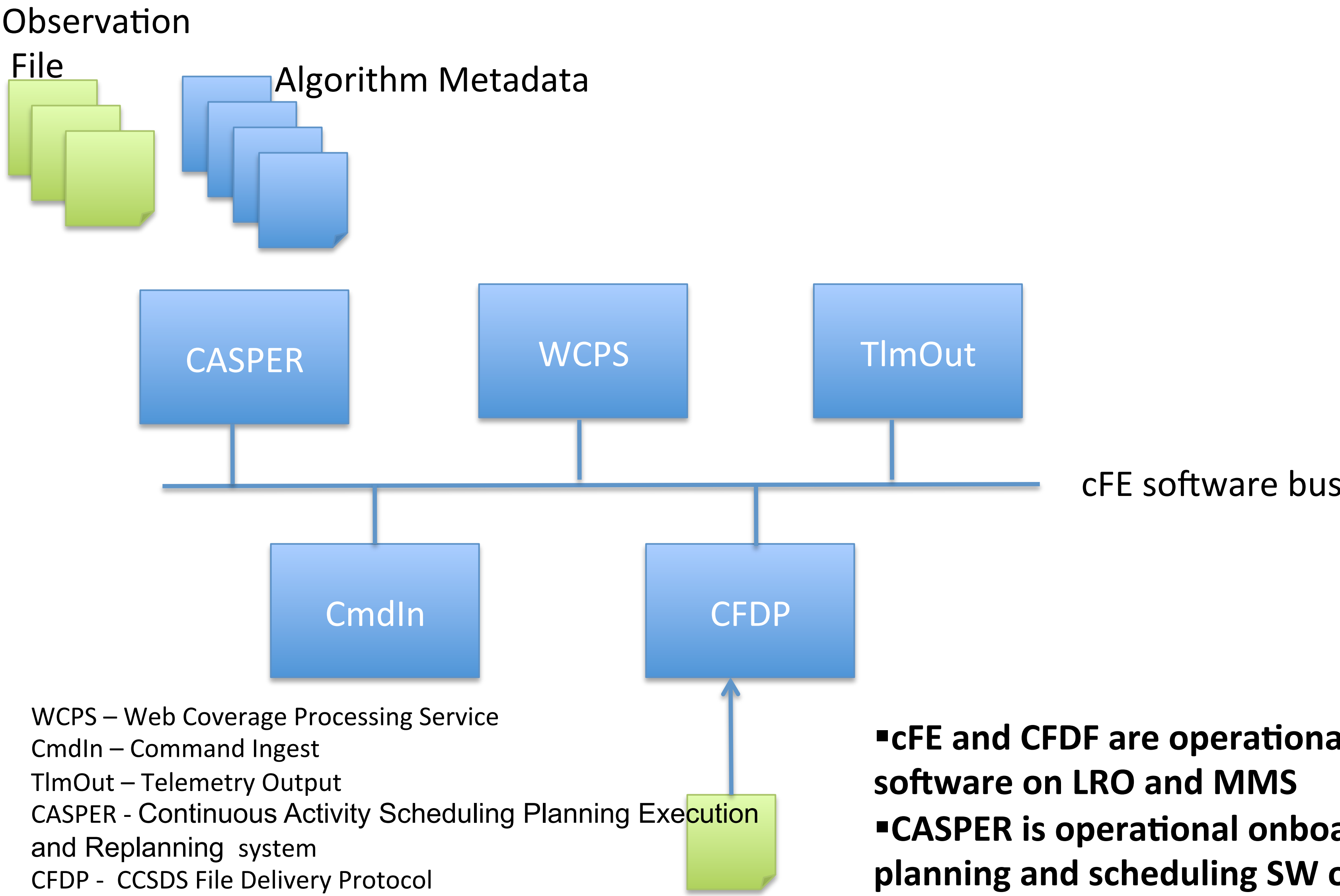

WCPS – Web Coverage Processing Service
CmdIn – Command Ingest
TlmOut – Telemetry Output
CASPER - Continuous Activity Scheduling Planning Execution and Replanning system
CFDP - CCSDS File Delivery Protocol
cFE- Core Flight Executive

- **cFE and CFDF are operational flight software on LRO and MMS**
- **CASPER is operational onboard planning and scheduling SW on EO-1**
- **WCPS is presently TRL 6**

Benchmarks for Use of Parallelization

- Tim Creech, Univ. of Maryland, Phd student
  - NASA Science and Technology Research Fellowship (NSTRF) 3 year grant awardee
- Investigating methods to automatically transform algorithms into parallel processes that can be applied to multicore architectures
  - AESOP is software research area
  - Used algorithms running against EO-1 ALI data on Tilera testbed
- Working towards integrating automatic parallelization into WCPS

AESOP Parallelization Test Results (1 of 2)

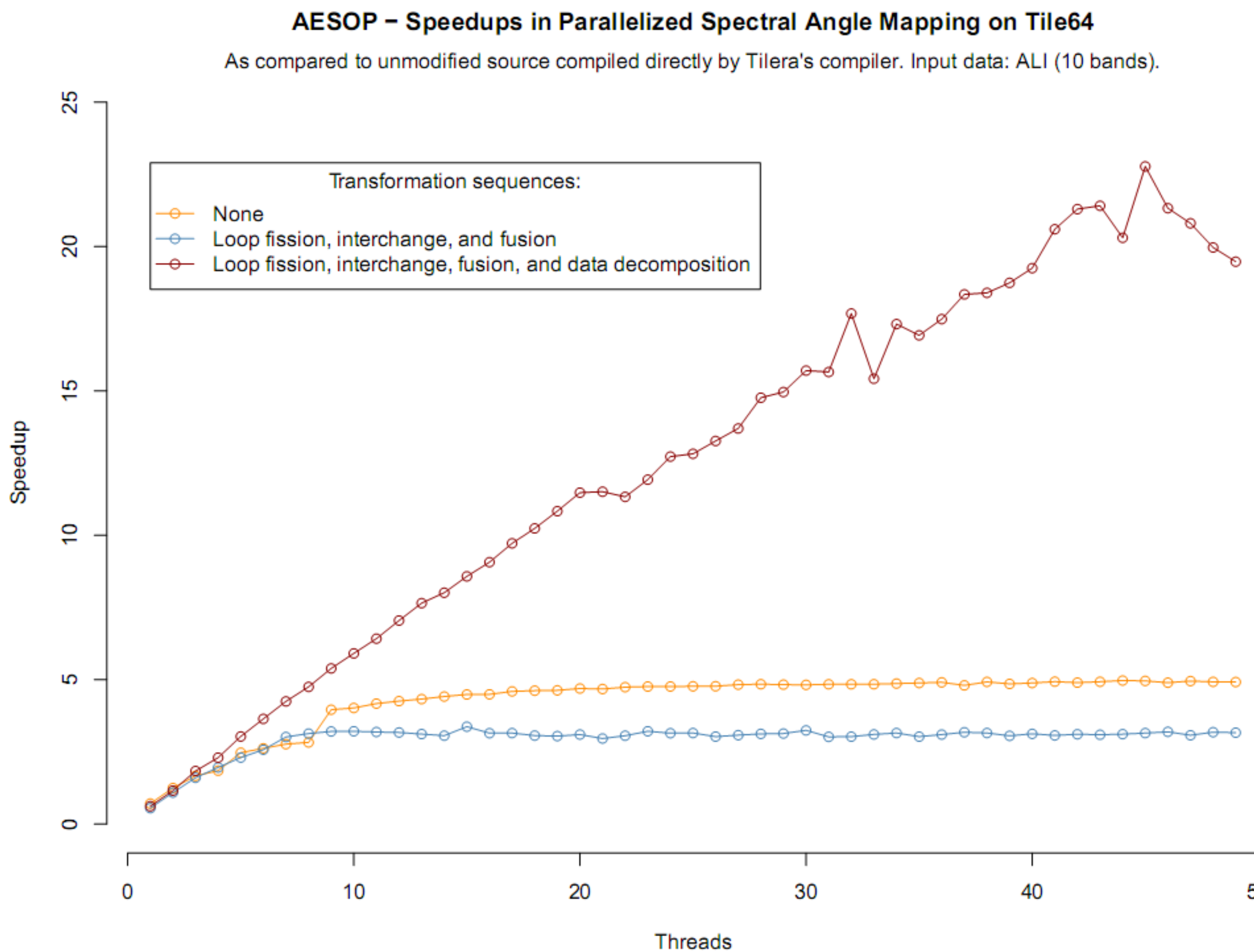

AESOP Parallelization Test Results (2 of 2)

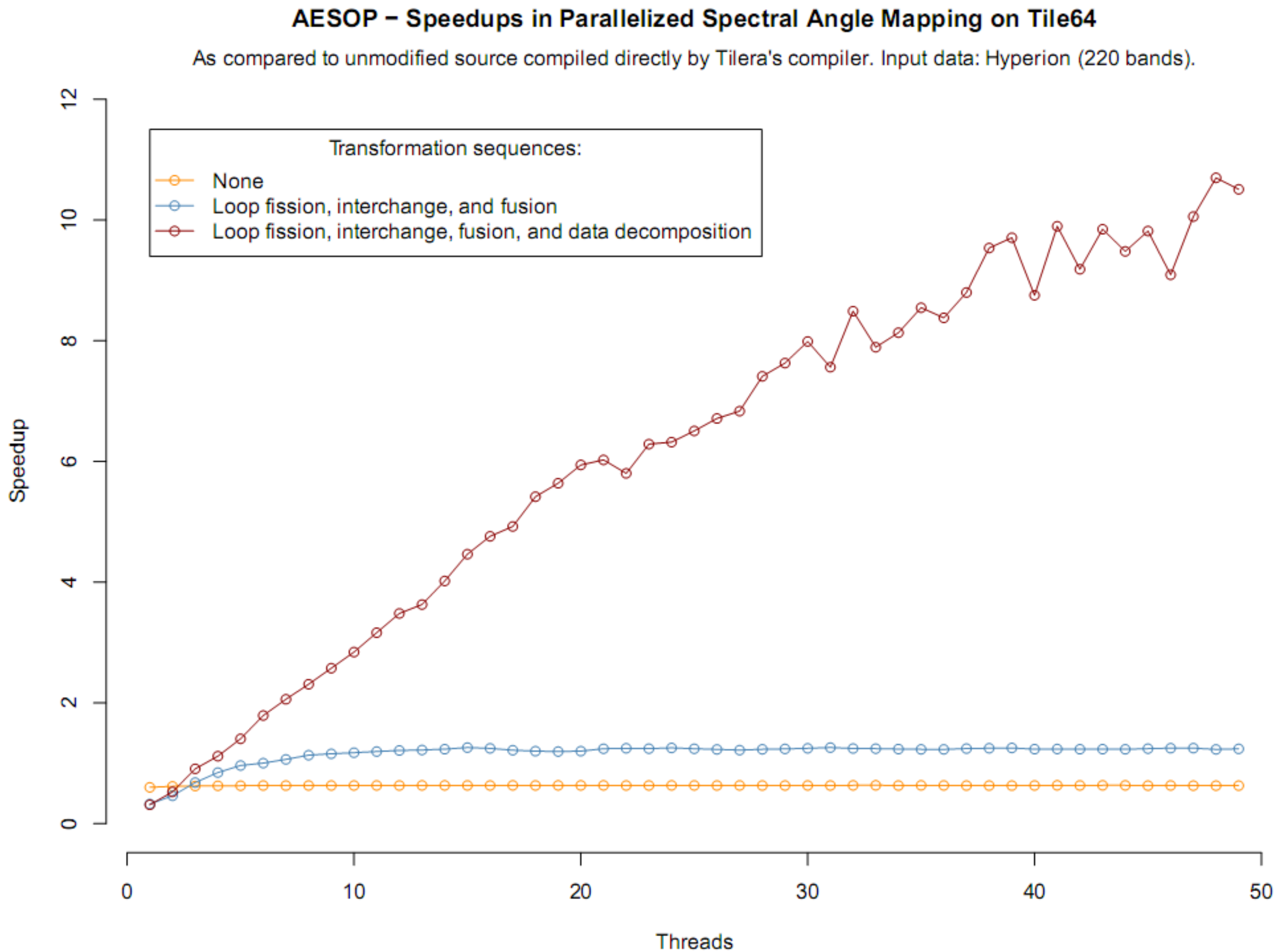

Conclusion

- Develop methods to provide low latency users of HyspIRI with quick look data products
  - Showed efforts with Maestro/Tilera, SpaceCube, WCPS
- Augment concept of Science As A Service by providing infrastructure, interfaces and services for non-programmer users to define new algorithms and select data sets and data feeds to run the algorithms against selected data
  - Showed WCPS client to build algorithms in realtime and WCPS runtime to use as adapters in various environments to enable algorithms to run against selected data
- Virtualize the interface to various environments with adapters that take into account the resources and methods to expose key data and data products
  - - Showed WCPS runtime
- Experiment with high performance multicore space computing architectures in order to meet the future significantly higher data rates.
  - - Showed a little of benchmarking to see how much performance can be enhanced with a multicore space computing architecture while designing in low power

Prototyping Science As A Service with **Cloud Data Distribution and Tools**

Daniel Mandl - NASA\GSFC
May 17, 2012

Team

Daniel Mandl – NASA/GSFC - lead

Robert Sohlberg – Univ. of Maryland/Dept. of Geography – SensorWeb scientist

Pat Cappelaere – Vightel Corporation – SensorWeb architecture

Stuart Frye – NASA/GSFC – SGT Inc. – systems engineer

Vuong Ly – NASA/GSFC – system engineer, software developer

Matthew Handy – NASA/GSFC – software developer

Steve Chien – NASA/JPL – algorithms

Tim Creech – Univ. of Maryland – NASA Science and Technology Research Fellow

Chris Flatley – NASA/GSFC summer intern

Neil Shaw – NASA/GSFC summer intern

Joshua Bronston – NASA/GSFC co-op

Objectives

- Experiment with Elastic Compute Cloud and demonstrate Science As A Service by virtualizing data processing pipeline processes
- Experiment and demonstrate automation and increased efficiency for large data set distribution and data product production
- Collaborate with Open Cloud Consortium and their Open Science Data Cloud
  - OCC provides Science as a Service (SAAS) or more accurately the infrastructure, platform and services to support science as a service.
- Using commercial cloud (Joyent) also
- Demonstrate various user run tools on the cloud

SensorWeb High Level Architecture

Sensors, Algorithms and Models Wrapped in Web Services Provide Easy Access to Sensor Data and Sensor Data Products

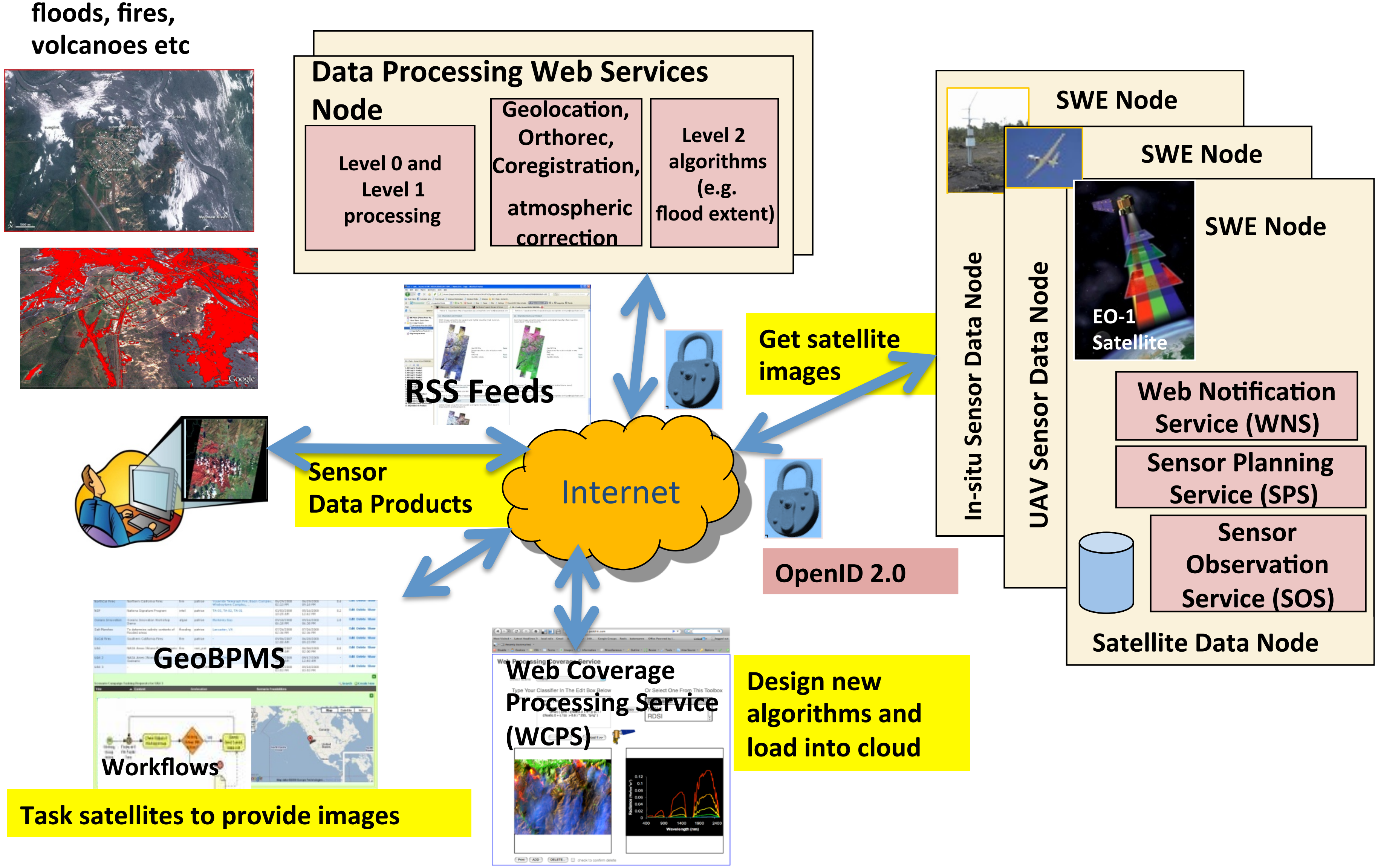

Integrate SensorWeb with Open Cloud Consortium Components

www.opencloudconsortium.org

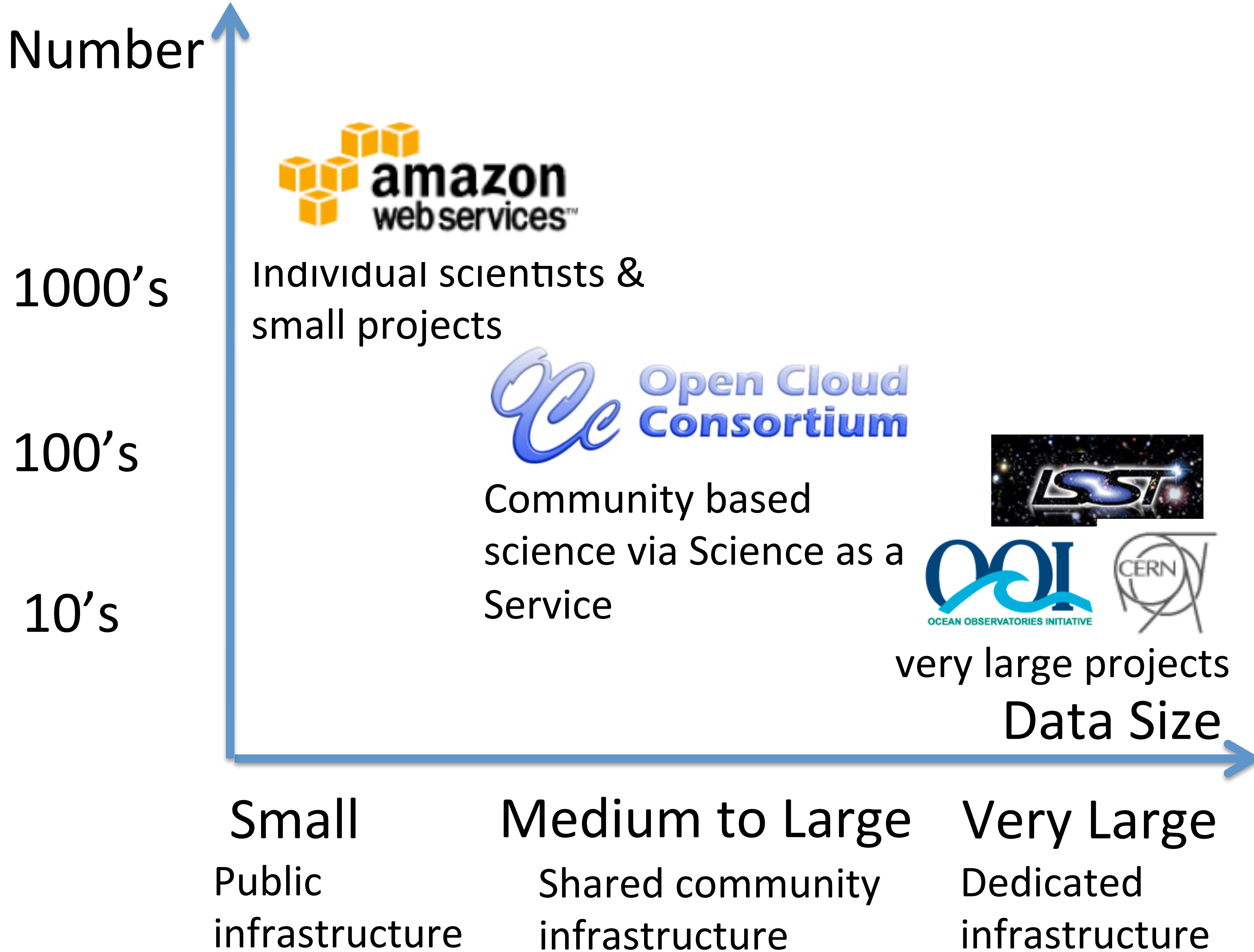
Number
1000's
100's
10's
Individual scientists &
small projects
Community based
science via Science as a
Service
very large projects
Data Size
Small
Public
infrastructure
Medium to Large
Shared community
infrastructure
Very Large
Dedicated
infrastructure

Open Cloud Consortium

- U.S based not-for-profit corporation.
- Manages cloud computing infrastructure to support scientific, environmental, medical and health care research, such as the Open Science Data Cloud.
- Manages cloud computing testbeds such as the Open Cloud Testbed.
- Develops reference implementations of standards based software for clouds
- Engages in outreach and education to support cloud computing.

www.opencloudconsortium.org

OCC Members

- Companies: Cisco, Yahoo!, Citrix, …
- Universities: University of Chicago, Northwestern Univ., Johns Hopkins, Calit2, ORNL, University of Illinois at Chicago, …
- Federal agencies and labs: NASA, LLNL, ORNL
- International Partners: AIST (Japan)
- Partners: National Lambda Rail

Global Lambda Integrated Facility (GLIF)
OCC Collaboration with Starlight (part of GLIF)

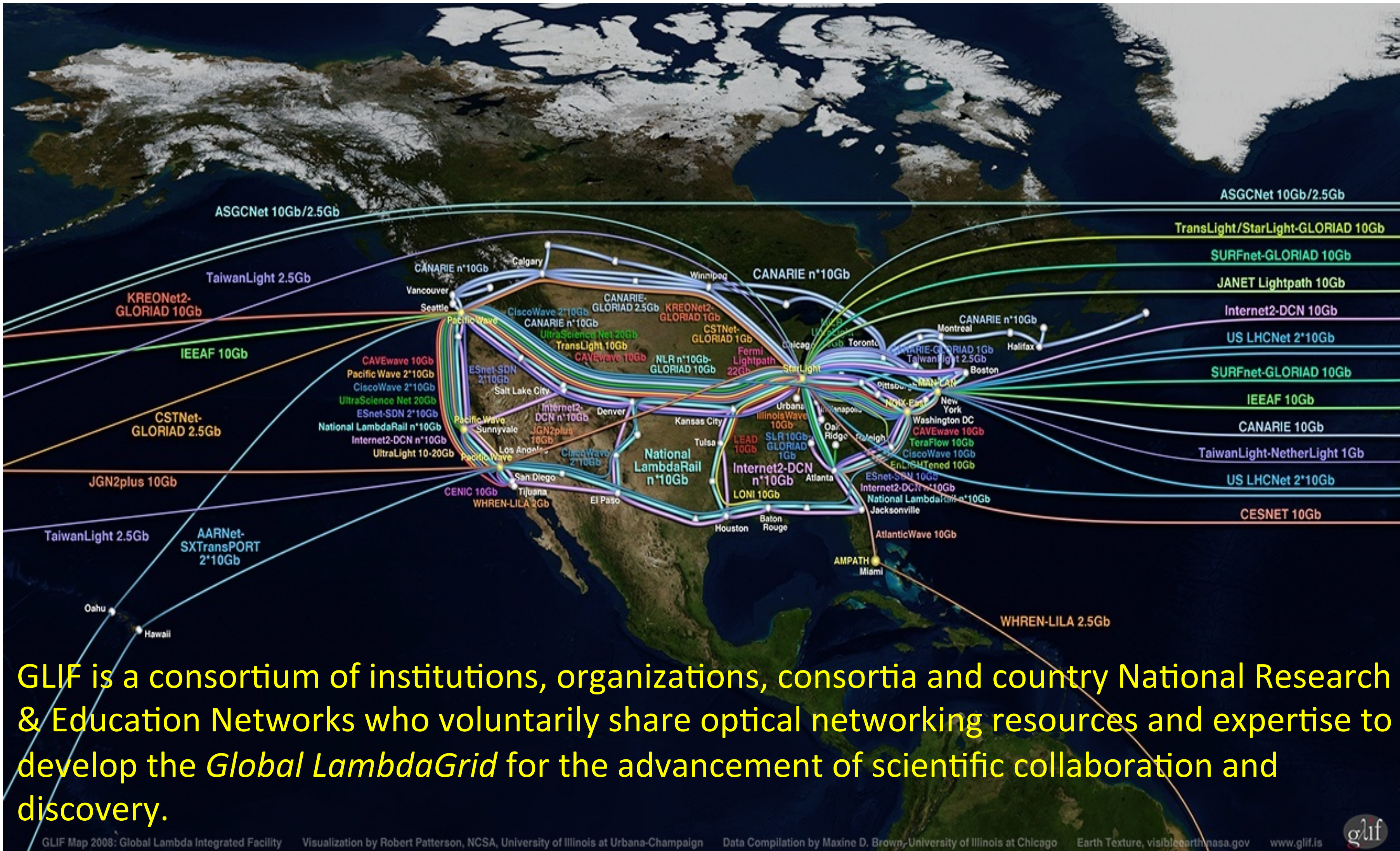

GLIF is a consortium of institutions, organizations, consortia and country National Research & Education Networks who voluntarily share optical networking resources and expertise to develop the *Global LambdaGrid* for the advancement of scientific collaboration and discovery.

OSDC Distribution of Scientific Data

- By the end of the 2012, the OSDC will make available approximately 1.5 PB of scientific and data to the research community.
- The data is available through both the commodity internet and through high performance research networks, including NLR and Internet2
- The data is from a variety of scientific disciplines:
  - 100+ TB of earth science through Project Matsu (joint with NASA)
  - 500 TB of genomic data, including the 1000 Genomes data set
  - 100 TB of astronomy data
  - 100 TB of web related data

OCC Investments

Year	Organization	$M	Comment
2009	Cisco	c. $1M+	Cisco provides access to the Cisco C-Wave to connect OCC data centers and partners with 10G wide area networks
2009	Yahoo!	c. 1.2M	Yahoo! donated a 2000 core cluster to the OCC
2011	NSF	$3.5M	NSF grant “Training and Workshops in Data Intensive Computing Using The Open Science Data Cloud”
2011	Yahoo!	c. $1M	Approximately $1M of equipment for OCC-Y Hadoop Cluster
2011	Moore Foundation	$2M	$1M per year for 2 years for equipment to support OCC-Adler & OCC-Sullivan

The Open Science Data Cloud (OSDC) is a hosted distributed facility managed by the OCC that:

- Manages & archives medium and large size datasets.
- Provides computational resources to analyze them.
- Provides networking to share the datasets with your colleagues and with the public.

Matsu Cloud Configuration

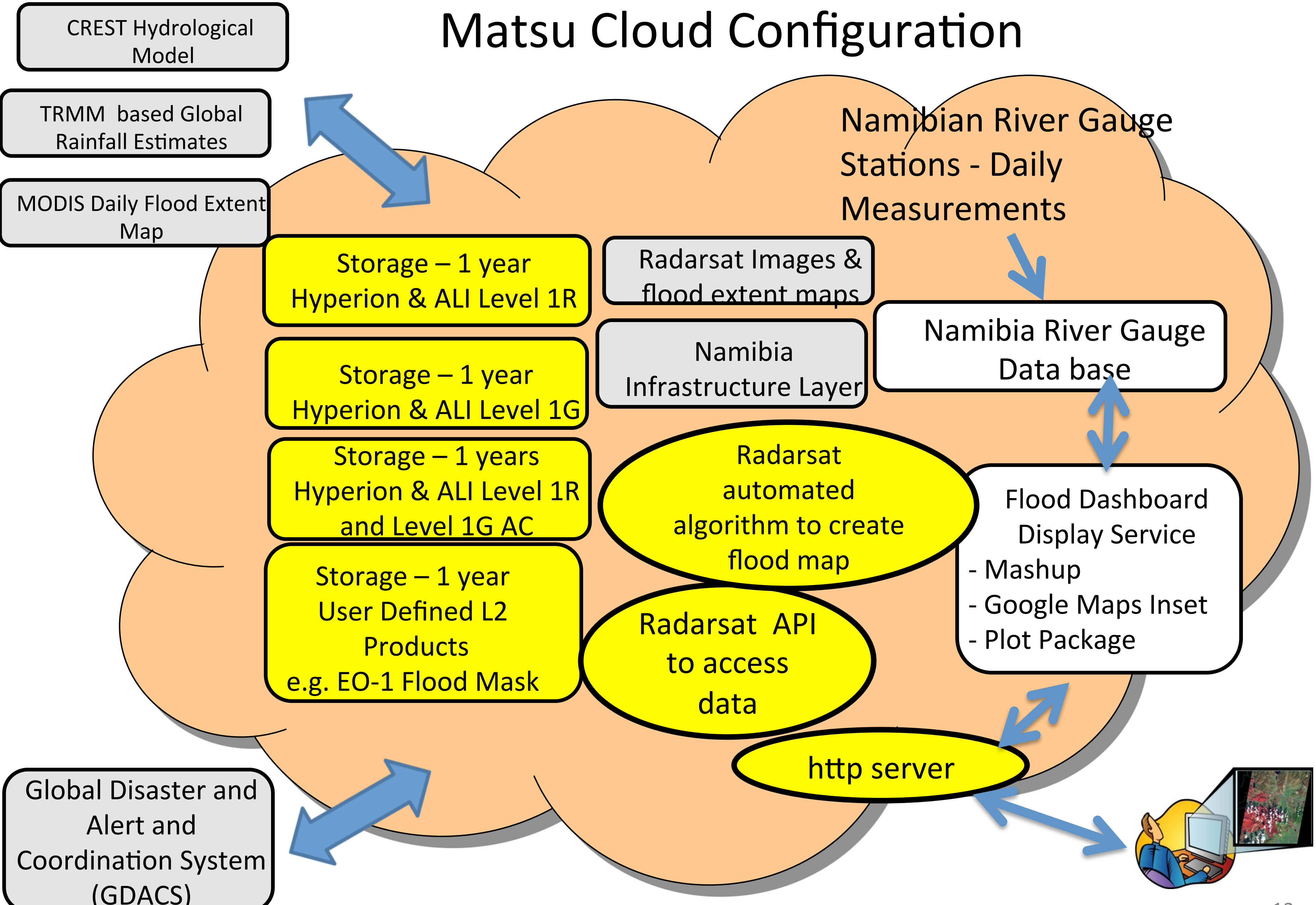

Matsu Cloud (In process)
Hadoop and Tiling Handles Large Dataset Displays

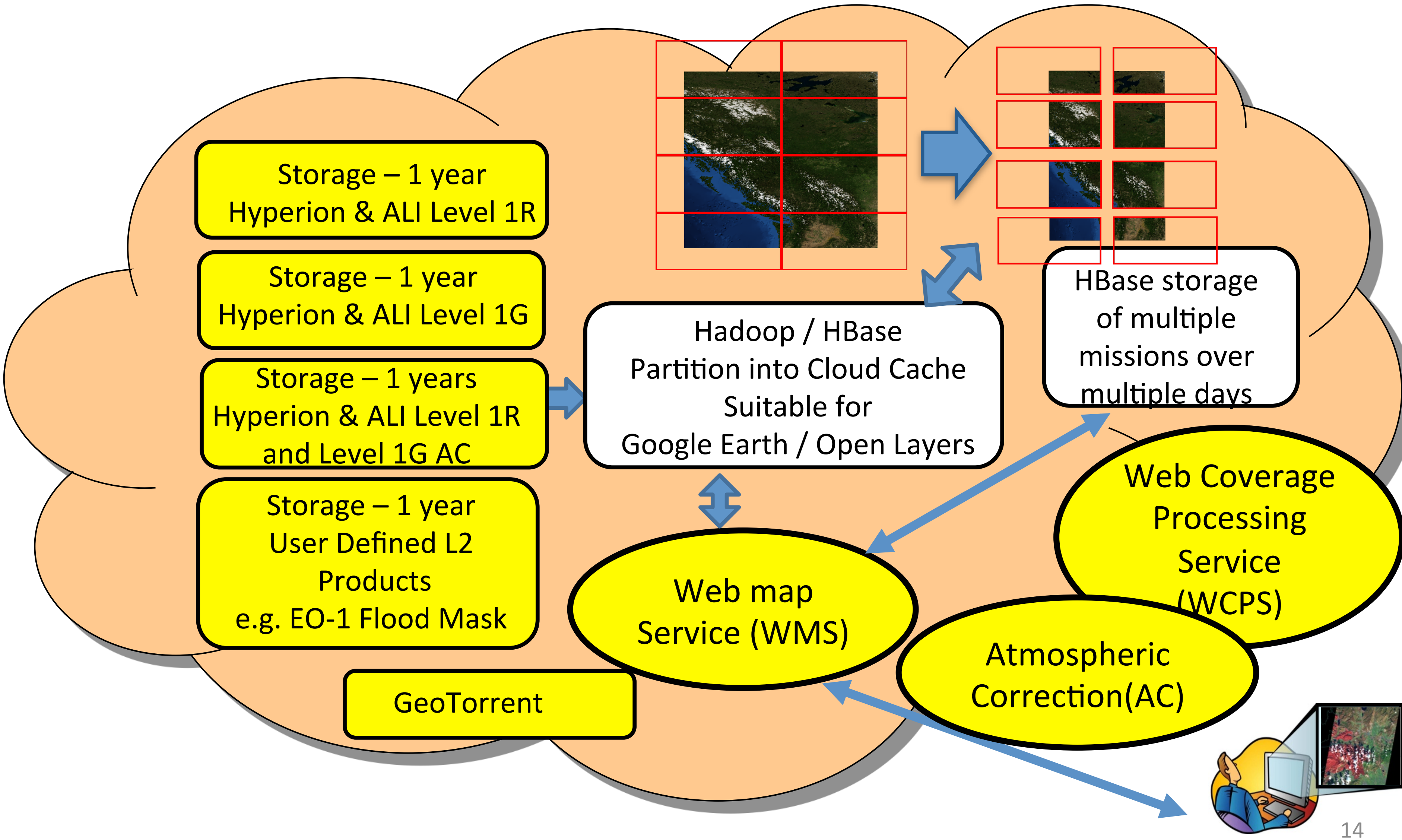

Joyent Cloud (commercial)

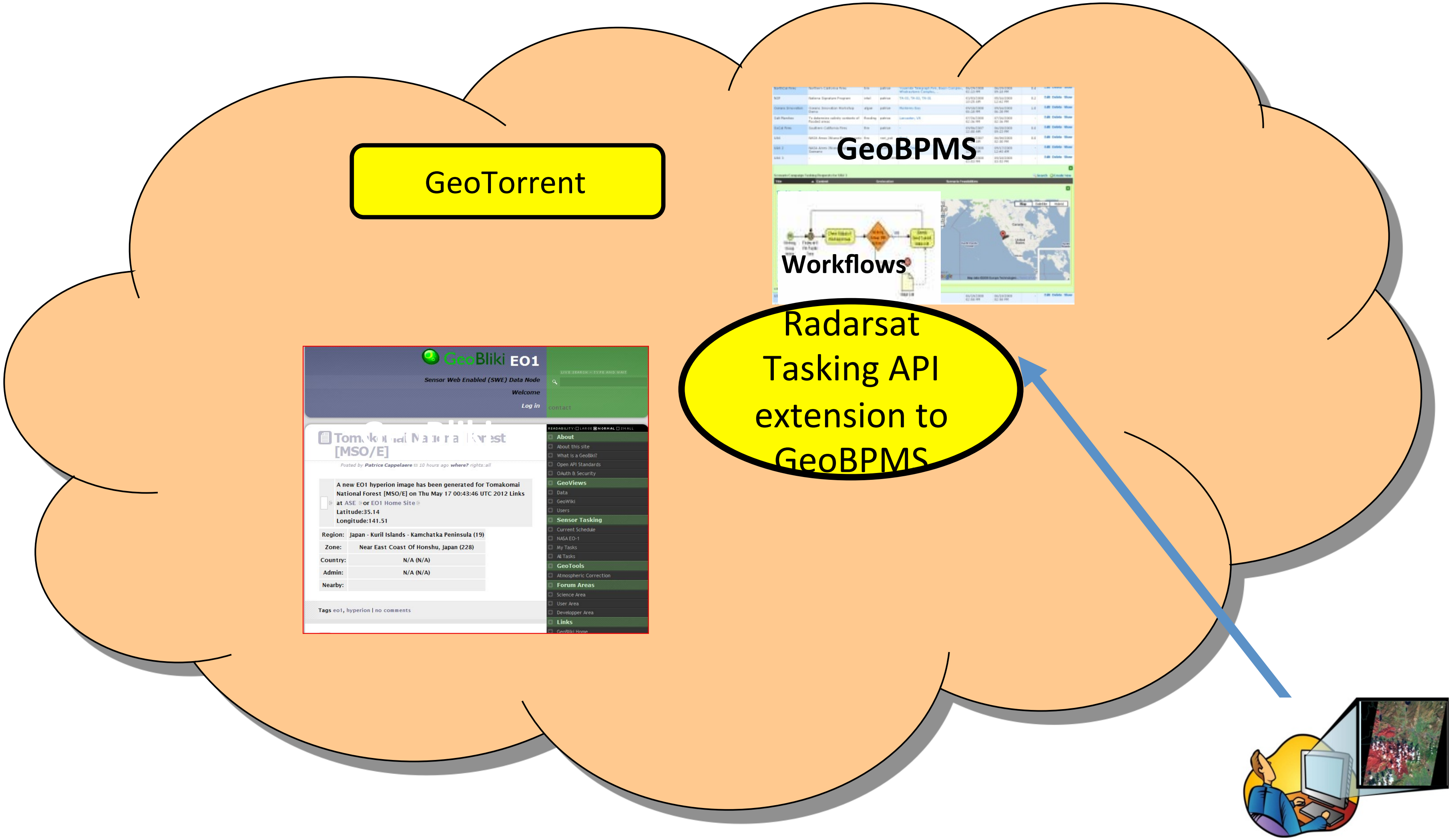

Namibia Flood Dashboard

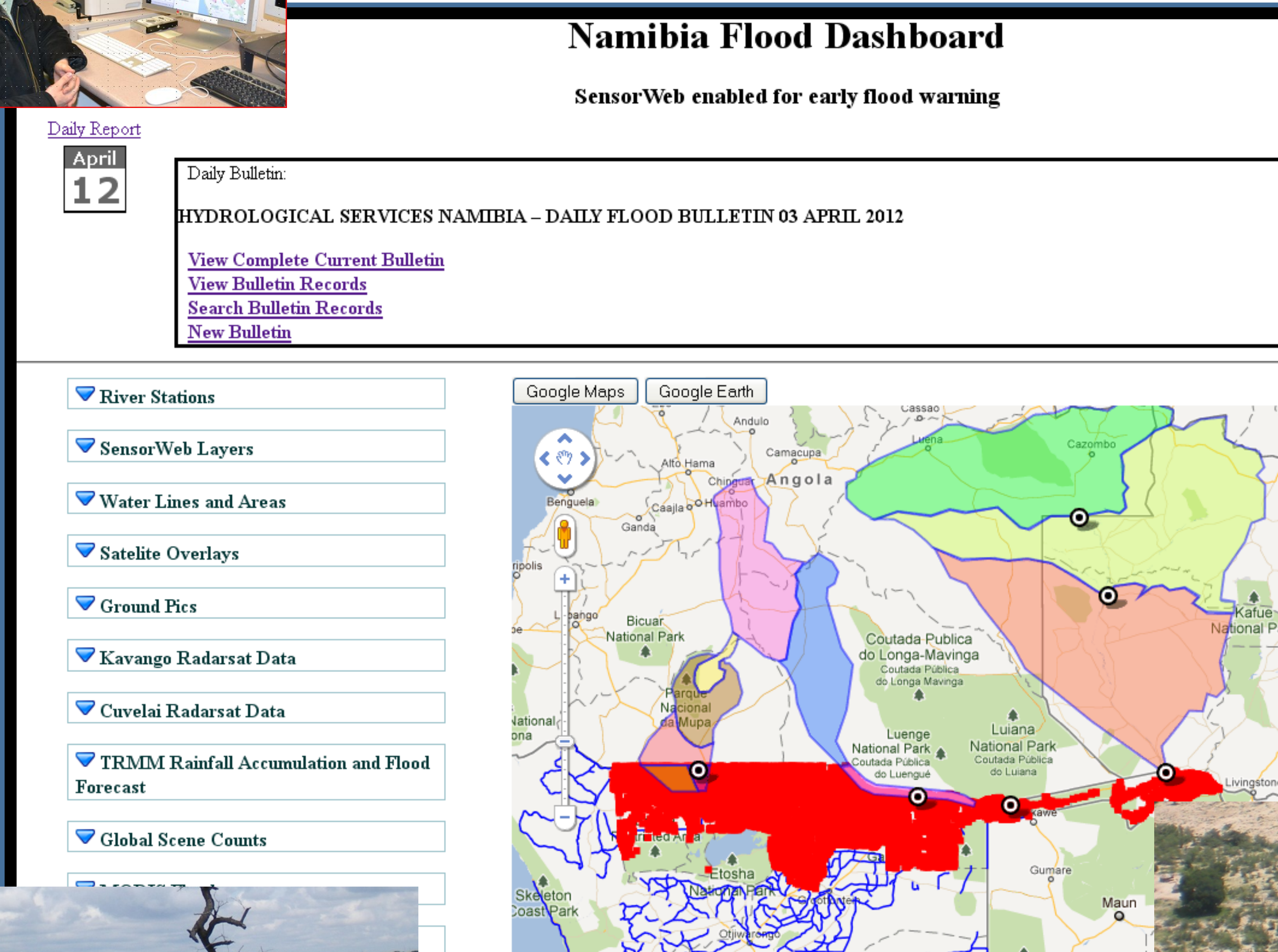

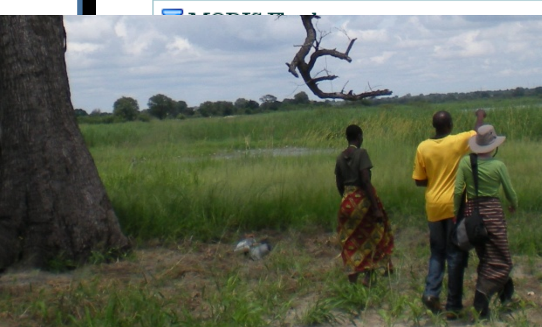

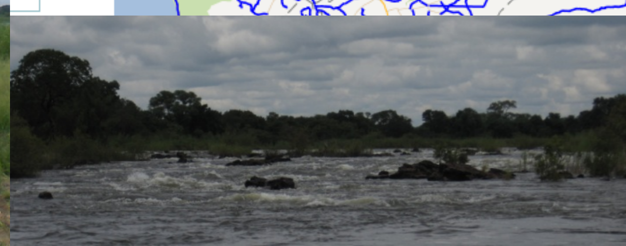

Matsu Cloud Functionality Enhancements

- Began developing method for automated co-registration using WCPS in Matsu Cloud
- Radarsat tasking Application Processing Interface (API) integrated with GeoBPMS (due in summer or fall 2012)
  - Funded by AIST ESTO QRS 2011
- Radarsat processing, and data distribution API
  - Display Radarsat data on IPAD
  - Funded by AIST ESTO QRS
- Waterpedia for Architecture Implementation Pilot 2 (AIP-5) (due summer/fall 2012)
  - High resolution water mask on map
  - Open street format
  - Crowd sourcing to validate and calibrate
  - Funded by AIST QRS 2011
- EO-1 tasking API for Pacific Data Center (due summer/fall 2012)
  - Funded by AIST ESTO QRS 2011

Matsu Cloud Functionality Enhancements

- Data distribution API for SERVIR nodes
  - CATHALAC (SERVIR in Caribbean)
  - RCMRD (SERVIR in Africa)
  - ICIMOD (SERVIR in Asia)

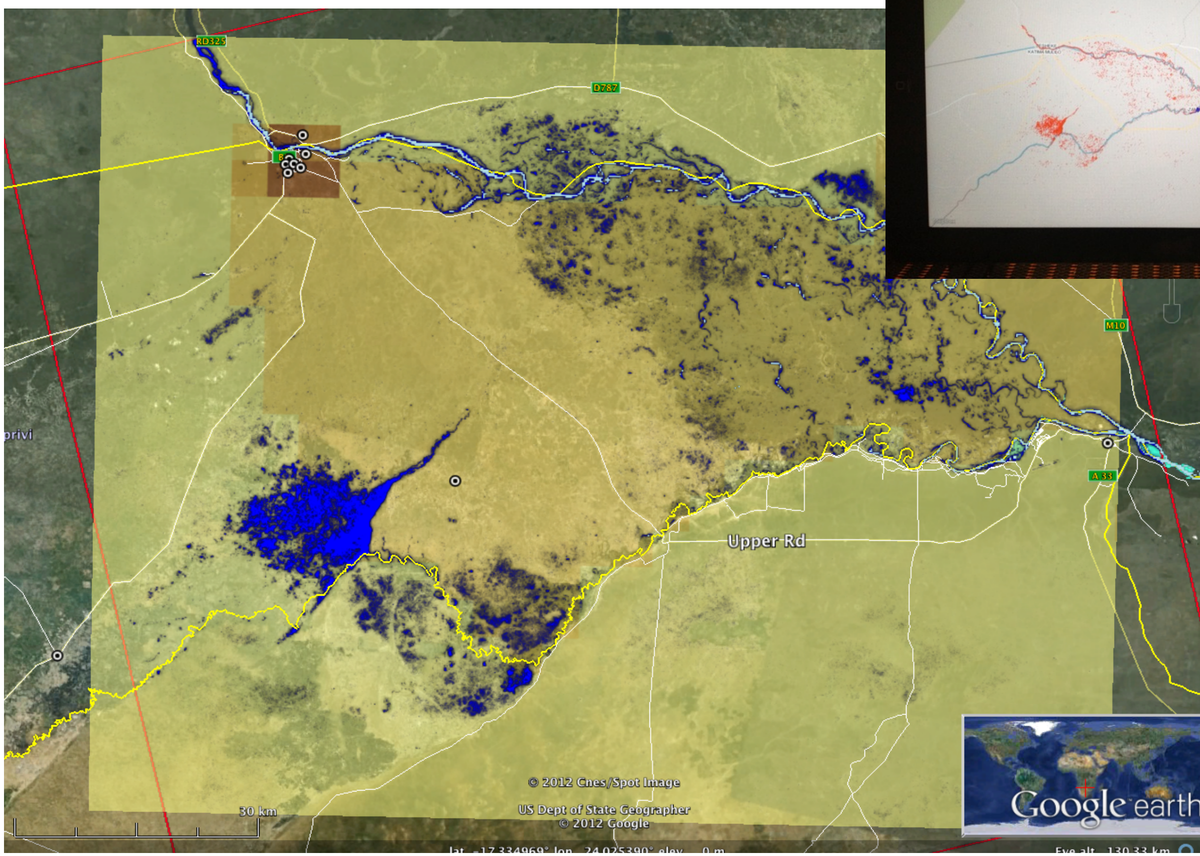

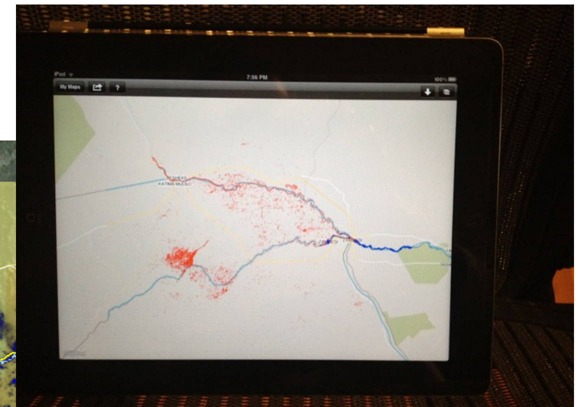

Radarsat data processed in cloud and tiled displayed on Ipad for field work and in preparation for Waterpedia with crowdsourcing

Conclusion: Relevance to HyspIRI

- HyspIRI will have large data sets
- Experiment with managing, processing and distributing large data sets in cloud on a “do-it-yourself” basis
- Prototype Science As A Service for users of the HyspIRI large data sets

Backup

StarLight – "By Researchers For Researchers"

StarLight is an experimental optical infrastructure and
proving ground for network services optimized for high-performance applications
GE+2.5+10GE
Exchange
Soon:
Multiple 10GEs
Over Optics –
World's "Largest"
10GE Exchange
First of a Kind
Enabling Interoperability
At L1, L2, L3

View from StarLight

Abbott Hall, Northwestern University's Chicago downtown campus

iCAIR: Founding Partner of the Global Lambda Integrated Facility
Available Advanced Network Resources

GLIF is a consortium of institutions, organizations, consortia and country National Research & Education Networks who voluntarily share optical networking resources and expertise to develop the *Global LambdaGrid* for the advancement of scientific collaboration and discovery.

www.glif.is

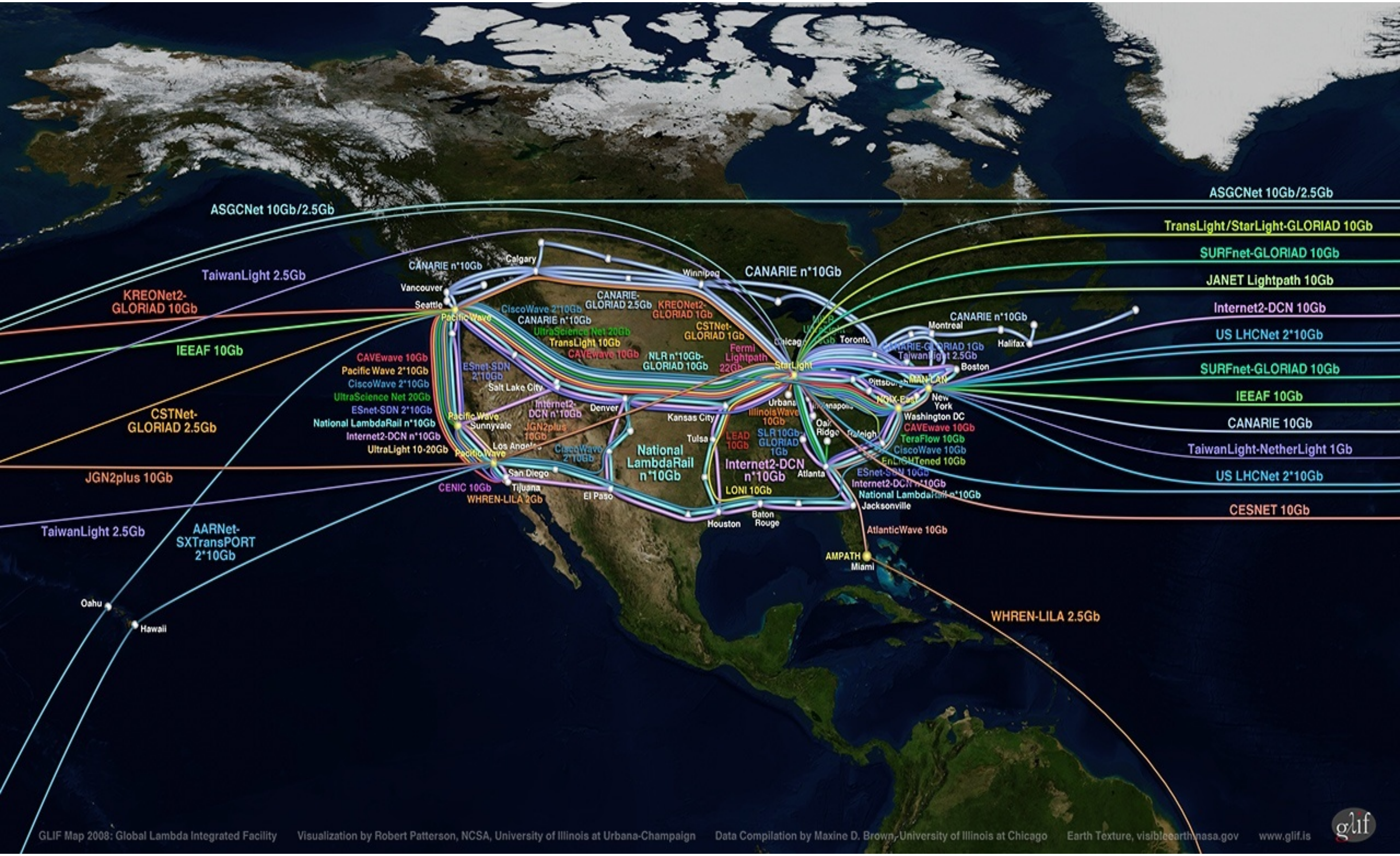
ASGCNet 10Gb/2.5Gb
TaiwanLight 2.5Gb
KREONet2-
GLORIAD 10Gb
IEEAF 10Gb
CSTNet-
GLORIAD 2.5Gb
JGN2plus 10Gb
TaiwanLight 2.5Gb
AARNet-
SXTransPORT
2*10Gb
Oahu
Hawaii
CANARIE n*10Gb
Calgary
Vancouver
Seattle
Pacific Wave
Winnipeg
CANARIE n*10Gb
CANARIE-
GLORIAD 2.5Gb
KREONet2-
GLORIAD 1Gb
CSTNet-
GLORIAD 1Gb
CiscoWave 2*10Gb
CANARIE n*10Gb
UltraScience Net 20Gb
TransLight 10Gb
CAVEwave 10Gb
NLR n*10Gb-
GLORIAD 10Gb
Fermi
Lightpath
22Gb
StarLight
Chicago
Toronto
CAVEwave 10Gb
Pacific Wave 2*10Gb
CiscoWave 2*10Gb
UltraScience Net 20Gb
ESnet-SDN 2*10Gb
National LambdaRail n*10Gb
Internet2-DCN n*10Gb
UltraLight 10-20Gb
ESnet-SDN
2*10Gb
Salt Lake City
Internet2-
DCN n*10Gb
Denver
Pacific Wave
Sunnyvale
JGN2plus
10Gb
Los Angeles
Pacific Wave
CiscoWave
2*10Gb
San Diego
Tijuana
CENIC 10Gb
WHREN-LILA 2Gb
El Paso
Kansas City
Tulsa
National
LambdaRail
n*10Gb
Urbana
IllinoisWave
10Gb
LEAD
10Gb
SLR 10Gb-
GLORIAD
1Gb
Internet2-DCN
n*10Gb
LONI 10Gb
Houston
Baton
Rouge
Atlanta
Raleigh
Jacksonville
CANARIE n*10Gb
Montreal
Halifax
Boston
Pittsburgh
MAN LAN
New
York
NGIX-East
Washington DC
CAVEwave 10Gb
TeraFlow 10Gb
CiscoWave 10Gb
Internet2-DCN n*10Gb
National LambdaRail n*10Gb
AtlanticWave 10Gb
AMPATH
Miami
WHREN-LILA 2.5Gb
ASGCNet 10Gb/2.5Gb
TransLight/StarLight-GLORIAD 10Gb
SURFnet-GLORIAD 10Gb
JANET Lightpath 10Gb
Internet2-DCN 10Gb
US LHCNet 2*10Gb
SURFnet-GLORIAD 10Gb
IEEAF 10Gb
CANARIE 10Gb
TaiwanLight-NetherLight 1Gb
US LHCNet 2*10Gb
CESNET 10Gb
GLIF Map 2008: Global Lambda Integrated Facility
Visualization by Robert Patterson, NCSA, University of Illinois at Urbana-Champaign
Data Compilation by Maxine D. Brown, University of Illinois at Chicago
www.glif.is

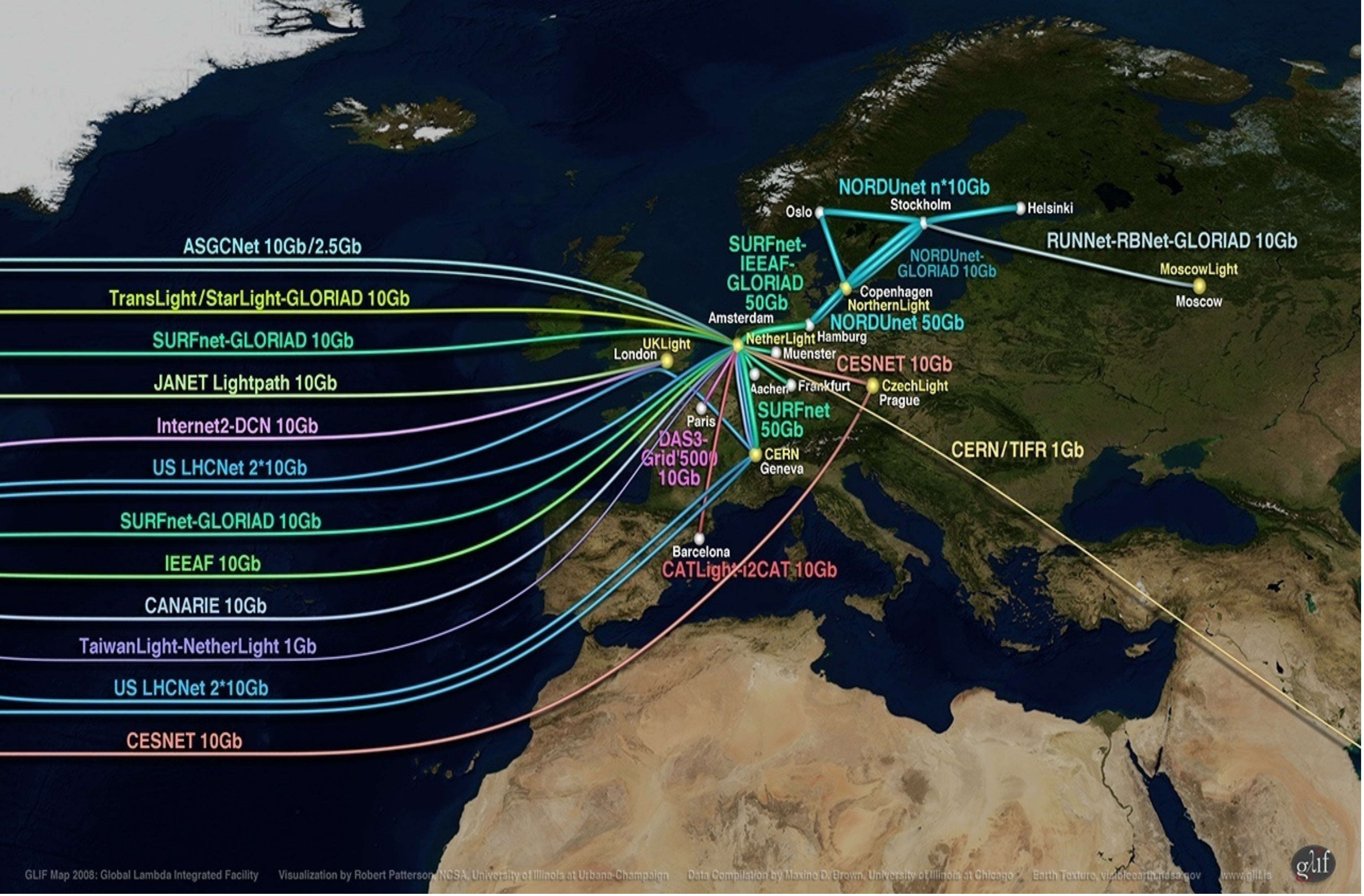

NORDUnet n*10Gb
Oslo
Stockholm
Helsinki
RUNNet-RBNet-GLORIAD 10Gb
MoscowLight
Moscow
SURFnet-IEEAF-GLORIAD 50Gb
NORDUnet-GLORIAD 10Gb
Copenhagen
NorthernLight
NORDUnet 50Gb
Amsterdam
NetherLight
Hamburg
Muenster
UKLight
London
CESNET 10Gb
Aachen
Frankfurt
CzechLight
Prague
Paris
SURFnet 50Gb
DAS3-Grid'5000 10Gb
CERN
Geneva
CERN/TIFR 1Gb
Barcelona
CATLight-i2CAT 10Gb
ASGCNet 10Gb/2.5Gb
TransLight/StarLight-GLORIAD 10Gb
SURFnet-GLORIAD 10Gb
JANET Lightpath 10Gb
Internet2-DCN 10Gb
US LHCNet 2*10Gb
SURFnet-GLORIAD 10Gb
IEEAF 10Gb
CANARIE 10Gb
TaiwanLight-NetherLight 1Gb
US LHCNet 2*10Gb
CESNET 10Gb
GLIF Map 2008: Global Lambda Integrated Facility
Visualization by Robert Patterson, NCSA, University of Illinois at Urbana-Champaign
Data Compilation by Maxine D. Brown, University of Illinois at Chicago
Earth Texture, visibleearth.nasa.gov
www.glif.is

TransLight/Pacific Wave/StarLight

10GE Wave Facilitates US West Coast Connectivity

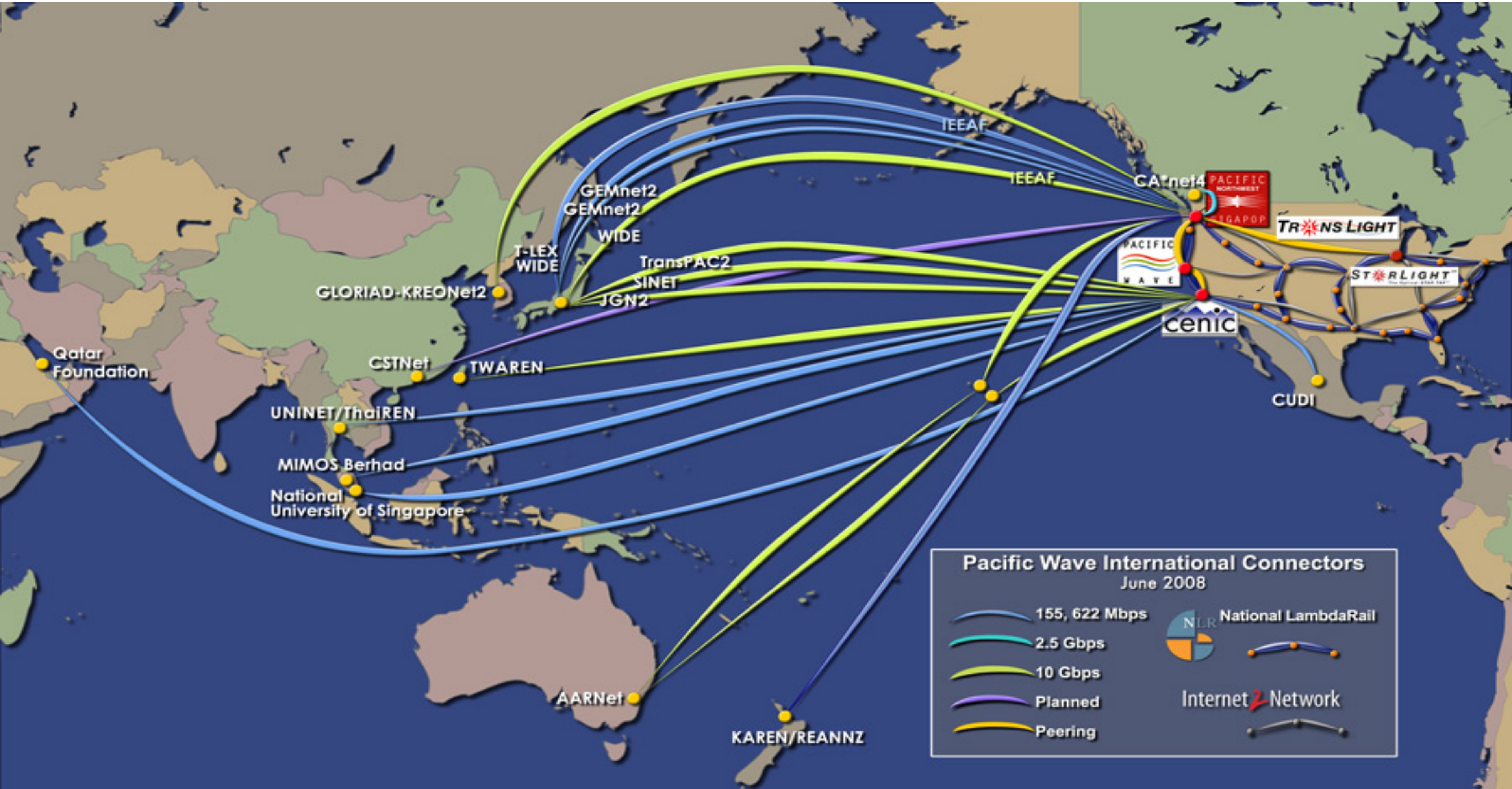

Sunnyvale and Los Angeles) to interconnect international and US research and education networks

www.pacificwave.net/participants/irnc/


CANARIE-
GLORIAD 2.5Gb
KREONet2-
GLORIAD 1Gb
CSTNet-
GLORIAD 1Gb
NLR n*10Gb-
GLORIAD 10Gb
CANARIE n*10Gb
MiLR-
UltraLight
10Gb
Chicago
StarLight
Kansas City
Urbana
IllinoisWave
10Gb
Tulsa
LEAD
10Gb
SLR 10Gb-
GLORIAD
1Gb
Indianapolis
Pittsburgh
NGIX
Oak
Ridge
Internet2-DCN
n*10Gb
Raleigh
LONI 10Gb
Atlanta

HyspIRI Low Latency Products Concept of Operation

Pat Cappelaere

SPACE FLIGHT CENTER

Get the free mobile app at
http://gettag.mobi

or http://youtu.be/EBlfwjz32sc

User Stories

- **Context**: A tsunami hits Japan, NASA scientists are called upon to image area and determine the impact of disaster.

1. Scientist requests low-latency imaging and specific product(s) by area and theme of interest. This generates one or more products that are immediately downloaded as soon as they are acquired and processed. User is notified upon product availability.
2. Much later, scientist [re-]processes existing data on the cloud using existing algorithms.
3. Scientist creates custom algorithm.
4. Algorithm is uploaded to satellite for subsequent ad-hoc product generation

1. Tasking Request

- ✓ User requests low-latency imaging and specific product(s) by area and theme of interest.
- ✓ HyspIRI is one of the available SensorWeb assets.
- ✓ Request is submitted to satellite(s).
- ✓ One or more products are immediately downloaded as possible.
- ✓ User is notified upon product availability via data feed.
- ✓ User displays product on Google Earth or IPAD or desktop.

2. Cloud Processing

- ✓ User decides to [re-] process data from specific area or specific task request.
- ✓ User picks algorithm to execute against specific data set.
- ✓ User is notified when product is generated
- ✓ User selects product from data feed and display it on Google Earth

3. New Algorithm on the Cloud

- ✓ User decides to customize an existing algorithm or create a new one.
- ✓ User could even use WEKA (Machine Learning Tool) and upload its output to WCPS.

3. New Algorithm Onboard

- ✓ User is satisfied with new algorithm.
- ✓ User submits algorithm for upload to HyspIRI
- ✓ Algorithm is now available for ad-hoc custom processing

HyspIRI

Low Latency Products

- Quick Response Ad-hoc Processing Where the Data is
  - On board
  - On the Cloud
  - Near Real-time
- Science (and Applications) As A Service
  - For Scientists
  - And Many Others…

Thank You!

SPACE FLIGHT CENTER

Examples of Higher level Products Possible from Existing Assets: Landsat, MODIS, ASTER, MASTER, AVIRIS, Hyperion, ALI

CQ5. **Surface Composition and Change**

John Car"Lyle" Mars[1], Anupma Prakash[2]

1) U.S. Geological Survey, jmars@usgs.gov

2) University of Alaska Fairbanks, Geophysical Institute, prakash@gi.alaska.edu

Members/contributors: Michael Abrams, Jim Crowley, Brian Bailey, Fred Kruse, Conrad Wright, Simon Hook, Woody Turner

science for a changing world

CQ5: Overarching Question

What is the composition of exposed terrestrial surface of the Earth and how does it respond to anthropogenic and non anthropogenic drivers?

MINERAL MAPS - HIGHER LEVEL PRODUCTS FOR HYSPIRI

RADIANCE - REFLECTANCE - EMISSIVITY

EXISTING PRODUCTS

LANDSAT TM - LAND COVER LAND USE – TRAINING SITES - DECISION TREE

MODIS MOD12 - LAND COVER LAND CHANGE – TRAINING SITES - DECISION TREE

ASTER - DECORRELATION STRETCH TIR DATA (DISCONTINUED)

AVIRIS - NONE

MASTER - NONE

ALI – NONE

HYPERION - NONE

SO WHAT DATA AND MAPPING METHODS HAVE BEEN DONE FOR EXPOSED TERRESTRIAL SURFACES THAT CAN BE USED FOR HYSPIRI SCIENCE INVESTIGATIONS INVOLVING CQ5?

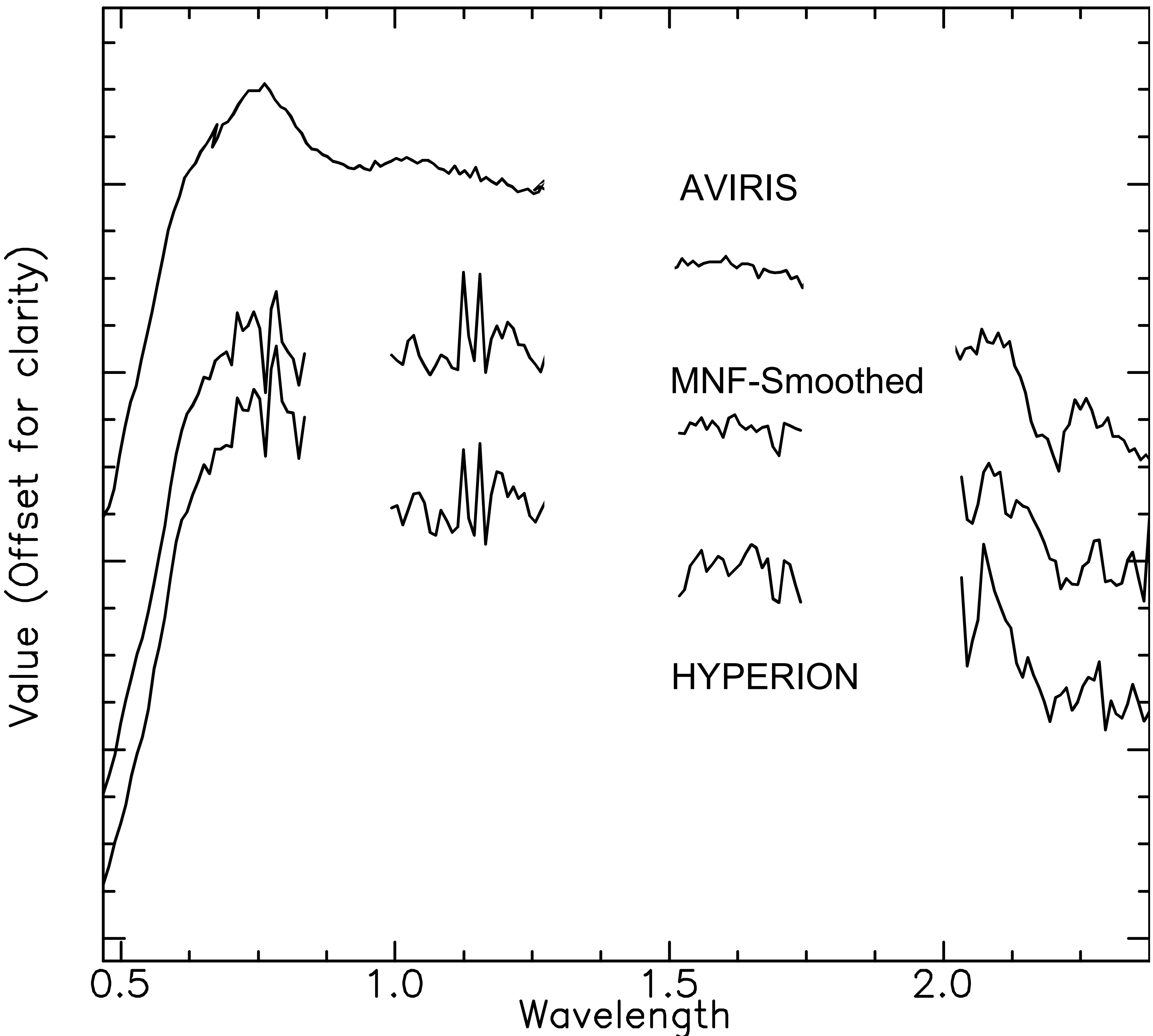

AVIRIS
MNF-Smoothed
HYPERION
Value (Offset for clarity)
Wavelength
0.5
1.0
1.5
2.0

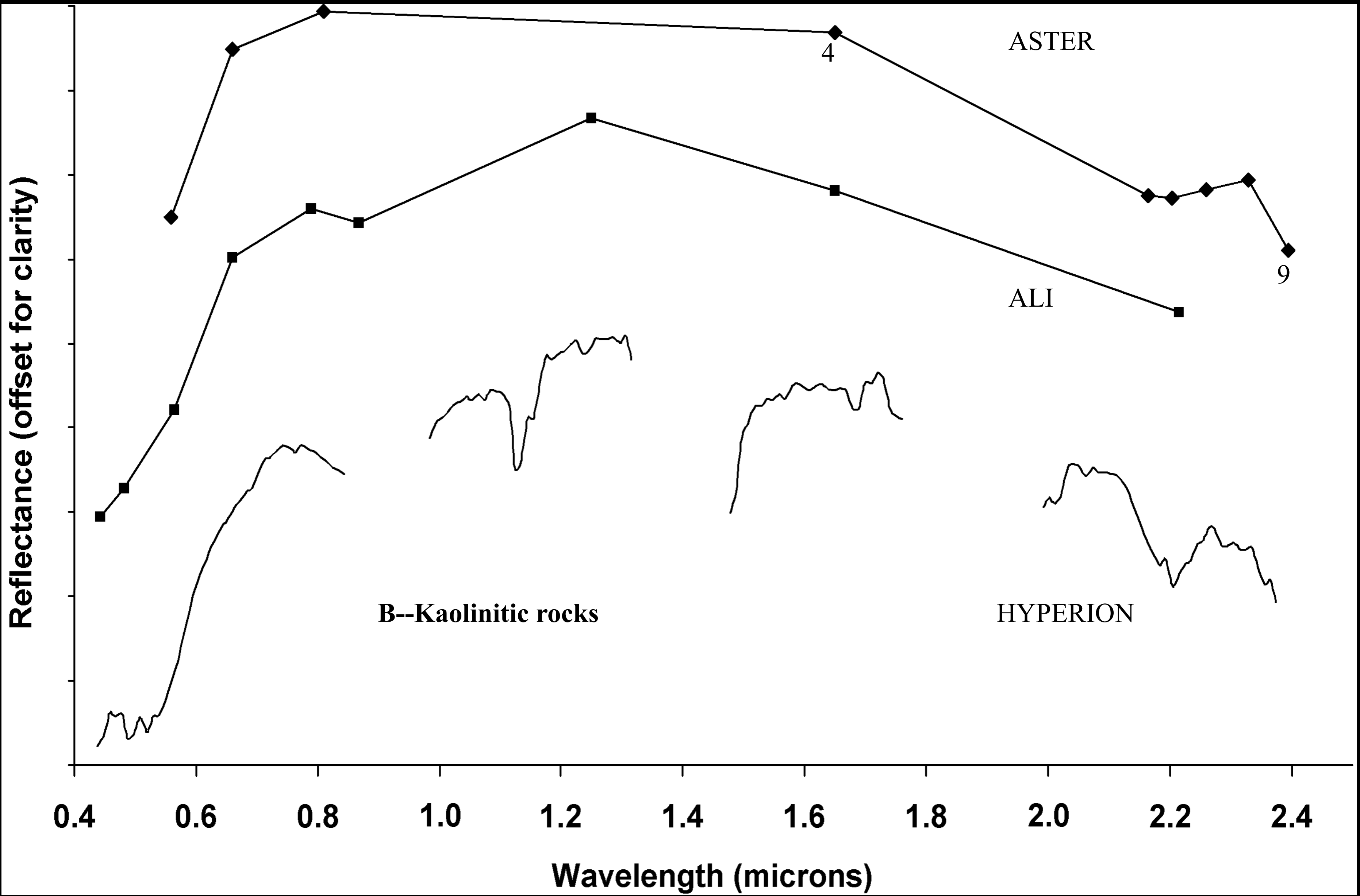

ASTER
4
9
ALI
B--Kaolinitic rocks
HYPERION
Reflectance (offset for clarity)
0.4
0.6
0.8
1.0
1.2
1.4
1.6
1.8
2.0
2.2
2.4
Wavelength (microns)

CQ5: Overarching Question

What is the composition of exposed terrestrial surface of the Earth and how does it respond to anthropogenic and non anthropogenic drivers?

AVIRIS Minerals Map of Elizabeth Mine, Vermont

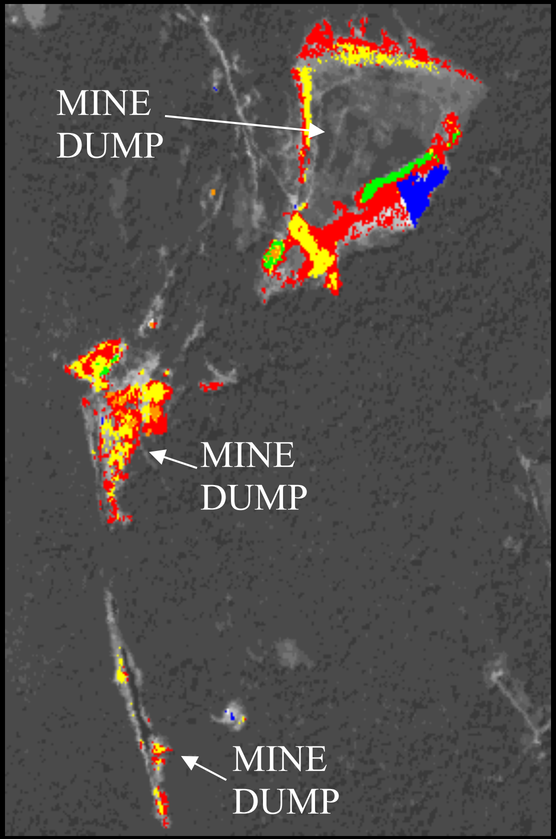

EXPLANATION:
- JAROSITE
- MUSCOVITE
- HEMATITE
- GOETHITE
- WATER

Crowley and others, 2001

Science Issue:
Mapping the mineralogical composition of the earth's surface is critical in understanding the distribution and formation economic ore deposits and hydrocarbons, and determining and monitoring processes that impact ecosystems such as acid runoff , desertification, and sediment flux into coastal and marine systems.

Tools:
VNIR-SWIR-TIR imagery, spectroscopy, mineral maps, false color composite band ratio images,

Approach:
The exposed terrestrial surface of the earth is composed of minerals that exhibit diagnostic spectroscopic absorption features in the 3.25 to 12.0 micrometer region. Mineral maps compiled from VNIR, SWIR and TIR spectroscopic data will be used to monitor desertification processes, determine soil quality, and map acid drainage and increased salinity. Rocks and sediments typically contain mixtures of different minerals and thus exhibit multiple absorption features in the VNIR-SWIR-TIR region. Band ratio false color composite images of VNIR-SWIR and TIR data will be used for rock and sediment type mapping.

Results:
Crowley and others used AVIRIS VNIR and SWIR data to map chemical weathering products of mine waste at the Elizabeth Mine, Vermont. Mineral maps show the distribution of jarosite, hematite and goethite which indicate low ph conditions around mine dumps that produce acid runoff.

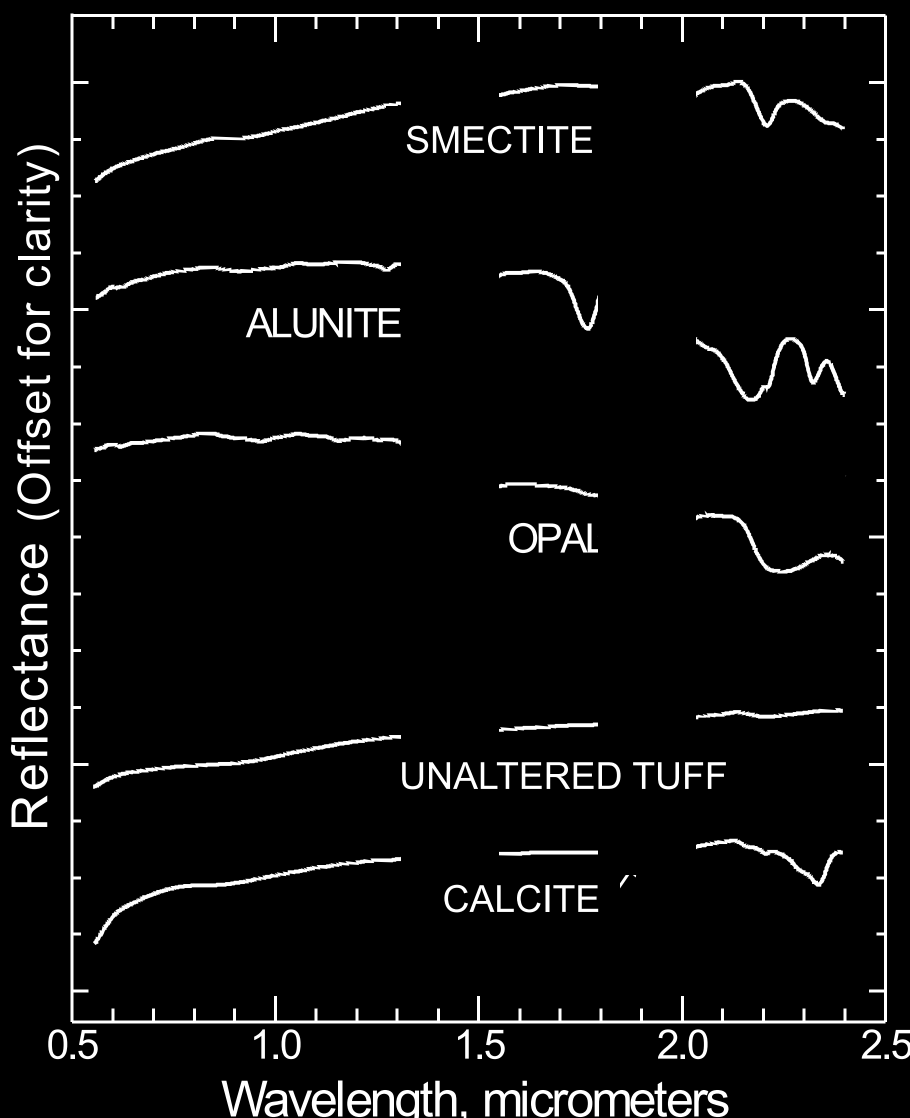
SMECTITE
ALUNITE
OPAL
UNALTERED TUFF
CALCITE
Reflectance (Offset for clarity)
0.5
1.0
1.5
2.0
2.5
Wavelength, micrometers

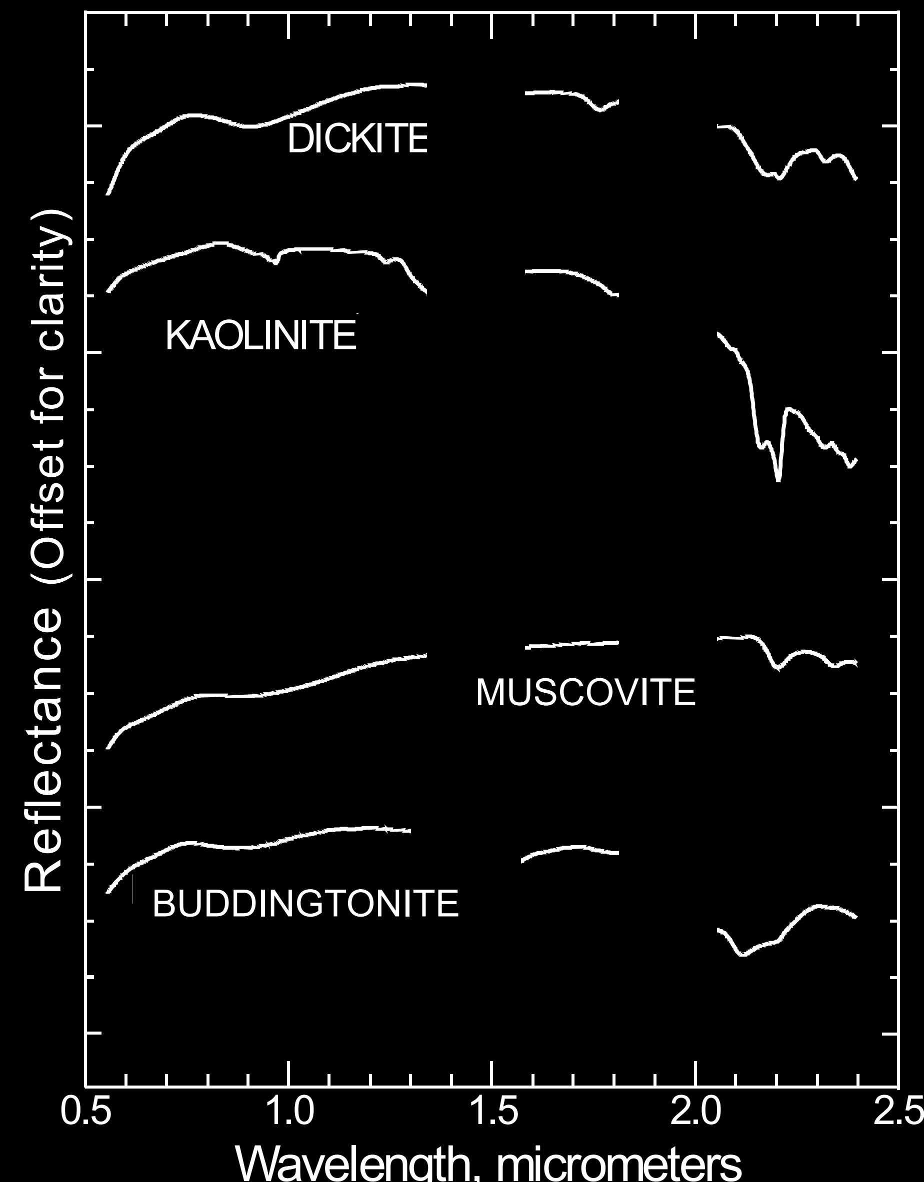
DICKITE
KAOLINITE
MUSCOVITE
BUDDINGTONITE
Reflectance (Offset for clarity)
0.5
1.0
1.5
2.0
2.5
Wavelength, micrometers

• What is the composition of the exposed terrestrial surface of the Earth? (DS 220)

False color composite HyspIRI simulated image of Grand Canyon, Arizona derived from TIR (red band - quartz-rich rocks), SWIR (green band - clay and muscovite-rich rocks; blue band - carbonate-rich rocks), and VNIR (dark green - green vegetation) data.

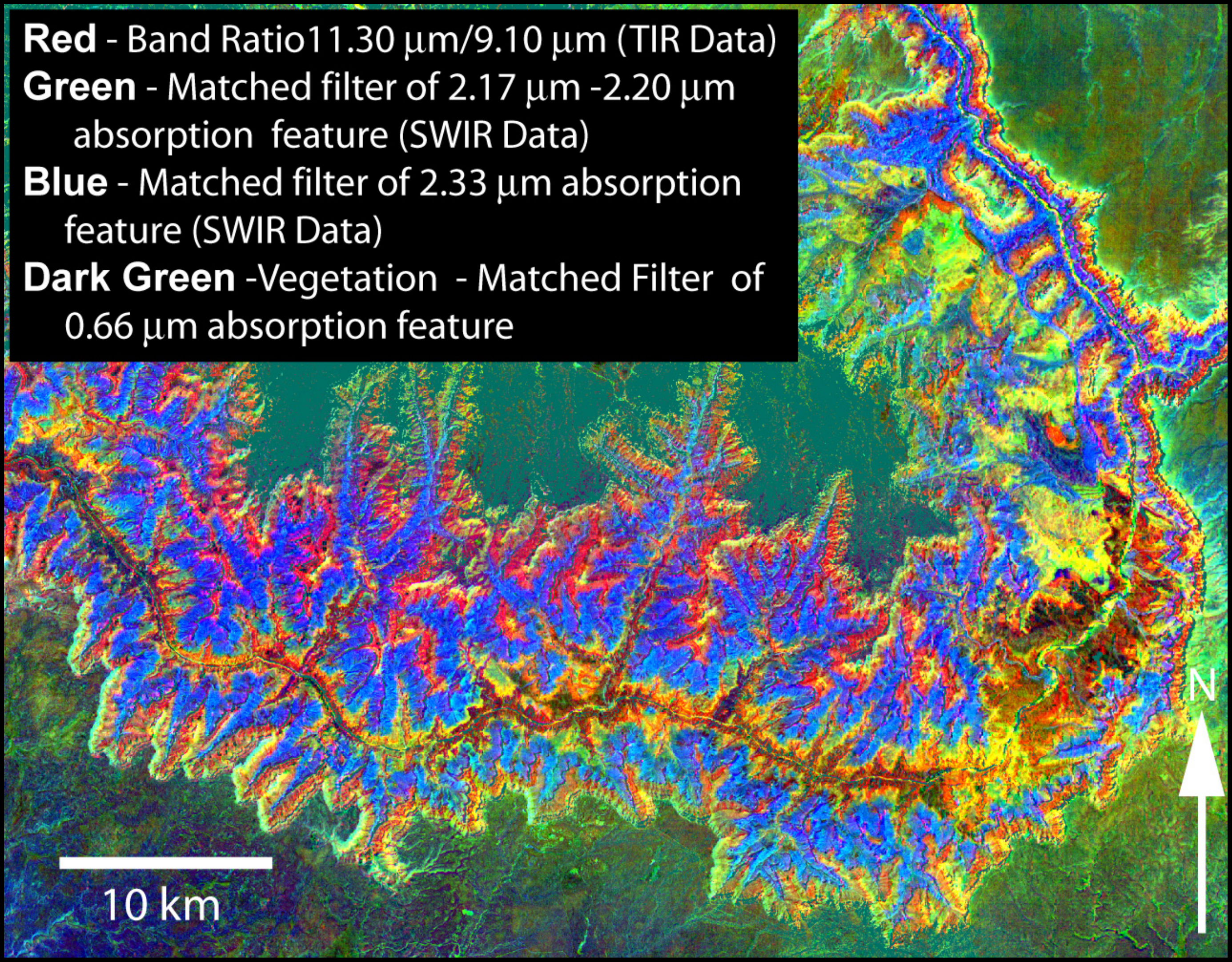

Science Issue:
How to compile more descriptive-detailed lithologic maps?

Tools:
With VINIR-SWIR-TIR capability, HyspIRI will be able to map the most common surficial minerals including quartz (TIR), carbonates (TIR, SWIR), clays (SWIR), oxides (VNIR) and evaporites (VNIR and SWIR).

Approach:
Use false color composite band ratio maps of common mineral groups

Results:
The Grand Canyon is an example where the quartz-rich sandstones were mapped using TIR data, and the clay-rich shale and carbonate rocks were mapped using SWIR data.


Sedimentary Rocks
Rocas sedimentarias
Roches sédimentaires

•How does the surface mineralogy and soil composition relate to the plant physiology and function on the terrestrial surface of the Earth? (DS 114)

Rowan and others, 1998

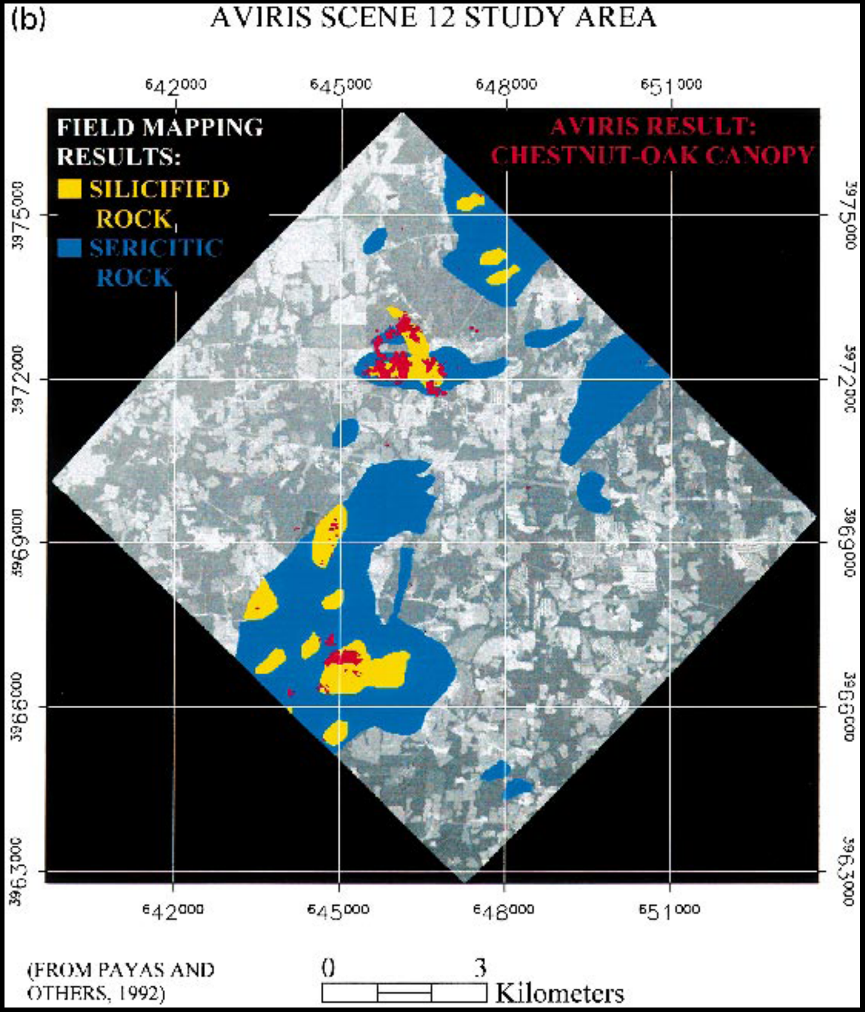

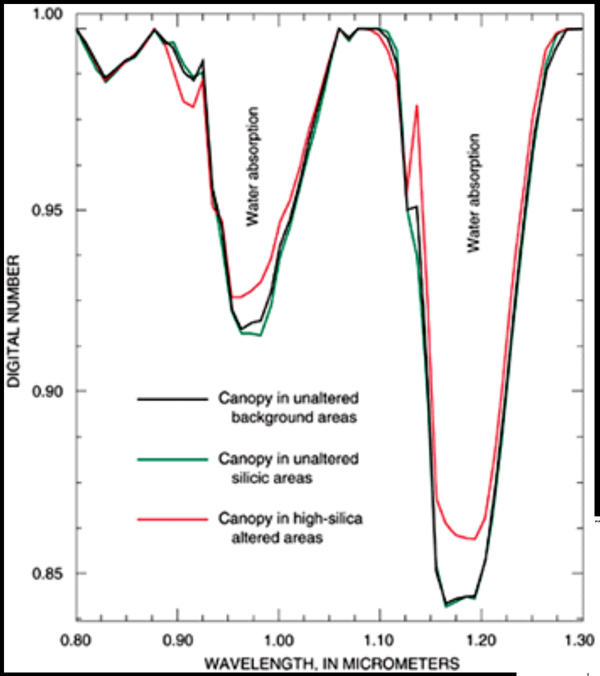

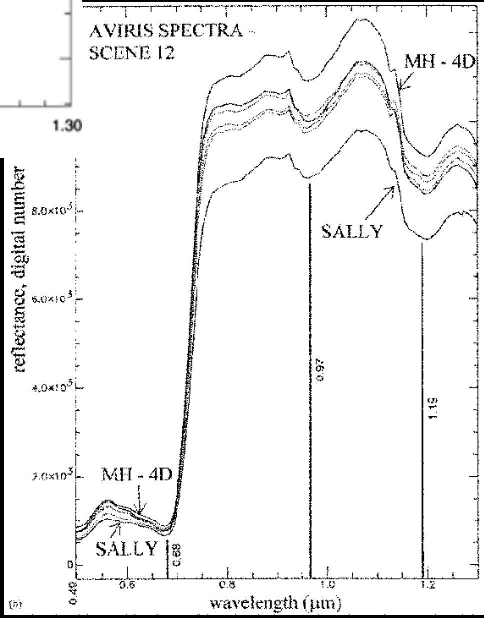

•How is the composition of exposed terrestrial surface responding to anthropogenic and non anthropogenic drivers (desertification, weathering, disturbance e.g. logging, mining)? (DS 114)

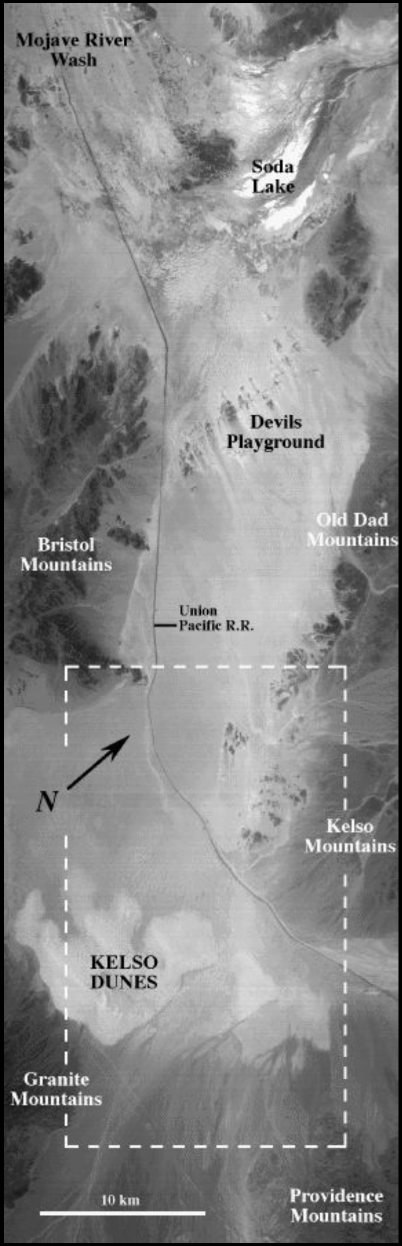

Ramsey and Lancaster, 1998

Monitoring dune migration in the Mojave Desert, California using TIMS (TIR) data

Science Issue:

Monitoring of desertification

Tools:

-Field spectral data

-HyspIRI VNIR, SWIR and TIR data, multiple temporal datasets

Approach:

-HyspIRI VNIR-SWIR data can be used to map vegetation, and clay, carbonate, and evaporite compositions of soils.

-HyspIRI TIR data can be used to map soil quartz content and quartz sand movement.

-Multiple HyspIRI data sets can be used to monitor landscape changes

Results:

-Chikhaoui and others used ASTER VNIR-SWIR field spectra and VNIR SWIR ASTER data to compile a land degradation index map.

-Ramsey and Lancaster used TIMS TIR data to monitor dune migration of quartz-rich sands.

Land Degradation Index Northern Morocco-Index compiled from ASTER VNIR-SWIR data

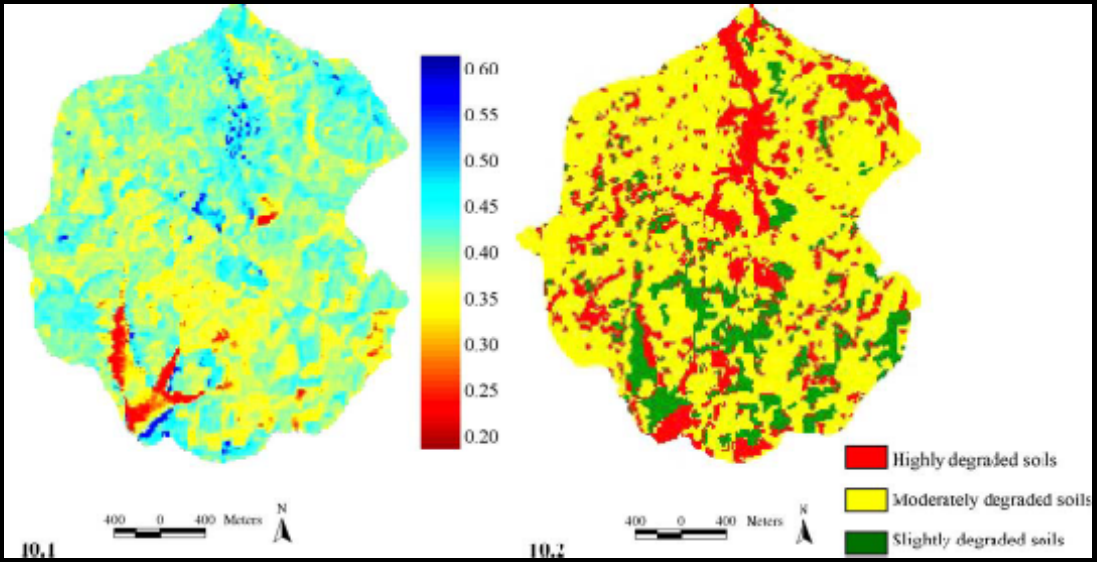

Chikhaoui and others, 2005

Ramsey and Lancaster, 1998

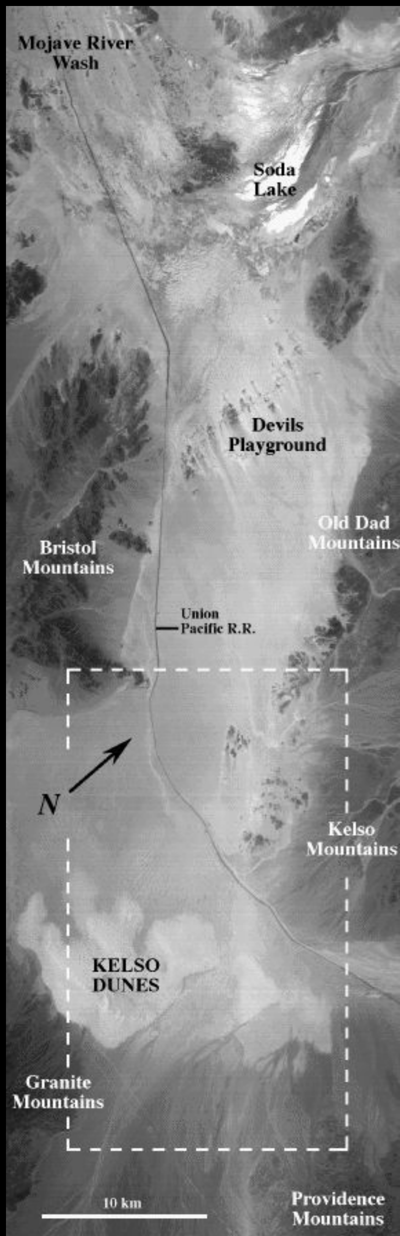

Dune migration in the Mojave Desert, California using TIMS data

Chikhaoui and others, 2005

Land Degradation Index Study, Northern Morocco

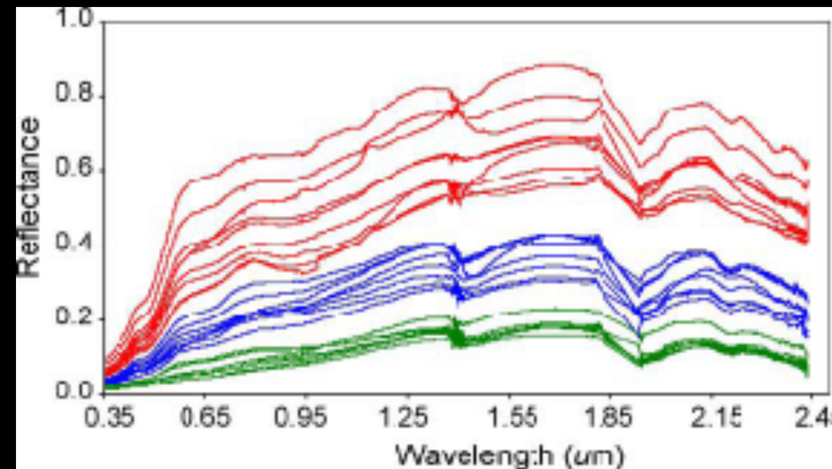

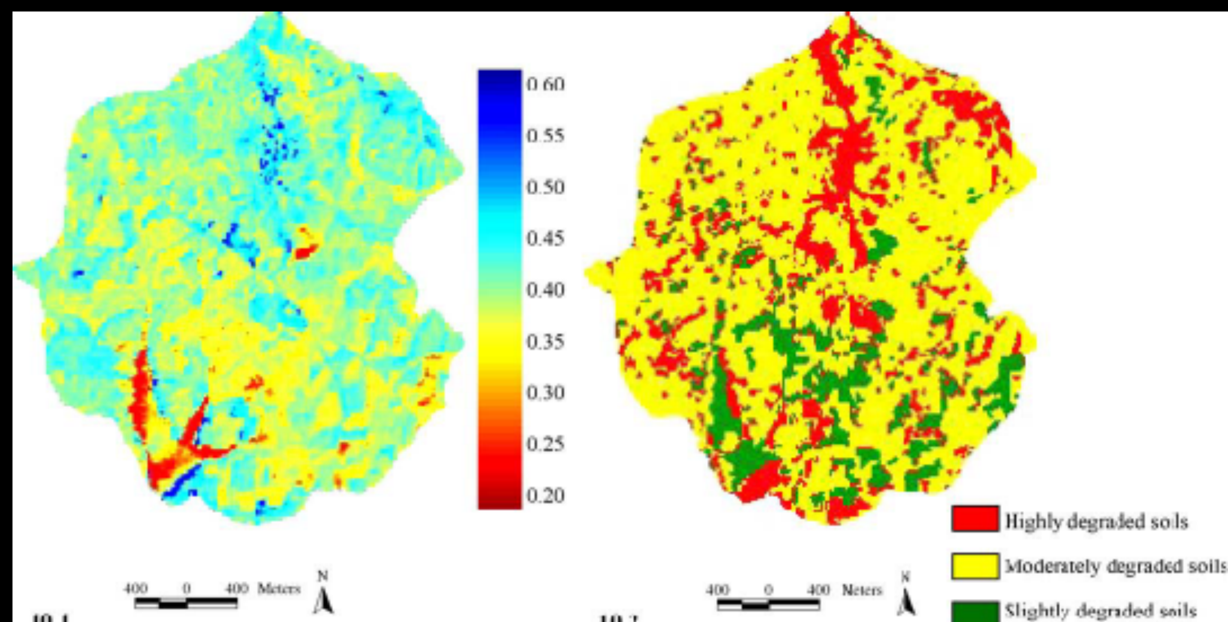

•How do types and distributions of altered rocks define regional trends in hydrothermal fluid flow for magmatic arcs and tectonic basins, better define hydrothermal deposit models, and assist in the discovery of new economic deposits? (DS 227)

Science Issue:

How can alteration be used to identify new economic deposits and better define hydrothermal fluid flow in hydrothermal systems?

Tools:

HyspIRI SWIR and TIR data

Approach:

- Deposit models such as Lowell and Guilbert (1970) suggest that most hydrothermal systems produce zones of different altered rocks based on geochemical conditions and alteration intensity.
- Propylitic, argillic, and phyillic-altered rocks have SWIR absorption features and potassic altered rocks have TIR absorption features. Thus, HyspIRI SWIR data could be used to map the propylitic, argillic and phyllic-altered rocks, and HyspIRI TIR data could be used to map potassic-altered and silicified rocks with the TIR detector.

Results:

Mars and Rowan (2006), have used ASTER data to regionally map argillic, phyllic, and potassic-altered and silicified rocks along magmatic arcs.

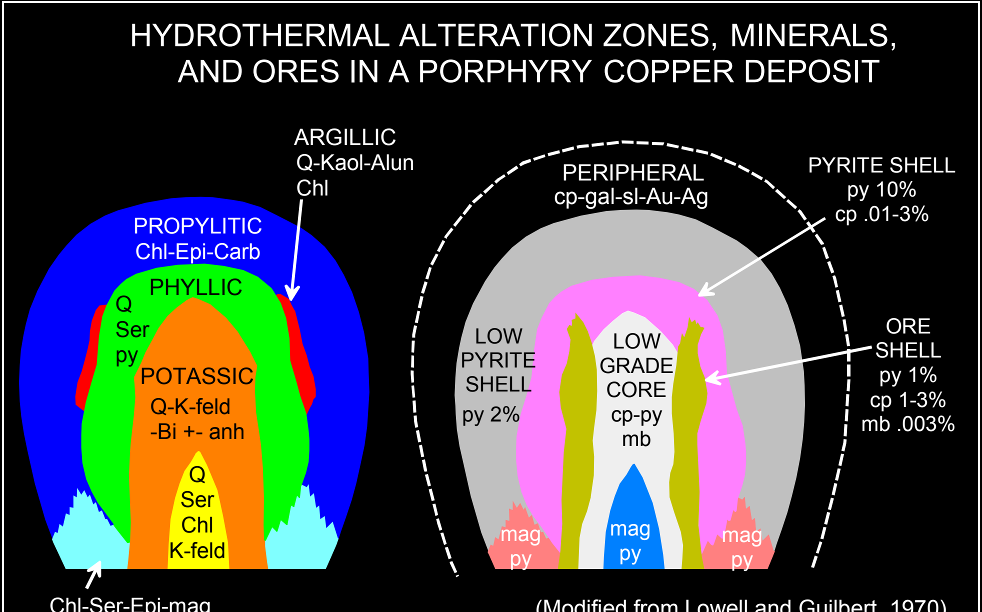

Deposit model cross section view

Results (cont.):

Porphyry copper deposits typically consist of circular to elliptical patterns of potassic, silicified, phyllic and argillic-altered rocks. Linear patterns of alteration have been associated with epithermal systems. Thus, the regional alteration data have been used to identify potential deposits and assess hydrothermal fluid flow.

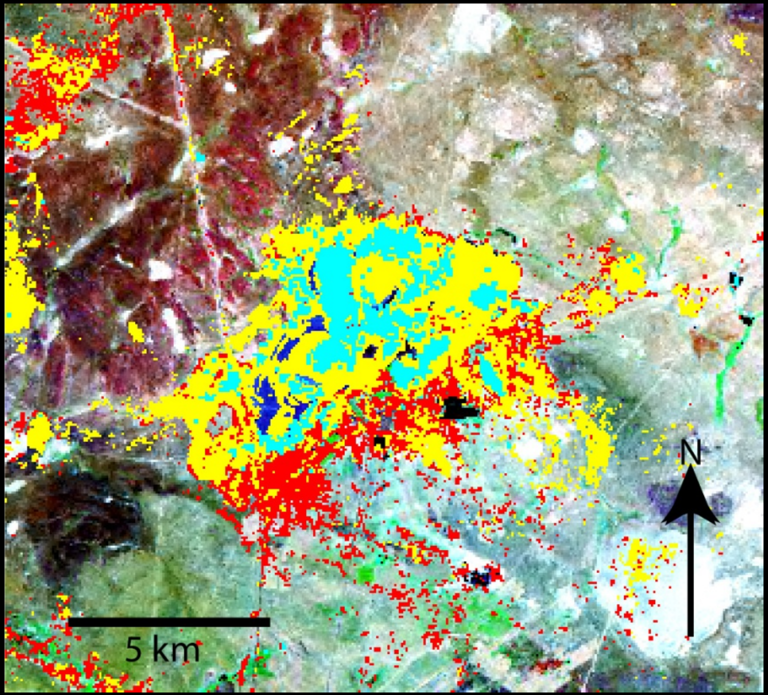

False color composite HyspIRI simulated image of the porphyry copper Konyrat Mine near Balquash, Kazakhstan. Elliptical patterns of altered rocks define the porphyry copper deposit at the surface (Mars and Rowan, 2006)

- Potassic-altered - Silicified rocks (TIR data)
- Argillic-altered rocks (SWIR data)
- Phyllic-altered rocks (SWIR data)

LOGICAL OPERATORS USED TO MAP MINERALS - HYDROTHERMAL SILICA-RICH

((float(b3)/b2)le1.55) and (b4gt2400) and ((float(b4)/b7)ge1.41) and ((float(b13)/b12)ge1.021)

(ge - greater than or equal to; gt - greater than; le - less than or equal to; float - floating point)

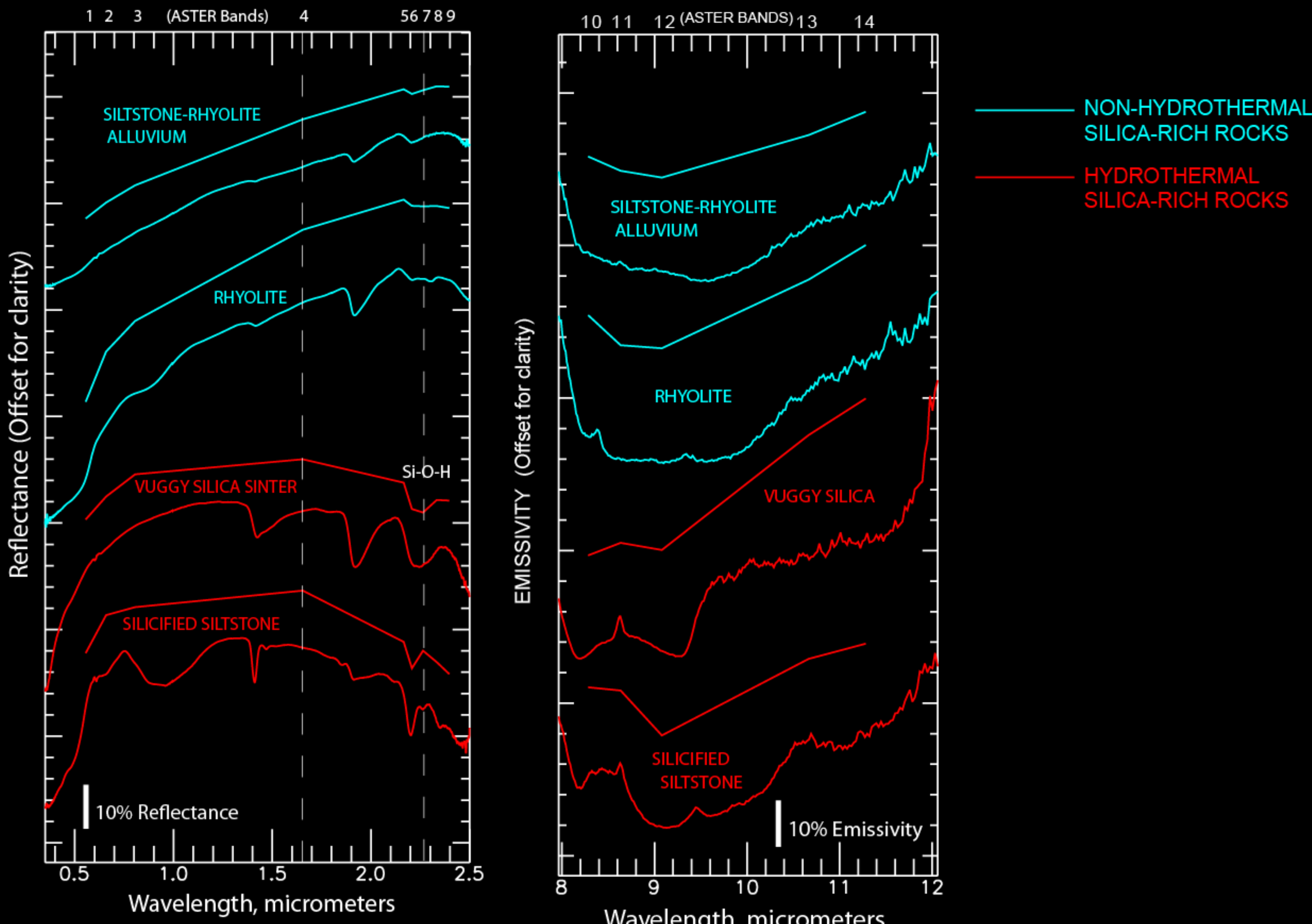

•How do regional trends of minerals and shale thermal maturity within basins better define depositional models and assist in the discovery of new hydrocarbon reserves? (DS 235)

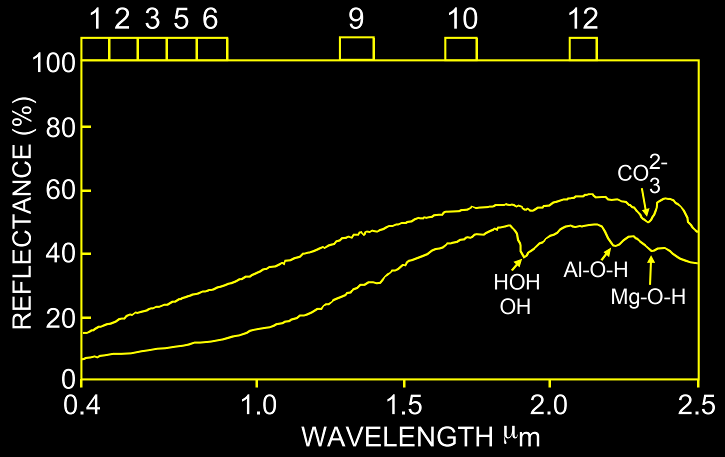

Compound Ratio:
(Ch3/Ch1+(Ch5/Ch3)
+(Ch6/Ch5)+(Ch10/Ch9)
-(Ch12/Ch10)

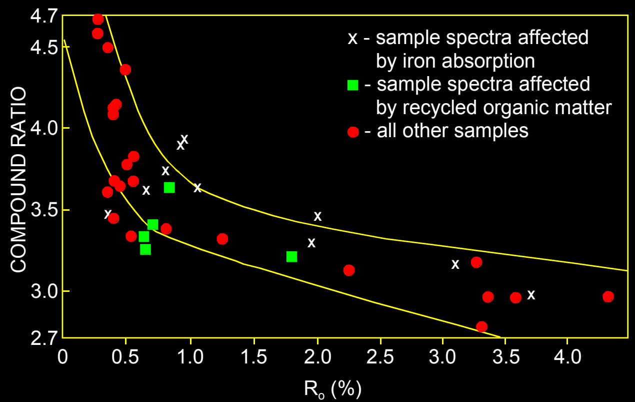

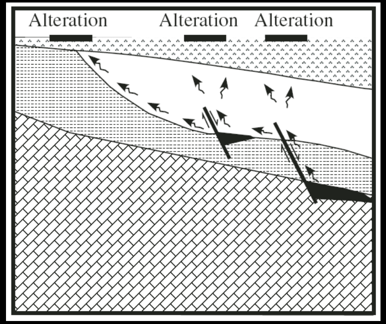

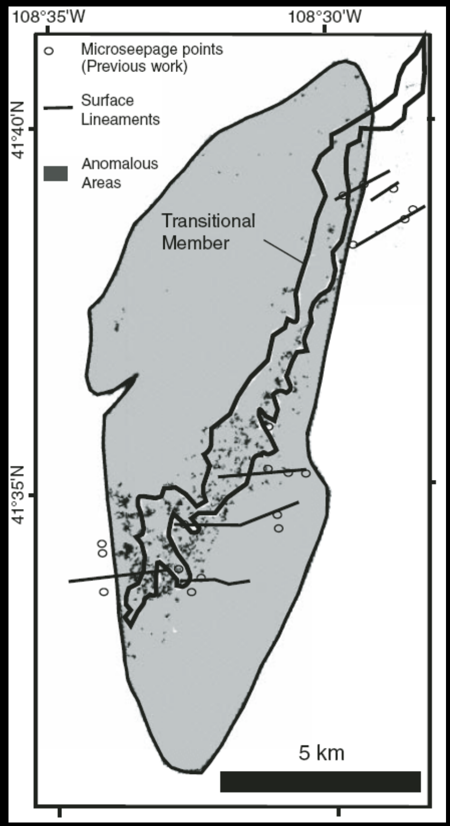

Khan and Jacobson, 2008

Science Issue:
How can mineral trends help identify new hydrocarbon reserves?

Tools:
HyspIRI VNIR, SWIR, and TIR data.

Approach:
-As hydrocarbons migrate, they alter rocks in the form of oxidation. Hyperspectral VNIR data could be used to identify bleached zones which may represent hydrocarbon seeps
-Determine thermal maturity of source rocks using VNIR, SWIR and TIR data by compiling vitrinite reflectance maps

Results:
- Khan and Jacobson (2008) have mapped bleached hydrocarbon seeps using VNIR-SWIR Hyperion (hyperspectral data.
- Rowan and others (1995) showed a relationship between vitrinite reflectance and reflectance. Using compound ratios they mapped thermal maturity using Landsat TM data in the Pieri Shale, Wyoming.

Science Issue:

How do changes in land composition affect coastal and inland aquatic ecosystems? [DS 25]

Tools:

HyspIRI VINIR, SWIR and TIR data

Approach:

VNIR data - map vegetation density and water turbidity

SWIR and TIR data – soil composition

Results:

Hubbard (2008) used ASTER VNIR, TIR, and ASTER data to map soil and vegetation characteristics of the Little Conestoga water shed. Farming practices expose large areas of smectite-rich soils venerable to erosion during periods of large storms and runoff.

MODIS image (04/09/00) of Chesapeake water shed during heavy rainfall. Yellow arrow illustrates location of increased sediment loading at the Little Conestoga water shed into the Susquehanna River and resulting sediment plume in the upper part of the Chesapeake Bay

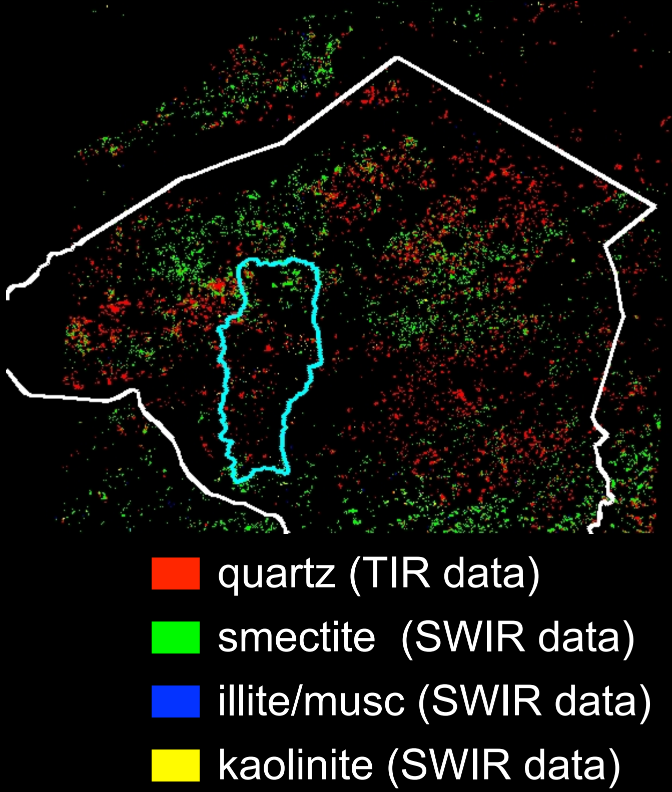

Endmember mapping of the Little Conestoga water shed area illustrates a large amount of smectite. Swelling clays tend to produce water impermeable crusts that increase runoff, rilling and gully development. The TIR and SWIR data allow for a more complete mineralogical analysis of the the soil including quartz, clays, carbonates and evaporites (Hubbard, 2008).

VNIR-SWIR LABORATORY SPECTRA AND RESAMPLED ASTER SPECTRA

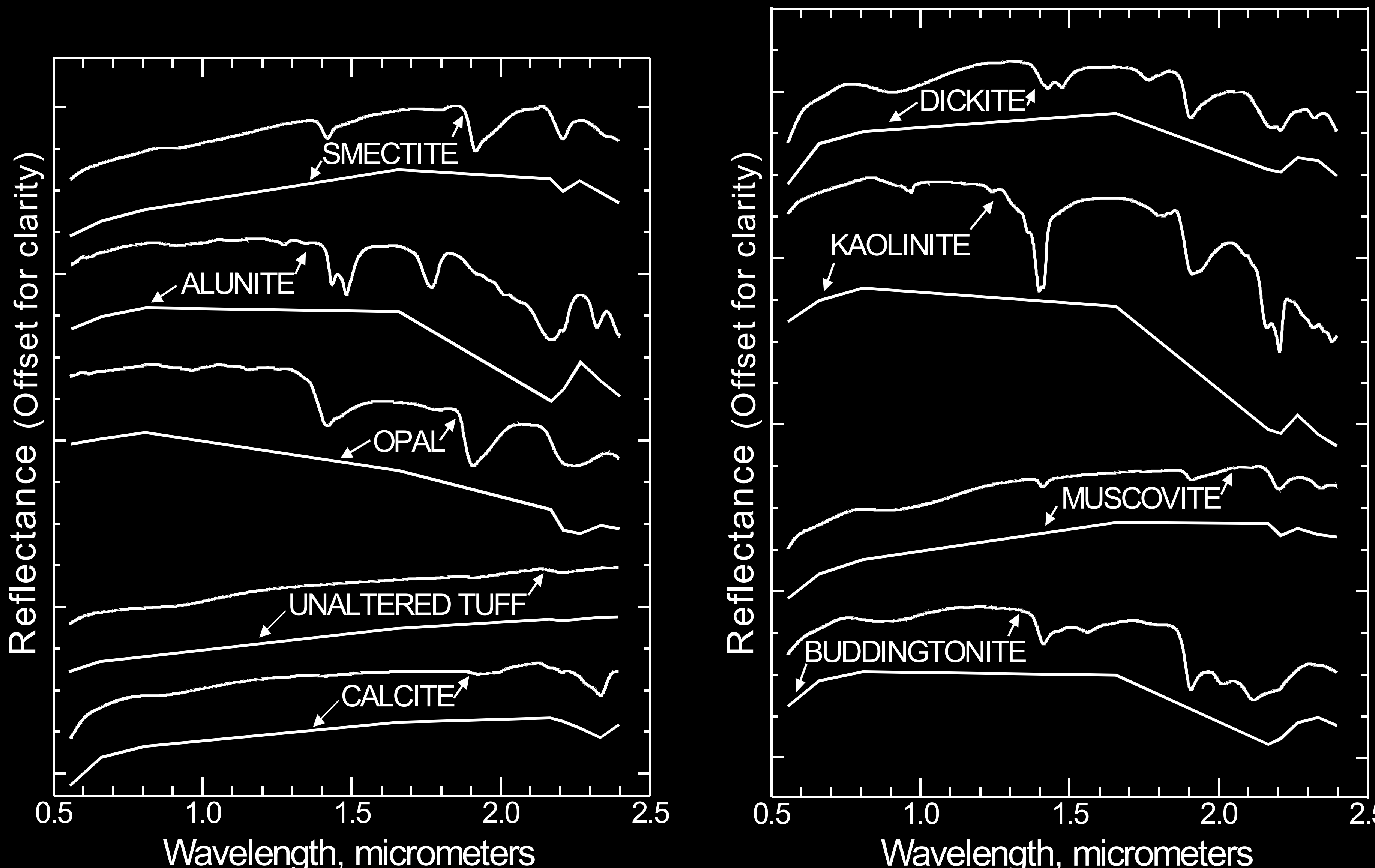

ASTER FALSE COLOR COMPOSITE IMAGE OF THE KHANNESHIN VOLCANO AREA

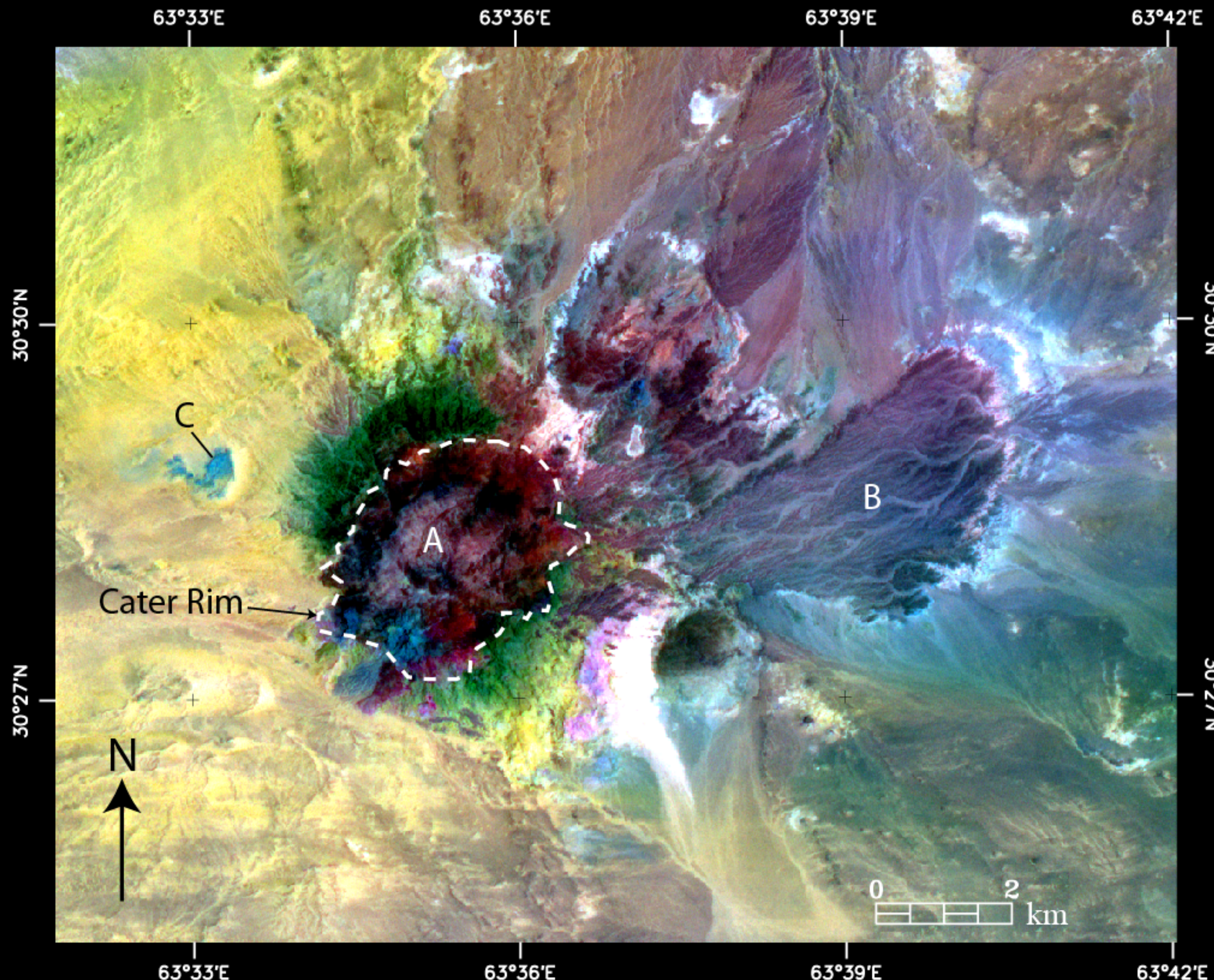

(RED = BAND 6, GREEN = BAND 3, BLUE = BAND 1)

(FROM, MARS AND ROWAN, 2011)

CARBONATITE VOLCANO - KHANNESHIN, AFGHANISTAN

DECORRELATION STRETCH OF ASTER TIR BANDS 13 -12-10

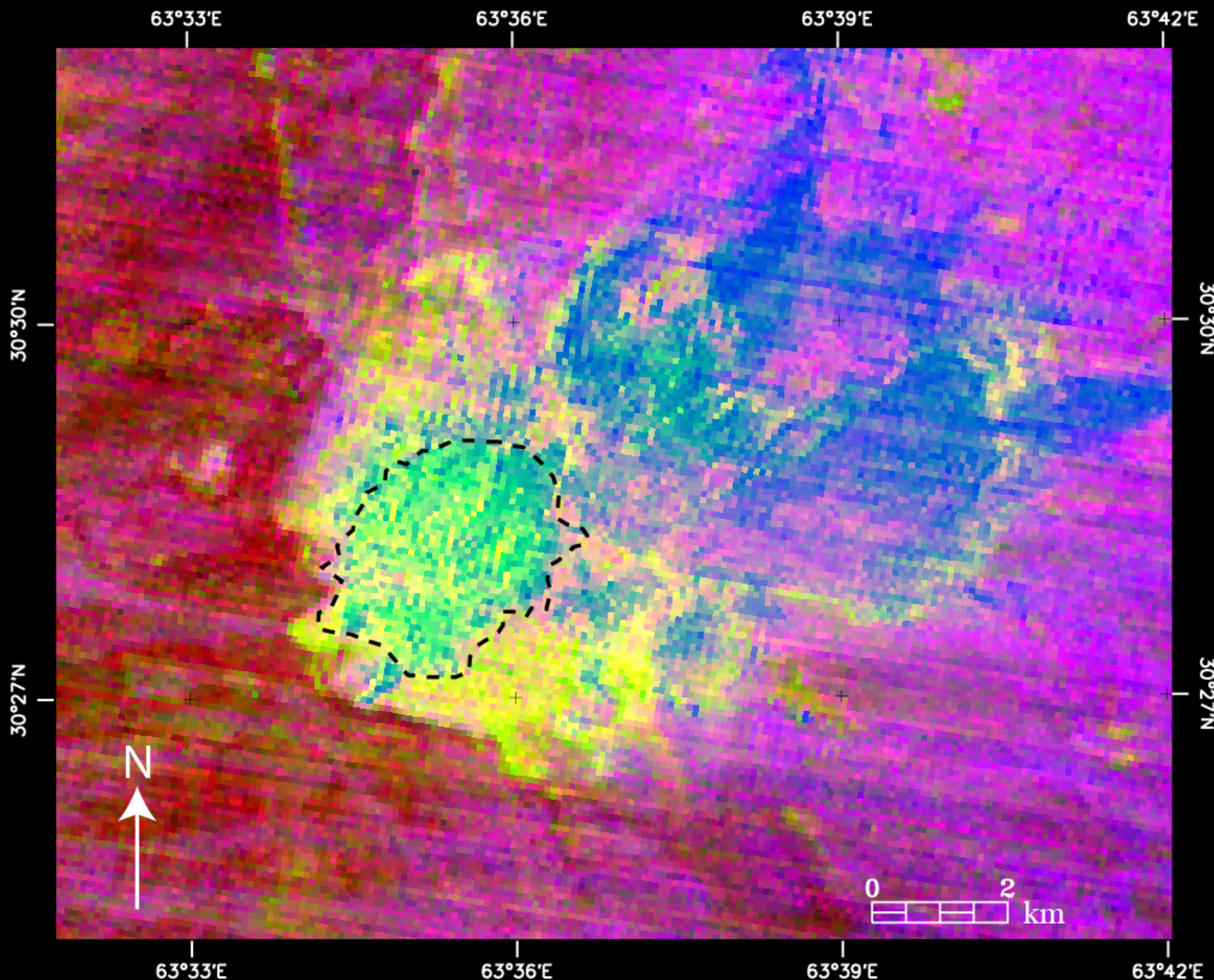

(FROM, MARS AND ROWAN, 2011)

REGIONAL MINERAL MAPPING

LOGICAL OPERATORS USED TO MAP MINERALS - HYDROTHERMAL SILICA-RICH

((float(b3)/b2)le1.55) and (b4gt2400) and ((float(b4)/b7)ge1.41) and ((float(b13)/b12)ge1.021)

(ge - greater than or equal to; gt - greater than; le - less than or equal to; float - floating point)

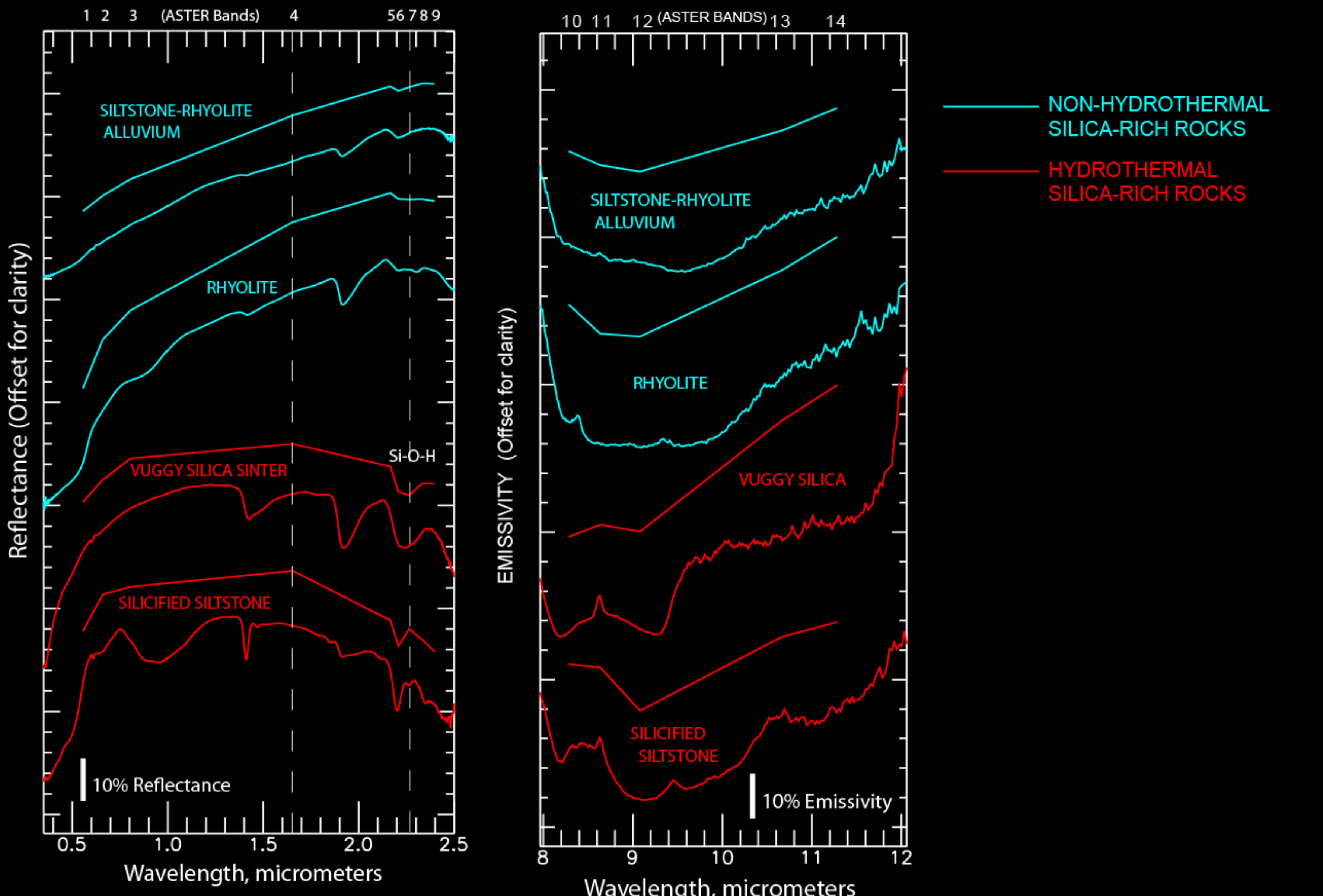

ASTER COVERAGE

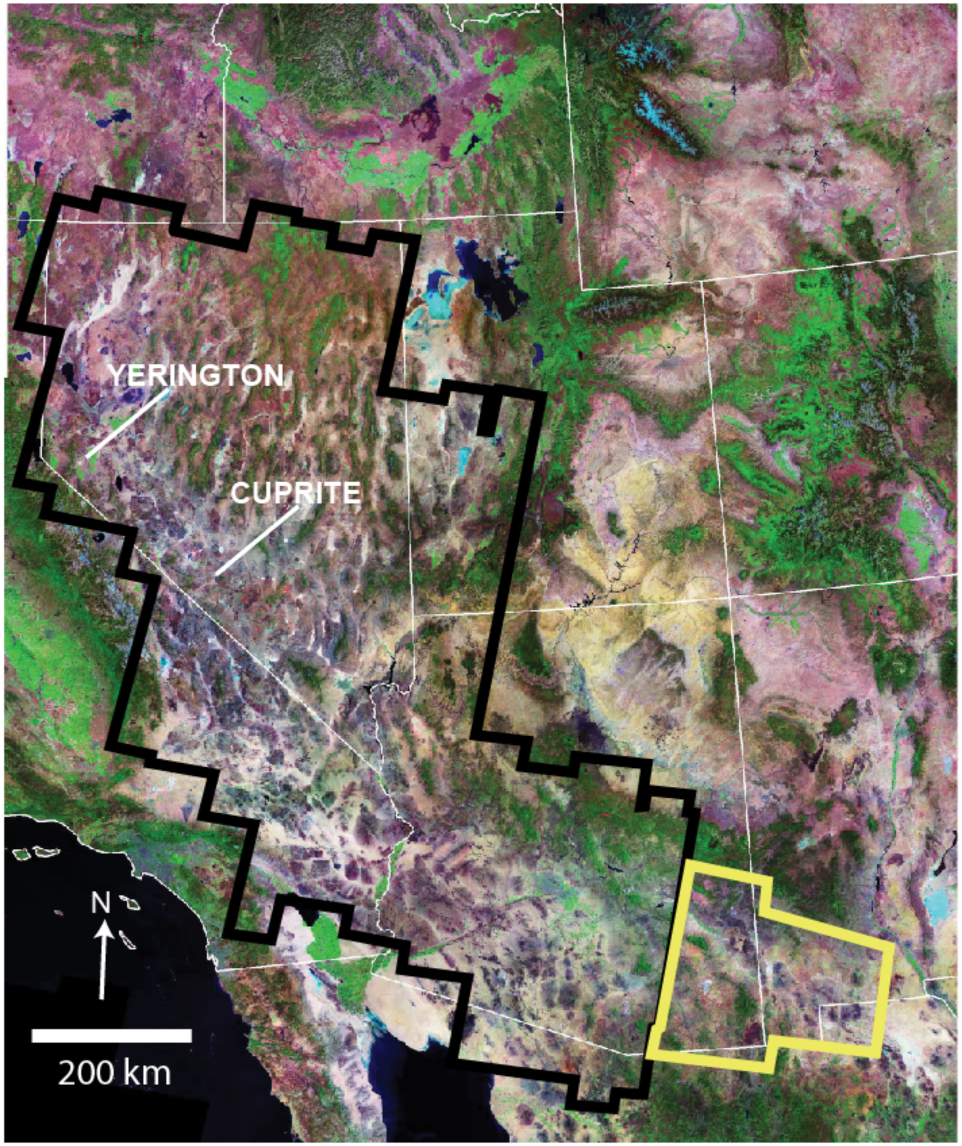

Landsat TM false color composite image (7=R, 4=G, 2=B) showing area mapped for hydrothermally altered rocks using ASTER data. Completed area outlined in black, area to be completed outlined in yellow, states are outlined in white.

ASTER MINERAL GROUPS MAP, BASIN AND RANGE

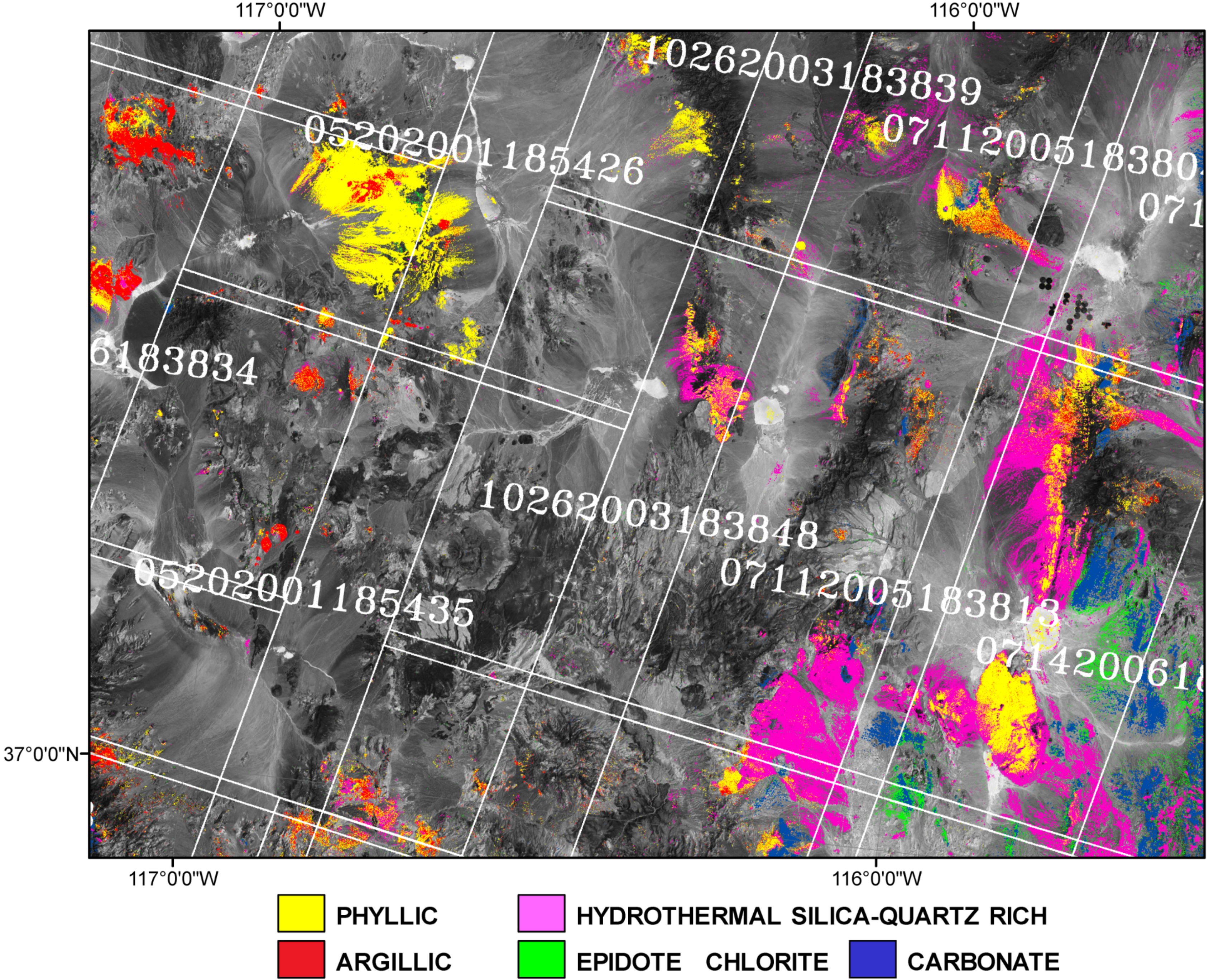

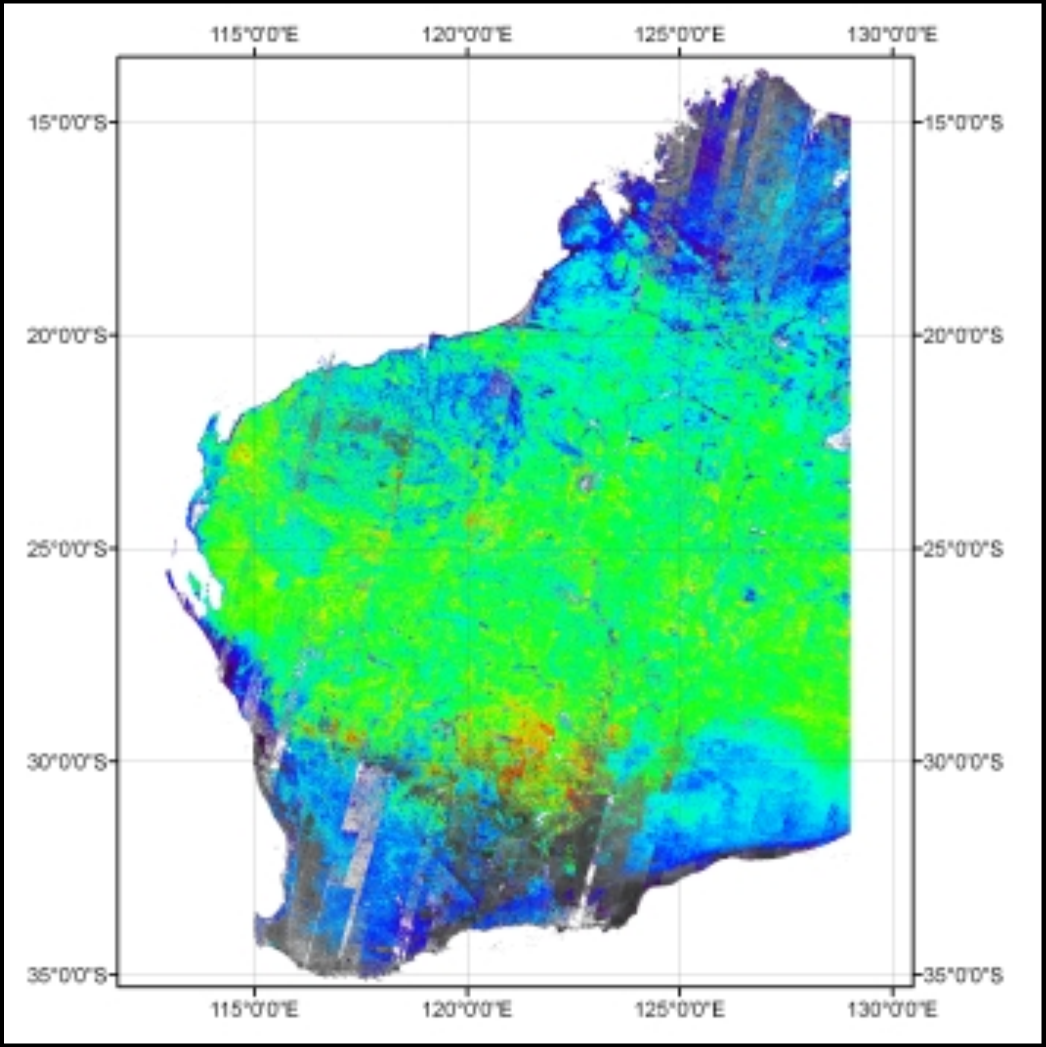

Satellite WA ASTER Geoscience map of iron oxide composition (blue: goethitic; red - hematitic).

GLOBAL SENSOR

NEED A UNIFORM MAPPING SYSTEM

NO INPUT – EXPERT SYSTEM – TETRATCORDER – LOGICAL OPERATORS – DÉCOR – BAND RATIOS (COLOR COMPOSITE)

INPUT – SPECTRA ? CONTROL FILE ?

Higher level products to support answering HyspIRI science questions: TQ1, TQ2, and CQ3

Robert Wright

Hawai'i Institute of Geophysics and Planetology, Honolulu

UNIVERSITY of HAWAI'I®
MĀNOA

TQ1. Volcanoes/Earthquakes

How can we help predict and mitigate earthquake and volcanic hazards through detection of transient thermal phenomena?

TQ1. How can we predict and mitigate earthquake and volcanic hazards through detection of transient thermal properties?

Science Issue:

•Volcanoes can exhibit idiosyncratic behaviors leading up to eruptions. For example, SO2 production can increase dramatically, or decrease dramatically. Thermal anomalies manifest themselves in many forms: crater lakes, fumaroles, domes, etc. Transient thermal anomalies may precede earthquakes. Systematic monitoring can provide potentially effective information to aid in predicting possible eruptions and improve earthquake forecasts.

Tools:

•Satellite observations from HyspIRI TIR; requires multispectral capability to separate volcano plume constituents; requires bands in 3-5um and 8-12um for temperature determinations in range -20 to 1200C

• Historical baseline of characteristic thermal and gas emission behavior for each volcano to compare with HyspIRI observations.

Approach:

•Schedule systematic day & night TIR observations with HyspIRI over several hundred up to 1000 active volcanoes.

• Implement automatic analysis algorithms to flag anomalous thermal or gas emission activity.

•Monitor potentially active faults with nighttime observations

Results:

• Unique, high spatial resolution TIR data from HyspIRI will improve our understanding of pre-eruption volcanic behavior; this will in turn lead to improvements in our ability to predict volcanic eruptions.

•Unique, high spatial resolution TIR data from HyspIRI will lead to improved earthquake forecasts.

TQ1a. Do volcanoes signal impending eruptions through changes in surface temperature or gas emission rates, and are such changes unique to specific types of eruptions?

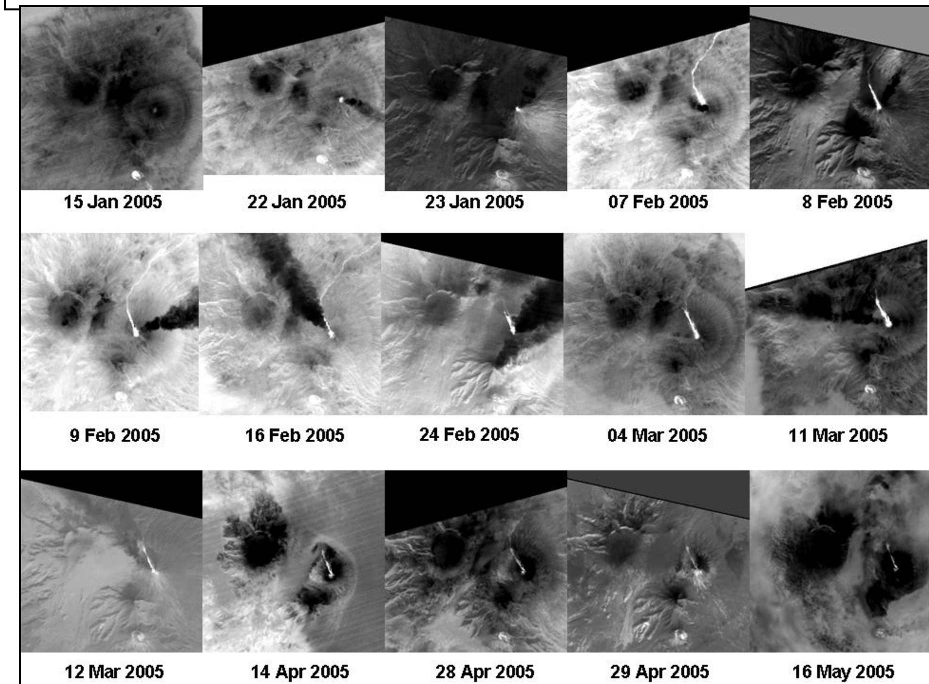

Kliuchevskoy and Bezymianny volcanoes in Siberia, observed by ASTER. 15 clear-sky nighttime observations in 5 months show changes in thermal behavior of summit domes, development of lava flows and pyroclastic flows, and presence of ash and SO2 plumes. Courtesy of M. Ramsey, U. Pittsburgh.

Science Issue:

•Volcanoes can exhibit idiosyncratic behaviors leading up to eruptions. For example, SO2 production can increase dramatically, or decrease dramatically. Thermal anomalies manifest themselves in many forms: crater lakes, fumaroles, domes, etc. Systematic monitoring can provide potentially effective information to aid in predicting possible eruptions.

Tools:

•Satellite observations from HyspIRI TIR; requires multispectral capability to separate plume constituents; requires bands in 3-5um and 8-12um for temperature determinations in range -20 to 100C

• Historical baseline of characteristic thermal and gas emission behavior for each volcano to compare with HyspIRI observations.

Approach:

•Schedule systematic day & night TIR observations with HyspIRI over several hundred up to 1000 active volcanoes.

• Implement automatic analysis algorithms to flag anomalous thermal or gas emission activity.

Results:

• Unique, high spatial resolution TIR data from HyspIRI will improve our understanding of pre-eruption volcanic behavior

• This will in turn lead to improvements in our ability to predict volcanic eruptions.

TQ1b: What do changes in the rate of lava effusion tell us about the maximum lengths that lava flows can attain, and the likely duration of lava flow-forming eruptions?

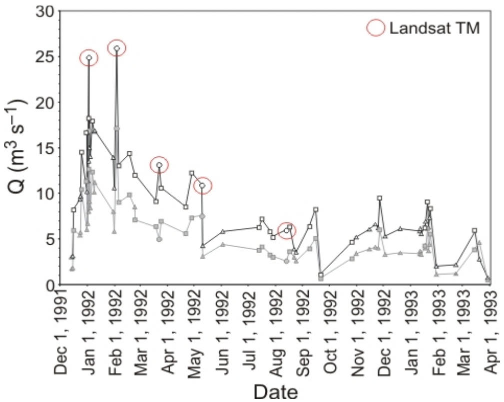

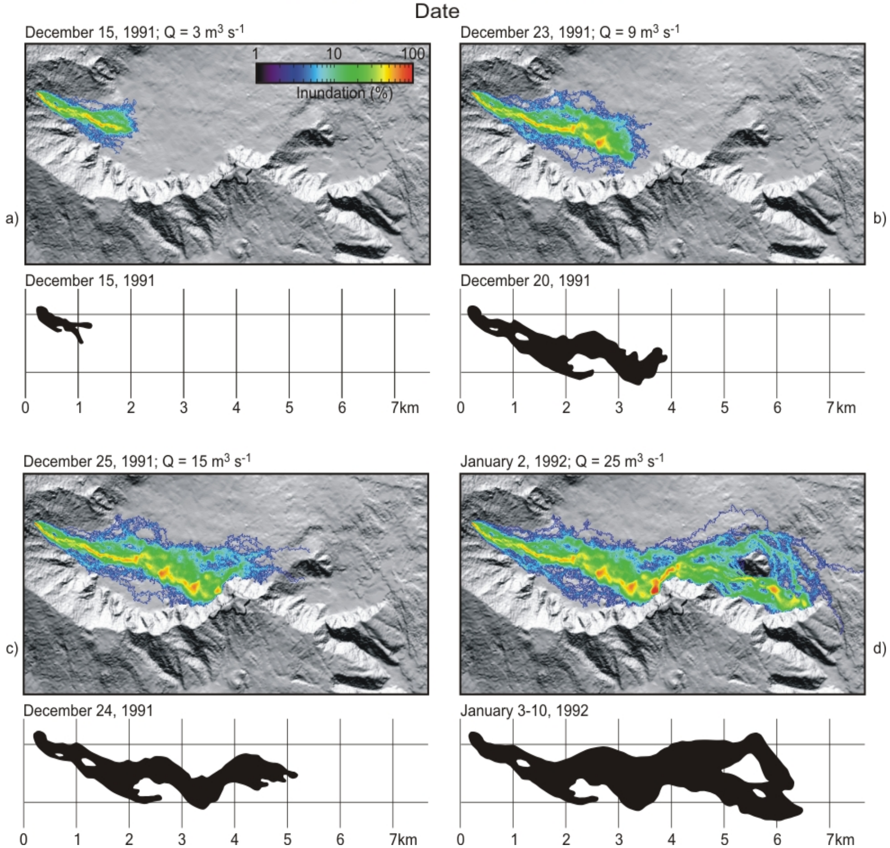

Wright et al. (2008). *Geophysical Research Letters,* 35, L19307.

Science Issue:

• After lava composition, the volumetric effusion rate (modulated by surface cooling) determines how far a lava flow can extend from the vent before it solidifies. Effusion rates vary dramatically during eruptions, but can be quantified using infrared satellite data (top left; AVHRR, ATSR and TM data). By acquiring high spatial resolution TIR data, HyspIRI will allow us to determine effusion rates twice every five days during a lava flow forming eruption for any volcano on Earth. These data can be used to drive numerical models that predict the hazards that these flows will pose

Tools:

• Satellite observations from HyspIRI TIR; requires band at ~4 μm (saturation temperature of ~1600 K) with moderate-high spatial resolution (<100 m) for determining the area of active lava at any given time during as eruption and estimating the radiant energy flux from the flow surface.

• Pre-HyspIRI DEMs (e.g. SRTM) of all volcanoes likely to erupt basaltic lava flows

• Time-series of effusion rates determined using higher temporal resolution MODIS data for calibration.

Approach:

• Implement automatic analysis algorithms to flag anomalous thermal activity, determine active lava area and thermal flux, and, subsequently, a HyspIRI-derived effusion rate. Using this, a DEM, the vent location as recorded in the HyspIRI data, and a numerical lava flow model, generate simulations of likely lava flow paths for the given effusion rate. Autonomously update the hazard simulation as most recent HyspIRI derived effusion rates become available (lower left).

Results:

• A global, near-real-time lava flow hazard assessment tool, driven by HyspIRI TIR data.

What do the transient thermal infrared anomalies that may precede earthquakes tell us about changes in the geophysical properties of the crust?

Science Issue:

- Prior to major earthquakes, the build-up of stresses deep below can manifest itself in the emission of spectroscopically distinct, narrow non-thermal IR bands. When volcanoes become activated, they are expected to exhibit the same type of non-thermal IR emission before the arrival of a thermal pulse at the surface.

Tools:

- Satellite observations; Narrow bands in the 10.7-12.5 μm range.

Approach:

- Schedule repetitive observation. Difference spectra.

Results:

- Spectroscopically distinct non-thermal IR bands can appear before earthquakes, mixing with the thermal signature. Same for volcanoes.

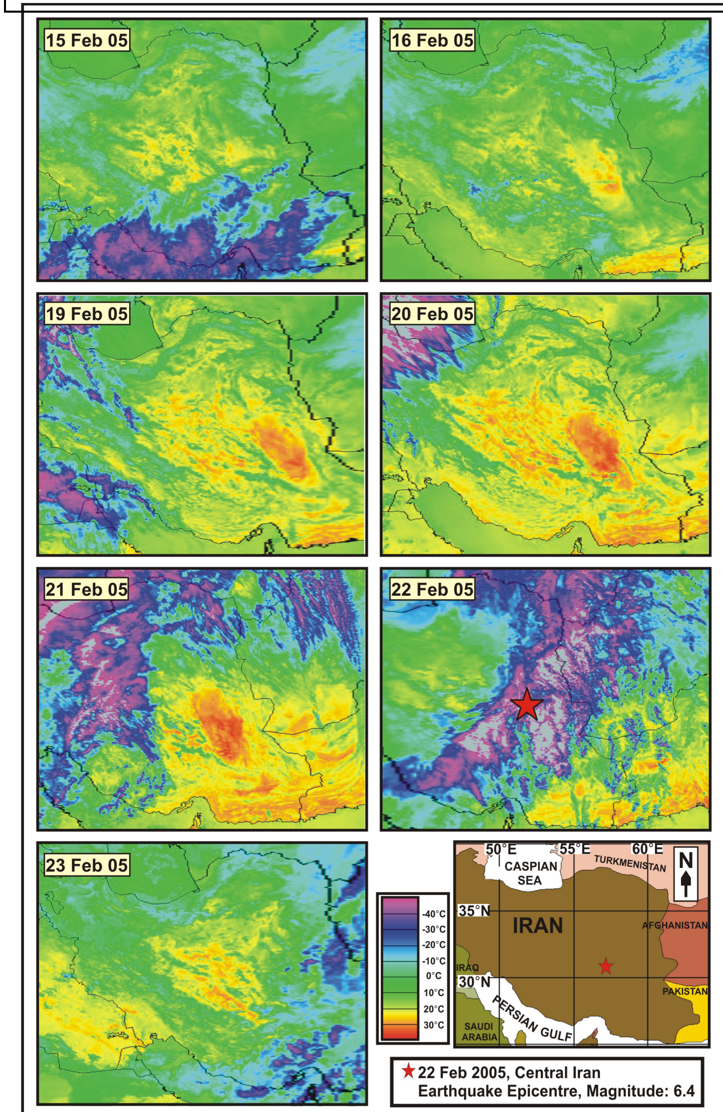

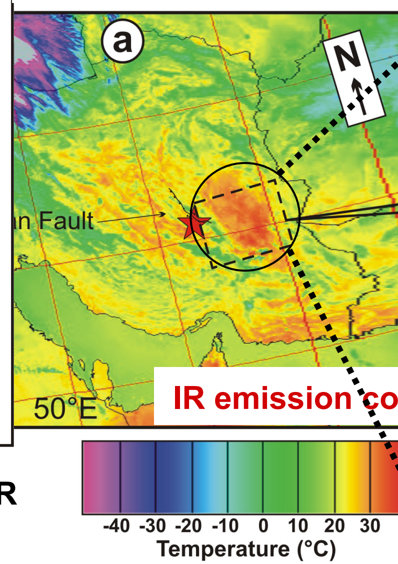

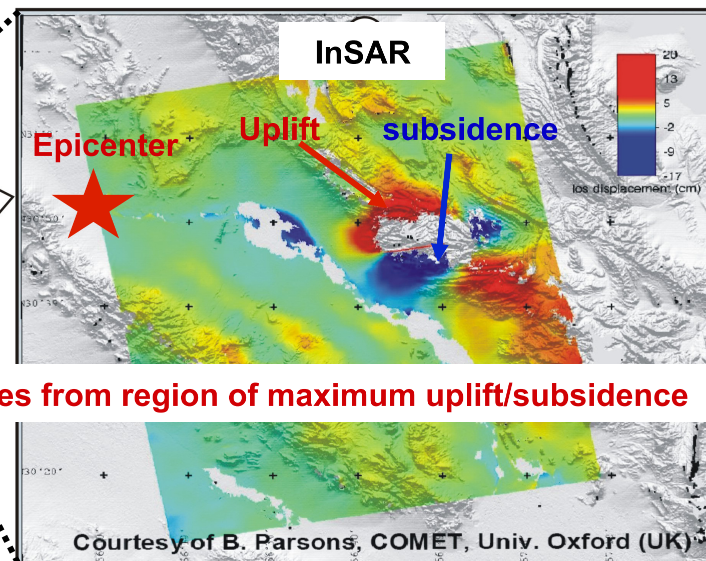

IR emission comes from region of maximum uplift/subsidence

M=6.4 earthquake in Iran 22 Feb. 2005
Good viewing conditions
(similar to Southern CA)

AVHRR

courtesy Saraf et al. 2008

TQ1d: What are the characteristic dispersal patterns and residence times for volcanic ash clouds and how long do such clouds remain a threat to aviation?

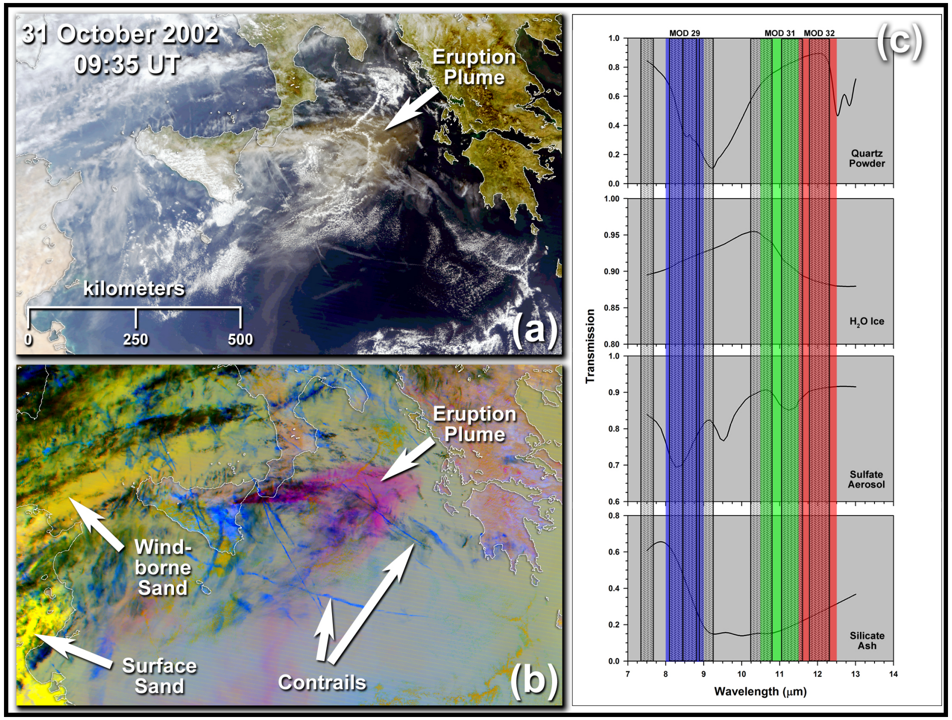

Detection of Eruption Plumes in the Thermal Infrared (TIR)

(a) MODIS true-color composite of data acquired over Mount Etna illustrating the difficulty of distinguishing a plume from surrounding meteorological clouds; (b) False-color composite of MODIS TIR data (Ch. 29, 31, 32 displayed in blue, green, and red, respectively) illustrating the unique spectral signatures of the eruption plume (silicate ash), jet contrails (ice), and windborne sand; (c) Model transmission spectra for silicate ash, sulfate aerosol, ice, and quartz powder (representing sand). The blue, green, and red color bars represent MODIS Ch. 29, 31, and 32, respectively; the shaded bars represent the proposed HyspIRI TIR channels. HyspIRI will have three channels in place of MODIS Ch. 29 and three channels in place of MODIS Ch. 31 and 32, enhancing our ability to detect and track eruption plumes and clouds.

Science Issue

The ash plumes generated by explosive volcanic eruptions pose a significant hazard to jet aircraft. Current air traffic protocol is to clear the airspace in the vicinity of the erupting volcano, but the ash plumes may be transported hundreds to thousands of kilometers from their sources. The use of true-color images to discriminate volcanic plumes from meteorological (met) clouds, and other suspended aerosols and particulates, is problematic (Panel (a), at left).

Tools

•HyspIRI multispectral TIR image data, 5-day revisit cycle (daytime acquisitions) at equator, spatial resolution of 60 m, and spectral channels as shown in Panel (c) (at left).

•Profiles of atmospheric temperature and water vapor, measured with radiosondes and spaceborne sounding instruments or model predictions.

•Radiative transfer model to predict radiance at the sensor given atmospheric profiles, length of optical path, and surface temperature, emissivity, and elevation (provided by DEM).

Approach

•Develop Internet portal to provide interactive plume analysis tools and on-demand modeling.

•Statistics-based enhancement of spectral contrast to discriminate eruption plume from met clouds (Panel (b), at left).

•Radiative transfer-based analysis tools to confirm presence of eruption plume and materials derived from plume

Results

On-demand detection and tracking of eruption plumes via Internet portal, with 2 (1 day + 1 night) HyspIRI revisits per 5 day cycle at equator, and more frequent coverage at higher latitudes.

TQ2. Global Biomass Burning

What is the impact of global biomass burning on the terrestrial biosphere and atmosphere, and how is this impact changing over time?

TQ2a: How are global fire regimes (fire location, type, frequency, and intensity) changing in response to changing climate and land use practices? [DS 198]

MODIS active fire detections 2000-2006 for Southern California

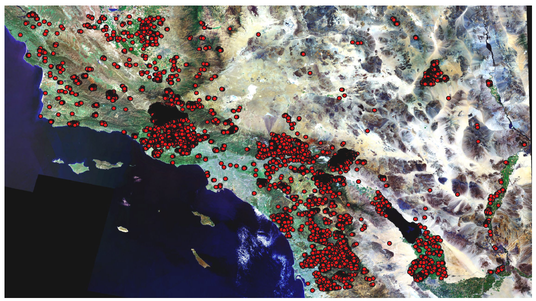

2001-2004 mean annual burned area derived from Terra MODIS active fire observations (top) and accompanying one-sigma uncertainties (bottom), expressed as fraction of grid cell that burns each year. From Giglio et al. (2005), *Atmos. Chem. Phys. Discuss.*, 5, 11091-11141

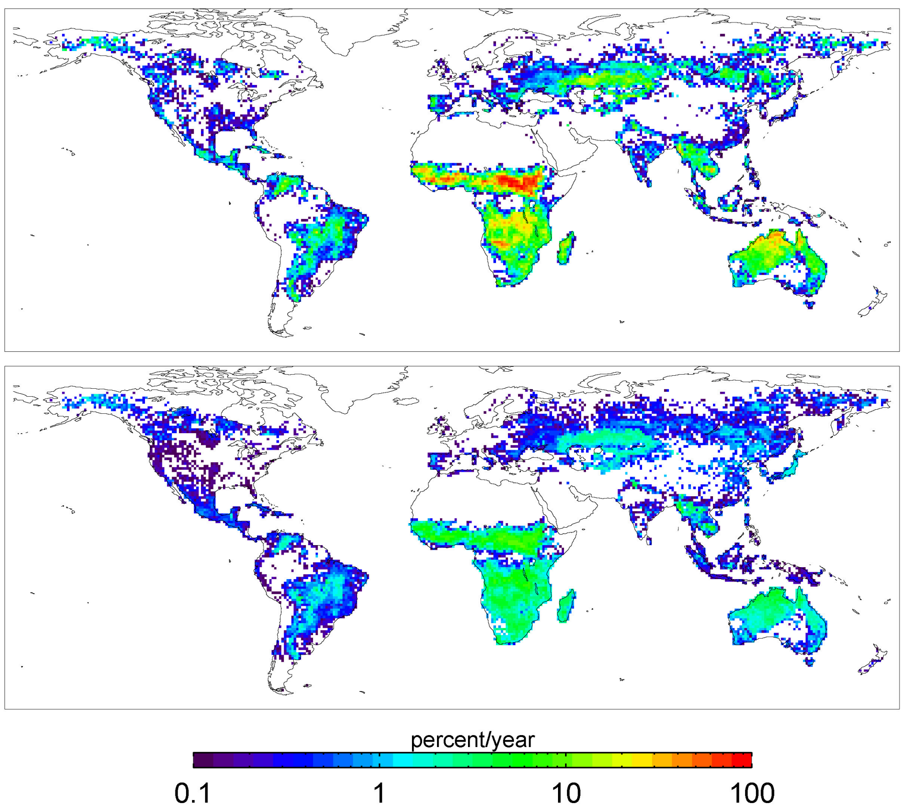

- Science issue
  Fire regimes vary considerably on a regional and global scale. Mapping fire location, type, frequency, and intensity at different times can contribute to an understanding of how they are affected by a changing climate and land use patterns.

- Tools
  Requires long-term regional or global data sets of thermal infrared imagery (low and normal gain channels at 4 and 11 μm). HyspIRI TIR data has a significantly improved capability of mapping flaming and smoldering fires. HyspIRIs greatly expanded spatial and temporal coverage can provide large sample sizes. Requires further pre-fire and post-fire thematic maps of climate variables and land use.

- Approach
  The HyspIRI thermal infrared data will provide large samples of detailed fire characteristics that are useful for statistical modeling of fires and their behavior. The database of fire detections can be analyzed in conjunction with thematic data sets of climate and land use.

TQ2b: Is regional and local fire frequency changing? [DS 196]

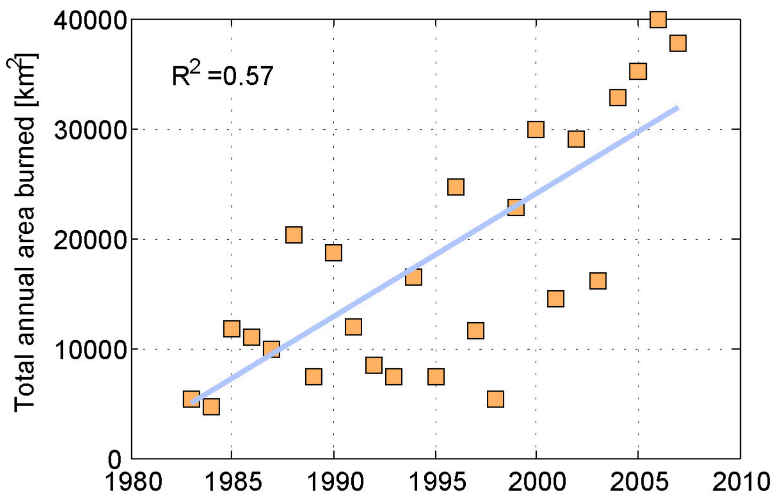

Total annual area burned in the United States 1983-2007. From Schneider (2008). Data from National Interagency Coordination Center

Precentage of total surface areas of each cell burned in the year 2000

From http://www-tem.jrc.it/Disturbance_by_fire/activities/occurglobal.htm

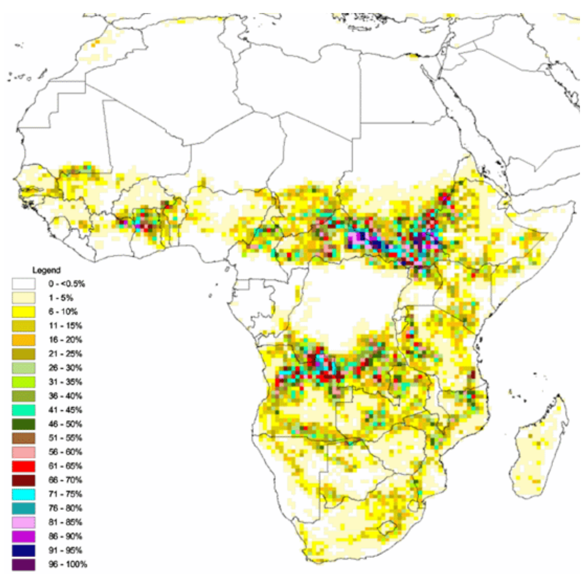

- Science Issue
  A warming climate has the potential for increased fire activity and more severe fires. Statistics show an increase in burned area in some regions but more accurate detection of fire events, in particular fire size, is necessary

- Tools
  Requires accurate detection of all fire types, including small agricultural fires and smoldering fires as small as ~10 sqm in size (difficult with coarser resolution sensors) and very hot fires, which often saturate existing sensors.
  HyspIRI TIR data has a greatly expanded spatial and temporal coverage compared to previous sensors, thus allowing for improved global fire mapping.
  Requires historical context from other sensors with measurement intercalibration to establish a baseline

- Approach
  Use HypsIRI TIR imagery to develop a comprehensive database of global fire events and compare with existing data sets of fire occurrence to determine trends in fire activity

TQ2c: What is the role of fire in global biogeochemical cycling, particularly trace gas emissions? [DS 195]

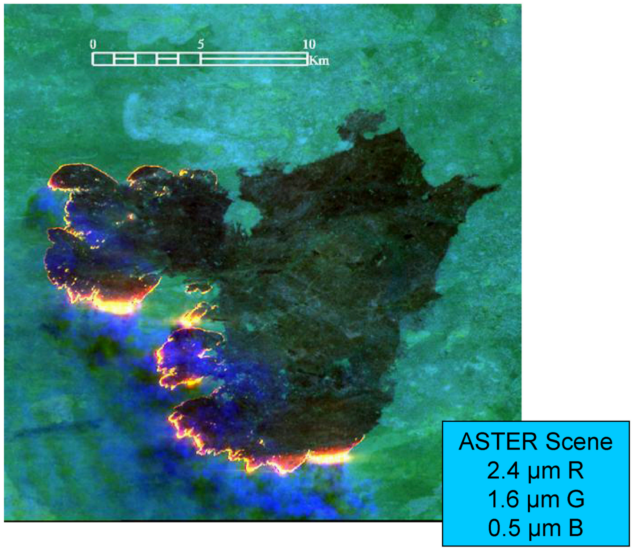

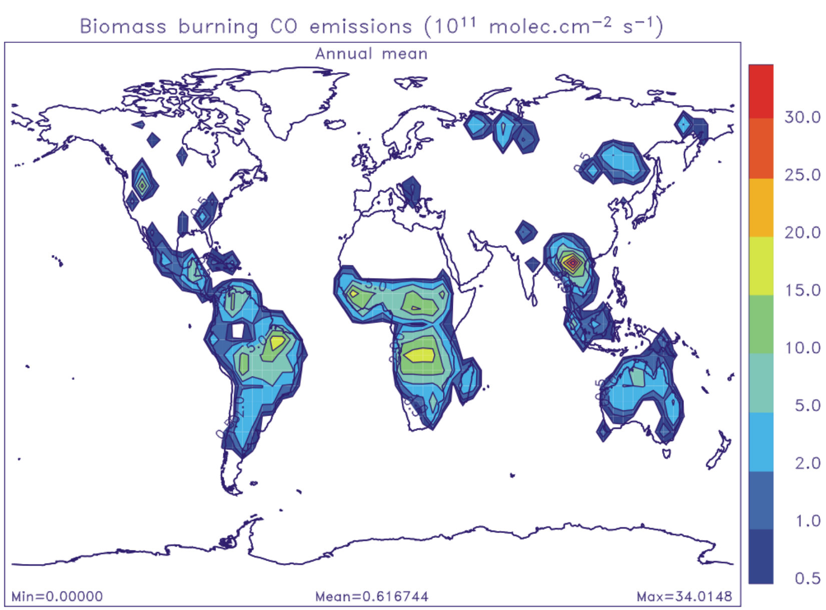

http://www.aeronomie.be/tropo/models/models_a_priori_emissions.htm

- Science issue
  Emissions from fires, such as carbon, carbon dioxide, carbon monoxide, methan, nitrogren oxides, particulate matter etc, affect the atmosphere on a local, regional and global scale. However, quantifying and modeling the impacts of such emissions is challenging and more detailed satellite imagery of fires, such as provided by HyspIRI, can contribute to this task.

- Tools
  Requires accurate fire detection including small and smoldering fires, fire monitoring, mapping of burn severity, and delineation of burned area. HyspIRI TIR data can detect fires as small as ~10 sqm in size. Also requires accurate measurements of fire temperature and fire area, as well as a fuel fire modeling element.

- Approach
  Use systematically acquired HyspIRI TIR data to develop a regional database of fire occurrence and characteristics of individual fire events. Model trace gas emission using the obtained fire characteristics

TQ2d: Are there regional feedbacks between fire and climate change?

HyspIRI can provide a more detailed database of fire events than traditional sensors (here the MODIS Active Fire Product)

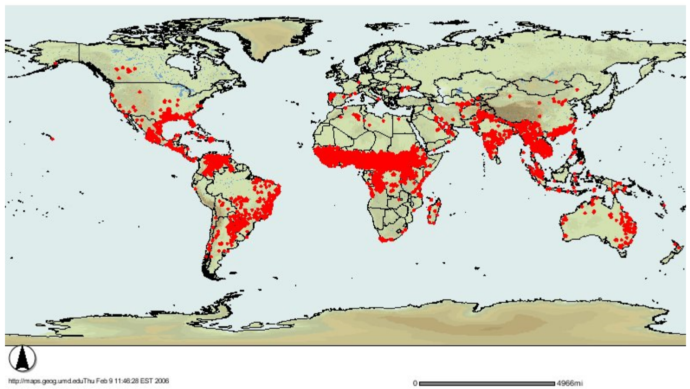

http://maps.geog.umd.edu/images/modis_fire_global.jpg

Regional climate models are improving and can be used in conjunction with a fire database to investigate potential feedbacks

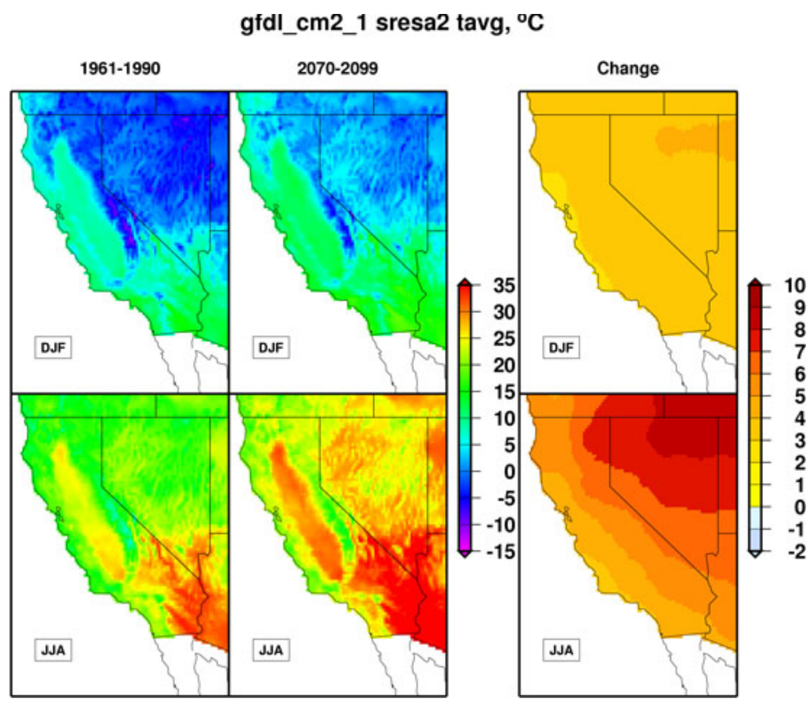

http://meteora.ucsd.edu/cap/images/CA_gfdl_cm2_1_sresa2_delta_tavg_1961_2070.jpg

- Science issue
  Regional and global fire activity has the potential to affect regional climate, in particular through impacts on atmospheric transmission. Furthermore, climate change has the potential to affect regional fire regimes.

- Tools
  The objectives for this task are mapping of the extent of the fire front and the confirmation of burn scars. Such measurements require the detection of flaming and smoldering fires as small as ~10 sqm in size
  Requires satellite observations from HyspIRI, in particular its multispectral TIR capability to detect fires and monitor fire activity, as well as mapping fire temperature and fire area. Further requires information on pre-fire vegetation cover, fuel condition and fuel load, as well as output from regional climate models.

- Approach
  Use systematically acquired HyspIRI TIR data to develop a regional database of fire occurrence and characteristics of individual fire events. Compare changes in regional fire activity with observed climate variables and with the output of regional climate models

CQ3. Volcanoes

Do volcanoes signal impending eruptions through changes in the temperature of the ground, rates of gas and aerosol emission, temperature and composition of crater lakes, or health and extent of vegetation cover?

CQ3: Do volcanoes signal impending eruptions through changes in the temperature of the ground, rates of gas and aerosol emission, temperature and composition of crater lakes, or health and extent of vegetation cover?

Left: Ground–based thermal image of the active lava dome at Sourfiere Hills volcano, Montserrat. Variations in thermal and gas flux from other lava domes have been shown to exhibit a cyclicity that is related to the periodic generation of explosive overpressures in the shallow conduit.

Left: Crater lake at Maly Semiachik, Kamchatka. Variations in the temperature, area, and color of crater lakes has been observed to change prior to significant changes in volcanic unrest

Science Issue:

• The replenishment of a shallow magma reservoir can herald a) the onset of an eruption at a previously inactive volcanic system or, b) significant changes in eruptive behavior at already active volcanoes. Rising magma ultimately results in a flux of volatiles (such as SO_2), particulate matter, and/or thermal energy, onto Earth's surface and into it's atmosphere. Detecting and characterizing these fluxes, and the indirect effects that they have on, for example, the health of local vegetation and the thermo–physical properties of volcanic crater lakes, is important for both basic science (as a means for quantifying aspects of magma ascent dynamics and shallow conduit processes) and hazard managers (for recognizing significant changes in a volcano's behavior and predicting volcanic hazards).

Tools:

• Moderate resolution (*i.e.* Landsat/ASTER class) data from the HyspIRI VSWIR and TIR instruments.
• In–situ observations to calibrate HyspIRI–derived measurements
• Published physical, geochemical, and field–based models of volcanic processes that will use the HyspIRI–derived measurements as input or for calibration/validation.
• Historical observational baseline, compiled over decadal time–scale via previous remote sensing missions, to place the HyspIRI observations in temporal context.

Approach:

• Develop and implement algorithms to extract key physical parameters (SO_2 flux, heat flux) from HyspIRI' s VSWIR/TIR data. Develop algorithms for detecting surface compositional changes that may signal an increase in volcanic unrest.

CQ3a: What do comparisons of thermal flux and SO_2 emission rates tell us about the volcanic mass fluxes and the dynamics of magma ascent? (DS 227; 230)

Oppenheimer et al. (2004) *Geology*, 32, 509-512.

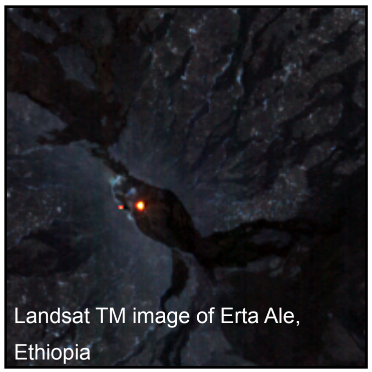

Landsat TM image of Erta Ale, Ethiopia

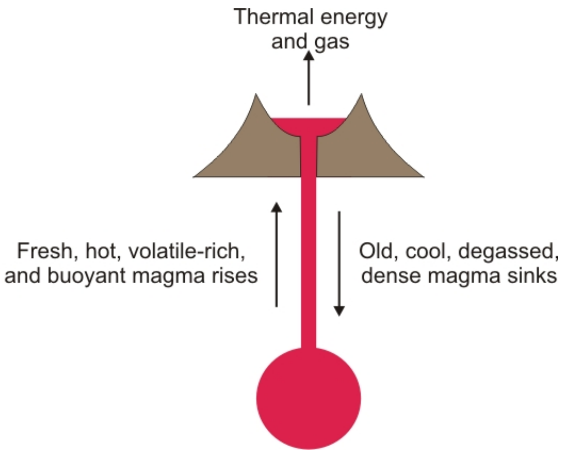

Francis et al. (1993). *Nature,* 366, 554-557.

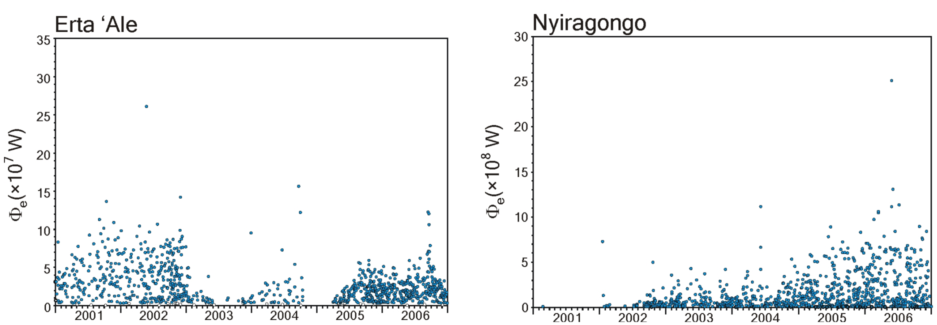

Wright & Pilger (2008). *J. Volcanol. Geotherm. Res.*, 177, 687-694.

Science Issue:

• The flux of gas and thermal energy from a volcano can be used to determine the mass of magma required to balance those fluxes. Over what time scales do mass fluxes at Earth's volcanoes vary and by how much? Does this vary as a function of tectonic setting? During ascent, how is magma partitioned between the surface (the erupted component) and the subsurface (the degassed but not erupted component)?

Tools:

•Requires multispectral TIR capability to detect, quantify, and monitor SO_2 flux. Requires hyperspectral VSWIR data as well as multispectral data in the 4 μm (saturation temperature of ~1600 K) and 8–12 μm (ideally, at least one band with a measurement temperature of ~800 K) regions for determining lava surface temperatures. This latter measurement will be used to determine the thermal flux at the magma/atmosphere interface.

• Published geochemical and enthalpy models relating these fluxes to the volume of magma cooled and degassed.

• Knowledge of local wind field and volcano altitude to aid computation of SO_2 flux.

• Historical baseline of characteristic thermal (*e.g.* from MODIS, lower left) and gas emission behavior for each volcano to provide multi–year/decadal context for the HyspIRI observations.

Approach:

• Use systematically acquired day and night VSWIR and TIR observations for several basaltic volcanoes that exhibit persistent lava lake activity (*e.g.* Erta Ale, Nyiragongo) and several volcanoes that frequently produce basaltic lava flows (*e.g.* Etna, Piton de la Fournaise).

• Field campaign to acquire in–situ SO_2 and thermal flux data at a single target for calibration purposes.

CQ3b: Does pressurization of the shallow conduit produce periodic variations in SO_2 flux and lava dome surface temperature patterns that may act as precursors to explosive eruptions? (DS 50; 227; 230)

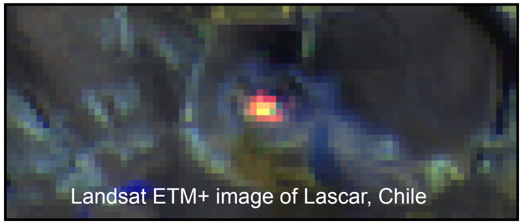

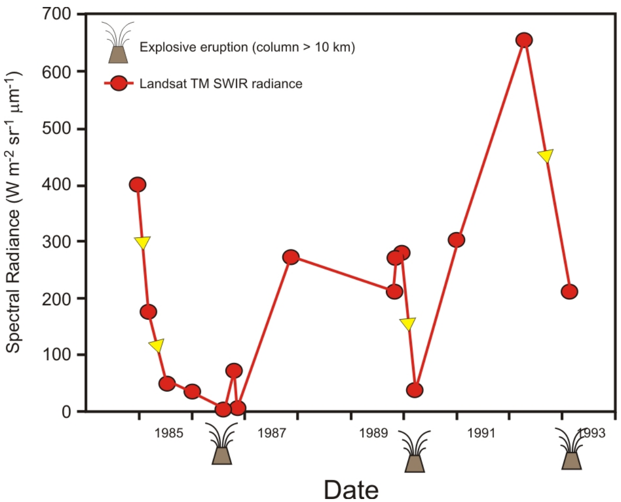

Oppenheimer et al. (1993), *J. Geophys. Res.*, 98, 4269-4286.

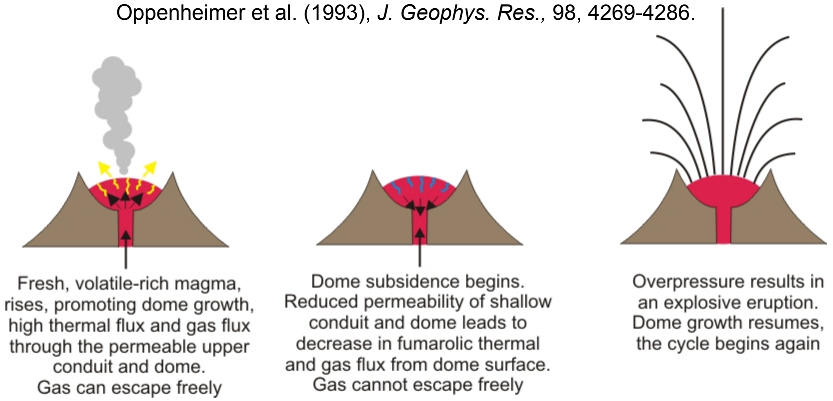

Matthews et al. (1997), *Bull. Volcanol.*, 59, 72-82.

Science Issue:

• Cyclicity is increasingly recognized as characteristic of explosive silicic dome–forming volcanoes. Precipitous drops in SWIR radiance detected by Landsat TM from Lascar's summit crater during the 1980s and 1990s were followed by significant explosive eruptions (middle left). A model, based on field observations, has been proposed to explain these cycles (bottom left). Explosive overpressure results when gas cannot escape freely from the shallow conduit resulting in a decreased gas flux *and* decreased abundance of high temperature fumaroles on the dome surface. Can we use HyspIRI to recognize similar patterns, at other potentially explosive volcanoes?

Tools:

• Satellite observations from HyspIRI. Requires multispectral TIR capability to detect and monitor SO_2 degassing rates over time; requires hyperspectral VSWIR data as well as multispectral data in the 4 μm (saturation temperature of ~1600 K) and 8–12 μm (ideally at least one band with a measurement temperature of 800 K) regions for determining the abundance of high temperature fumaroles on dome surfaces and how this changes through time.

Approach:

• Use systematically acquired day and night VSWIR and TIR observations for a subset of active volcanoes known to host silicic lava domes (*e.g.* Popocatepetl, Soufriere Hills Volcano) to determine temporal changes in degassing rate and the surface temperature characteristics of active lava domes.

• Use historic archive of thermal flux data from MODIS to place the HyspIRI observations in temporal context.

CQ3c: Can measurements of the rate at which lava flows cool allow us to improve forecasts of lava flow hazards? (DS 50; 226)

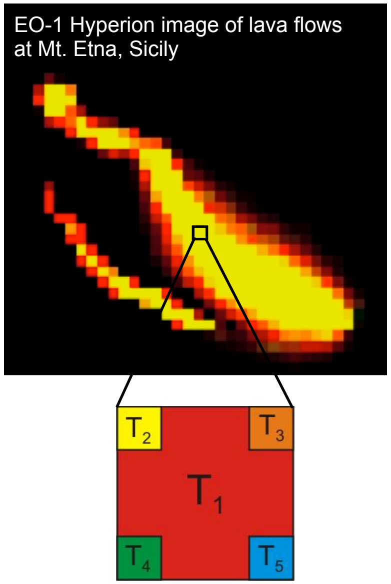

$$L(\lambda) = \sum_{i=1}^{n} f_i L(\lambda, T_i)$$

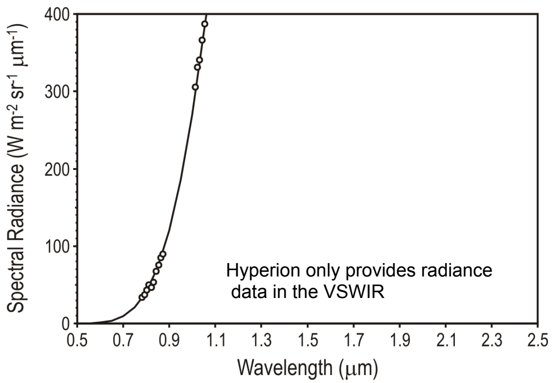

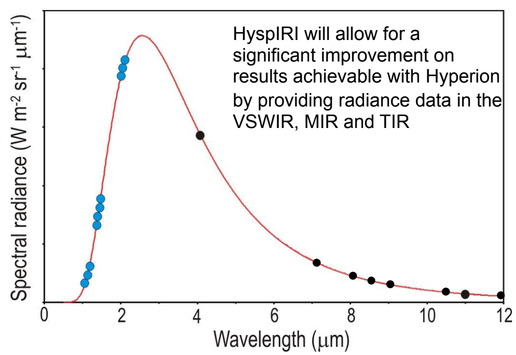

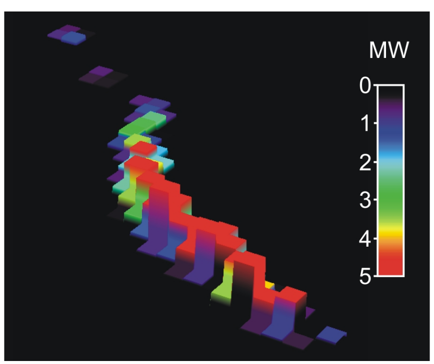

Radiant cooling of the active lava channel shown above, determined from the EO-1 Hyperion VSWIR imaging spectrometer

Science Issue:

• The rate at which a lava flow cools exerts a fundamental control on the distance from the vent at which it solidifies. The surface temperature of an active lava flow, and how this vary spatially and temporally, is therefore key information for parameterizing and validating numerical models that forecast lava flow hazards.

Tools:

• Satellite observations from HyspIRI. Requires hyperspectral VSWIR data as well as multispectral data in the 4 μm (saturation temperature of ~1600 K) and 8–12 μm (ideally, at least one band with an upper measurement temperature of 800 K) regions for un–mixing the sub–pixel radiative components of active lava flow surfaces (left). These temperature data can be used to estimate energy fluxes from flow surface and subsequently, lava cooling rates (left).

• Published numerical models of lava flow motion which will take the HyspIRI–derived temperature/cooling data as an input.

• Heat flux estimates derived from simultaneously acquired high temporal/low spatial resolution sensors (*e.g*. MODIS) as both a point calibration and to assess the short time scale variability of heat fluxes during eruptions.

Approach:

• Schedule nighttime VSWIR and TIR observations during eruptions that produce basaltic lava flows. Systematic nighttime VSWIR and TIR acquisitions for high priority volcanoes that frequently erupt lava flows (*e.g*. Kilauea, Etna, Piton de la Fournaise). Potential application for the JPL volcano sensor web and U. Hawaii's low resolution MODVOLC global volcano monitoring system as a means to autonomously perform the tasking for other volcanoes that erupt lava flows less frequently (*e.g*. Fernandina, Galapagos).

CQ3d: Does the temperature and composition of volcanic crater lakes change prior to eruptions? (DS 226; 227).

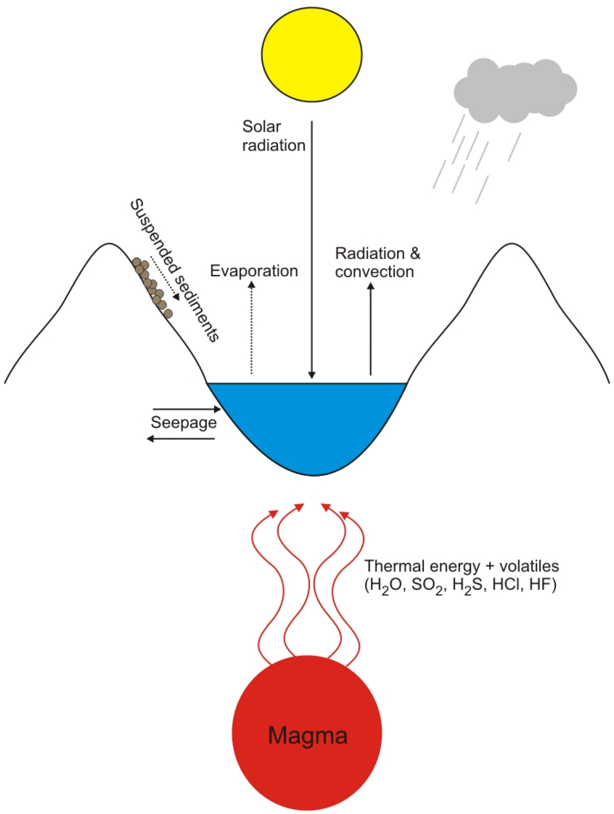

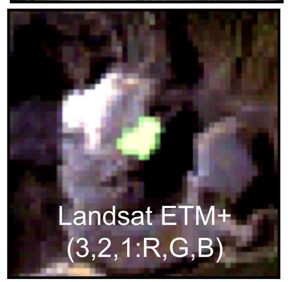

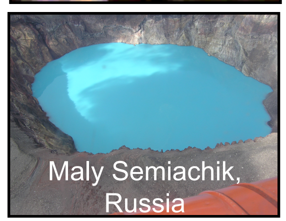

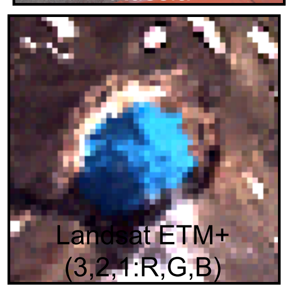

Science Issue:

• Some 100 Holocene active (*i.e.* within the last 10,000 years) volcanoes host crater lakes. These lakes act as chemical condensers and calorimeters that allow us to quantify energy and chemical fluxes from their associated magma bodies. Several eruptions have been observed to follow increases in lake water temperature. Variations in water color can result from increased suspended sediment content (caused by elevated seismicity and turbidation due to degassing through lake floor sediments), and changes in scattering properties due to changes in chemical composition. HyspIRI's TIR and VSWIR instruments will allow us to monitor these volcanoes to identify changes in the temperature, area, and color of volcanic crater lakes for changes that may indicate enhanced volcanic unrest.

Tools:

• HyspIRI's VSWIR (for quantifying lake color and area) and TIR (two bands in the 8–12 μm region) for monitoring lake water surface temperature.

• Published enthalpy models of crater lake systems to be used as the basis for converting lake water temperatures to thermal fluxes.

Approach:

• Systematic day (VSWIR) and day and night (TIR) observations of 100 Holocene active volcanoes know to host crater lakes.

• Field campaigns (Poas volcano, Costa Rica) to acquire ground based VSWIR spectra and thermal camera data for calibration purposes.

CQ3e: Do changes in the health and extent of vegetation cover indicate changes in the release of heat, gas, and ash from crater regions? (DS 230; 231)

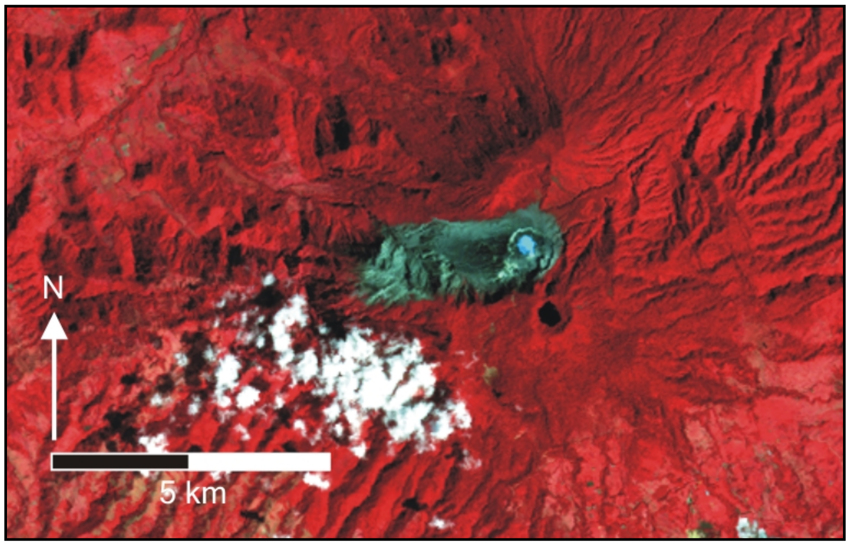

Landsat TM, Poas volcano, Costa Rica

Science Issue:

• Gaseous and particulate emissions from active volcanoes adversely impact surrounding ecosystems. SO_2 quickly converts to sulfuric acid aerosol, deposition of which is harmful to both humans and vegetation (left). Fluorine, adsorbed onto ash particles which may be distributed over a wide geographic area, is detrimental to both human and animal physiology. HyspIRI's VSWIR and TIR instruments will allow us to monitor SO_2 fluxes from active volcanoes and the dispersal and deposition of ash clouds, and quantify the effect that these processes have on the surrounding landscape.

Tools:

• HyspIRI's VSWIR instrument for monitoring vegetation health.
• TIR data (two bands in the 8–12 μm region) for mapping low temperature volcanogenic heat sources and the spatio–temporal distribution of volcanic ash.
• TIR data (7 bands in the 8–12 μm region) for quantifying and monitoring SO_2 degassing rates.
• Published data and modes regarding the rate at which SO_2 is converted to sulfate aerosol
• Pre–eruption/archival thematic maps/image maps showing how landscape disturbance has progressed through time prior to HyspIRI launch for a subset of volcanoes.

Approach:

• Automated vegetation health change detection algorithms for a selection of active and potentially active volcanoes.

High-Speed Atmospheric Correction for NASA Spectral Imaging Sensors

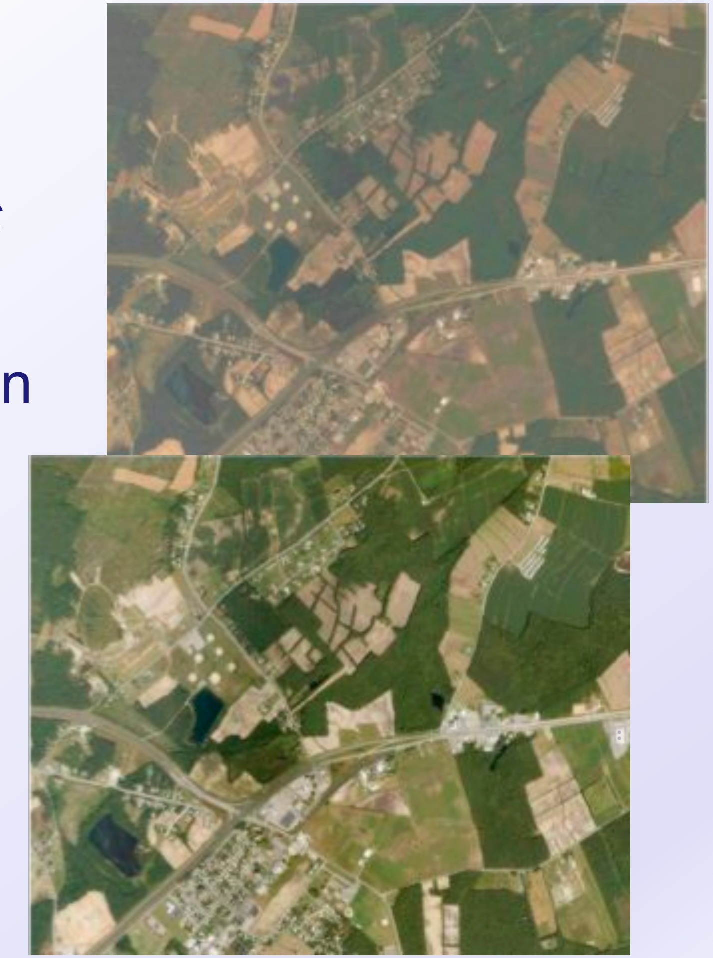

Tim Perkins and Steve Adler-Golden
Spectral Sciences, Inc., Burlington, MA

Pat Cappelaere
Vightel Corp., Ellicott City, MD

Dan Mandl
NASA Goddard SFC, Greenbelt, MD

HyspIRI Products Symposium
Greenbelt, MD, May 2012

Atmospheric Correction Enables Surface Characterization

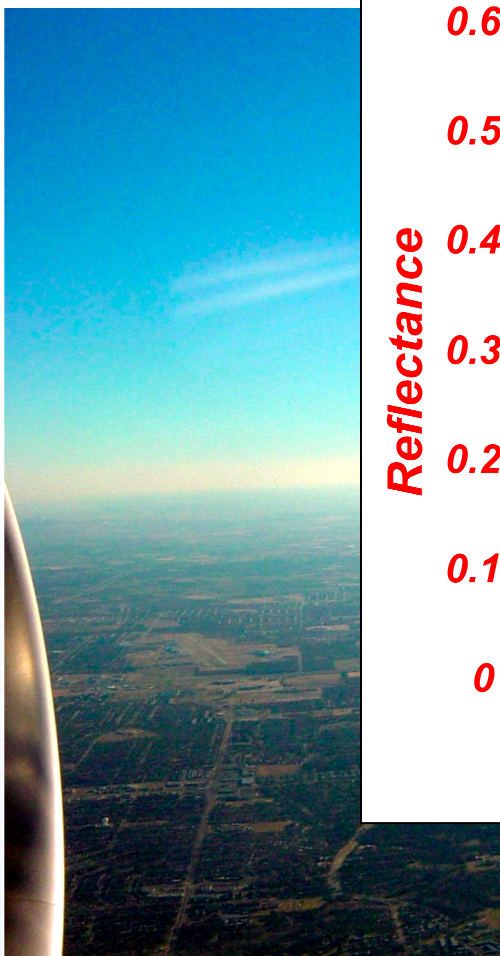

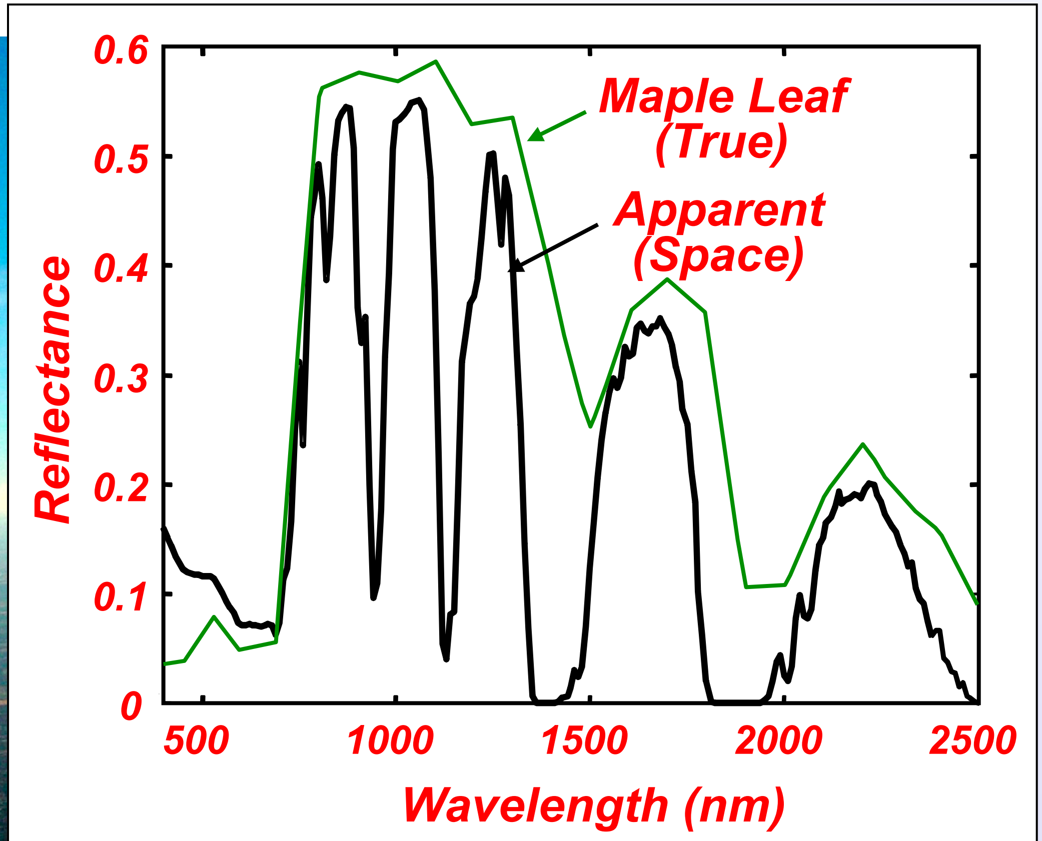

Observed Spectrum

↓

Atmospheric Correction

↓

True Reflectance Spectrum

Objectives & Approach

- **Use SSI's FLAASH code to address the challenges of automated, high-speed, high-accuracy atmospheric correction in both on-board and ground processing systems**
- **Simplify data processing and distribution to NASA scientists**
- **Support NASA's visible-through-shortwave-infrared (VSWIR) spectral imaging instruments, including**:
  - *Current EO-1 instruments Hyperion and ALI and operational Landsat satellites; Landsat Data Continuity Mission (LDCM)*
  - *HyspIRI and associated test missions;*
  - *AVIRIS, MODIS on Terra and Aqua*
- **Approach**
  - *Giant look-up tables (LUTs) of MODTRAN5 radiative transfer simulations enable near-real-time processing*
  - *Newly released C++ version of FLAASH for portability and speed, supports ground-based and onboard processing*

Needs: Emergency Response

Mobile Bay Oil Spill Detection Using EO-1 Advance Land Imager Data

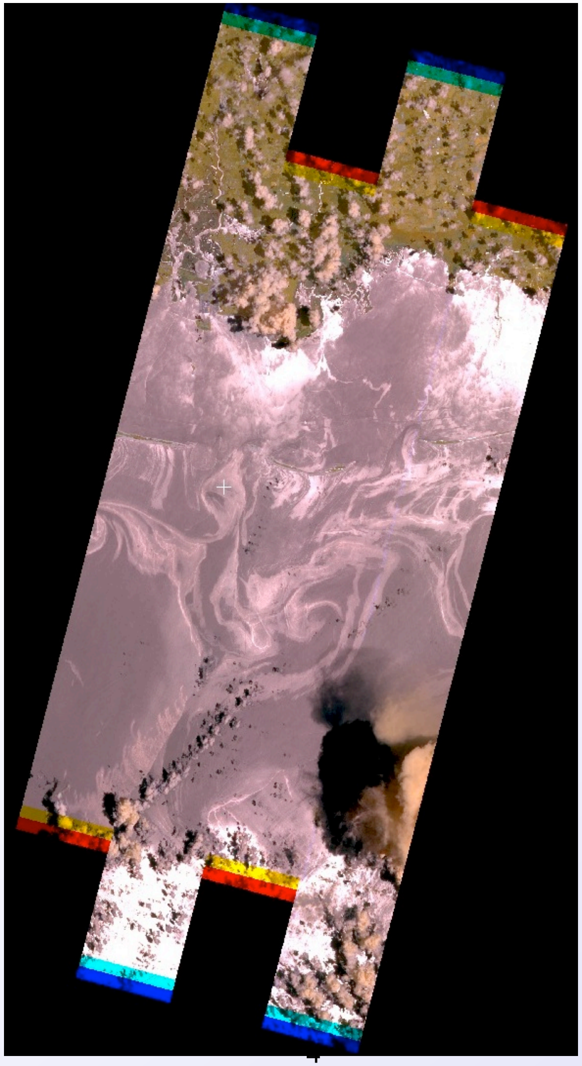

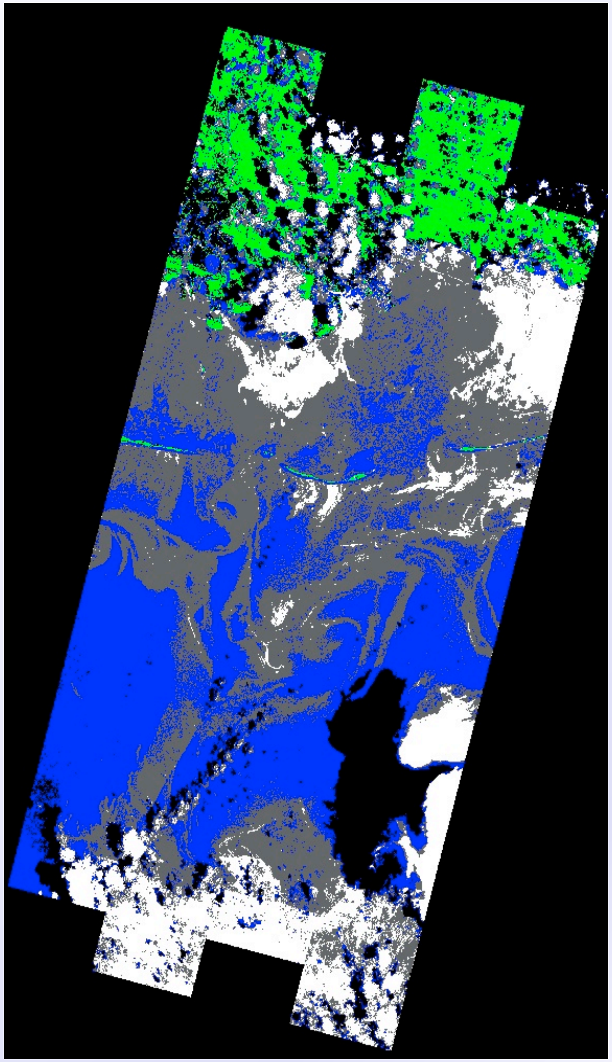

green = land

white = cloud & sand

black = cloud shadow

blue = clear water

grey = surface oil

NASA Archive Processing

- Example: Hyperion image of the 2011 New Mexico wildfires
- SWIR wavelengths diminish the effects of haze and smoke, highlight active hotspots and burn scars.

Visible

SWIR

FLAASH Overview

- **Codes**
  - Originally developed by SSI with primary support from AFRL, additional support from NGA, NASA, SSI
  - ENVI commercial product developed from the original IDL code
  - FLAASH-C developed with DoD support; public release May 2011
- **Science/Features**
  - MODTRAN-5 radiative transfer; pixel-by-pixel water retrieval; scene visibility retrieval; adjacency effect and spectral smile compensation; spectral polishing; wavelength self-calibration
- **Operating Modes**
  - Interactive (IDL) or batch (FLAASH-C)
  - High-speed MODTRAN lookup-table option (ongoing development)
- **Demonstrated Sensor Support**
  - AISA-ES, ALI, ARTEMIS, ASAS, ASTER, AVHRR, AVIRIS, CASI, Compass, GeoEye-1, HYDICE, HyMap, Hyperion, IKONOS, Landsat, LASH, MaRS, MASTER, MODIS, MTI, Probe-1, QuickBird, RapidEye, SPOT, TRWIS, WorldView-2

Atmospheric Modeling

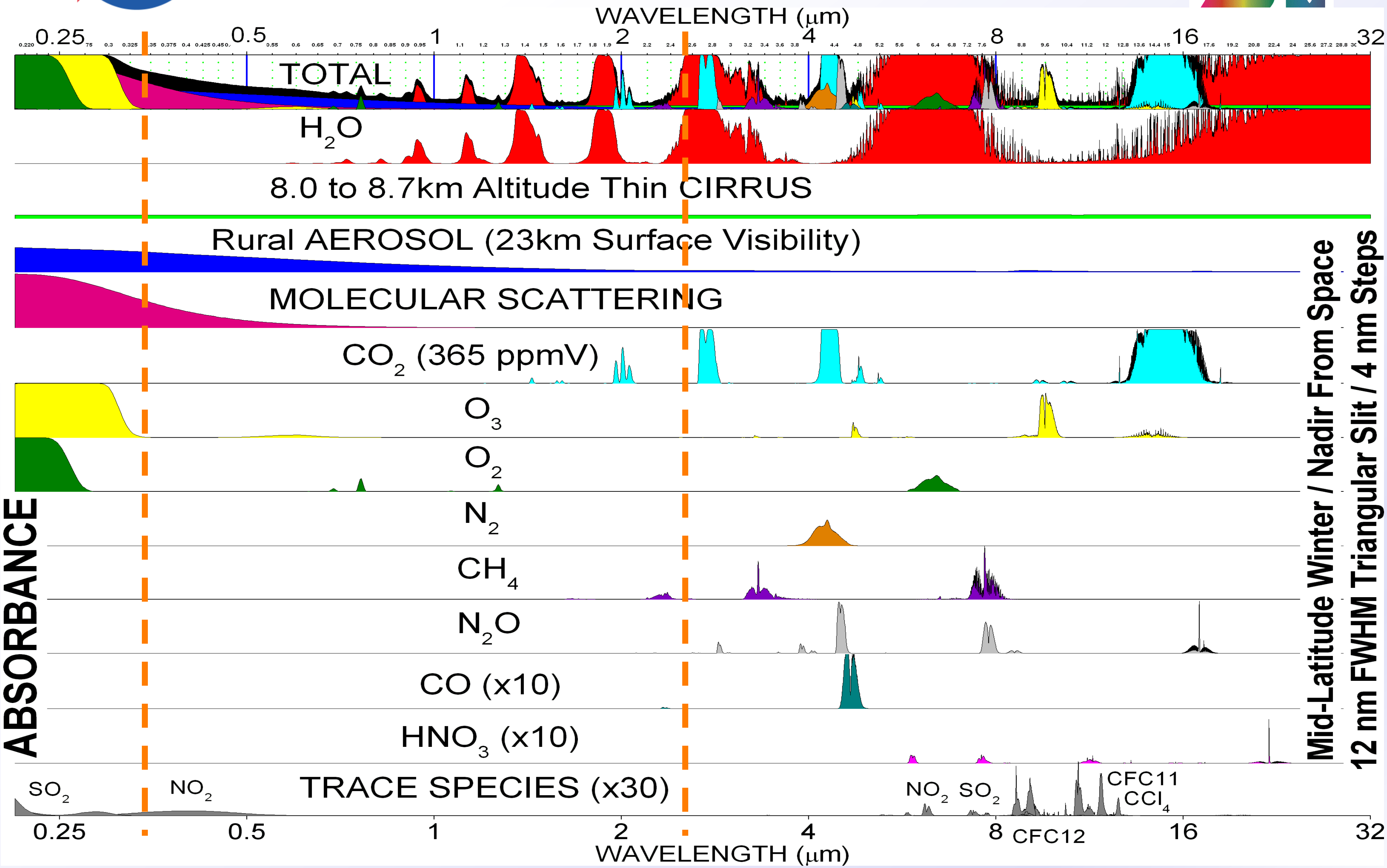

FLAASH Processing

- RT Equation

$$L^* = \frac{a\,\rho}{1-\rho_e S} + \frac{b\,\rho_e}{1-\rho_e S} + L_a^*$$

MODTRAN-derived

- Adjacency compensation reduces signature mixing

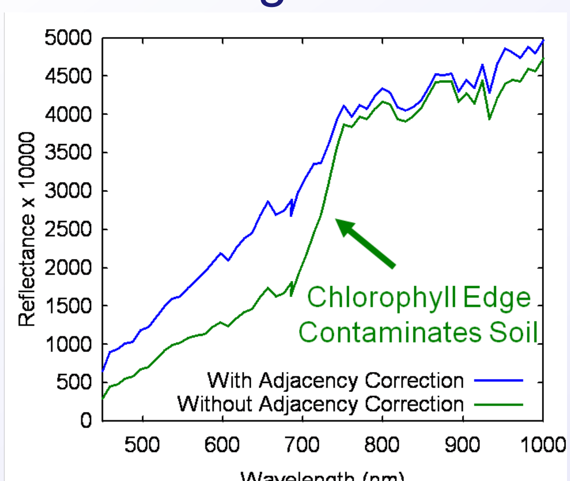

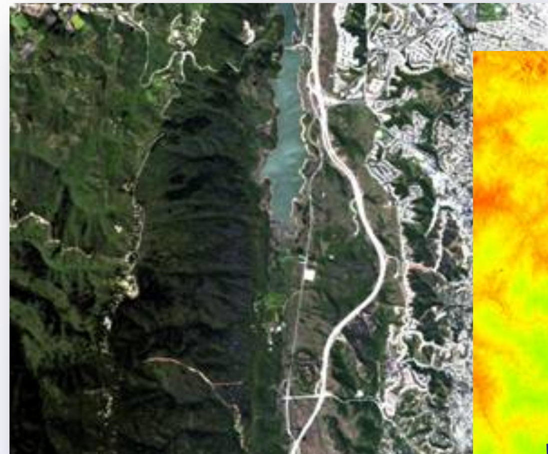

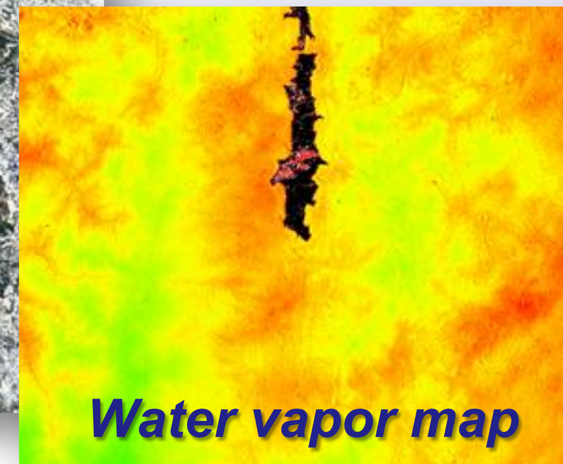

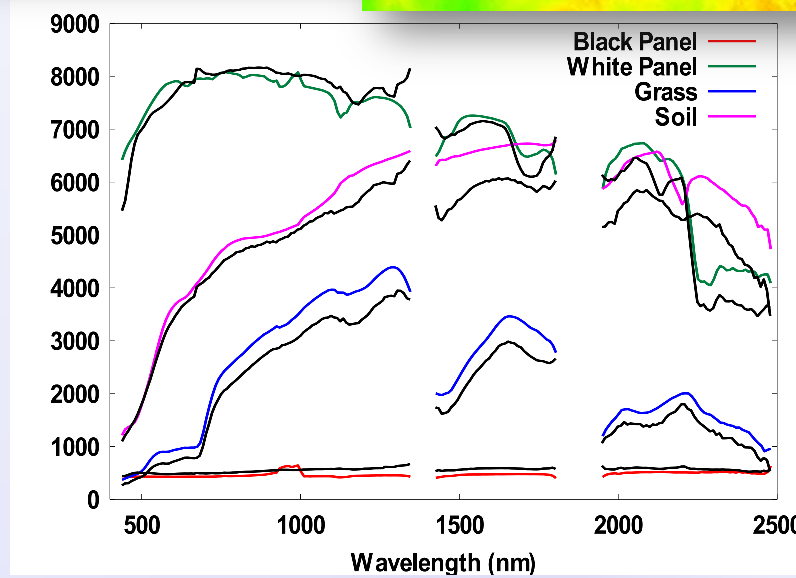

Retrieval vs. Ground Truth

Wavelength and Smile Calibration

- Molecular absorption features are used to estimate wavelength calibration errors based on a Normalized Optical Depth Derivative (NODD) error metric.
- Smile-compensation factors are determined by analyzing the image in narrow, cross-track segments.

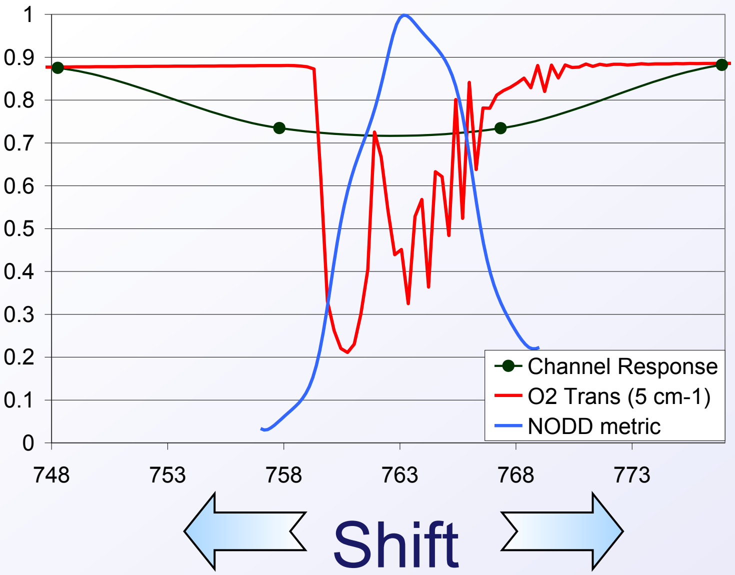

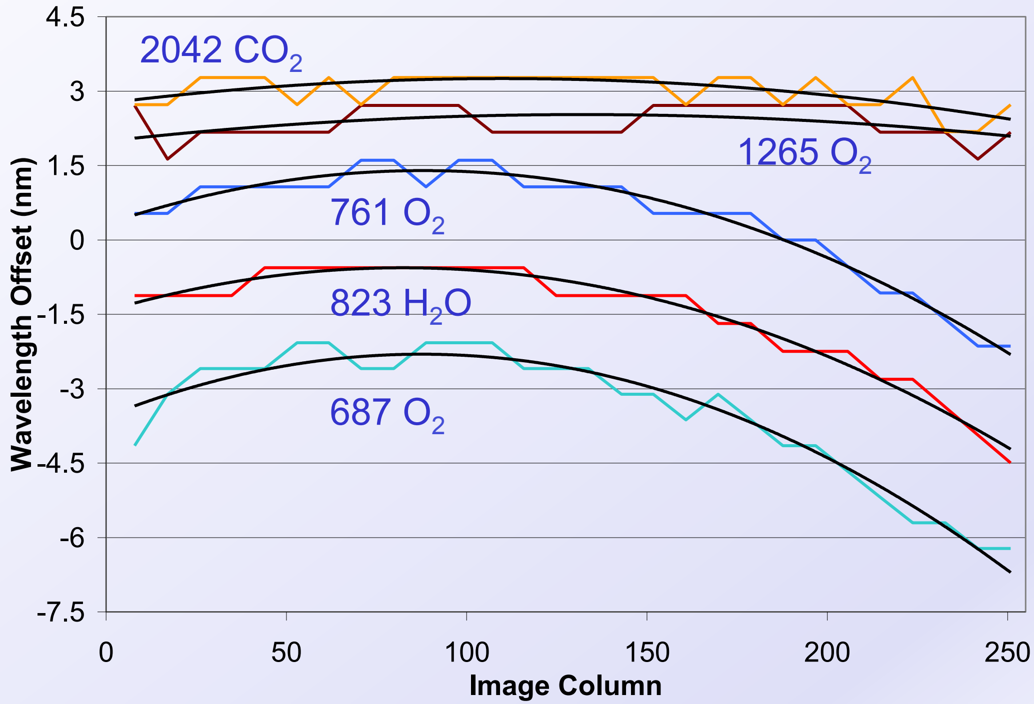

Hyperion Smile Adjustments

Ground-Leaving Radiance
2011 Los Alamos Fire

- Hyperion spectral radiance *before* and *after* atmospheric correction.
- *Thermal radiance* emitted by the ground, gases, and smoke in an active fire pixel (red) was estimated by simple background subtraction

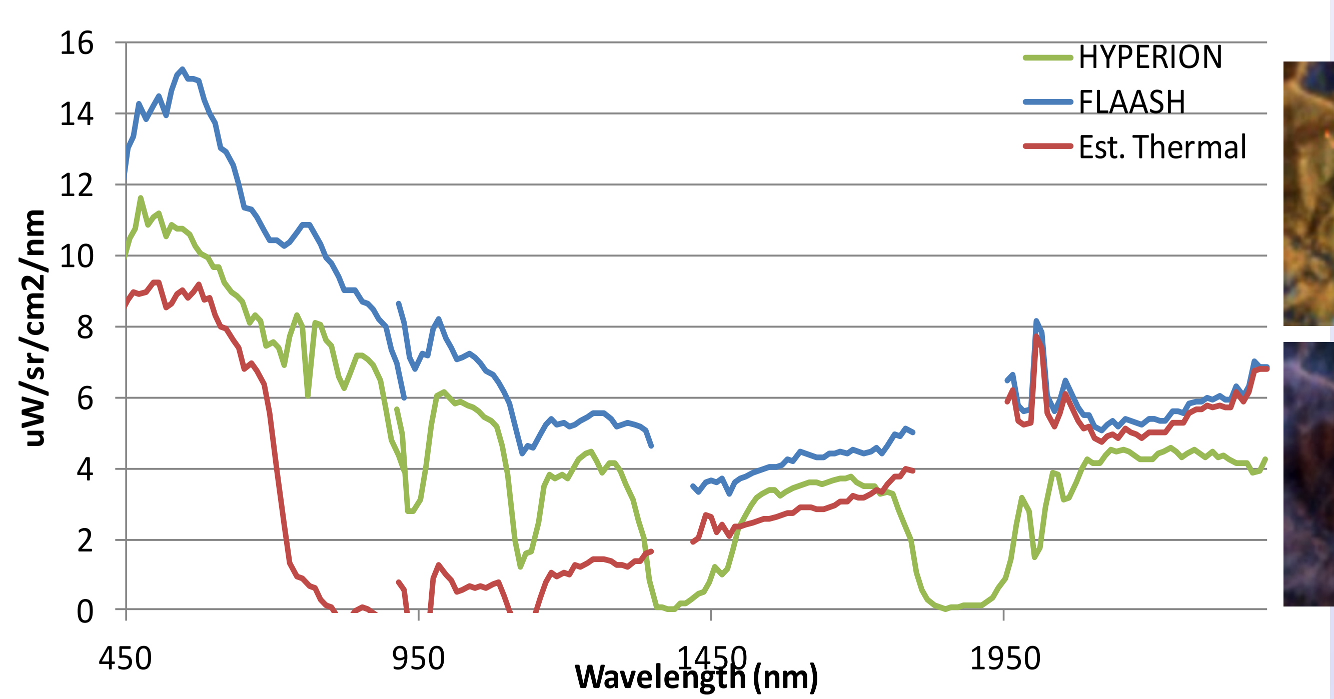

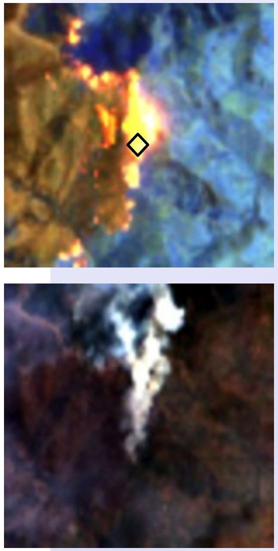

Phase I Program Accomplishments

- **Giant LUT Development**
  - Developed LUT for rural aerosol – ~1CPU-week of MODTRAN calculations
  - >100-fold compression with PCA (16 Gbytes → 100 Mbytes)
- **FLAASH-C Development**
  - Introduced support for compressed LUT format
  - Timing improved for MSI and HIS processing
  - *New feature*: atmospherically corrected radiance (blackbody emission in “hot” pixels for characterizing fires, volcanoes, etc.)
- **Demonstrations:** EO-1 Data (Hyperion, and ALI) - LUT and/or MODTRAN versions
  - On NASA Elastic Cloud automatically processing new scenes
  - As a WCPS algorithm re-processing archived scenes on-demand
  - Embedded on the Intelligent Payload Module (IPM), Telera

Speedup via Look-up Tables (LUTs)

- **Large pre-calculated LUTs replace the custom MODTRAN simulations in the FLAASH atmospheric retrievals**

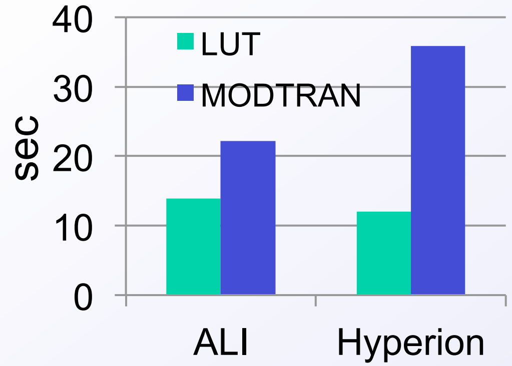

PC Run Time (2.7 GHz)

- **Space-based LUTs supporting nadir and off-nadir viewing**
  - *Initial LUTs constructed for a rural aerosol model (5-300 km visibility)*
  - *~146,000 MODTRAN calculations, 5 cm^{-1} resolution*
  - *Required ~1 week of serial runtime on a PC*
  - *Generated 800 GB of raw MODTRAN output (text)*
  - *Extracting the FLAASH LUT parameters reduced the data to 16 GB (binary)*

LUT Compression

- Reduced the LUT data volume using a principal component analysis (PCA) transformation
  - Manageable size for onboard processing (100 – 200 MB)
  - Improve lookup and interpolation runtime performance by reducing file I/O
- PCA translates the LUT dimensions onto orthonormal basis vectors, ordered by variance:
  - Matrix diagonalization / inversion of high-dimensional data is challenging
  - Iterative methods are more efficient when a limited number of basis vectors are needed
  - **N**on-linear **I**terative **PA**rtial **L**east **S**quares (NIPALS) algorithm
- Compressed each LUT component separately
  - Six 2.7 GB matrices, ~1 day to compute 64 eigenvectors

LUT Compression Analysis

- Data compressed with 32 basis functions, 150x reduction
- Compressed data is roughly the size of a single Hyperion image
- Worst-case error localized around the 760 nm oxygen feature

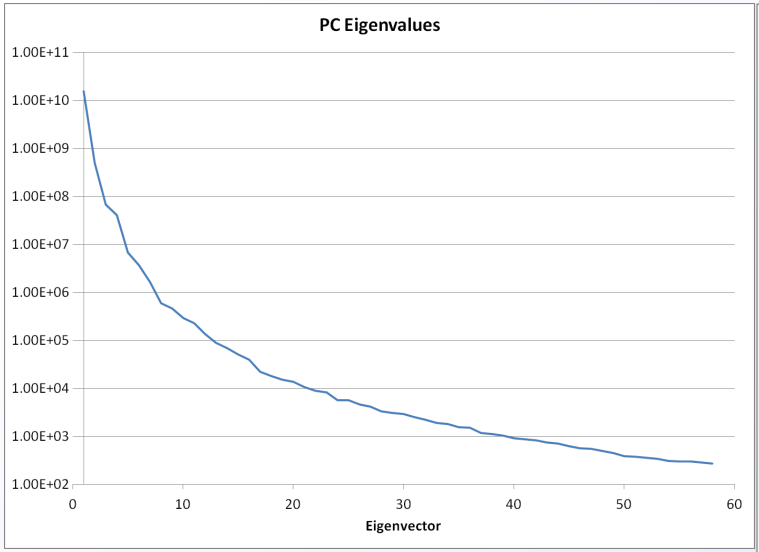

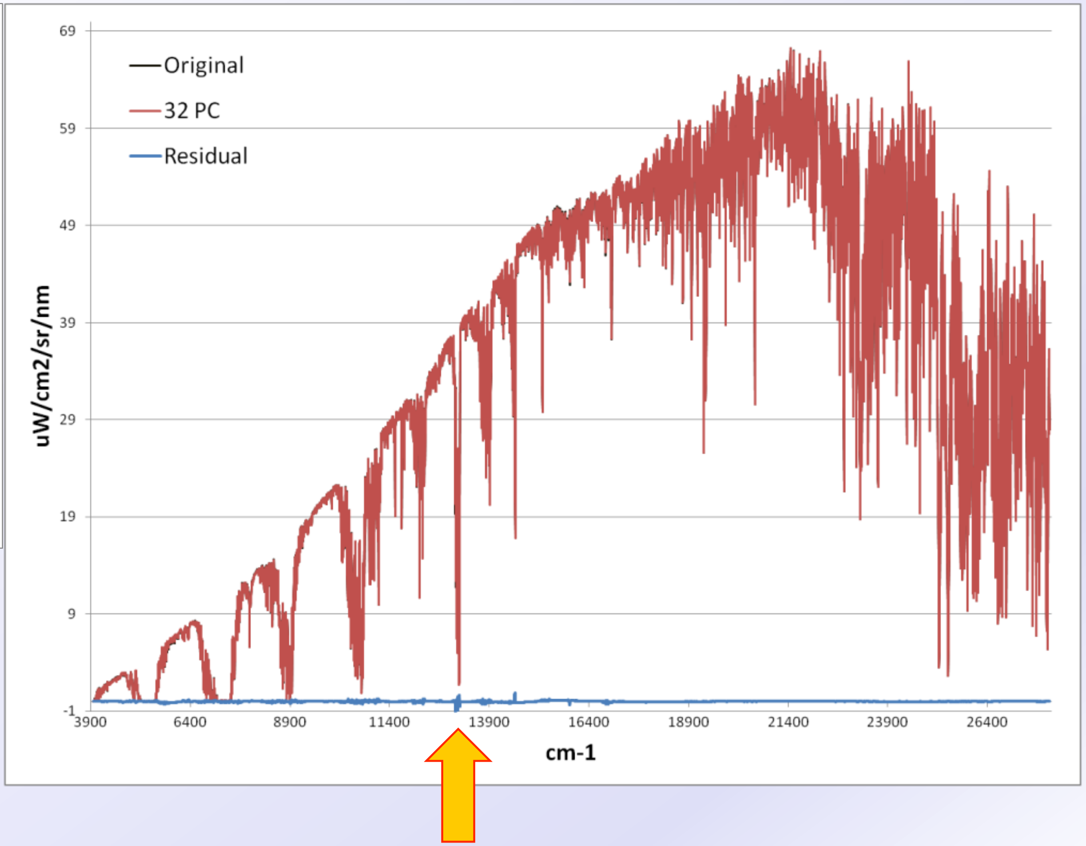

LUT Evaluation

- RT parameters interpolated and extracted from the compressed LUTs
- Hyperion reflectance spectra compared against MODTRAN results
  - *Retrieved Hyperspectral reflectance values agree to within +/- 0.01*
  - *Differences dominated by interpolation error, not compression*

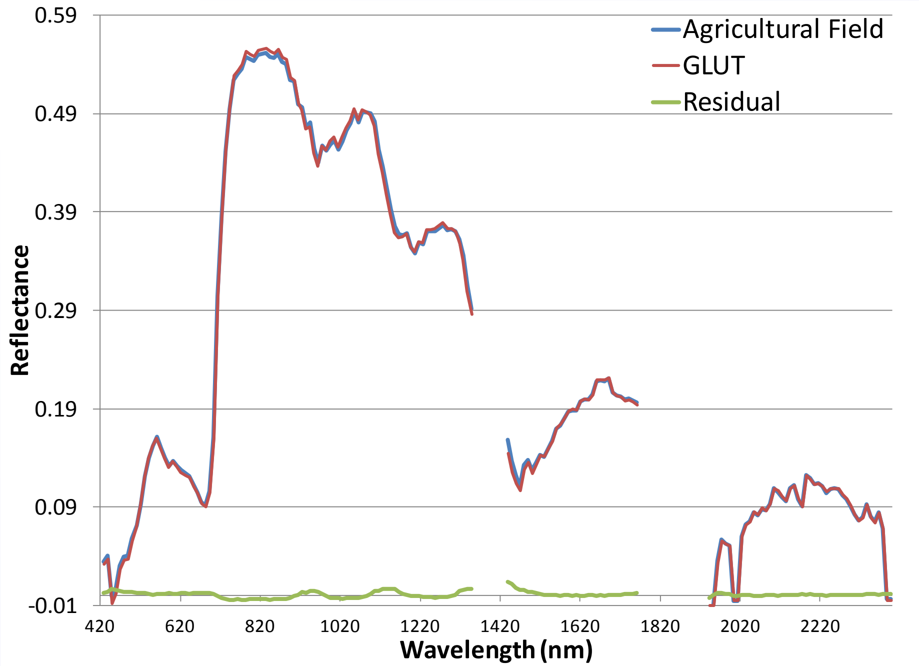

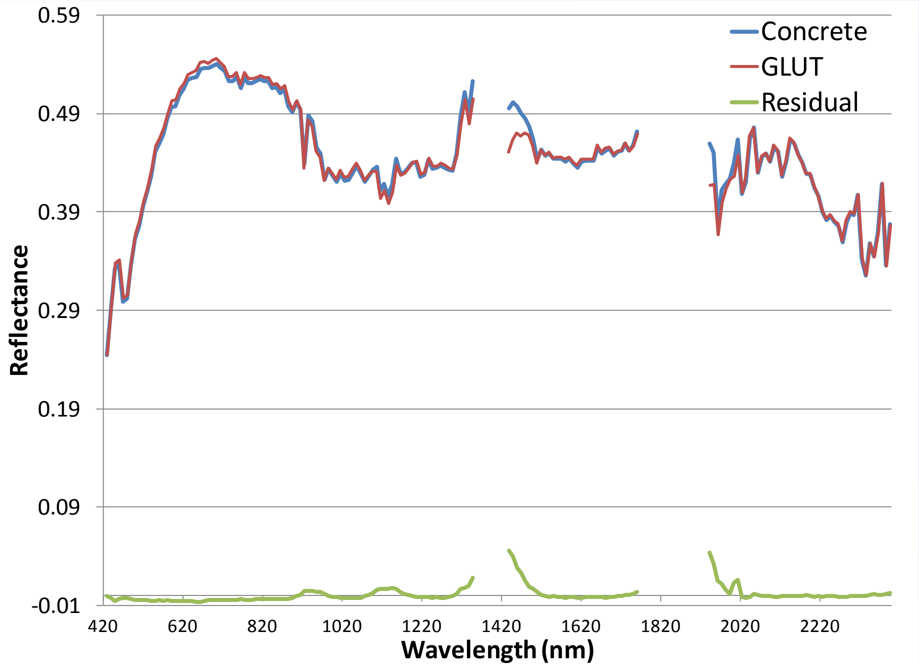

Future Plans

- **Code Development**
  - *Expand LUTs to include more aerosols/dusts (rural, maritime, urban, desert), extend to lower altitudes for aircraft (e.g. EMAS)*
  - *Parallelize for multiprocessor systems (Tilera)*
  - *Include Thermal IR (TIR) atmospheric correction options*
    - *Fusion of VNIR/SWIR with TIR would benefit the AC process*
  - Radiometric *re*-calibration, image de-striping
- **Code Integration**
  - *Fully operational Sensor Web and IAAS data processing, distribution*
  - *Prototype demonstration for HyspIRI flight system using Space Cube and/or Maestro testbeds*
  - *Cloud data product generation and distribution*
    - *Water vapor mapping, cloud cover, vegetation analysis, coastal studies*

End

Backup Slides

Proposed System Concept

- ***Ground-based system:***
  - Cloud computing and distribution
  - Support Hyperion, Landsat, ALI, MODIS, ASTER
- ***On-board system:***
  - For direct broadcast of products from HyspIRI, LDCM in near real-time

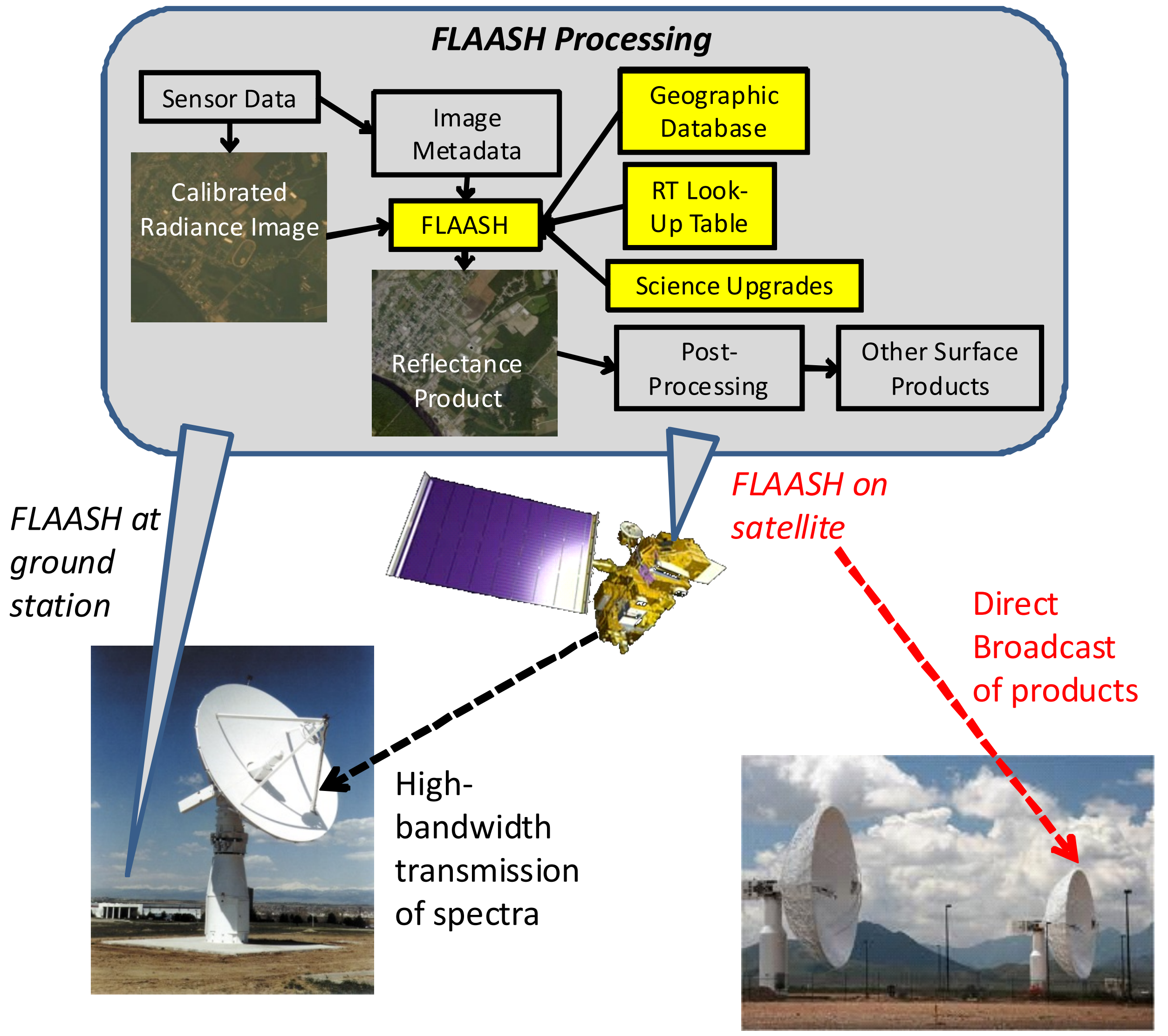

FLAASH Deployment at NASA

- Automated FLAASH processing and distribution of archival data products via Elastic Cloud and Sensor Web
- Web Coverage Processing Service (WCPS) integration grants control over the FLAASH correction process at the user's request

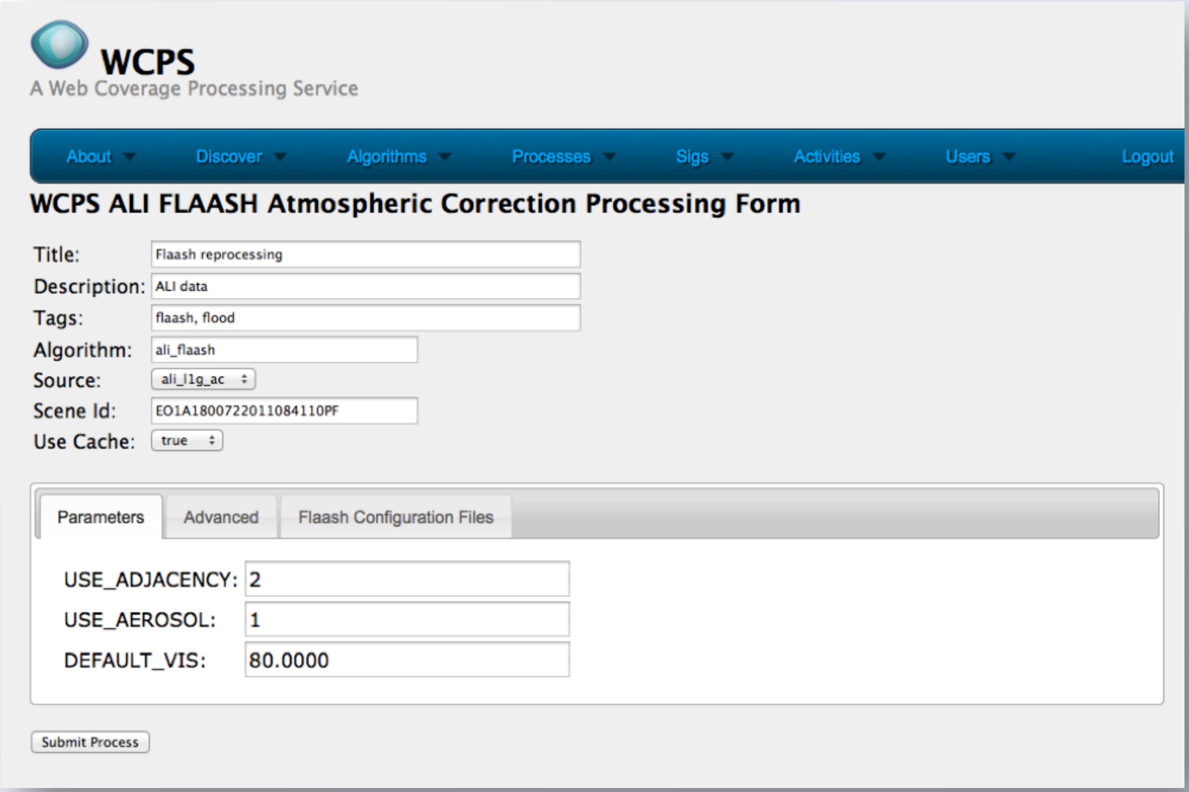

ASTER Standard TIR Data Products

Terra Satellite
Operating since December 1999

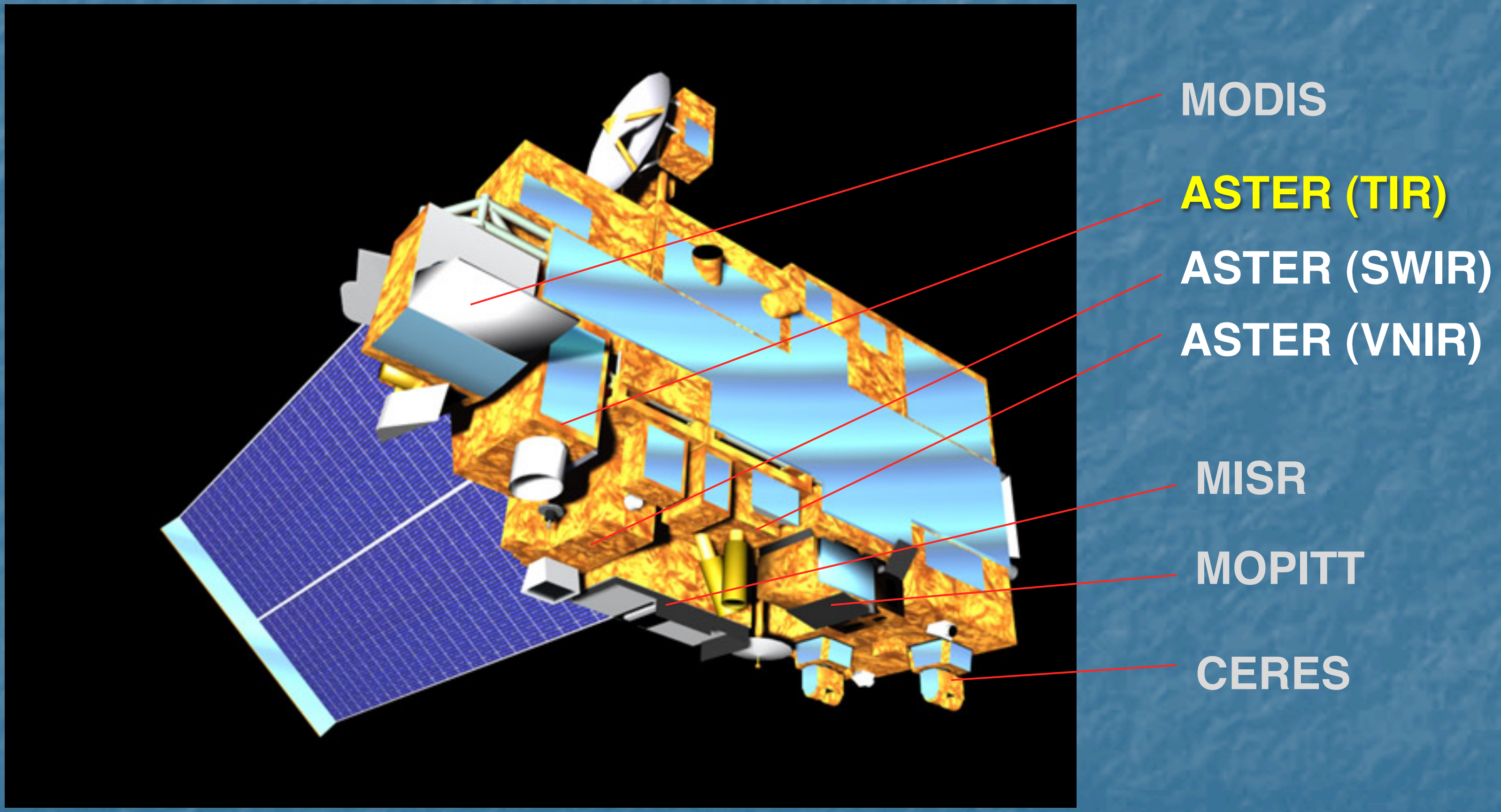

ASTER Characteristics

- **Wide Spectral Coverage**
  - 3 VNIR bands, 8-bit (0.52 – 0.86 µm)
  - 6 SWIR bands, 8-bit (1.6 – 2.43 µm)
  - 5 TIR bands, 16-bit (8.125 – 11.65 µm)
- **High Spatial Resolution**
  - 15m for VNIR bands
  - 30m for SWIR bands
  - 90m for TIR bands
- **Other Characteristics**
  - 60 km swath width
  - Along-track Stereo for DEM
  - Daily programming of acquisitions

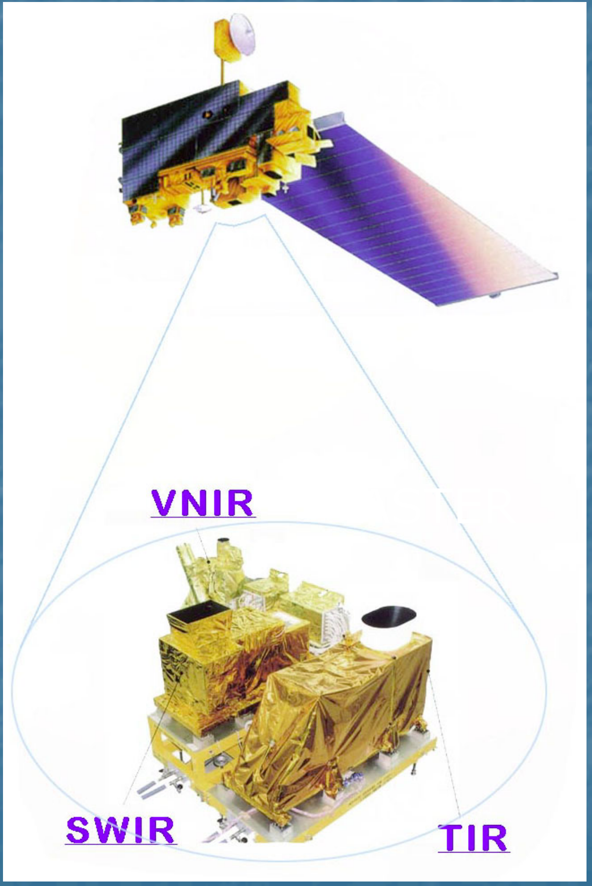

ASTER Bands

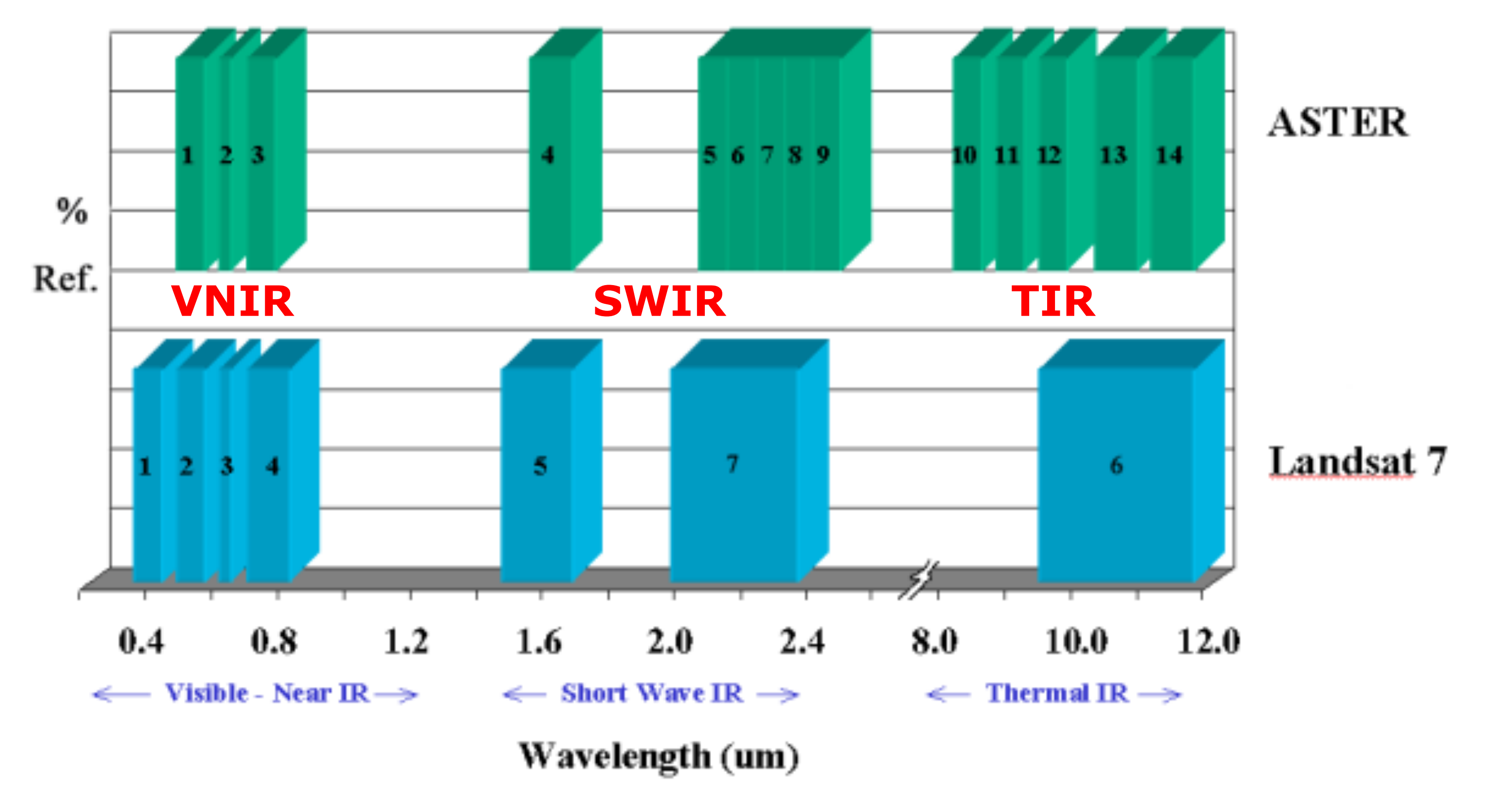
ASTER
1 2 3
4
5 6 7 8 9
10 11 12 13 14
%
Ref.
VNIR
SWIR
TIR
Landsat 7
1 2 3 4
5
7
6
0.4 0.8 1.2 1.6 2.0 2.4 8.0 10.0 12.0
Visible - Near IR
Short Wave IR
Thermal IR
Wavelength (um)

Data Acquisition Strategy

- Daily acquisition schedule uploaded every day: ~500 scenes/day
- Automatic priority function determines which scenes are acquired; acquisition request data base has ~3000 orders: global background mapping, large area monitoring, individual scientist requests, etc. Each order is assigned priorities based on who requested, amount of resources, percent of area already acquired…..
- Expedited data scheduling put in place after launch. Allows "last minute" additions to daily acquisition schedule for natural disasters, national security, field campaigns. Data can be processed and delivered to requester in 2-4 hours after acquisition.

Data Processing Strategy

- All higher level data products (except for Level 1) are produced "on-demand" when a user order is placed
- This is a throw-back to early 90s when the data system was being designed, and disk storage was very expensive
- User has ability to customize most products, selecting projection, resampling, ancillary data inputs, etc.
- Data products can be ordered from LPDAAC or Japan GDS; only electronic delivery is supported

Level	Product Name	Description
1A	Radiance at Sensor	Image data plus radiometric and geometric coefficients, separated by telescope
1B	Registered radiance at sensor	1A data with coefficients applied
2	AST09 Surface radiance VNIR,SWIR	Radiance corrected for atmosphere
2	AST09T Surface Radiance-TIR	Radiance corrected for atmosphere
2	AST09XT Surface radiance-VNIR,SWIR crosstalk corrected	VNIR & Crosstalk corrected SWIR
2	AST07 Surface Reflectance-VNIR,SWIR	Surface radiance with topo corrections
2	AST07XT Surface reflectance-VNIR,SWIR crosstalk corrected	AST07 VNIR & crosstalk corrected SWIR
2	AST08 Surface Kinetic Temperature	Temperature-emissivity separation applied to atmospherically corrected surface radiance
2	AST05 Surface Emissivity	Temperature-emissivity separation applied to atmospherically corrected surface radiance
3	ASTER GDEM	Global Digital elevation model
3	ASTER Digital Elevation Model	Single scene DEMs
3	AST14OTH Orthoimage	L1B Orthorectified

Level 1A

Radiance at the Sensor

- Geometric and radiometric calibration coefficients are in the metadata
- VNIR, SWIR and TIR data are included
- TIR data are 16-bit integer: L1A can be converted to radiance units by applying calibration coefficients, then scaling with conversion coefficient
- Data are not registered between telescopes
- Data are distributed in HDF format

Level 1B

Registered Radiance at the Sensor

- Geometric and radiometric calibration coefficients are applied to the L1A data
- VNIR, SWIR and TIR data are included
- TIR data are 16-bit integer: L1B can be converted to radiance units by applying a gain and offset (same values all through mission): *radiance = (DN-1) x conversion coefficient*
- Map projection and resampling have default values (UTM and CC), but are also user specifiable
- Data are distributed in HDF format

AST09T

Surface Radiance

- Corrects at-sensor radiance for effects of atmospheric transmission, path radiance and scattering using MODIS or NCEP atmospheric profiles
- Input data are Level 1
- 16-bit data are converted from DN to radiance by multiplying by conversion factor
- Data are distributed in HDF format

AST05

Surface Emissivity

- Corrects measured at-sensor radiance for effects of atmospheric transmission, path radiance and scattering using NCEP profiles or MODIS atmospheric water vapor and temperature profiles.
- TES algorithm hybridizes two established algorithms, first estimating the temperature and band emissivities by the Normalized Emissivity Method, and then normalizing the emissivities by their average value. Next, an empirical relationship adapted from the Alpha Residual method is used to predict the minimum emissivity from the spectral contrast (min-max difference or MMD) of the normalized values,
- TIR data are 16-bit integer; they can be converted to emissivity units by multiplying by 0.001
- Data are distributed in HDF or GeoTIFF format

AST08

Surface Kinetic Temperature

- Iteratively corrects calculated land-leaving radiance for effects of downwelling atmospheric irradiance as it calculates and refines the temperatures and emissivities.
- Uses temperature-emissivity algorithm
- TIR data are 16-bit integer: data can be converted to surface temperature degrees Kelvin by multiplying by 0.1
- Data are distributed in HDF or GeoTIFF format

AST14OTH

Orthorectified L1B

- ASTER DEM is used to orthorectify the L1B bands
- 14 bands of data are distributed in GeoTIFF format

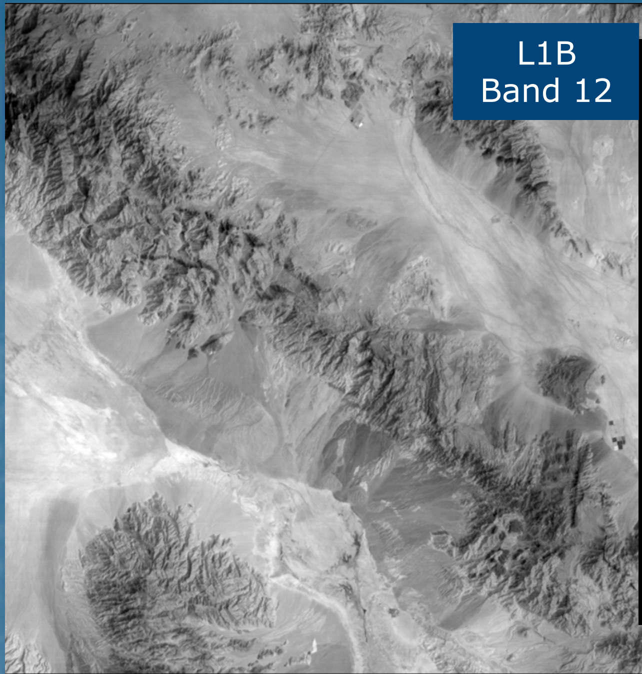
L1B
Band 12

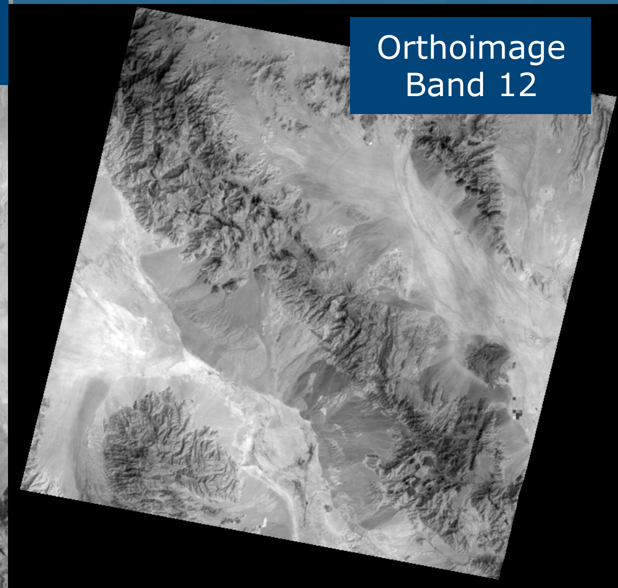
Orthoimage
Band 12

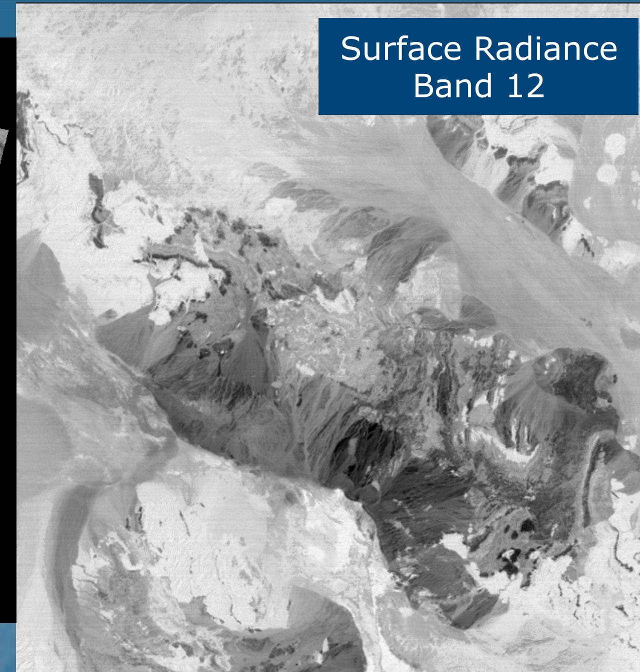
Surface Radiance
Band 12

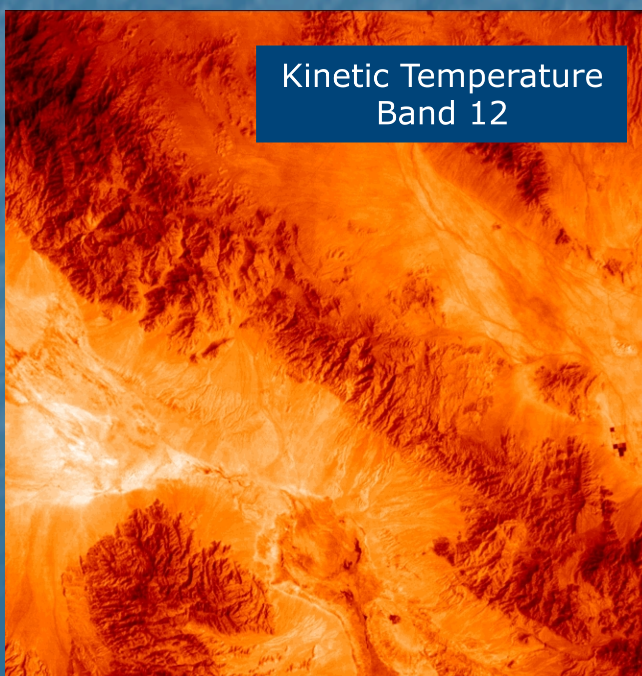
Kinetic Temperature
Band 12

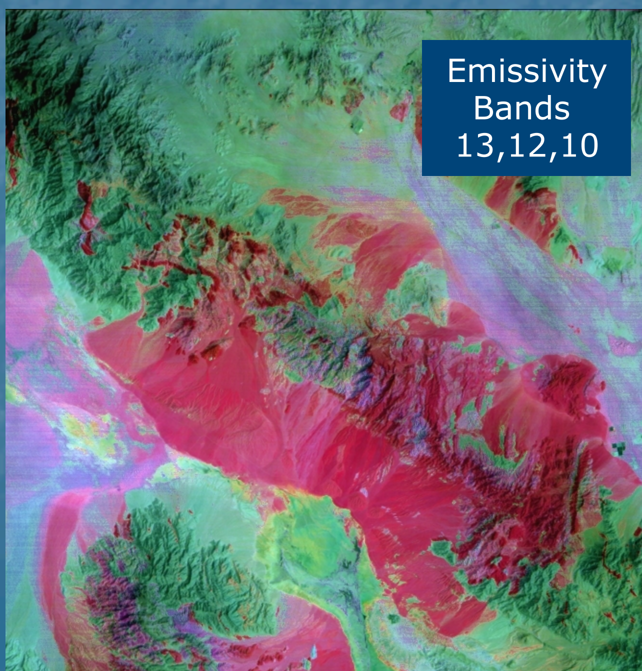
Emissivity
Bands
13,12,10

Data Volume per Image

Data Product	Volume
L1A	110 MB
L1B	125 MB
AST09T Surface Radiance-TIR	14 MB
AST08 Surface Kinetic Temperature	4 MB
AST05 Surface Emissivity	9 MB
AST14OTH Orthorectified L1B	132 MB

Number of images ordered in 2009

Data Product	Volume
L1A	4,000
L1B	230,000
AST09T Surface Radiance-TIR	13,000
AST08 Surface Kinetic Temperature	40,000
AST05 Surface Emissivity	28,000
AST14OTH Orthorectified L1B	13,000

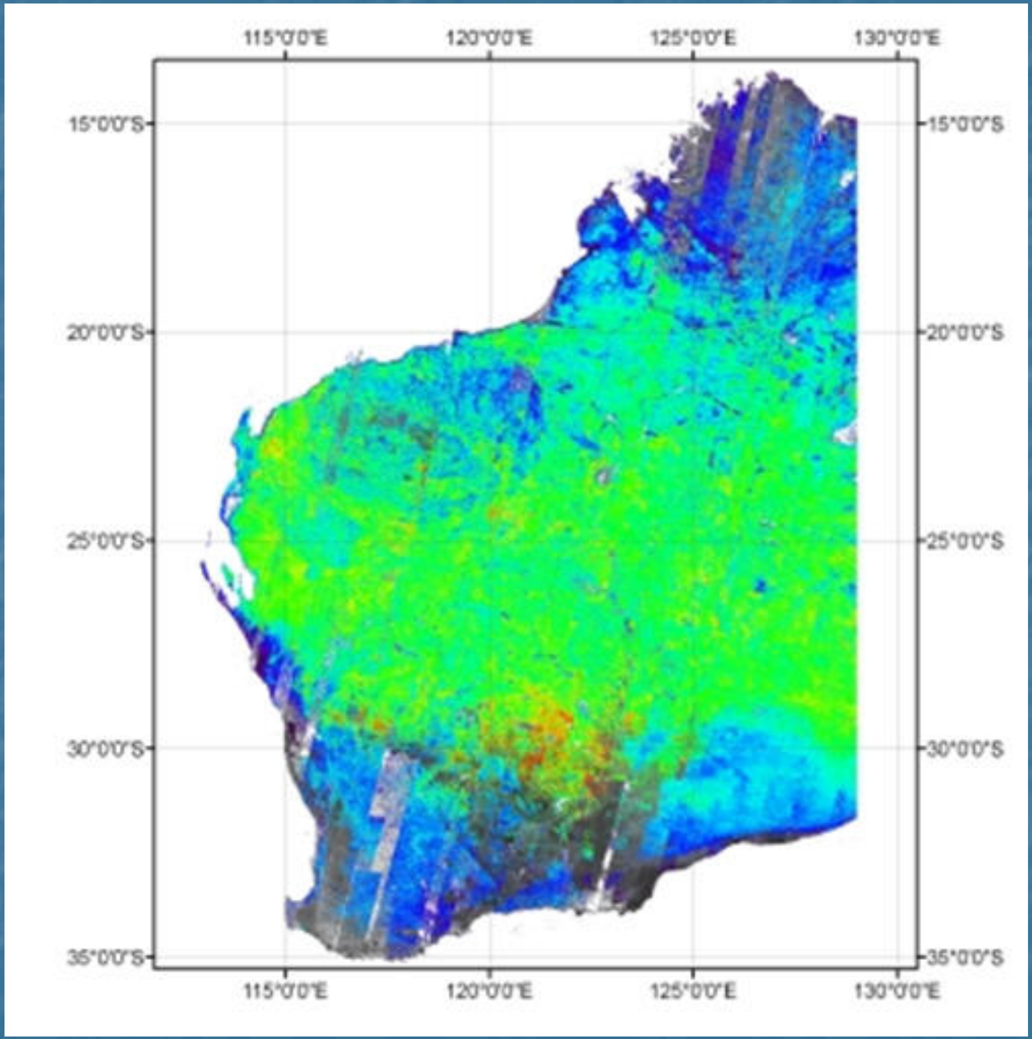

CSIRO Australia Satellite ASTER Geoscience Maps

Uses all 14 ASTER bands – VNIR, SWIR, TIR

Final products are "mineral group" information: clays, carbonate, iron minerals, etc.

Maps are continental scale, available for free over the internet, in TIF, JPG or BSQ formats

Specific products: ferric and ferrous oxide composition, opaque index, ALOH content, Kaolin group index, FeOH content, MgOH content, Silica index, Carbonate index, Mafic index,

Results of increased spatial, spectral & temporal observations of volcanic activity: Implications for HyspIRI TIR data

Michael Ramsey

Department. of Geology and Planetary Science
University of Pittsburgh, Pittsburgh, PA, USA

Kliuchevskoi volcano (ASTER-URP data): 28 May 07

Overview

Kizimen volcano (ASTER-URP data): March 2011

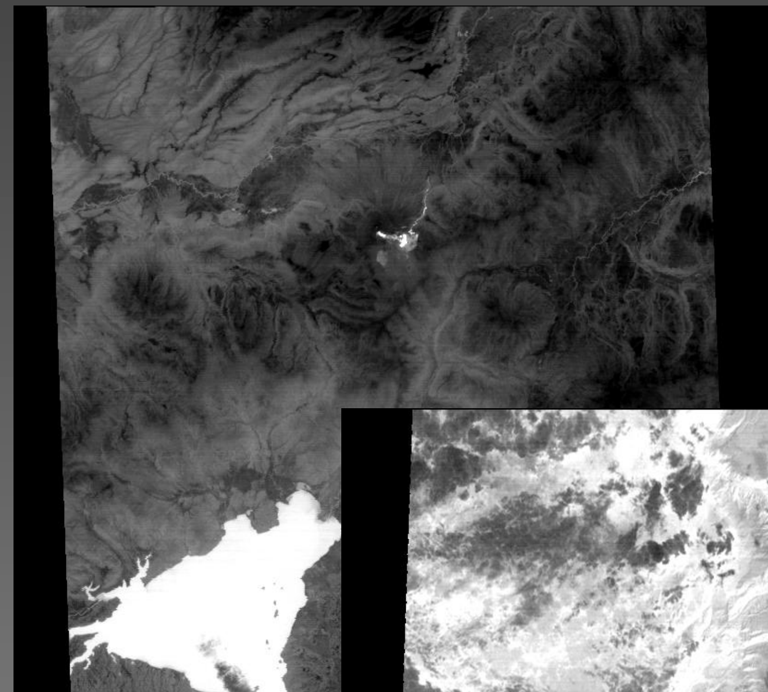

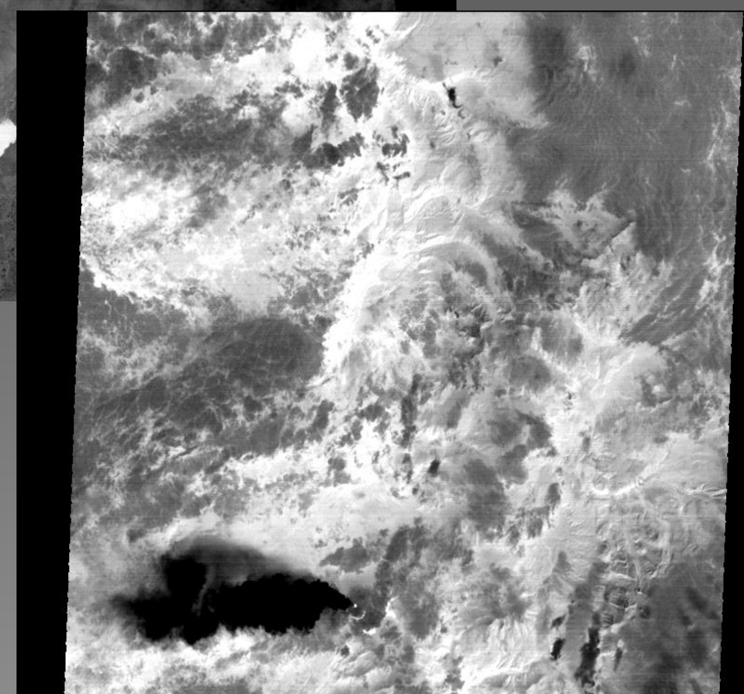

- **Spatial Resolution**
  - volcano science returned from multispectral TIR data
    - the ASTER URP Program
    - 8 year archive
    - cloud vs. anomaly statistics for volcanoes
- **Spectral Resolution**
  - trade studies of spectral resolution and band positions
    - MAGI and SEBASS airborne data

Thermal Anomaly Detection

- **Operational Algorithms**
  - used for routine thermal anomaly detection
    - based on three end-member algorithms:

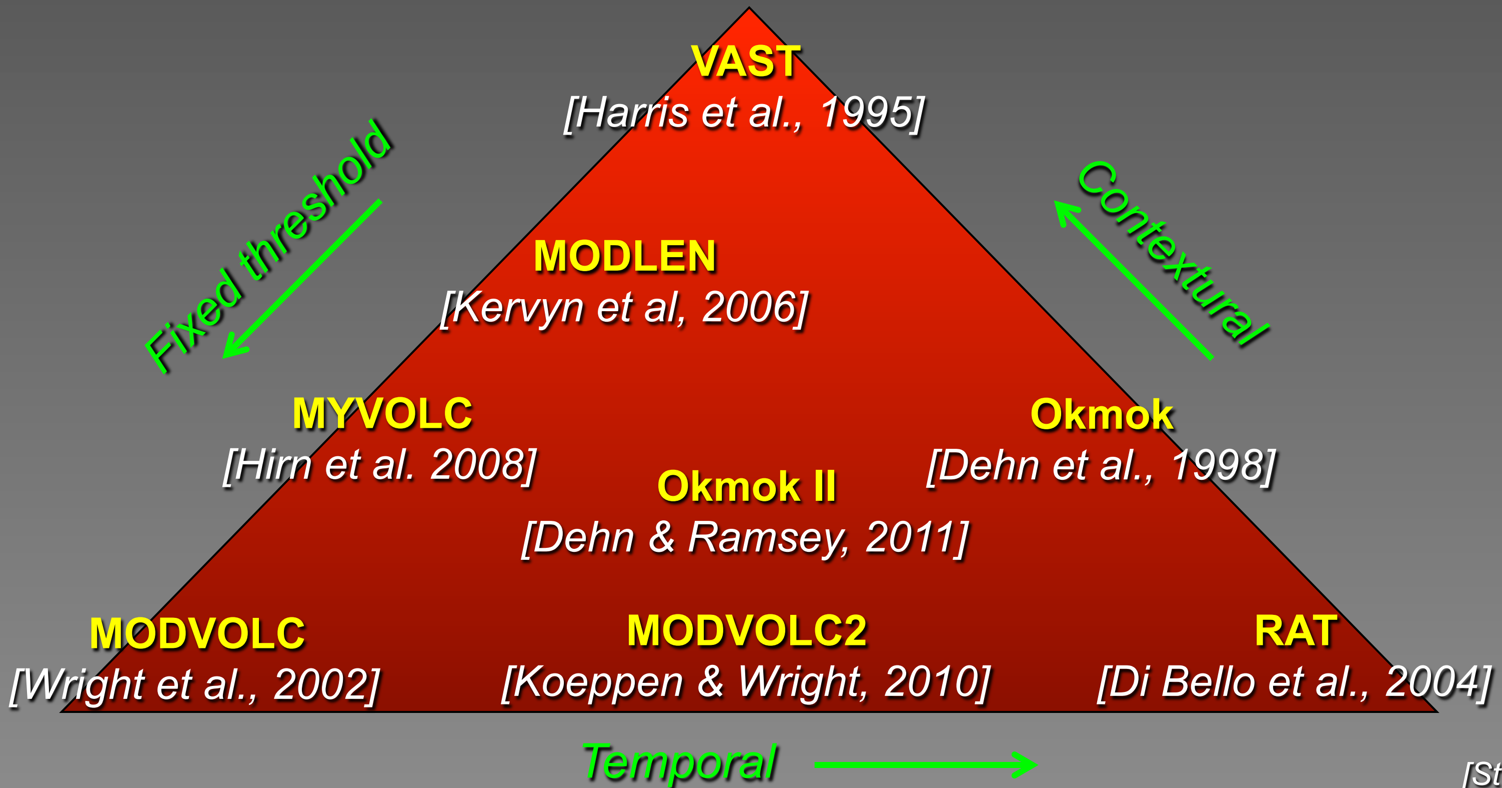

[Steffke, 2009]

URP Summary

- **ASTER Urgent Request Protocol (URP) Program**
  – integrates Alaska Volcano Observatory monitoring into the ASTER Urgent Request stream
    - focused on the northern Pacific volcanic arc
      - trigger automated ASTER requests → sent to the LP DAAC → ASTER scheduled
      - 1 – 5 day repeat times
      - several thousand high spatial, high temporal scenes in the URP archive
    - now integrated with MODVOLC

Kluichevskoi time series

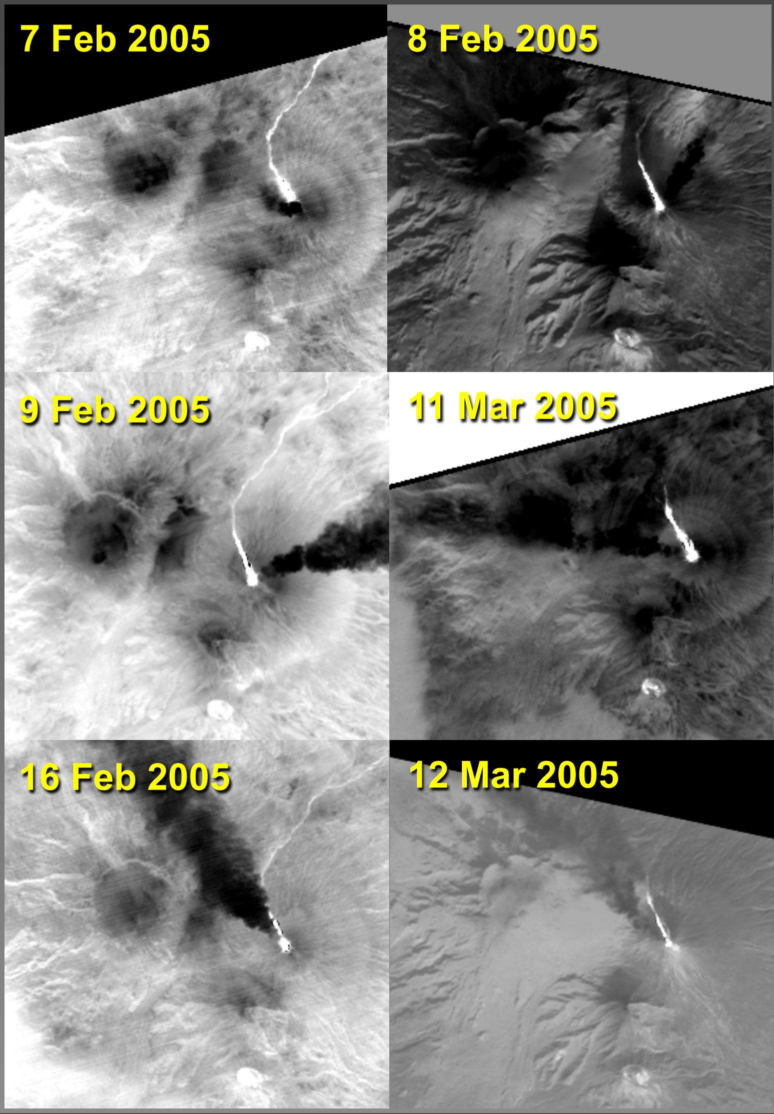

ASTER URP Flowchart

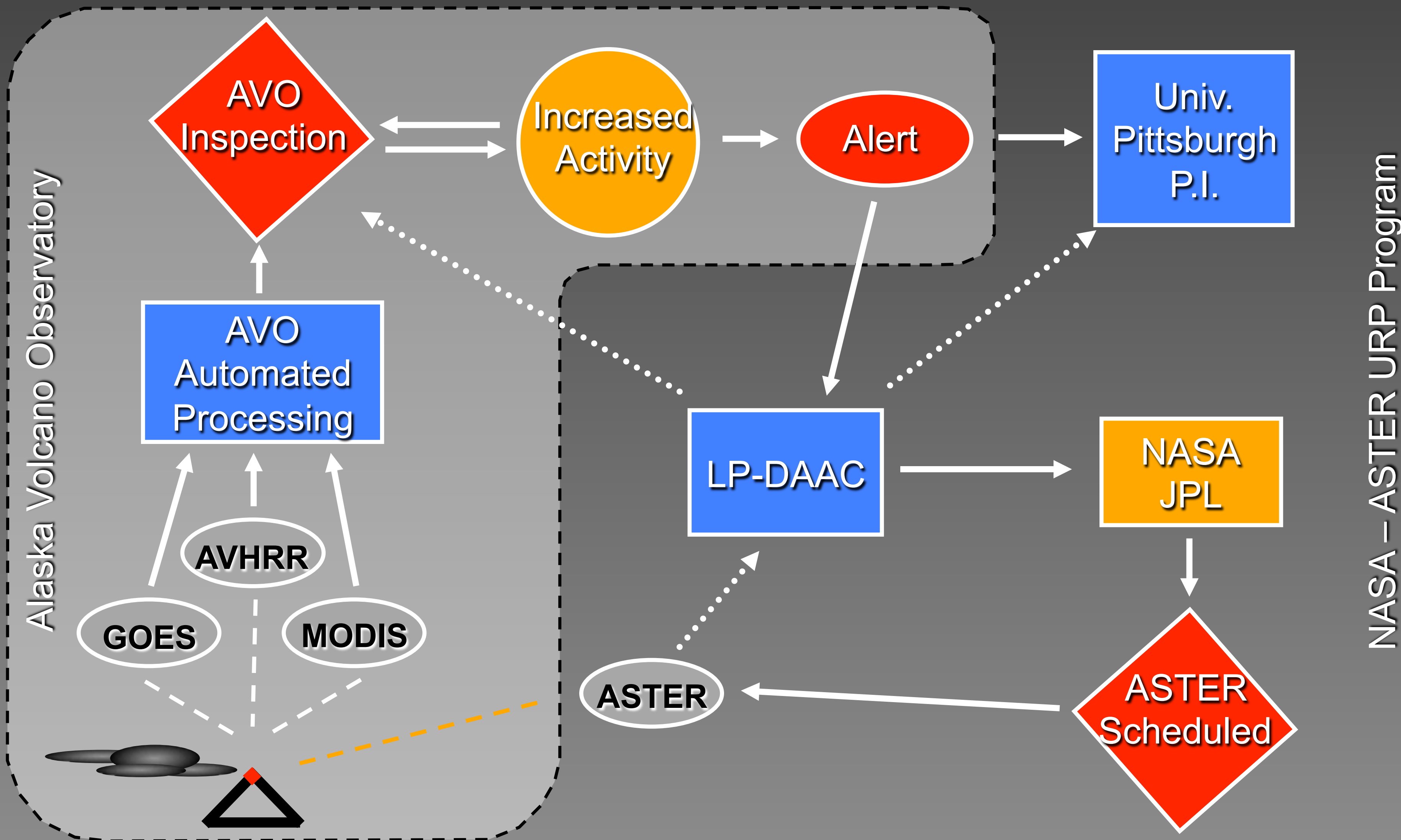

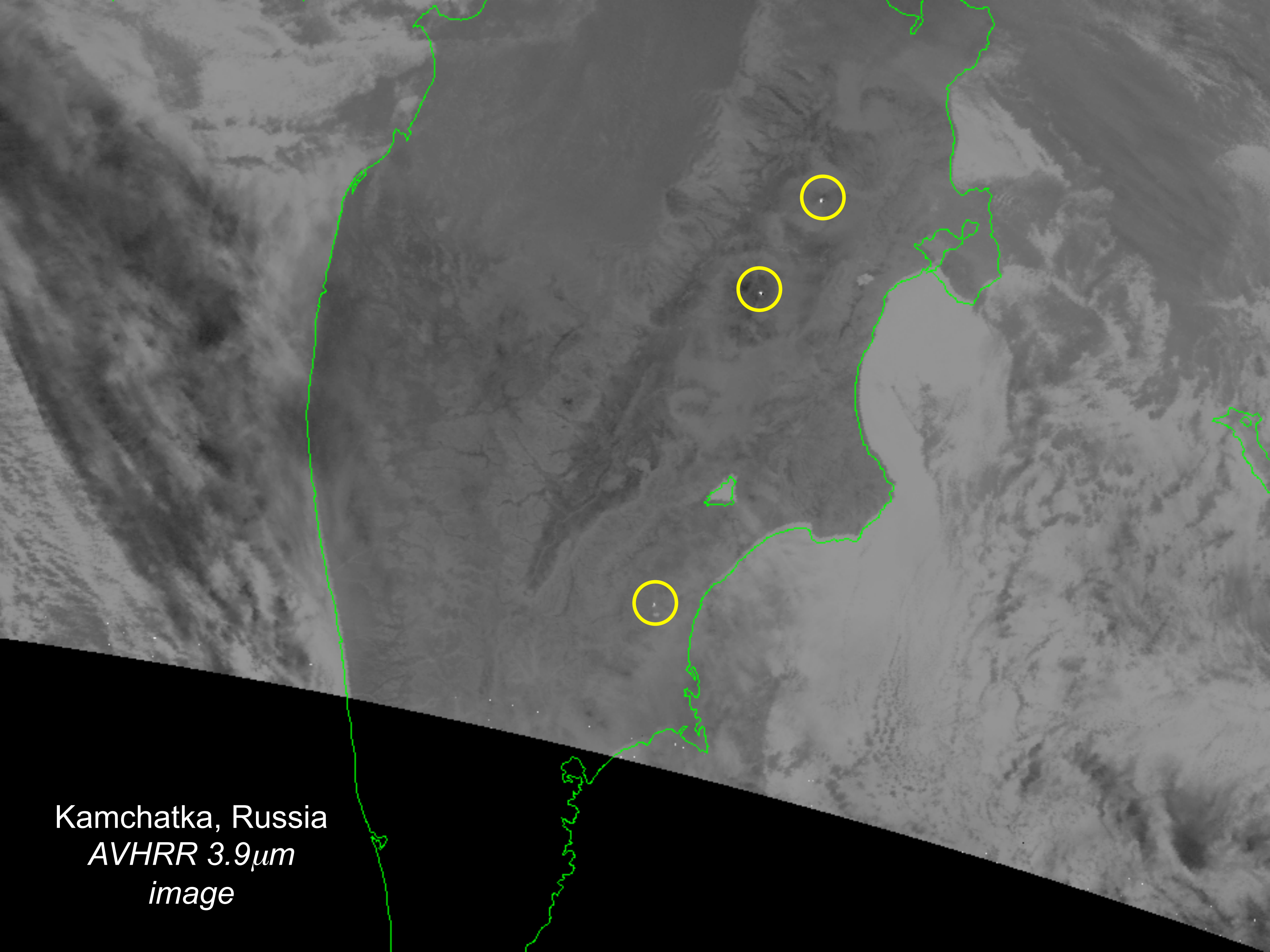
Kamchatka, Russia
AVHRR 3.9µm
image

TIR/SWIR UPR Data

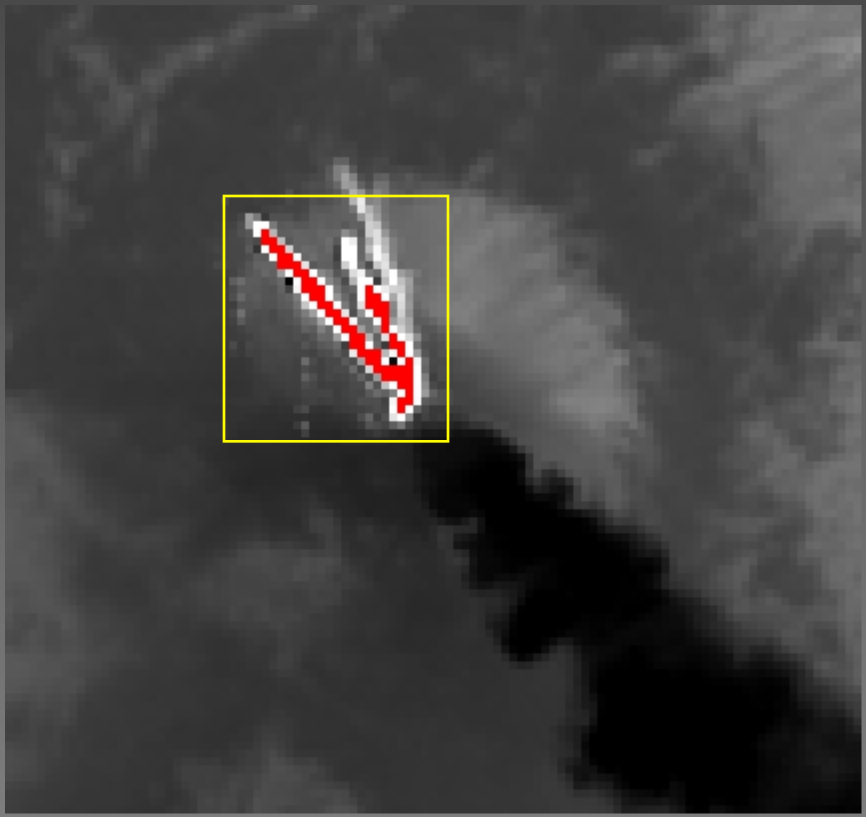

TIR temp (90m)
T_{TIR} (max detected) = 100 °C
saturated pixels (red)

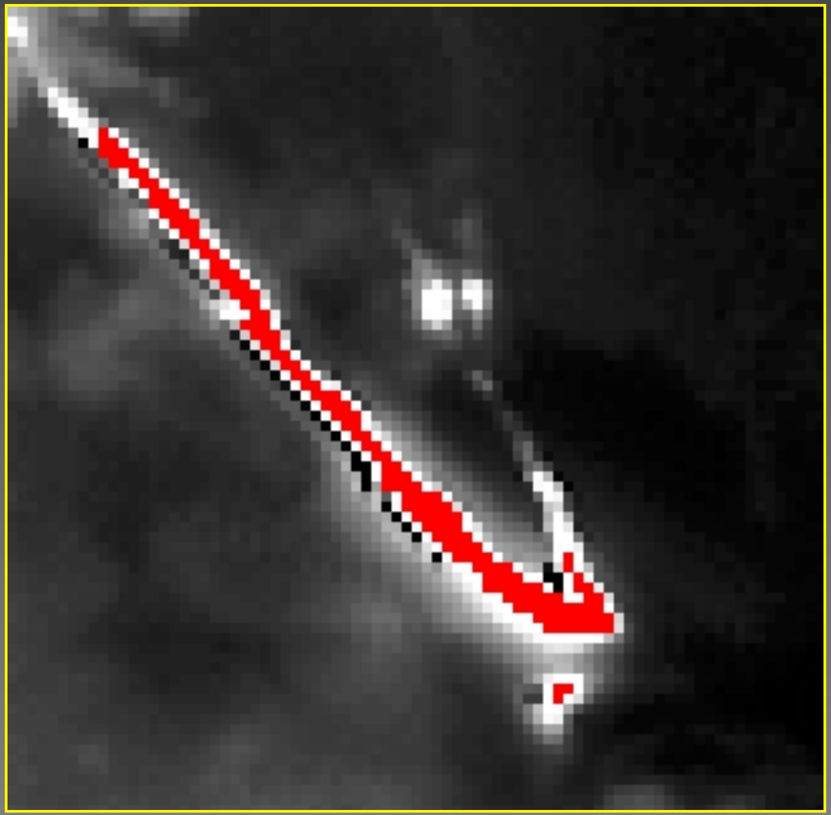

Band 4 *(LO2 gain)* temp (30m)
T_{b4} (max detected) = 464 °C
saturated pixels (red)

ASTER URP Statistics

- **Kizimen Volcano *(new eruption)***
  - – 1 Jan 2011 to 30 Apr 2012
  - – 49 ASTER observations
    - average: 1 scene / 9 days
    - 40 contained clouds (7 had no anomaly)
      - 7 *(thermal)*, 13 *(plume)*, 22 *(both)*

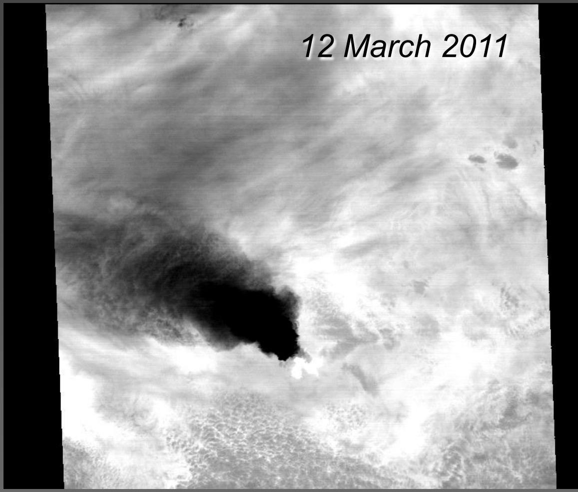

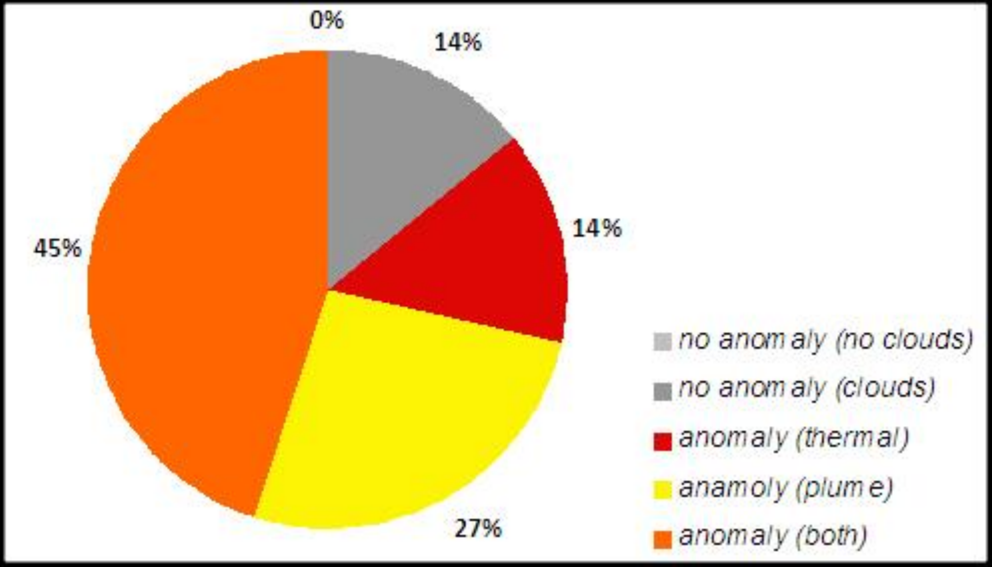

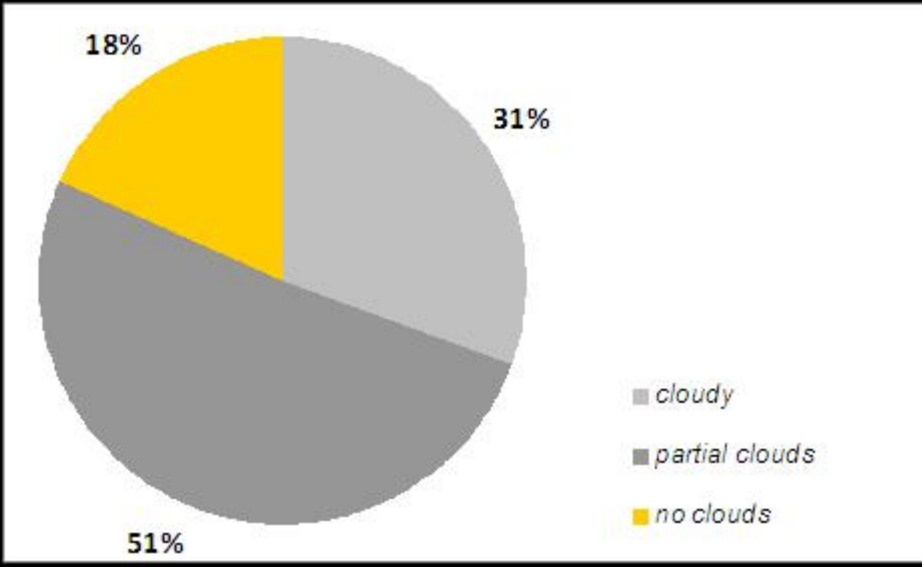

ASTER URP Statistics

- **Karymsky Volcano *(ongoing eruption)***
  - 1 Jul 2007 to 30 Apr 2012
  - 96 ASTER observations *(not continuous)*
    - average: 1 scene / 18 days *(1 / 5 days)*
    - 71 contained clouds (45 had no anomaly)
      - 19 *(thermal)*, 11 *(plume)*, 20 *(both)*

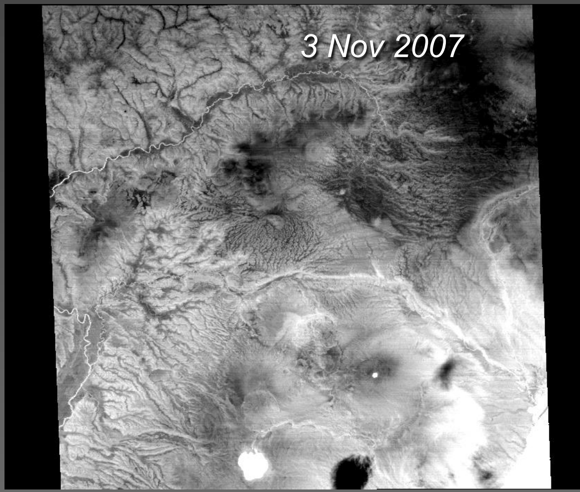

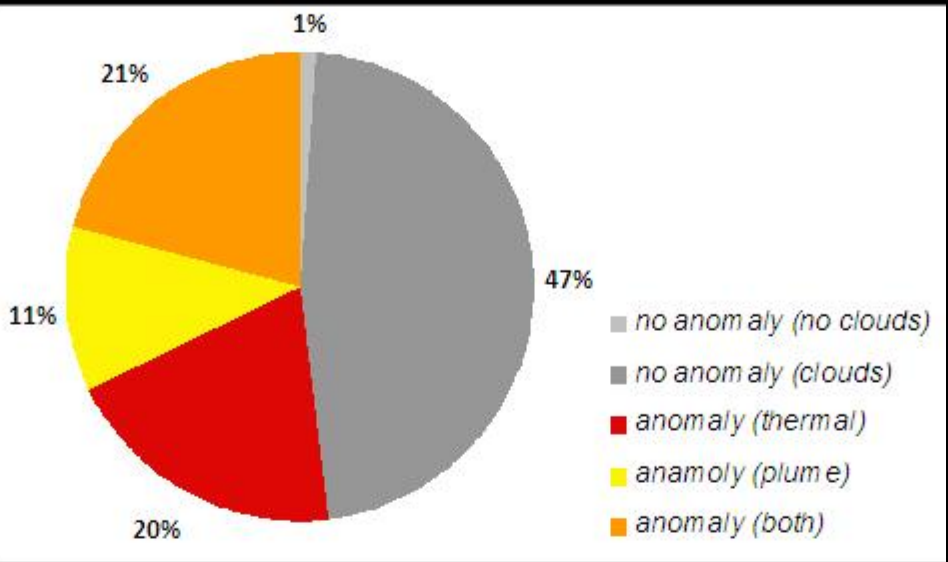

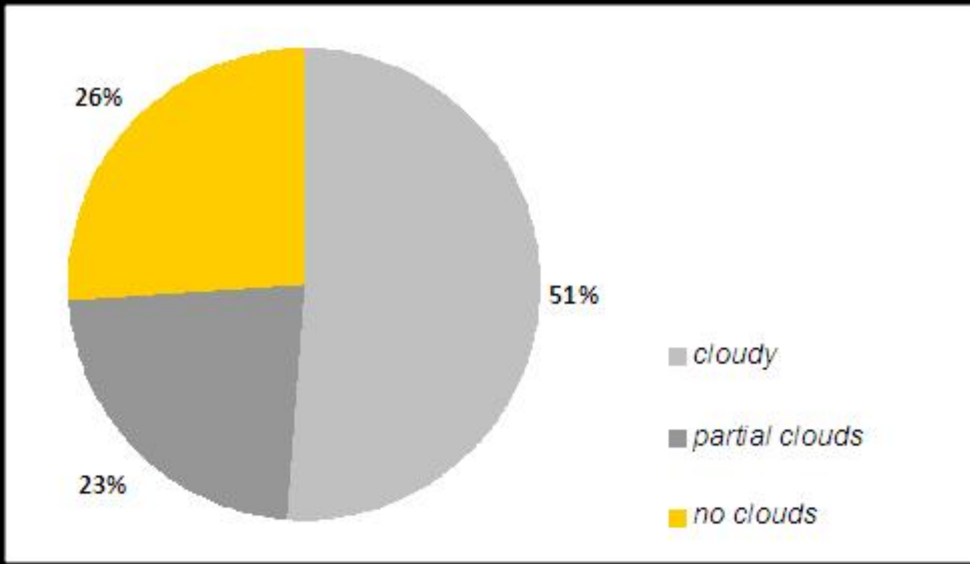

ASTER URP Statistics

- **URP Expansion Now Underway**
  - MODVOLC-based targets:
    - Cordon Caulle *(Chile)*
    - Erta Ale *(Ethiopia)*
    - Etna *(Italy)*
    - Nyamuragira *(DR Congo)*
    - Nyiragongo *(DR Congo)*
    - Pu’u O’o / Kilauea *(Hawaii, USA)*
    - Reventador *(Ecuador)*
    - Santa Maria *(Guatemala)*
    - Semeru *(Indonesia)*
    - Stromboli *(Italy)*
    - criteria
      - volcanoes with high activity / danger potential
      - globally distributed
      - 10 targets initially chosen to test the scheduling demand
        - will grow based upon capacity of the system

Spectral Analysis

Salton Sea Geothermal Field (SSGF)

SEBASS data

MAGI data

Spectral Analysis

- **Salton Sea Geothermal Field (SSGF)**
  - diversity of thermal/compositional targets
  - SEBASS TIR data *(26 Mar 2009 & 6 Apr 2010)*
  - geology validation target for new airborne MAGI instrument
    - funded by the NASA IIP
    - built by Aerospace Corp.
    - 32 TIR channels
    - initial flights: Nov. 2011
  - this study
    - TIR band positions of HyspIRI
    - spectral deconvolution

"sandbar" geothermal site
Salton Sea, CA (6 Apr 2010)

Spectral Analysis

- **Proposed HyspIRI TIR Bands (*μm*)**
  - 3.98, 7.35, 8.28, 8.63, 9.07, 10.53, 11.33, 12.05
- **Suggested Variant (*μm*)** *[Ramsey & Rose, 2009]*
  - 3.98, 7.35, 8.28, 8.55, 9.07, 10.05, 11.35, 12.05
    - better discrimination of:
      - SO_2 (8.55), silicates (10.05), carbonates (11.35)

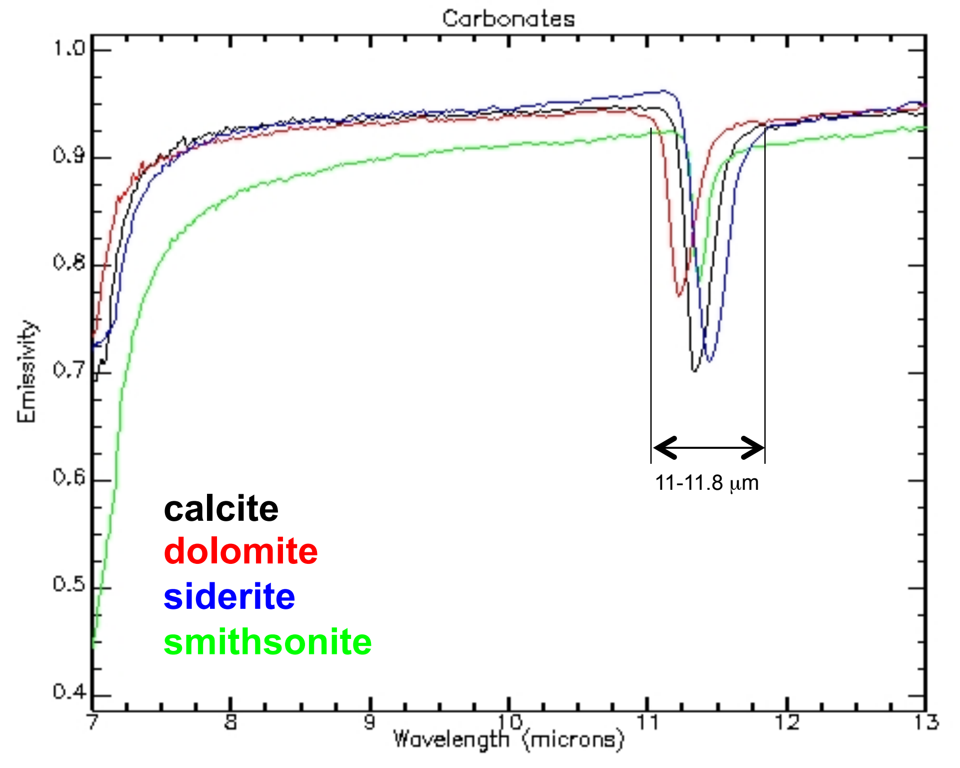

- **Focus of This Study**
  - only varying the 10 μm band (10.18)

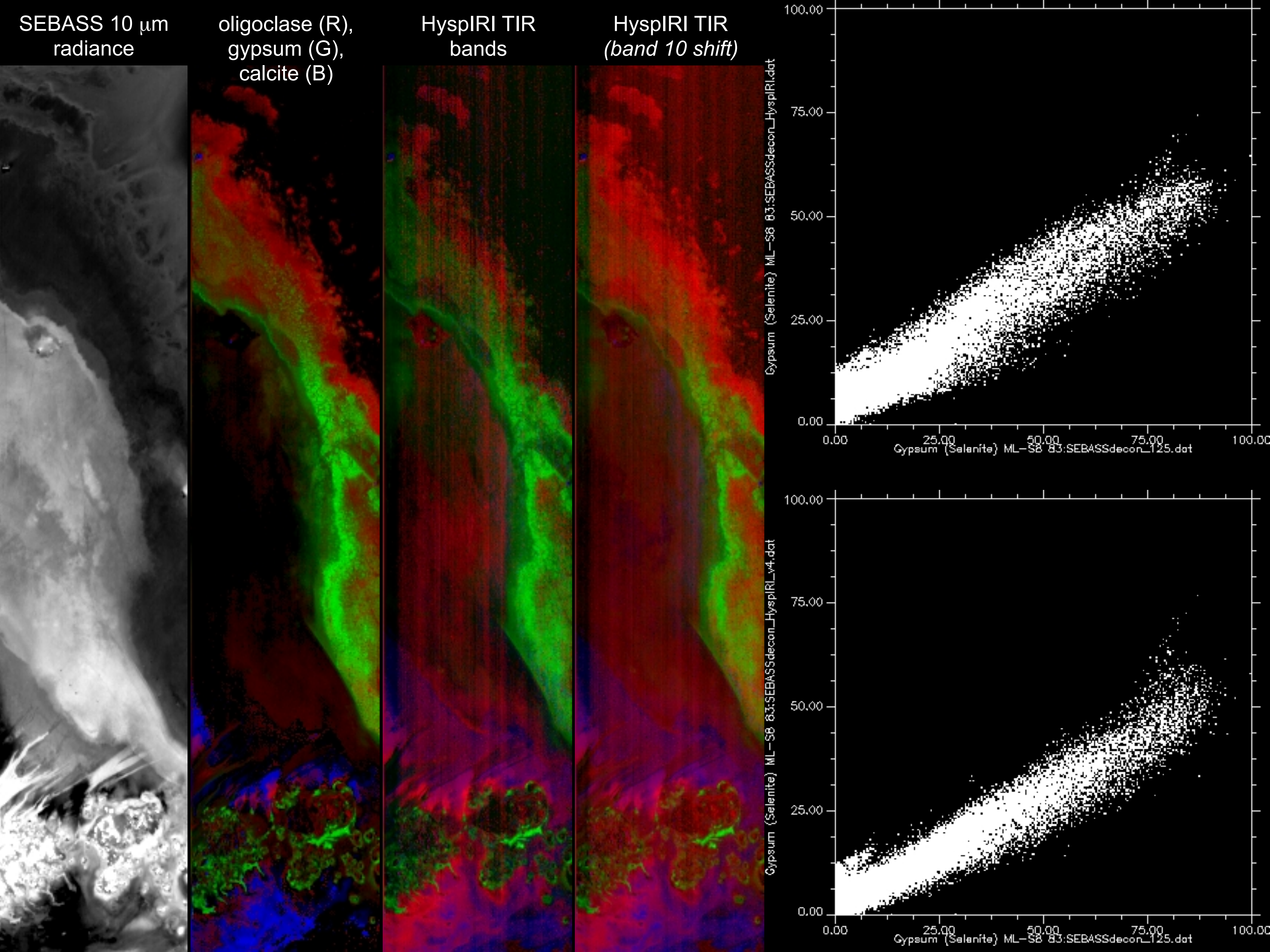
SEBASS 10 μm radiance
oligoclase (R), gypsum (G), calcite (B)
HyspIRI TIR bands
HyspIRI TIR (band 10 shift)
Gypsum (Selenite) ML-S8 83:SEBASSdecon_HyspIRI.dat
Gypsum (Selenite) ML-S8 83:SEBASSdecon_125.dat
Gypsum (Selenite) ML-S8 83:SEBASSdecon_HyspIRI_v4.dat
Gypsum (Selenite) ML-S8 83:SEBASSdecon_125.dat
0.00
25.00
50.00
75.00
100.00

MAGI On The Twin Otter

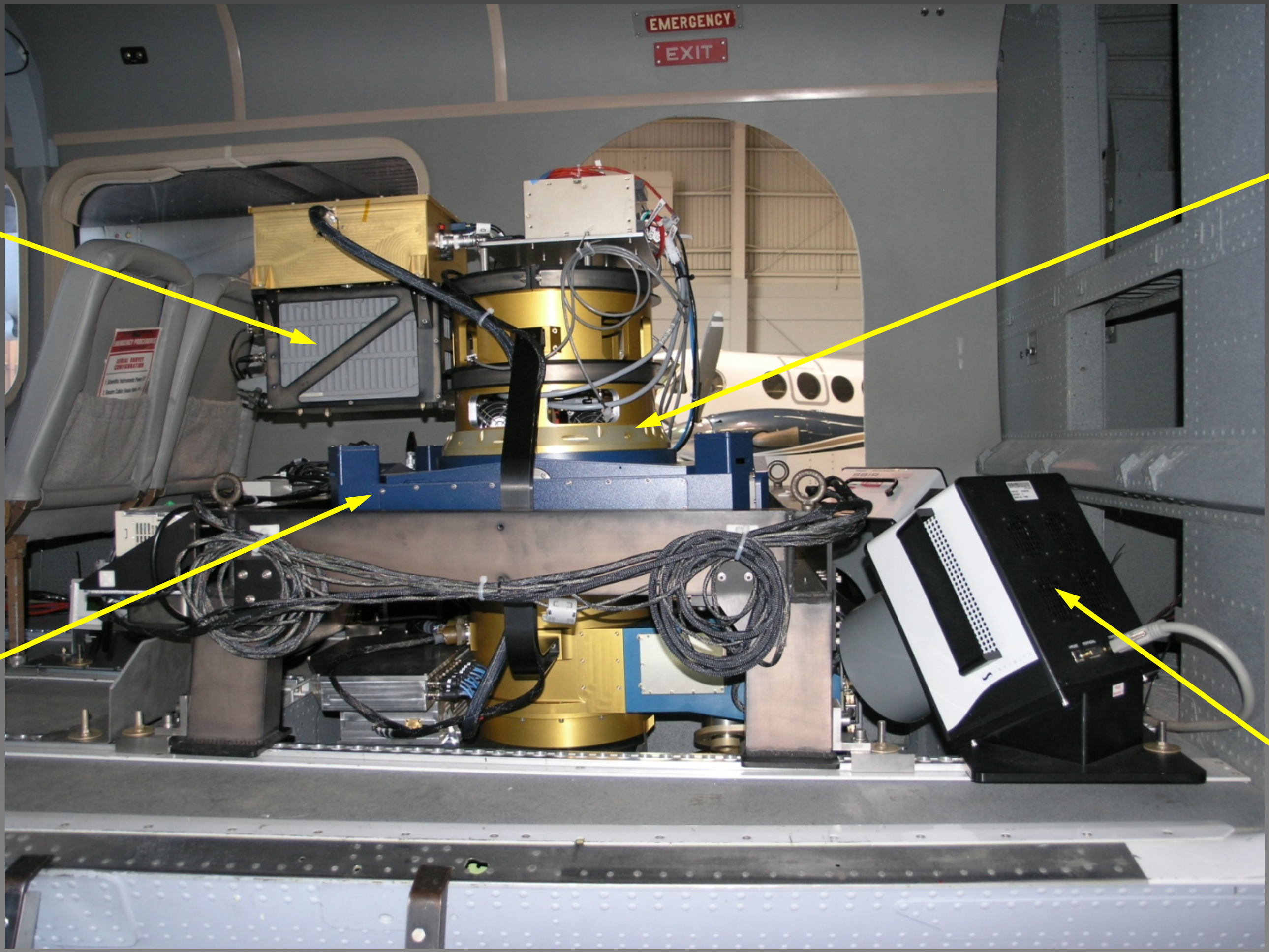

Inertial Navigation System

Sensor

Commercial Stabilization Platform

Calibration Blackbody

MAGI L0 Data *(10 μm Band)*

Salton Sea, CA
(~ 1-meter GSD)

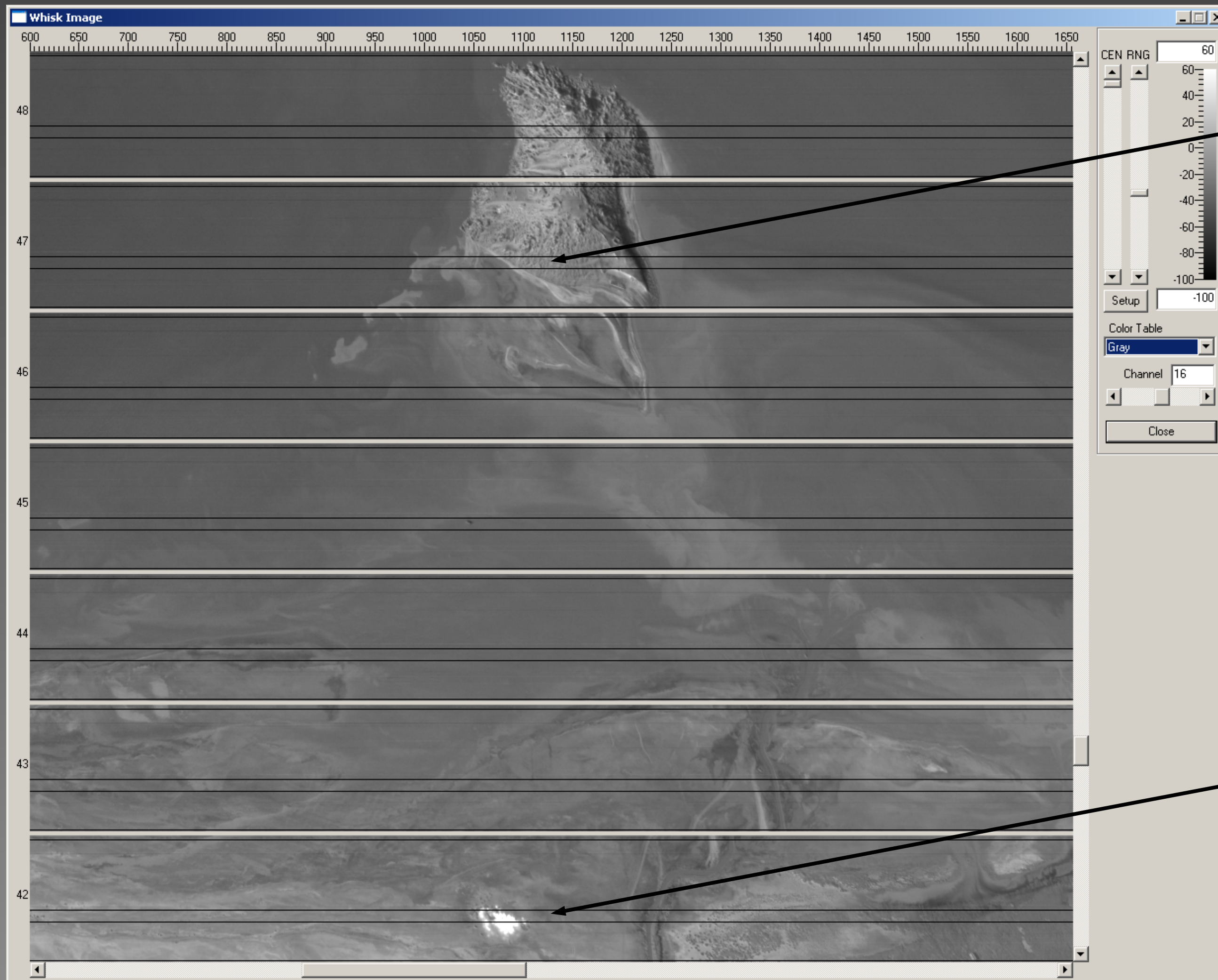

Mullet Island

fumarole region

MAGI Analysis

- **Initial Analysis**
  - limited amount of data processed from L1
  - some detector line noise
  - temperature/emissivity data appear very good
  - compositional diversity matches well with SEBASS mineral maps

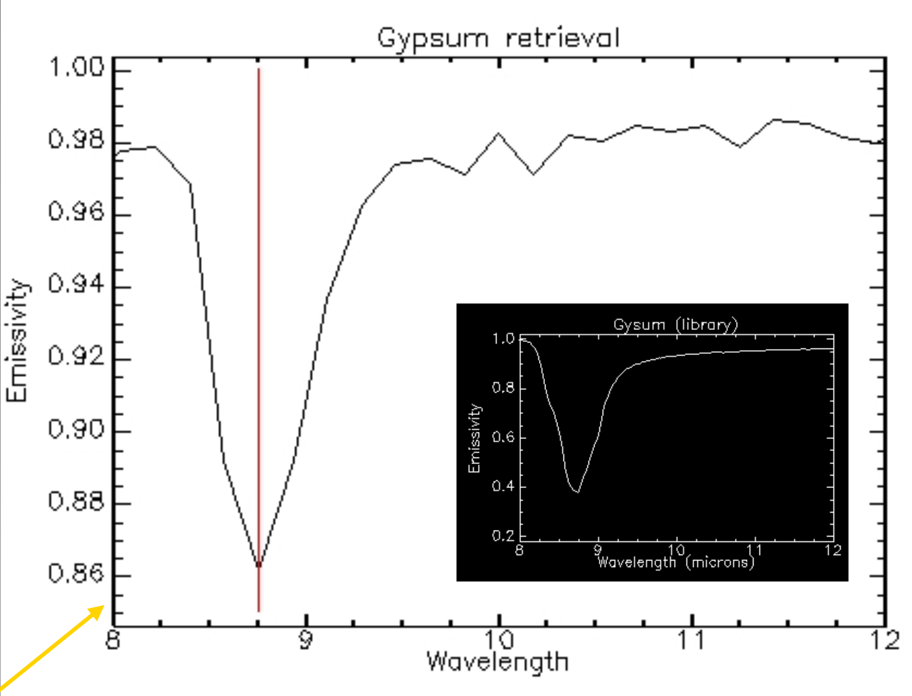

Conclusions

- **TIR Observations of Volcanic Targets**
  - temporal
    - 8 year volcano archive from the URP Program
    - several 1000 scenes available for analysis
    - TIR observations of numerous volcanic eruptive styles *(nearly identical to HyspIRI spatial/spectral/temporal)*
    - clouds are always an issue (74 – 82% of URP scenes)
      - *high repeat time is critical (52 – 86% of scenes show anomalies)*
  - spectral
    - new instruments/tools to simulate HyspIRI TIR bands
    - slight tweaking of band positions needs to be studied
      - greatly improves detection of feldspar silicate minerals
      - carbonates and SO_2 as well

Quantifying global volcanic unrest with HyspIRI: near-real-time algorithms and products

Robert Wright

Hawai'i Institute of Geophysics and Planetology, Honolulu

UNIVERSITY of HAWAI'I MĀNOA

What are we trying to detect, quantify, and monitor?

-1500 potentially active volcanoes distributed around the globe

- Can display high temperature (1100 ^{o}C) and/or low temperature (<100 ^{o}C) manifestations of unrest

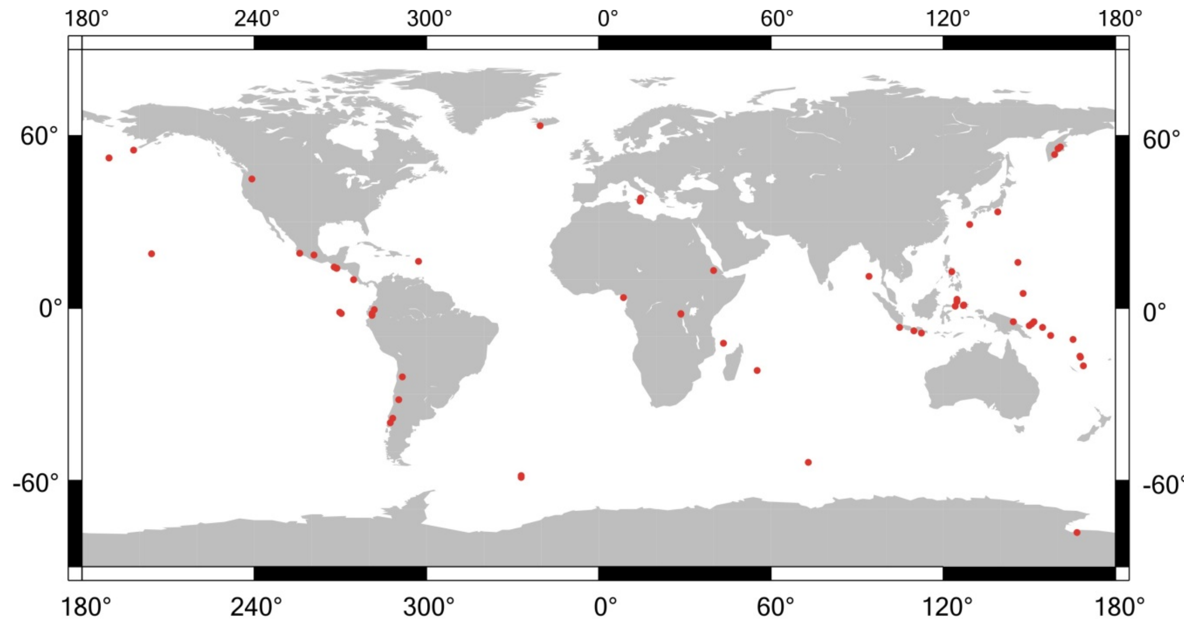

What are we trying to detect, quantify and monitor?

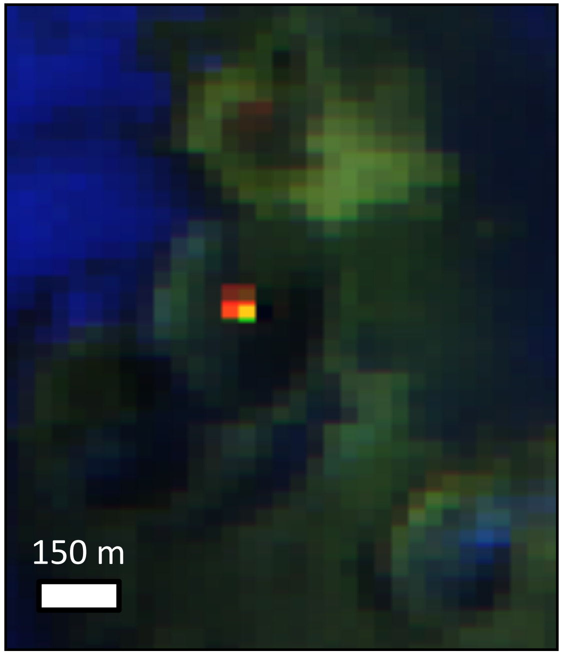

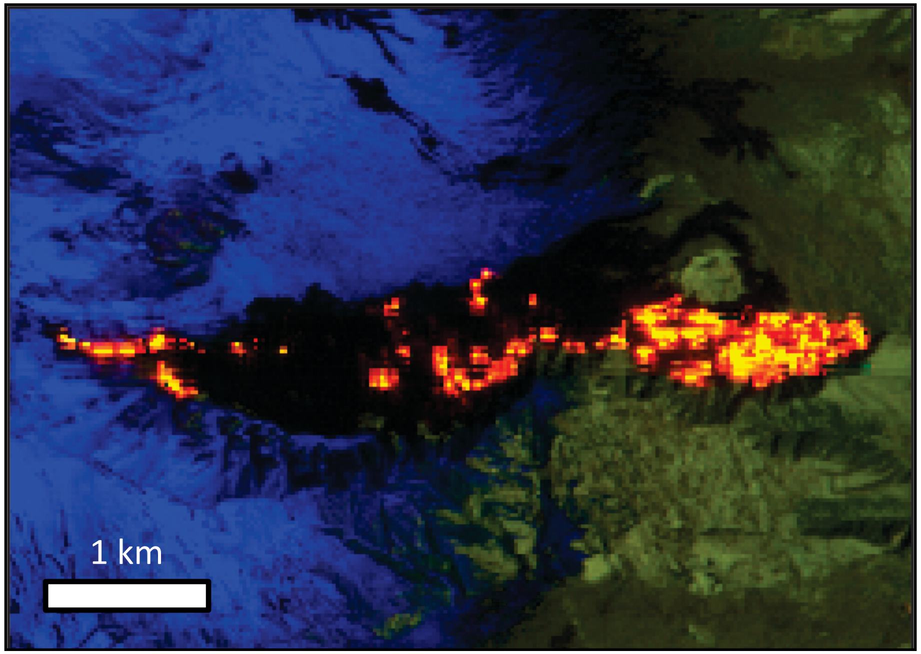

Volcanic activity can be on small spatial scales (decameter) or large (kilometer)

What are we trying to detect, quantify and monitor?

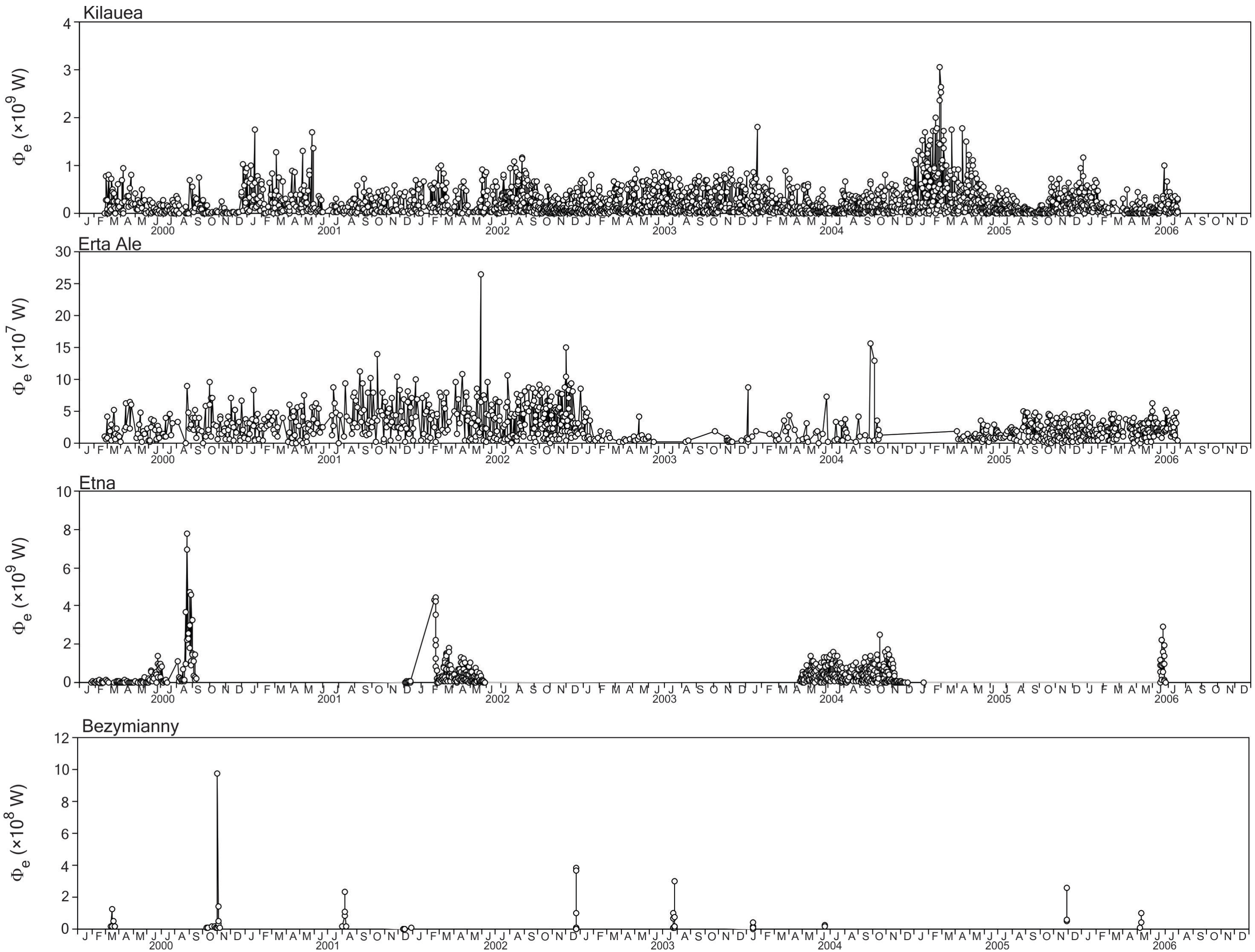

Volcanic activity can be episodic or persistent

What are we trying to detect, quantify and monitor?

Eruptions can take us by surprise

Photo: T. Fischer (Univ. New Mexico)

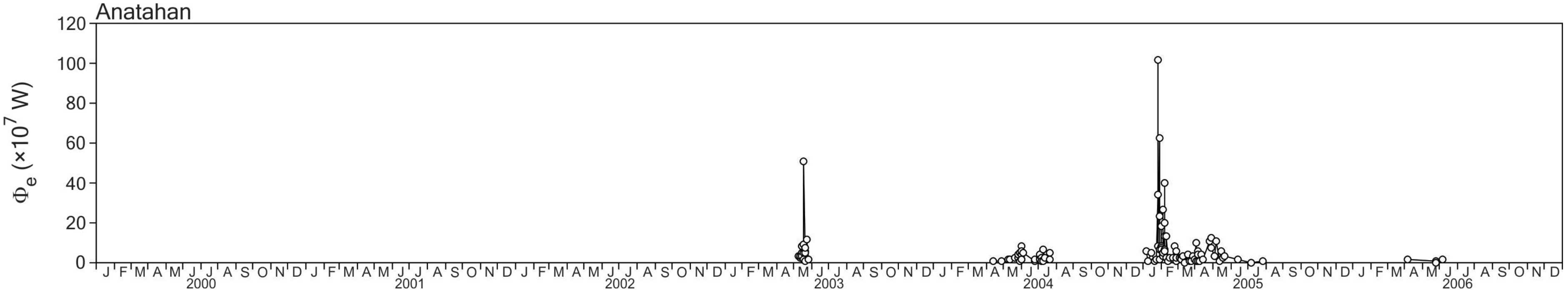

Resulting requirements for a monitoring algorithm

Global mapping mission

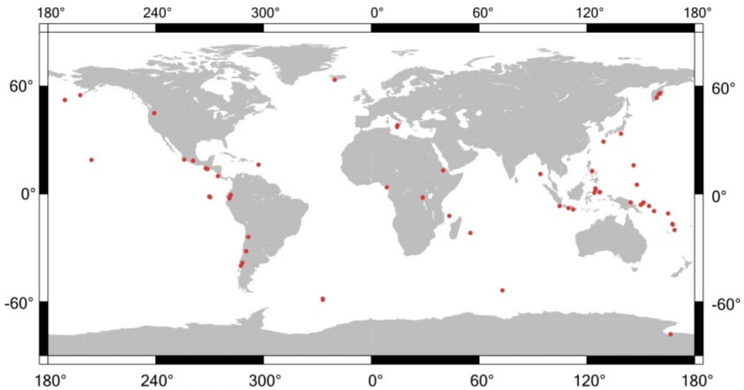

Night and day

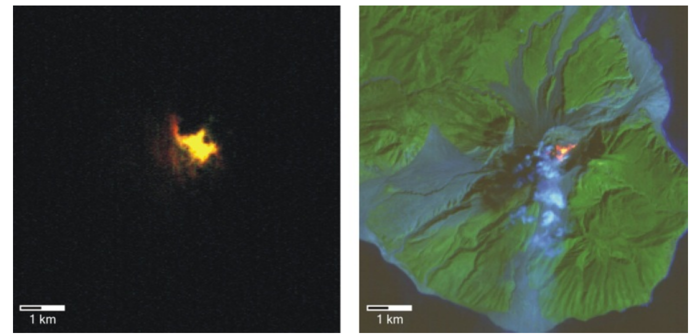

Timely delivery of information to users (direct broadcast; on-board

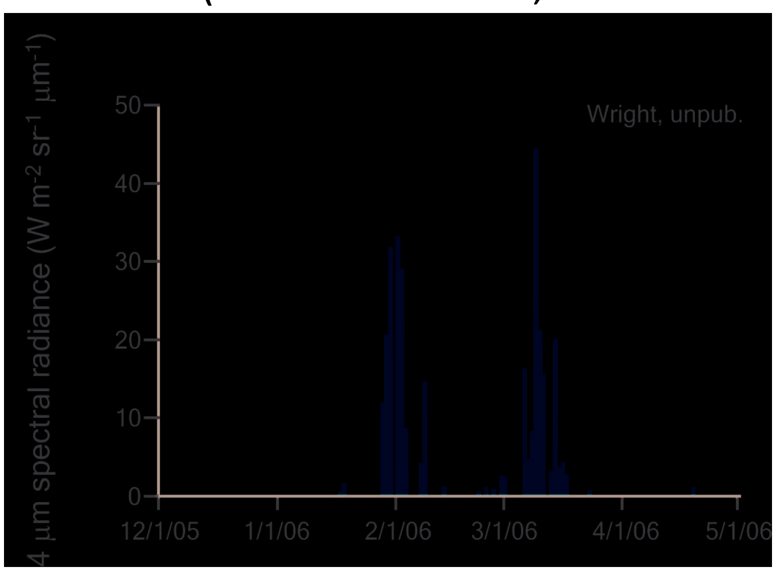

Results/data delivered in a useable (and useful) format

Unix time	Satellite	Longitude	Latitude	L_{21} (W m^{-2} sr^{-1} μm^{-1})	L_{22}	L_6	L_{31}	L_{32}
1089853500	A	159.424927	54.047855	0.775	0.802	177.015	7.087	6.790
1089838800	T	159.439728	54.049419	2.228	-10.000	166.546	8.392	7.967
1089853500	A	159.448288	54.052444	1.440	1.453	177.015	7.786	7.453
1089853500	A	159.453903	54.045853	1.218	1.235	177.015	7.558	7.156

The past

Reliant on low spatial resolution data because of its high temporal resolution

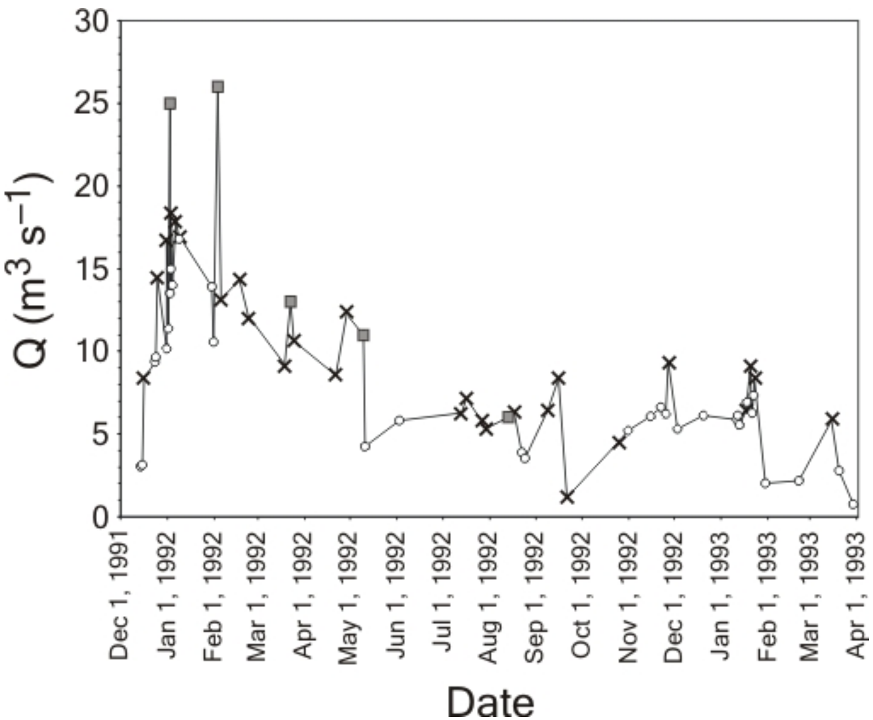

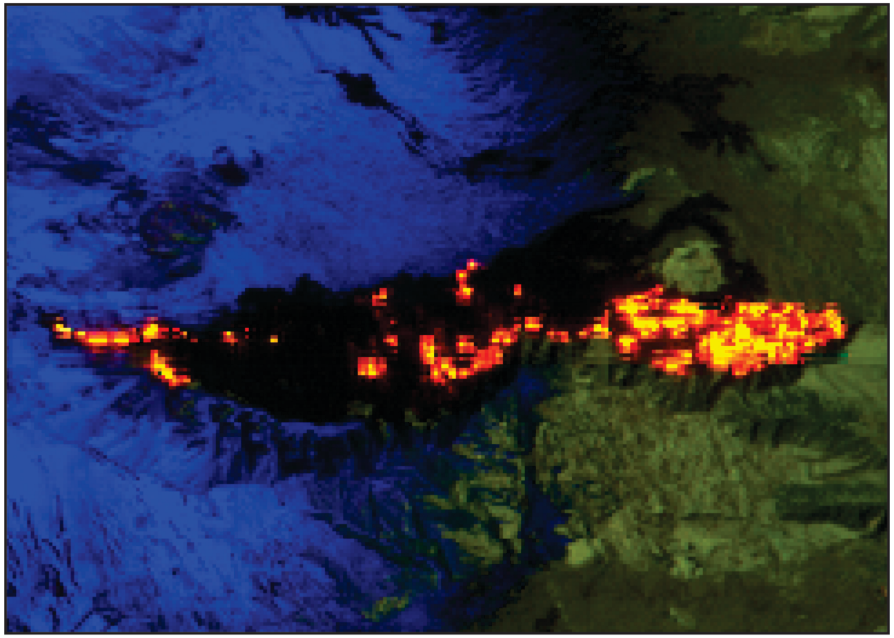

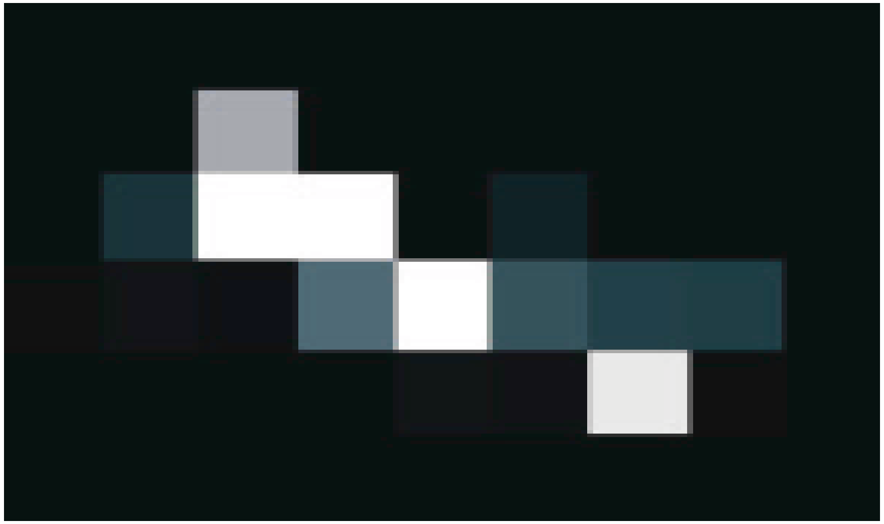

HyspIRI fills the gap between MODIS and LDCM/ASTER

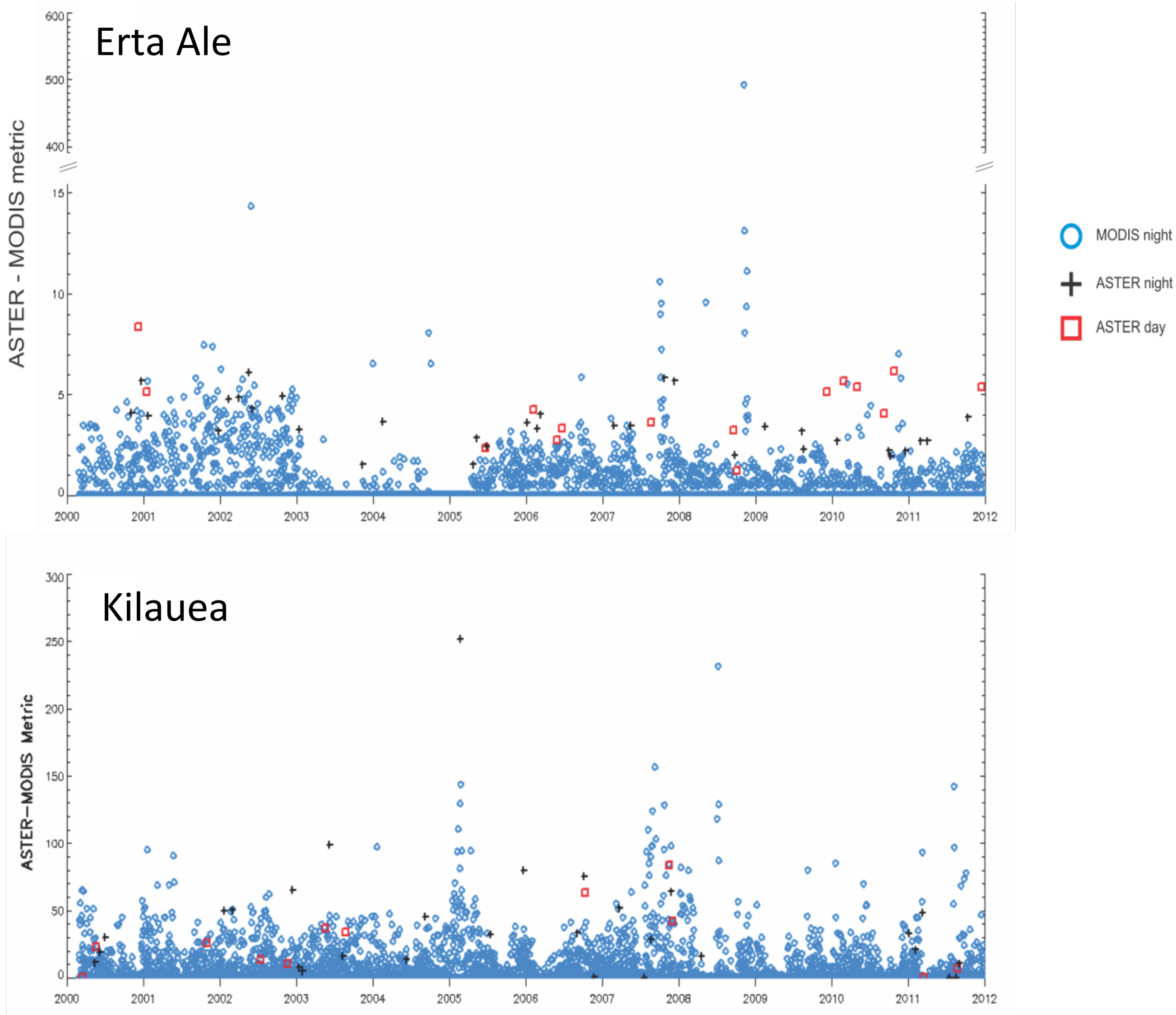

Hulme, Wright, Oppenheimer & De Souza (in review)

HyspIRI fills the gap between MODIS and LDCM/ASTER

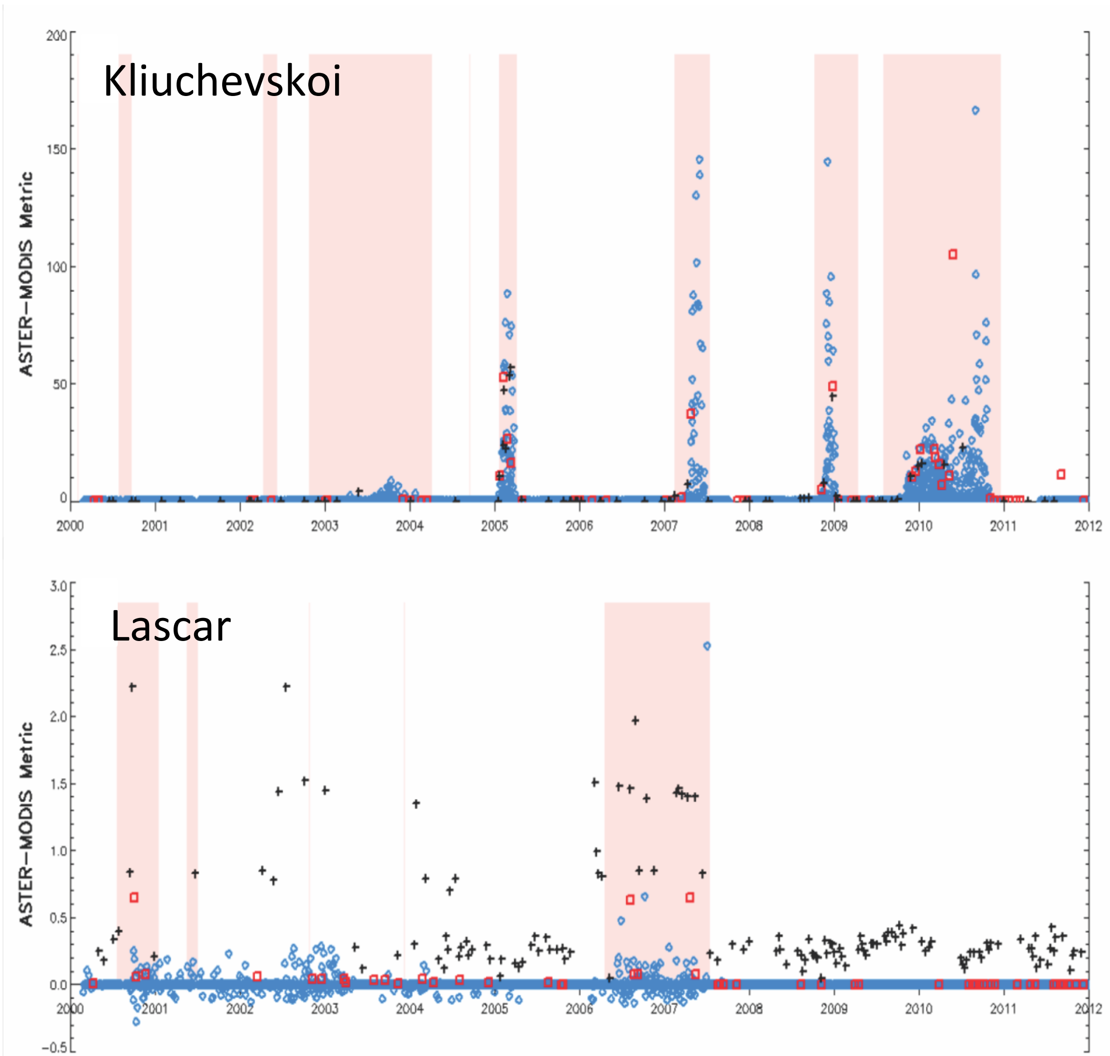

Hulme, Wright, Oppenheimer & De Souza (in review)

HyspIRI fills the gap between MODIS and LDCM/ASTER

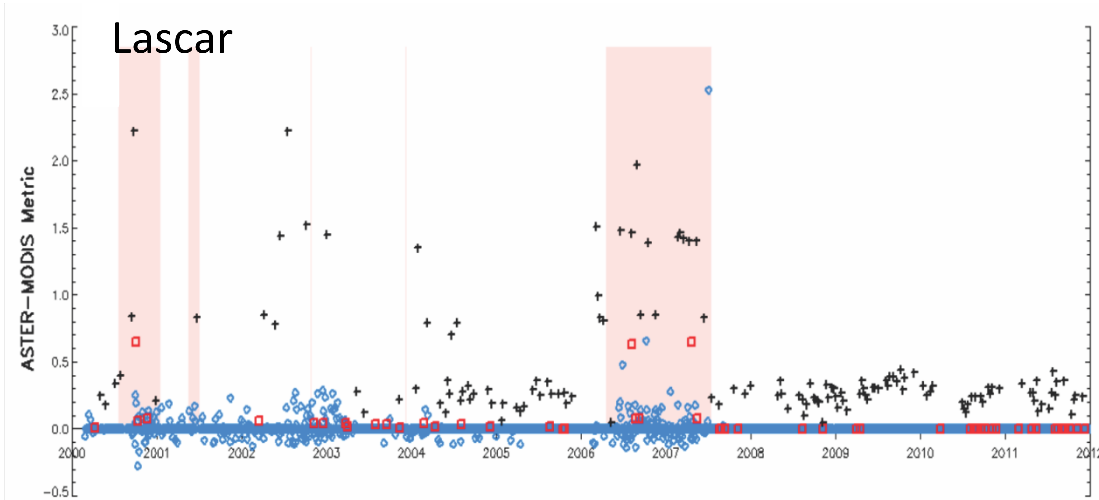

Anatahan

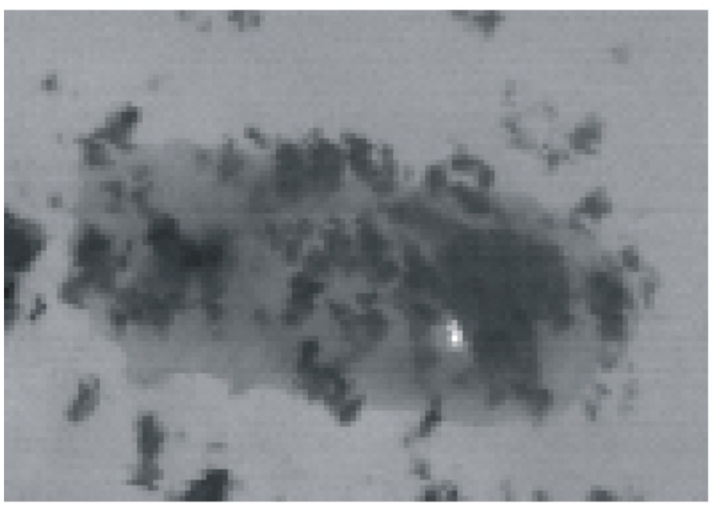

ASTER

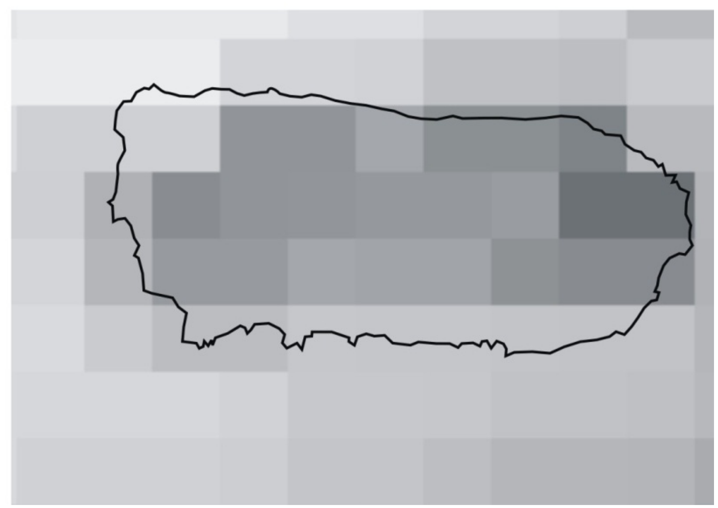

MODIS

Potential HyspIRI hot-spot detection algorithms

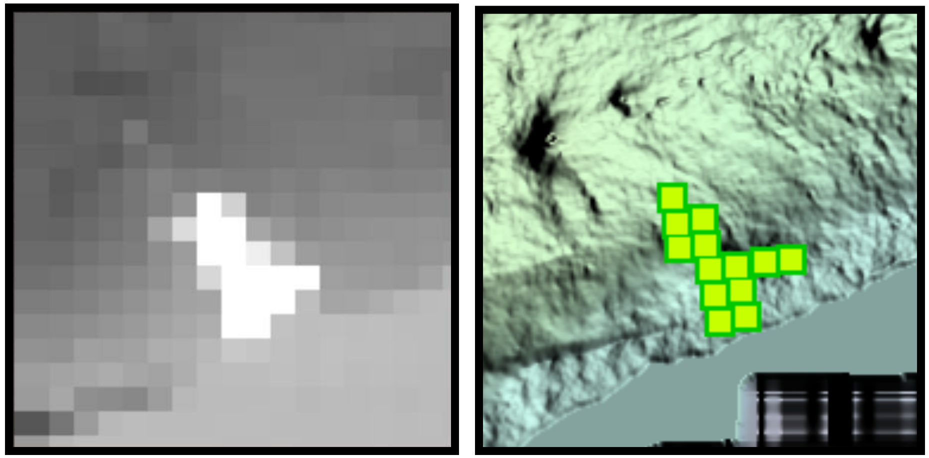

1. Class of algorithm
2. "Plug and play" with the HyspIRI data stream?
3. Computational complexity

The basis of existing, low resolution algorithms

At 11 μm, L_λ = 9.5 W m^{-2} sr^{-1} μm^{-1}
At 4 μm, L_λ = 0.4 W m^{-2} sr^{-1} μm^{-1}

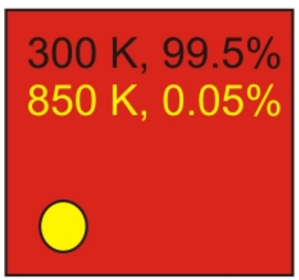

At 11 μm, L_λ = 9.6 W m^{-2} sr^{-1} μm^{-1}
At 4 μm, L_λ = 1.3 W m^{-2} sr^{-1} μm^{-1}

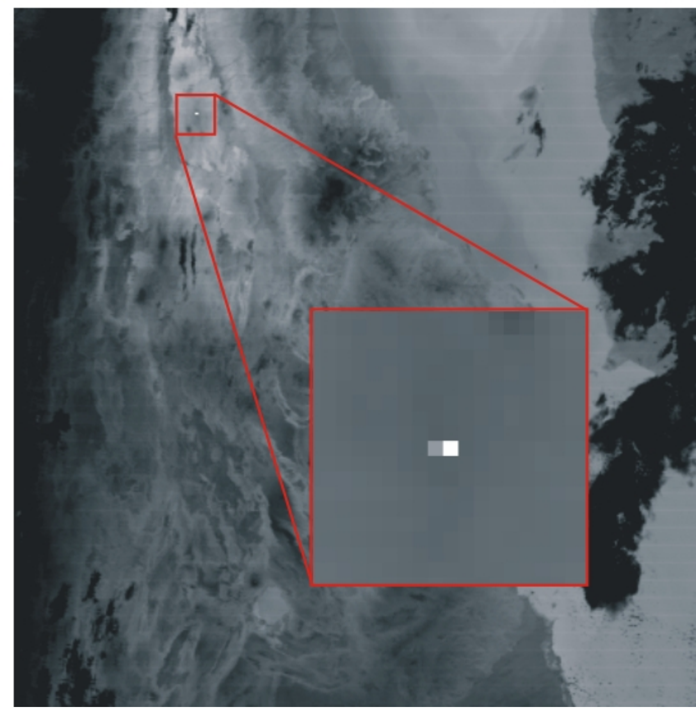

The basis of existing, low resolution algorithms

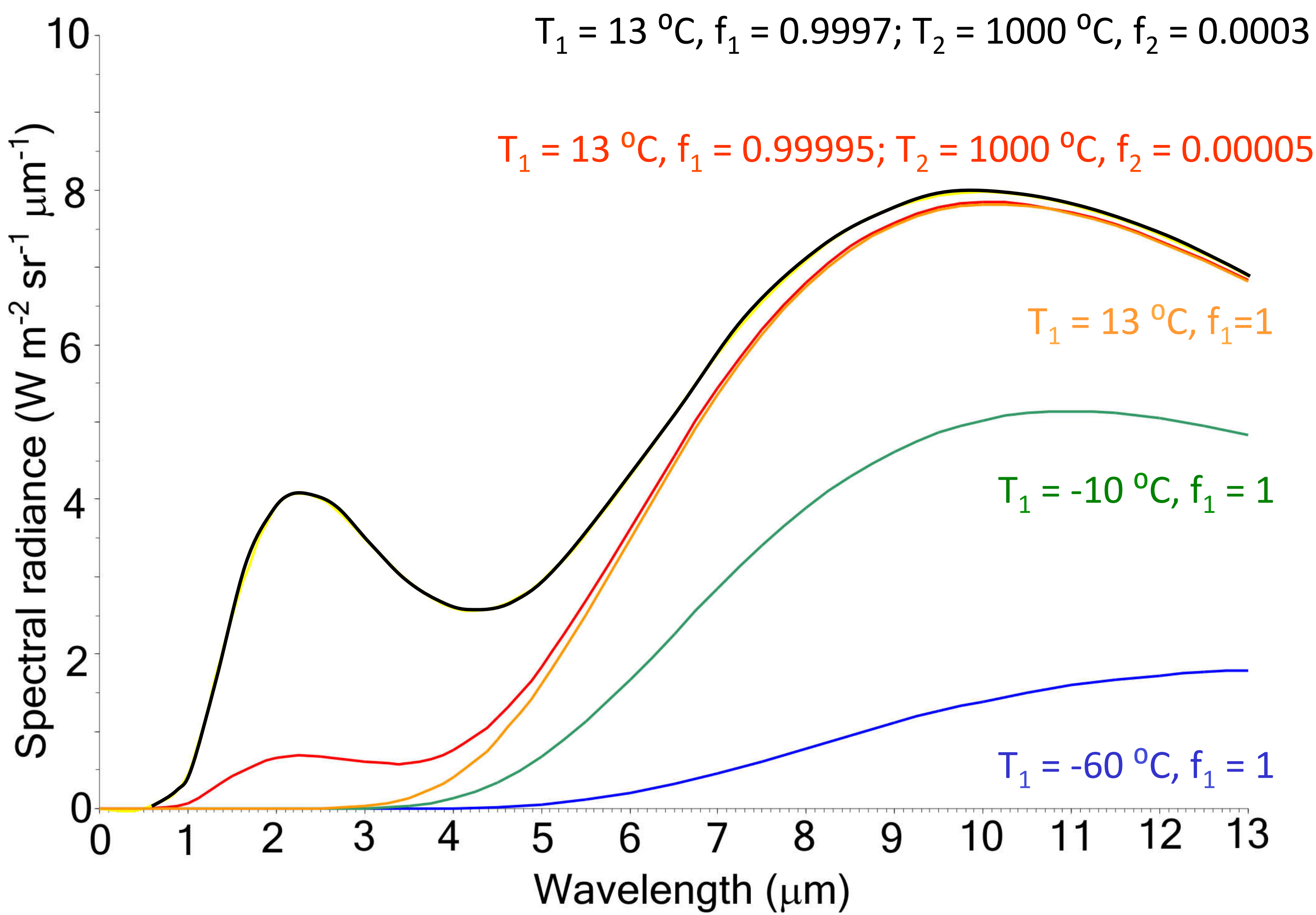

Spectral-contextual hot-spot detection algorithm

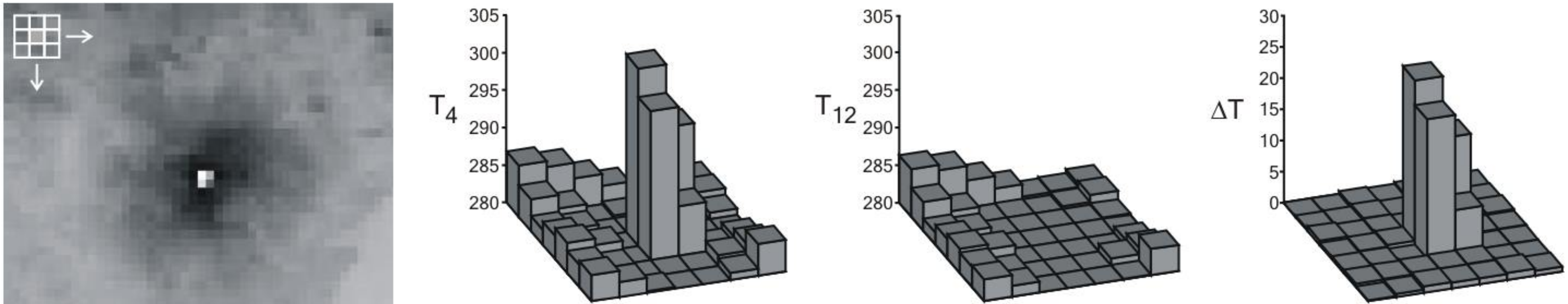

e.g. MODIS Fire Product

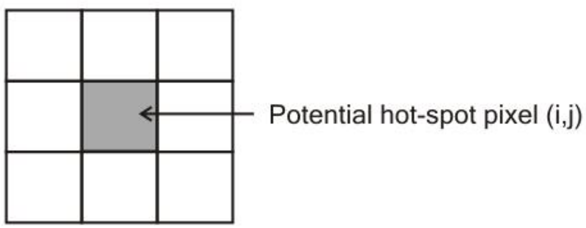

How does ΔT still work when the hot-spots are no longer sub-pixel-sized?

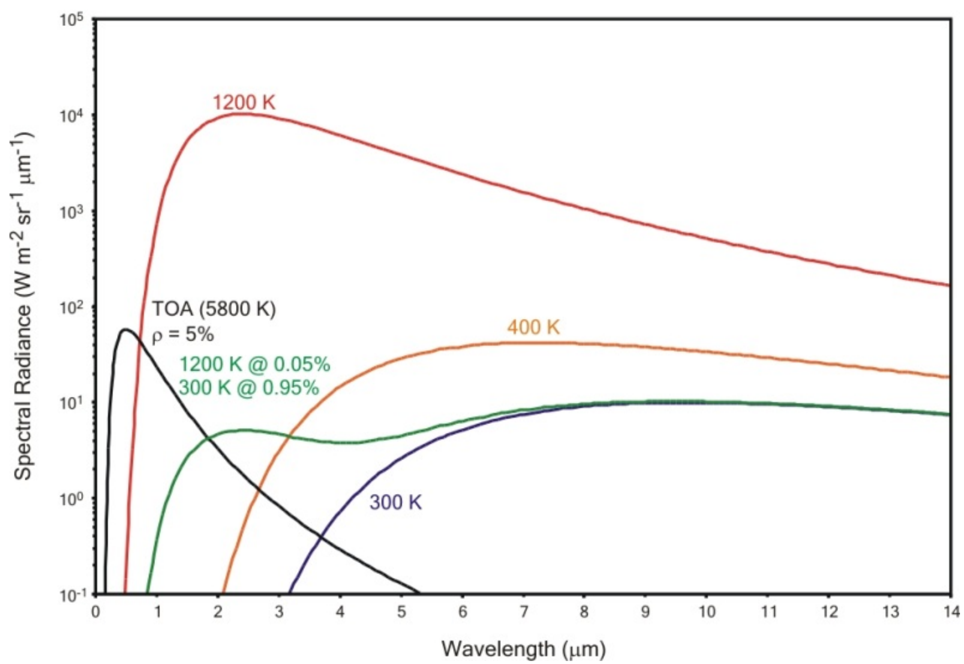

Dealing with daytime 4 μm data

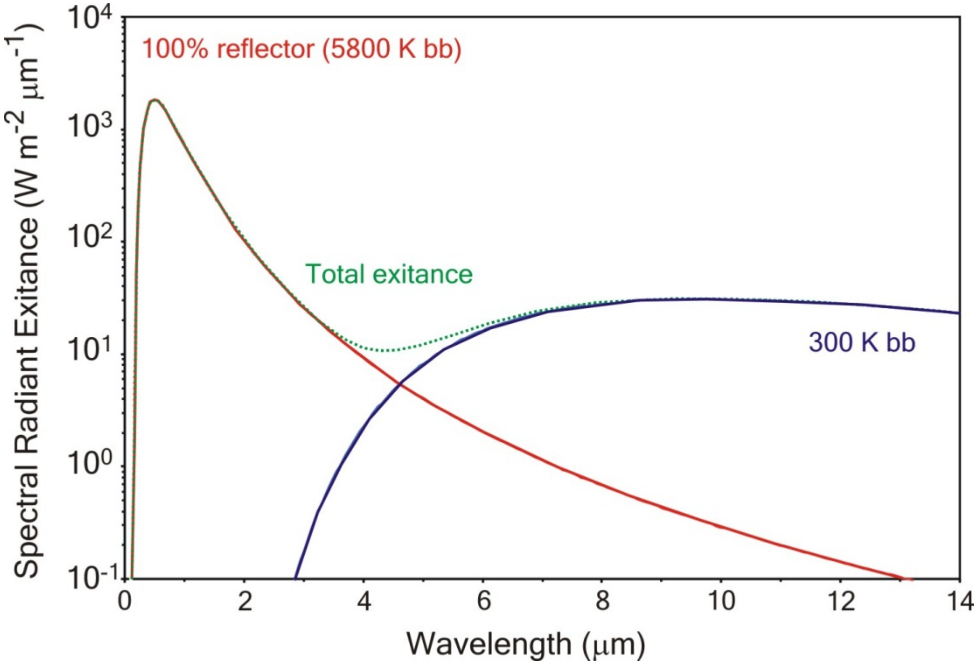

How to estimate excess radiance in the presence of reflected sunlight, while just using the HyspIRI TIR subsystem?

'Raw' 4 μm daytime data

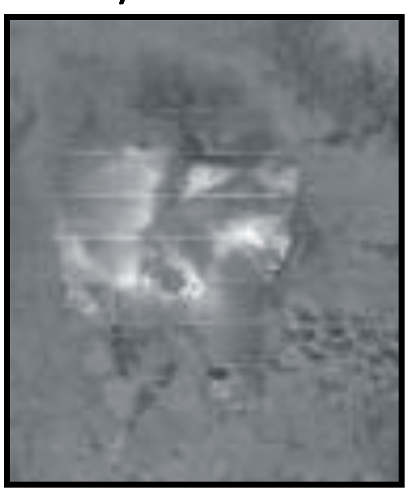

$$L_{4corr} = L_4 - 0.0426 \times L_{1.6}$$

Corrected 4 μm daytime data

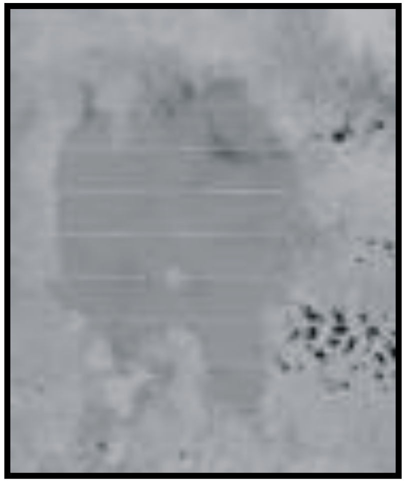

Must also account for sunglint in daytime data

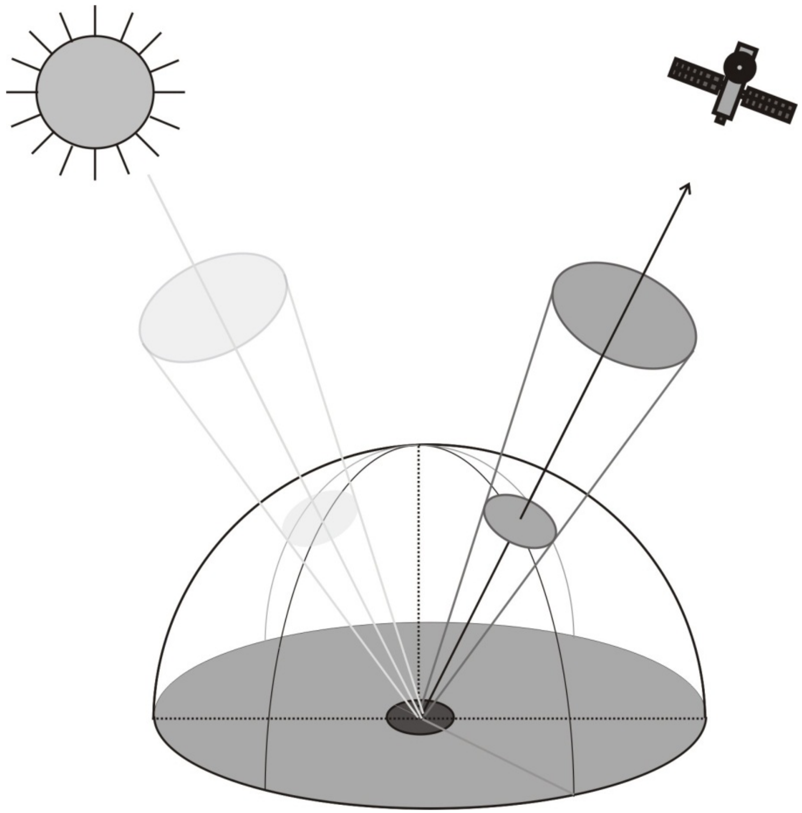

Just use an angular threshold

MODVOLC: spectral point operation, algorithm, and output

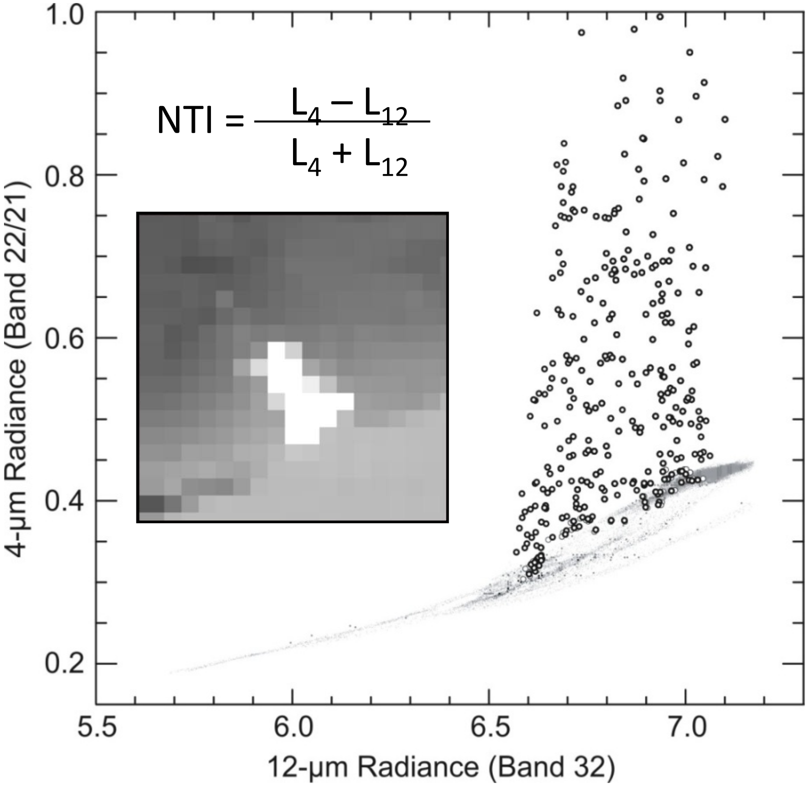

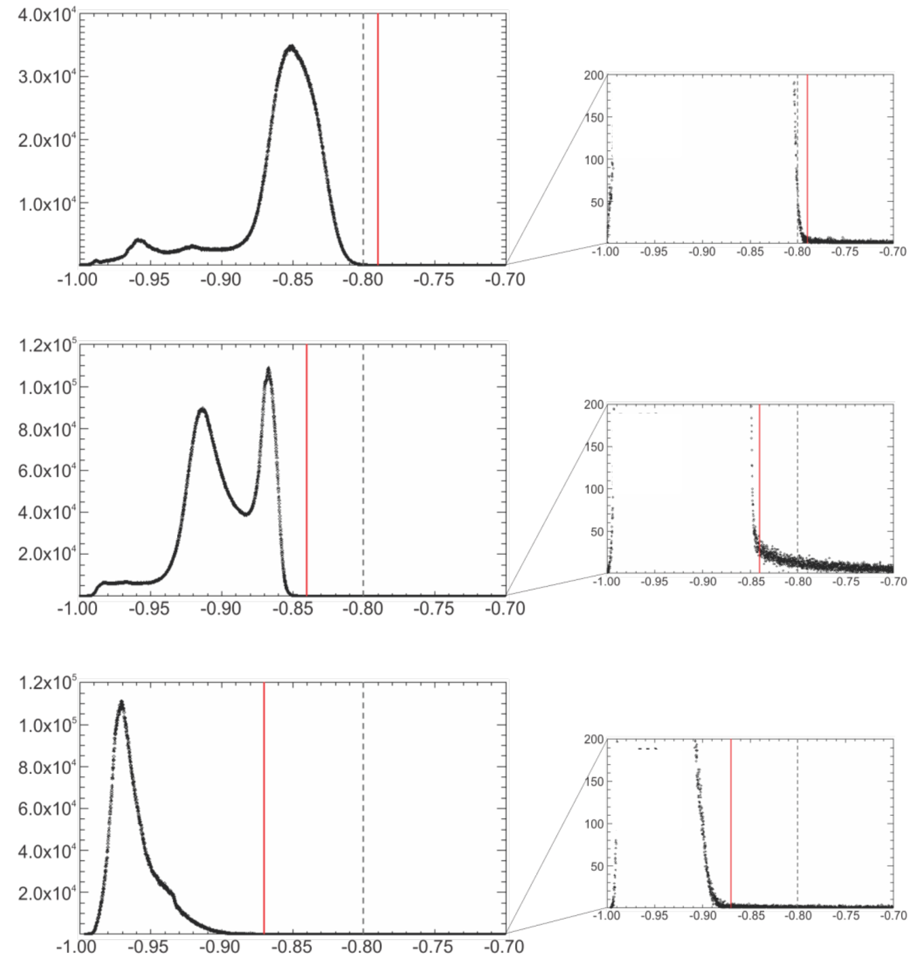

Unix time	Satellite	Year	Month	Day	Hour	Minute	Longitude	Latitude	L_{21} (W m^{-2} sr^{-1} μm^{-1})	L_{22}	L_6	L_{31}	L_{32}	Satellite zenith	Satellite azimuth	Sunzenith	Sun azimuth	Line	Sample	NTI	Glint vector
1089853500	A	2004	07	14	15	05	159.424927	54.047855	0.775	0.802	177.015	7.087	6.790	42.97	96.49	101.53	22.91	329	210	-0.789	109.602
1089838800	T	2004	07	14	11	00	159.439728	54.049419	2.228	-10.000	166.546	8.392	7.967	5.88	75.11	98.09	325.58	793	743	-0.563	95.933
1089853500	A	2004	07	14	15	05	159.448288	54.052444	1.440	1.453	177.015	7.786	7.453	42.97	97.57	101.53	22.93	331	211	-0.674	108.869
1089853500	A	2004	07	14	15	05	159.453903	54.045853	1.218	1.235	177.015	7.558	7.156	42.97	96.49	101.53	22.93	329	211	-0.706	109.617

Time-series hot-spot detection algorithms

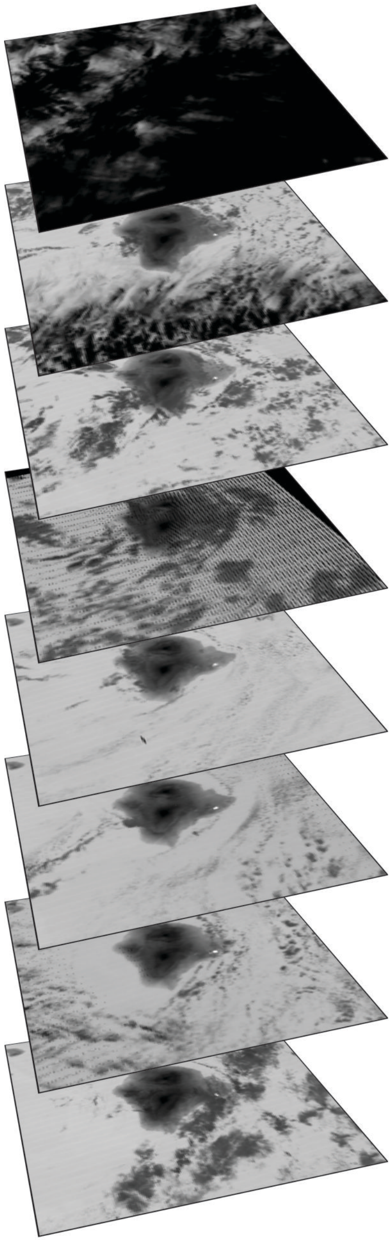

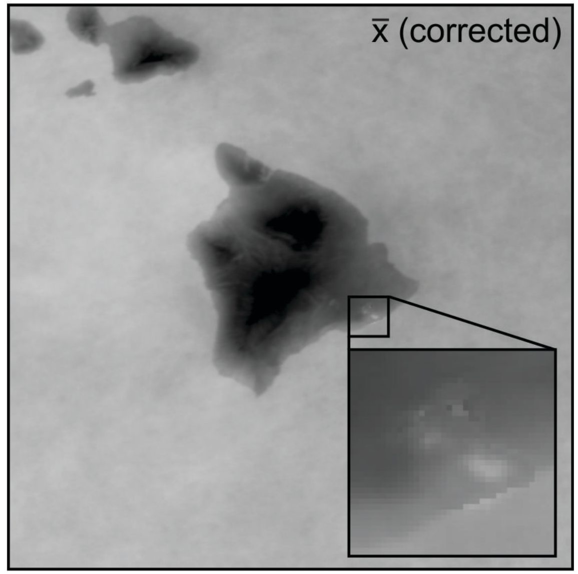

$$\otimes T_4(x,y,t) = \frac{T_4(x,y,t) - \bar{T}_4(x,y)}{\sigma_4(x,y)}$$

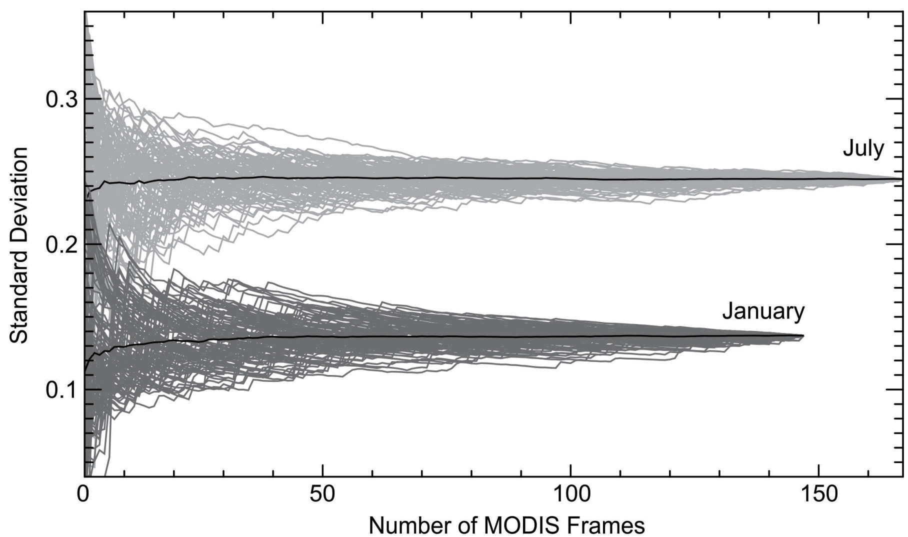

Koeppen et al., 2010, after Pergola et al., 2004

Path forward: simulate HyspIRI data, test algorithms

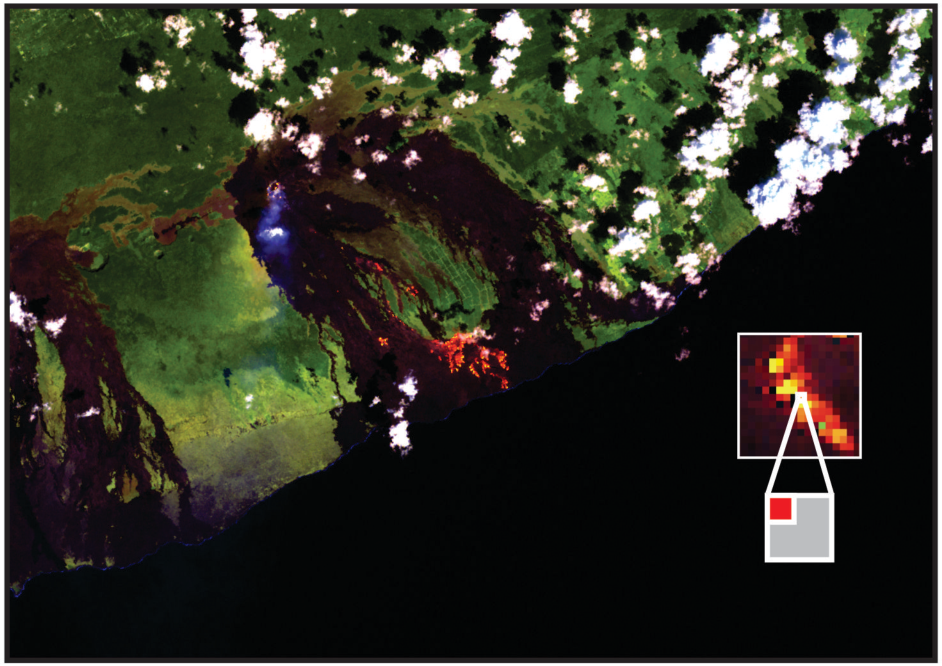

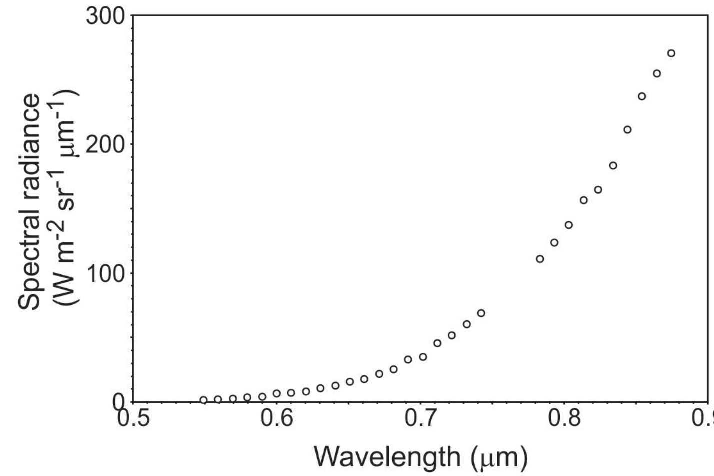

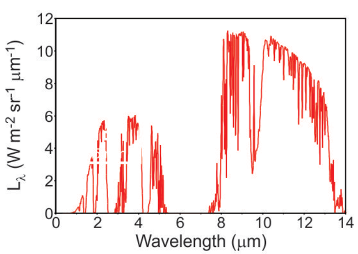

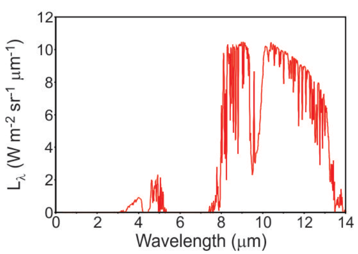

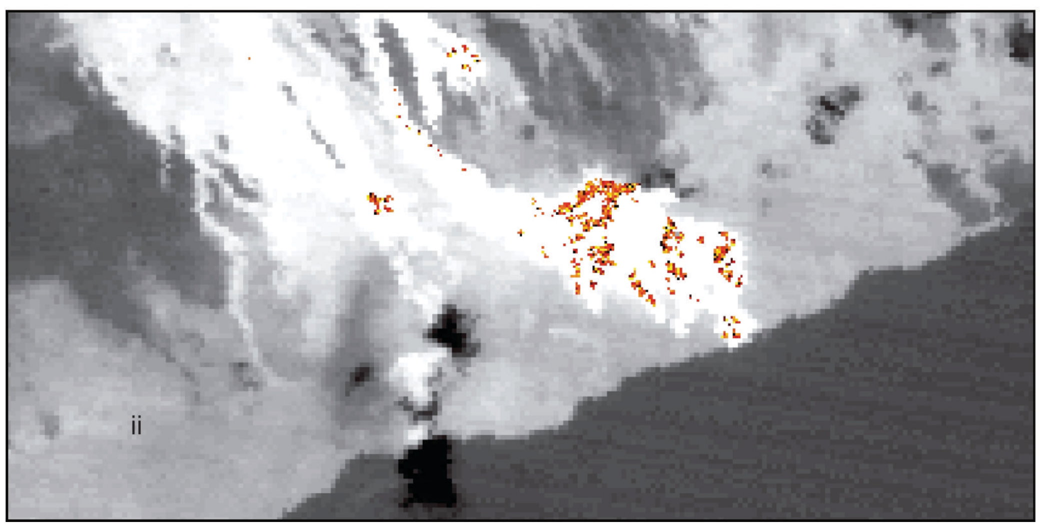

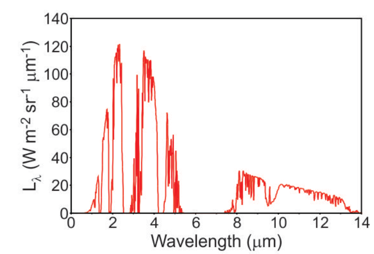

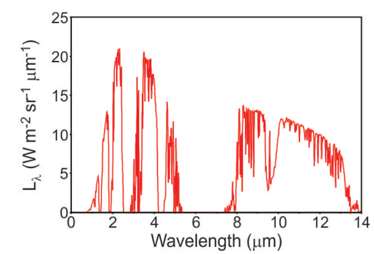

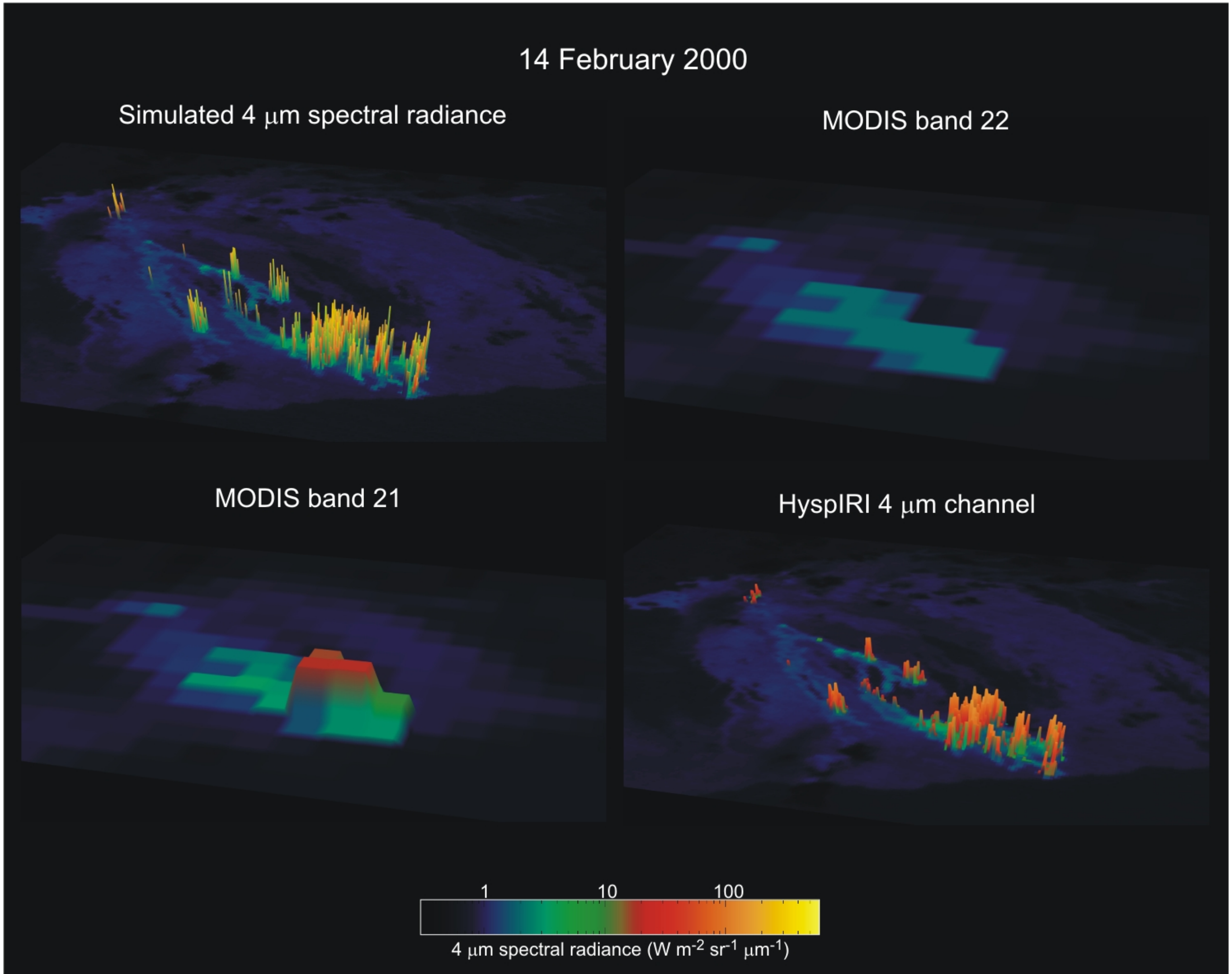
14 February 2000
Simulated 4 μm spectral radiance
MODIS band 22
MODIS band 21
HyspIRI 4 μm channel
1
10
100
4 μm spectral radiance (W m-2 sr-1 μm-1)

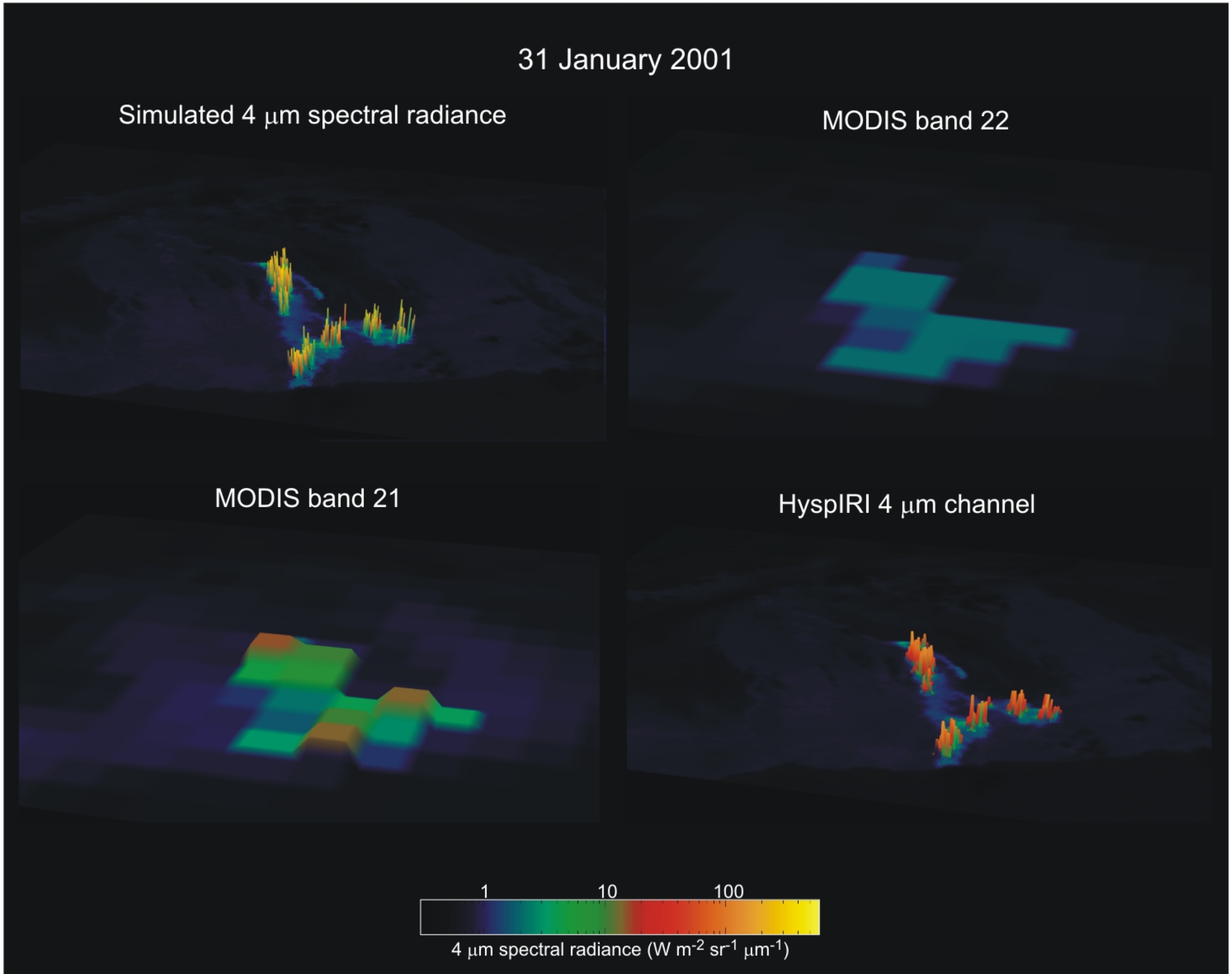

31 January 2001
Simulated 4 μm spectral radiance
MODIS band 22
MODIS band 21
HyspIRI 4 μm channel
1
10
100
4 μm spectral radiance (W m-2 sr-1 μm-1)

Products: useful and useable

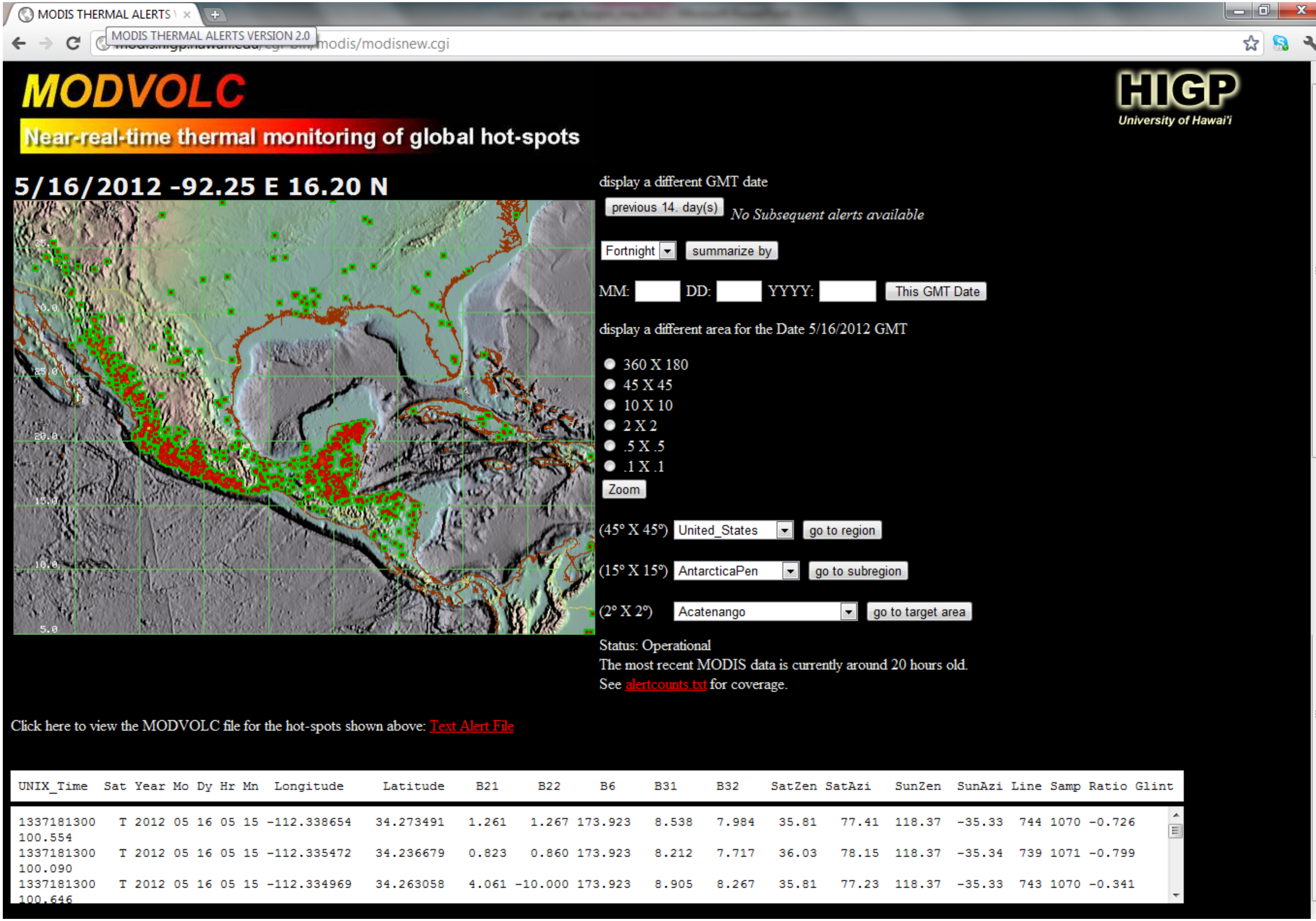

Summary

1. HyspIRI is an important bridge between MODIS class and Landsat class mission, with respect to detecting, quantifying and monitoring global wildfires and volcanic hot-spots

2. Existing algorithms are not directly portable to the analysis of HyspIRI data (smaller IFOV; algorithms must operate independently of the VSWIR sensor) but will need to be tested, compared and adapted

In preparation for the follow-up breakouts we present:

HyspIRI and the Art of Geo-Location

Dealing with substantial differences between the VSWIR and TIR measurement patterns

Steve Ungar

Pat Cappelaere

HyspIRI Science Symposium – NASA GSFC – May 17, 2010

What I am going to present and why I am presenting it to <u>you</u> !

- The geometric properties of HyspIRI level-1 data.
- Exposing the myth of *(defining limitations in)* achieving coincident individual observations between instruments and over time.
- Options for generating VSWIR, TIR and combined level-1 *(calibrated)* products.
- <u>**You**</u> determine higher level product requirements needed to meet your research goals.
- Higher level products depend, both qualitatively and quantitatively, on the level-1 products from which they are generated.

Geometric Factors Influencing VSWIR/TIRS Combined Product Utility

- Final Satellite Orbit
- Satellite Pointing Accuracy
  - Attitude Control System (ACS)
  - Star Trackers
- Satellite Positioning Accuracy
  - GPS
- Instrument Models & Geometry
- **Science Users Geolocation Expectations??**
- Low-latency Product Geolocation Expectations!

Preliminary Geometric *Nominal* Parameters for the HyspIRI

The Satellite

- Platform: Sun-synchronous Circular Ground-track Repeat Orbit
- Altitude: 623 km (mean sea-level)
- Velocity: ~7 km/sec (ground speed)
- Repeat Cycle:19 days
- 10:30 am MLT at Equator (descending node crossing)

The VSWIR Spectrometer

- Pushbroom Technology
- Revisit Cycle at Equator: 19 days
- Detectors/wavelength: 2*1280 (2 FPAs)
- Swath Width: 145 km
- Pixel size/GSD: 60 m

The TIR Instrument

- Whiskbroom *(2-sided rotating mirror)*
- Revisit Cycle at Equator: 5 days
- Detector Elements/band: 256
- Mirror Scan Frequency: 14.2 RPM
- Swath Width: 600 km
- Long-track Swath: 15.4 km at Nadir
- Nadir Pixel GSD: 60 m

Pushbroom Observing System

Depiction
-Grids are the detectors
-Spots are the IFOV centers
-Colors are the wavelengths

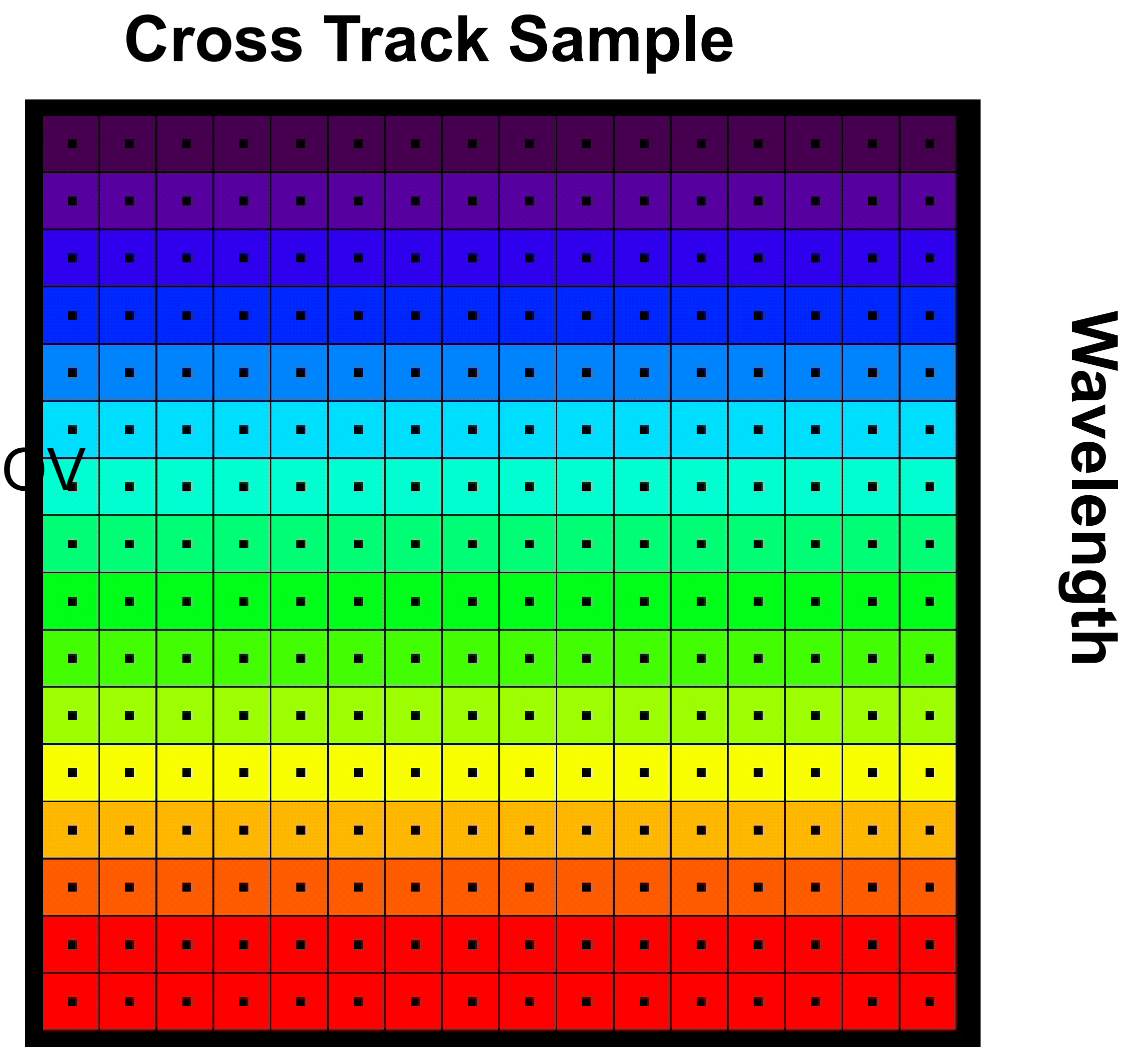

Pushbroom Observing System

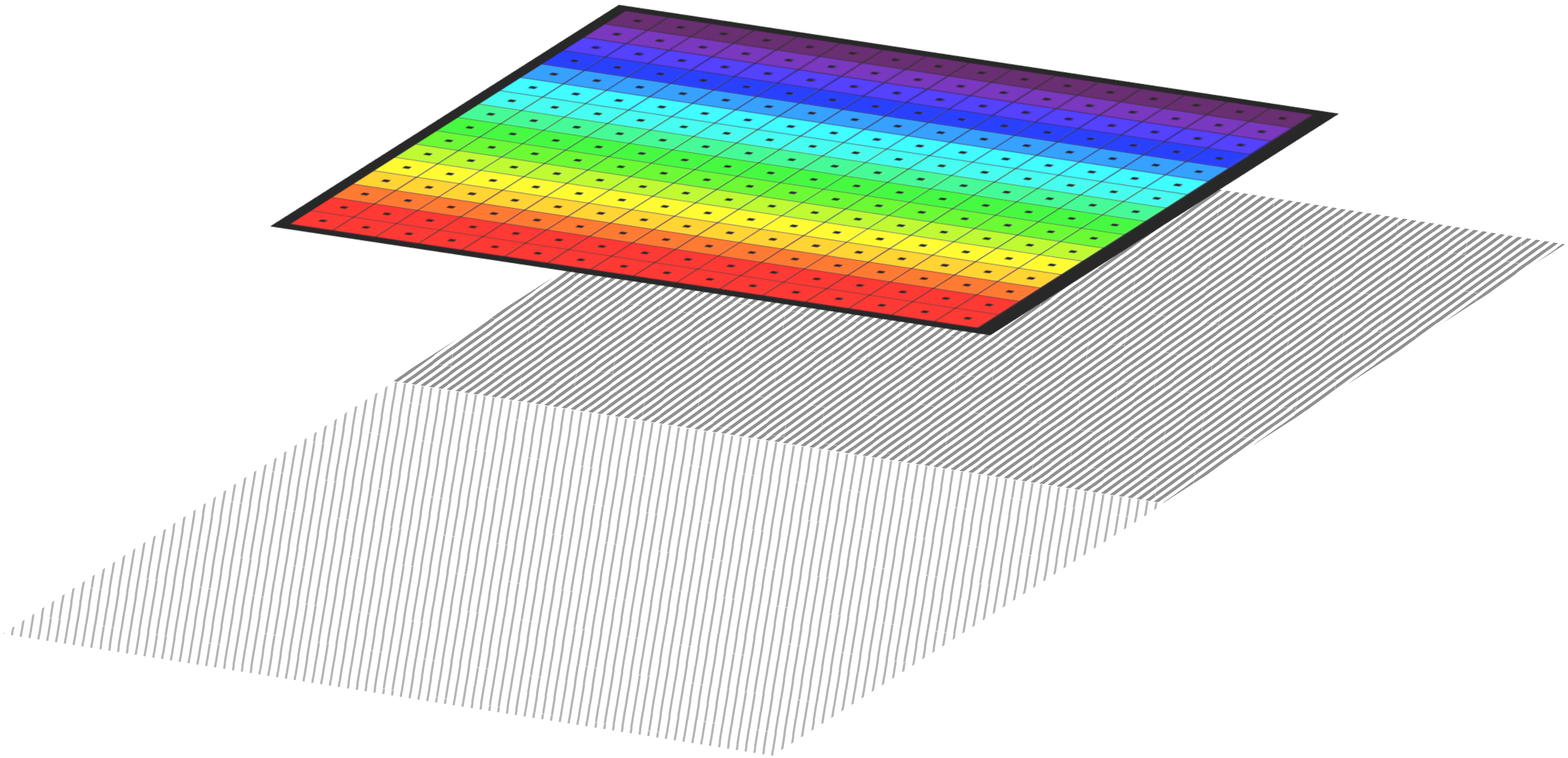

Pushbroom Observing System

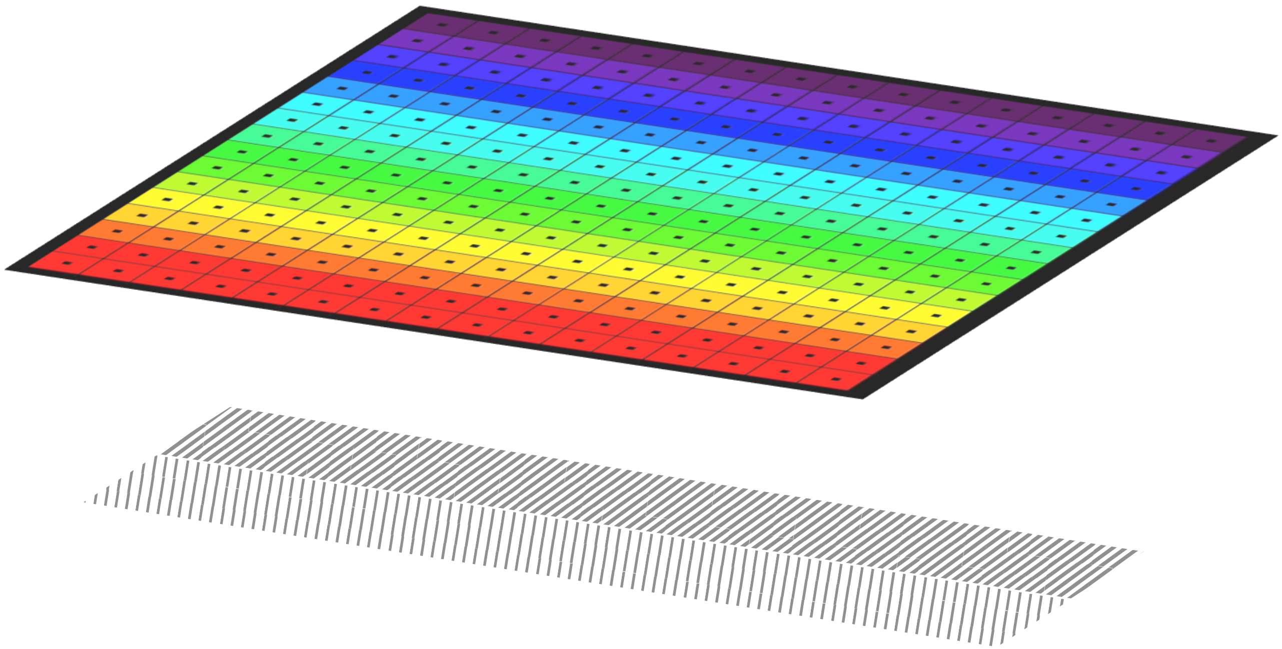

Pushbroom Observing System

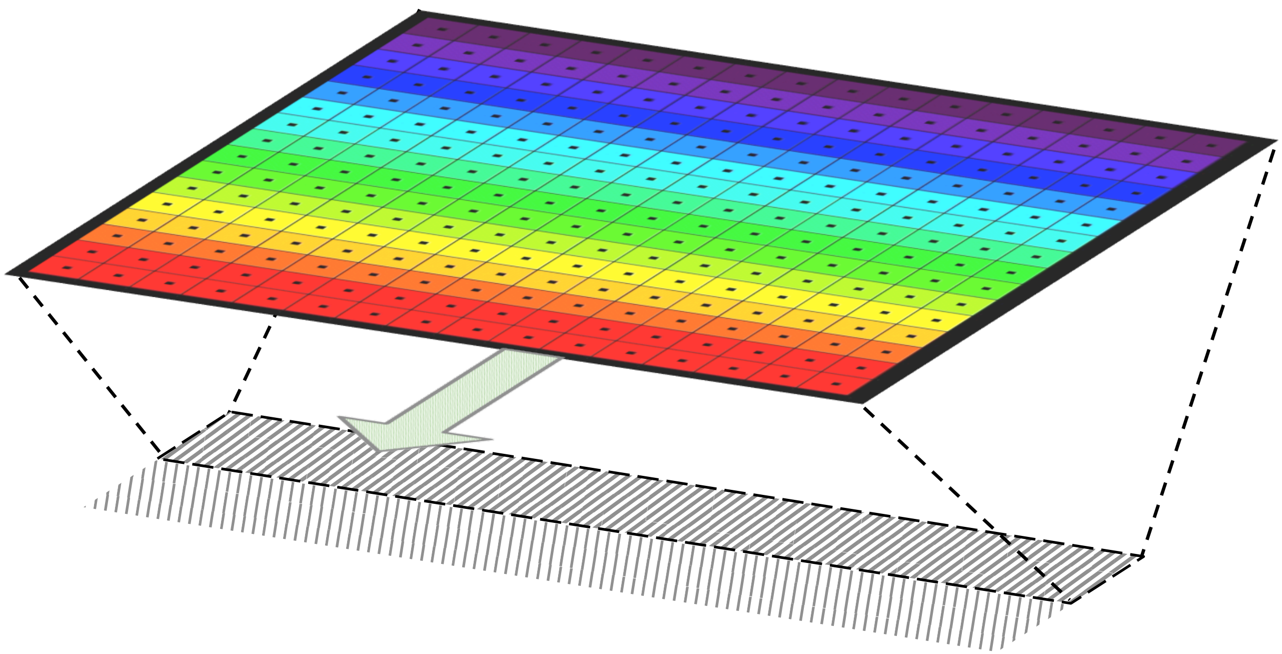

Pushbroom Observing System

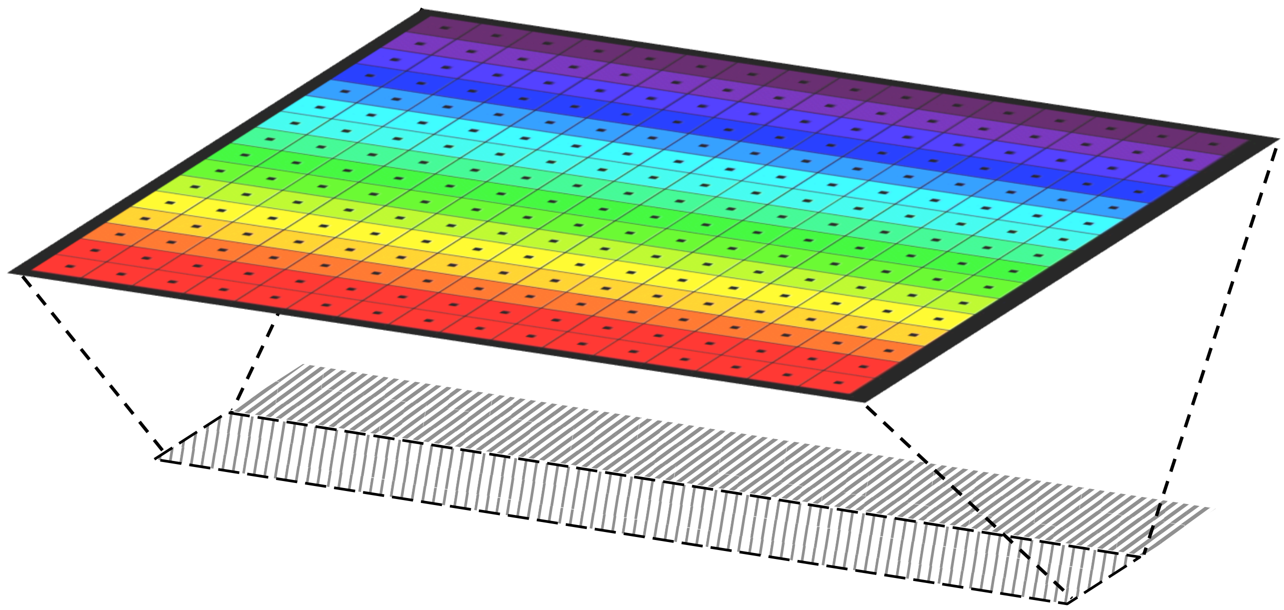

HyspIRI TIR Scan Method

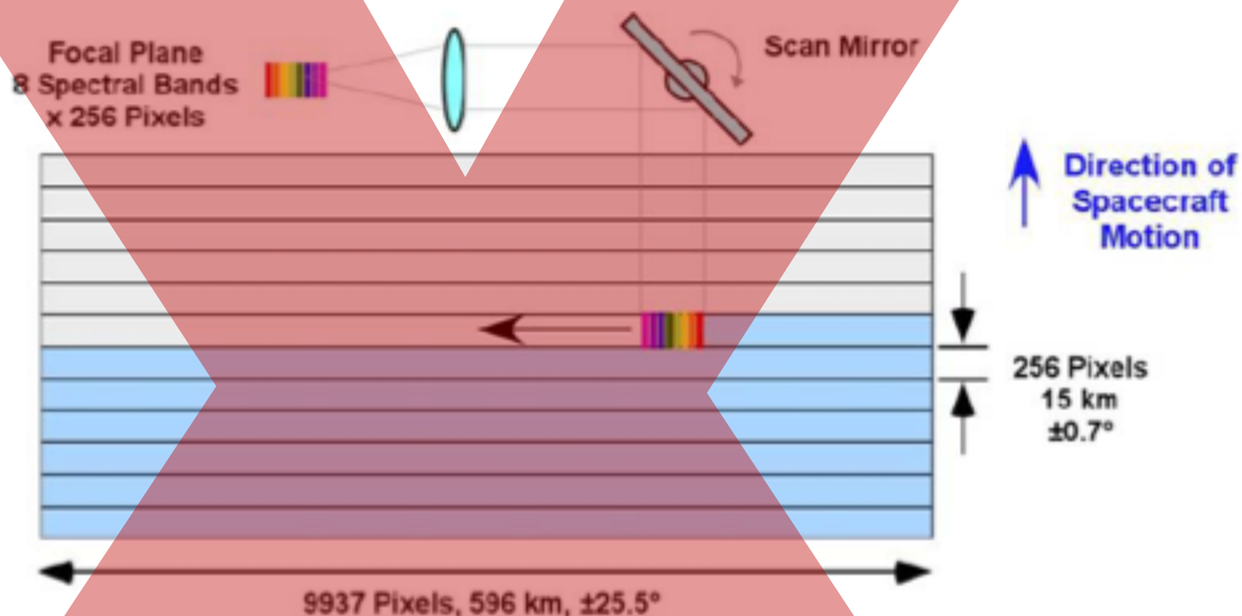

8 Thermal bands
Band to band co-registration: 0.2 pixels (12m)
Pointing Knowledge: 10 arcsec (0.5 pixels, 30m)

HyspIRI TIR Scan Method

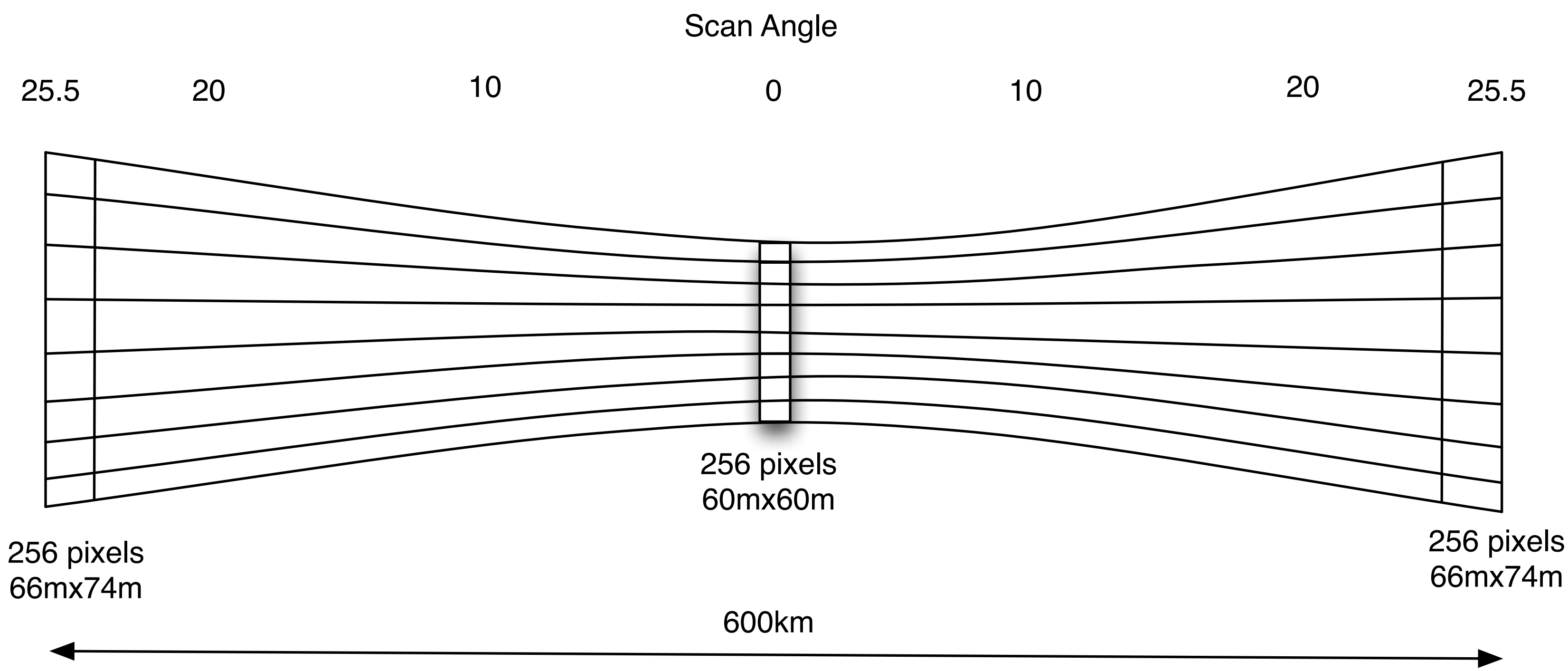

HyspIRI TIR Scan Method

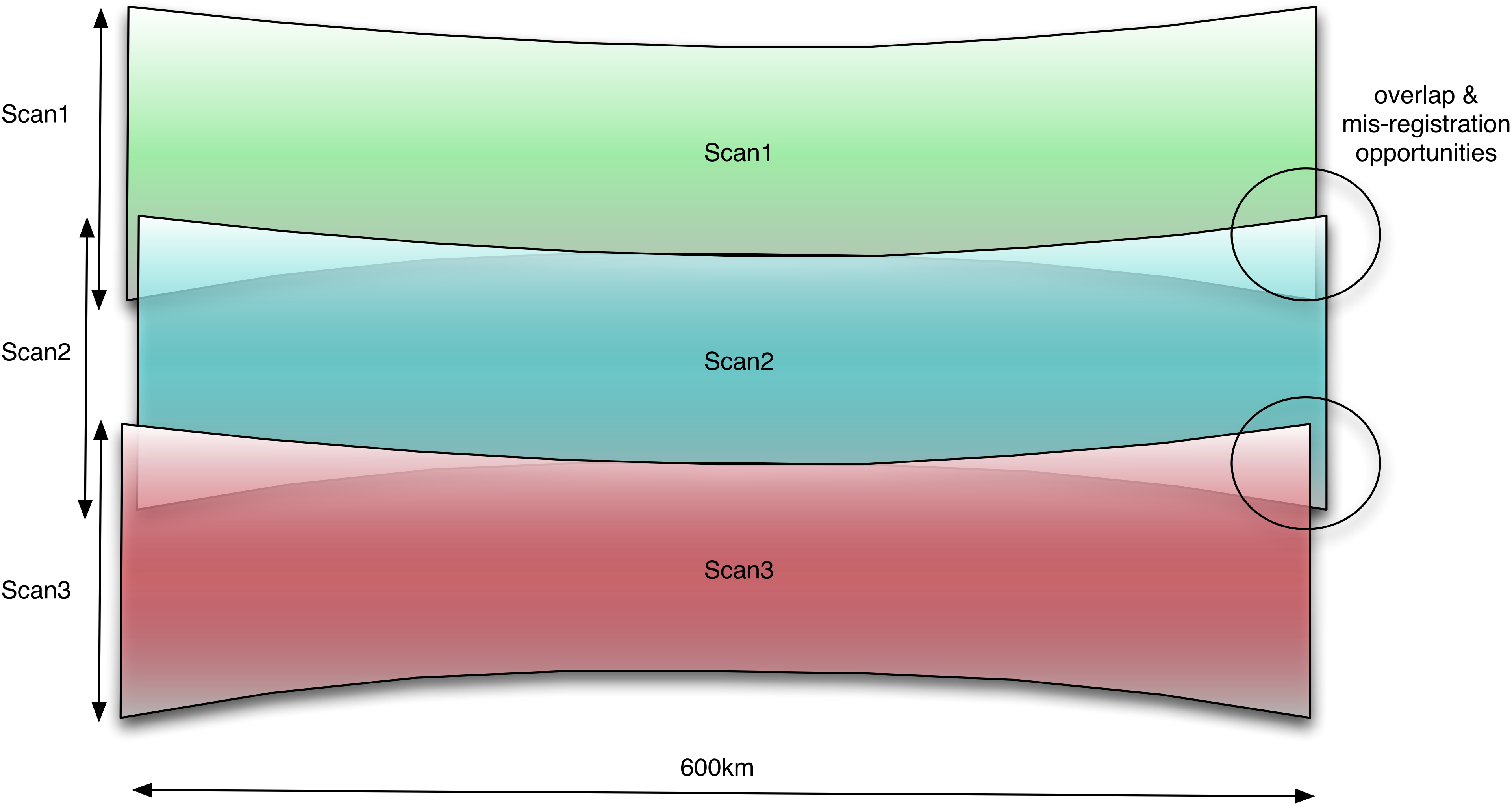

HyspIRI TIR Scan Method

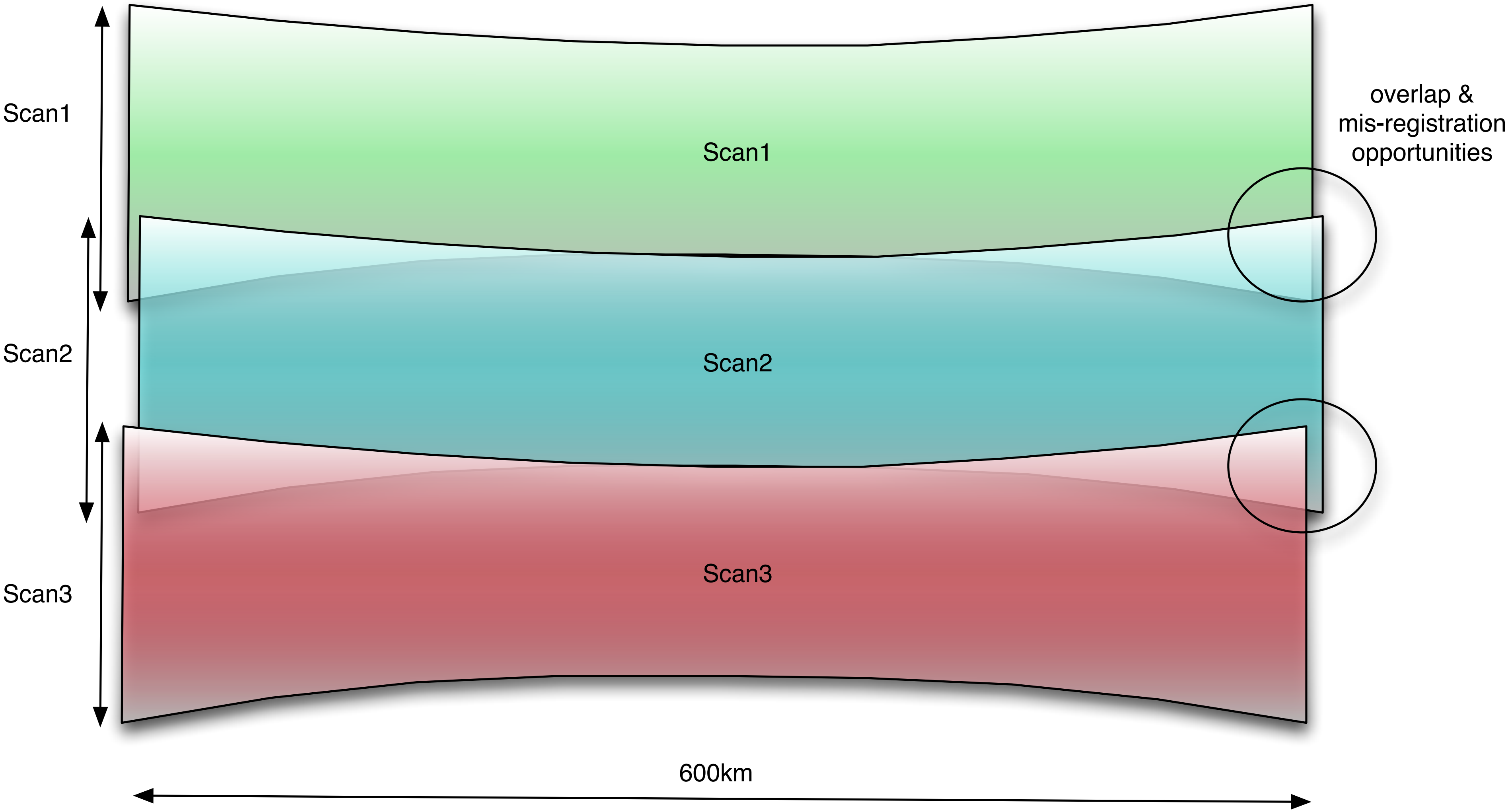

Odd numbered scans are acquired with scan mirror side 1
Even numbered scans are acquired with scan mirror side 2

The Bow-Tie effect is an artifact of the arrangement of sensors on the MODIS instrument.

An example of the bow-tie effect (near the right-hand edge of a 250 m band) :

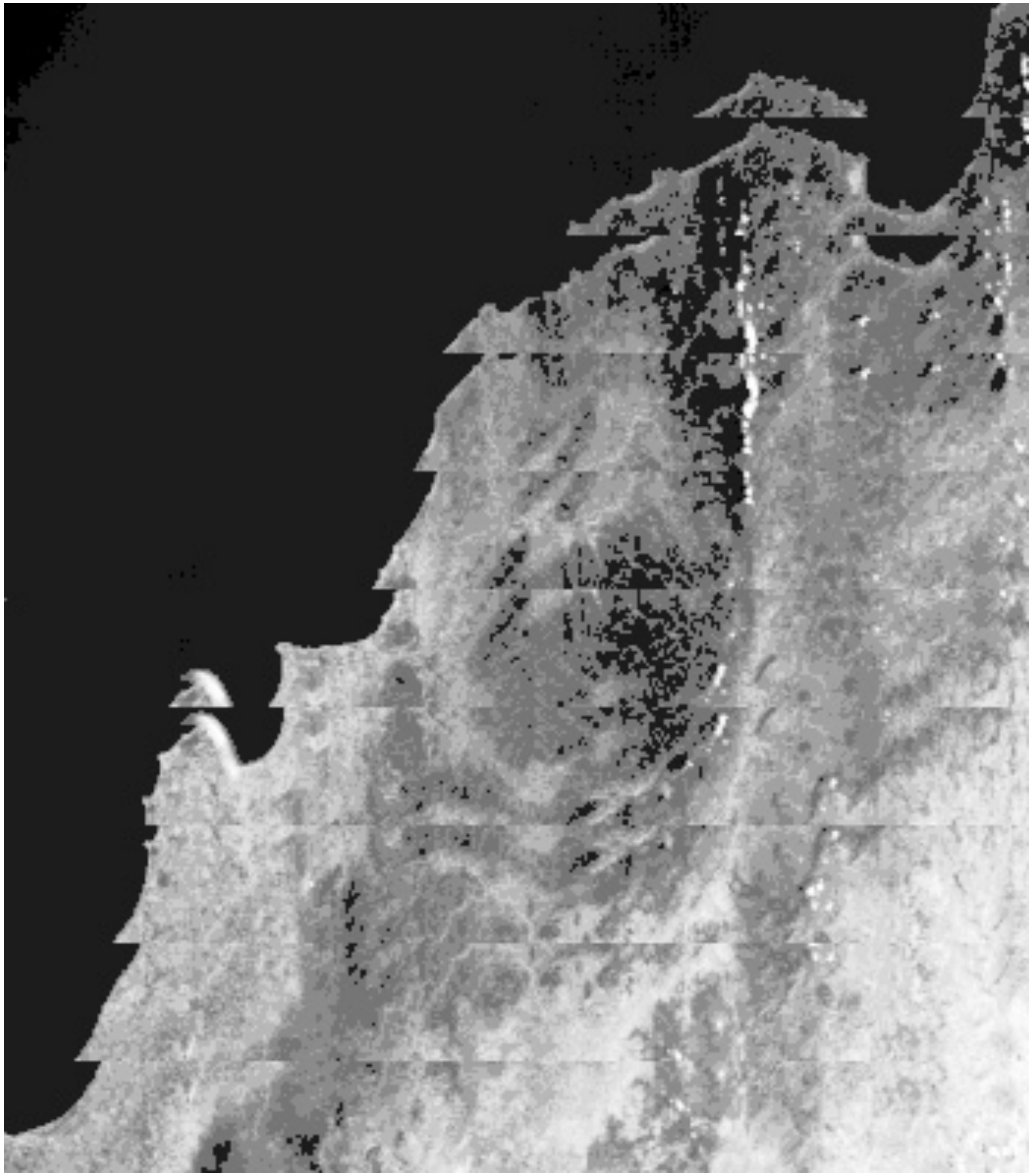

Stationary View

How the VSWIR and TIR would image if HyspIRI were able to hover

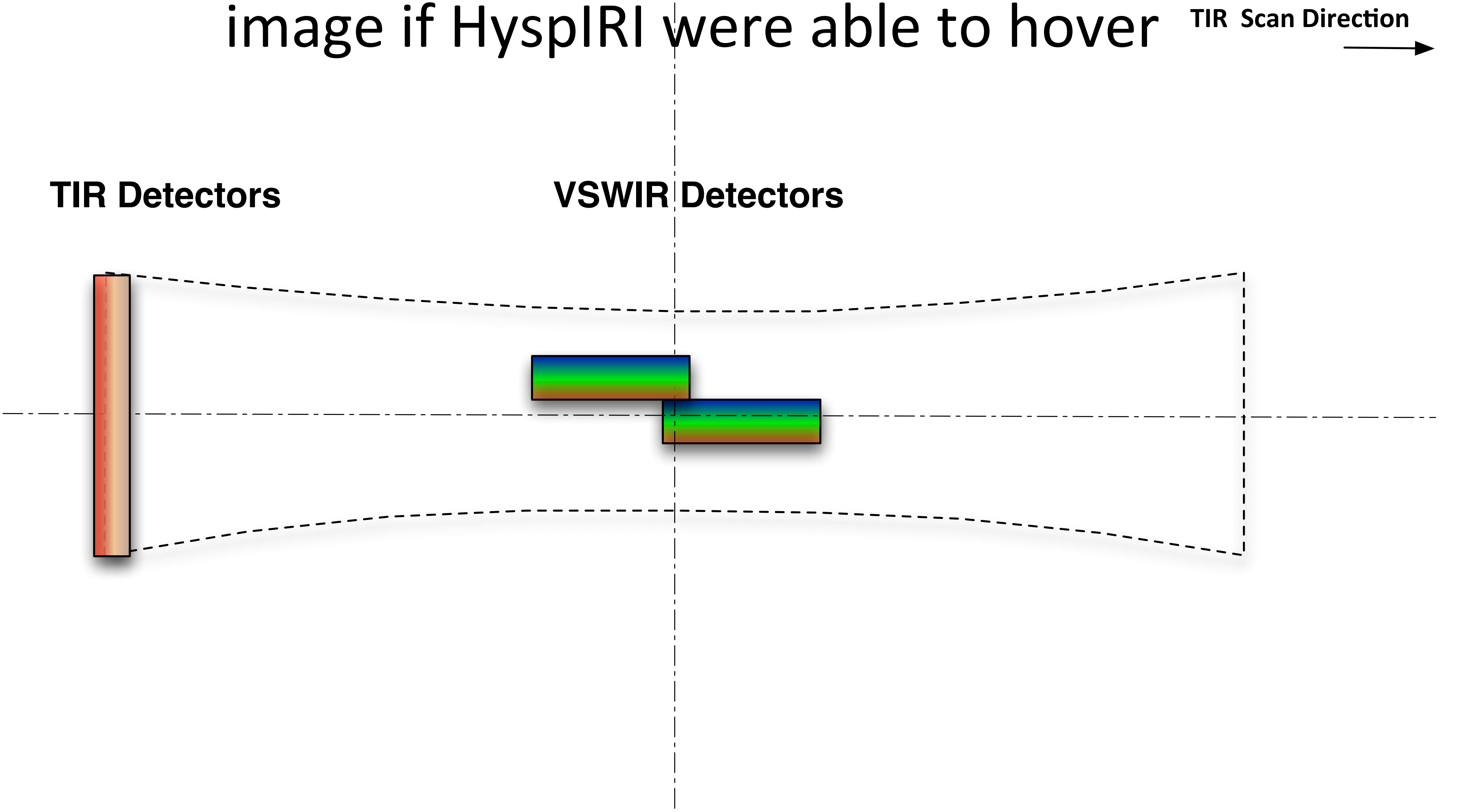

Stationary View

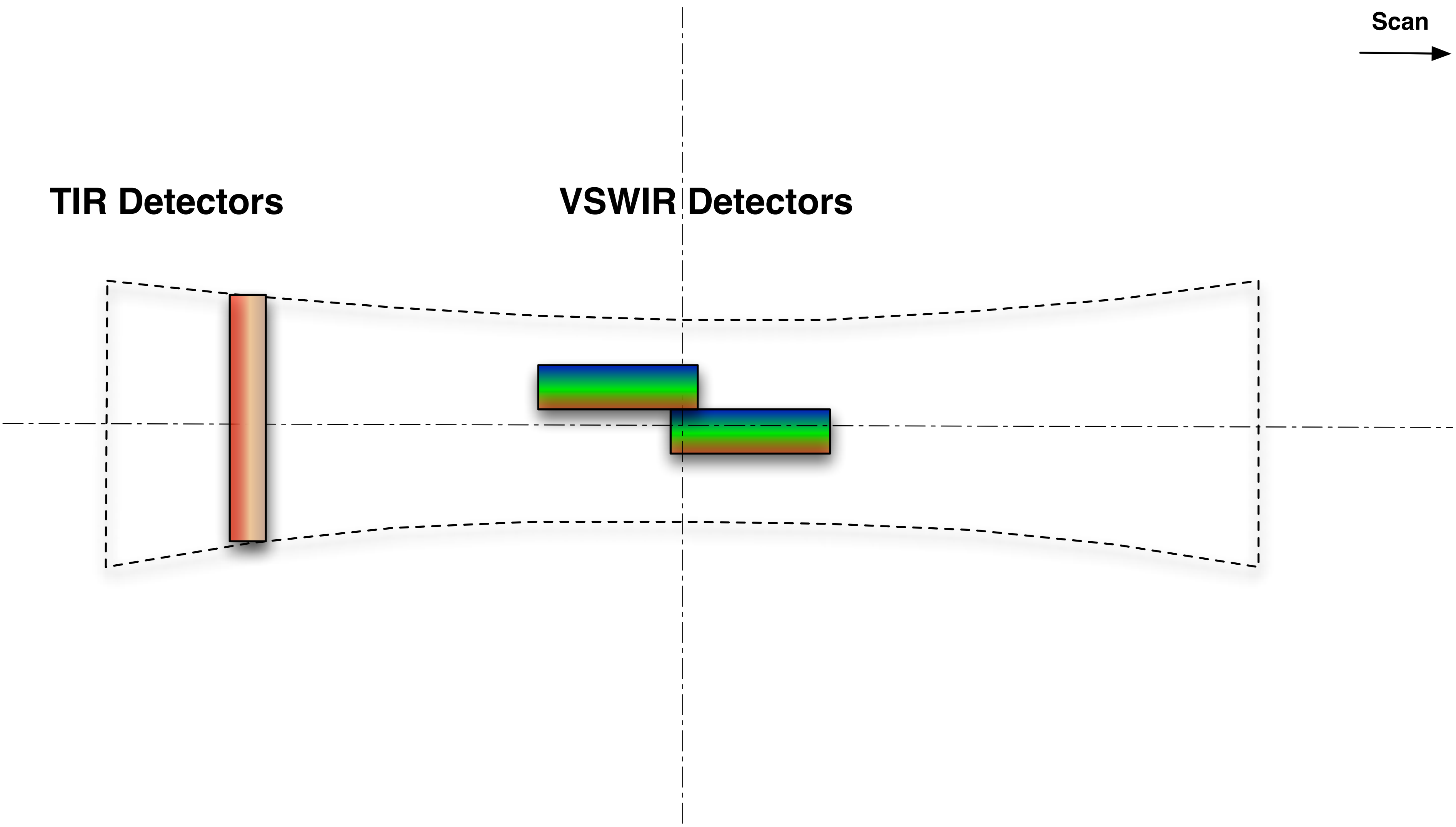

Stationary View

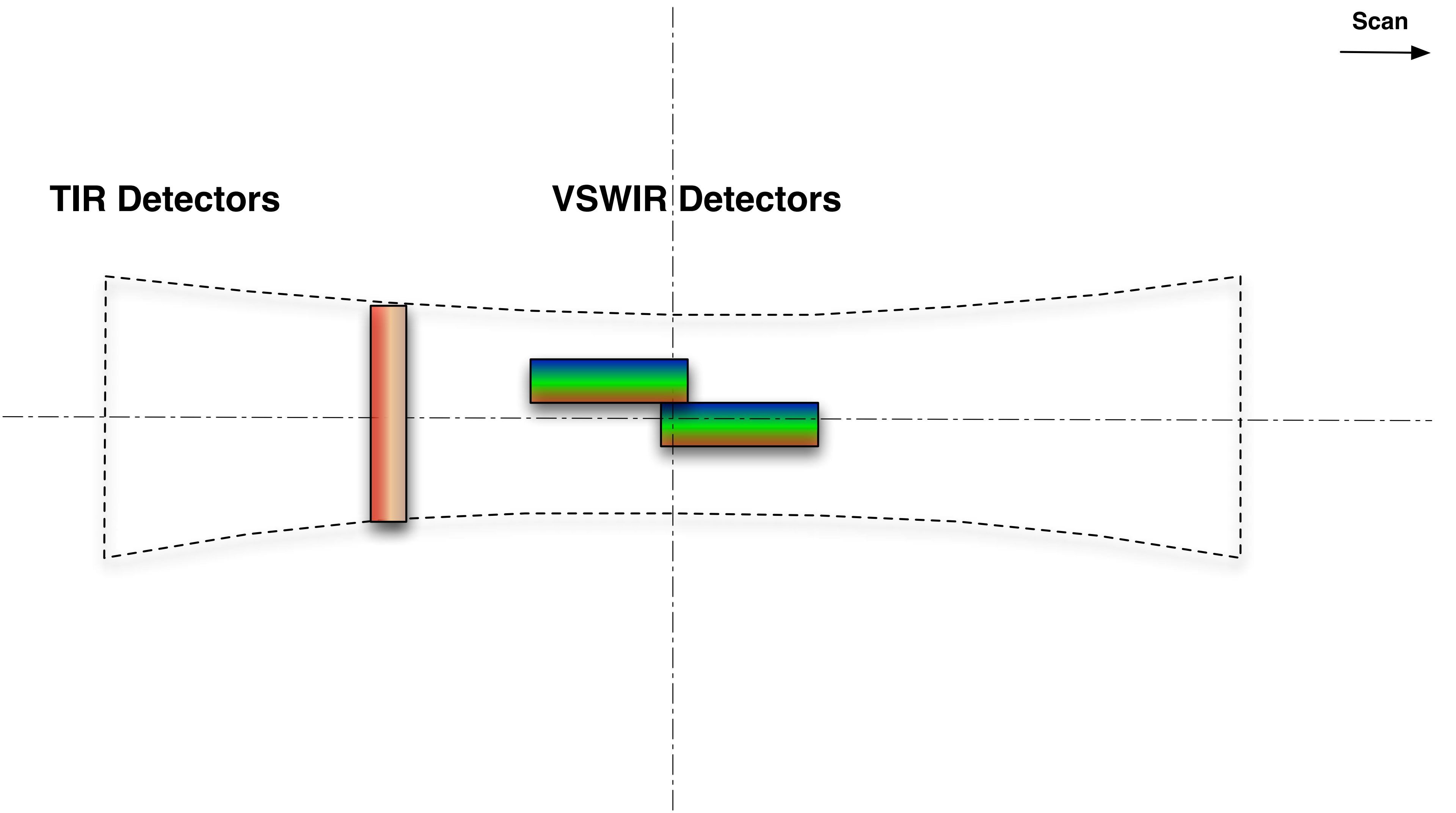

Stationary View

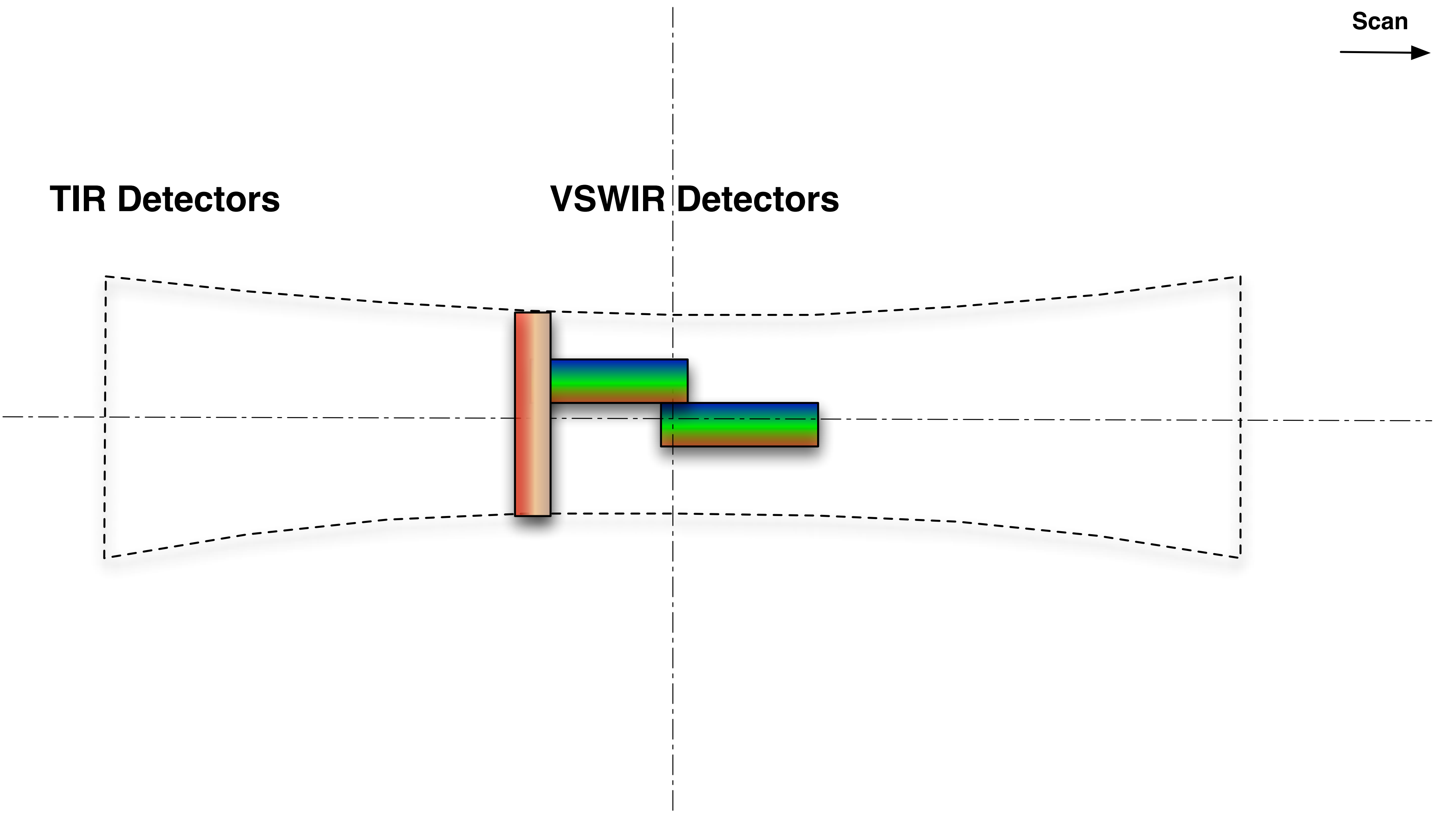

Stationary View

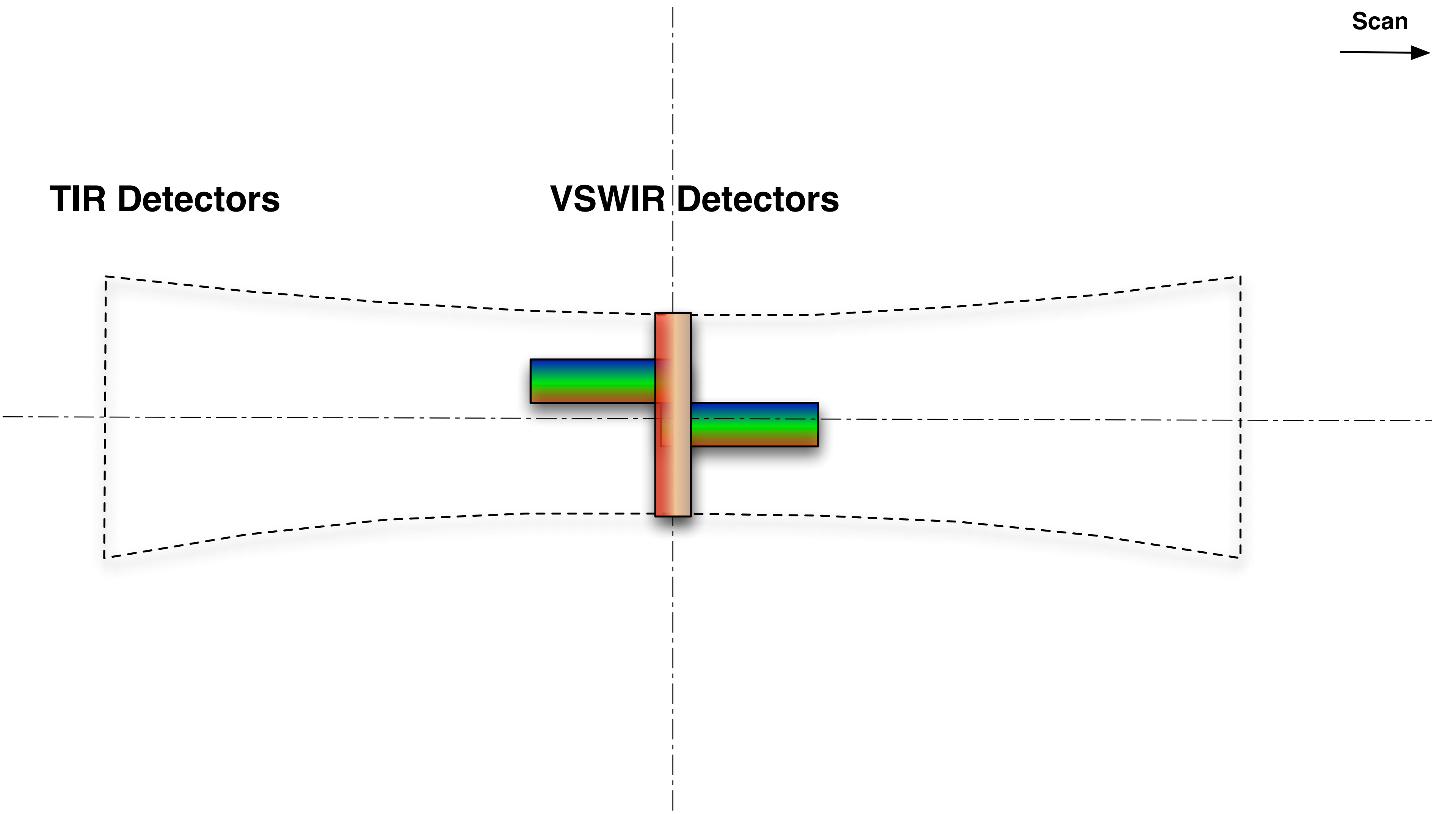

Stationary View

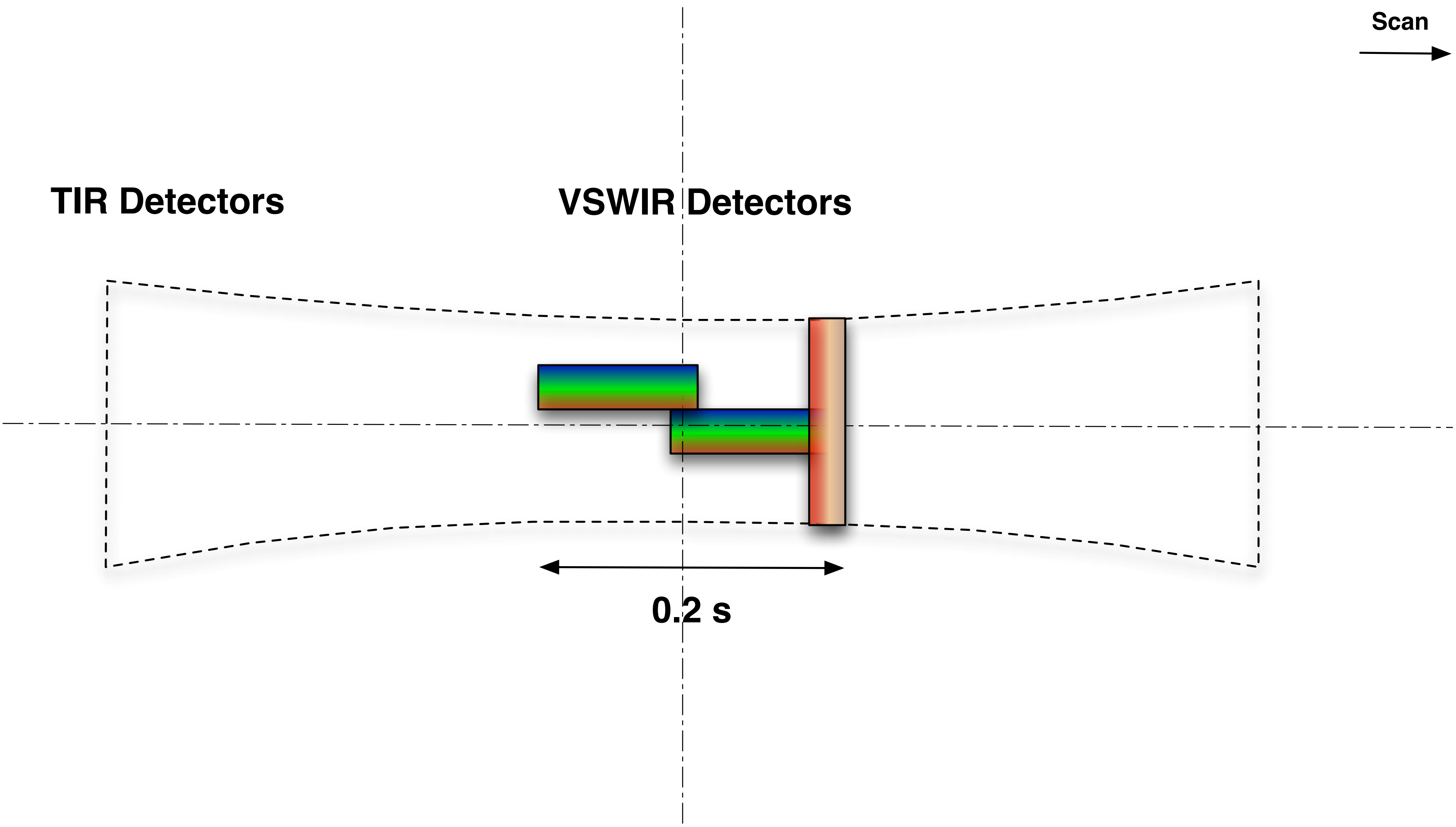

Stationary View

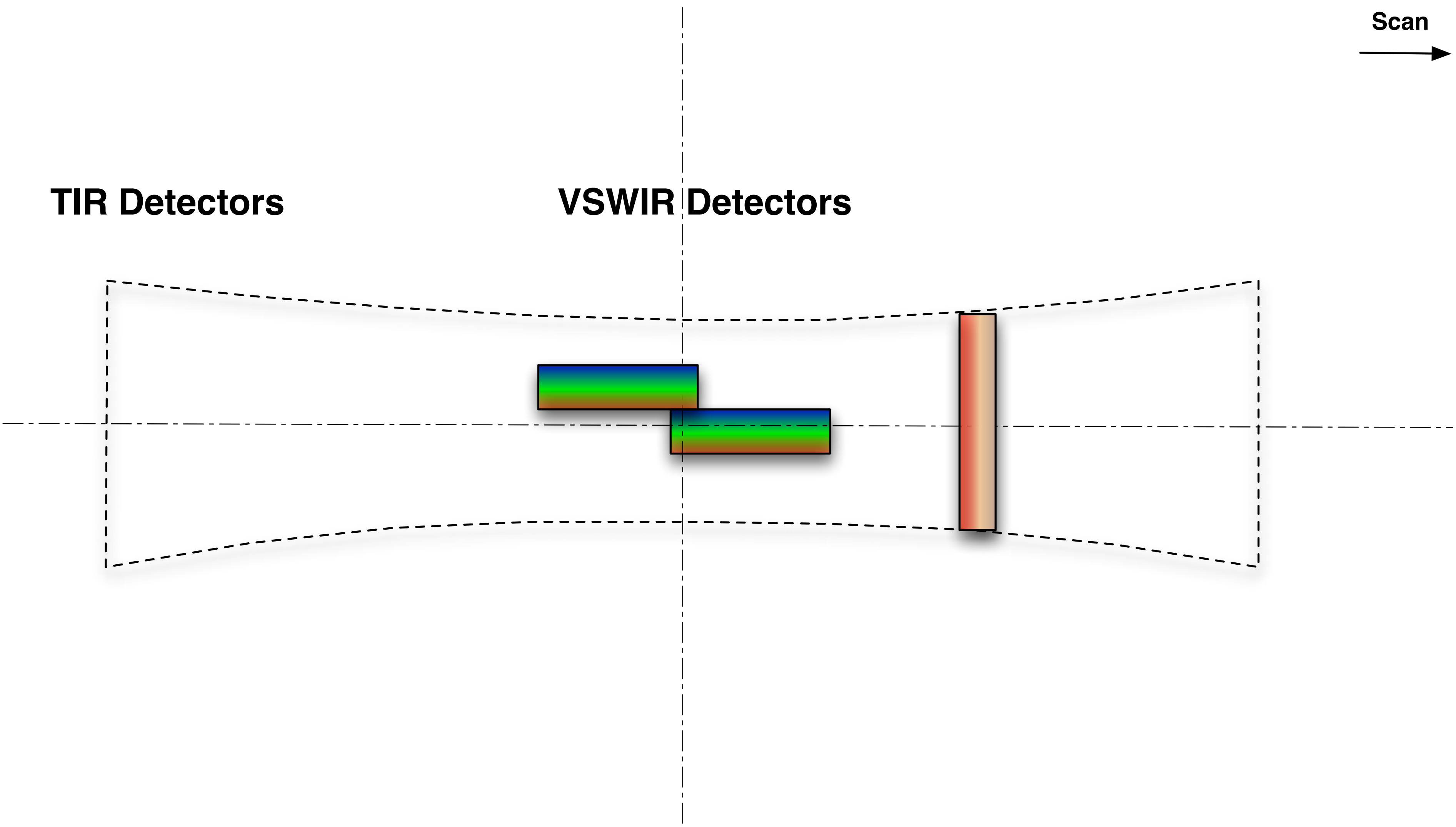

Stationary View

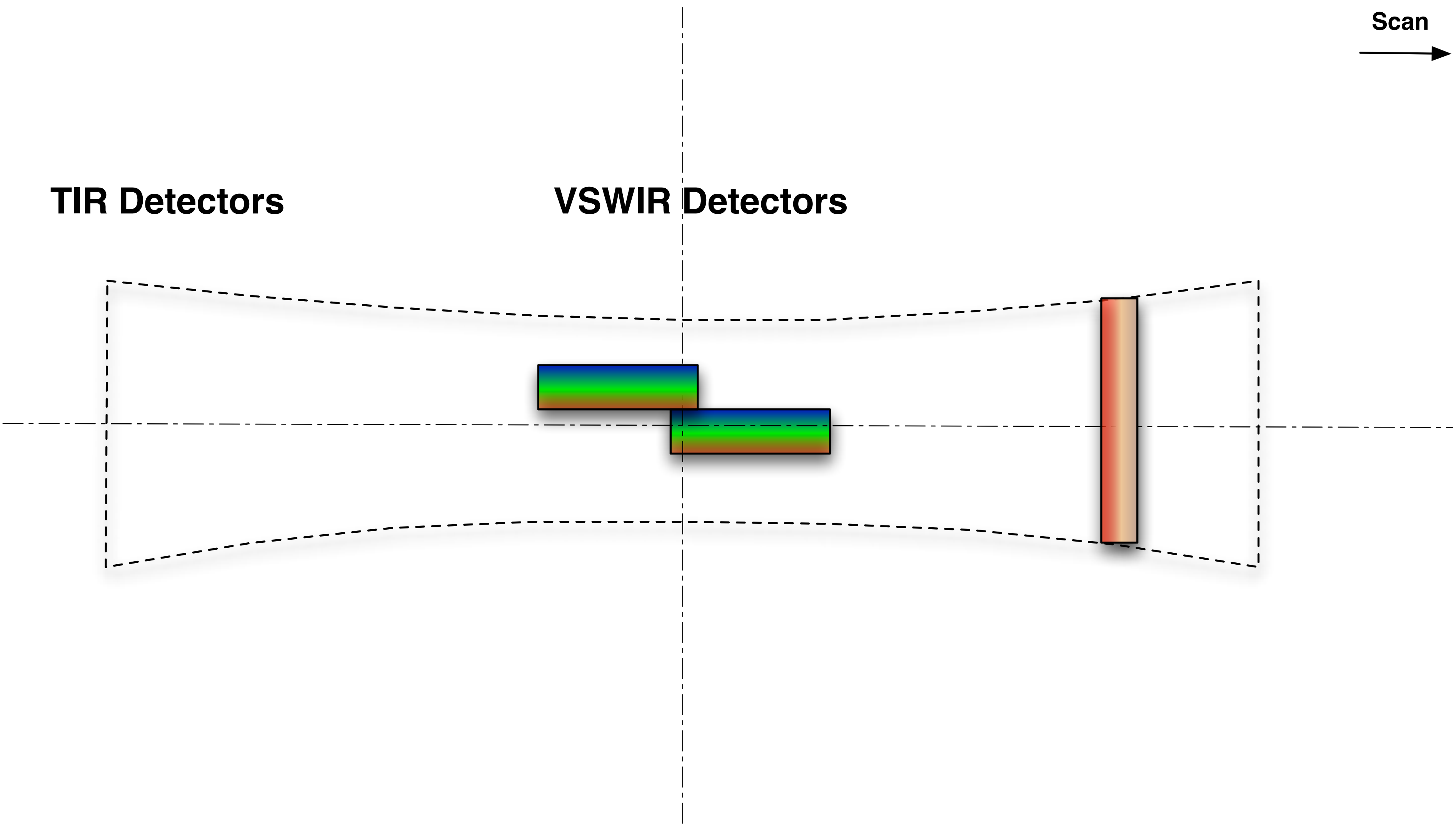

Stationary View

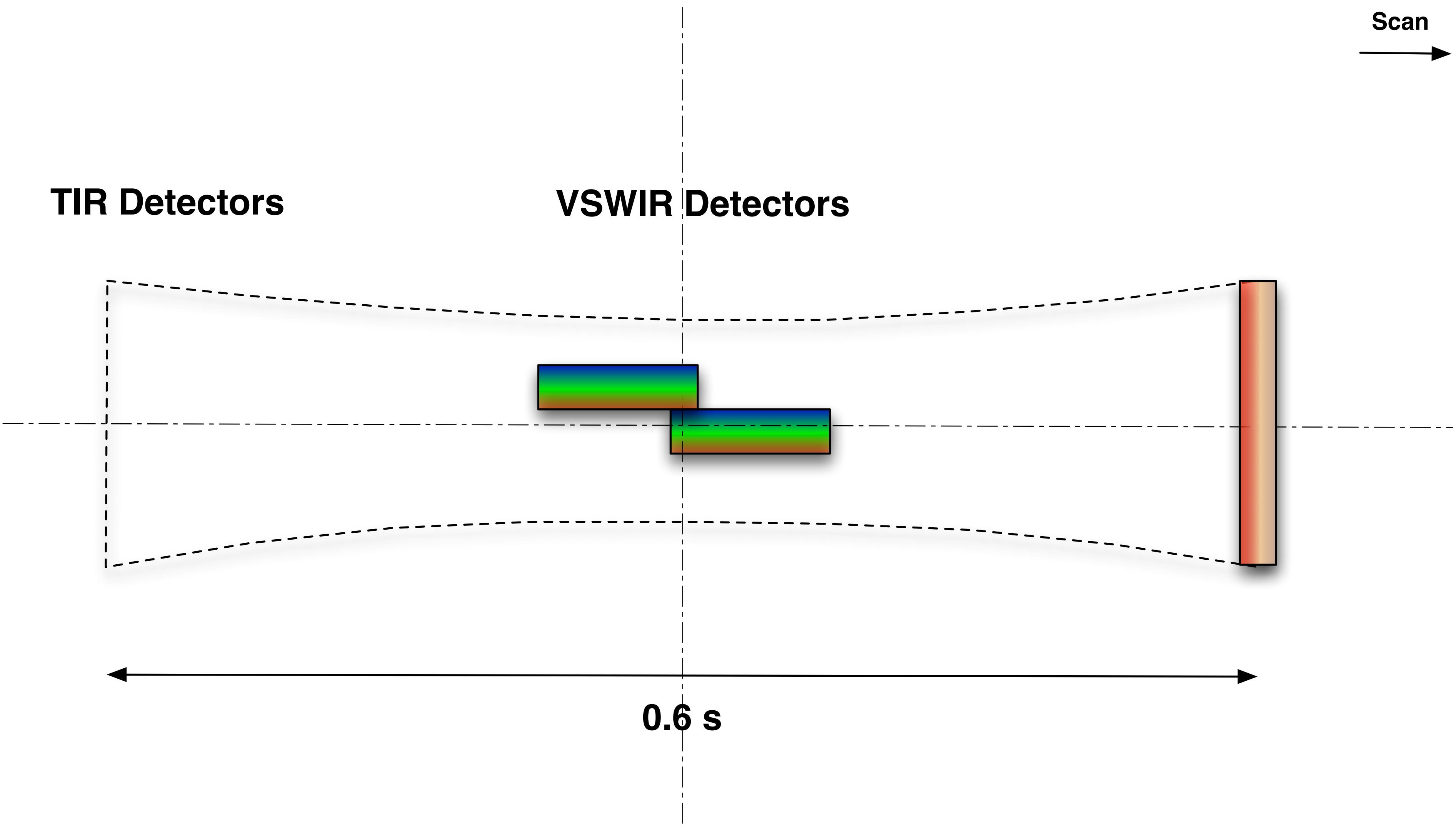

Stationary View

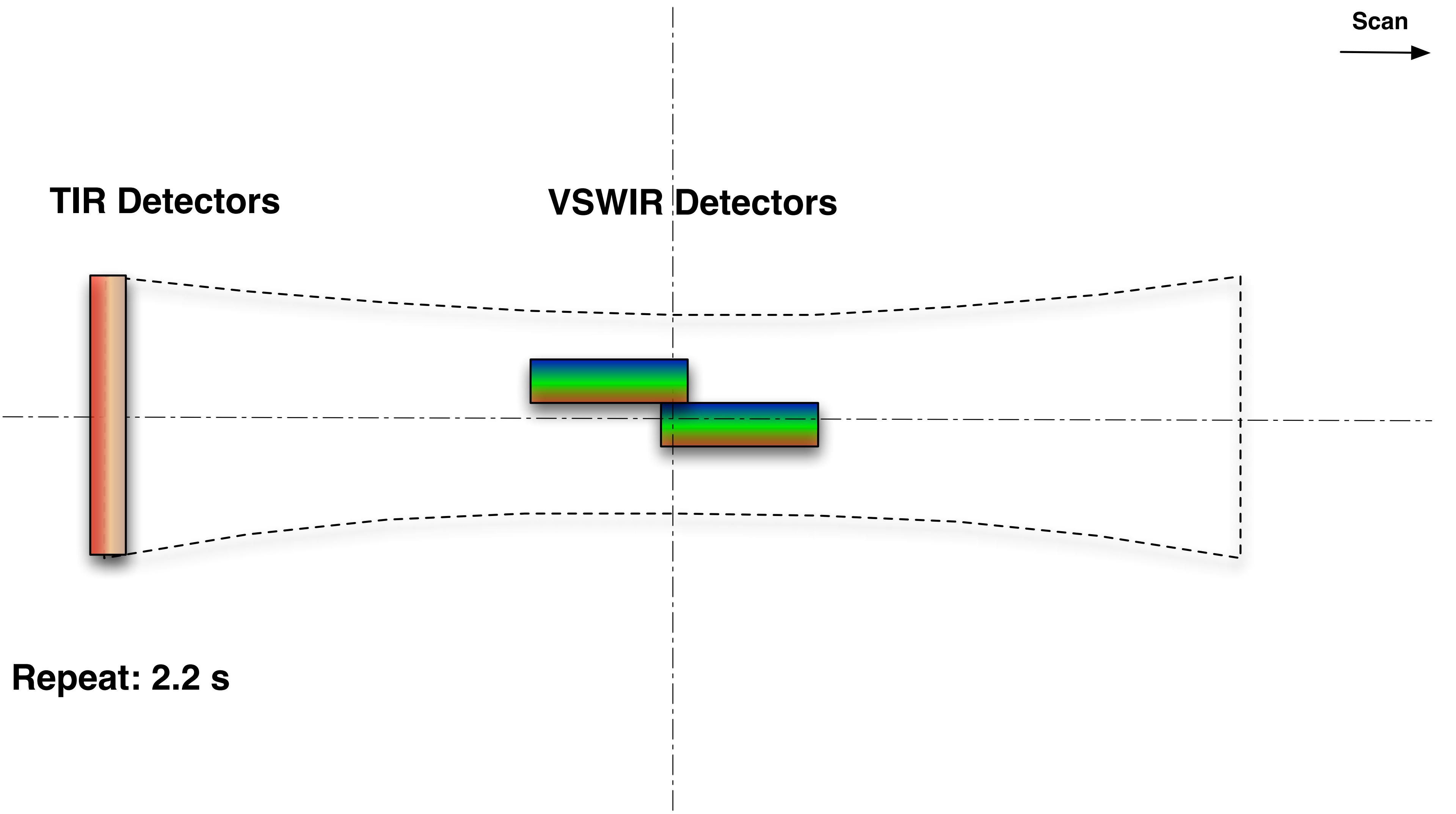

With Spacecraft Forward Movement

How the VSWIR and TIR image when HyspIRI moves in orbit

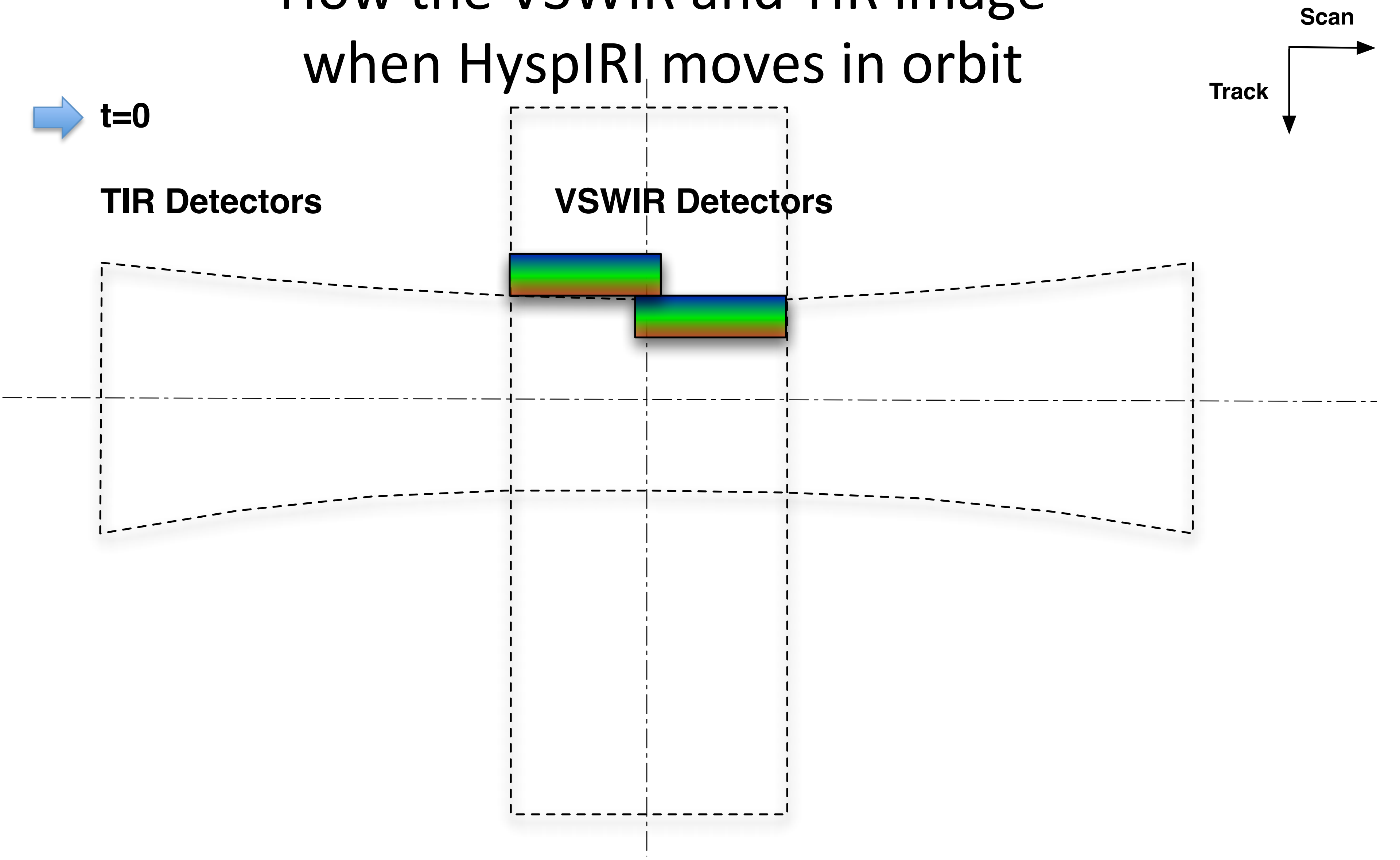

With Spacecraft Forward Movement

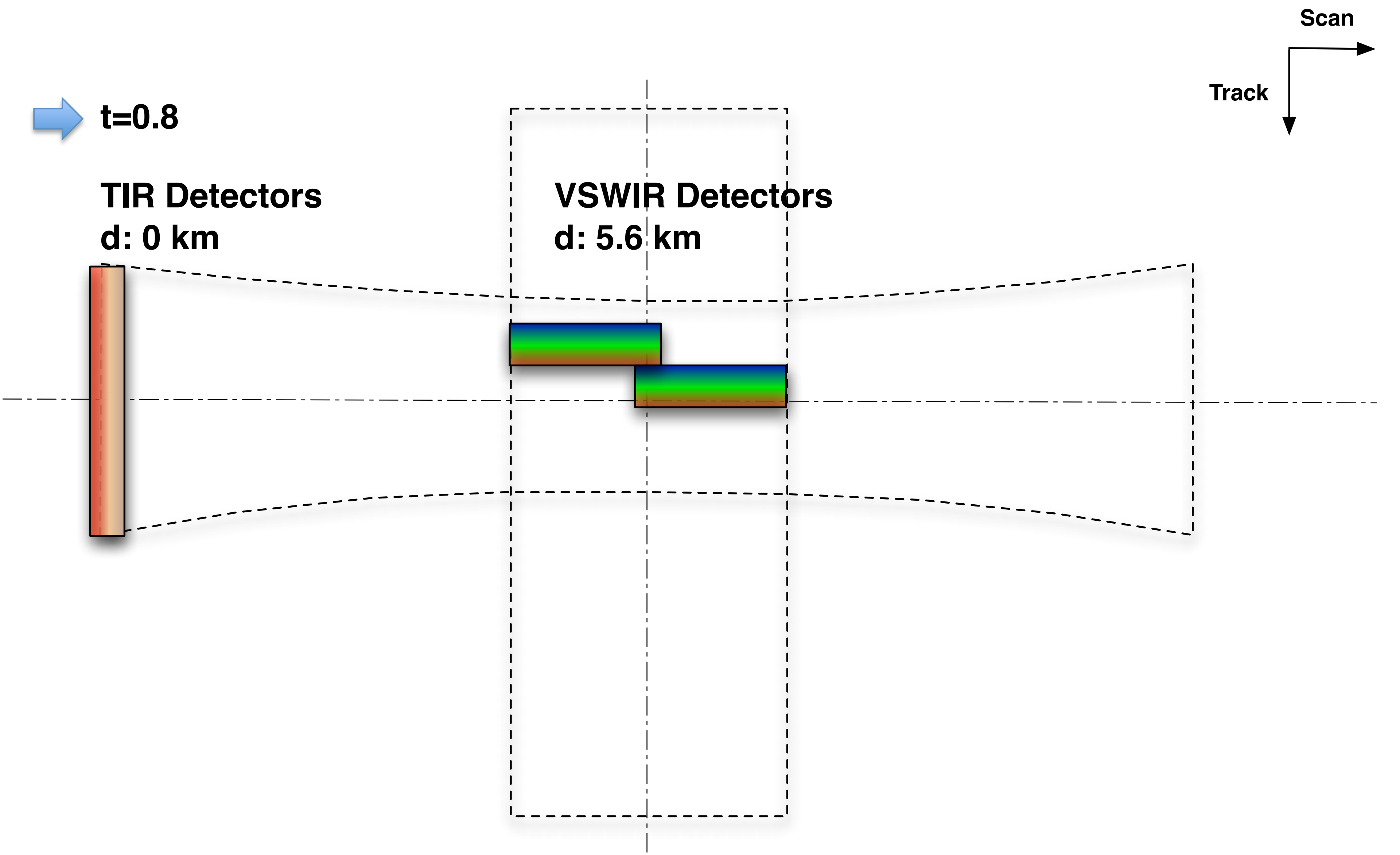

With Spacecraft Forward Movement

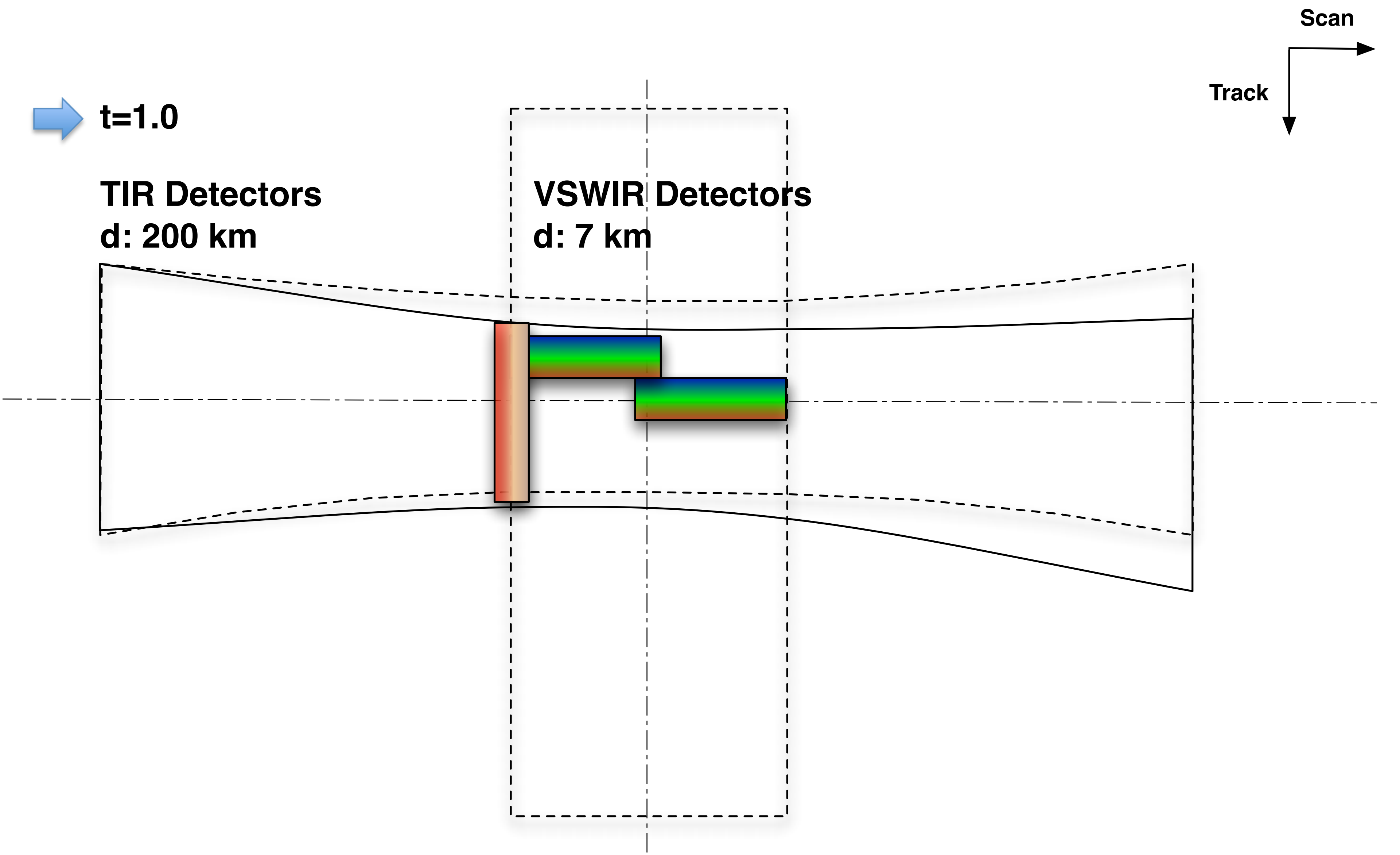

With Spacecraft Forward Movement

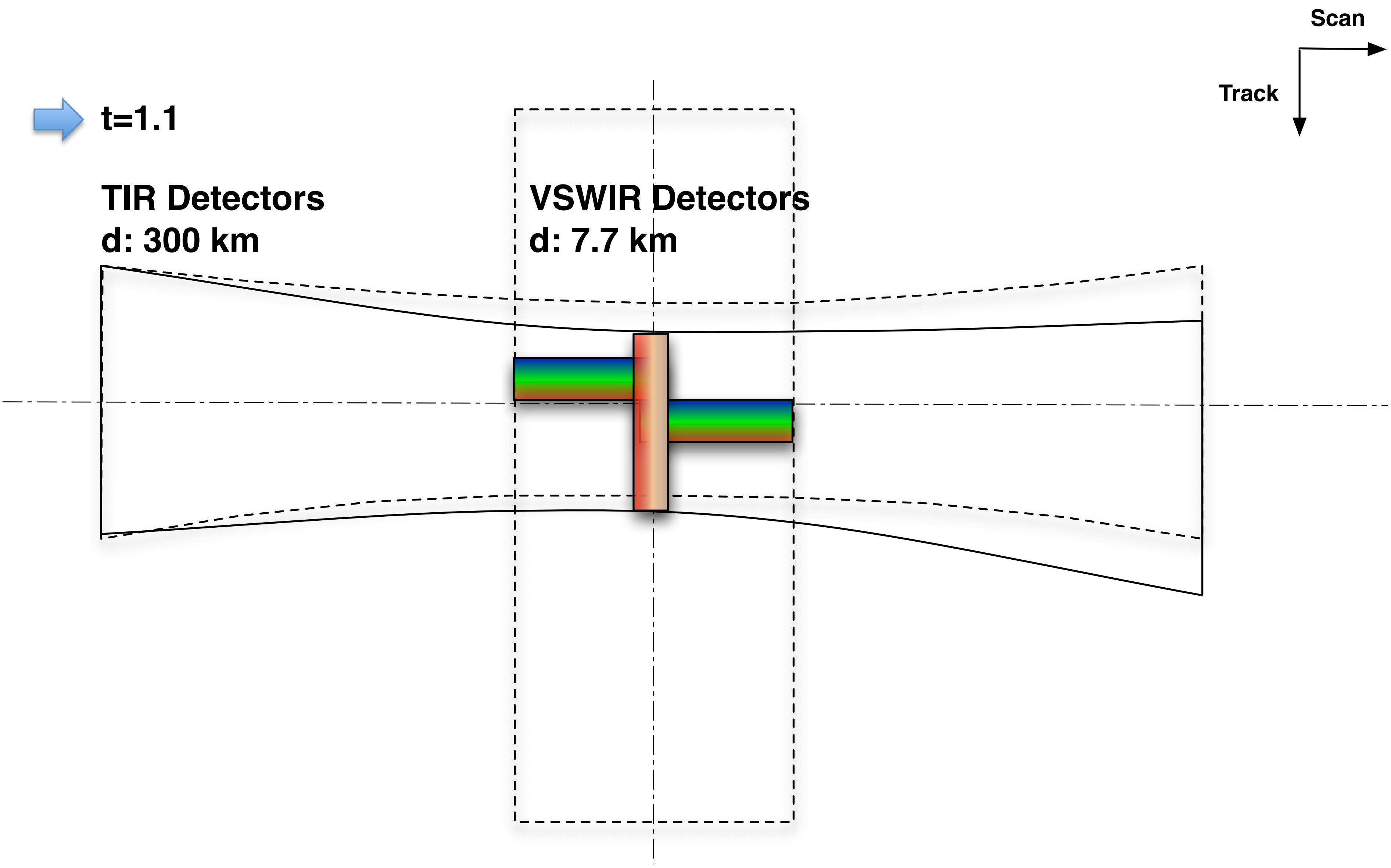

With Spacecraft Forward Movement

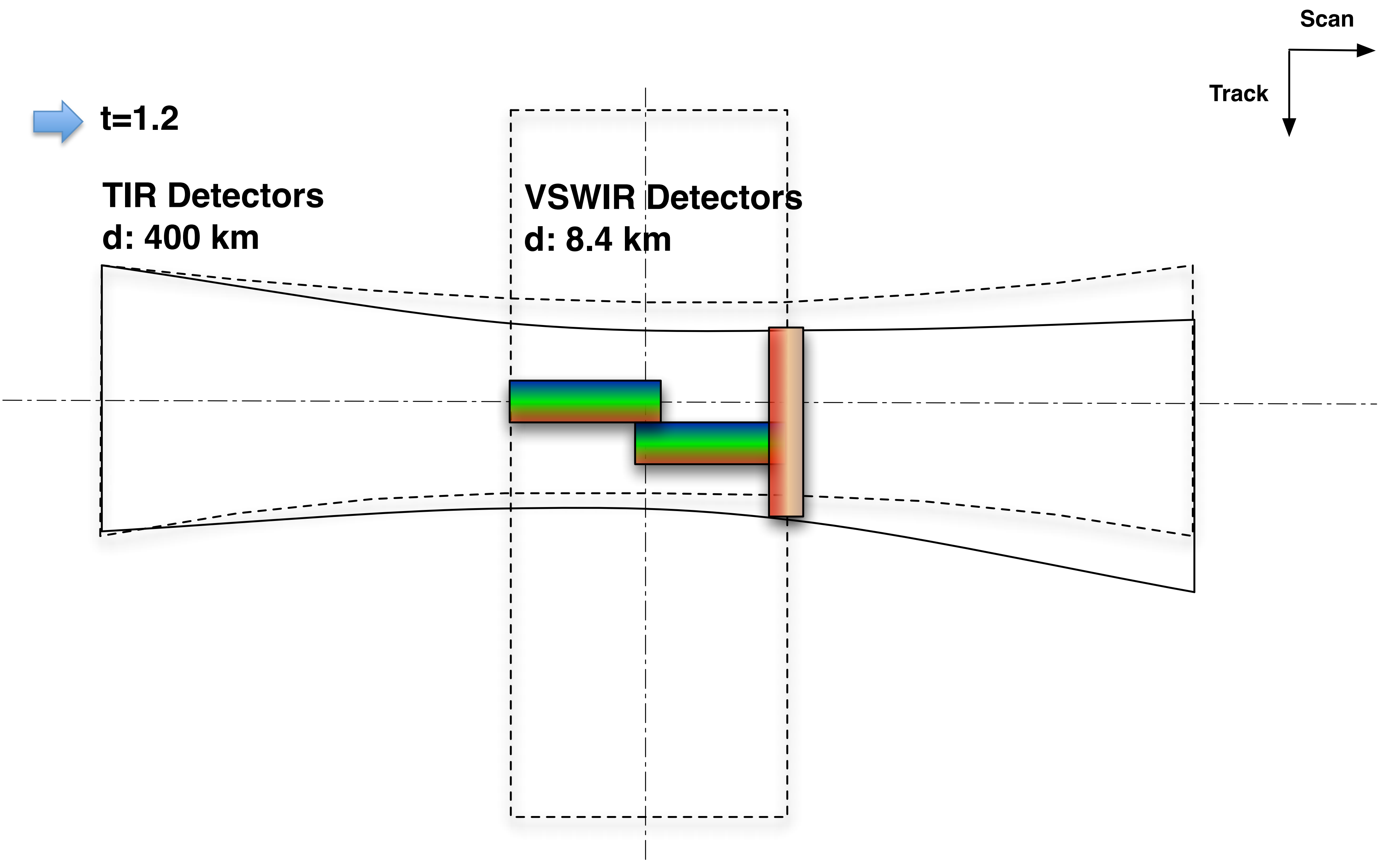

With Spacecraft Forward Movement

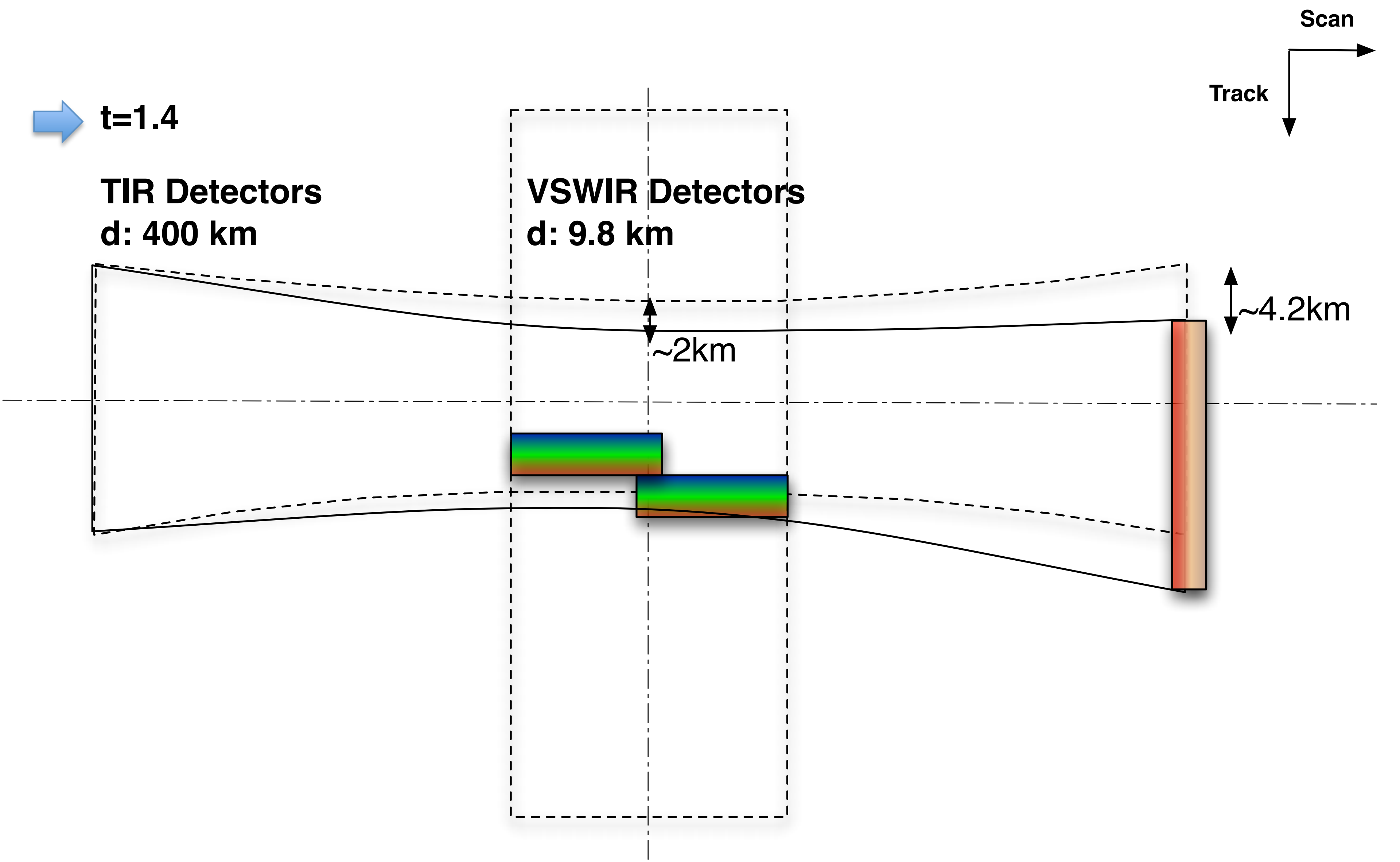

With Spacecraft Forward Movement

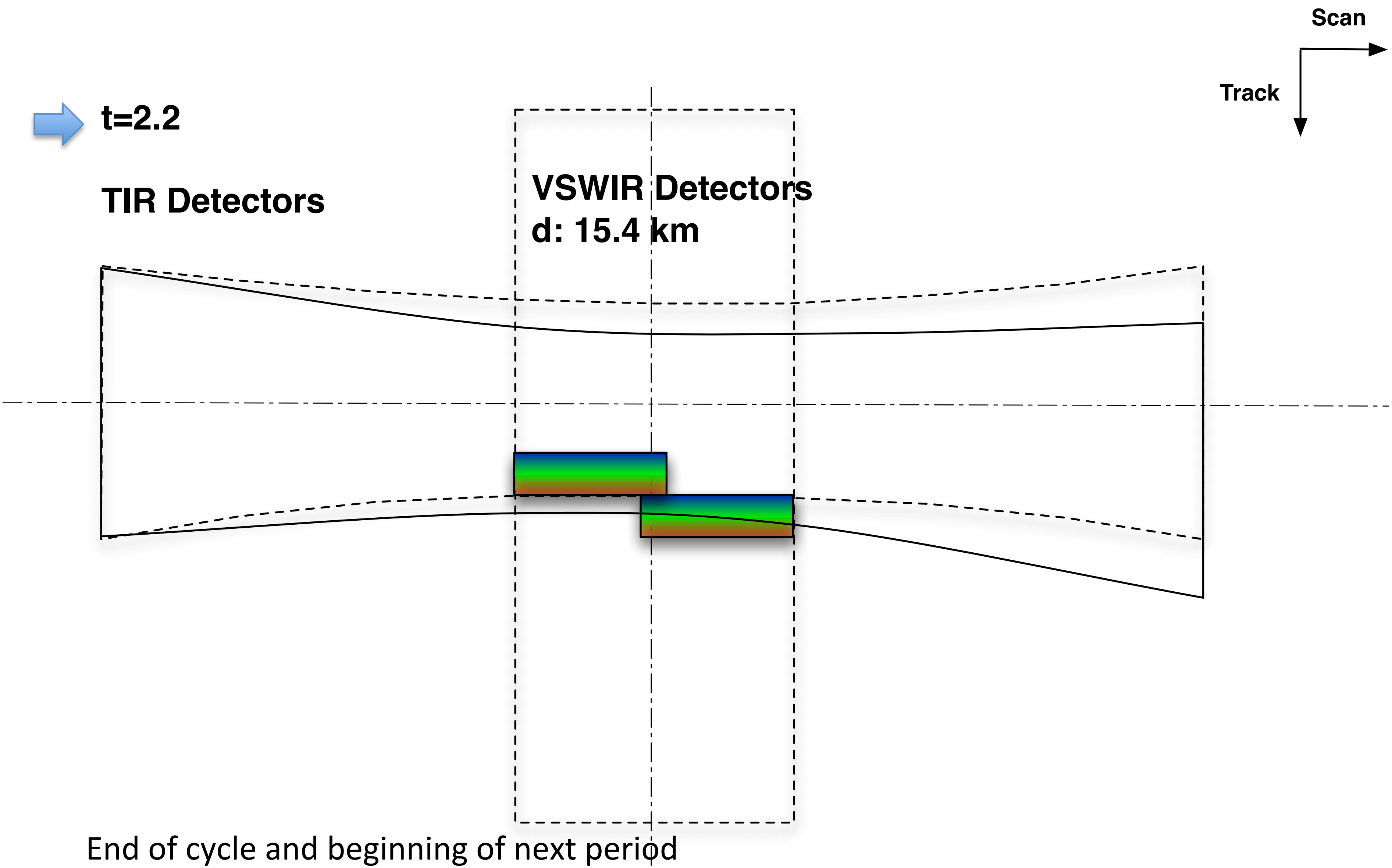

End of cycle and beginning of next period

VSWIR / TIR Alignment Correction?

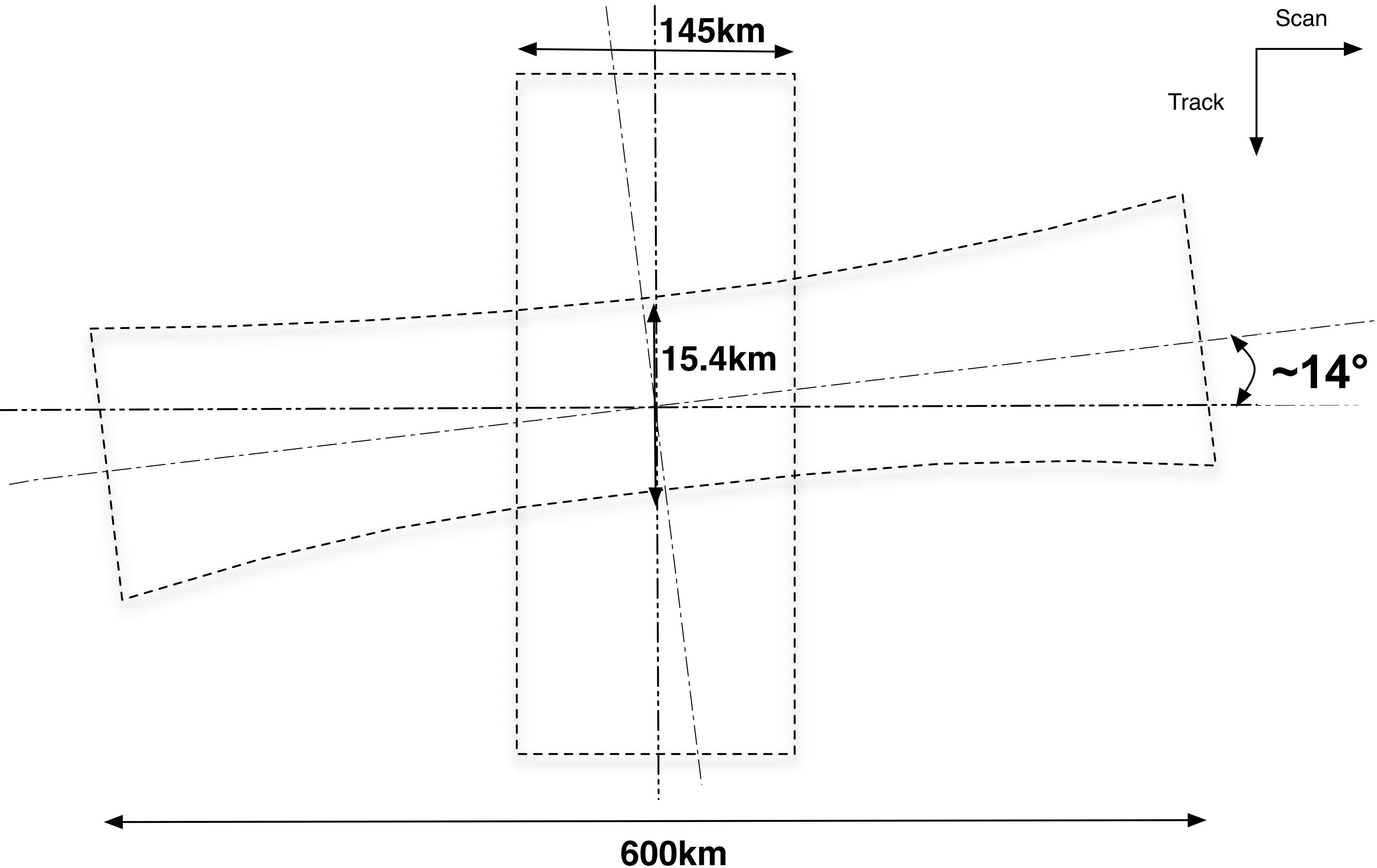

How the VSWIR and TIR would image if TIR bore sight were rotated by ~14°

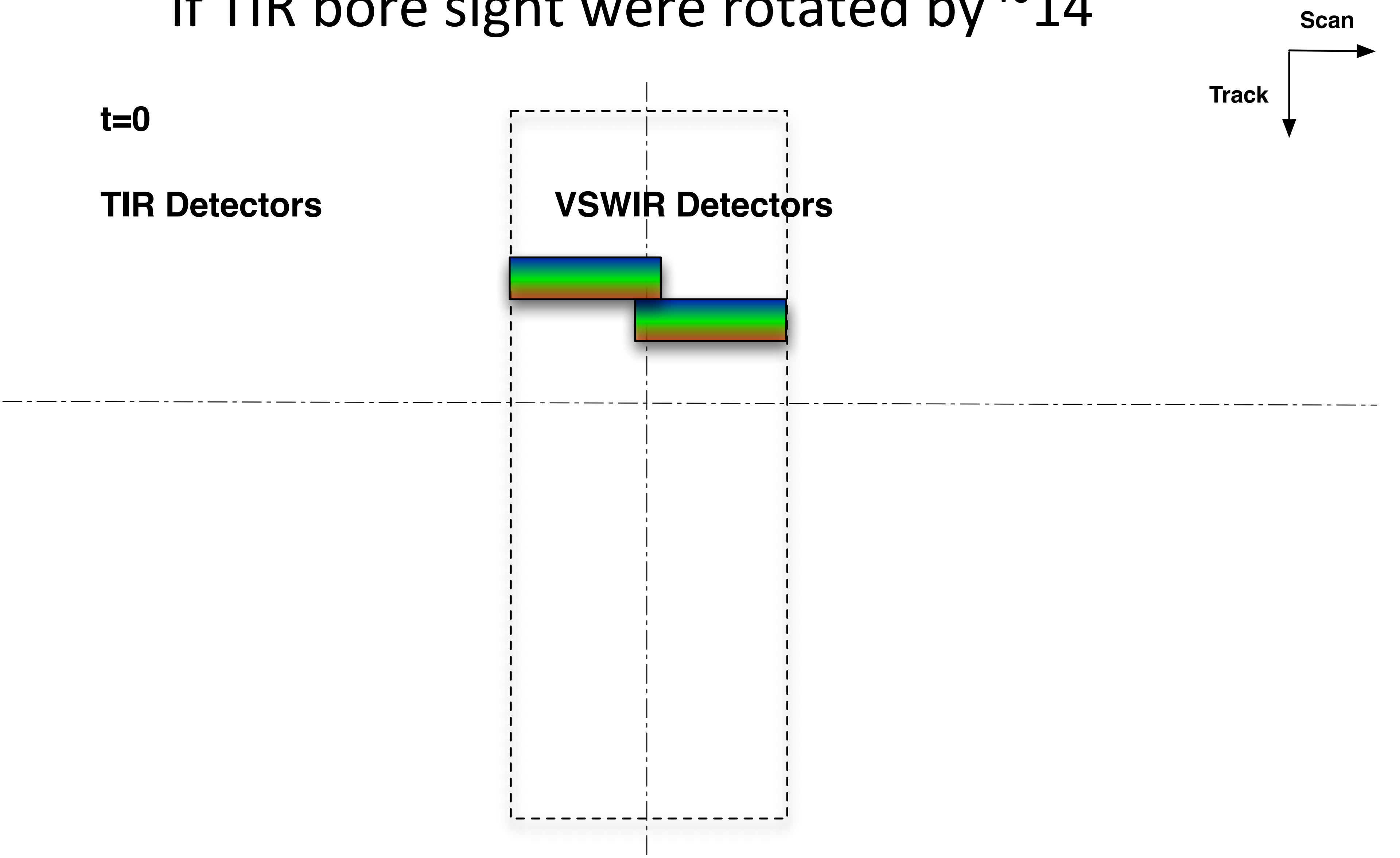

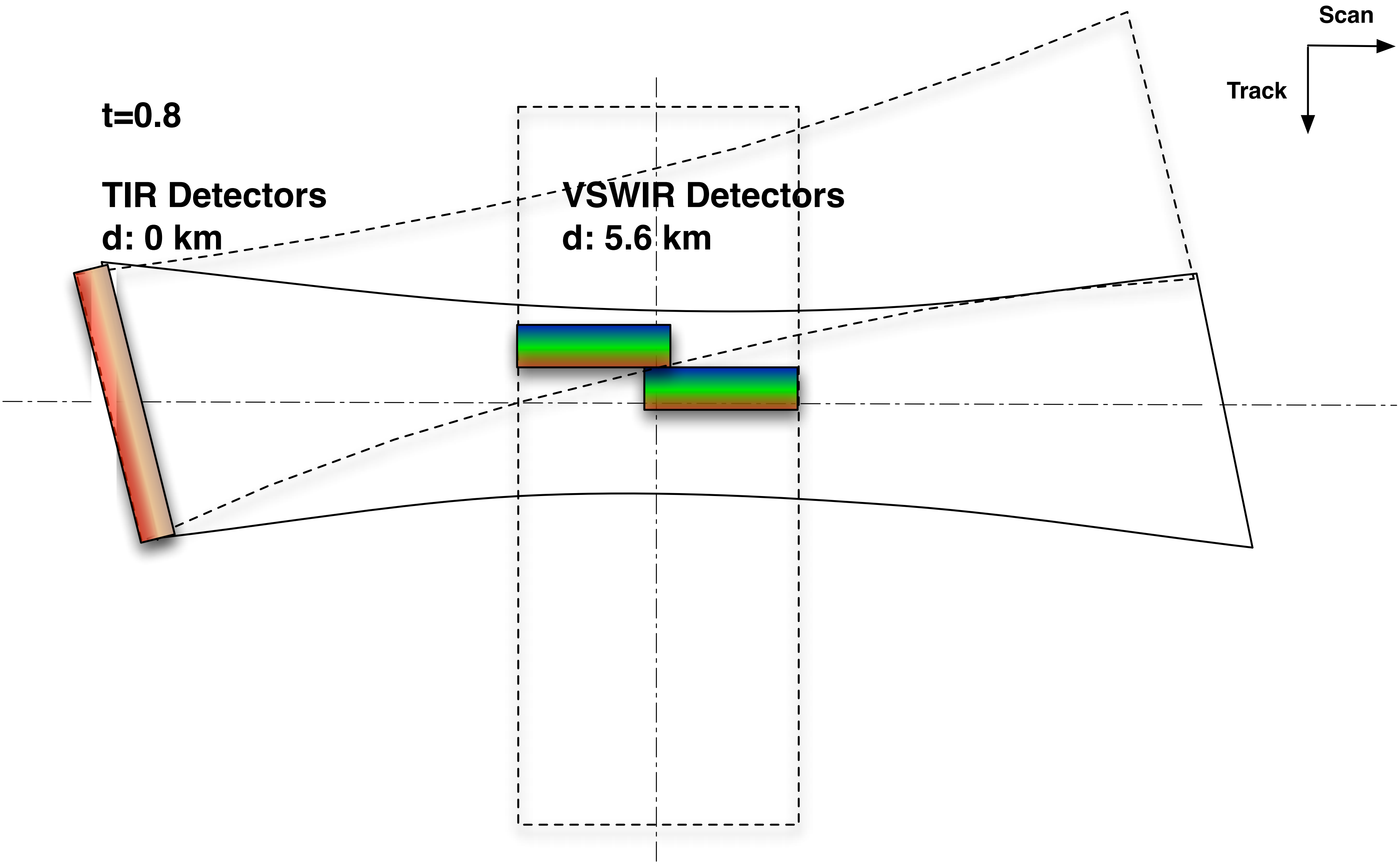
t=0.8
TIR Detectors
d: 0 km
VSWIR Detectors
d: 5.6 km
Scan
Track

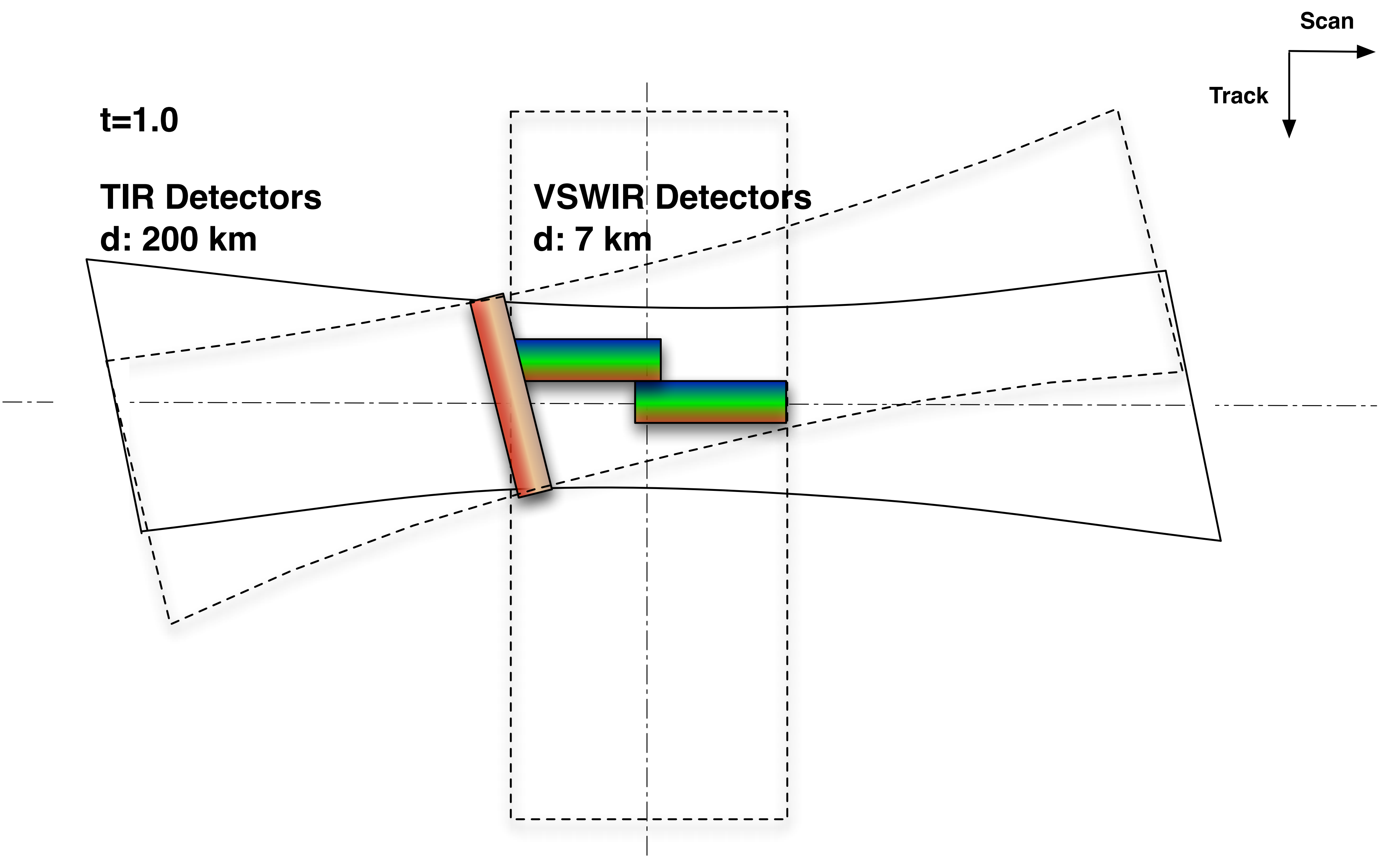

t=1.0
TIR Detectors
d: 200 km
VSWIR Detectors
d: 7 km
Scan
Track

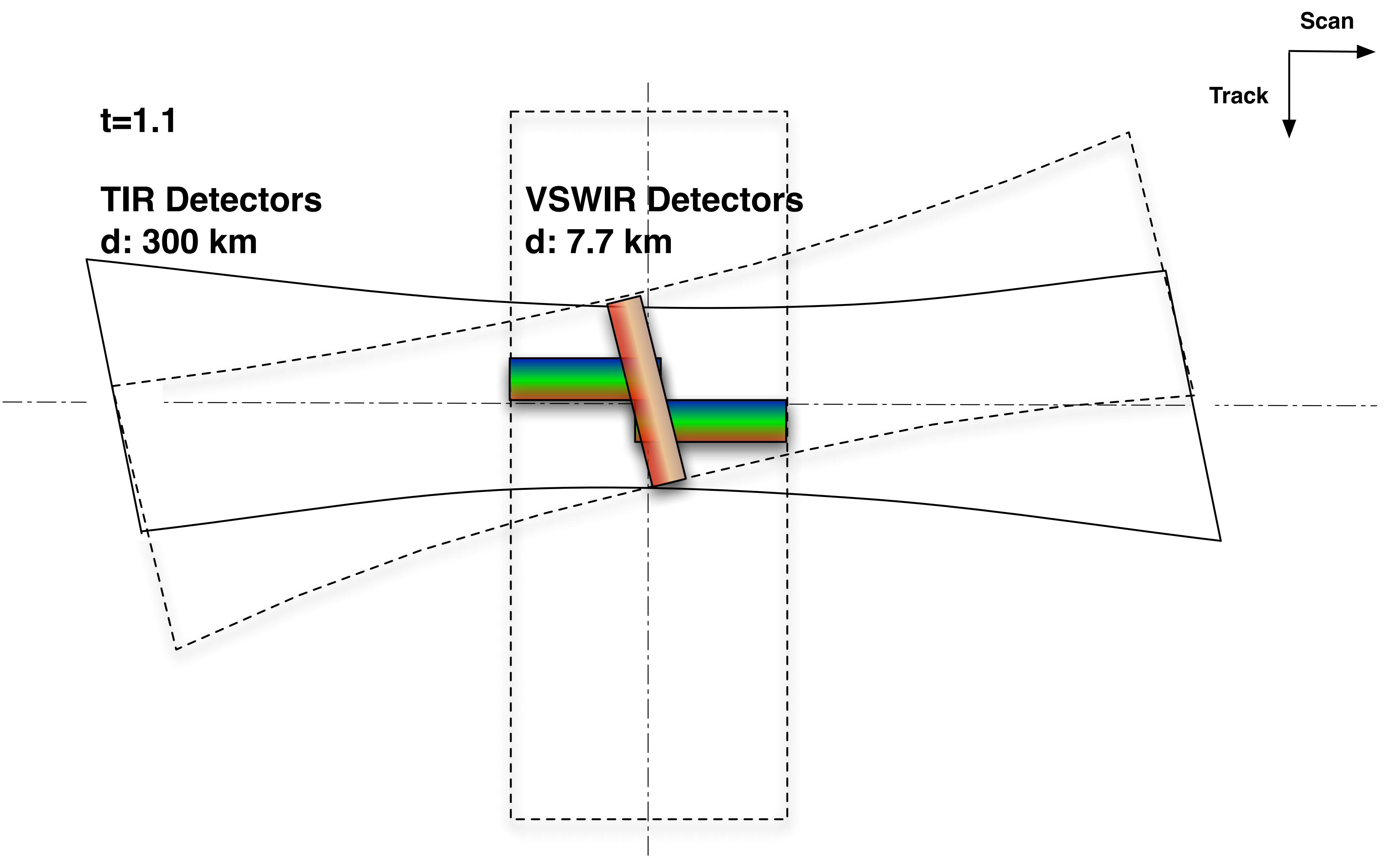
t=1.1
TIR Detectors
d: 300 km
VSWIR Detectors
d: 7.7 km
Scan
Track

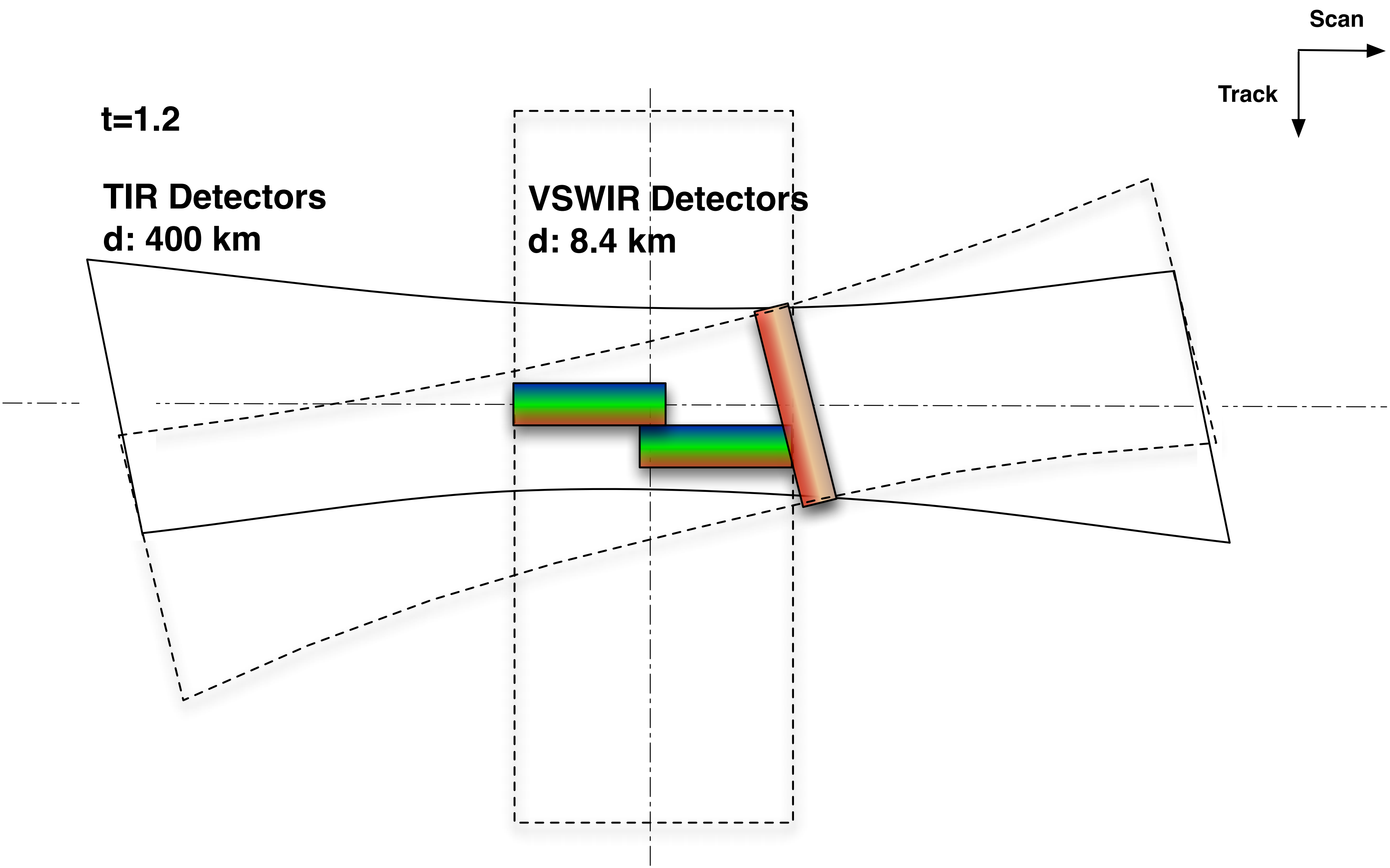
t=1.2
TIR Detectors
d: 400 km
VSWIR Detectors
d: 8.4 km
Scan
Track

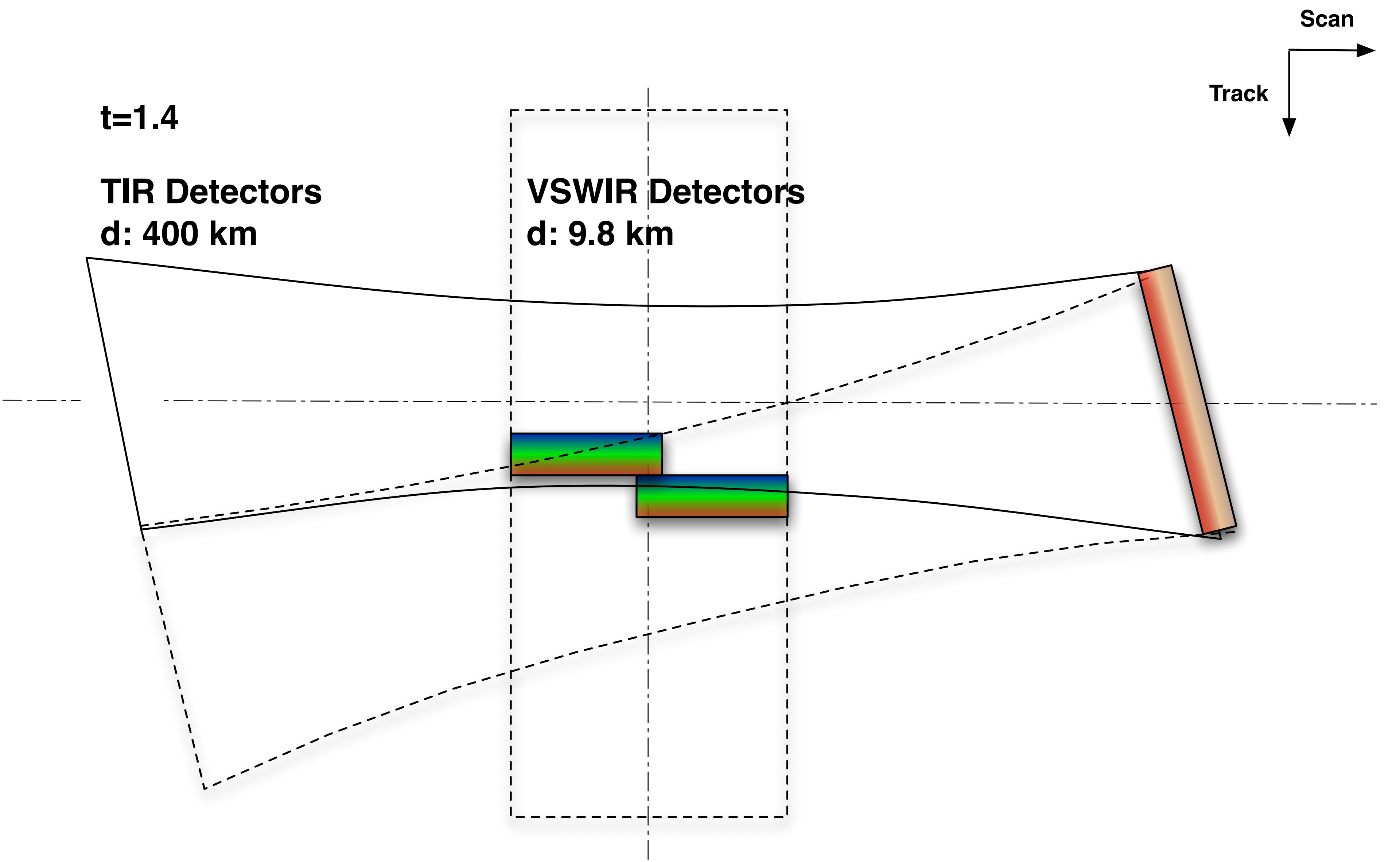

t=1.4
TIR Detectors
d: 400 km
VSWIR Detectors
d: 9.8 km
Scan
Track

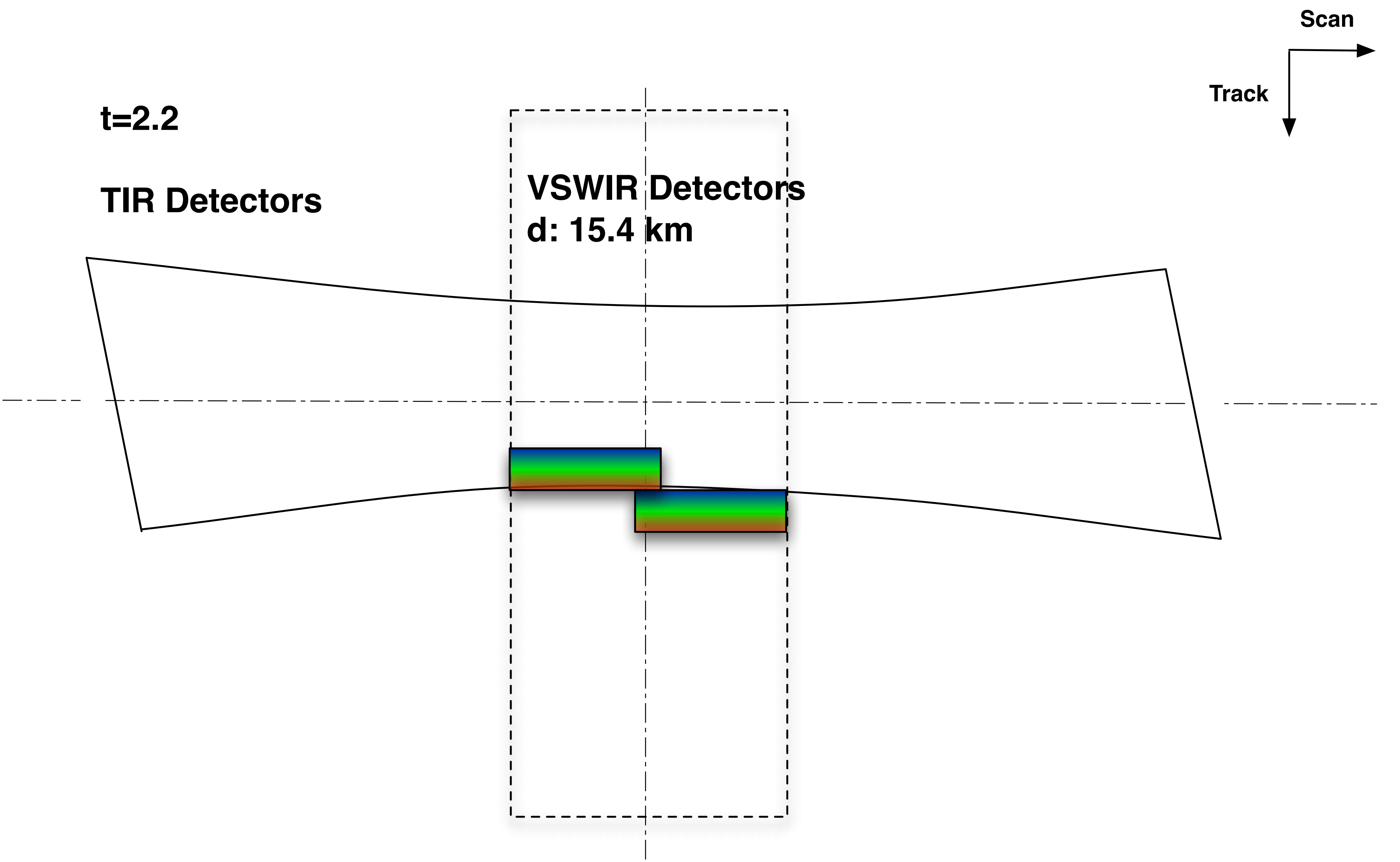

t=2.2
TIR Detectors
VSWIR Detectors
d: 15.4 km
Scan
Track

What's the problem with making level-1 VSWIR, TIR and combined products?

- By definition level-1 data must be entirely reversible back to the original level-0 data.
  - Geo-tag *radiometrically* corrected data.
  - Re-grid data using nearest neighbor values and geo-tag back to original pixel data positions *(need to deal with multiple values for the TIR)*.
- VSWIR and TIR observations are inherently misaligned in a manner which is both geographically and temporally sensitive.

Issues with sun synchronous orbits which impact geo-location control

- The selected 19 day sun synchronous circular repeat cycle orbit is not truly synchronous.
  - All sun-sync orbits are designed *(and must be maintained)* to have a fixed precession rate which will exactly match the target MLT only 2X annually
- Many factors influence the position of the sub-satellite ground track and variations of several kilometers are tolerated even in high resolution platforms (e.g. Landsat)

Why a 19 day repeat cycle and how do we determine the satellite altitude?

- We want global coverage in the shortest amount of time commensurate with achievable FOVs within the mission's cost constraints.
- There are a variety of altitudes which produce the same repeat cycle.
  - Orbital with period **T** that divide into 19 days as an exact integer **N** provide a perfect repeat cycle.
  - If **T** is in minutes, then **N*T = 12360** (= **19***24*60)
  - $\mathbf{N > 2\pi R_{Earth} / Swath\text{-}width}$ ensures global coverage

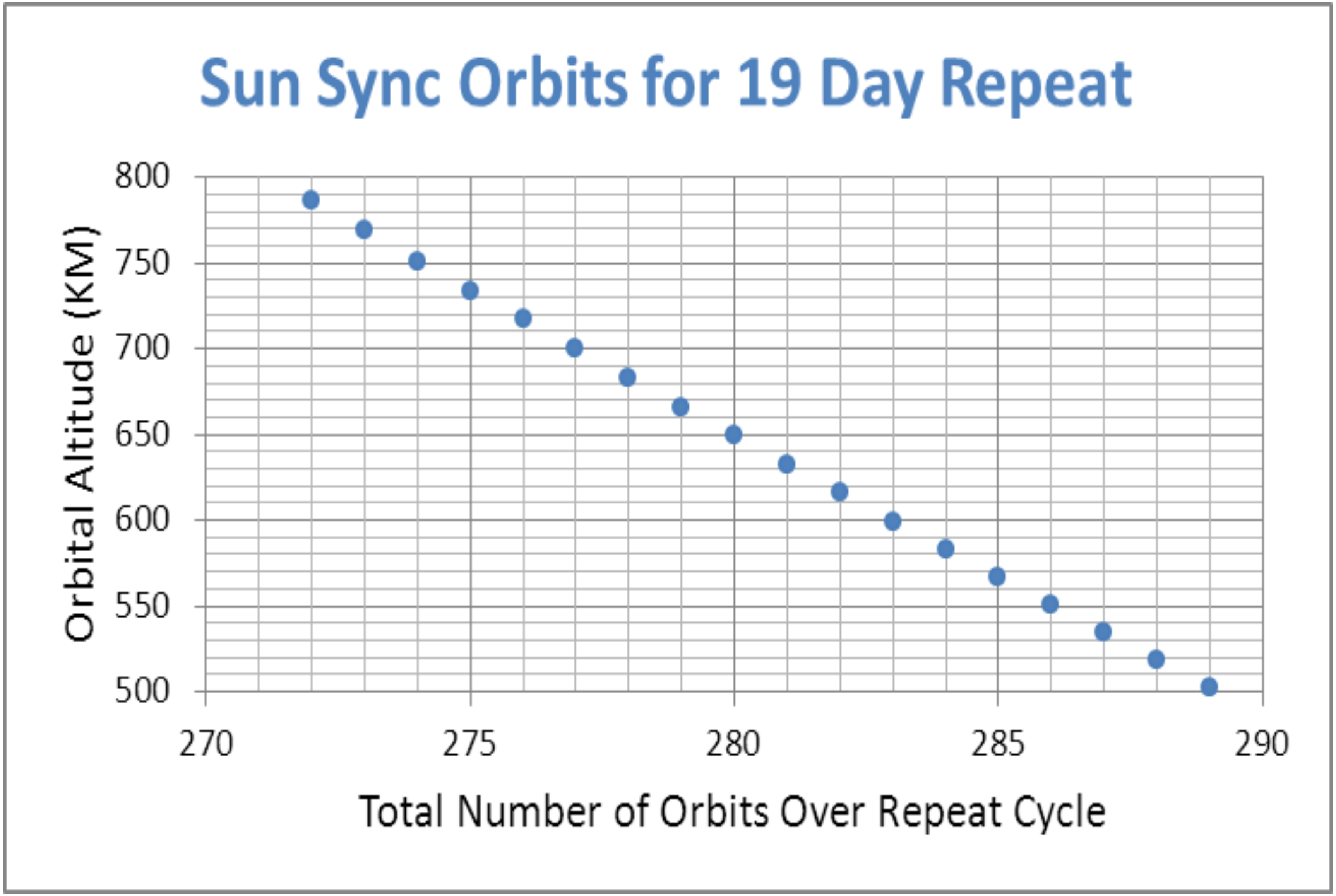
Sun Sync Orbits for 19 Day Repeat
Orbital Altitude (KM)
800
750
700
650
600
550
500
270
275
280
285
290
Total Number of Orbits Over Repeat Cycle

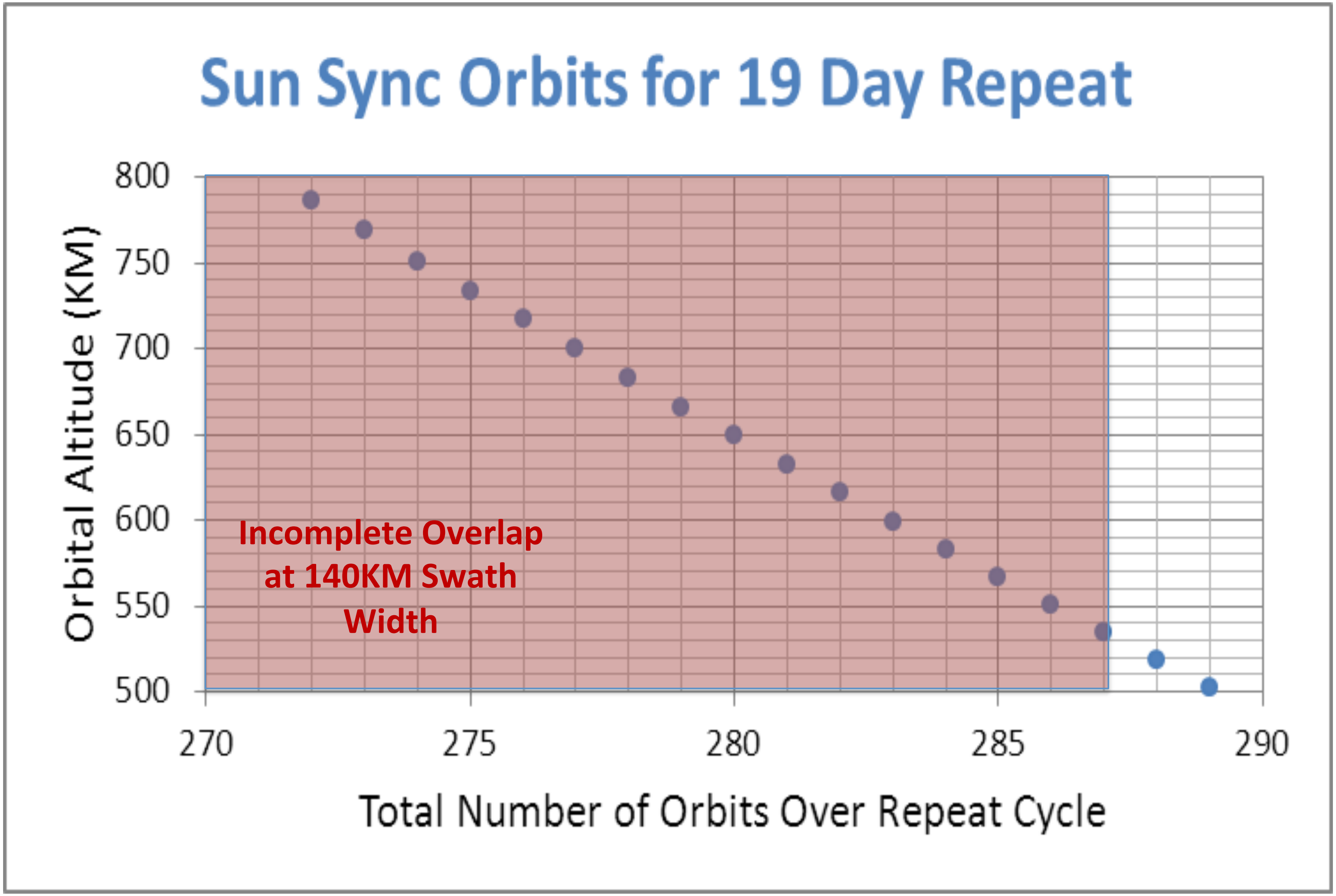
Sun Sync Orbits for 19 Day Repeat
Orbital Altitude (KM)
800
750
700
650
600
550
500
Incomplete Overlap at 140KM Swath Width
270
275
280
285
290
Total Number of Orbits Over Repeat Cycle

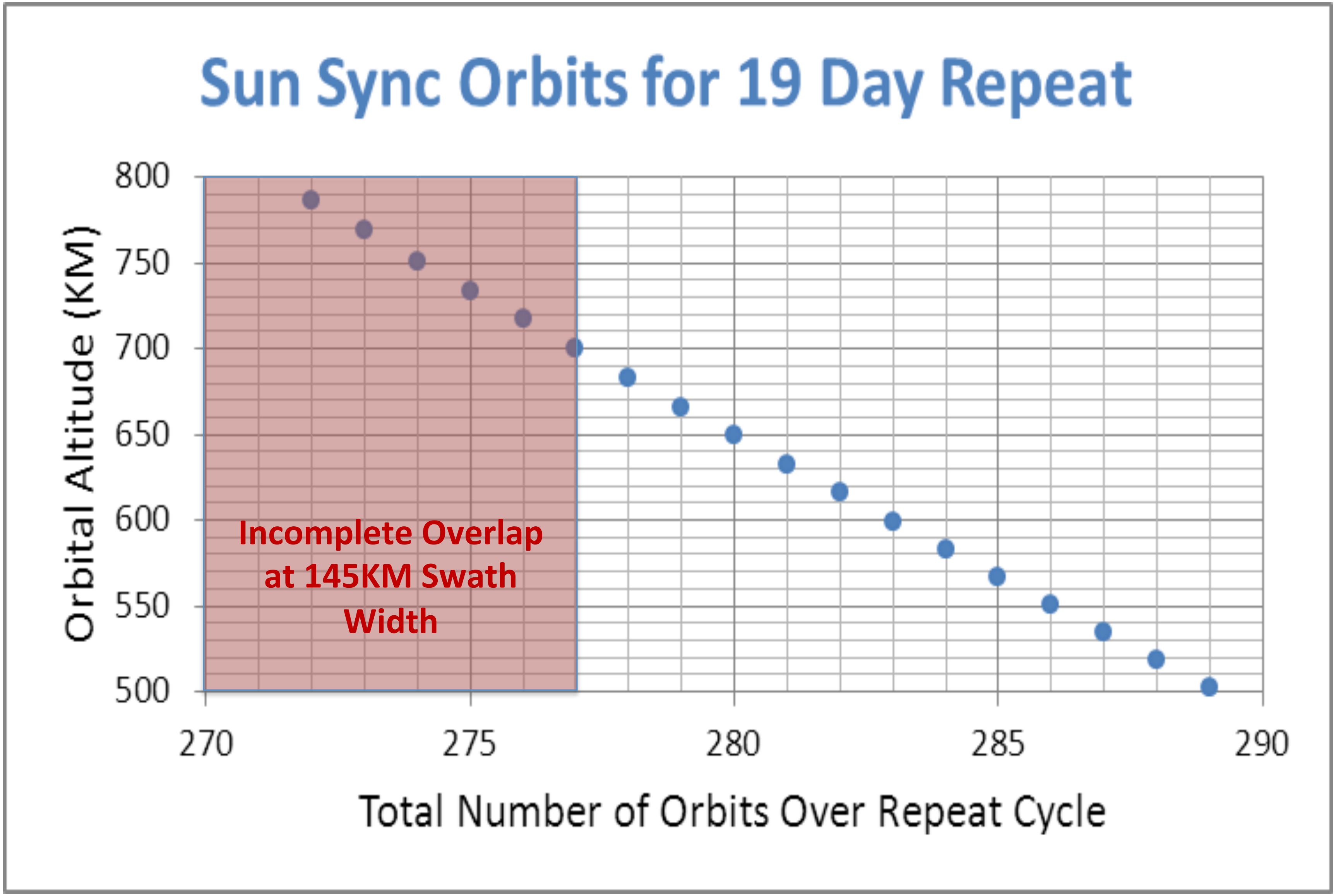

Sun Sync Orbits for 19 Day Repeat
Orbital Altitude (KM)
800
750
700
650
600
550
500
Incomplete Overlap at 145KM Swath Width
270
275
280
285
290
Total Number of Orbits Over Repeat Cycle

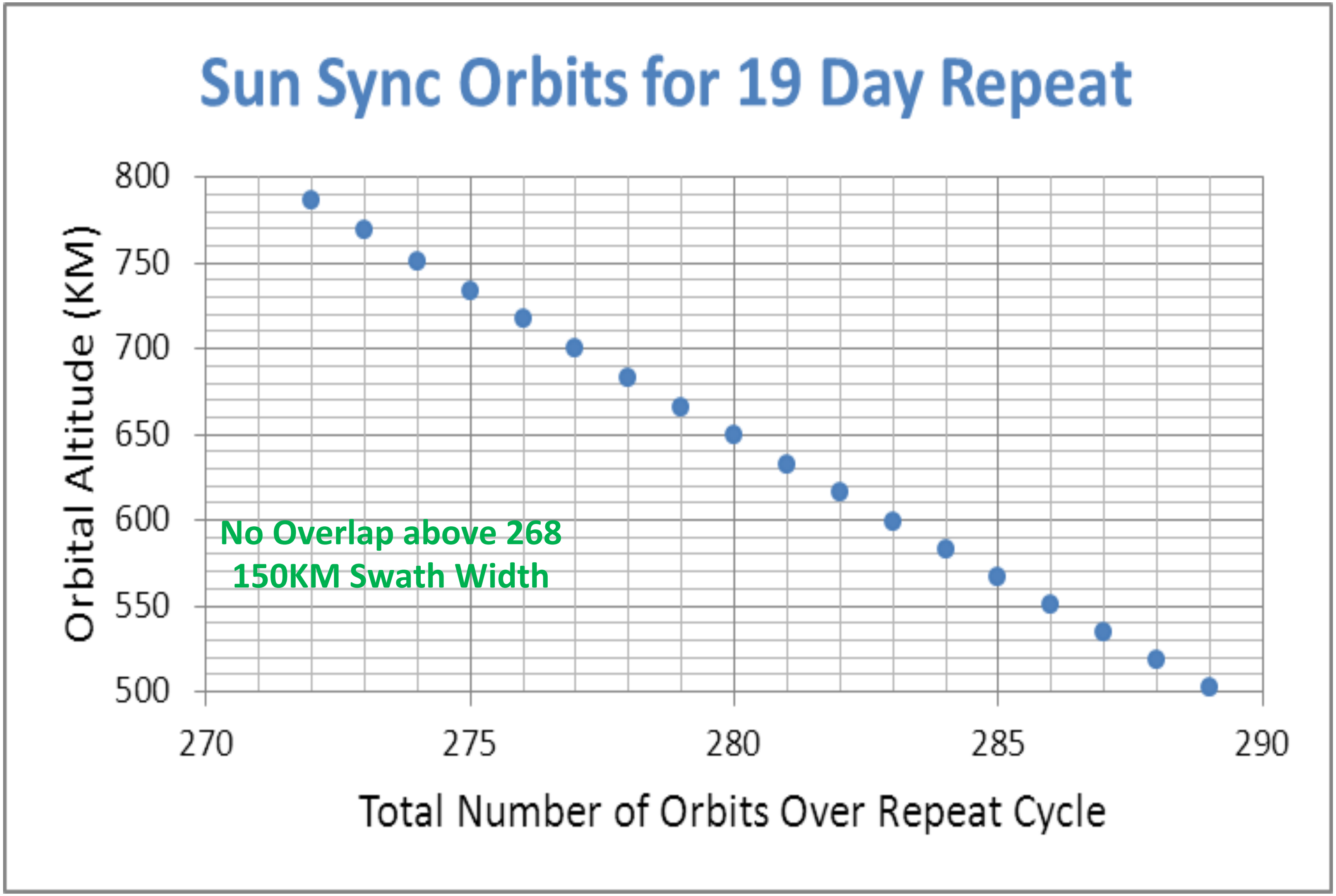
Sun Sync Orbits for 19 Day Repeat
Orbital Altitude (KM)
800
750
700
650
600
550
500
No Overlap above 268
150KM Swath Width
270
275
280
285
290
Total Number of Orbits Over Repeat Cycle

Can we have a shorter repeat cycle consistent with the current concept

- Maybe?

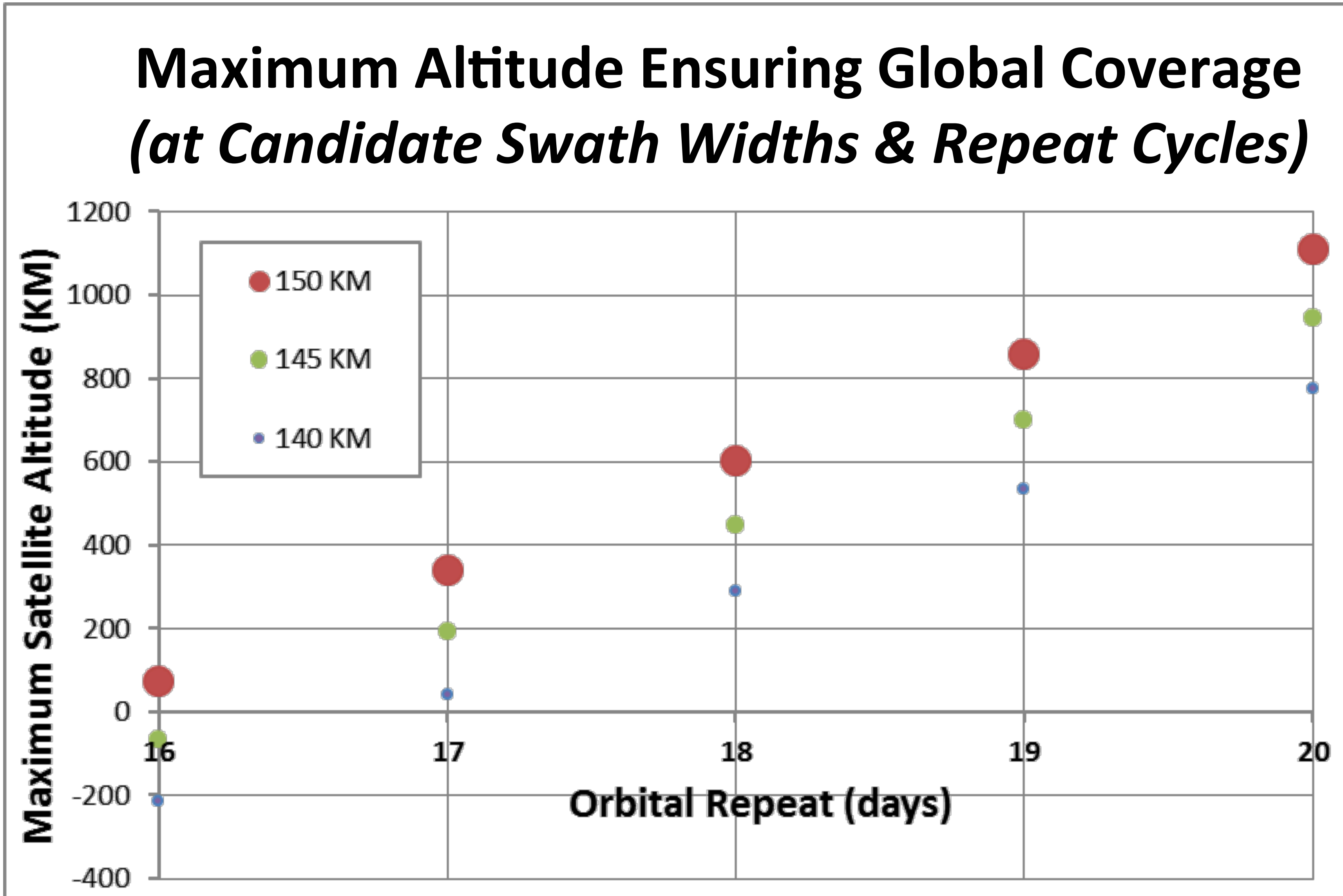
Maximum Altitude Ensuring Global Coverage
(at Candidate Swath Widths & Repeat Cycles)
Maximum Satellite Altitude (KM)
1200
1000
800
600
400
200
0
-200
-400
150 KM
145 KM
140 KM
16
17
18
19
20
Orbital Repeat (days)

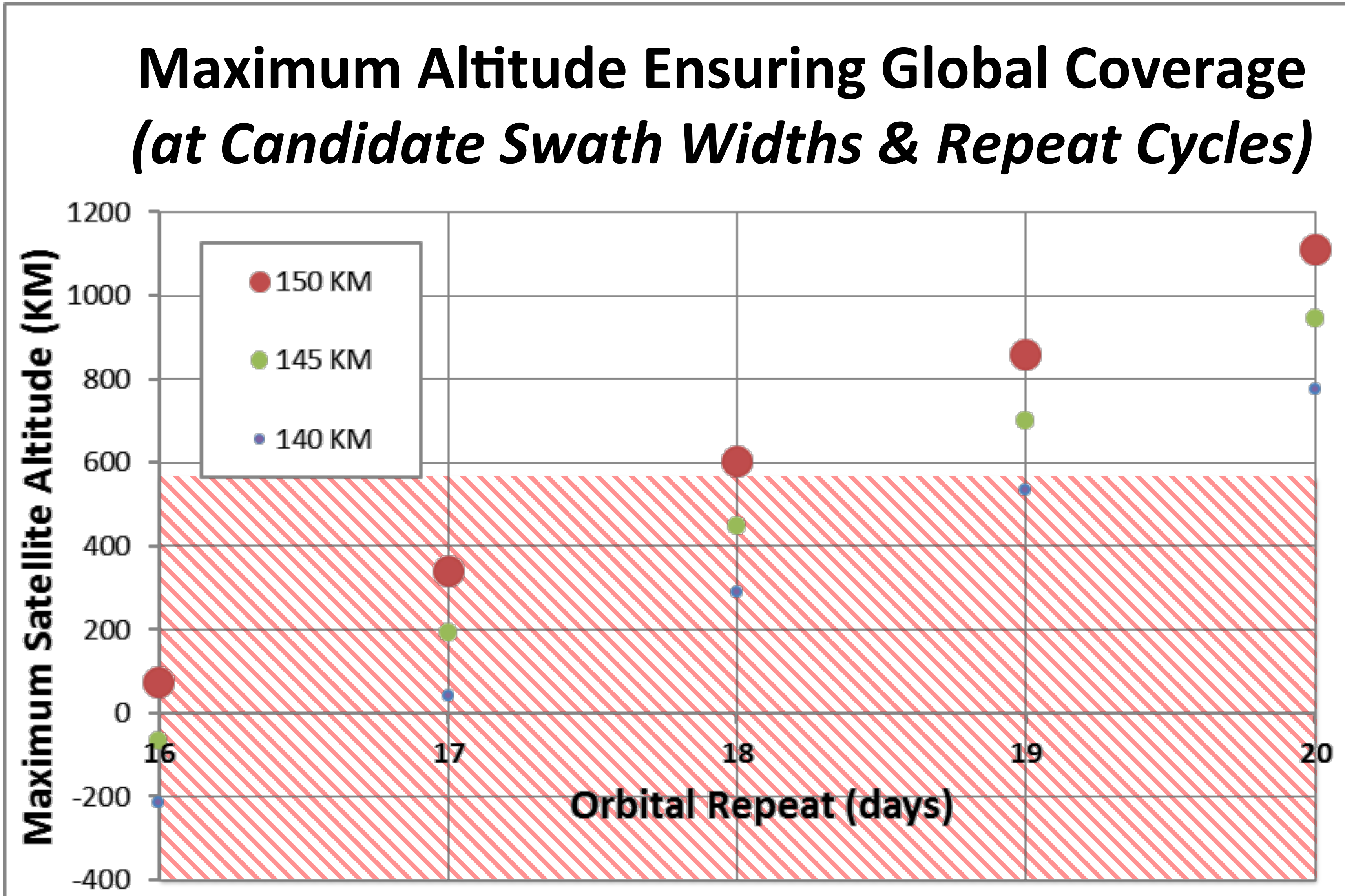
Maximum Altitude Ensuring Global Coverage
(at Candidate Swath Widths & Repeat Cycles)
1200
1000
800
600
400
200
0
-200
-400
Maximum Satellite Altitude (KM)
150 KM
145 KM
140 KM
16
17
18
19
20
Orbital Repeat (days)

Onboard Low Latency Products

- VSWIR, TIR, VSWIR / TIR Gridded?
- > 15.4km?
- Radiometric Correction
- Atmospheric Correction (VSWIR)
- AC TIR?
- DEM Corrected?
- VSWIR/TIR Co-Registration?
- Actual Product Generation (WCPS)

Finally!!

- The preceding descriptions are not merely a simplification --- they are an oversimplification.
- We need to take the effects of the Earth's rotation into account.
  - The ground sampling distance (GSD) for each instrument and the VSWIR pixel shape vary with latitude.
  - The nadir TIR and VSWIR ground tracks will not be congruent because of acquisiton time differences.
- Effects related to Earth's shape and topography
- **In my opinion none of these effects need impede the scientific utility of the data provided that we use them intelligently.**

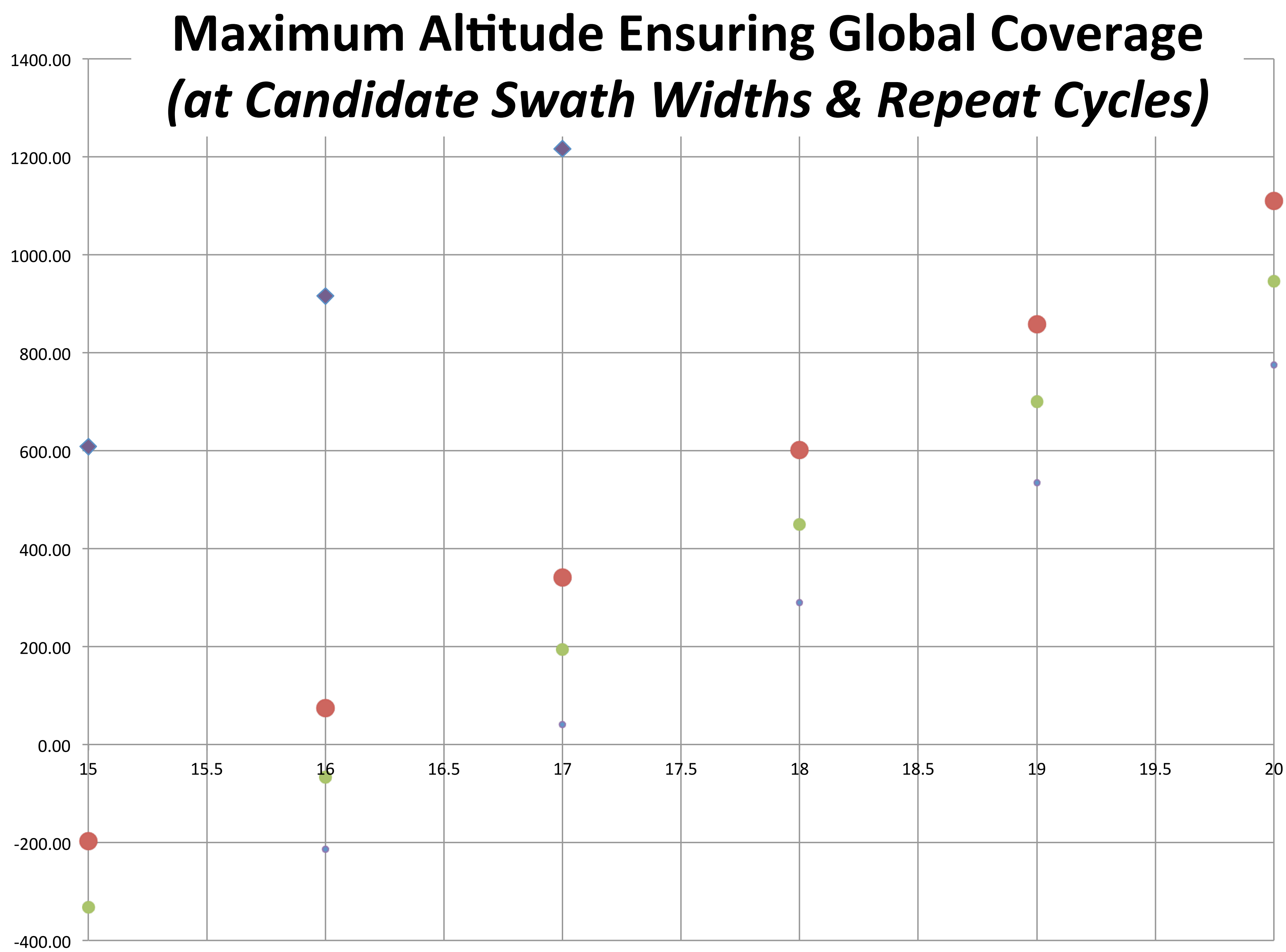

Maximum Altitude Ensuring Global Coverage
(at Candidate Swath Widths & Repeat Cycles)
1400.00
1200.00
1000.00
800.00
600.00
400.00
200.00
0.00
-200.00
-400.00
15
15.5
16
16.5
17
17.5
18
18.5
19
19.5
20

19 Day Sun Synchronous Repeat Orbits

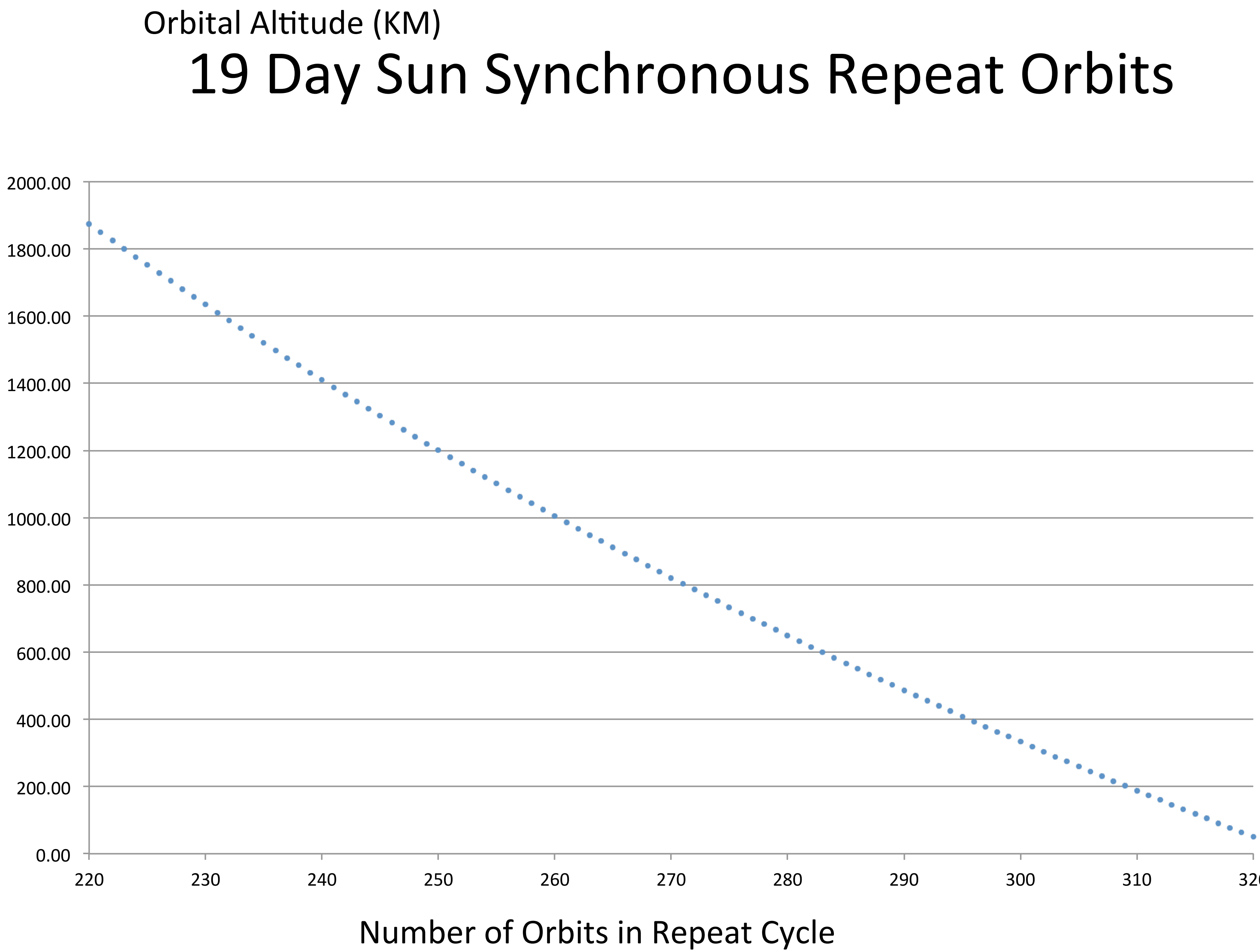

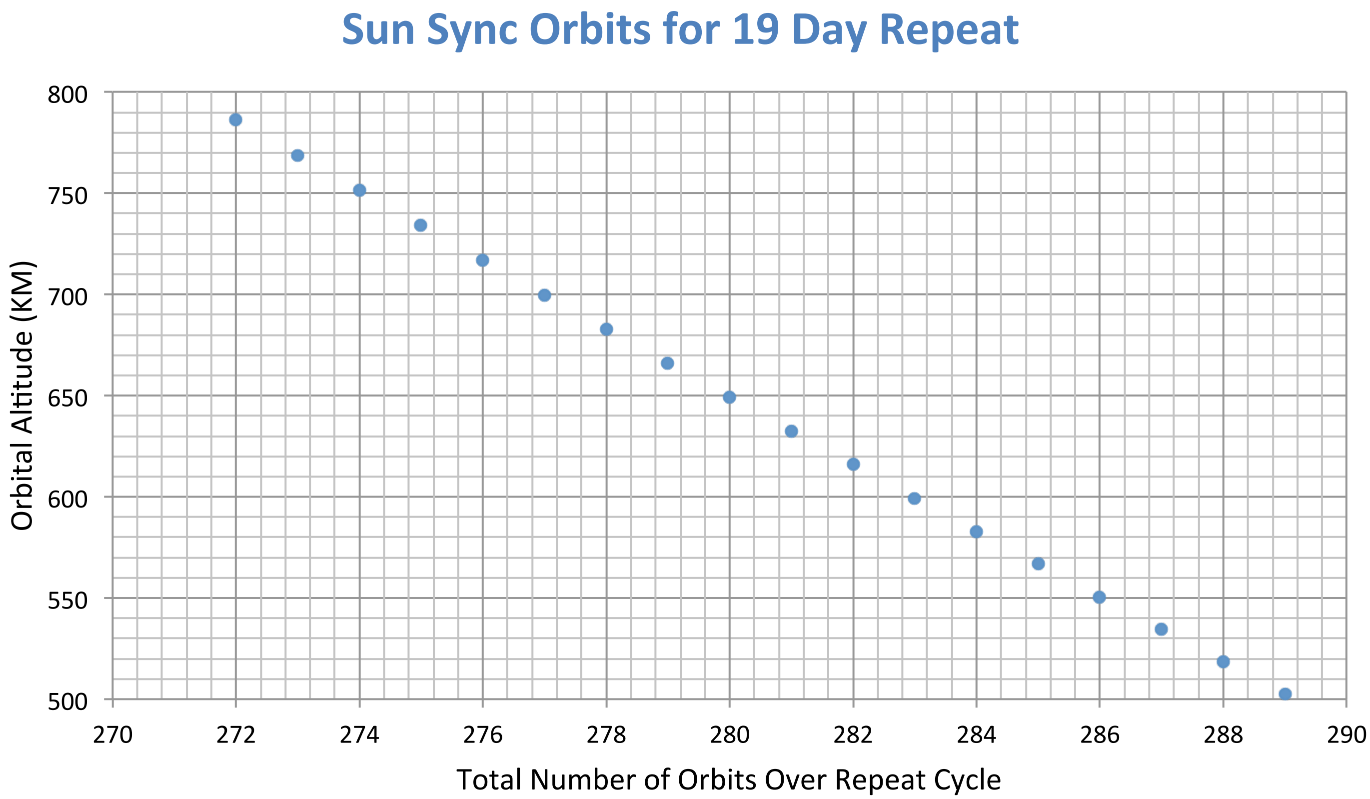

Sun Sync Orbits for 19 Day Repeat
Orbital Altitude (KM)
800
750
700
650
600
550
500
270
272
274
276
278
280
282
284
286
288
290
Total Number of Orbits Over Repeat Cycle

All you need to know about spatial impact without going into way too much detail !

Steve Ungar – NASA/GSFC Scientist Emeritus

HyspIRI Science Symposium – NASA GSFC – May 17, 2012